VOLUME 66
NUMBER 9 / NUMÉRO 9
SEPTEMBER / SEPTEMBRE
2009

An NRC Research Press
JOURNAL
Une REVUE des
Presses scientifiques du CNRC

Canadian Journal of FISHERIES AND AQUATIC SCIENCES

cjfas.nrc.ca

Journal canadien des SCIENCES HALIEUTIQUES ET AQUATIQUES

jcsha.cnrc.ca

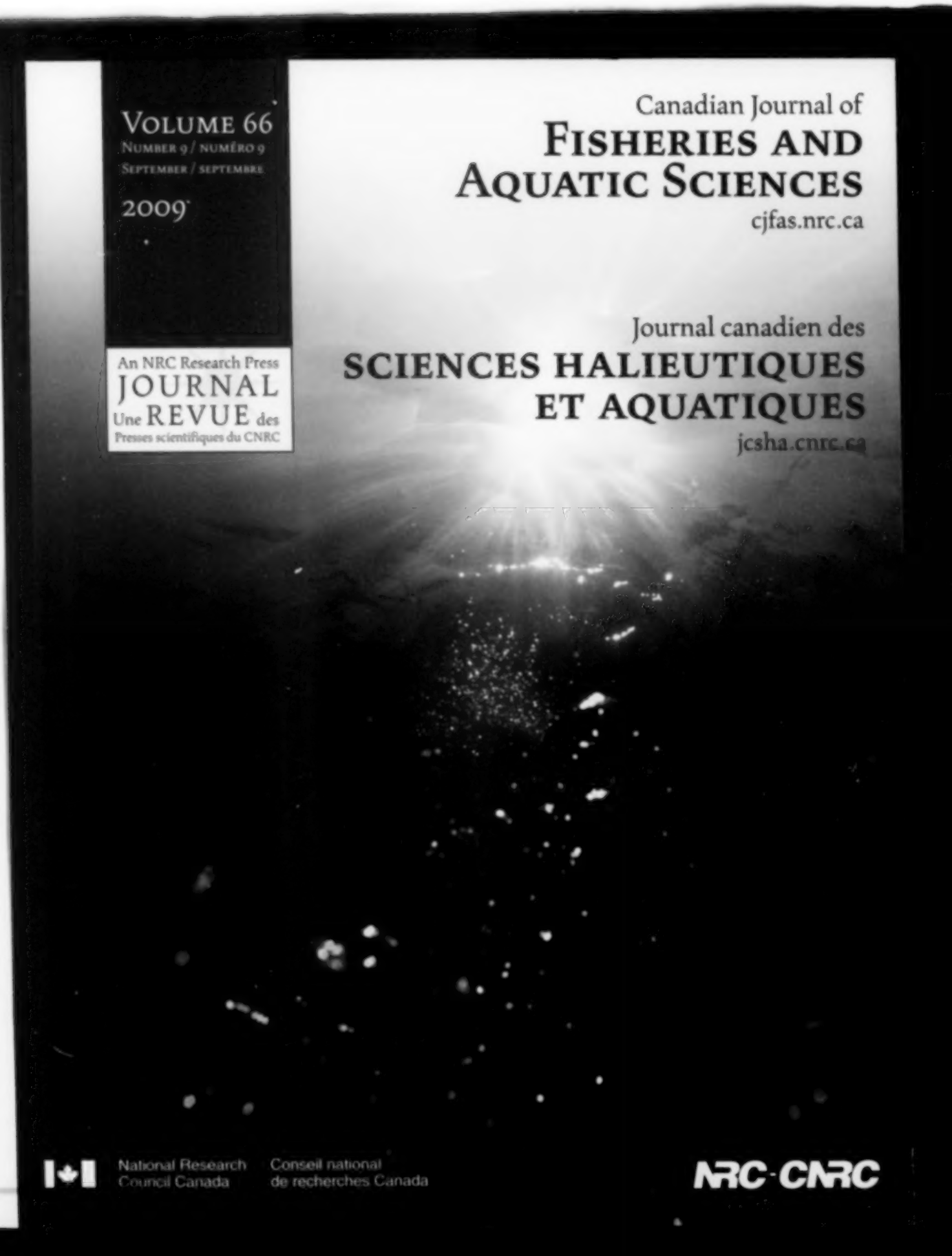

National Research Council Canada
Conseil national de recherches Canada
NRC·CNRC

ISSN 0706-652X / CJFSDX 66(9) 1399–1633 (2009)

The *Canadian Journal of Fisheries and Aquatic Sciences*, previously published as *Contributions to Canadian Biology* 1901–1925, *Contributions to Canadian Biology and Fisheries* 1926–1934, *Journal of the Biological Board of Canada* 1934–1937, and *Journal of the Fisheries Research Board of Canada* 1938–1979, is issued monthly to form annual volumes of 12 numbers plus supplements.

Editorial policy. The *Journal* publishes original research articles, perspectives (syntheses, critiques, reevaluations), discussions (comment and reply), and rapid communications. Manuscripts may concern cells, organisms, populations, communities, ecosystems, or processes that affect aquatic systems. They may cover a range of disciplines including biology and ecology of marine and freshwater organisms, limnology, oceanography, physiology, toxicology, genetics, economics, disease, and management. Preference will be given to manuscripts that emphasize understanding of observed phenomena and interpretation of experimental results. The Journal encourages papers that lead from clearly stated purpose or rationale and from testable hypotheses, concepts, or questions to identifiable conclusions or syntheses. Such papers may amplify, modify, question, or redirect accumulated knowledge embodied in contemporary perceptions of a particular state of aquatic sciences. The Journal discourages papers that are essentially descriptive, except in emerging disciplines; have only site-specific or local applications (a certain year, place, taxon, chemical compound, etc.); only confirm previously established principles; or apply standard techniques without breaking new methodological ground.

Manuscripts for publication should be submitted to the Editorial Office via NRC Research Press' online submission and peer review system (**OSPREY**) at http://pubs.nrc-cnrc.gc.ca/cjfas/osprey. Alternatively, manuscripts may be submitted to the Editor, *Canadian Journal of Fisheries and Aquatic Sciences*, Department of Ecology and Evolutionary Biology, University of Toronto, Toronto, ON M5S 3G5, Canada (416-946-0609; fax: 866-523-4174 (Canada and United States) or 416-946-0509; e-mail: cjfas@utoronto.ca).

Submissions in either English or French are acceptable. The information must be original, that is, not copyrighted, published, or submitted elsewhere except in abstract form or unless by written consent of the Editor.

Correspondence concerning accepted manuscripts and corrected proofs should be sent to NRC Research Press, National Research Council of Canada, Ottawa, ON K1A 0R6, Canada (fax: 613-952-7656; e-mail: pubs@nrc-cnrc.gc.ca).

Instructions to Authors are published at cjfas.nrc.ca. The **Publishing Policy** of NRC Research Press is available at pubs.nrc-cnrc.gc.ca.

The *Canadian Journal of Fisheries and Aquatic Sciences*, ISSN 0706-652X, is published monthly, 12 times per year, by NRC Research Press, c/o USACAN Media Dist. Srv. Corp. at 26 Power Dam Way, Suite S1-S3, Plattsburgh, NY 12901, USA. Periodicals postage paid at Plattsburgh, NY. POSTMASTER: Send address changes to *Canadian Journal of Fisheries and Aquatic Sciences*, c/o NRC, P.O. Box 2888, Plattsburgh, NY 12901, USA.

Publié sans interruption depuis 1901, le *Journal canadien des sciences halieutiques et aquatiques* a paru sous plusieurs titres : *Contributions to Canadian Biology* 1901–1925, *Contributions to Canadian Biology and Fisheries* 1926–1934, *Journal of the Biological Board of Canada* 1934–1937, et *Journal of the Fisheries Research Board of Canada* 1938–1979. Le Journal paraît tous les mois, formant ainsi un volume de 12 numéros, et offre en plus jusqu'à deux suppléments par année.

Politique éditoriale. On publie, dans le Journal, des articles rendant compte de recherche originale, des perspectives (synthèses, critiques et réévaluations), des discussions (commentaires et réponses) et des communications rapides. Les documents peuvent porter sur les cellules, organismes, populations, communautés, écosystèmes ou processus qui affectent les systèmes aquatiques. Ils peuvent relever de divers domaines y compris la biologie et l'écologie des organismes marins et d'eau douce, la limnologie, l'océanographie, la physiologie, la toxicologie, la génétique, l'économie, la pathologie et la gestion. On accorde la préséance aux articles qui contribuent à la compréhension de phénomènes observés et à l'interprétation de résultats expérimentaux. On invite les auteurs à soumettre des articles ayant des objectifs précis ou relevant d'hypothèses, de concepts ou de questions vérifiables et se terminant par de solides conclusions ou d'utiles synthèses. Ces articles enrichissent, changent, mettent en question ou réorientent les connaissances acquises sur divers aspects des sciences aquatiques. On décourage toutefois la soumission d'articles simplement descriptifs (à moins qu'il ne s'agisse de nouvelles disciplines), d'application très limitée (applicables à une seule année, une seule région ou un seul taxon, portant sur un unique composé chimique, etc.); d'articles qui ne font que reprendre les principes énoncés dans des articles précédents; et d'articles rendant compte de l'application de normes sans gain de méthodologie.

Les auteurs sont invités à soumettre leur **manuscrit** au Bureau de la rédaction par le truchement du Système de soumission et d'examen en direct des articles (**OSPRE**Y) des Presses scientifique du CNRC à http://pubs.nrc-cnrc.gc.ca/jcsha/osprey. Sinon, ils peuvent transmettre leur manuscrit par la poste au rédacteur en chef, *Journal canadien des sciences halieutiques et aquatiques*, Département d'écologie et de biologie évolutive, Université de Toronto, Toronto, ON M5S 3G5, Canada (416-946-0609; télécopieur : 866-523-4174 (Canada et États-Unis) ou 416-946-0509; courriel : cjfas@utoronto.ca).

Les contributions peuvent être en anglais ou en français. Elles doivent être originales, c.-à.-d. qu'elles ne doivent pas avoir fait l'objet d'un copyright, avoir été publiées ou soumises ailleurs, sauf sous forme abrégée ou avec le consentement du rédacteur en chef.

La correspondance ayant trait aux manuscrits acceptés et les **épreuves corrigés** doivent être envoyées aux Presses scientifiques du CNRC, Conseil national de recherches du Canada, Ottawa, ON K1A 0R6, Canada (télécopieur : 613-952-7656; courriel : pubs@nrc-cnrc.gc.ca).

Les **Recommandations aux auteurs** sont publiées au jcsha.cnrc.ca. La **Politique éditoriale** est disponible auprès des Presses scientifiques du CNRC ou au pubs.nrc-cnrc.gc.ca.

This Journal is indexed or abstracted in / Cette revue est signalée ou résumée dans

Aqualine; Aquatic Sciences and Fisheries Abstracts; BIOBASE; Biological and Agricultural Index; BIOSIS; CAB Abstracts; Canadian Fisheries Abstracts; Chemical Abstracts; Current Awareness in Biological Sciences; Current Abstracts; Current Contents; General Science Index; Oceanic Abstracts; PASCAL; Pollution Abstracts; Referativnyi Zhurnal; Science Citation Index; Water Resources Abstracts

Volume 66, Number 9, September 2009

Canadian Journal of Fisheries and Aquatic Sciences

Published by the National Research Council of Canada

Volume 66, numéro 9, septembre 2009

Journal canadien des sciences halieutiques et aquatiques

Publié par le Conseil national de recherches du Canada

Editors / Rédacteurs en chef **Don Jackson and Rolf Vinebrooke**

Assistant to the Editors / Adjointe au rédacteur en chef **Holly Foster**

Associate Editors / Comité de rédaction

M.J. Bradford, *DFO/MPO and Simon Fraser University*
D. Brickman, *DFO/MPO, Dartmouth*
S.E. Campana, *DFO/MPO, Dartmouth*
X. Chen, *Shanghai Fisheries University, Shanghai, China*
Y. Chen, *University of Maine, Orono, Maine*
B. Gillanders, *University of Adelaide, Australia*
J.W.A. Grant, *Concordia University*
M.M. Hansen, *Aarhus University, Denmark*
R. Hilborn, *University of Washington*
J.M. Jech, *NFSC/NOAA, Woods Hole, Mass.*
B. Jonsson, *Norwegian Institute for Nature Research, Oslo, Norway*
K.A. Kidd, *University of New Brunswick*
C. Kraft, *Cornell University, Ithaca, N.Y.*
D.L. MacLatchy, *University of New Brunswick, Saint John*
P. Magnan, *Université du Québec à Trois Rivières*
C.T. Marshall, *University of Aberdeen*
J. Post, *University of Calgary*
Y.T. Prairie, *Université du Québec à Montréal*
T.J. Quinn II, *University of Alaska–Fairbanks, Juneau, Alaska*
C.W. Ramcharan, *Laurentian University*
J.S. Richardson, *The University of British Columbia*
M.-J. Rochet, *IFREMER, Nantes, France*
K. Rose, *Louisiana State University, Baton Rouge, La.*
J. Rosenfeld, *British Columbia Ministry of Fisheries*
B. Sainte-Marie, *DFO/MPO, Mont-Joli*
R.E.H. Smith, *University of Waterloo*
S.J. Smith, *DFO/MPO, Dartmouth*
W.G. Sprules, *University of Toronto at Mississauga*
E.B. Taylor, *The University of British Columbia*
W. Tonn, *University of Alberta*
M. Trudel, *DFO/MPO, Pacific Biological Station, Nanaimo*
A. Vasemägi, *University of Turku, Turku, Finland*
C.J. Walters, *The University of British Columbia*
G. Weyhenmeyer, *Uppsala University, Sweden*

NRC Research Press / Presses scientifiques du CNRC

Fax / Télécopieur : 613-952-7656; e-mail / courriel : pubs@nrc-cnrc.gc.ca; URL / URL : pubs.nrc-cnrc.gc.ca

Editor-in-Chief / Directeur de la publication **Bruce P. Dancik**
Deputy Editor-in-Chief / Sous-directrice de la publication **Cindy E. Prescott**
Publisher / Éditeur **Cameron D. Macdonald**
Deputy Director / Directrice adjointe **Suzanne Kettley**

Business Manager / Gestionnaire des affaires commerciales **Mike Boroczki**
Advertising / Annonces publicitaires **Roxanne Landriault** (613-990-2254)
Subscriptions / Abonnements **Eileen Evans-Nantais** (613-990-7873)

Manager, Journals Program / Gestionnaire du Programme des revues **Carolyn Brown**
Managing Editor / Directrice de la rédaction **Cecily M. Pearson** (613-993-9099)
Scientific Publishing Editors / Réviseurs de publications scientifiques **Jennifer McColl, Thad Costigan, Peter Burke**
Editorial Publication Technicians / Techniciens à la publication éditoriale **Diana Leck, Luc Julien**
Editorial Applications Training and Support Officer / Agente de formation et de soutien à l'éditique **Mary Seligy**

Production Manager / Gestionnaire de la production **Judy Hum**
Acting Application Support Technician / Technicien au soutien de la production par intérim **Greg Boyce**
e-Publishing Technician / Technicien à l'édition électronique **Cory Klinkenberg**
Graphics Technician / Technicien en graphisme **Dario Ferrara, Davin P. Henrikson**
Web Technician / Technicien Web **Dennis Cafferty**

The National Research Council of Canada accepts no responsibility for statements or opinions expressed by a contributor. Acceptance of an advertisement, announcement, or other material does not imply endorsement by either the Journal's Editor or the National Research Council of Canada.

2009 National Research Council Canada or its licensors

For articles published in 2009 and later, copyright remains with the authors, whereas for articles published before 2009, copyright is held by the National Research Council Canada.

No part of the NRC Research Press journals may be reproduced, stored, or transmitted in any form or by any means, without the written permission of the publisher, except as stated below.

Under the Canadian *Copyright Act*, individuals may download or print single copies of articles for personal research or study. Any person may reproduce short excerpts from articles in the journals for any purpose that respects the moral rights of authors, provided that the source is fully acknowledged. As a courtesy, the consent of authors of such material should be obtained directly from the author.

Authorization to reproduce items for other than personal research or study, as stated above, may be obtained by clicking on the "Reprints and Permissions" link in the table of contents of the electronic article in question or via Access Copyright (http://www.accesscopyright.ca).

NRC Research Press also extends certain additional rights to authors.

The above rights do not extend to copying or reproduction for general distribution, for advertising or promotional purposes, for creating new collective works, or for resale. For such copying or reproduction, arrangements must be made with NRC Research Press (National Research Council Canada, Ottawa, ON K1A 0R6, Canada).

Subscription information

The *Canadian Journal of Fisheries and Aquatic Sciences* (ISSN 0706-652X) is published monthly by the National Research Council of Canada. The 2009 subscription rates are as follows. Institutional: electronic $1125; print, $1250; electronic + print, $1560. Personal: electronic, $290, print + electronic, $380. For all orders outside Canada, rates are in U.S. dollars. Print subscriptions include second class postage. For air mail add US$180 to the foreign rate. Canadian customers please include GST (business no. 12149 1807 RT 0275). Subscriptions are entered for the calendar year. Remittances should be made payable to the Receiver General for Canada, credit NRC. Price for regular single issues: institutional, $120.00; personal, $40.00. Supplements will be priced separately. Special rates apply to members of Canadian scientific and engineering societies if they subscribe through their respective societies.

Issues of the *Canadian Journal of Fisheries and Aquatic Sciences* are available on the Web. Pricing information can be found at pubs.nrc-cnrc.gc.ca.

There are no refunds on cancelled subscriptions once delivery has begun. Claims for missing issues should be made within four months (North America) or six months (outside North America) following the date of publication. The publisher expects to supply missing issues only when losses have occurred in transit and when the reserve stock will permit. For change of address and subscription enquiries: Subscription Office, NRC Research Press, National Research Council of Canada, Ottawa, ON K1A 0R6, Canada; tel.: 613-993-9084; fax: 613-952-7656; e-mail: pubs@nrc-cnrc.gc.ca.

Microform backfiles are available from UMI, P.O. Box 1346, Ann Arbor, MI 48106-1346, USA, and Micromedia Ltd., 20 Victoria St., Toronto, ON M5C 2N8, Canada.

Le Conseil national de recherches du Canada ne se tient en aucune façon responsable des opinions exprimées par un collaborateur ou des déclarations que pourrait faire ce dernier. La publication d'annonces publicitaires, d'avis et autres n'implique pas l'endossement de leur contenu par le rédacteur en chef de la Revue ou le Conseil national de recherches du Canada.

2009 Presses scientifiques du CNRC ou ses concédants de licence

Les auteurs détiennent les droits d'auteur sur les articles publiés en 2009 et plus tard, tandis que les Presses scientifiques du CNRC détiennent les droits d'auteurs sur les articles publiés avant 2009.

Il est interdit de reproduire, de sauvegarder ou de transmettre toute partie des revues des Presses scientifiques du CNRC dans quelque format ou de quelque façon que ce soit sans le consentement écrit de l'éditeur, sauf dans les cas énoncés ci-après.

Aux termes de la *Loi sur le droit d'auteur* du Canada, les particuliers peuvent télécharger ou imprimer des copies individuelles d'articles pour leurs études ou leurs recherches personnelles. Toute personne peut reproduire de courts extraits des articles d'une revue pourvu que les droits moraux de l'auteur soient respectés et que la source soit clairement indiquée. Il convient de demander directement à l'auteur son consentement.

On peut obtenir l'autorisation de reproduire du contenu à d'autres fins que l'usage personnel (tel que décrit ci-dessus), en cliquant sur le lien « Réimpressions et autorisations » dans la table des matières de l'article électronique en question ou par l'intermédiaire d'Access Copyright (http://www.accesscopyright.ca).

Les Presses scientifiques du CNRC accordent aussi des privilèges supplémentaires aux auteurs.

Les droits ci-dessus ne s'appliquent pas à la reproduction à grande échelle aux fins de distribution générale, de publicité ou de promotion, de compilation de nouveaux ouvrages collectifs ou de revente, par exemple. Les droits de reproduction de ce genre doivent faire l'objet d'une entente particulière avec les Presses scientifiques du CNRC (Conseil national de recherches du Canada, Ottawa, ON K1A 0R6, Canada).

Renseignements sur l'abonnement

Journal canadien des sciences halieutiques et aquatiques (ISSN 0706-652X) est une publication mensuelle du Conseil national de recherches du Canada. En 2009, les tarifs d'abonnement pour les organismes sont : 1125 $ pour la version électronique; 1250 $ pour l'imprimé; 1560 $ pour les deux versions. Pour leur part, les particuliers paient les tarifs suivants : 290 $ pour la version électronique; 380 $ pour la version électronique et l'imprimé. Les tarifs des commandes provenant de l'extérieur du Canada sont en dollars des États-Unis. L'abonnement à l'imprimé comprend le tarif du courrier de deuxième classe. L'expédition par avion exige des frais de 180 $ US en sus du prix d'abonnement à l'étranger. Les clients du Canada doivent ajouter la TPS (numéro d'entreprise 12149 1807 RT 0275). Les abonnements sont pour l'année civile. Tout paiement doit être adressé au Receveur général du Canada, crédit du CNRC. Le prix par numéro est de 120,00 $ pour les organismes et de 40,00 $ pour les particuliers. Le prix des hors-série varie. Les membres des sociétés canadiennes de sciences et de génie bénéficient de taux préférentiels en s'abonnant via leurs sociétés respectives.

Les numéros de *Journal canadien des sciences halieutiques et aquatiques* sont accessibles sur le Web. On trouvera des renseignements sur les tarifs à pubs.nrc-cnrc.gc.ca.

Aucun remboursement ne sera accordé ni aucune annulation acceptée une fois que les livraisons auront commencé. Les réclamations de numéros manquants devront être soumises dans les quatre mois (Amérique du Nord) ou dans les six mois (à l'extérieur de l'Amérique du Nord) suivant la date de publication. L'éditeur ne fournira de numéros manquants que si le document a été perdu pendant l'expédition et que si le stock le permet. Adressez tout changement d'adresse ou toute question quant à l'abonnement au : Bureau des abonnements, Presses scientifiques du CNRC, Conseil national de recherches Canada, Ottawa, ON K1A 0R6, Canada; téléphone : 613-993-9084; télécopieur : 613-952-7656; courriel : pubs@nrc-cnrc.gc.ca.

On peut obtenir les fichiers rétrospectifs sur **microforme** auprès de UMI, P.O. Box 1346, Ann Arbor, MI 48106-1346, É.-U., et auprès de Micromedia Ltée, 20, rue Victoria, Toronto, ON M5C 2N8, Canada.

RAPID COMMUNICATION / COMMUNICATION RAPIDE

Striking the *right* balance in right whale conservation

Robert S. Schick, Patrick N. Halpin, Andrew J. Read, Christopher K. Slay, Scott D. Kraus, Bruce R. Mate, Mark F. Baumgartner, Jason J. Roberts, Benjamin D. Best, Caroline P. Good, Scott R. Loarie, and James S. Clark

Abstract: Despite many years of study and protection, the North Atlantic right whale (*Eubalaena glacialis*) remains on the brink of extinction. There is a crucial gap in our understanding of their habitat use in the migratory corridor along the eastern seaboard of the United States. Here, we characterize habitat suitability in migrating right whales in relation to depth, distance to shore, and the recently enacted ship speed regulations near major ports. We find that the range of suitable habitat exceeds previous estimates and that, as compared with the enacted 20 nautical mile buffer, the originally proposed 30 nautical mile buffer would protect more habitat for this critically endangered species.

Résumé : Malgré de nombreuses années d'étude et de protection, la baleine franche du nord (*Eubalaena glacialis*) de l'Atlantique Nord demeure au bord de l'extinction. Il y a une faille essentielle dans notre compréhension de leur utilisation de l'habitat dans le corridor de migration le long de la côte est des États-Unis. Nous caractérisons ici la convenance des habitats pour les baleines franches en migration en relation avec la profondeur, la distance de la rive et la réglementation récemment en vigueur sur la vitesse des navires près des ports principaux. Nous trouvons que la gamme d'habitats adéquats dépasse les estimations précédentes et que, par comparaison à la zone tampon de 20 milles marins présentement en vigueur, la zone tampon de 30 milles marins proposée à l'origine protégerait plus d'habitats pour cette espèce sérieusement menacée de disparition.

[Traduit par la Rédaction]

Introduction

Despite many years of study and protection, the North Atlantic right whale (*Eubalaena glacialis*) remains on the brink of extinction (Fujiwara and Caswell 2001; Kraus et al. 2005). Although a more complete understanding of right whale movement, feeding, and distribution patterns on their northern foraging and southern calving grounds has emerged (Kraus and Rolland 2007), the space used by right whales along their migratory corridor remains almost entirely unknown. This lack of knowledge impedes management of the segment of this critically endangered species, namely pregnant females and nursing mothers, whose death most impacts population survival (Fujiwara and Caswell 2001). As right whales migrate, they pass several of the largest ports on the eastern seaboard (Knowlton et al. 2002) (Fig. 1). Ship strikes are one of the primary factors limiting recovery of this species; more than a quarter of known ship strike mortalities for right whales occur in this region (Knowlton

Received 13 March 2009. Accepted 2 July 2009. Published on the NRC Research Press Web site at cjfas.nrc.ca on 14 August 2009. J21103

R.S. Schick,[1] **J.J. Roberts, and B.D. Best.** Nicholas School of the Environment and Earth Sciences, Box 90328, Levine Science Research Center, Duke University, Durham, NC 27708-0328, USA.
P.N. Halpin and C.P. Good. Nicholas School of the Environment and Earth Sciences, Box 90328, Levine Science Research Center, Duke University, Durham, NC 27708-0328, USA; Duke University Marine Laboratory, 135 Duke Marine Lab Road, Beaufort, NC 28516-9721, USA.
A.J. Read. Duke University Marine Laboratory, 135 Duke Marine Lab Road, Beaufort, NC 28516-9721, USA.
C.K. Slay. Coastwise Consulting, Athens, GA 30601, USA.
S.D. Kraus. Edgerton Research Laboratory, New England Aquarium, Boston, MA 02110, USA.
B.R. Mate. Marine Mammal Institute, Oregon State University, Newport, OR 97365, USA.
M.F. Baumgartner. Biology Department, Woods Hole Oceanographic Institution, Woods Hole, MA 02543, USA.
S.R. Loarie. Department of Global Ecology, Carnegie Institution, 260 Panama Street, Stanford, CA 94305, USA.
J.S. Clark. Nicholas School of the Environment and Earth Sciences, Box 90328, Levine Science Research Center, Duke University, Durham, NC 27708-0328, USA; Department of Biology, Duke University, Durham, NC 27708-0338, USA; Department of Statistical Science, Duke University, Durham, NC 27708-0251, USA.

[1]Corresponding author (e-mail: robert.schick@duke.edu).

Fig. 1. The portions of two movement paths that cross the migratory corridor are depicted in relation to the proposed (red) and enacted (blue) seasonal management areas (SMA). Light grey and dark grey circles are estimated locations of NEA 1812 and NEA 2320. Major ports are in beige. The upper inset map shows the last four locations of NEA 2320's track in grey with the buffered track shown in light grey. The lower inset map highlights the study area. TEU, twenty foot equivalent units; EEZ, exclusive economic zone.

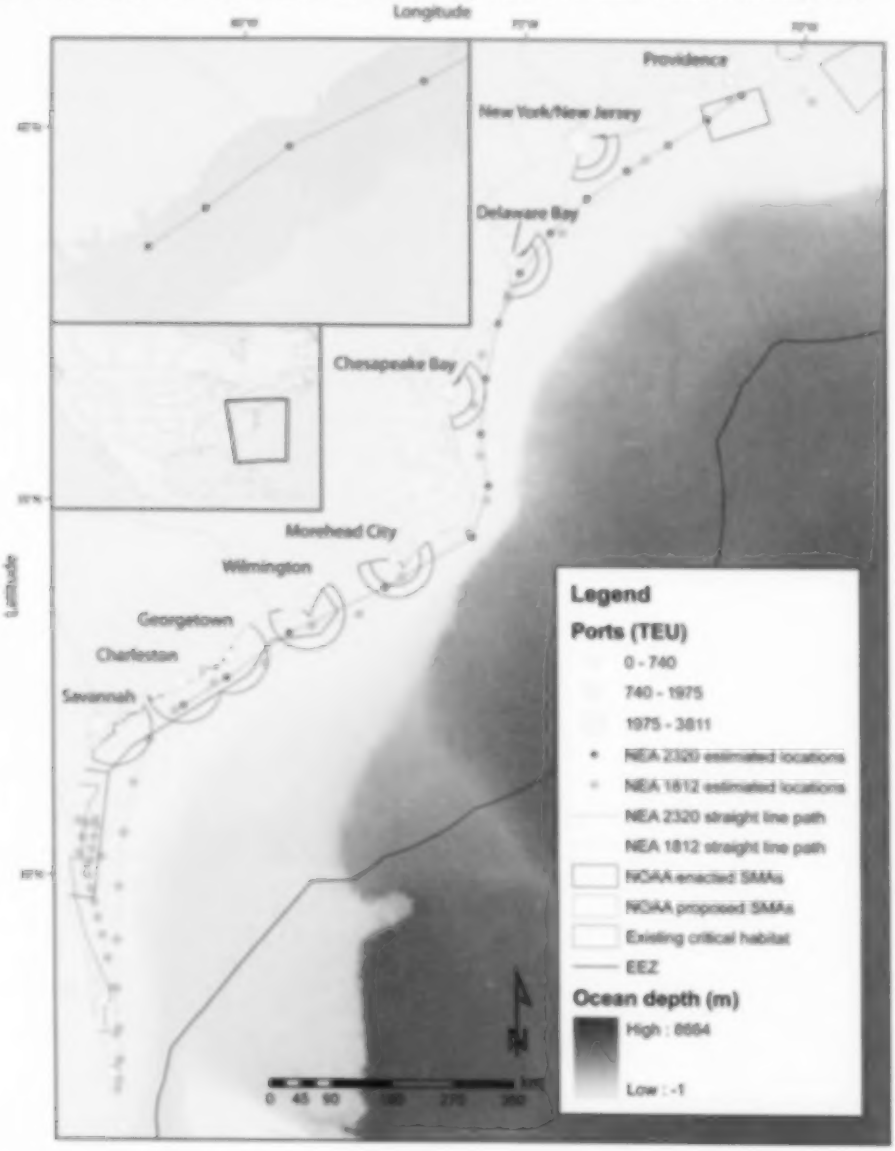

et al. 2002). Knowledge of how right whales perceive and move through this area will help inform the risk of ship strikes near these ports. Accordingly, we fit a new movement model to the migratory paths of two female right whales to estimate habitat suitability along the Mid-Atlantic corridor. In fitting this model, we emphasize (*i*) the general suitability of this important migratory corridor and (*ii*) the spatial relationship between habitat suitability and recently enacted vessel speed restrictions near shipping ports along the east coast (NOAA 2008).

Data

The data used here come from portions of movement paths from two female right whales: NEA 1812, tagged in 1996 (C.K. Slay and S.D. Kraus, unpublished data), and NEA 2320, tagged in 2000 (Baumgartner and Mate 2005). Both animals were tagged with ARGOS satellite-monitored radio tags. NEA 1812 is a reproductively active female at least 20 years old. She was first identified in Roseway Basin on the Nova Scotian Shelf in September 1988 and was last seen in August 2008 in the Bay of Fundy. NEA 1812 was

accompanied by a newborn calf at the time of tagging. NEA 2320 is a reproductively active female first identified in January 1993 off Florida and last seen in March 2008 in Cape Cod Bay. Information about age, sighting history, and reproductive status comes from The North Atlantic Right Whale Catalog (http://rwcatalog.neaq.org/Default.aspx, last accessed 12 December 2008). The track of NEA 1812 originated off Fernandina Beach, Florida, on 21 February 1996 and ended in the Gulf of Maine on 2 June 1996 (Fig. 1). (Note that the ports are symbol coded according to TEU (twenty foot equivalent units), where 1 TEU approximately represents the capacity of a standard shipping container, or 1360 ft^3, information taken from the United States Army Corps of Engineers, Navigation Data Center (http://www.iwr.usace.army.mil/ndc/wcsc/by_portname06.htm, last accessed 19 February 2009).) The track of NEA 2320 originated in the Bay of Fundy on 11 August 2000 and ended just north of the calving grounds in Florida and Georgia on 15 December 2000 (Fig. 1). In both cases, we ignored the Gulf of Maine portion of the tracks because this comprised a demonstrably different behavioral state and locations were no longer in the migratory corridor. For NEA 1812, 24 locations spanned the calving ground and migratory corridor; for NEA 2320, 16 locations spanned the migratory corridor. NEA 1812 transmitted for 103 days and covered 2676 km (average of 26.0 km·day^{-1}). NEA 2320 transmitted for 127 days and covered 5612 km (average of 44.2 km·day^{-1}).

Methods

Because the model from Schick et al. (2008) assumes equal time intervals between locations, we fit the model from Jonsen et al. (2005) to the data as a first-stage filter to obtain an estimate of the true path. The model from Jonsen et al. (2005) is a state-space model that uses a directed correlated random walk as the process model and that returns daily estimates of the animal's true position and, where appropriate, estimates of a behavioral state. We then buffered positions along this estimated path to compare actual location visited at time t versus a range of possible locations. We chose a 100 km spatial buffer around each location at time t because this distance slightly exceeded the maximum daily distance covered by the individual whales (97 km). Using GIS, we sampled two environmental covariates, water depth (metres) and distance to shore (kilometres), at each of these possible locations along the path of the individual as well as at the centroid of each 4 km grid cell within the buffered track (Fig. 1, inset). Because there is no literature describing the response of migrating right whales to dynamic covariates such as sea surface temperate, we did not include them in our model. In certain cases where shorter movements by the animal resulted in overlap of the spatial buffers, a separate time index was derived for each of the points. In other words, at time $t = 3$, the possible locations were, for example, 100. At $t = 4$, the locations were also 100, but since the animal only moved 5 km, 90 of these 100 possible locations were the same as the previous time step. In this case, we calculated and kept the space and time index of each patch in relation to when it could have been visited by the moving animal (Fig. 1, inset). We built upon these two covariates by separately calculating quadratic terms for both water depth and distance to shore. We used quadratic terms to see if there was an optimal range for each of these covariates and because without them, the assumption would be that right whales prefer the smallest possible values for each covariate, i.e., the closer right whales are to shore, the higher the suitability. In addition, we calculated the distance from the animal's position at time $t - 1$ to the current location of possible patches at time t. This allowed us to make inference on how distance from the animal affects suitability.

To these data, we applied the Bayesian movement model from Schick et al. (2008) that embeds a resource selection function (Manly and McDonald 2002) inside a movement model in an effort to infer the parameters governing relative habitat suitability h, where h is a function of environmental covariates. That is, how does the suitability of the patch chosen differ from those the animal could have chosen to visit? We modeled suitability as a function of the two environmental covariates, including both linear and quadratic terms for both. The model from Schick et al. (2008) exploits observed movement relative to the options available as the basis for inference on habitat preference.

We used these covariates and regression parameters to model the suitability h of areas along the track. At each point along the movement track, the animal chooses one location of many possible locations. We used a multinomial for the likelihood based on the assumption that the animal chooses the location with probability θ. Probability θ was mechanistically derived from the relative suitability h of the visited patch. Suitability h was normalized by dividing by the sum of h for all other patches. Suitability h had a functional form $\mathbf{X}\beta$. We constructed $\mathbf{X}$, and in a Gibbs sampling framework, we drew βs from a truncated multivariate normal distribution with mean values based on the current values of $\beta^{(g)}$, where the g superscript represents the current step in the Gibbs loop. The density a of the proposed value is determined in relation to the current value, and if $a > 1$, the proposed values were accepted. We derived and used an empirical covariance matrix $\mathbf{V}$ for this multivariate distribution. A default covariance matrix was used at the start of the Gibbs sampler, and we then twice calculated and employed the empirical covariance matrix after 1000 and 100 000 steps through the Gibbs sampler. We used uninformative flat priors centered on 0 with large variance. We ran the Gibbs sampler for 250 000 steps, saving the last thinned 150 000 values. Summary statistics were calculated for each of the posterior estimates of the parameters. To display habitat suitability, we used median estimates of the regression parameters and plotted estimates of suitability around each point. For the global suitability, we fixed distance and depth at their mean values while calculating suitability as a function of distance to shore.

Results

Results from the two migratory tracks analyzed here (whales NEA 1812 and NEA 2320) indicate that the estimate of habitat suitability should be revised farther offshore (Fig. 2*a*). Peak suitability values for distance to shore are slightly farther offshore for NEA 1812 than for NEA 2320 (Fig. 2*a*). In particular, NEA 1812, a migrating female with a newborn calf, occurred relatively far offshore during some

Fig. 2. (*a*) Posterior estimates of habitat suitability as a function of distance to shore across the entire migration for NEA 2320 (blue line) and NEA 1812 (red line). The vertical grey line corresponds to 75 km (40 nautical miles) offshore. Posterior estimates of habitat suitability are shown for (*b*) NEA 2320 near the mouth of Delaware Bay, and (*c*) NEA 1812 near the mouth of Chesapeake Bay. Suitable habitat is colored from high (dark green colors) to low (light blue colors). Shown are the southbound (Fig. 2*b*) and northbound (Fig. 2*c*) paths of the animal (grey dots and lines) as well as the 37 km (20 nautical miles) and the originally proposed 55.6 km (30 nautical miles) buffer around these two ports (blue line and red line, respectively). SMA, seasonal management area.

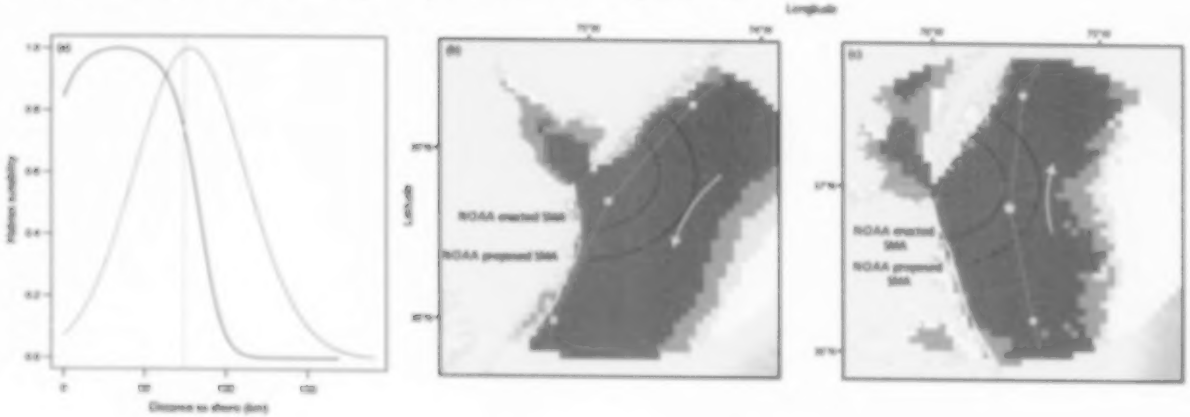

points in her migration (Figs. 1 and 2*a*). Because the analysis was Bayesian, uncertainty the parameters indicate a range of peak suitability as a function of distance to shore from 32 to 200 km for NEA 1812 and from 14 to 75 km for NEA 2320. Results thus indicate that the migratory corridor may be broader than originally thought (Fig. 2) (Knowlton et al. 2002).

Discussion

We estimated habitat suitability around all seasonal management areas (NOAA 2008) in relation to the new 37 km (20 nautical miles) speed restriction buffers and earlier proposed 55.6 km (30 nautical miles) buffers (NOAA 2006). Our analysis indicates that the enacted seasonal management area boundary covers only a small portion of suitable habitat. Enacting the original proposed zones over the Mid-Atlantic would protect an additional 15 453 km^2 of suitable habitat as follows: (*i*) 3849 km^2 around the southeastern United States, a 22% increase, (*ii*) 3042 km^2 around Morehead City, a 135% increase, (*iii*) 2052 km^2 around Chesapeake Bay, a 123% increase, (*iv*) 2188 km^2 around Delaware Bay, a 119% increase, and (*v*) a 1761 km^2 around New York/New Jersey, a 107% increase (see detailed views for Chesapeake Bay and Delaware Bay presented herein). We prefer the contiguous border for the seasonal management areas from Savannah to Wilmington but feel it would be improved by extending the boundary the full 30 nautical miles from shore, as it is clear that peak suitability for both whales ranges farther than 20 nautical miles.

While we do not undertake a full model selection analysis herein, the fact that there is a Pearson *r* correlation value of 0.45 between the covariates bears some discussion. To determine the effect this has on the analysis, we reran the model using one environmental covariate at a time, e.g., distance to future patch and depth, distance to future patch and distance to shore. For example, the estimate for the β governing depth for NEA 1812 is 0.12 (Bayesian credible interval 0.02, 0.27) with just depth in the model and 0.069 (Bayesian credible interval 0.005, 0.21) with depth and distance to shore. Results are similar for distance to shore: 0.47 (Bayesian credible interval 0.05, 1.14) with just distance to shore and 0.68 (Bayesian credible interval 0.1, 1.56) with both covariates. In both cases, the credible intervals for the single-covariate model contain the parameters estimated in the two-covariate model, thereby giving us confidence in the model formulation.

By taking a new approach to inference, we find that habitat suitability for migrating right whales extends farther offshore than previously thought (Knowlton et al. 2002). In addition, we show that the original proposed boundary of 30 nautical miles would protect more suitable habitat near ports. Future management and conservation activities should take these two findings into account. While we cannot draw too much inference from analysis of two tracks, we note the following. First, the entire population is extremely small, comprised of approximately 300–400 individuals, so two tagged reproductively active females represent a significant portion (2%) of the most valuable segment of the population (current estimate is 97 breeding females, Philip Hamilton, Edgerton Research Laboratory, New England Aquarium, Central Wharf, Boston, Massachusetts, personal communication). Previous estimates of population viability have stressed that if two females per year can be saved, the population growth will become positive (Fujiwara and Caswell 2001). Second, the migratory section of the species' range is the least understood but critical for pregnant females migrating southward from the Gulf of Maine to calving grounds and for mothers with newborn calves migrating northward to feeding grounds. Because these north- and southbound migration routes pass close to several of the largest shipping ports on the eastern seaboard, and because a substantial number of ship strike mortalities occur in this area (Knowlton et al. 2002), we argue that the speed restric-

tion boundaries be revisited. While we are not estimating risk of ship strike, previous work has documented the successful reduction in risk of ship strike to right whales with a combination of traffic separation schemes and speed restrictions (Fonnesbeck et al. 2008; Vanderlaan et al. 2008). Incorporating the results presented here in conservation and management schemes would protect a larger portion of right whale habitat in this critical yet understudied area of their range.

Acknowledgements

We thank Martin Biuw and two anonymous reviewers whose comments considerably strengthened this manuscript. This work was supported in part by SERDP/DoD grant W912HQ-04-C-0011 to A.J. Read and P.N. Halpin as well as a James B. Duke Fellowship and a Harvey L. Smith Dissertation Year Fellowship to R.S. Schick.

References

Baumgartner, M.F., and Mate, B.R. 2005. Summer and fall habitat of North Atlantic right whales (*Eubalaena glacialis*) inferred from satellite telemetry. Can. J. Fish. Aquat. Sci. **62**(3): 527–543. doi:10.1139/f04-238.

Fonnesbeck, C.J., Garrison, L.P., Ward-Geiger, L.I., and Baumstark, R.D. 2008. Bayesian hierarchichal model for evaluating the risk of vessel strikes on North Atlantic right whales in the SE United States. Endanger. Species Res. **6**: 87–94. doi:10.3354/esr00134.

Fujiwara, M., and Caswell, H. 2001. Demography of the endangered North Atlantic right whale. Nature, **414**(6863): 537–541. doi:10.1038/35107054. PMID:11734852.

Jonsen, I., Flemming, J.M., and Myers, R. 2005. Robust state-space modeling of animal movement data. Ecology, **86**(11): 2874–2880. doi:10.1890/04-1852.

Knowlton, A., Ring, J., and Russell, B. 2002. Right whale sightings and survey effort in the mid-atlantic region: migratory corridor, time frame, and proximity to port entrances. A report submitted to the NMFS Ship Strike Working Group. Available from www.nero.noaa.gov/shipstrike/ssr/midatanticreportrFINAL.pdf

Kraus, S., and Rolland, R. 2007. The urban whale: North Atlantic right whales at the crossroads. Harvard University Press, Cambridge, Mass.

Kraus, S.D., Brown, M.W., Caswell, H., Clark, C.W., Fujiwara, M., Hamilton, P.K., Kenney, R.D., Knowlton, A.R., Landry, S., Mayo, C.A., McLellan, W.A., Moore, M.J., Nowacek, D.P., Pabst, D.A., Read, A.J., and Rolland, R.M. 2005. North Atlantic right whales in crisis. Science, **309**(5734): 561–562. doi:10.1126/science.1111200. PMID:16040692.

Manly, B., and McDonald, T. 2002. Resource selection by animals: statistical design and analysis for field studies. Kluwer Academic Publishers, Boston, Mass.

NOAA. 2006. Endangered Fish and Wildlife; Proposed rule to implement speed restrictions to reduce the threat of ship collisions (26 June 2006). Federal Register Vol. 71. No. 122. pp. 36299–36313.

NOAA. 2008. Endangered Fish and Wildlife; Final rule to implement speed restrictions to reduce the threat of ship collisions with North Atlantic right whales (10 October 2008). Federal Register Vol. 73. No. 198. pp. 60173–60191.

Schick, R.S., Lourie, S.R., Colchero, F., Best, B.D., Boustany, A., Conde, D.A., Halpin, P.N., Joppa, L.N., McClellan, C.M., and Clark, J.S. 2008. Understanding movement data and movement processes: current and emerging directions. Ecol. Lett. **11**(12): 1338–1350. doi:10.1111/j.1461-0248.2008.01249.x. PMID: 19046362.

Vanderlaan, A., Taggart, C., Serdynska, A., Kenney, R., and Brown, M. 2008. Reducing the risk of lethal encounters: vessels and right whales in the Bay of Fundy and on the Scotian Shelf. Endanger. Species Res. **4**: 283–297. doi:10.3354/esr00083.

RAPID COMMUNICATION / COMMUNICATION RAPIDE

A new method to identify the fluvial regimes used by spawning salmonids

Hamish J. Moir, Christopher N. Gibbins, John M. Buffington, John H. Webb, Chris Soulsby, and Mark J. Brewer

Abstract: Basin physiography and fluvial processes structure the availability of salmonid spawning habitat in river networks. However, methods that allow us to explicitly link hydrologic and geomorphic processes to spatial patterns of spawning at scales relevant to management are limited. Here we present a method that can be used to link the abundance of spawning salmonids to fluvial processes at the mesoscale. We show that the frequency of spawning activity at individual morphological units (riffles, pools, runs) is quantitatively related to a number of fluvial parameters. Of these, bankfull excess shear stress (τ_{xs}) was the best predictor of spawning frequency. Results suggest that τ_{xs} can be used to represent the fluvial regimes that spawning salmon are responsive to as well as to assess the likely impacts of altered flow regimes.

Résumé : La physiographie du bassin et les processus fluviaux sont responsables de la disponibilité de l'habitat de fraie des salmonidés dans les réseaux de rivières. Il y a cependant peu de méthodes qui permettent de relier explicitement les processus hydrologiques et géomorphiques aux patrons spatiaux de la fraie à des échelles qui sont pertinentes à la gestion. Nous présentons ici une méthode qui peut servir à relier l'abondance de salmonidés en fraie aux processus fluviaux à une échelle moyenne. Nous démontrons que la fréquence de l'activité de fraie dans des unités morphologiques particulières (les rapides, fosses et couloirs) est associée quantitativement à un certain nombre de variables fluviales. Parmi celles-ci, la contrainte de cisaillement en excès à pleins bords (τ_{xs}) est la meilleure variable prédictive de la fréquence de fraie. Nos résultats indiquent que τ_{xs} peut servir à représenter les régimes fluviaux auxquels les saumons réagissent, ainsi qu'à évaluer les impacts probables des modifications des régimes d'écoulement.

[Traduit par la Rédaction]

Introduction

Sustainable river management is only possible if we understand the links between species, the habitats they use, and the physical processes creating these habitats. This understanding is needed most for life stages that exert an important influence on species' reproductive success. Moreover, our understanding needs to be at scales relevant to management, whether it be the development of environmental flow regimes in regulated systems or habitat restoration in physically degraded channels.

Spawning is a critical stage in the life cycle of salmonid fish (Quinn 2005). Salmonids generally spawn in gravel- and cobble-bed rivers, preferentially within pool–riffle channels (Montgomery et al. 1999). The hydraulic and sedimentary characteristics of the specific locations used by spawning fish are well documented (e.g., Moir et al. 2002) but this microscale analysis is data intensive and hence costly. Conversely, reach-scale analysis does not capture the subreach conditions that fish are selecting when spawning. An intermediate, mesoscale analysis applied to individual morphologic units (e.g., riffles, bars, runs) may be most appropriate for determining meaningful relationships between physical conditions and spawning (Fig. 1). We used this scale of analysis to investigate fluvial controls on spawning activity of Atlantic salmon (*Salmo salar*) in an upland Scottish stream. We do not aim to understand why salmon use some areas and not others; the broad geomorphic controls on spawning and nonspawning locations within river systems and the microhabitat conditions selected and avoided by fish are already known and detailed in the literature (e.g., Montgomery et al. 1999; Moir et al. 2004). Rather,

Received 27 March 2009. Accepted 1 July 2009. Published on the NRC Research Press Web site at cjfas.nrc.ca on 14 August 2009. J21125

H.J. Moir,[1] The Macaulay Land-Use Research Institute, Craigiebuckler, Aberdeen AB15 8QH, UK.
C.N. Gibbins. Northern Rivers Institute, University of Aberdeen, Aberdeen AB24 3UF, UK.
J.M. Buffington. US Forest Service, Rocky Mountain Research Station, Boise, ID 83702, USA.
J.H. Webb. Atlantic Salmon Trust, Marine Scotland, Marine Laboratory, Aberdeen, AB11 9BD, UK.
C. Soulsby. Northern Rivers Institute, Department of Geography and Environment, University of Aberdeen, Aberdeen AB24 3UF, UK.
M.J. Brewer. BioSS Office, The Macaulay Land-Use Research Institute, Craigiebuckler, Aberdeen AB15 8QH, UK.

[1]Corresponding author (e-mail: h.moir@macaulay.ac.uk).

Fig. 1. Conceptual diagram of the nested hierarchy of spatial scales present in river systems that influence the spatial distribution of salmonid spawning habitat. Spatial scales decrease from the top left corner in a clockwise direction. Our study focuses on mesoscale morphological units (e.g., riffle, run).

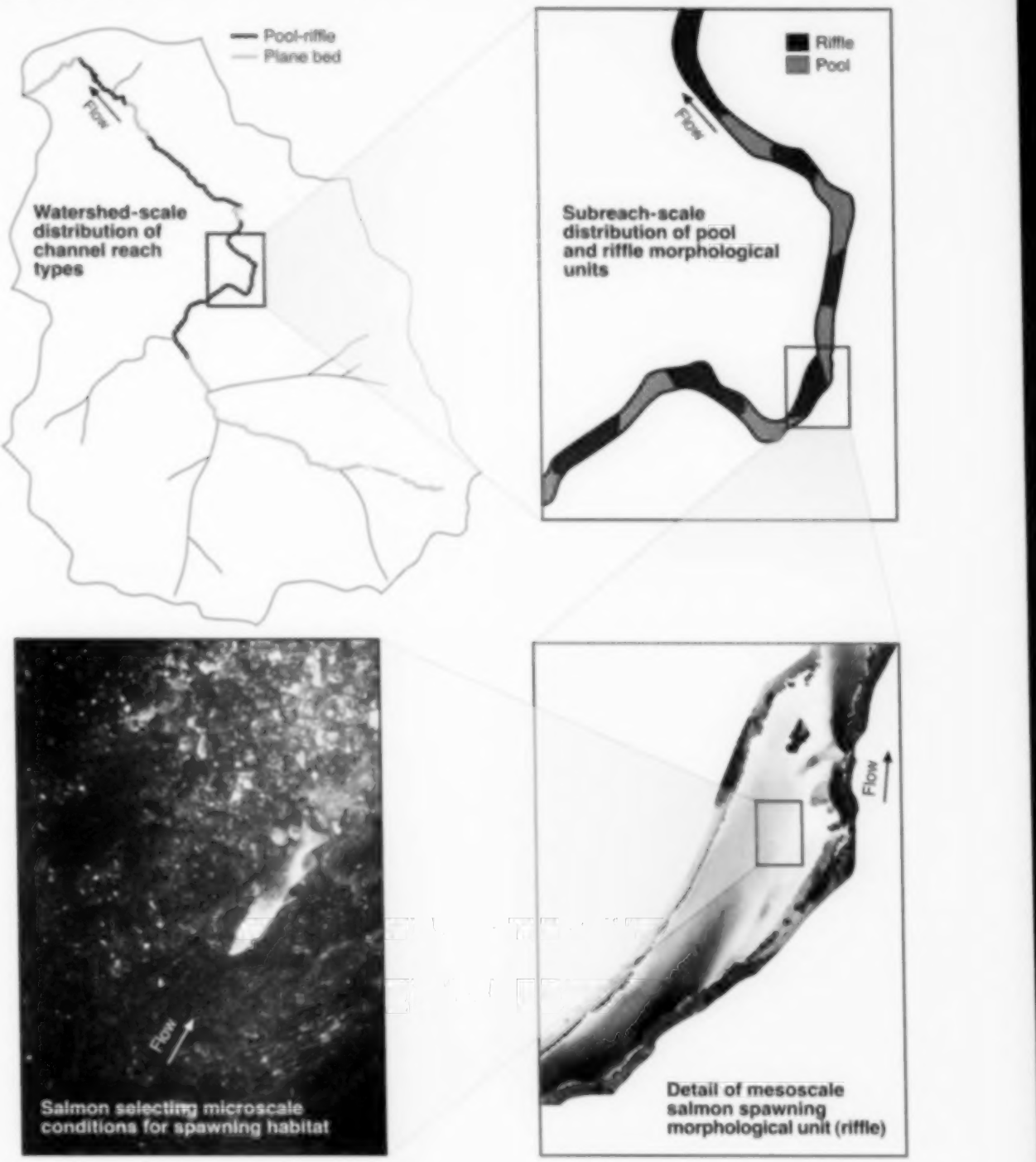

we aim to relate observed mesoscale variation of spawning activity to fluvial characteristics that create spawning habitat.

Materials and methods

Study area and spawning observations

The Allt a' Ghlinne Bhig (56°49′N, 3°27′W) is a small (27 km^2), unregulated mountain tributary of the River Tay. Spawning observations were made in the stream in five years (2000–2003, 2006, and 2007). In each year, surveys began on the day of commencement of spawning activity and continued until only sporadic incidents were detected (Moir et al. 2006). On each day, the same experienced observer walked the stream from the mouth (335 m above mean sea level) to the upstream limit of spawning (a waterfall impassable to fish 9.1 km upstream at 510 m above mean sea level) in daylight hours (08:00 to 16:00); on average, surveys were conducted on 86% of the days over the studied spawning periods. Spawning (initial cutting and oviposition) was defined using recognized criteria (Jones 1959). The location of spawning incidents was determined using a hand-held Global Positioning System.

Study locations

Spawning sites in upland streams occur over a continuum of spatial scales from entire morphological units to small (<3 m^2) localized gravel accumulations (Moir et al. 2004). Spawning incidents in the gravel accumulations do not reflect morphological unit scale processes but, rather, much smaller scale factors (e.g., localized deposition of gravels behind large boulders) that result in transient areas of suitable habitat. For this analysis, we used only locations that supported, on average, one or more spawning incidents per year per unit channel length over the course of the study (i.e., greater than five spawning incidents in total). This criterion provided a clear division between clusters of spawning activity associated with specific morphological units (the focus of this study) and more sporadic incidents in small gravel accumulations.

A total station was used to conduct topographical surveys of potential sites in September and October 2003. The surveys determined mean bank-full width, depth, and longitudinal bed slope (the latter measured between geomorphically equivalent topographic highs, e.g., riffle/bar crests or boulder steps). Once the subsample of these sites that met the greater than five spawning incident criterion was determined, an assessment was made from photographic time series as to whether significant morphological change had occurred between 2000 and 2007; sites where such change had occurred (either before or after the 2003 survey) were removed. The same observer walked the entire stream on each day in each year and became sufficiently familiar with the characteristics of the channel to identify significant morphological change. Although small variations in the structure and sedimentology of bedforms occurred, the mesoscale focus of study sites meant that marked change to general channel geometry (e.g., bank-full width and depth and bed slope) would be required for exclusion of sites from the study. The 37 sites that were identified by this two-stage procedure accounted for 552 of the 726 (76%) observed spawning incidents. The sites extended across an 8.2 km length of the stream (from the mouth to within 0.9 km of the farthest upstream point accessible to adult salmon).

Characterization of fluvial regime

Our analysis focused on fluvial characteristics that create spawning habitat. As such, five channel-forming parameters were examined: total stream power (Ω), specific stream power (ω), shear stress (τ), excess specific stream power (ω_{xs}), and excess shear stress (τ_{xs}), with the latter two describing the degree of bed mobility at a given flow. All parameters were calculated using standard equations available in the literature and are further defined in the list of symbols. The parameters were evaluated for bank-full flow, since the hydraulic conditions at this flow exert a dominant control on channel morphology in many alluvial rivers (Wolman and Miller 1960), i.e., bank-full is a geomorphically significant flow. So that ω_{xs} and τ_{xs} were relevant to salmon spawning habitat, we expressed these parameters as the difference between bank-full conditions and critical values for mobilizing the median size of sediment used by spawning fish (D_{50} = 41.1 mm, determined from nearby spawning tributaries; Moir et al. 2002). It is important to note that the above parameters do not describe the microscale physical conditions at the time of spawning but rather describe the mesoscale fluvial regime of spawning habitats during channel-forming flows.

Results

Parameter τ_{xs} was the best predictor of spawning frequency (Ω, R^2 = 0.11; ω, R^2 = 0.45; τ, R^2 = 0.53; ω_{xs}, R^2 = 0.57; τ_{xs}, R^2 = 0.67; all n = 37). However, there was still an appreciable amount of the variation that remained unexplained by this parameter alone, particularly at τ_{xs} < 50 N·m^{-2} (Fig. 2). The data set was therefore subdivided to show separate relationships for river sections upstream and downstream of a major tributary confluence within the study basin (the rationale for separating the stream at this point was that the confluence marked an abrupt change in drainage area and, hence, channel discharge and dimensions). Separate curves fitted to each of the two sections (downstream: R^2 = 0.90, P < 0.001, n = 15; upstream: R^2 = 0.71, P < 0.001, n = 23) showed a significantly improved fit over the single regression (R^2 = 0.67). Many more fish used locations with τ_{xs} < 50 N·m^{-2} in the downstream river section compared with the upstream one.

Discussion

Our analysis demonstrates that the frequency of spawning by Atlantic salmon is inversely related to τ_{xs}. Given the explicit mesoscale of our analysis and the fact that τ_{xs} was indexed to a single discharge (bank-full flow), this relationship should not be interpreted as meaning that fish construct redds at points that have particular values of τ_{xs} at the time of spawning. Rather, the results indicate that spawning occurs most frequently in morphological units that, at a geomorphically effective flow, have low mobility of spawning sediment. Low sediment mobility has several possible consequences for salmon habitat. It may influence the availability of spawning gravels, particularly for bank-full threshold

Fig. 2. Regressions between spawning frequency and excess shear stress. Open squares, downstream river section; solid squares, upstream river section; thick curve, overall regression for entire data set; broken curve, regression for upstream section; thin curve, regression for downstream section.

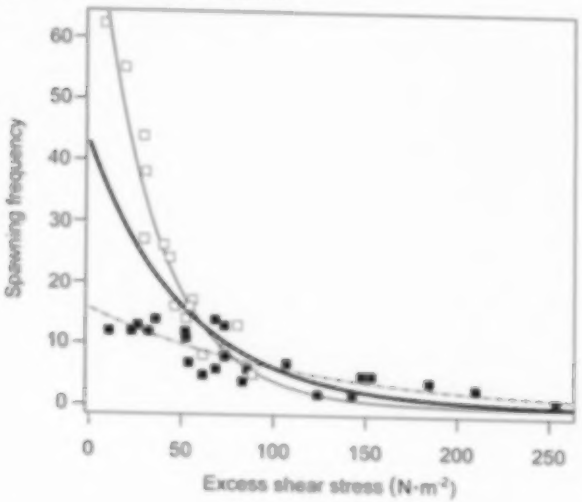

channels, where the size of material on the bed will approach the spawning sediment size as τ_{ss} approaches zero (Buffington and Montgomery 1999), assuming no sediment supply limitations. Alternatively, τ_{ss} is directly related to probability of scour (Haschenburger 1999), with potentially greater productivity and higher numbers of fish returning to sites that are less likely to scour incubating eggs. The τ_{ss} can also be an index of channel morphology (García et al. 2000) and associated depth and velocity regimes (Moir et al. 2006). Our analysis does not allow examination of these factors, so further investigation of the biological significance of low τ_{ss} values is warranted.

At lower τ_{ss} values, the number of fish using particular locations differed markedly between the two sections of the stream. This divergence, as well as the improved fit of the relationship when subdivided by river section, indicates that there are location-specific factors that influence the interaction between fish and physical habitat conditions. Our data do not allow us to isolate the cause of the different relationships in the two sections, but there are a number of possible explanations. The larger drainage area of the downstream section will produce relatively larger channel dimensions with potentially more spawning area per mesoscale unit and thus a greater carrying capacity. However, in this study, a similar number of locations with $\tau_{ss} < 50$ N·m^{-2} were present in both the downstream and upstream sections, and differences in area between channel units in the two sections were not sufficient to explain variations in spawning frequency. The explanation therefore may be a biological one. For example, differences in juvenile production and their fine-scale homing behaviour when they return as adults (Youngson et al. 1994) may lead to different patterns of occupancy along the stream. There may also be differences in competition and predation between the stream sections that contribute to differences in frequency of use.

Overall, the results indicate that there are clear relationships between τ_{ss} and spawning frequency, and the strength of these improve when spawning locations are grouped according to position within the stream network. Indexing the fluvial regime in this way has management value. In Europe and North America, legislation for river management is based increasingly on ecological considerations, so a thorough understanding of species habitat requirements and habitat-forming processes is needed. Our index is at a scale most often targeted by river managers (that of the habitat unit) and captures the physical controls on spawning habitat availability relatively rapidly. It can be used to set ecological targets or objectives as well as to assess potential ecological response to natural and anthropogenic disturbances that alter stream flow and shear stress patterns. It may also be useful in river restoration initiatives, which often fail because of the lack of explicit links between fluvial processes and biota (Wohl et al. 2005).

Acknowledgements

The authors thank Nikolai Friberg and Martyn Futter for their comments on the manuscript and Pat Carnegie for help with the illustrations. This work was partly funded by the Scottish Government Rural and Environment Research and Analysis Directorate.

References

Buffington, J.M., and Montgomery, D.R. 1999. Effects of sediment supply on surface textures of gravel-bed rivers. Water Resour. Res. **35**(11): 3523–3530. doi:10.1029/1999WR900232.

García, M.H., Laursen, E.M., Michel, C., and Buffington, J.M. 2000. The legend of A.F. Shields. J. Hydraul. Eng. **126**(9): 718–723. doi:10.1061/(ASCE)0733-9429(2000)126:9(718).

Haschenburger, J.K. 1999. A probability model of scour and fill depths in gravel-bed channels. Water Resour. Res. **35**(9): 2857–2869. doi:10.1029/1999WR900153.

Jones, J.W. 1959. The salmon. Collins, London, U.K.

Moir, H.J., Soulsby, C., and Youngson, A.F. 2002. Hydraulic and sedimentary controls on the availability and use of Atlantic salmon (*Salmo salar*) spawning habitat in the River Dee system, north-east Scotland. Geomorphology, **45**(3–4): 291–308. doi:10.1016/S0169-555X(01)00160-X.

Moir, H.J., Gibbins, C.N., Soulsby, C., and Webb, J.H. 2004. Linking channel geomorphic characteristics to spatial patterns of spawning activity and discharge use by Atlantic salmon (*Salmo salar* L.). Geomorphology, **60**(1–2): 21–35. doi:10.1016/j.geomorph.2003.07.014.

Moir, H.J., Gibbins, C.N., Soulsby, C., and Webb, J.H. 2006. Discharge and hydraulic interactions in contrasting channel morphologies and their influence on site utilization by spawning Atlantic salmon (*Salmo salar*). Can. J. Fish. Aquat. Sci. **63**(11): 2567–2585. doi:10.1139/F06-137.

Montgomery, D.R., Beamer, E.M., Pess, G.R., and Quinn, T.P. 1999. Channel type and salmonid spawning distribution and abundance. Can. J. Fish. Aquat. Sci. **56**(3): 377–387. doi:10.1139/cjfas-56-3-377.

Quinn, T.P. 2005. The behavior and ecology of Pacific salmon and trout. American Fisheries Society, Bethesda, Md.

Wohl, E., Angermeier, P.L., Bledsoe, B., Kondolf, G.M., MacDonnell, L., Merritt, D.M., Palmer, M.A., Poff, N.L., and Tarboton, D. 2005. River restoration. Water Resour. Res. **41**(10): W10301. doi:10.1029/2005WR003985.

Wolman, M.G., and Miller, J.P. 1960. Magnitude and frequency of forces in geomorphic processes. J. Geol. **68**: 54–74.

Youngson, A.F., Jordan, W.C., and Hay, D.W. 1994. Homing of Atlantic salmon (*Salmo salar* L.) to a tributary spawning stream in a major river catchment. Aquaculture, **121**(1–3): 259–267. doi:10.1016/0044-8486(94)90025-6.

List of symbols used in the text and their definitions

Symbol	Definition
D_{50}	median size of spawning sediment, 41.1 mm in this analysis
d_{c50}	critical depth for incipient motion of spawning sediment, $\tau_{c50}/\rho_w gS$
g	gravitational acceleration
n	Manning's roughness coefficient
R	hydraulic radius
S	channel slope
v_{c50}	critical velocity for incipient motion of spawning sediment determined from the Manning equation, $d_{c50}^{0.67} S^{0.5}/n$
ρ_s	sediment density, 2650 kg·m^{-3}
ρ_w	water density, 1000 kg·m^{-3}
τ_{xs}	excess bank-full shear stress, $\tau - \tau_{c50}$
τ	shear stress determined from the depth–slope product, $\rho_w RgS$, evaluated at bank-full flow
τ_{c50}	critical shear stress for incipient motion of spawning sediment, $\tau^*_c g D_{50}(\rho_s - \rho_w)$
τ^*_c	critical Shields parameter for incipient motion, 0.045
Ω	total stream power, $\rho g S Q_{bf}$, where Q_{bf} is bank-full discharge
ω	specific stream power, Ω/w_{bf}, where w_{bf} is bank-full channel width
ω_{xs}	excess specific stream power, $\omega - \omega_{c50}$, evaluated at bank-full flow
ω_{c50}	critical specific stream power for incipient motion of spawning sediment, $v_{c50}\tau_{c50}$

Seasonal dispersion of Pacific halibut (*Hippoglossus stenolepis*) summering off British Columbia and the US Pacific Northwest evaluated via satellite archival tagging

Timothy Loher and Calvin L. Blood

Abstract: Fisheries for eastern Pacific halibut (*Hippoglossus stenolepis*) occur over a 9-month season that is closed in winter to protect spawners. The industry has requested season extension, but conventional tag data suggest that 67% of Canada's fishable biomass may comprise Alaskan spawning stock vulnerable to out-of-area interception. Seventy-eight halibut were tagged during summer in Canada and the US Pacific Northwest (USPNW) with archival tags programmed to report via satellite on 1 February, 15 February, and 1 March. Fifty-seven tags (44 Canadian and 13 USPNW) escaped recapture and reported on or near their scheduled reporting dates. Only 7% out-of-area dispersion was observed for Canadian-tagged halibut; light-based geolocations suggested that an additional 4% may have emigrated prior to February and then returned. Halibut that emigrated were located north of their tagging location. From the USPNW, 46% dispersion was observed. Eighty-nine percent of the tagged halibut displayed depth profiles consistent with migration to offshore spawning areas during the winter, and the majority (78%) were located on the continental slope (>200 m) immediately prior to tag reporting, suggesting locations on or near spawning grounds. There was no detectable difference in dispersion by date, but the mean central position of Canadian-tagged halibut shifted progressively farther southeast over time.

Résumé : La pêche commerciale du flétan du Pacifique (*Hippoglossus stenolepis*) dans l'est de l'océan s'étend sur une saison de pêche de 9 mois qui est fermée en hiver pour la protection des reproducteurs. L'industrie de la pêche a demandé une extension de la saison, mais les données obtenues des étiquettes ordinaires laissent croire que 67 % de la biomasse disponible à la pêche au Canada provient d'un stock reproducteur d'Alaska qui est vulnérable à l'interception dans les zones extérieures. Soixante-dix-huit flétans ont été munis pendant l'été au Canada et dans la région pacifique du Nord-Ouest des États-Unis (USPNW) d'étiquettes d'archivage programmées pour émettre un rapport par satellite les 1 février, 15 février et 1 mars. Cinquante-sept étiquettes (44 canadiennes et 13 d'USPNW) ont échappé à la capture et ont émis un rapport aux dates prévues ou à des dates rapprochées. Chez les flétans marqués au Canada, on a observé une dispersion hors zone de seulement 7 %; des géolocalisations estimées par la lumière indiquent qu'un pourcentage additionnel de 4 % a pu émigrer avant février pour revenir plus tard. Les flétans qui avaient émigré ont été retrouvés au nord de leur site de marquage. Dans la région USPNW, on a observé une dispersion de 46 %. Quatre-vingt-neuf pourcent des flétans porteurs d'étiquettes ont des profils de répartition en profondeur compatibles avec une migration au large vers les zones de fraie durant l'hiver et les poissons se retrouvaient en majorité (78 %) sur le plateau continental (>200 m) juste avant le rapport des étiquettes, ce qui laisse croire qu'ils étaient sur les lieux de fraie ou à proximité. Il n'y a pas de différence décelable de dispersion en fonction de la date, mais la position moyenne centrale des flétans marqués au Canada se déplace progressivement vers le sud-est avec le temps.

[Traduit par la Rédaction]

Introduction

Pacific halibut (*Hippoglossus stenolepis*) (hereafter halibut) are one of the world's largest flatfish with a maximum reported size approaching 3 m and over 200 kg (Mecklenburg et al. 2002). They are believed to have diverged from Atlantic halibut (*Hippoglossus hippoglossus*) during the Pleistocene roughly 2–4 millions years ago (Grant et al. 1984) and are presently distributed from northern California through the Bering Sea and Sea of Okhotsk and into the northern Sea of Japan (Mecklenburg et al. 2002). Whereas North American stocks of Atlantic halibut are experiencing depressed abundance (Department of Fisheries and Oceans 2001; Brodziak and Col 2005), Pacific halibut support one of the most important fisheries on the west coast of the United States and Canada. Commercial fisheries are supported by annual stock productivity that has averaged approximately 3300 t over the past decade. The stock is

Received 23 June 2008. Accepted 3 March 2009. Published on the NRC Research Press Web site at cjfas.nrc.ca on 20 August 2009. J20637

Paper handled by Associate Editor C. Walters.

T. Loher[1] and C.L. Blood. International Pacific Halibut Commission, P.O. Box 95009, Seattle WA 98145, USA.

[1]Corresponding author (e-mail: tim@iphc.washington.edu).

jointly managed by the United States and Canada via the International Pacific Halibut Commission (IPHC). Harvest is restricted to hook-and-line fisheries, and for much of the IPHC's 83-year history, total catch was controlled by adjusting annual season length to fishing effort levels. Historically, the fishery lasted for months. Economic incentives and increased fishing power led to rapidly shrinking seasons throughout the 1980s, culminating in a Canadian halibut season lasting only 10 days in 1990 and just 2 or 3 days, twice per year, in Alaska. Ex-vessel prices were relatively low because large volumes of product were landed over short periods, fresh product was only briefly available each year, and fishery safety became a major concern as fishers raced to land fish regardless of weather conditions.

Seeking to increase the overall resource value and fleet safety, managers established an individual vessel quota system in Canada in 1991 that allowed the season to be increased to 213 days. In 1995, a quota system was implemented in Alaska, resulting in a 245 day fishery. Since the inception of quota management, these sectors of the fishery have experienced season lengths ranging from 245 to 262 days with a closed period during the North American winter (December–February) to protect spawning fish. In 1998, economic concerns prompted the fishing industry to formally request that the IPHC substantially extend the commercial season (Leaman and Clark 2000), and an interagency working group was convened to review issues associated with implementing that proposal (Gilroy and Sadorus 2000). Extending commercial halibut harvest into the winter spawning season would present a number of challenges.

While halibut spend the summer feeding on the continental shelf (<200 m), spawning occurs during winter in deeper slope waters (250–600 m; Loher and Seitz 2008*a*) from at least the Queen Charlotte Islands, British Columbia, to the Pribilof Canyon in the southeast Bering Sea (St. Pierre 1984). The primary management concern expressed by IPHC staff regarding season extension is the possibility that winter fisheries would intercept halibut as they move among regulatory areas during seasonal migrations. Catch limits are presently established within regulatory areas on the basis of midsummer distribution, as determined from catch per unit effort in annual stock assessment surveys. In addition to clearly documented onshore–offshore movements associated with spawning (Loher and Seitz 2006, 2008*a*; Seitz et al. 2007), conventional tagging studies (Leaman et al. 2002) and recent archival tagging data (Loher and Seitz 2006; Seitz et al. 2007) indicate that halibut can also move considerable distances alongshore on a seasonal basis. Specifically, the autumn spawning migration in the Gulf of Alaska appears to possess a northward component. Analyses of conventional tag data have suggested that up to two thirds of Canada's fishable summer biomass may ultimately join spawning aggregations located in southeastern and south-central Alaskan waters (Leaman et al. 2002). Likewise, it has been hypothesized that a substantial proportion of fish that summer in the US Pacific Northwest (USPNW) (Washington and Oregon) may emigrate seasonally to Canadian waters.

If the magnitude of net northward seasonal redistribution is significantly large, fishing conducted on winter spawning grounds or during migratory periods could effectively transfer exploitable biomass (i.e., quota) from Canada to Alaska and from the USPNW to Canada and alter area-specific exploitation rates relative to target levels (Leaman et al. 2002). The concept is simple: interception of migratory fish will reduce source abundance. Additionally, differential mortality among population components could alter stock demographics in fisheries executed during the active spawning season. Spawning season hook-and-line fisheries for Tasmanian calamary (*Sepioteuthis australis*) have been shown to alter size structure within the male population component (Hibberd and Pecl 2007), and sex-specific selectivity within aggregations of spawning Gulf of Mexico grouper (Serranidae) may cause seasonal changes in population sex ratio (Coleman et al. 1996). For halibut, spatially explicit seasonal catch limits may be necessary to minimize interception and shifts in spawning stock distribution and demographics.

Developing strategies that account for seasonal redistribution will require a refined understanding of seasonal dispersal. Migration distance, timing, and rates of interarea mixing are critical features that can govern the potential impacts of a winter fishery. Unintended impacts are more likely if a large proportion of a population emigrates to distant spawning grounds, as opposed to being composed primarily of local spawners. For example, Atlantic bluefin tuna (*Thunnus thynnus*) are presently managed as distinct eastern and western management units based on indices (Sissenwine et al. 1998) suggesting low rates of interchange (<4%; Stokesbury et al. 2004) between spatially segregated spawning grounds. However, tagging data suggesting that rates of mixing may be an order of magnitude greater (Block et al. 2001) have led to debate regarding the potential for cross-basin recruitment and the degree to which fishing mortality might affect productivity between management units (Sissenwine et al. 1998). The longer the spawning and migratory periods, the greater the likelihood of fish being intercepted during transit. Seasonal redistribution can result in mixing on extensive scales, such as the cross-basin migration of Atlantic bluefin tuna, or be confined within smaller areas, such as demonstrated for North Sea plaice (*Pleuronectes platessa*) (Hunter et al. 2003) and Bay of Biscay sole (*Solea solea*) (Koutsikopoulos et al. 1995). Ideally, management actions should match these scales, both spatially and temporally.

For halibut, average seasonal migration distance, rates of emigration, and timing of migration relative to fishing season dates are poorly understood. The conventional tag analysis that led to the hypothesis of high rates of interarea migration (Leaman et al. 2002) has not been validated with fishery-independent data. Conventional tag analysis is highly sensitive to spatial artifacts of recovery effort and tag reporting and requires that various assumptions be made with respect to these factors (sensu Hilborn et al. 1995). Acknowledging this, Leaman et al. (2002) stated that recovery data were "not corrected to account for potential differences in reporting rates or fishing effort" and were "likely to be biased (perhaps strongly so) by differences...across the stock range." Electronic pop-up archival transmitting (PAT) tags represent an ideal technique for examining temporally explicit movement in a manner free from recovery and reporting biases. PAT tags report to satellites at the end of

their chosen deployment period and therefore do not need to be recaptured to produce endpoint locations. However, the only such study conducted to date (Loher and Seitz 2006) was too limited in scope to draw quantitative conclusions and there has been no such research in the USPNW.

The aim of the present study was to gain a better understanding of late winter dispersal of halibut that summer in Canada and the USPNW via fisheries-independent tagging. Specifically, we sought to quantify the potential for commercial fisheries prosecuted in February, 1 month prior to recent fishery openings, to intercept halibut that emigrate from their summer grounds in adjacent management areas. The project used PAT tags to examine the relative proportion of Canadian summer-resident halibut likely to be found in Alaskan waters on three different potential season opening dates: 1 February, 15 February, and 1 March. In addition, a smaller number of tags were deployed to investigate the likelihood that halibut summering in the USPNW emigrate into Canadian waters. In addition to producing endpoint locations, PAT tags collect ambient light data that can be used to generate geolocation estimates on a subset of days between tagging and recovery. For fish that appear to exhibit little net movement, light-based geopositions can provide information on whether the fish might have departed their tagging site prior to the chosen recovery date and then returned. This is particularly relevant to the present work considering that halibut have been shown to display a strong tendency to home to their summer grounds following the spawning season (Loher 2008). For fish that clearly depart their tagging region, geopositions can also provide an indication of migration timing.

Materials and methods

Tag deployments

Wildlife Computers PAT tags were deployed during the summer of 2006 on 60 Pacific halibut in Canadian waters and 18 Pacific halibut in USPNW waters (Fig. 1*a*). Fish were captured using commercial longline gear during the IPHC's stock assessment setline survey from 1 June through 31 July. Tags were programmed to record depth (4 m resolution), temperature (0.1 °C resolution), and light level every minute and were attached to halibut via an 18 cm leader of 130 kg test monofilament line coated in black adhesive-lined heat-shrink tubing anchored to the fish using a surgical-grade titanium dart inserted through the pterygiophores on the eyed-side of the fish roughly 2.5 cm medial to the dorsal fin.

In Canada, halibut were tagged between west-central Vancouver Island (49.00°N) and northern Graham Island (54.33°N) with deployments partitioned into four independent subregions. Tags were distributed among subregions in proportion to the relative abundance of halibut ≥100 cm fork length (FL) encountered during the 2004 and 2005 IPHC stock assessment surveys within those subregions as follows: Graham Island, $n = 15$ tags; southern Hecate, $n = 21$; Queen Charlotte Sound, $n = 12$; Vancouver Island, $n = 12$. Only halibut ≥100 cm FL were tagged because that was the minimum size that has historically been deemed appropriate for PAT tagging based on behavioral studies of captive halibut (A. Seitz, University of Alaska-Fairbanks, School of Fisheries and Ocean Sciences, Fairbanks, AK 99775, USA, unpublished data). In each subregion, an equal number of tags were programmed to detach from their host fish (i.e., "report") on each of three dates: 1 February, 15 February, and 1 March 2007.

In the USPNW, six halibut ≥100 cm FL were tagged in each of three subregions, spaced roughly equidistantly along the coast, that generated relatively high catch rates in prior stock assessment surveys: Cape Johnson (Washington), the Columbia River Entrance (Washington), and Yaquina (Oregon). Due to small sample sizes at these locations, tags were programmed to report on only two dates: 1 February and 15 February. The March reporting date was eliminated because our primary objective was to determine possible winter spawning locations; fish were most likely to be on those grounds on earlier dates. In all treatments in all tagging areas, tags were randomly assigned their reporting dates and the personnel conducting the tagging were unaware of any tag's programmed date. Tag rewards were offered for tags captured on fish or found adrift or awash.

Location estimates

On the programmed reporting dates, properly functioning tags that had escaped recovery by commercial and sport fisheries detached from their host, floated to the surface, and began broadcasting to the US National Oceanic and Atmospheric Administration's polar-orbiting satellites, administered by the Advanced Research and Global Observation System (ARGOS). Endpoint positions were estimated by Service ARGOS using the Doppler shift of each tag's signal as received on successive satellite passes (Hays et al. 2001). Each position estimate was assigned a "location class" by Service ARGOS, which indicated its positional accuracy; locations and distances reported here rely upon first broadcasts for which positional accuracy was <1000 m. For each tagging region and reporting date, total dispersion was calculated as the proportion of tags reporting from out-of-area relative to the total number of tags reporting from within the tagging area. The designation "dispersion" has been chosen in this context to specifically denote movement of multiple individuals away from a central area of origin (i.e., the tagging region). Elsewhere, the more general term "dispersal" is used to denote movement of individuals or group movement without reference to a specific point of origin. In addition to reporting final positions for individual tags and regional date-specific dispersion rates, mean displacement (distance between tag deployment and reporting locations) and mean central latitude and longitude are reported for each temporal (1 February, 15 February, and 1 March) and spatial (Canada and USPNW) treatment group.

Horizontal displacement during time at liberty was estimated using archived ambient light data, which were used to generate daily longitude estimates via Wildlife Computers' proprietary software Global Position Estimator. Global Position Estimator was used to identify daily sunrise and sunset events; days with sunrise–sunset data that did not exhibit smoothly sloping light levels from high to low or from low to high were rejected. Longitude was calculated for the remaining days by comparing local noon of the tag (mean of the sunrise and sunset times) with 1200 UTC (Coordinated Universal Time). Estimated longitude values that

Fig. 1. (*a*) Locations at which 78 Pacific halibut were tagged (diamonds) with PAT tags in the summer of 2006. The size of each symbol indicates the number of tags deployed at each site (smallest $n = 1$, largest $n = 8$). An equal number of tags from each temporal treatment group were randomly deployed in each tagging subregion for tag reporting dates of 1 February, 15 February, and, in the case of Canadian-tagged halibut, 1 March. (*b* and *c*) Reporting locations for tags deployed in Canadian waters (crosses) and USPNW waters (circles) on 1 February and 15 February, respectively. Reporting locations for the two tags that detached from their host fish prematurely (during January 2007) are included in Fig. 1*b* and the tag that reported late in Fig. 1*c*, as indicated. (*d*) 15 March reporting locations for tags deployed in Canadian waters (crosses) and the mean central position (shaded circles) of all tags that reported on each programmed tag release date by region.

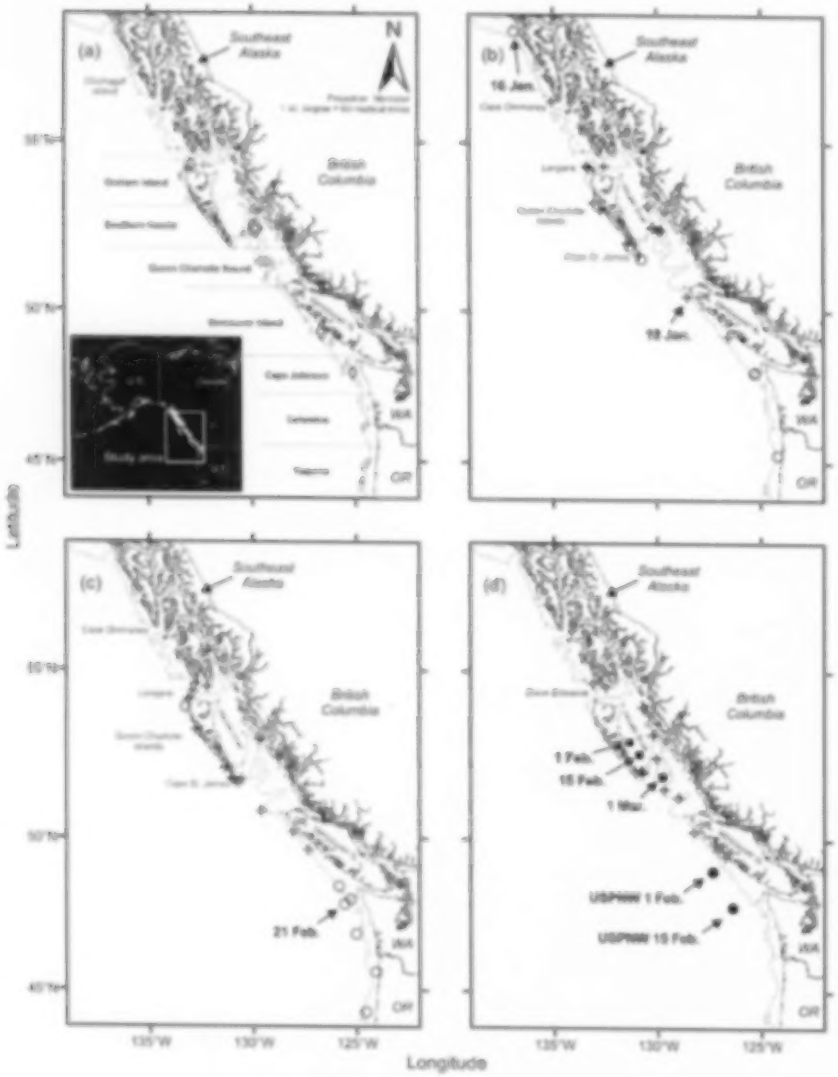

were outside the published range of the halibut (i.e., 140°E to 117°W; Mecklenburg et al. 2002) were rejected. Latitude estimates for halibut have been found to be highly variable in previous experiments (Seitz et al. 2006) and were therefore not calculated. Inferring displacement from geoposition estimates is somewhat subjective for halibut because variable cloud cover, water clarity, and the fish's vertical movements can all skew light level readings taken at depth and introduce considerable variability into location estimates, even for relatively stationary tags (Seitz et al. 2006). Individual position estimates must be considered cautiously, whereas series of positions located consistently away from a point of reference are more likely to indicate displacement of the fish. Here, halibut were deemed to have moved into Alaskan waters if their archived light data generated five consecutive geoposition estimates west of 136°W; this is the westernmost Canadian continental slope habitat that is <800 m in depth (i.e., Bowie Seamount). A depth of 800 m

was chosen as the maximum allowable depth because it approximates the deepest winter depth recorded for halibut in all prior IPHC archival tagging studies (T. Loher, unpublished data). Halibut were deemed to have moved from the USPNW into Canadian waters if five consecutive geoposition estimates placed them west of 126°30′W.

Depth and temperature data

Archived environmental data were broadcast during satellite transmissions in the form of summaries during consecutive 8 h "binning" periods. These summaries included information on the amount of time spent within user-defined depth and temperature bins, absolute minimum and maximum depths and temperatures during each summary period, and ambient light levels. Depth bins were defined as follows: surface and 0–10.0, 10.5–50.0, 50.5–100.0, 100.5–150.0, 150.5–200.0, 200.5–250.0, 250.5–300.0, 300.5–400.0, 400.5–500.0, 500.5–600.0, 600.5–700.0, 700.5–800.0, and 800.5–1000.0 m. Temperature bins were defined as <2, 2.1–3.0, 3.1–4.0, 4.1–5.0, 5.1–6.0, 6.1–7.0, 7.1–8.0, 8.1–10.0, 10.1–12.0, 12.1–16.0, 16.1–20.0, 20.1–33.0, and 33.1–60.0 °C.

Depth data collected by the tags were examined for evidence of offshore seasonal migration that would be consistent with spawning activity (Loher and Seitz 2006, 2008*a*; Seitz et al. 2007). Fish were designated as having conducted a migration consistent with spawning if they inhabited waters >200 m depth for a period of at least 7 consecutive days after 1 November, as these depths have been established as consistent with active spawning (Loher and Seitz 2008*a*) and 1 November represents a conservative estimate of the onset of spawning season (St. Pierre 1984). Maximum depth recorded immediately prior to tag reporting (hereafter "terminal depth") was used as an indication of whether halibut were still on their deepwater grounds (>200 m) at the end of their time at liberty or had returned to the continental shelf. Average terminal depth was calculated and compared among treatment groups to determine the extent to which the timing of tag reporting might have either preceded or followed the return of halibut to their shallow summer grounds. Tags that did not generate depth data within 3 days of scheduled reporting were omitted from analysis of terminal depth.

Archived temperature data were examined in an attempt to identify patterns of thermal habitat use that might be regionally specific. Average proportion of time spent in each archival temperature bin was calculated for each of four basic migration categories: halibut tagged in Canada whose tags reported from Canada, halibut tagged in the USPNW whose tags reported from the USPNW, halibut tagged in either Canada or the USPNW whose tags reported from Alaska, and halibut tagged in the USPNW whose tags reported from Canada. Proportions were calculated on a monthly basis by summing all values that were received for all fish for each 8 h summary period within each month; data were not weighted to account for summary periods that were not received.

Statistical analyses and maturity estimation

Differences in mean lengths of fish tagged, displacement distances, and terminal depths were examined via one-factor analysis of variance in which either tagging region (Canada and USPNW) or tag reporting date (1 February, 15 February, and 1 March) was established as an independent variable; lack of balanced design (i.e., absence of a 1 March treatment group in the USPNW) precluded two-factor analysis. Errors associated with mean values are reported as 1 standard error unless otherwise specified. The total number of fish tagged in any treatment group that were likely to have been immature (Im_{sum}), and therefore not expected to conduct a substantial seasonal migration, was estimated using size-specific maturity data collected during the 2006 IPHC setline survey in the Gulf of Alaska as follows:

$$Im_{sum} = \sum_{1}^{n} (FL_n \times P_{il})$$

where FL_n is the fork length of the nth fish and P_{il} is the proportion of the surveyed population at the given length that was deemed immature via macroscopic gonad examination.

Results

Tagged population and tag recoveries

Tagged Pacific halibut ranged from 104 to 163 cm FL (Fig. 2). For halibut whose tags subsequently produced location and depth data, mean length (±1 SD) in the USPNW (112.9 ± 9.15 cm FL) was significantly smaller (n = 13 and 44, $p < 0.001$) than in Canada (127.2 ± 12.25 cm). No significant difference ($\alpha = 0.05$) in mean length was detected among temporal treatments. Given size-specific sex ratios and size-at-maturity observed in the 2006 IPHC Gulf of Alaska stock assessment survey (Fig. 3), halibut of tagged size were estimated to possess >77% probability of being female. Females possessed >80% probability of being mature and males essentially 100% probability of being mature (Fig. 3). Size-at-maturity data from the setline survey suggested that fewer than four fish (Im_{sum} = 3.4) were likely to be immature across all tagging treatments; no treatment was expected to contain more than one immature fish. Im_{sum} by treatment group was as follows: Canadian waters, 1 February tag reporting = 0.6; USPNW, 1 February tag reporting = 0.6; Canada, 15 February tag reporting = 0.6; USPNW, 15 February tag reporting = 0.9; Canada, 15 March tag reporting = 0.7.

Seven tags were recaptured by the commercial fishery prior to their reporting date: six from Canadian deployments and one from the USPNW. In all cases, recapture occurred in the same region as the fish was tagged at distances ranging from 3 to 110 km from the tagging location. Eleven tags (seven Canadian and four USPNW) detached from their host fish prematurely on dates ranging from 25 July to 6 January. Ten of these tags reported from within the region of tagging at distances ranging from 25 to 275 km from the tagging location. One tag, deployed in Canadian waters and detached on 21 December, reported from Alaska 996 km from the tagging location. Two tags detached prematurely during midwinter, close enough to their programmed release dates to be included in the region-specific results that follow: one tag deployed in the USPNW detached on 16 January and one from Canada detached on 18 January. One tag deployed

Fig. 2. Stacked length frequency distribution of Pacific halibut tagged in Canadian waters (solid bars) and the USPNW (shaded bars) during the summer of 2006.

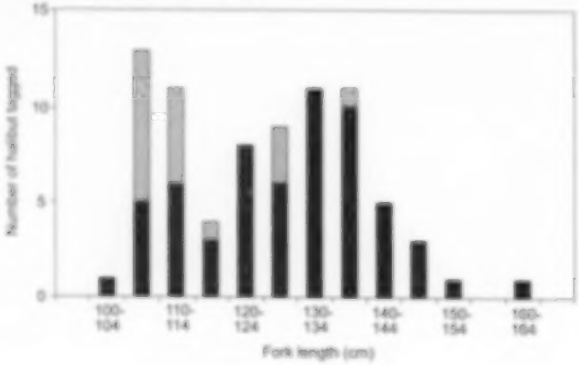

Fig. 3. (*a*) Size-specific sex ratio of Pacific halibut (n = 54 224) encountered during the IPHC's 2006 Gulf of Alaska stock assessment survey; (*b*) proportion mature at size for males (circles, n = 22 696) and females (diamonds, n = 31 528) based on external gonad examinations. On each panel, the minimum size of fish tagged in the present study (104 cm) is indicated by an arrow and the shaded portion of each graph represents the range of sizes tagged.

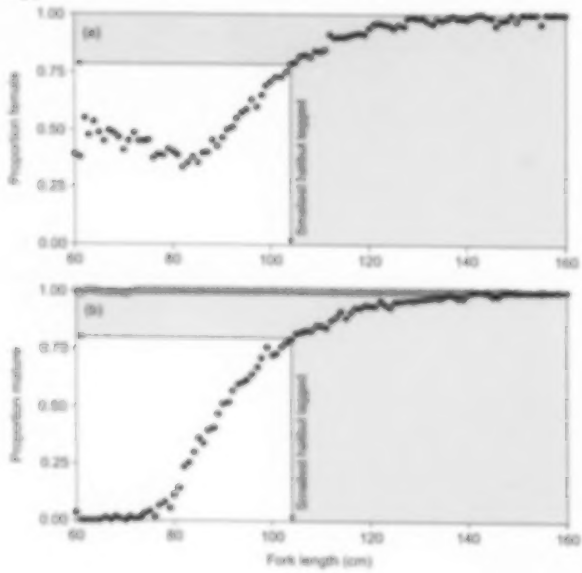

in the USPNW reported on 21 February, 6 days after its programmed release date, and was also included with its scheduled release group (15 February) in the region-specific results that follow: 54 tags (43 Canadian and 11 USPNW) functioned as programmed and reported on their scheduled dates (19 tags on 1 February, 22 on 15 February, and 13 on 1 March) (Figs. 1*b*–1*d*); three tags failed to report.

For 39 of the 57 tags providing useful broadcast data, the first position that was broadcast was accurate to within 1000 m and was accepted. For the remaining 18 tags, a total of 33 position estimates were rejected due to lower estimated accuracy. For 12 of these tags, only the initial broadcast was rejected, whereas two to seven estimates were rejected for each of the other six tags. Total delay in time between receipt of the tags' initial rejected positions and their final accepted positions ranged from 16 to 371 min; for only one tag was the delay more than 2 h. None of the rejected positions were found to be in a different region than the tag's accurate and accepted position.

Canadian dispersion

Individual displacement distances for fish tagged in Canadian waters ranged from a minimum of 1 km to a maximum of 511 km (Fig. 4). The halibut whose tag reported on 18 January was located in Canadian waters on that date (Fig. 1*b*). A total of three tags, one from each programmed reporting date, reported from southeast Alaskan waters, resulting in a total out-of-area dispersion rate of approximately 7%. Although a large number of fish were tagged close to the northern Canadian border, thus generating the possibility that high out-of-area dispersion rates could have been observed in the presence of relatively little net movement, this did not occur. One fish tagged in the Graham Island subregion did move only a moderate distance (80 km) to produce an endpoint position at the very southern extreme of Alaskan waters (Fig. 1*d*). However, all remaining Graham Island tags (n = 10) reported from Canadian waters, having displayed dispersal distances of 1–192 km. The remaining two fish that moved out of Canadian waters had been tagged in the southern Hecate subregion and displayed relatively large displacements (375 and 477 km; Figs. 1*b* and 1*c*, respectively).

While there was no apparent difference in out-of-area dispersion rate by date (Table 1), there was an indication of southward contraction of the overall distribution. For tags that reported from Alaskan waters, the farthest north occurred on 1 February at Cape Ommaney (Fig. 1*b*) and the farthest south occurred on 1 March in northwestern Dixon Entrance (Fig. 1*d*). Most fish found in Canadian waters on 1 February were clustered near the Queen Charlotte Islands or eastern Hecate Strait, with a single fish off western Vancouver Island. On subsequent dates, aggregation in the northern Queen Charlotte Islands began to erode and a progressively greater number of fish were observed off western Vancouver Island. Mean central position of all temporal treatments (Table 1; Fig. 1*d*) was in Canadian waters but shifted 52 km to the southeast (bearing = 141° from true north) between 1 February and 15 February and another 106 km to the southeast (bearing = 134° from true north) between 15 February and 1 March. Mean displacement distances, by date, were as follows: 1 February, 114.6 ± 37.6 km; 15 February, 140.1 ± 35.2 km; 1 March, 74.8 ± 39.0 km. No significant difference was detected between treatments (n = 14, 16, and 13, p = 0.442). At the subregional level (Table 1), there was little indication of a relationship between summer tagging location and mean displacement. However, irrespective of temporal treatment, fish tagged in northerly subregions displayed more northerly mean central winter locations than those tagged in southern subregions.

Light-based longitudinal estimates during time at liberty provided strong evidence that at least one Canadian-tagged

Fig. 4. Stacked frequency distribution of displacement distances associated with Pacific halibut tagged in Canadian waters (solid bars) and the USPNW (hatched bars). In both cases, fish whose tags reported from within their tagging area are denoted by dark shading (black in the case of Canada and thick hatching for USPNW) and tags that reported from out-of-area by light shading (gray in the case of Canada and thin hatching for USPNW). Note that, for the most part, movement out-of-area is associated with relatively long-distance displacment.

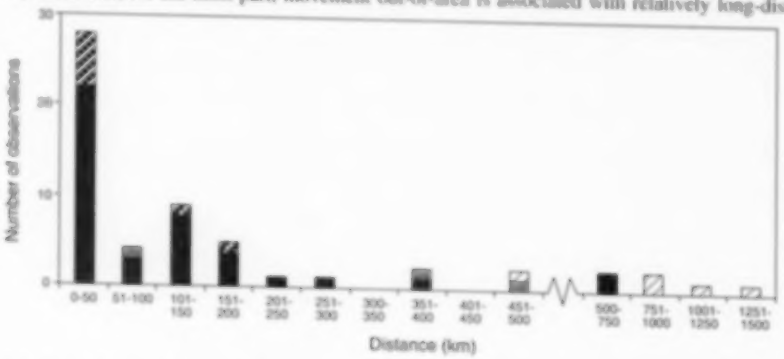

Table 1. Sample size (n), dispersion rate, mean displacement, and mean central position (latitude and longitude) of late-winter locations of Pacific halibut tagged with satellite-transmitting archival tags during the summer in Canada and the USPNW.

Location and date	n	Dispersion rate	Mean displacement	Mean central latitude	Mean central longitude
Canada	44	0.068	115.0±21.1	52.461	130.635
1 February	14	0.071	114.6±37.6	53.004	131.368
15 February	16	0.063	140.1±35.2	52.634	130.887
1 March	13	0.077	74.8±39.0	51.815	129.698
Graham Island	11	0.091	38.4±16.8	54.015	132.747
Southern Hecate	14	0.143	125.5±40.8	53.136	131.008
Queen Charlotte Sound	8	0.000	94.1±17.9	51.675	130.402
Vancouver Island	11	0.000	193.3±17.9	50.619	128.219
USPNW	13	0.385	384.5±136.7	49.106	127.482
1 February	5	0.400	377.6±184.4	49.023	127.350
15 February	7	0.286	241.6±155.9	47.893	126.237
Cape Johnson	5	0.200	299.6±280.2	50.033	127.660
Columbia Entrance	4	0.500	373.8±212.6	49.452	128.306
Yaquina	4	0.500	501.8±243.7	47.603	126.438

Note: Data are broken down according to tag reporting date and according to region (Canada and USPNW) and subregion for all reporting dates combined. Note that the total sample size for regional data is 1 greater than for the sum of all temporal treatments; in each region, one tag that reported in January is included, which is absent from the February–March temporal treatments.

halibut moved to Alaska during the winter spawning season and then returned prior to the reporting date (1 February). Tag S-06029 generated a series of six consecutive estimates that placed the fish in Alaska from at least 2 November to 22 January (Fig. 5*a*). Although the tag generated relatively few other estimates, it produced an easterly estimate on 30 October that could have placed it in either Alaskan or Canadian waters, and upon reporting on 1 February, it had clearly returned to British Columbia. These data suggest northward transboundary movement in late October and a return to Canadian waters in late January. A second tag (S-06033) produced three consecutive geoposition estimates west of 136°W from 4 December to 14 January (Fig. 5*b*). Although this was too few positions to meet the preestablished criterion for designating the fish an emigrant, it is possible that the fish departed Canadian waters before returning in late January. The tag produced a relatively large number of geopositions (n = 20) earlier in the deployment, all of which were east of 136°W and whose 90% confidence intervals (2 SE) were only ±0.55° of the mean. This variance was low compared with the displacement observed in the three later geopositions, which ranged from 3.93 to 8.95° west of the reference longitude. If this fish emigrated to Alaska, it presumably did so in late November or very early December and returned to Canada in the latter half of January. Assuming that both of the aforementioned halibut emigrated to Alaskan waters, the total emigration rate for all temporal treatment groups would be 11%. No other tag, including the three that reported from Alaskan waters, produced more than one or two isolated geoposition estimates west of 136°W.

USPNW dispersion

Individual displacement distances for fish tagged in the USPNW ranged from a minimum of 14 km to a maximum of 1420 km (Fig. 4). The halibut whose tag reported on 16 January was located in southeast Alaskan waters near northwestern Chichagof Island (Fig. 1*b*). This was the only Alaskan report for halibut tagged in the USPNW. A total of four tags reported from Canadian waters, two on 1 February 1 and two on 15 February, resulting in a total out-of-area dis-

Fig. 5. Light-based longitude estimates during time at liberty for the three Pacific halibut displaying evidence of having departed their tagging region while at liberty and then having returned prior to tag reporting: (*a*) tag S-06029, (*b*) tag S-06033, and (*c*) tag S-06074. Diamonds at the top and bottom of each plot indicate tagging and reporting locations, respectively. Vertical lines indicate reference longitudes west of which fish were considered to have departed their tagging region. Open circles indicate positions within a fish's tagging region and shaded circles positions outside the tagging region.

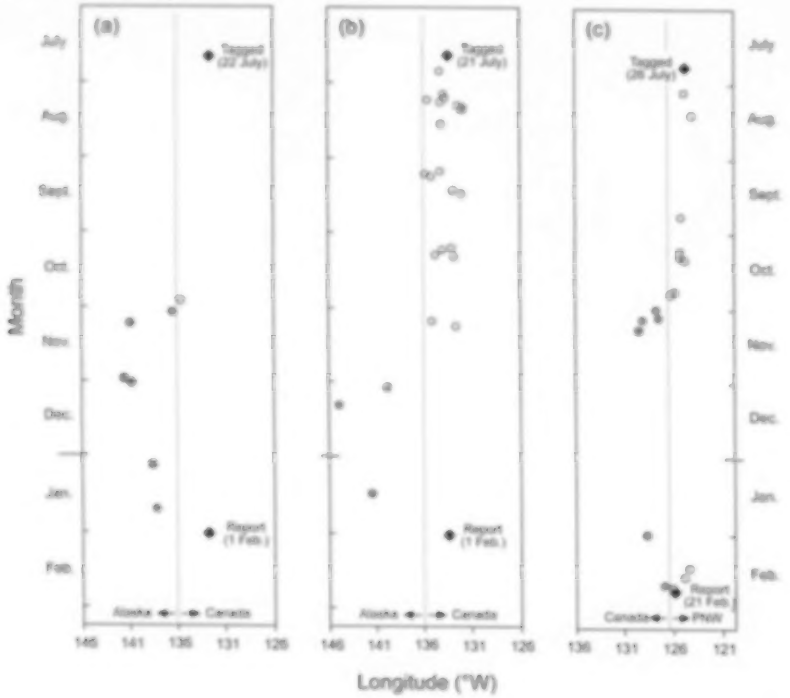

persion rate of approximately 39% (8% to Alaska coupled with 31% to Canada). The fish whose tags reported from out-of-area were those that displayed the greatest net displacements (Fig. 4), ranging from 470 to 1420 km. Similar to that observed for Canadian-tagged fish, the large number of fish tagged near the northern US border did not contribute markedly to total out-of-area dispersion: only one fish tagged in the northern subregion (Cape Johnson) dispersed out-of-area, and it was the fish that displayed the greatest overall displacement (1420 km).

Mean displacement distances, by reporting date, were as follows: 1 February, 377.6 ± 184.4 km; 15 February, 241.6 ± 155.9 km. No significant difference was detected between temporal treatments (n = 5 and 7, p = 0.586), but for tags reporting on their scheduled dates, overall mean displacement from USPNW tagging sites (298 ± 170.5 km) was found to be significantly greater (n = 12 and 43, p = 0.012) than displacement from Canadian tagging sites (111 ± 43.8 km). At the subregional level (Table 1), there was some indication that halibut tagged in more southerly subregions dispersed the farthest, but variance was high and sample sizes too low to reach definitive conclusions. Similar to Canadian-tagged halibut, fish tagged in northerly subregions displayed more northerly mean central winter locations than those tagged in southern subregions.

For the fish whose tag (S-06074) reported from USPNW waters on 21 February, light-based geopositions suggested emigration to Canadian waters and return to the USPNW prior to tag detachment. A series of five consecutive positions placed the fish in Canadian waters from at least 29 October to 30 January (Fig. 5*c*). Considering this fish an emigrant would result in a total out-of-area dispersion rate of approximately 46% (39% to Canada).

Depth data

Five general depth profiles (Fig. 6) were observed from the 57 halibut whose tags reported via satellite. A total of 51 fish (89% of the tagged population) displayed depth profiles consistent with migration to offshore spawning areas during the winter. Forty halibut displayed the typical pattern of summertime continental shelf residence followed by an autumn offshore migration to deeper continental slope waters. The majority of these fish (n = 36) did not show marked evidence of having yet returned to shallow water by the end of tagging period (Fig. 6*a*). Twenty-nine of these 36 fish had been tagged in Canadian waters, and two were individuals whose tags reported from Alaska. The remaining seven fish in this category had been tagged in the USPNW, and of these fish, two produced final tag locations in Canada and one in Alaska. Four halibut that moved to deep water in winter appeared to have completed their deepwater residence phase by the tag pop-up date (Fig. 6*b*); all had been tagged in Canadian waters and produced final reporting locations in Canada. A total of 10 fish showed no evidence of

Fig. 6. Profiles of maximum depth within 8 h binning periods for five Pacific halibut that demonstrate the general seasonal behaviors observed across all tagged fish (n = 57). (*a*) Summer residence on the continental shelf with an offshore autumn migration and occupation of deeper slope waters in winter (n = 36); (*b*) summer shelf residence followed by winter slope residence with evidence of return to shelf waters at the end of the period at liberty (n = 4); (*c*) use of continental slope habitat throughout the year (n = 10); (*d*) use of slope habitat in summer and shelf residence in autumn and winter (n = 3); (*e*) full-time shelf residence (n = 3).

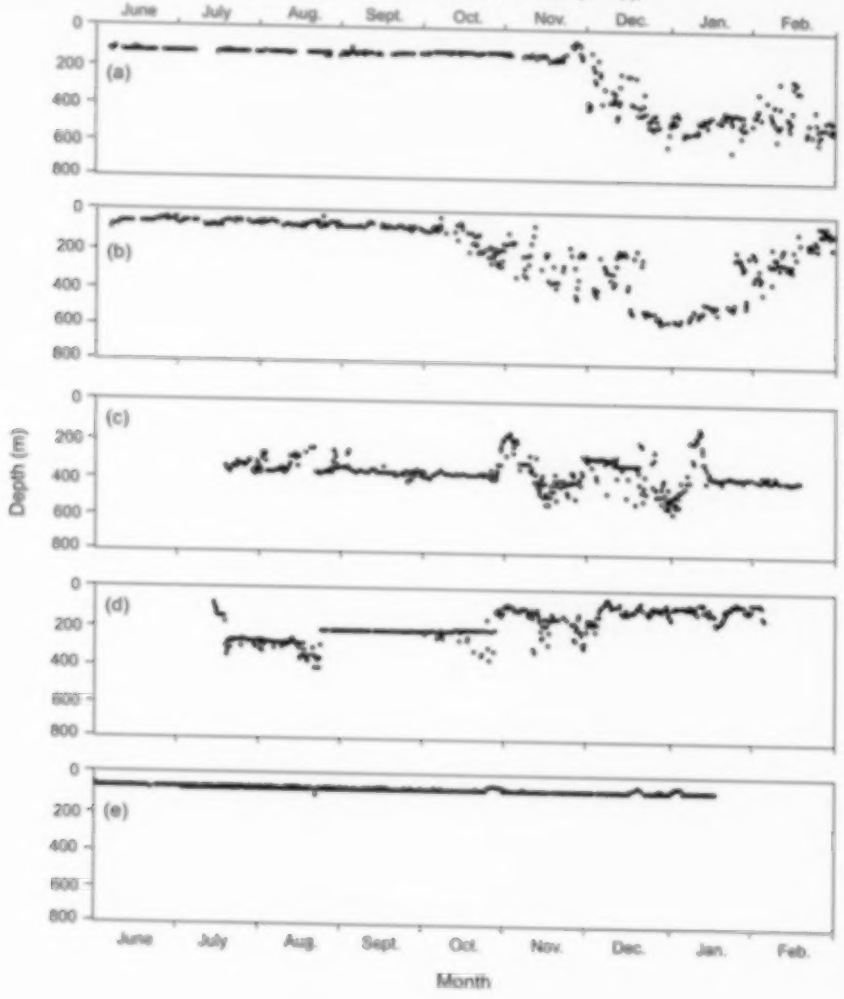

having moved to markedly deeper water during winter but had inhabited continental slope waters throughout their time at liberty (Fig. 6*c*) and were therefore still deemed to possess a depth profile consistent with spawning. Seven of these had been tagged in Canadian waters, of which one produced a final tag location in Alaska. The remaining three fish were tagged in the USPNW, and two produced final tag locations in Canada.

Six halibut failed to display migration patterns consistent with known spawning behavior. Three fish, all of which were tagged in USPNW waters and produced USPNW final tag locations, demonstrated an inverted depth profile in which slope waters were inhabited in the summer and shelf waters during the winter spawning season (Fig. 6*d*). Three fish, all of which were tagged in Canadian waters and produced Canadian final tag locations, inhabited shallow shelf waters throughout their time at liberty (Fig. 6*e*).

For 54 of the tagged fish, reliable depth data were produced within 3 days of scheduled reporting. One tag from the 15 February treatment of Canadian-tagged halibut did not produce data at the end of the reporting period, and the two tags that reported prematurely were excluded from analysis of terminal depth. The majority of fish were located in relatively deep water on the continental shelf (i.e., >200 m) immediately prior to tag reporting (Fig. 7). For halibut tagged in Canadian waters, mean terminal depths, by date, were as follows: 1 February, 307 ± 34.1 m; 15 February, 307 ± 32.9 m; 1 March, 252 ± 35.3 m. No significant difference was detected among dates (n = 4, 15, and 13, p = 0.441). No halibut exhibited a terminal depth associated

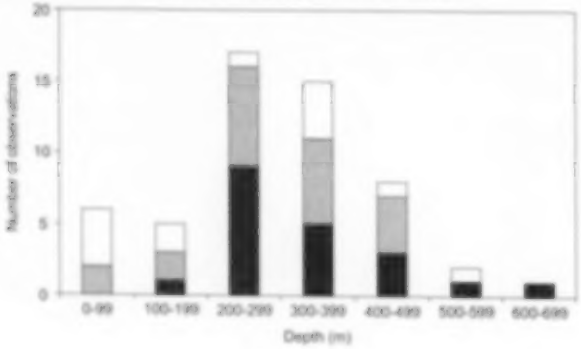

Fig. 7. Stacked frequency distribution of maximum depths visited by Pacific halibut immediately prior to the end of their time at liberty (i.e., terminal depth) for fish whose tags broadcast reliable depth data within 3 days of their reporting dates; solid bars, 1 February; shaded bars, 15 February; open bars, 1 March.

with continental shelf residence (<200 m) immediately prior to a 1 February reporting date (depth range = 208–472 m). Two of 15 fish displayed shelf depths immediately prior to 15 February reporting (depth range = 64–632 m). Six of 13 fish displayed shelf depths immediately prior to 1 March reporting (depth range = 56–440 m). For fish tagged in the USPNW, mean terminal depths were as follows: 1 February, 338 ± 68.1 m; 15 February, 286 ± 57.5 m. Two of five fish were located on the continental shelf immediately prior to 1 February reporting (depth range = 144–576 m) and two of seven prior to 15 February reporting (depth range = 88–456 m). All of the halibut that were tagged in the USPNW and found in Canadian waters upon reporting were located on the continental slope (depth range = 224–456 m), as was the fish whose tag detached prematurely in Alaskan waters on 16 January (depth = 480 m). No significant differences in mean terminal depth were detected among dates for either area (Canada: n = 14, 15, and 13, p = 0.441; USPNW: n = 5 and 7, p = 0.573) or between areas (n = 12 and 42, p = 0.694).

Temperature data

Tagged halibut experienced temperatures ranging from 3.6 to 13.6 °C. Some general patterns of thermal habitat use were observed, related to summer tagging region and final winter tag reporting location (Fig. 8). Halibut that appeared to remain resident in the USPNW throughout their tagging period (including both final tag reporting location and at-liberty light-based longitude estimates, n = 7) experienced temperatures primarily between 6 and 8 °C through October and then a broader and generally warmer temperature distribution (5–12 °C) during the winter spawning season. For Canadian residents (n = 38), this pattern was somewhat reversed: a broader range of temperatures (5–12 °C) was experienced through November followed by generally cooler conditions (4–10 °C) in winter. Out-of-area migrants experienced a mixture of conditions that appeared to be consistent with their source and destination locations. Emigrants from the USPNW to Canada (n = 5) experienced a narrower range of temperatures in summer than in winter as well as cooler conditions later in the tagging period. Migrants to Alaska (n = 6) (note that one Canadian-tagged fish was excluded due to a final position very near the Canada–Alaska border) experienced the narrowest and coldest observed winter temperature range (4–8 °C). Despite these general patterns of thermal habitat usage, close inspection of individual records suggested little opportunity to use these data for individual-based assessments of interarea movements during time at liberty. Individual profiles ranged considerably within regions, and there was excessive overlap in the temperatures experienced by fish that appeared to remain segregated by considerable distance. The ranges of temperatures experienced by halibut were very similar whether fish were tagged in Canadian (3.6–13.6 °C) or USPNW (4.2–13.0 °C) waters.

Discussion

The results of the present research did not support our hypothesis that a high proportion of Canadian-tagged Pacific halibut would be found in Alaskan waters on the selected late-winter dates. The data suggest a relatively low probability that halibut ≥100 cm FL summering on Canadian feeding grounds would be intercepted by halibut longline fisheries commencing later than 15 February and conducted in Alaskan waters. Dispersion rates observed in February and early March were roughly an order of magnitude lower than estimated in earlier conventional tag analysis (Leaman et al. 2002). The present results do suggest a substantially greater probability that Canadian fisheries prosecuted prior to 15 February would intercept fish emigrating from the USPNW and that fisheries conducted in either region during February–March could target fish on deepwater grounds and still spawning.

Archived light and depth data did not support the hypothesis that the tagged fish had emigrated and returned to their summer grounds, although it should be noted that light-based geolocation is not ideal for addressing this hypothesis. The accuracy of light-based geoposition estimates can be substantially reduced during the winter in northern latitudes due to low-light conditions and light attenuation at depth (Seitz et al. 2006), with resolution decreasing further around the winter solstice (Hill and Braun 2001). However, predominantly deepwater distribution for tagged halibut at the end of their times at liberty is inconsistent with completion of an onshore migration prior to tag reporting, and most fish tagged in Canadian waters were aggregated near the well-documented spawning grounds off Langara Island and Cape St. James (VanCleve and Seymour 1953; Skud 1977; St. Pierre 1984). Analysis of high-resolution archived depth data from physically recovered tags (Loher and Seitz 2008*a*) further suggests that many of the same individuals were actively engaged in spawning (i.e., gamete release) at the time of tag reporting: peak spawning was observed at depths of >250 m in late January to early February and extended until at least mid-March.

The observation of greater mean displacement and higher out-of-area dispersion of USPNW-tagged halibut relative to Canadian fish further indicates that the tag reporting dates were appropriate for detecting seasonal emigration. While migration and spawn timing might be expected to vary geographically across the stock's range (sensu Stephenson et al.

Fig. 8. Monthly temperature ranges experienced by Pacific halibut that were (*a*) tagged in the USPNW and showed no evidence of having departed the region during time at liberty ($n = 7$), (*b*) tagged in Canada and showed no evidence of having departed ($n = 38$), (*c*) tagged in the USPNW and moved to Canada in winter ($n = 5$), and (*d*) tagged in either the USPNW or Canada and moved to Alaska in winter ($n = 6$). The width of each bar represents the proportion of all observations falling into each temperature range (bin) during that month. Warmer temperatures are represented by darker bars cooler temperatures by lighter bars.

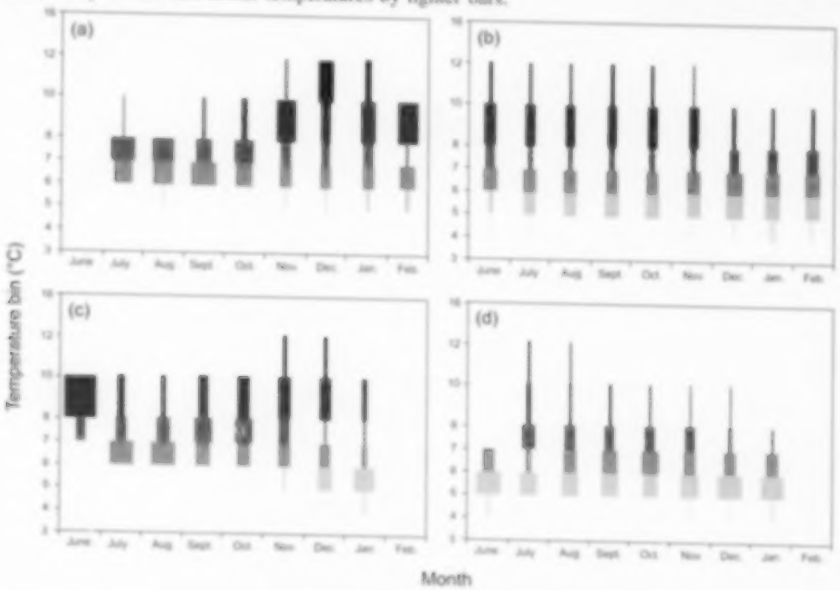

2001; Porter 2005), there is little reason to believe that halibut emigrating from Canada to join the Alaskan spawning stock would return to summer grounds prior to those emigrating from the USPNW to Canada. It has been suggested that spawning in marine fishes should be timed to deliver planktotrophic larvae into peak seasonal plankton productivity (Cushing 1990). Abundance of zooplankton, particularly copepods, over the continental shelf of British Columbia appears to peak earlier and decline more rapidly (Mackas 1992) than on the northern Gulf of Alaska shelf (Coyle and Pinchuk 2005). Spawning of flathead sole (*Hippoglossoides elassodon*) has been shown to occur progressively later along an east-to-west gradient in the western Gulf of Alaska (Porter 2005). Thus, it is reasonable to hypothesize that halibut would spawn later on Alaskan than on Canadian spawning grounds and that the majority of Canadian-tagged halibut would have been on or near their spawning sites.

Although the final sample size was disappointingly small in the USPNW, more emigrants were identified here than in a Canadian deployment that comprised four times as many tags. This occurred despite the fact that halibut tagged in the USPNW were significantly smaller and therefore more likely to be immature and forego the spawning migration. All USPNW emigrants exhibited terminal depths (296–576 m) consistent with slope spawning (Loher and Seitz 2008*a*) and those located off the Queen Charlotte Islands and in southeast Alaskan waters were at documented spawning grounds (St. Pierre 1984), supporting the hypothesis that emigration from the USPNW was for the purpose of spawning. A number of apparently nonmigratory individuals were aggregated near Cape Johnson at the end of the tagging period. Given that no major spawning has been identified south of Cape St. James (St. Pierre 1984), it is possible that these fish, and the others that remained in the USPNW, were either large immature individuals or exhibiting spawning omission (i.e., skip-spawning) for which an extensive migration would have been energetically disadvantageous. However, this seems unlikely based on maturity data from the IPHC's annual setline survey. If a large proportion of large fish were immature or not in spawning condition, this should have appeared in the survey data as a substantial skew in regional size-at-maturity; this was not the case. However, the location of the Cape Johnson aggregation does correspond to anecdotal reports of a winter ground historically fished by the Makah tribe, and the terminal depths experienced by these fish were consistent with documented spawning depths (Loher and Seitz 2008*a*). A more detailed investigation may be warranted to determine to what extent spawning takes place south of previously documented grounds and to determine abundance within such aggregations.

Small aggregations of nonmigratory fish may be susceptible to early-season depletion if subjected to concentrated commercial fishing effort. If such sites support spawning, it may be advisable to delay onset of commercial fishing until emigrants have returned to their summer grounds to offset fishing mortality. In essence, target exploitation rates will not be realized until the region's abundance has returned to true summer levels; in advance of immigration, exploitation rates will be amplified within the nonmigratory stock component. Although spawning on small grounds at the southern range edge might comprise a minor contribution to overall recruitment from a numerical perspective, degradation of spawning population complexity has been implicated in re-

ducing resilience of other commercially important stocks (Parrish et al. 1998; Smedbol and Wroblewski 2002), and Stephenson (1999) suggested that "preservation of the full suite of spawning areas and times should be considered a general biodiversity issue" and "become a principle of management."

Differences in estimated emigration rates derived from the present study and prior conventional tag analyses (Leaman et al. 2002) may have resulted from either methodological factors or biological variance. Of considerable importance may be differences in the size composition of fish tagged in each study. Whereas the conventional tag analysis was based on fish of all commercially exploitable sizes (>82 cm FL), the fish tagged here were larger (>103 cm FL) due to the size of the PAT tags and therefore likely biased towards females (refer to Fig. 3). Sex-specific migratory behavior occurs in many species, mediated by annual energy budgets, potential for long-distance dispersal, and mating systems. The nature of sex-specific dispersal may be taxa specific (Greenwood 1980) or scale dependent (Bekkevold et al. 2004), and in fishes, both male-biased (Knight et al. 1999; Hutchings 2003; Bekkevold et al. 2004) and female-biased (Dorazio et al. 1994; Bekkevold et al. 2004) dispersal have been identified. Migration distances that appear to be sex specific can be confounded by covariates such as mean body size or growth rate (Dorazio et al. 1994), an observation that is particularly relevant to species such as halibut, which are characterized by marked sexually dimorphic growth rates (Clark et al. 1999). We have no information regarding sexual bias in the dispersal of halibut, but it is reasonable to caution that the present results might only be applicable to the tagged demographic. Future work should seek to tag smaller individuals and a larger proportion of males.

Whereas the present results may be influenced by a demographic bias, prior conventional tagging results were likely affected by spatial tag recovery and reporting biases (Hilborn et al. 1995) and by data that were collected over temporal scales unable to resolve among multiple dispersal processes. Fishery recruitment, and therefore conventional tag recapture, occurs at sizes approximately 10 cm below length at 50% maturity for females, juveniles are known to migrate primarily to the southeast (Skud 1977), and recent analyses suggest that persistent eastward migration may also occur in mature individuals (Valero and Hare 2009). It is impossible to resolve the relative contributions of seasonal versus ontogenetic redistribution from conventional tag data wherein fish have been at liberty for periods sometimes in excess of 10 years. The unique nature of PAT tags allowed us to design the present study so that all recovery information was obtained in less than a year, isolating seasonal migration to the greatest degree possible and completely eliminating recovery biases.

In conclusion, the results of the present work depart markedly from previous analyses and additional resolution on this topic is warranted. Examinations of the timing of spawning (Loher and Seitz 2008*a*) and of onshore–offshore migration (Loher and Seitz 2008*b*) suggest that, since the establishment of quota management systems, commercial fishery openings in the Gulf of Alaska have preceded by weeks to months the termination of spawning and return of halibut to shallow summer grounds. A certain degree of seasonal interarea interception has presumably been a feature of both Canadian and Alaskan halibut fisheries for roughly 15 years. However, potential rates of those interceptions remain very much in question, both presently and historically. It is also unknown if halibut migratory behavior is heritable and whether rates of fishing mortality or the duration of interception fisheries have been great enough to have discernible effects upon the population. Simulation modeling of North Sea plaice (*P. platessa*) has demonstrated the degree to which seasonal mixing between adjacent stock components can contribute to interception fisheries and, in turn, yield incorrect estimates of relative productivity and management effectiveness (Kell et al. 2004). Satellite tagging represents an idea tool for calibrating such models in an unbiased manner, and archival tag data have proven a powerful resource for elucidating the nature and timing of dispersal in a variety of pelagic (Block et al. 2001; Rooker et al. 2007; Svedäng et al. 2007) and benthic (Hunter et al. 2003, 2006) species. For eastern halibut, a full understanding of seasonal mixing rates will require tagging fish across the range of sizes that comprise mature and exploitable biomass, sexual identification at time of tagging (sensu Martin-Robichaud and Rommens 2001), and temporal replication to resolve questions of interannual variance. Fishery independence should remain a priority to eliminate the recovery biases that have hampered the interpretation of conventional tagging studies. Development of methods that provide more frequent and reliable midpoint locations during time at liberty would also add considerable power and scope to future work.

Acknowledgements

Kathy Bareza, Drew Barrett, Jen Lucke, Dan Rafla, and Tucker Soltau conducted the tagging described in this study aboard the fishing vessels *Blackhawk*, *Pender Isle*, *Proud Venture*, and *Star Wars II*. Claude Dykstra, Tracee Geernaert, Eric Soderlund, and Erica Anderson provided valuable logistical assistance through the IPHC setline survey program.

References

Bekkevold, D., Hansen, M.M., and Mensberg, K.L. 2004. Genetic detection of sex-specific dispersal in historical and contemporary populations of anadromous brown trout *Salmo trutta*. Mol. Ecol. **13**(6): 1707–1712. doi:10.1111/j.1365-294X.2004.02156.x. PMID:15140113.

Block, B.A., Dewar, H., Blackwell, S.B., Williams, T.D., Prince, E.D., Farwell, C.J., Boustany, A., Teo, S.L.H., Seitz, A., Walli, A., and Fudge, D. 2001. Migratory movements, depth preferences, and thermal biology of Atlantic bluefin tuna. Science (Washington, D.C.), **293**(5533): 1310–1314. doi:10.1126/science.1061197.

Brodziak, J., and Col, L. 2005. Atlantic halibut. *In* Assessment of 19 Northeast Groundfish Stocks through 2004. NEFSC Ref. Doc. 05-13. *Edited by* R.K. Mayo and M. Terceiro. US National Marine Fisheries Service, Woods Hole, Mass. pp. 424–431. Available at www.nefsc.noaa.gov/nefsc/publications/crd/crd0513/crd0513.pdf.

Clark, W.G., Hare, S.R., Parma, A.M., Sullivan, P.J., and Trumble, R.J. 1999. Decadal changes in growth and recruitment of Pacific halibut (*Hippoglossus stenolepis*). Can. J. Fish. Aquat. Sci. **56**(2): 242–252. doi:10.1139/cjfas-56-2-242.

Coleman, F.C., Koenig, C.C., and Collins, L.A. 1996. Reproductive styles of shallow-water groupers (Pisces: Serranidea) in the eastern Gulf of Mexico and the consequences of fishing spawning

aggregations. Environ. Biol. Fishes, **47**(2): 129–141. doi:10.1007/BF00005035.

Coyle, K.O., and Pinchuk, A.I. 2005. Seasonal cross-shelf distribution of major zooplankton taxa in the northern Gulf of Alaska shelf relative to water mass properties, species depth preferences and vertical migration behavior. Deep-Sea Res. Part II. Top. Stud. Oceanogr. **52**(1–2): 217–245. doi:10.1016/j.dsr2.2004.09.025.

Cushing, D.H. 1990. Plankton production and year-class strength in fish populations: an update of the match/mismatch hypothesis. Adv. Mar. Biol. **26**: 249–293. doi:10.1016/S0065-2881(08)60202-3.

Department of Fisheries and Oceans. 2001. Atlantic halibut on the Scotian Shelf and southern Grand Bank (Div. 4VWX3NOP). DFO Stock Stat. Rep. A3-23. Department of Fisheries and Oceans, Dartmouth, N.S. Available at www.mar.dfo-mpo.gc.ca/science/rap/internet/SSR_2006_038_E.pdf.

Dorazio, R.M., Hattala, K.A., McCollough, C.B., and Skjeveland, J.E. 1994. Tag recovery estimates of migration of striped bass from spawning areas of the Chesapeake Bay. Trans. Am. Fish. Soc. **123**(6): 950–963. doi:10.1577/1548-8659(1994)123<0950:TREOMO>2.3.CO;2.

Gilroy, H.L., and Sadorus, L.L. 2000. Impacts of an extension to the IPHC commercial fishing season. Part II. Report from the interagency work group meeting on the implications of extending the halibut season. *In* Report of assessment and research activities 1999. *Edited by* L. Sadorus. International Pacific Halibut Commission, Seattle, Wash. pp. 87–94. Available at www.iphc.washington.edu/halcom/pubs/rara/1999rara/99rara.htm.

Grant, W.S., Teel, D.J., Kobayashi, T., and Schmitt, C. 1984. Biochemical population genetics of Pacific halibut (*Hippoglossus stenolepis*) and comparison with Atlantic halibut (*H. hippoglossus*). Can. J. Fish. Aquat. Sci. **41**(7): 1083–1088. doi:10.1139/f84-127.

Greenwood, P.J. 1980. Mating systems, philopatry and dispersal in birds and mammals. Anim. Behav. **28**(4): 1140–1162. doi:10.1016/S0003-3472(80)80103-5.

Hays, G.C., Akesson, S., Godley, B.J., Luschi, P., and Santidrian, P. 2001. The implications of location accuracy for the interpretation of satellite-tracking data. Anim. Behav. **61**(5): 1035–1040. doi:10.1006/anbe.2001.1685.

Hibberd, T., and Pecl, G.T. 2007. Effects of commercial fishing on the population structure of spawning southern calamary (*Sepioteuthis australis*). Rev. Fish Biol. Fish. **17**(2-3): 207–221. doi:10.1007/s11160-006-9028-4.

Hilborn, R., Skalski, J., Anganuzzi, A., and Hoffman, A. 1995. Movements of juvenile halibut in IPHC regulatory areas 2 and 3. IPHC Tech. Rep. 31. International Pacific Halibut Commission, Seattle, Wash. Available at www.iphc.washington.edu/halcom/pubs/techrep/tech0031.pdf.

Hill, R.D., and Braun, M.J. 2001. Geolocation by light level, the next step: latitude. *In* Electronic tagging and tracking in marine fisheries. *Edited by* J.R. Sibert and E.D. Stevens. Kluwer Academic Press, Dordrecht, the Netherlands. pp. 315–330.

Hunter, E., Metcalfe, J.D., and Reynolds, J.D. 2003. Migration route and spawning area fidelity by North Sea plaice. Proc. R. Soc. Lond. B Biol. Sci. **270**(1529): 2097–2103. doi:10.1098/rspb.2003.2473.

Hunter, E., Berry, F., Buckley, A.A., Stewart, C., and Metcalfe, J.D. 2006. Seasonal migration of thornback rays and implications for closure management. J. Appl. Ecol. **43**(4): 710–720. doi:10.1111/j.1365-2664.2006.01194.x.

Hutchings, J.A. 2003. Sex-biased dispersal in a salmonid fish: implications for growth rate and survival. J. Fish Biol. **63**(Suppl. 1): 233. doi:10.1111/j.1095-8649.2003.0216q.x.

Kell, L.T., Scott, R., and Hunter, E. 2004. Implications for current management advice for North Sea plaice: Part I. Migration between the North Sea and English Channel. J. Sea Res. **51**(3–4): 287–299. doi:10.1016/j.seares.2003.10.004.

Knight, M.E., Oppen, M.J., Smith, H.L., Rico, C., Hewitt, G.M., and Turner, G.F. 1999. Evidence for male-biased dispersal in lake malawi cichlids from microsatellites. Mol. Ecol. **8**(9): 1521–1527. doi:10.1046/j.1365-294x.1999.00740.x. PMID: 10564458.

Koutsikopoulos, C., Dorel, D., and Desaunay, Y. 1995. Movement of sole (*Solea solea*) in the Bay of Biscay: coastal environment and spawning migration. J. Mar. Biol. Assoc. U.K. **75**(01): 109–126. doi:10.1017/S002531540001523X.

Leaman, B.L., and Clark, W.G. 2000. Impacts of an extension to the IPHC commercial fishing season part I: biological issues. *In* Report of assessment and research activities 1999. *Edited by* L. Sadorus. International Pacific Halibut Commission, Seattle, Wash. pp. 81–85. Available at www.iphc.washington.edu/halcom/pubs/rara/1999rara/99rara.htm.

Leaman, B.L., Geernaert, T.O., Loher, T., and Clark, W.G. 2002. Further examination of biological issues concerning an extended commercial fishing season. *In* Report of assessment and research activities 2004. *Edited by* L. Sadorus. International Pacific Halibut Commission, Seattle, Wash. pp. 53–74. Available at www.iphc.washington.edu/halcom/pubs/rara/2002rara/2002rara.htm.

Loher, T. 2008. Homing and summer feeding site fidelity of Pacific halibut (*Hippoglossus stenolepis*) in the Gulf of Alaska, established using satellite-transmitting archival tags. Fish. Res. **92**(1): 63–69. doi:10.1016/j.fishres.2007.12.013.

Loher, T., and Seitz, A. 2006. Seasonal migration and environmental conditions of Pacific halibut *Hippoglossus stenolepis*, elucidated from pop-up archival transmitting (PAT) tags. Mar. Ecol. Prog. Ser. **317**: 259–271. doi:10.3354/meps317259.

Loher, T., and Seitz, A. 2008*a*. Characterization of active spawning season and depth for eastern Pacific halibut (*Hippoglossus stenolepis*), and evidence of probable skipped spawning. J. Northwest Atl. Fish. Sci. **41**: 23–36. doi:10.2960/J.v41.m617.

Loher, T., and Seitz, A. 2008*b*. Characterization of seasonal onshore-offshore migration timing, and active spawning depth and period of Gulf of Alaska halibut, with evidence of possible skipped spawning. *In* Report of assessment and research activities 2007. *Edited by* L. Sadorus. International Pacific Halibut Commission, Seattle, Wash. pp. 433–449. Available at www.iphc.washington.edu/halcom/pubs/rara/2007rara/2007rara.htm.

Mackas, D.L. 1992. Seasonal cycle of zooplankton off southwestern British Columbia. Can. J. Fish. Aquat. Sci. **49**(5): 903–921. doi:10.1139/f92-101.

Martin-Robichaud, D.J., and Rommens, M. 2001. Assessment of sex and evaluation of ovarian maturation of fish using ultrasonography. Aquacult. Res. **32**(2): 113–120. doi:10.1046/j.1365-2109.2001.00538.x.

Mecklenburg, C.W., Mecklenburg, T.A., and Thorsteinson, L.K. 2002. Fishes of Alaska. American Fisheries Society, Bethesda, Md.

Parrish, D.L., Behnke, R.J., Gephard, S.R., McCormick, S.D., and Reeves, G.H. 1998. Why aren't there more Atlantic salmon (*Salmo salar*)? Can. J. Fish. Aquat. Sci. **55**(Suppl. 1): 281–287. doi:10.1139/cjfas-55-S1-281.

Porter, S.M. 2005. Temporal and spatial distribution and abundance of flathead sole (*Hippoglossoides elassodon*) eggs and larvae in the western Gulf of Alaska. Fish. Bull. **103**: 648–658.

Rooker, J.R., Bremer, J.R.A., Block, B.A., Dewar, H., de Metrio, G., Corriero, A., Kraus, R., Prince, E.D., Rodriguez-Marin, E., and Secor, D.H. 2007. Life history and stock structure of Atlan-

tic bluefin tuna (*Thunnus thynnus*). Rev. Fish. Sci. **15**(4): 265–310. doi:10.1080/10641260701484135.

Seitz, A.C., Norcross, B.L., Wilson, D., and Nielsen, J.L. 2006. Evaluating light-based geolocation for estimating demersal fish movements in high latitudes. Fish. Bull. **104**: 571–578.

Seitz, A., Loher, T., and Nielsen, J.L. 2007. Seasonal movements and environmental conditions experienced by Pacific halibut in the Bering Sea, examined by pop-up satellite tags. IPHC Sci. Rep. 84. International Pacific Halibut Commission, Seattle, Wash. Available at www.iphc.washington.edu/halcom/pubs/scirep/SciReport0084.pdf.

Sissenwine, M.P., Mace, P.M., Powers, J.E., and Scott, G.P. 1998. A commentary on western bluefin tuna assessments. Trans. Am. Fish. Soc. **127**(5): 838–855. doi:10.1577/1548-8659(1998)127<0838:ACOWAB>2.0.CO;2.

Skud, B.E. 1977. Drift, migration, and intermingling of Pacific halibut stocks. IPHC Sci. Rep. 63. International Pacific Halibut Commission, Seattle, Wash. Available at www.iphc.washington.edu/halcom/pubs/scirep/SciReport0063.pdf.

Smedbol, R.K., and Wroblewski, J.S. 2002. Metapopulation theory and northern cod population structure: interdependency of subpopulations in recovery of a groundfish population. Fish. Res. **55**(1–3): 161–174. doi:10.1016/S0165-7836(01)00289-2.

St. Pierre, G. 1984. Spawning locations and season for Pacific halibut. IPHC Sci. Rep. 70. International Pacific Halibut Commission, Seattle, Wash. Available at www.iphc.washington.edu/halcom/pubs/scirep/SciReport0070.pdf.

Stephenson, R.L. 1999. Stock complexity in fisheries management: a perspective of emerging issues related to population sub-units. Fish. Res. **43**(1–3): 247–249. doi:10.1016/S0165-7836(99)00076-4.

Stephenson, R.L., Clark, K.J., Power, M.J., Fife, F.J., and Melvin, G.D. 2001. Herring stock structure stock discreteness, and biodiversity. *In* Herring: expectations for a new millenium. *Edited by* F. Funk, J. Blackburn, D. Hay, A.J. Paul, R. Stephenson, R. Torresen, and D. Witherell. University of Alaska Sea Grant, AK-SG-01-04, Fairbanks, Alaska. pp. 559–571.

Stokesbury, M.J.W., Teo, S.L.H., Seitz, A., O'Dor, R.K., and Block, B.A. 2004. Movement of Atlantic bluefin tuna (*Thunnus thynnus*) as determined by satellite tagging experiments initiated off New England. Can. J. Fish. Aquat. Sci. **61**(10): 1976–1987. doi:10.1139/f04-130.

Svedäng, H., Righton, D., and Jonsson, P. 2007. Migratory behaviour of Atlantic cod *Gadus morhua*: natal homing is the prime stock-separating mechanism. Mar. Ecol. Prog. Ser. **345**: 1–12. doi:10.3354/meps07140.

Valero, J.L., and Hare, S.R. 2009. Exploring the effects of fishing and migration on the distribution of Pacific halibut. *In* Report of assessment and research activities 2008. *Edited by* L. Sadorus. International Pacific Halibut Commission, Seattle, Wash. pp. 265–297. Available at www.iphc.washington.edu/halcom/pubs/rara/2008rara/2008rara.htm.

VanCleve, R., and Seymour, A.H. 1953. The production of halibut eggs on the Cape St. James spawning bank off the coast of British Columbia, 1935–1946. IPHC Sci. Rep. 19. International Pacific Halibut Commission, Seattle, Wash. Available at www.iphc.washington.edu/halcom/pubs/scirep/Report0019.pdf.

Rainbow trout (*Oncorhynchus mykiss*) invasion in Hokkaido streams, northern Japan, in relation to flow variability and biotic interactions

Mikio Inoue, Hiroshi Miyata, Yousuke Tange, and Yoshinori Taniguchi

Abstract: Factors controlling invasion success of rainbow trout (*Oncorhynchus mykiss*) and interactions with native masu salmon (*Oncorhynchus masou*) were examined by field investigations. The results suggested that flow regime has a major role in controlling rainbow trout invasion success. Although competitive relationships were found between the two species, masu salmon were not likely to prevent trout invasion. Analyses on the distributions and abundances of the two species indicated that the occurrence of rainbow trout was limited to streams with stable flows, and the density of each species was negatively related with that of the other. Habitat use and diet analyses revealed a pattern of their resource partitioning; rainbow trout occupy positions near the bottom or cover, foraging benthic prey, while masu salmon feed drifting prey at the middle layers of the water column. This resource partitioning was suggested to reflect a diet shift by rainbow trout. Our results also have a management implication that dams, which control flow regime, can be a key factor in managing rainbow trout invasion and its effects.

Résumé : Des observations de terrain ont permis d'examiner les facteurs qui contrôlent le succès de l'invasion de la truite arc-en-ciel (*Oncorhynchus mykiss*) et ses interactions avec le saumon masou (*Oncorhynchus masou*) indigène. Les résultats font croire que le régime d'écoulement des eaux a un rôle majeur dans le contrôle du succès de l'invasion des truites. Bien qu'il existe des relations de compétition entre les deux espèces, il est peu probable que les saumons masou empêchent l'invasion des truites. Des analyses de la répartition et de l'abondance des deux espèces indiquent que la présence de la truite arc-en-ciel est restreinte aux cours d'eau à écoulement stable; il y a aussi une relation négative entre les densités des deux espèces. Des analyses de l'utilisation de l'habitat et du régime alimentaire montrent un patron de partage des ressources : les truites arc-en-ciel se tiennent près du fond ou des abris et se nourrissent de proies benthiques, alors que les saumons masou s'alimentent de proies en dérive dans les couches intermédiaires de la colonne d'eau. Ce partage des ressources semble refléter un changement de régime alimentaire chez la truite arc-en-ciel. Nos résultats ont aussi des conséquences sur la gestion, puisque les barrages, qui contrôlent le régime d'écoulement, peuvent être un facteur essentiel pour gérer l'invasion des truites arc-en-ciel et ses effets.

[Traduit par la Rédaction]

Introduction

Invasions by non-native species are a major threat to biodiversity and ecosystem health. Once non-native species establish self-reproducing populations, they can exert strong impacts on native communities at various levels through competition, predation, and indirect cascade effects (Crowl et al. 1992; Townsend 2003). However, introduced species cannot always become successful invaders; some species fail to be established (e.g., Brown and Moyle 1997) or may not have strong, detectable impacts on native communities even if they are established. Therefore, understanding factors affecting success and failure of invasion and variation in impacts by invaders is an important subject in invasion biology (Fausch et al. 2001; Light 2003; Marchetti et al. 2004).

Rainbow trout (*Oncorhynchus mykiss*), which is native to the Pacific coast of North America and Kamchatka Peninsula (Russian Far East), is one of the most widely introduced species in cool-temperate regions of the world (Fausch et al. 2001), with evidence of its negative impacts on native biota having been frequently reported (e.g., Crowl et al. 1992; Weigel et al. 2003; Morita et al. 2004). Fausch et al. (2001) analyzed geographic patterns in invasion success of rainbow trout at a broad scale, using four regions where their invasions varied from highly successful (southern Appalachians, USA) to moderate (Colorado, USA, and Hokkaido, Japan) or failed (Honshu, Japan). They showed that the region where invasions failed has flow regimes that are not favorable for reproductive life history of rainbow trout (e.g., frequent high flows after their emergence period). The match between invasion success and flow regime across the regions strongly suggests that flow disturbance limits the trout's invasion success. However, because their comparison was made at a large, regional scale, various factors may differ distinctly among the regions (e.g., temperature regimes, biota), and the differences in invasion success might be explained also

Received 11 September 2008. Accepted 22 June 2009. Published on the NRC Research Press Web site at cjfas.nrc.ca on 20 August 2009.
J20770

M. Inoue,[1] **H. Miyata, and Y. Tange.** Department of Biology, Faculty of Science, Ehime University, Bunkyo-cho 2-5, Matsuyama 790-8577, Japan.
Y. Taniguchi. Department of Environmental Science and Technology, Faculty of Science and Technology, Meijo University, Tenpaku, Nagoya 468-8502, Japan.

[1]Corresponding author (e-mail: inom@sci.ehime-u.ac.jp).

by similar other factors. Therefore, their flow disturbance hypothesis needs to be examined at a smaller spatial scale (i.e., within a region) so that possible confounding factors that vary among regions can be ruled out. If presence or absence of rainbow trout among streams within a region can be explained by differences in flow regimes, this provides strong support for the flow disturbance hypothesis.

In Japan, rainbow trout has been stocked extensively over the four main islands (Hokkaido, Honshu, Shikoku, and Kyushu), with varying success of establishment among the regions (Kitano 2004). In Honshu, Shikoku, and Kyushu, only a few cases of their establishment have been reported (Kato and Yanagawa 2000), despite repeated stocking for fisheries and recreational purposes in most river systems through the last several decades (Kawanabe 1980; Kitano 2004). In Hokkaido, however, their self-sustaining populations are not rare (e.g., Kitano et al. 1993; Aoyama et al. 1999; Takami and Aoyama 1999); they have been successfully established in certain streams, but not in others. This situation is ideal to test the flow disturbance hypothesis. The objective of our study is to identify factors controlling invasion success of rainbow trout in Hokkaido streams, considering the flow disturbance hypothesis and biotic interactions with native salmonids.

It is important to examine interactions between native and non-native salmonids, not only in terms of impacts of invaders but also of biotic resistance from native species. Because competition for food and space is common among salmonids (Fausch 1988; Nakano 1995), native salmonids may prevent invasion by non-native salmonids through competitive interactions. On the Asian side of the Pacific coast, masu salmon (*Oncorhynchus masou*) and whitespotted charr (*Salvelinus leucomaenis*) are the two most widely distributed native salmonids (Kawanabe 1989). Recently, a growing number of studies, both empirical (Taniguchi et al. 2000; Morita et al. 2004) and experimental (Hasegawa et al. 2004; Hasegawa and Maekawa 2006), have revealed negative effects of non-native rainbow trout on whitespotted charr populations in Japan. These studies suggest that whitespotted charr is unable to prevent rainbow trout invasion. However, studies on interactions with masu salmon are scarce and limited to small-scale, controlled experiments in artificial channels (Taniguchi et al. 2002; Hasegawa et al. 2004; Hasegawa and Maekawa 2006); empirical data from the field are still largely lacking (but see Nakano and Kaeriyama 1995).

Nakano and Kaeriyama (1995) described resource partitioning among four salmonid species, including rainbow trout (juvenile steelhead (i.e., sea-run rainbow trout)) and masu salmon in a Kamchatkan stream, which provided a unique case where both species were native. Their data suggest that masu salmon occupied suitable feeding positions despite the presence of rainbow trout, although their study did not adopt a comparative approach in which competitive effects can be examined (i.e., comparison of resource use between sympatric and allopatric sites; e.g., Gatz et al. 1987). Recent experimental studies using laboratory channels reported that masu salmon matched rainbow trout in behavioral competitive ability (Hasegawa et al. 2004), and rainbow trout did not affect habitat use of masu salmon (Hasegawa and Maekawa 2006). Such evidence suggests that effects of rainbow trout on masu salmon populations may be weak (but see Taniguchi et al. 2002). Rather, masu salmon may offer biotic resistance to rainbow trout invasions.

Fig. 1. Location of the study sites in the Iburi District, southwestern Hokkaido, northern Japan. Fish distribution and abundance were examined using 24 sites (solid circles and open squares); open squares indicate six sites used for habitat use and diet analyses.

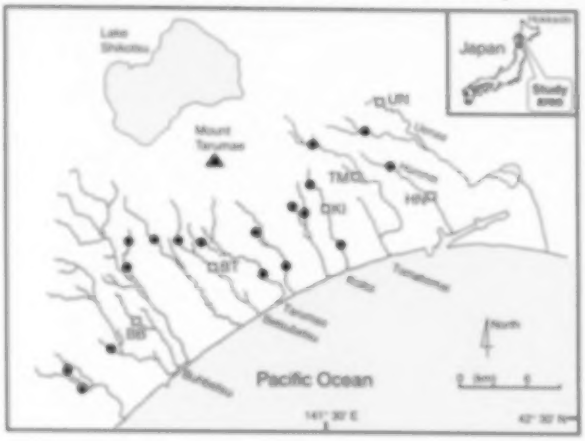

In this study, we examined (*i*) distribution and abundance of rainbow trout in relation to flow variability, masu salmon abundance, and other habitat factors, and (*ii*) habitat use and diet of rainbow trout and masu salmon in both sympatric and allopatric sites. Because we assume that life history of rainbow trout does not perfectly fit to the seasonal pattern of stream discharge in Hokkaido (high flows in spring and summer; see Fausch et al. 2001), we predict that rainbow trout would fail to establish in streams with higher flow variability, and therefore, the occurrence of rainbow trout would be limited to streams with stable flows. If masu salmon offers strong biotic resistance to rainbow trout invasion, we predict that a complementary occurrence would be found in their distributions. In addition, investigations on habitat use and diet of the two species would provide information on elaborating their interactions.

Materials and methods

Study area

The study was conducted using 13 streams in the Iburi District in southwestern Hokkaido, Japan (Fig. 1). The mean annual precipitation in this region is ~1200 mm, dominated by summer rainfall (70%) and winter snowfall (25%). In streams, high flows occur in the snowmelt season (April–May) and between August and October by rainfall (Kishi et al. 1999; Shibata et al. 2001). Although precipitation regime and the seasonal pattern of stream discharge are similar within the study area, the degree of fluctuation in stream discharge differs between eastern and western parts of the area owing to geological conditions. In the eastern side, the soil is dominated by clastic pumice derived from volcanic ejecta of Mt. Tarumae. Because this soil has high water permeability, surface runoff during precipitation is negligible, and stream discharge is derived mainly from deeper groundwater (Shibata et al. 2001). As a result, streams on this volcanic

deposit have stable flow. Distribution of the thick deposits of the Mt. Tarumae volcanic ejecta is limited to the eastern side of Tarumae Stream, and thus flow fluctuation in the western side streams is higher than in the eastern side.

Twenty-four study sites were established over the 13 streams to investigate fish distribution, abundance, habitat use, and diet (Fig. 1). Streams at the study sites were generally small (first- to third-order), with low or moderate channel gradient (Table 1). All study sites were located in deciduous broad-leaved forests dominated by oak (*Quercus crispula*) and maple (*Acer* spp.), and stream channels were generally shaded by riparian canopy. Masu salmon or rainbow trout and Siberian stone loach (*Barbatula barbatulus*) or sculpin (*Cottus nozawae*) were common among the study sites. Two other salmonids, whitespotted charr and exotic brown trout (*Salmo trutta*), were found at a few sites.

In Hokkaido, rainbow trout are strictly stream residents that spawn during spring (late January – early May: Aoyama et al. 1999; Taniguchi et al. 2000), whereas most masu salmon are anadromous. Masu salmon adults ascend rivers and spawn in small tributaries in autumn (late August – early October). Fry emerge in spring (February–May), earlier than rainbow trout (June–July). Juvenile masu salmon generally spend 1 year as age-0 parr and descend to the sea in the following spring (i.e., most masu salmon in streams are age-0), although some individuals stay in streams more than 1 year. Owing to these differences in life history traits, size structure differs between the two species in streams (see Taniguchi et al. 2002). Masu salmon (mostly age-0) are larger than age-0 rainbow trout but smaller than age-1 and older rainbow trout.

Distribution and abundance

Field surveys

A study reach including at least two sets of pool–riffle sequences (reach length: 50–150 m) was established at each site to quantify fish abundance and habitat characteristics. Fish abundance was estimated during June–July 2003 using the removal method of DeLury (1951). Each study reach was blocked with 5 mm mesh seines at the upper and lower ends, and three removal passes were made using an electrofishing unit (Model 12 Backpack Electrofisher, Smith-Root Inc.). The fork length of captured fish was measured. Population estimates of rainbow trout and masu salmon were calculated separately for fry (age-0) and parr (age > 0) and converted to density (N·100 m^{-2}).

Summer water temperature, channel gradient, stream size, and the area of habitat types (pool and cover) were quantified at each site during June–August 2003. A maximum–minimum thermometer was placed in each study reach, and the maximum temperature was recorded every 10–14 days (four times) from 18 June to 6 August 2003. The channel gradient, expressed as percent change in relative height to reach length, was measured with a level and leveling rod. Equally spaced transects were set along the study reaches (3–5 m intervals depending on stream size), and bank-full and wetted channel widths were measured. The boundaries of bank-full channels were determined by scour lines, vegetation limits, or changes between developed organic soils and inorganic alluvium. Each study reach was divided into channel units, classified as riffle, glide, or pool. The length of each channel unit was measured, and each channel unit area was estimated by multiplying the length and the mean wetted width of the transects within the channel unit. Cover is generally considered as any object that conceals fish from predators or provides shelter from strong current (e.g., Shirvell 1990). In this study, we considered course woody debris, brush (often structured by twigs and grass stems), undercut banks, and overhanging vegetation (instream or within 40 cm of the water surface) as cover materials. The length and several widths of each cover material were measured to calculate the occupied area within the wetted channel surface.

Table 1. Habitat variables characterizing each study site.

Habitat variable	Mean (SD), range
Channel gradient (%)	1.0 (0.6), 0.2–2.1
Stream size (m)	
Mean wetted width	4.1 (1.3), 1.5–7.1
Water temperature (°C)	
Maximum in summer	13.5 (2.1), 9.3–18.5
Habitat component (%)	
Pool area	45.4 (15.9), 15.7–80.7
Cover area	9.7 (6.5), 1.9–29.3
Flow variability index	
Wetted/bank-full width ratio	0.74 (0.22), 0.24–1.00

Habitat variables

Habitat characteristics of the study reaches were expressed by summer maximum water temperature (mean of the four maximum temperatures recorded), channel gradient, mean wetted width, the areal percentage of pools and that of cover (Table 1), which can affect the abundance of rainbow trout (Urabe and Nakano 1998, 1999) and masu salmon (Inoue et al. 1997; Inoue and Nakano 1998). In addition to these five variables, wetted/bank-full width ratio (*W*/*B* ratio), calculated as the ratio of mean wetted width at low flow to mean bank-full channel width, was used as an index of flow variability. Bank-full channel is the region of wetted area at high flows occurring once every few years (Gordon et al. 2004). Therefore, lower values of *W*/*B* ratio indicate greater differences between peak and baseflow discharges, suggesting higher flow variability. At locations near 9 of the 24 study sites, seasonal variations in discharge had been recorded (Hayakawa and Sato 1978). Our *W*/*B* ratio was negatively correlated with coefficient of variation (SD/mean) of the discharges (r = –0.79, P = 0.011, n = 9), suggesting that this measure can be used as an index of flow variability in this region.

Data analyses

Distribution and abundance of fishes were analyzed using discriminant and regression analyses. First, a stepwise discriminant function analysis was used to examine factors affecting presence or absence of rainbow trout. The above habitat variables and masu salmon density were used to discriminate presence or absence of rainbow trout at the study sites. The correct classification rate by the discriminant model was estimated by a leave-one-out cross-validation method (jackknife method in Olden et al. 2002). Second, effects of habitat and biotic interactions (rainbow trout vs.

Fig. 2. Differences in habitat conditions (water depth and current velocity: *a*, 2003; *c*, 2004) and food availability (*b*, 2003; *d*, 2004) among the study sites: rainbow trout allopatric sites (solid squares: TM, Tomakomai; UN, Uenae), masu salmon allopatric sites (open circles: BB, Buhbetsu; BT, Betsubetsu), and sympatric sites (crosses: HN, Horonai; KI, Koitoi). Bars indicate ± standard deviation (SD).

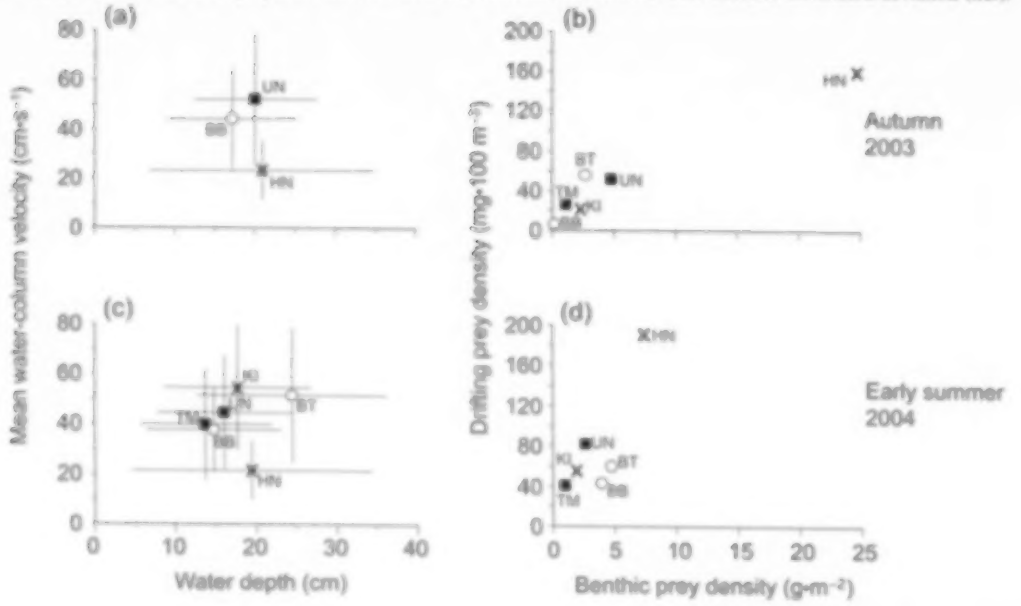

masu salmon) on rainbow trout abundance were examined by a stepwise multiple regression analysis, using study sites inhabited by rainbow trout. Rainbow trout density was used as a dependent variable and the habitat variables and masu salmon density as independent variables. Similarly, effects of rainbow trout on masu salmon abundance were examined using rainbow trout density with the habitat variables as independent variables; rainbow trout density was expressed by not only total density but also density of age-1 and older trout (removing age-0 trout from total density), because only larger trout may have significant effects on masu salmon (Taniguchi et al. 2002). In addition, effects of habitat variables on total salmonid density (rainbow trout and masu salmon combined) were examined. Fish densities, channel gradient, and mean wetted width were $\log_{10}$-transformed to improve normality; the percentages of pool and cover and *W*/*B* ratio were arcsin-square-root-transformed. All analyses were performed using SPSS (version 13, SPSS Inc., Chicago, Illinois).

Habitat use and diet

Field observation and sampling

Habitat use and diet of rainbow trout and masu salmon were surveyed using six study sites in autumn (September–October 2003) and early summer (June–July 2004) (habitat use survey in autumn was conducted at only three sites) to examine their interspecific interactions (Fig. 1). The six sites represented the three cases of allopatric–sympatric situations (two sites per case): sites inhabited only by rainbow trout (trout allopatric site: Tomakomai, TM; Uenae, UN), only by masu salmon (salmon allopatric site: Buhbetsu, BB; Betsubetsu, BT), and by both species (sympatric site: Koitoi, KI; Horonai, HN). Some distinct differences were found among the study sites in both habitat characteristics and food abundance. HN and BT had slower current and deeper water, respectively, than other sites (Fig. 2). HN was characterized also by abundant food.

Habitat use was surveyed by underwater observation. Underwater observations were made by snorkeling in an upstream direction, with the focal points of fish being identified for all undisturbed individuals (rainbow trout or masu salmon) encountered. Distance from the bottom to the focal points (vertical position) and the fish total length were estimated visually, and the focal points were marked by putting a numbered flag on the streambed. In each site, the observation was made in a reach including at least two pool–riffle sequences; in case the reach did not harbor sufficient number of fish, the observation reach was expanded so that data of at least 30 individuals per species were obtained (length of observation reaches: 80–500 m). After the observation, water depth, current velocity at the surface, mid-depth (0.5 depth), bottom and fish vertical position, and the distance from the nearest cover were measured at the marked focal points. Focal points were then characterized by water depth, focal point velocity, distance from cover, and the relative vertical position (distance from the bottom/total depth). To describe differences in habitat characteristics among the study sites, water depth and current velocity were measured over the observed reach using transects. Equally spaced transects (3–6 m) with equally spaced measuring points (0.3–0.5 m) were established, and water depth and the surface, mid-depth, and bottom velocities were measured.

Fish were sampled using an electrofishing unit for analysis of their diet. Captured fish were anesthetized with FA100 (Tamura-Seiyaku Pharmaceutical), and stomach contents were sampled using a stomach pumping method. Fish were

Table 2. Summary of stomach contents of rainbow trout and masu salmon in allopatry and sympatry.

	Rainbow trout		Masu salmon	
Prey category	Allopatry	Sympatry	Allopatry	Sympatry
Terrestrial invertebrates	63.0–78.0	7.6–73.7	41.8–85.4	62.1–89.1
Aquatic invertebrates				
Gammaridae	1.3–27.3	0.4–87.3	0–0.1	0.2–2.3
Other invertebrates	9.7–29.8	5.1–26.0	14.6–38.0	9.1–37.7
Others	0	0–4.6[a]	0–41.7[b]	0

Note: Relative abundance (%) of each category by dry weight is expressed as the range of four values from each site (two sites by two seasons).

[a]Fish (rainbow trout fry) in early summer.

[b]Eggs (masu salmon) in autumn.

then released alive. Benthic and drifting invertebrates were also sampled to examine differences in food availability among the study sites. Six samples of benthic invertebrates were sampled from riffles and pools (three samples per habitat type) in each site using a Surber sampler (25 cm × 25 cm quadrat, 0.3 mm mesh). Drift was sampled once at each site using drift nets (25 cm × 25 cm opening, 0.3 mm mesh). Four drift nets were placed in a riffle for 30–40 min during the daytime (1000–1500 h), with current velocity measured at the center of net opening to estimate the volume of sieved water. Samples of stomach contents, benthic invertebrates, and drifts were preserved in 10% formalin in the field and sorted (benthic and drift samples were washed onto 1 mm mesh), identified to family or order, and weighed (dry weight) in the laboratory.

Data analyses

Habitat and diet data were used to examine resource partitioning between rainbow trout and masu salmon and effects of interspecific interactions on it. To identify habitat variables related to their habitat partitioning in the sympatric sites, a stepwise discriminant function analysis was used. Focal points of rainbow trout and those of masu salmon in each sympatric site were discriminated using water depth, focal point velocity, distance from cover, and the relative vertical position as potential discriminant variables, with the correct classification rate being assessed by a leave-one-out cross-validation. On the basis of the results of this analysis, key variables related to their habitat partitioning were identified. These variables were then compared among allopatric rainbow trout and allopatric masu salmon using one-way analysis of variance (ANOVA) with Tukey's honestly significant difference (HSD) multiple comparison test to examine whether their habitat partitioning in the sympatric sites were mediated by habitat shift by either species. Water depth, focal point velocity, and distance from cover were $\log_{10}$ transformed to improve normality; the relative vertical position was arcsin-square-root-transformed.

In the diet analysis, we focused on two prey categories, terrestrial invertebrates and gammarids, which were major components of stomach contents (Table 2) and may reflect foraging behavior of fish. For stream fishes, terrestrial invertebrates are provided as drifts, and thus their dominance in stomach contents is indicative of drift feeding. On the other hand, gammarids, which also made up large proportions in some sites (Table 2), are a typical inhabitant of leaf litter patches on the bottom (see Konishi et al. 2001). Therefore, gammarids are likely consumed by benthic feeding rather than drift feeding. To examine whether the food resource use differs between rainbow trout and masu salmon in each sympatric site, the percentage of terrestrial invertebrates and that of gammarids in stomach contents (by dry weight) of individual fish were compared between the two species using Mann–Whitney *U* test. Similarly, the percentage of terrestrial invertebrates and that of gammarids were compared among allopatric rainbow trout and allopatric masu salmon using Kruskal–Wallis test and subsequent pairwise comparisons (Mann–Whitney *U* test with Bonferroni correction). All analyses were performed using SPSS (version 13, SPSS Inc., Chicago, Illinois).

Fig. 3. The presence (solid squares) and absence (open circles) of rainbow trout in relation to wetted/bank-full width ratio and masu salmon density. The axes of masu salmon density and wetted/bank-full width ratio are logarithmic and arcsin-square-root scales, respectively.

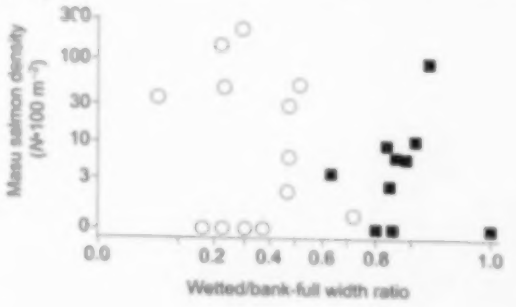

Results

Distribution and abundance

Among the 24 study sites, rainbow trout occurred in 11 sites. The stepwise discriminant function analysis indicated that the presence or absence of rainbow trout was discriminated by the *W/B* ratio but not by masu salmon abundance (Fig. 3); the discriminant function, of which correct classification rate was 91.7%, retained only *W/B* ratio as the discriminant variable (Wilks' $\lambda = 0.282$, $\chi^2 = 27.19$, $P < 0.001$). The study sites inhabited by rainbow trout were characterized by a higher value of *W/B* ratio.

Table 3. Results of stepwise multiple regression analysis on the densities of rainbow trout, masu salmon, and total salmonids (both species combined).

Species	Independent variable	Standardized coefficient	Significance		
			R^2	F	P
Rainbow trout	Mean wetted width	–0.64	0.75	11.72	0.004
	Masu salmon density	–0.45			
Masu salmon	Age-1 and older trout density	–0.79	0.62	14.85	0.004
Total salmonids	Cover area	0.67	0.45	7.38	0.024

Note: Data were transformed prior to analysis.

The stepwise multiple regression analysis on the 11 sites revealed negative relationships between rainbow trout and masu salmon densities (Table 3; Fig. 4). The variation of rainbow trout density was best explained by a combination of mean wetted width and masu salmon density; rainbow trout increased with decreasing wetted width and masu salmon density. Masu salmon density was best modeled by a negative effect of the density of age-1 and older rainbow trout. For total salmonids, cover area was detected as the single best predictor. The density of rainbow trout and masu salmon combined increased with cover area.

Habitat use

In the sympatric sites, differences in the total body length between rainbow trout and masu salmon varied among the sites and seasons (Fig. 5). In HN, rainbow trout was smaller than masu salmon in autumn 2003, whereas rainbow trout was larger than masu salmon in early summer 2004. In KI in early summer, the sizes of the two species were comparable, although the shape of frequency distribution differed (bimodal vs. unimodal). The stepwise discriminant function analysis showed that although variables discriminating between focal points of rainbow trout and those of masu salmon in sympatry varied among the sites and seasons, focal points of rainbow trout were generally characterized as lower vertical positions or locations closer to cover (Table 4; Fig. 6). In HN in autumn, focal points of the two species were best discriminated by relative vertical position, with rainbow trout occupying lower vertical position than masu salmon. In HN in early summer, where rainbow trout was larger in body size than masu salmon, their focal points were best discriminated by water depth and distance from cover. Rainbow trout occupied locations with deeper water and closer to cover than masu salmon. In KI, where their sizes were comparable, the discriminant function retained all four variables, with the highest contribution of relative vertical position followed by distance from cover; their habitat partitioning in terms of the two variables was similar to those in HN.

Relative vertical position and distance from cover were considered as key variables in habitat partitioning between the two species, and these variables were compared among the allopatric sites (Fig. 7). In autumn 2003, relative vertical position of allopatric rainbow trout (UN) was significantly lower than that of allopatric masu salmon (BB) (one-way ANOVA, $F = 4.80$, $P < 0.032$). Although the same result was obtained from early summer 2004 (i.e., trout in UN < salmon in BB; Tukeys' HSD test, $P = 0.021$), relative vertical position of rainbow trout in another allopatric site (TM)

Fig. 4. The density of rainbow trout (*a*, *b*), masu salmon (*c*), and both combined (*d*) in relation to explanatory variables detected by multiple regression analysis. The axes of fish densities and mean wetted width are logarithmic scale, while that of cover area is arc-sin-square-root scale. In panel (*b*), trout and salmon densities are expressed by residuals after removing effects of mean wetted width.

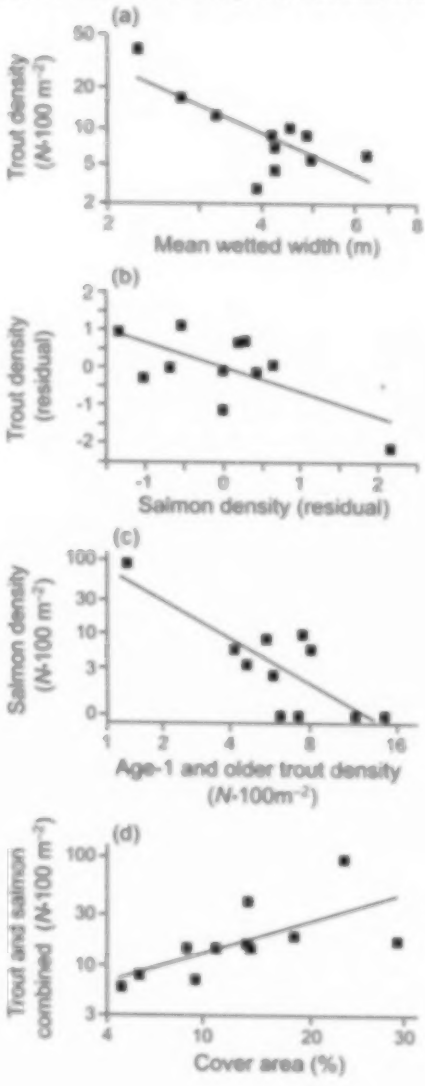

Fig. 5. Frequency distributions of body size for rainbow trout (solid columns) and masu salmon (open columns) in each sympatric site: HN (Horonai) in autumn 2003 (*a*), HN in early summer 2004 (*b*), and KI (Koitoi) in early summer 2004 (*c*).

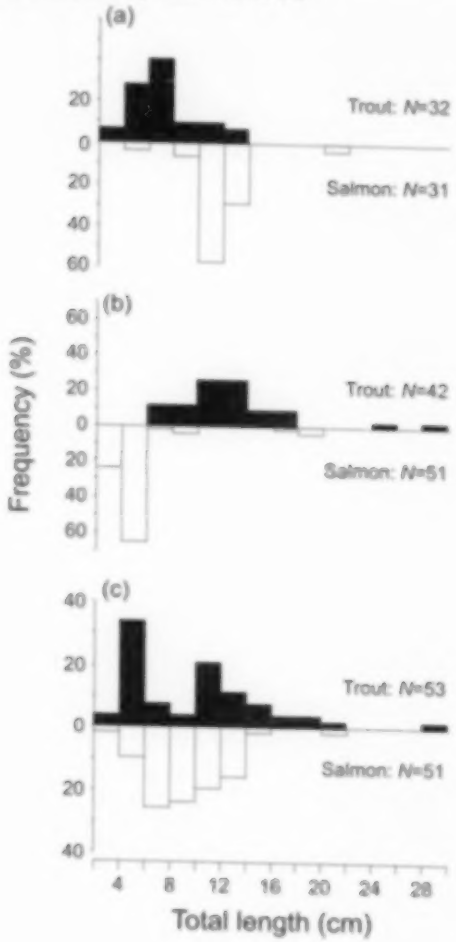

was not significantly different from that of allopatric masu salmon in BB and BT (Tukey's HSD test, $P = 0.198$–0.999). Distance from cover was not significantly different between the two species in autumn 2003 (one-way ANOVA, $F = 0.265$, $P = 0.609$). However, in early summer 2004, distance from cover for allopatric rainbow trout in both TM and UN was significantly shorter than that for allopatric masu salmon in BB and BT (Tukey's HSD test, $P < 0.03$).

Diet

The diet analysis indicated that in the sympatric sites, stomach contents differed between rainbow trout and masu salmon (Fig. 8). The percentage of terrestrial prey in stomach contents of rainbow trout was significantly lower than that of masu salmon in both sites in both seasons (Mann–Whitney *U* test, see Fig. 8). From 20% to 50% of rainbow trout stomachs included no terrestrial invertebrates, while many individuals of masu salmon had terrestrial prey in their stomachs. In particular, in autumn 2003, more than 40% of masu salmon stomachs were filled with terrestrial prey by 90%–100%. In contrast with the case of terrestrial prey, the percentage of gammarids in stomach contents was significantly higher for rainbow trout than for masu salmon in all cases except KI in autumn 2003 (Fig. 8). Most masu salmon had no gammarids in their stomachs, whereas stomach contents of several individuals of rainbow trout were dominated by gammarids, especially in HN.

Table 4. Results of stepwise discriminant function analysis discriminating focal points of rainbow trout and those of masu salmon in each sympatric site.

	Autumn 2003	Early summer 2004	
Variable–statistic	HN	HN	KI
Variable			
Water depth	—	−0.95	0.41
Focal-point velocity	—	—	0.40
Distance from cover	—	0.81	0.56
Relative vertical position	1.00	—	0.99
Statistics			
Wilks' λ	0.590	0.513	0.703
χ^2	31.96	60.06	35.24
P	<0.001	<0.001	<0.001
Correct classification rate (%)	87.3	80.6	77.9

Note: Standardized coefficients, significance, and correct classification rate based on a leave-one-out cross-validation are shown for each discriminant function. Data were transformed prior to analysis. HN, Horonai; KI, Koitoi.

In the allopatric sites (Fig. 9), contribution of terrestrial prey to diet of rainbow trout was greater than that of sympatric rainbow trout. In autumn 2003, the percentage of terrestrial prey in rainbow trout stomachs in both TM and UN was larger than that of masu salmon in BB (Mann–Whitney *U* test, $P = 0.003$, 0.006, respectively; see Fig. 9) and not significantly different from that of masu salmon in BT (Mann–Whitney *U* test, $P = 0.155$, 0.467, respectively). This is attributable to lower contribution of terrestrial prey to masu salmon diet, as well as higher contribution of terrestrial prey to rainbow trout diet. In autumn 2003, the study sites in BB and BT were used for spawning by adult masu salmon, and stomachs of several masu salmon sampled were filled with salmon eggs (see Table 2), which is a reason for the low contributions of terrestrial prey to masu salmon diet in these sites.

In early summer 2004, no significant difference was found in the percentage of terrestrial prey among the species and sites (Kruskal–Wallis test, $P = 0.398$). In every case of rainbow trout and masu salmon under allopatric situations, more than 30% of stomachs were filled with terrestrial prey by >80%. Differences in gammarid contribution between the two species in allopatric sites were similar to those in sympatric sites (Fig. 9). In both seasons, the percentage of gammarids in stomach contents of rainbow trout was higher than that of masu salmon (Mann–Whitney *U* test, $P < 0.005$).

Fig. 6. Differences in focal point characteristics between rainbow trout (solid squares) and masu salmon (open circles) in Horonai in autumn 2003 (*a*), Horonai in early summer 2004 (*b*), and Koitoi in early summer 2004 (*c*), based on the results of discriminant function analysis. The axes of distance from cover and water depth are logarithmic scale, while that of relative vertical position is arcsin-square-root scale.

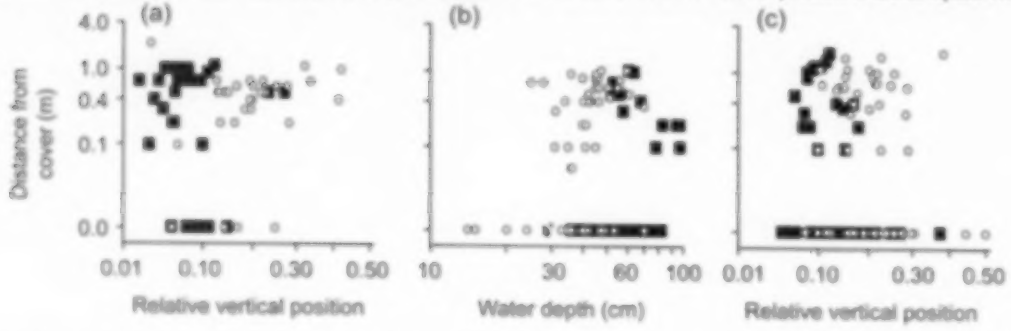

Fig. 7. Comparisons of relative vertical position (*a*) and distance from cover (*b*) for focal points held by rainbow trout (RT, solid squares) and masu salmon (MS, open circles) among allopatric sites (TM, Tomakomai; UN, Uenae; BB, Buhbetsu; BT, Betsubetsu). Bars indicate ± standard deviation (SD). Data denoted by the same letter (a, b; x, y, z) are not significantly different ($P > 0.05$) by one-way analysis of variance (ANOVA) or Tukey's honestly significant difference (HSD) test.

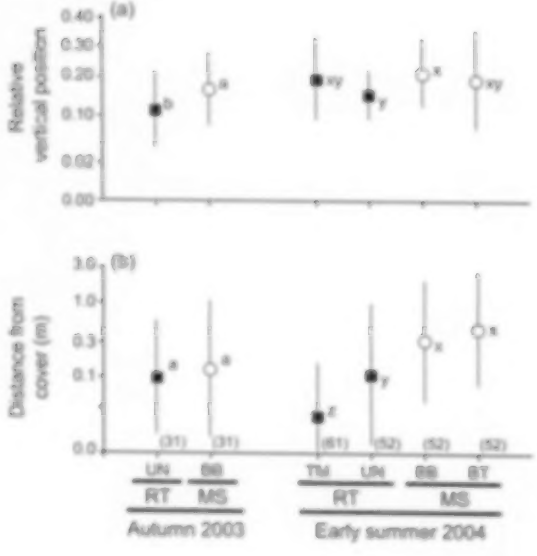

Discussion

Factors controlling invasion success

In our study area, the sites with and without rainbow trout were clearly separated by *W/B* ratio, with sites inhabited by rainbow trout having higher values. This result suggests that stable discharge favors establishment of rainbow trout populations, supporting the flow disturbance hypothesis by Fausch et al. (2001). Life history of rainbow trout is thought to adapt to flow regimes in their native range (Fausch et al. 2001). For example, in Pacific Coast of North America, where rainbow trout is native, flow regimes of streams are characterized by winter high flows and summer low flows (see Fausch et al. 2001; Light 2003), and spawning and emergence season of rainbow trout is from late winter to early summer, the period of declining flow (Fausch et al. 2001). This match decreases the risk of mortality caused by high flows at egg and fry stages. On the other hand, in our study area in Hokkaido, northern Japan, high flows occur in April–May by snowmelt and in August–October by rainfall (Kishi et al. 1999; Shibata et al. 2001). Therefore, high flows by snowmelt, coincident with the spawning and emergence period of rainbow trout in this area (Kitano et al. 1993; Taniguchi et al. 2000), have potential to limit establishment of their populations. In the eastern side of the study area, however, owing to the high water permeability of the soil, stream flow variability is low, which was expressed by a higher *W/B* ratio. For example, Shibata et al. (2001) reported the lack of snowmelt peak in the hydrograph of Horonai Stream, a typical spring-fed stream in the eastern side. Probably, such a moderate hydrological condition in the spawning and emergence period is an important factor allowing rainbow trout to establish their self-reproducing populations.

Presence or absence of rainbow trout was not related to masu salmon density, suggesting that biotic resistance from the native salmonid plays no role or a lesser role in controlling rainbow trout invasion. In general, where two species of stream salmonids exhibit complementary distributions (occurrences or abundances), interference competition often plays an important role (Fausch et al. 1994; Taniguchi and Nakano 2000; Rieman et al. 2006). Superiority in interference competition is largely determined by body size (e.g., Nakano 1995). In the case of competition between rainbow trout and masu salmon, the latter has a clear advantage over the former, because masu salmon fry emerge earlier than rainbow trout. This advantage allows masu salmon to have a great potential to prevent rainbow trout invasion. However, most masu salmon in Hokkaido are anadromous, staying in streams generally for only 1 year. Therefore, rainbow trout that survive 1 year can grow larger than masu salmon, resulting in a competitive advantage over masu salmon. An experimental study by Taniguchi et al. (2002) demonstrated that growth and survival of age-0 masu salmon were reduced by age-1 rainbow trout through aggressive interference and predation. Anadromy of masu salmon may be one reason why they cannot offer biotic resistance to rainbow trout invasion in our study area.

Fig. 8. Relative abundance of terrestrial prey and gammarids in the diet of rainbow trout (solid columns) and masu salmon (open columns) individuals in each sympatric site (HN, Horonai; KI, Koitoi). Results (P value) of Mann–Whitney U test comparing between the two species in each site are indicated in parentheses. An asterisk indicates statistically significant ($P < 0.05$).

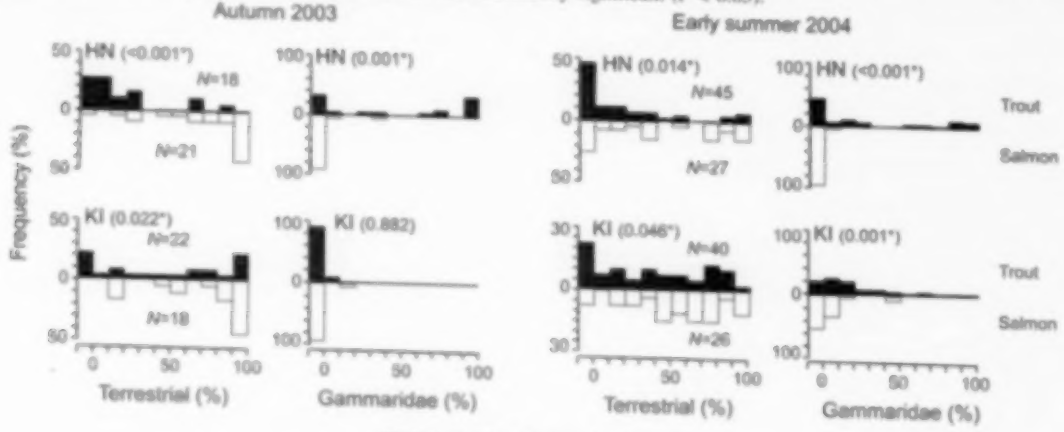

Fig. 9. Relative abundance of terrestrial prey and gammarids in the diet of rainbow trout (solid columns) and masu salmon (open columns) individuals in each allopatric site (TM, Tomakomai; UN, Uenae; BB, Bubbetsu; BT, Betsubetsu). Significant differences among the four sites based on Mann–Whitney U test after Kruskal–Wallis test are denoted by letters (a, b; x, y); sites denoted by the same letter are not significantly different at $P = 0.0083$ (= 0.05/6; Bonferroni correction).

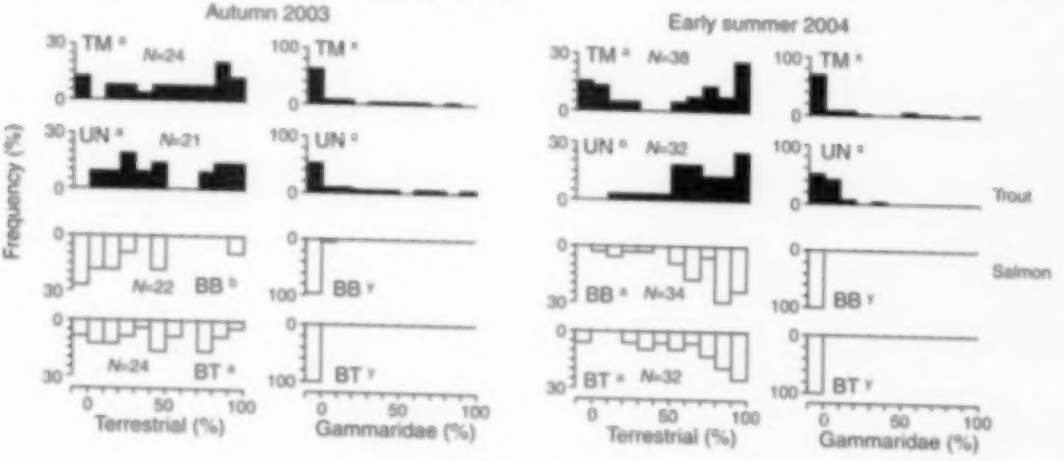

Importance of abiotic factors, rather than biotic interactions, in controlling invasion and its impacts has frequently been reported in other regions. For example, in New Zealand and Australia, both drought and spate are suggested to limit invasion of brown trout (*Salmo trutta*) and prevent them from eliminating native galaxiid fishes (Closs and Lake 1996; McIntosh 2000; Lepricur et al. 2006). In California, 5-year annual surveys of fishes in a regulated stream revealed that the abundance of non-native fishes decreased with increasing stream flow, suggesting flushing effects on non-native fishes (Marchetti and Moyle 2001). Such effects of high flows were reported also for non-native crayfish in other streams of California (Light 2003). Our results are consistent with these previous studies and the view that flow regime has a major role in controlling invasion success.

Interactions with native masu salmon

In our study area, masu salmon were distributed regardless of the presence of rainbow trout. This lack of complementary occurrences between the two species indicates that competitive exclusion is not likely to have occurred. However, the regression analysis on the abundance variations showed significant negative effects of each density on the other's. Previous studies have shown that masu salmon abundance is limited by the abundance of cover or pool in northern Hokkaido streams where other salmonids were rare (Inoue et al. 1997; Abe and Nakamura 1999; Abe 2007).

Similarly for rainbow trout, importance of pool and cover in determining their abundance has been shown in southern Hokkaido streams, where rainbow trout numerically dominated (Urabe and Nakano 1998, 1999). In the present study, however, the abundance variation of each species was explained by the density of the opponent, rather than such habitat factors, although the density of the two species combined was explained by cover abundance. These results suggest that rainbow trout and masu salmon have a competitive relationship with each other and share the same carrying capacity that increases with cover abundance. In other words, establishment of rainbow trout can decrease masu salmon abundance by forcing to share the capacity, although masu salmon is not likely inferior to rainbow trout in competitive interactions (see discussion below).

The habitat use and diet analyses in the sympatric sites describe resource partitioning between the two species. Major variables related to their habitat partitioning were vertical position and proximity to cover. Rainbow trout generally occupied positions closer to the bottom or cover than masu salmon. Further, the diet analysis showed that contribution of terrestrial prey to the diet of rainbow trout was lower than that of masu salmon. Instead, rainbow trout tended to consume gammarids. These results illustrate that in the sympatric sites, many individuals of rainbow trout occupied positions near the bottom or cover, foraging benthic prey, while the majority of masu salmon fed drifting prey at the middle layers of the water column. Although information on their interactions is limited, the pattern of their resource partitioning described here is largely consistent with existing data from a field study (Nakano and Kaeriyama 1995) and an experimental work (Hasegawa and Maekawa 2006). Nakano and Kaeriyama (1995) described distinct differences in diet between rainbow trout (juvenile steelhead) and masu salmon, with the former characterized by aquatic invertebrates of large body size (caddisfly larvae) and the latter by terrestrial invertebrates. They also reported higher selectivity for cover habitats by rainbow trout than by masu salmon. Furthermore, an experiment using an artificial channel showed that rainbow trout occupied lower vertical positions relative to masu salmon when they were in sympatry (Hasegawa and Maekawa 2006).

Although we also examined resource use by the two species in allopatry, it is difficult to clarify whether the habitat partitioning in sympatry is mediated by shift by either species. Results of interspecific comparisons of habitat use among the allopatric sites were equivocal, possibly owing to among-site differences in habitat conditions and food availability (Fig. 2). For example, in autumn 2003, vertical position of allopatric trout (in UN) was lower than that of allopatric salmon (in BB), suggesting that the vertical segregation in the sympatric site is due to species-specific habitat preference, rather than habitat shift by either species, whereas the data from 2004 showed that vertical position of allopatric rainbow trout in TM was as high as that of masu salmon in BB and BT. Despite such equivocality, our data suggest, at least, that masu salmon is unlikely to have shifted their resource use under the influence of rainbow trout. The pattern of resource partitioning we described is analogous to that between masu salmon and whitespotted charr (Nakano 1995; Miyasaka et al. 2003), where masu salmon are competitively dominant and do not shift their resource use (masu salmon occupy higher vertical positions than charr, feeding on drifting terrestrial prey). That is, higher vertical position is suitable for masu salmon. Therefore, the vertical segregation between masu salmon and rainbow trout in our sympatric sites suggests that masu salmon held their preferred position. This is supported by previous experiments showing that competitive ability of masu salmon in interference interactions was comparable to that of rainbow trout (Hasegawa et al. 2004), and rainbow trout did not elicit habitat shift by masu salmon (Hasegawa and Maekawa 2006).

In the experiment by Hasegawa and Maekawa (2006), vertical position of allopatric rainbow trout was lower than that of allopatric masu salmon, and they concluded that their vertical segregation in sympatry simply reflects a difference in species-specific habitat preference by each species. In addition, selective use of cover has often been reported for rainbow trout in allopatric situation (Gatz et al. 1987; Fausch 1993) and in streams where effects of other salmonids are negligible (Kitano et al. 1993; Urabe and Nakano 1999). Considering these previous studies, the habitat partitioning along vertical position and proximity to cover in our sympatric sites is also not likely attributable to habitat shift by rainbow trout. However, our analysis on stomach contents suggests a diet shift by rainbow trout in the sympatric sites. Contribution of terrestrial invertebrates to the diet of sympatric rainbow trout was relatively low, whereas that of allopatric rainbow trout was as high as that of both allopatric and sympatric masu salmon. Such differences in diet can be caused by differences in food availability, rather than by the presence of opponent species. For example, it is reported that stream salmonids shifted their foraging behavior from drift interception to benthic foraging when drifting prey abundance declined (Nakano et al. 1999*a*, 1999*b*). In our study, however, the difference in terrestrial prey contribution to rainbow trout diet between sympatric and allopatric situations cannot be explained by differences in drift availability. Drifting prey density in the sympatric sites (KI and HN) was not always lower than that in the allopatric sites (UN and TM). Rather, exceedingly high densities of drifting prey were recorded in a sympatric site (HN) where contribution of terrestrial prey to rainbow trout diet was lowest. Although rainbow trout is thought to feed primarily on drifting terrestrial prey (Nakano et al. 1999*c*; Baxter et al. 2007), these data were obtained from streams where effects of other salmonids were negligible (very low density of other salmonids or sympatry with competitively inferior species). Our results suggest that rainbow trout shift their resource use from drifting prey to benthic prey when they are sympatry with masu salmon. Although, in general, competitive effects on resource use cannot be fully elucidated by only comparative analyses as ours, our empirical data corroborate results of previous controlled experiments on interactions between rainbow trout and masu salmon (Hasegawa et al. 2004; Hasegawa and Maekawa 2006).

Management implications

Overall results of our study suggest that (*i*) flow regime has an important role in controlling success and failure of rainbow trout invasion, as hypothesized by Fausch et al. (2001), and (*ii*) masu salmon has competitive effects on

rainbow trout and vice versa, although native anadromous masu salmon cannot offer strong biotic resistance to rainbow trout invasion. Our results have important implications for habitat management, especially associated with dams. In general, natural flow regime is thought to favor native assemblages, and alterations of flow can facilitate invasions by non-natives (Poff et al. 1997; Marchetti and Moyle 2001). In regions where flow regimes are different from those in the native range of rainbow trout, altered flow may facilitate invasion by rainbow trout, which is otherwise suppressed by natural flow regimes. In addition, reservoirs created by dams may prevent rainbow trout that are flushed from inlet streams from being lost downstream. Therefore, dams may lead to the trout's higher invasibility (see also Marchetti et al. 2004). However, dams, as a flow-controlling device, are usable to prevent or mitigate invasion effects by manipulating discharge to mimic natural flow regimes. It is important to consider both negative and positive aspects of dams to seek better ways to manage non-natives and conserve native biota.

Acknowledgements

We are grateful to K.D. Fausch, C.V. Baxter, M. Murakami, and H. Urabe for useful suggestions during the fieldwork. We also thank the staff and graduate students, especially M. Miura, at the Tomakomai Research Station, Hokkaido University, for help in conducting the fieldwork. Critical and helpful comments from two reviewers and an editor greatly improved the manuscript. This research was planned on the basis of a preliminary survey on fish fauna in the Iburi District conducted by Y. Shibata, H. Miyasaka, H. Urabe, H. Onishi, Y. Taniguchi, Y. Kawaguchi, T. Saito, Y. Miyake, T. Iwata, D. Kishi, H. Saito, K. Murakami, and S. Nakano and was supported by a Grant-in-Aid for Scientific Research from the Japan Society for the Promotion of Science (No. 15770009).

References

Abe, T. 2007. Effects of riparian deforestation on habitat of juvenile masu salmon (*Oncorhynchus masou*) in a small watershed, northern Japan. J. Jpn. For. Soc. **89**(2): 85–91. [In Japanese with English abstract.] doi:10.4005/jjfs.89.85.

Abe, T., and Nakamura, F. 1999. Effects of experimental removal of woody debris on channel morphology and fish habitats. Ecol. Civil. Eng. **2**: 179–190. [In Japanese with English abstract.]

Aoyama, T., Takami, T., Fujiwara, M., and Kawamura, H. 1999. Natural reproduction of rainbow trout, *Oncorhynchus mykiss*, in the Shiribetsu River in Hokkaido, Japan. Sci. Rep. Hokkaido Fish. Hatchery, **53**: 29–38. [In Japanese with English abstract.]

Baxter, C.V., Fausch, K.D., Murakami, M., and Chapman, P.L. 2007. Invading rainbow trout usurp a terrestrial prey subsidy from native charr and reduce their growth and abundance. Oecologia (Berlin), **153**(2): 461–470. doi:10.1007/s00442-007-0743-x.

Brown, L.R., and Moyle, P.B. 1997. Invading species in the Eel River, California: successes, failures, and relationships with resident species. Environ. Biol. Fishes, **49**(3): 271–291. doi:10.1023/A:1007381027518.

Closs, G.P., and Lake, P.S. 1996. Drought, differential mortality and the coexistence of a native and an introduced fish species in a south east Australian intermittent stream. Environ. Biol. Fishes, **47**(1): 17–26. doi:10.1007/BF00002376.

Crowl, T.A., Townsend, C.R., and McIntosh, A.R. 1992. The impact of introduced brown and rainbow trout on native fish: the case of Australasia. Rev. Fish Biol. Fish. **2**(3): 217–241. doi:10.1007/BF00045038.

DeLury, D.B. 1951. On the planning of experiments for the estimation of fish populations. J. Fish. Res. Board Can. **8**: 281–307.

Fausch, K.D. 1988. Tests of competition between native and introduced salmonids in streams: what have we learned? Can. J. Fish. Aquat. Sci. **45**: 2238–2246. doi:10.1139/f88-260.

Fausch, K.D. 1993. Experimental analysis of microhabitat selection by juvenile steelhead (*Oncorhynchus mykiss*) and coho salmon (*O. kisutch*) in a British Columbia stream. Can. J. Fish. Aquat. Sci. **50**(6): 1198–1207. doi:10.1139/f93-136.

Fausch, K.D., Nakano, S., and Ishigaki, K. 1994. Distribution of two congeneric charrs in streams of Hokkaido Island, Japan: considering multiple factors across scales. Oecologia (Berlin), **100**(100): 1–12. doi:10.1007/BF00317124.

Fausch, K.D., Taniguchi, Y., Nakano, S., Grossman, G.D., and Townsend, C.R. 2001. Flood disturbance regimes influence rainbow trout invasion success among five holarctic regions. Ecol. Appl. **11**(5): 1438–1455. doi:10.1890/1051-0761(2001)011[1438:FDRIRT]2.0.CO;2.

Gatz, A.J., Jr., Sale, M.J., and Loar, J.M. 1987. Habitat shifts in rainbow trout: competitive influences of brown trout. Oecologia (Berlin), **74**(1): 7–19. doi:10.1007/BF00377339.

Gordon, N.D., McMahon, T.A., Gippel, C.J., and Nathan, R.J. 2004. Stream hydrology: an introduction for ecologists. 2nd ed. John Wiley & Sons, Ltd., Chichester, UK.

Hasegawa, K., and Maekawa, K. 2006. The effect of introduced salmonids on two native stream-dwelling salmonids through interspecific competition. J. Fish Biol. **68**(4): 1123–1132. doi:10.1111/j.0022-1112.2006.00997.x.

Hasegawa, K., Yamamoto, T., Murakami, M., and Maekawa, K. 2004. Comparison of competitive ability between native and introduced salmonids: evidence from pairwise contests. Ichthyol. Res. **51**(3): 191–194. doi:10.1007/s10228-004-0214-x.

Hayakawa, F., and Sato, I. 1978. Hydrological survey on rivers in the southeast of Lake Shikotsu, Hokkaido, Japan. Scientific Report of Geological Survey of Hokkaido, **50**: 109–132. [In Japanese with English abstract.]

Inoue, M., and Nakano, S. 1998. Effects of woody debris on the habitat of juvenile masu salmon (*Oncorhynchus masou*) in northern Japanese streams. Freshw. Biol. **40**(1): 1–16. doi:10.1046/j.1365-2427.1998.00346.x.

Inoue, M., Nakano, S., and Nakamura, F. 1997. Juvenile masu salmon (*Oncorhynchus masou*) abundance and stream habitat relationships in northern Japan. Can. J. Fish. Aquat. Sci. **54**(6): 1331–1341. doi:10.1139/cjfas-54-6-1331.

Kato, K., and Yanagawa, T. 2000. A reproductive population of rainbow trout introduced into the Sanjo River, western Japan. Suisanzoshoku, **48**: 603–608. [In Japanese with English abstract.]

Kawanabe, H. 1980. Rainbow trout: they fail to establish despite stocking. *In* Freshwater organisms in Japan: their ecology of invasion and disturbance. *Edited by* T. Kawai, H. Kawanabe, and N. Mizuno. Tokai University Press, Tokyo, Japan. pp. 44–48. [In Japanese.]

Kawanabe, H. 1989. Japanese char(r(r))s and masu-salmon problems: a review. Physiol. Ecol. Jpn. **1**: 13–24.

Kishi, C., Nakamura, F., and Inoue, M. 1999. Budgets and retention of leaf litter in Horonai Stream, southwestern Hokkaido, Japan. Jpn. J. Ecol. **49**: 11–20. [In Japanese with English abstract.]

Kitano, S. 2004. Ecological impacts of rainbow, brown and brook trout in Japanese inland waters. Glob. Environ. Res. **8**: 41–50.

Kitano, S., Nakano, S., Inoue, M., Shimoda, K., and Yamamoto, S. 1993. Feeding and reproductive ecology of exotic rainbow trout *Oncorhynchus mykiss* in the Horonai Stream in Hokkaido, northern Japan. Nippon Suisan Gakkai Shi, **59**: 1837–1843. [In Japanese with English abstract.]

Konishi, M., Nakano, S., and Iwata, T. 2001. Trophic cascading effects of predatory fish on leaf litter processing in a Japanese stream. Ecol. Res. **16**(3): 415–422. doi:10.1046/j.1440-1703.2001.00406.x.

Leprieur, F., Hickey, M.A., Arbuckle, C.J., Closs, G.P., Brosse, S., and Townsend, C.R. 2006. Hydrological disturbance benefits a native fish at the expense of an exotic fish. J. Appl. Ecol. **43**(5): 930–939. doi:10.1111/j.1365-2664.2006.01201.x.

Light, T. 2003. Success and failure in a lotic crayfish invasion: the roles of hydrologic variability and habitat alteration. Freshw. Biol. **48**(10): 1886–1897. doi:10.1046/j.1365-2427.2003.01122.x.

Marchetti, M.P., and Moyle, P.B. 2001. Effects of flow regime on fish assemblages in a regulated California stream. Ecol. Appl. **11**(2): 530–539. doi:10.1890/1051-0761(2001)011[0530:EOFROF]2.0.CO;2.

Marchetti, M.P., Light, T., Moyle, P.B., and Viers, J.H. 2004. Fish invasions in California watersheds: testing hypotheses using landscape patterns. Ecol. Appl. **14**(5): 1507–1525. doi:10.1890/03-5173.

McIntosh, A.R. 2000. Habitat- and size-related variations in exotic trout impacts on native galaxiid fishes in New Zealand streams. Can. J. Fish. Aquat. Sci. **57**(10): 2140–2151. doi:10.1139/cjfas-57-10-2140.

Miyasaka, H., Nakano, S., and Furukawa-Tanaka, T. 2003. Food habit divergence between white-spotted charr and masu salmon in Japanese mountain streams: circumstantial evidence for competition. Limnology, **4**(1): 1–10. doi:10.1007/s10201-002-0088-4.

Morita, K., Tsuboi, J., and Matsuda, H. 2004. The impact of exotic trout on native charr in a Japanese stream. J. Appl. Ecol. **41**(5): 962–972. doi:10.1111/j.0021-8901.2004.00927.x.

Nakano, S. 1995. Competitive interactions for foraging microhabitats in a size-structured interspecific dominance hierarchy of two sympatric stream salmonids in a natural habitat. Can. J. Zool. **73**(10): 1845–1854. doi:10.1139/z95-217.

Nakano, S., and Kaeriyama, M. 1995. Summer microhabitat use and diet of four sympatric stream-dwelling salmonids in a Kamchatkan stream. Fish. Sci. **61**: 926–930.

Nakano, S., Fausch, K.D., and Kitano, S. 1999*a*. Flexible niche partitioning via a foraging mode shift: a proposed mechanism for coexistence in stream-dwelling charrs. J. Anim. Ecol. **68**(6): 1079–1092. doi:10.1046/j.1365-2656.1999.00355.x.

Nakano, S., Miyasaka, H., and Kuhara, N. 1999*b*. Terrestrial–aquatic linkages: riparian arthropod inputs alter trophic cascades in a stream food web. Ecology, **80**: 2435–2441.

Nakano, S., Kawaguchi, Y., Taniguchi, Y., Miyasaka, H., Shibuta, Y., Urabe, H., and Kuhara, N. 1999*c*. Selective foraging on terrestrial invertebrates by rainbow trout in a forested headwater stream in northern Japan. Ecol. Res. **14**(4): 351–360. doi:10.1046/j.1440-1703.1999.00315.x.

Olden, J.D., Jackson, D.A., and Peres-Neto, P.R. 2002. Predictive models of fish species distributions: a note on proper validation and chance predictions. Trans. Am. Fish. Soc. **131**(2): 329–336. doi:10.1577/1548-8659(2002)131<0329:PMOFSD>2.0.CO;2.

Poff, N.L., Allan, J.D., Bain, M.B., Karr, J.R., Prestegaard, K.L., Richter, B.D., Sparks, R.E., and Stromberg, J.C. 1997. The natural flow regime. Bioscience, **47**(11): 769–784. doi:10.2307/1313099.

Rieman, B.E., Peterson, J.T., and Myers, D.L. 2006. Have brook trout (*Salvelinus fontinalis*) displaced bull trout (*Salvelinus confluentus*) along longitudinal gradients in central Idaho streams? Can. J. Fish. Aquat. Sci. **63**(1): 63–78. doi:10.1139/f05-206.

Shibuta, H., Mitsuhashi, H., Miyake, Y., and Nakano, S. 2001. Dissolved and particulate carbon dynamics in a cool-temperate forested basin in northern Japan. Hydrol. Process. **15**(10): 1817–1828. doi:10.1002/hyp.241.

Shirvell, C.S. 1990. Role of instream rootwads as juvenile coho salmon (*Oncorhynchus kisutch*) and steelhead trout (*O. mykiss*) cover habitat under varying streamflows. Can. J. Fish. Aquat. Sci. **47**(5): 852–861. doi:10.1139/f90-098.

Takami, T., and Aoyama, T. 1999. Distributions of rainbow and brown trouts in Hokkaido, northern Japan. Wildl. Conserv. Japan, **4**: 41–48. [In Japanese with English abstract.]

Taniguchi, Y., and Nakano, S. 2000. Condition-specific competition: implications for the altitudinal distribution of stream fishes. Ecology, **81**: 2027–2039.

Taniguchi, Y., Miyake, Y., Saito, T., Urabe, H., and Nakano, S. 2000. Redd superimposition by introduced rainbow trout, *Oncorhynchus mykiss*, on native charrs in a Japanese stream. Ichthyol. Res. **47**(2): 149–156. doi:10.1007/BF02684235.

Taniguchi, Y., Fausch, K.D., and Nakano, S. 2002. Size-structured interactions between native and introduced species: can intraguild predation facilitate invasion by stream salmonids? Biol. Invasions, **4**(3): 223–233. doi:10.1023/A:1020915416559.

Townsend, C.R. 2003. Individual, population, community, and ecosystem consequences of a fish invader in New Zealand streams. Conserv. Biol. **17**(1): 38–47. doi:10.1046/j.1523-1739.2003.02017.x.

Urabe, H., and Nakano, S. 1998. Contribution of woody debris to trout habitat modification in small streams in secondary deciduous forest, northern Japan. Ecol. Res. **13**(3): 335–345. doi:10.1046/j.1440-1703.1998.00273.x.

Urabe, H., and Nakano, S. 1999. Linking microhabitat availability and local density of rainbow trout in low-gradient Japanese streams. Ecol. Res. **14**(4): 341–349. doi:10.1046/j.1440-1703.1999.00311.x.

Weigel, D.E., Peterson, J.T., and Spruell, P. 2003. Introgressive hybridization between native cutthroat trout and introduced rainbow trout. Ecol. Appl. **13**(1): 38–50. doi:10.1890/1051-0761(2003)013[0038:IHBNCT]2.0.CO;2.

Phytoplankton productivity across prairie saline lakes of the Great Plains (USA): a step toward deciphering patterns through lake classification models

Courtney R. Salm, Jasmine E. Saros, Sherilyn C. Fritz, Christopher L. Osburn, and David M. Reineke

Abstract: We investigated patterns of primary production across prairie saline lakes in the central and northern Great Plains of the United States. Based on comparative lake sampling in 2004, seasonal predictors of algal primary productivity were identified within subsets of similar lakes using a combination of Akaike's information criterion (AIC) and classification and regression trees (CART). These models indicated complex patterns of nutrient limitation by nitrogen (N), phosphorus (P), and iron (Fe) within different lake groups. Nutrient enrichment assays (control, + Fe, + N, + P, + N + P) were performed in spring and summer of 2006 to determine if phytoplankton in selected lakes followed predicted patterns of nutrient limitation. Both the comparative lake sampling and experimental results indicated that N limitation was widespread in these prairie lakes, with evidence for secondary P limitation in certain lakes. In the experiments, iron did not stimulate primary production. Our results suggest that given the diverse geochemical nature of these lakes, classification models that separate saline lakes into subsets may be an effective method for improving predictions of algal production.

Résumé : Nous avons étudié les patrons de production primaire dans des lacs salés de prairie répartis dans le centre et le nord des Grandes Plaines des États-Unis. À partir d'un échantillonnage comparatif des lacs en 2004, nous avons identifié les variables prédictives saisonnières de la production primaire des algues dans des sous-ensembles de lacs en utilisant conjointement le critère d'information d'Akaike (AIC) et des arbres de classification et de régression (CART). Ces modèles identifient des patrons complexes de limitation par les nutriments d'azote (N), de phosphore (P) et de fer (Fe) dans les différents groupes de lacs. Nous avons fait des tests d'enrichissement de nutriments (témoin, + Fe, + N, + P, + N + P) au printemps et à l'été 2006 afin de déterminer si le phytoplancton dans les lacs sélectionnés suivait les patrons prédits de limitation par les nutriments. Tant l'échantillonnage comparatif des lacs que les résultats expérimentaux indiquent que la limitation par N est commune dans ces lacs de prairie, avec des indications d'une limitation secondaire par P dans certains lacs. Dans les expériences, le fer ne stimule pas la production primaire. Nos résultats indiquent qu'étant donné la nature géochimique diverse de ces lacs, les modèles de classification qui séparent les lacs salés en sous-ensembles peuvent être des méthodes efficaces pour améliorer les prédictions de production des algues.

[Traduit par la Rédaction]

Introduction

Prairie saline lakes are widely distributed across semi-arid regions of the world (Williams 1981) and are important habitats for migratory waterfowl and carbon sequestration (Batt et al. 1989; Euliss et al. 2006). Fossil algal records from these lakes are often used to reconstruct drought frequency and severity over time scales ranging from centuries to millennia (Cumming and Smol 1993; Laird et al. 1998; Fritz et al. 2000). However, although some of these lakes are limited by phosphorus or trace metals (Waiser and Robarts 1995; Evans and Prepas 1997), broad trends in the factors that control algal production across suites of these systems are not yet apparent (Bierhuizen and Prepas 1985; Campbell

Received 7 July 2008. Accepted 3 March 2009. Published on the NRC Research Press Web site at cjfas.nrc.ca on 20 August 2009. J20656

Paper handled by Associate Editor Yves Prairie.

C.R. Salm.[1,2] Department of Biology, University of Wisconsin – La Crosse, La Crosse, WI 54601, USA.
J.E. Saros. Climate Change Institute, University of Maine, Orono, ME 04469, USA.
S.C. Fritz. Department of Geosciences and School of Biological Sciences, University of Nebraska – Lincoln, Lincoln, NE 68588-0340, USA.
C.L. Osburn.[3] Marine Biogeochemistry Section, US Naval Research Laboratory, Washington, DC 20375, USA.
D.M. Reineke. Department of Mathematics, University of Wisconsin – La Crosse, La Crosse, WI 54601, USA.

[1]Corresponding author (e-mail: courtney.salm@umit.maine.edu).
[2]Present address: Climate Change Institute, 135 Sawyer Environmental Research Center, University of Maine, Orono, ME 04469, USA.
[3]Present address: Department of Marine, Earth, and Atmospheric Sciences, North Carolina State University, Raleigh, NC 27695, USA.

and Prepas 1986). Commonly, these lakes do not follow the paradigm established for freshwater lakes (Waiser and Robarts 1995) in which spring total phosphorus (TP) concentrations predict summer chlorophyll *a* (Chl *a*) concentrations (Dillon and Rigler 1974; Smith 1979). In prairie saline lakes, TP concentrations are often greater than 50 $\mu g \cdot L^{-1}$, and total nitrogen (TN) concentrations can exceed 1000 $\mu g \cdot L^{-1}$ (Campbell and Prepas 1986). Despite these high concentrations of nutrients, the algal biomass is lower than predicted based on freshwater models (Campbell and Prepas 1986; Robarts et al. 1992; Evans and Prepas 1997).

Several factors may account for the poor performance of the freshwater spring TP – summer Chl *a* model in saline lakes. Although total nutrient concentrations are high, a substantial fraction of the nutrients may not be bioavailable (Waiser and Robarts 1995), particularly because concentrations of dissolved organic material (DOM) are very high in these lakes, ranging from 20 to 800 mg $C \cdot L^{-1}$ (measured as dissolved organic carbon (DOC); Curtis and Adams 1995; Evans and Prepas 1997; Arts et al. 2000). DOM can complex with nutrients and alter their bioavailability (Hessen and Tranvik 1998; Bushaw-Newton and Moran 1999; Findlay and Sinsabaugh 2003). In addition, the ionic composition and high salinity of saline lakes affects nutrient cycling and availability, as well as uptake by algae (Caraco et al. 1989; Waiser and Robarts 1995; Saros and Fritz 2000). Chlorophyll concentrations may be affected by intense zooplankton grazing on standing phytoplankton crops in saline lakes (Anderson 1958), and limited information is available on rates of primary production rather than chlorophyll concentrations alone (Armstrong et al. 1966; Hammer 1981). These conditions suggest that measuring total and dissolved nutrient pools may not provide enough information to discern the factors that drive algal production in these lakes; physiological parameters of algal production and nutrient status may be more useful in clarifying any patterns (Waiser and Robarts 1995).

An additional factor that may hinder the development of a predictive model of phytoplankton production in saline lakes is the assumption that one model and one variable can have sufficient explanatory power to model phytoplankton response in these chemically complex systems. Unlike marine systems, the dominant ions in saline lakes vary extensively (Fritz et al. 1993; Gosselin 1997), and the cycling of phosphorus and nitrogen can differ greatly, for example, between bicarbonate- and sulfate-dominated systems (Cole et al. 1986; Caraco et al. 1989). These differences suggest the need to develop a classification system to separate these diverse lakes into subsets based on similar characteristics. Lake classification has been used for a variety of applications, from assessing trophic state to managing water quality (Emmons et al. 1999; Søndergaard et al. 2005; Bulley et al. 2007).

We examined patterns of primary production in phytoplankton across a suite of lakes in the central and northern Great Plains of the United States in the spring and summer of 2004. In addition to measuring environmental parameters, physiological methods were used to assess the nutrient status of phytoplankton by measuring alkaline phosphatase activity and seston nutrient ratios. Rather than employing chlorophyll measurements alone as in other studies, we directly measured phytoplankton primary production across all lakes via ^{14}C uptake rates. Subsequently, we tested the model predictions from the survey data in Cubitainer experiments in a set of lakes in the spring and summer of 2006.

Materials and methods

Study sites

Prairie saline (>3 $g \cdot L^{-1}$) and subsaline (0.5–3 $g \cdot L^{-1}$) lakes included in this study are located in the central (Nebraska) and northern (North Dakota, South Dakota, and Montana) Great Plains (CGP and NGP, respectively) (Fig. 1). On average, the Great Plains are characterized as semi-arid with a negative effective moisture balance (precipitation minus evapotranspiration, $P - E$). Land-use patterns vary across the region and include primarily cropland, rangeland, and undisturbed native grassland.

In the NGP, thousands of lakes occur east of the Missouri River; most of these are morainal depressions or dammed river valleys formed upon retreat of the Pleistocene ice margin (Bluemle and Clayton 1984). In eastern and central North Dakota and South Dakota, the majority of saline lakes are sulfate-dominated as a result of the widespread presence of pyrite in bedrock and surface deposits (Fritz et al. 1993). Major cation concentrations and proportions are highly variable. A smaller number of lakes are found in the glaciated regions of northeastern Montana – northwestern North Dakota immediately north of the Missouri River. The majority is in paleochannels of the Missouri River system and is dominated by carbonates because of inflow from shallow groundwater systems in calcareous outwash and till (Donovan 1994).

Lakes are also widespread in the Nebraska Sandhills of the CGP, a large region of Holocene eolian sands overlying Pleistocene and late-Tertiary alluvial sands and silts, which is the principal recharge area of the High Plains (Ogallala) Aquifer. Here lakes are formed by deflation and blockage of interdune valleys by eolian sands, and most lakes are thought to have formed during dry intervals during the Holocene (Loope et al. 1995; Mason et al. 1997). The majority of lakes is dominated by bicarbonate, although a small number of sulfate-enriched lakes occur. Sodium and potassium are the most abundant cations (LaBaugh 1986; Gosselin 1997).

Lakes across the NGP and CGP are topographically closed, but many are hydrologically connected to groundwater. Salinities range from 0.1 to greater than 100 $g \cdot L^{-1}$ (note that for simplicity, we use the term "prairie saline lakes" to refer to the entire group of lakes, recognizing that technically some of the lakes are subsaline). Lakes were selected to maximize variation in conductivity, ion composition, and nutrient concentrations. In the spring, these lakes were primarily dominated by diatoms (largely *Fragilaria crotonensis* and *Cyclotella quillensis/meneghiniana*) with some cyanobacteria (*Gloeocapsa* sp. and *Aphanocapsa* sp.). In the summer, cyanobacteria dominated the phytoplankton assemblages (*Aphanizomenon* sp. and *Aphanocapsa* sp.) with some diatoms (*Cyclotella quillensis* and *Surirella* sp.) (Salm et al. 2009).

Fig. 1. Map of central Great Plains, USA. Ellipses indicate study sites for the 2004 survey. NGP, northern Great Plains; CGP, central Great Plains.

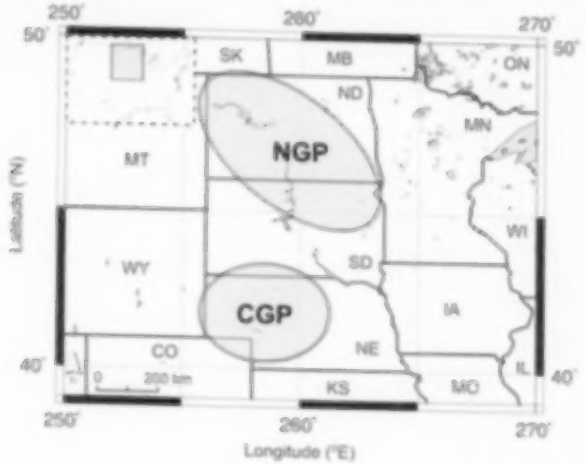

Lake sampling and model development

Data collection

Data for approximately 30 parameters were collected for lakes across the study area in both spring (24 lakes) and summer (30 lakes), including temperature, conductivity, pH, total alkalinity, ion composition, Chl *a*, nutrients (total, particulate, and dissolved), DOM characteristics, alkaline phosphatase activity (APA), and rates of primary production. For these analyses, approximately 10 L of lake water were collected with a van Dorn horizontal bottle from a depth of 1 m in lakes that were at least 2 m deep and from the midpoint of the water column in lakes that were <1 m deep.

Temperature and conductivity were measured with a portable conductivity meter (WTW MultiLine P4); pH was measured with a pH meter (Corning); and total alkalinity was determined by titration (American Public Health Association (APHA) 1998). Cations were measured via atomic absorption spectroscopy (Varian 220FS with a GTA-110 graphite furnace and a VGA-77 vapor generation unit), and anions were measured by ion chromatography (Dionex ICS-90).

In the field, whole water samples were collected for total P and total N and acidified with H_2SO_4. Samples for total dissolved P, soluble reactive P, nitrate + nitrite, and dissolved Si were filtered through 0.45 μm Millipore membrane filters. Samples for total P, dissolved P, and particulate P were first digested with potassium persulfate and measured by ascorbic acid methods (Lind 1985; APHA 1998), as were those for soluble reactive P. Total N was measured by alkaline potassium persulfate digestion (D'Elia et al. 1977) and the ultraviolet (UV) absorption method (APHA 1998), and nitrate + nitrite N was determined by the hydrazine reduction method (Downes 1978). Dissolved Si was measured following the methods of Wetzel and Likens (1991). Water was also filtered through 0.7 μm glass-fiber filters (Whatmann GF/F) for analysis of Chl *a*, as well as particulate carbon and nitrogen analyses (in duplicate). Filters were collected onto Petri dishes and either wrapped in foil and frozen (Chl *a*) or refrigerated (particulate C and N) until processing. Chlorophyll was analyzed spectrophotometrically after pigment extraction with 90% acetone (Varian Cary-50 UV-VIS Spectrophotometer; APHA 1998) within two weeks of collection to maintain sample integrity. Filters for particulate C and N were fumed with concentrated HCl in a glass desiccator and measured by combustion and gas chromatography with an elemental analyzer (Costech).

Dissolved iron was quantified in samples that were filtered through 0.45 μm Millipore membrane filters and acidified at the time of collection. Total recoverable iron was determined on separate acidified samples prepared by mixing unfiltered lake water with hydrochloric acid and nitric acid to improve the solubility of iron during digestion. Samples were covered and digested overnight (~12 h) at 90 °C on a hotplate and diluted in 1% nitric acid prior to analysis. Samples for total and dissolved iron were analyzed with an inductively coupled plasma mass spectrometer (GV Instruments Platform XS). Total iron was quantified based on the response of ^{56}Fe. Potential interferences were monitored in samples and blanks fortified with these elements, and Indium was added to all samples and standards to monitor for additional matrix effects. The method detection limit was 1.0 ppb.

Samples for DOM characterization were prefiltered through 0.2 μm pore-size membranes before analysis. DOC concentration (mg C·L^{-1}) was measured by wet chemical oxidation on an OI Analytical 1010 TOC analyzer, following the recommendations of Osburn and St. Jean (2007) for high-salinity samples. Sodium persulfate (450 g·L^{-1}; cleaned by heating to a near-boil and then rapidly cooling) was added to the reactor and allowed to react for 10 min, converting all DOC to CO_2. The CO_2 was quantified by nondispersive IR detection and calibrated to potassium biphthalate standards over the range of 1–100 mg C·L^{-1}. Sample volumes of 100–2000 μL were injected to stay within this calibration range.

Absorption of water samples was measured from 250 to 650 nm on a dual-beam spectrophotometer (Shimadzu UV1601) against Milli-Q water in 1 cm cuvets due to the strong absorbance of these samples. Raw absorbance was converted to absorption coefficients:

$$a(\lambda) = A(\lambda) \times 2.303/D$$

where $A(\lambda)$ is the raw absorbance of the sample at wavelength λ, and D is the pathlength of the 1 cm cuvet (in metres) (Kirk 1994). The constant of 2.303 converts from the natural logarithm. The ratio of absorption at 250–365 nm has been used to observe relative changes in molecular weight of DOC (De Haan and De Boer 1987). An increase in the ratio indicates a decrease in molecular weight.

Bulk alkaline phosphatase activity was measured in the field with the 4-methylumbelliferyl phosphate method (Hill et al. 1968) on a field fluorometer (Turner Designs Model 10-AU Field Fluorometer). Bulk APA:Chl *a* ratios were used to normalize enzyme activity to the amount of algal biomass.

Rates of primary productivity in each lake were assessed using a modified light–dark bottle ^{14}C uptake assay (Wetzel and Likens 1991). Bottles (300 mL) were incubated under a

suspended light bank (Freshwater AquaLight by Coralife, ~450 $\mu E \cdot cm^{-2} \cdot s^{-1}$) in a water bath held at a temperature consistent with ambient seasonal lake conditions (2004: spring, 15 °C; summer, 20 °C). We chose this approach, rather than in situ incubations in each lake, to maintain similar light and temperature conditions across all lakes. Bottles were filled with lake water prescreened through 212 μm Nitex mesh to remove large grazers. During the summer, when colonial cyanobacteria populations were present in lakes, prefiltering was not possible for some lakes. In these instances, grazers were handpicked from bottles with a pipette. Each bottle was inoculated with 0.5–2.0 mL $NaH^{14}CO_3$ solution (Perkin Elmer, 1 $\mu Ci \cdot mL^{-1}$) and incubated onshore for 3 h at some point between 0900 and 1500 h (within the diurnal period of maximum algal productivity). After incubation, two aliquots (the size of which depended on algal densities) were collected from each bottle on 0.45 μm Millipore HA filters, which were dried in a desiccator overnight and stored in a cool, dry location until processing in the laboratory. Filters were fumed with concentrated HCl in a glass desiccator to remove residual inorganic ^{14}C and carbonates. They were dissolved in 10 mL of Filter-Count scintillation cocktail (Perkin Elmer) and read on a scintillation counter (Beckman Coulter LS 6500; 32 768 channels with 0.06 keV per channel resolution), with primary production rates calculated according to Wetzel and Likens (1991).

Data analysis

Values for all variables except pH, seston ratios, and $a_{250}:a_{365}$ were $\log_{10}$-transformed to correct for unequal variance after Levene's homogeneity of variance test, and simple and stepwise multiple regression were used to identify predictors of primary production ($\alpha = 0.05$). In addition to these methods, Akaike's information criterion (AIC; Burnham and Anderson 2002) was used to explore how multiple factors may control primary production across all lakes in the data set. Although a priori hypotheses are strongly suggested when using AIC, in cases such as this when it is difficult to formulate reasonable a priori models, AIC may be used in conjunction with secondary studies to confirm important predictor variables (Burnham and Anderson 2002). A program for running AIC analyses in SAS (version 9.1; SAS Institute Inc., Cary, North Carolina) was written by Episystems, Inc. (St. Paul, Minnesota) and used to analyze the spring and summer comparative lake sampling data. The best set of approximating models was found from a larger set of candidate models by selecting those with the lowest AIC. It has been suggested that models for which the AIC value is within 4 units of the lowest would constitute an approximate 95% confidence set of top models (Burnham and Anderson 2002); thus this criterion was used to determine which models were retained, parameter weights, and model-averaged parameter estimates.

Exploratory classification models also were developed with classification and regression trees (CARTs; De'ath and Fabricius 2000) using the program R (version 2.1.1; http://www.r-project.org/), with the rate of primary production as the predictor variable for regression trees and phosphorus limitation status (severely limited or not limited) as the predictor variable for classification trees. An APA : Chl *a* value above 0.005 is considered indicative of severe P limitation (Healey and Hendzel 1980); hence this was used as the dividing value between lakes that were potentially P-limited (APA : Chl $a > 0.005$) or not (APA : Chl $a \leq 0.005$). Simple regressions were then performed in SPSS (version 11.5 for Windows; SPSS Inc., Chicago, Illinois) to identify parameters controlling primary production within each of the resulting groups.

Experiments and model testing

Experimental design

Using the groups identified in the CART analyses (see Results below), nutrient enrichment experiments were conducted in spring and summer 2006 as a test of these models. Assays were similar in spring and summer, with five treatments created with the following additions: control (no nutrient addition), Fe, N, P, and N + P ($n = 3$). For the spring and summer experiments, a subset of two or three lakes was chosen from within each group identified by the CART analyses. Water from each lake was filtered through a 212 μm mesh to remove large zooplankton and incubated in 4 L Cubitainers (VWR TraceClean™ Cubitainer™ containers, made of low-density polyethylene) in Coldwater Lake at approximately 0.5 m depth in the spring (15 °C) and just below the surface in the summer (20 °C). Appropriate iron (11.7 μmol $Fe \cdot L^{-1}$ in the form of $FeCl_3 \cdot 6H_2O$, added along with 11.7 μmol $EDTA \cdot L^{-1}$), nitrogen (18 μmol $N \cdot L^{-1}$ in the form of $NaNO_3$), and phosphorus (5 μmol $P \cdot L^{-1}$ in the form of NaH_2PO_4) additions were made to each Cubitainer. Transmission scans of Cubitainer plastic on a spectrophotometer (Varian Cary-50 UV-VIS Spectrophotometer) indicated that for the visible spectrum, approximately 60%–75% of ambient light was allowed through the plastic, whereas at lower wavelengths (~300 nm), 40%–50% of ambient light was allowed through. For each Cubitainer, rates of primary production (^{14}C uptake assay) were measured initially and 3 days after nutrient additions, because preliminary laboratory experiments indicated that, based on daily measurements over a 7-day period, the greatest changes in production rates occurred on day 3 (data not shown). One light bottle was analyzed for each Cubitainer, and two dark-bottle replicates were analyzed for each lake. The dark-bottle replicates were taken from a random control Cubitainer and a random N + P Cubitainer for each lake to assess whether the higher biomass in nutrient addition treatments affected the ^{14}C measurements. Previous use of this method during the comparative lake sampling in 2004 showed very little variation among dark-bottle replicates.

Data analysis

Results from these experiments were statistically analyzed using analysis of variance (ANOVA) in SPSS (version 11.5 for Windows; SPSS Inc., Chicago, Illinois) to determine if rates of primary production were significantly different among treatments ($\alpha = 0.05$). Levene's homogeneity of variance test was used to check for equal variances, and rates of primary production were $\log_{10}$-transformed to correct for unequal variances. Tukey's post-hoc analysis was also used to compare mean values across treatments.

Results

Lake sampling and model development

Rates of primary production were generally higher across lakes in summer compared with spring (Table 1). Regional differences among lakes also were evident, as CGP lakes had much higher rates of productivity than those of the NGP based on the ^{14}C uptake assays (spring average rates of primary productivity: CGP, 263.4 mg $C \cdot m^{-3} \cdot h^{-1}$; NGP, 33.0 mg $C \cdot m^{-3} \cdot h^{-1}$; summer average rates: CGP, 526.5 mg $C \cdot m^{-3} \cdot h^{-1}$; NGP, 124.9 mg $C \cdot m^{-3} \cdot h^{-1}$). CGP lakes had high concentrations of nutrients and DOC and were shallow (<1 m) and very turbid, making filtration difficult (only possible to filter 1–2 mL at most through 0.45 µm filters). Some of these systems dried out in the summer, preventing parallel seasonal studies. Given these difficulties with the CGP lakes, we examined patterns in the full data set of lakes, as well as the subset of lakes ($n = 18$) found in the NGP alone.

Simple regressions between rates of primary production and key nutrients did not indicate strong limitation by a single nutrient (Table 2), with the exception of NO_3^- for all lakes in the spring ($R^2 = 0.519$, $F = 28.08$, df = 1,22, $p < 0.001$). Other low R^2 but significant simple regressions with nutrient parameters included total P ($R^2 = 0.306$, $F = 9.718$, df = 1,22, $p = 0.005$) and total N ($R^2 = 0.202$, $F = 5.561$, df = 1,22, $p < 0.028$) for all lakes in the spring, total P ($R^2 = 0.316$, $F = 12.951$, df = 1,28, $p < 0.001$) and total N ($R^2 = 0.168$, $F = 5.634$, df = 1,28, $p = 0.025$) for all lakes in the summer, and total N ($R^2 = 0.238$, $F = 4.985$, df = 1,16, $p = 0.040$) for NGP lakes only.

Multiple regressions revealed variable predictors of primary production by season and region. For the spring, NO_3^- was the only variable selected by stepwise regression for all lakes ($R^2 = 0.519$, $F = 22.66$, df = 1,21, $p < 0.001$), with a positive relationship between this parameter and primary production rates. This relationship was not found for the subset of NGP lakes alone, in which no variables were significant predictors of primary production. In the summer, stepwise selection indicated C:P and dissolved Fe as the best predictors for all lakes ($R^2 = 0.606$, $F = 20.75$, df = 1,28, $p < 0.001$), and absorptivity at 350 nm (indicative of chromophoric dissolved organic matter) for NGP lakes alone ($R^2 = 0.311$, $F = 7.23$, df = 1,16, $p = 0.016$). These parameters were positively correlated to rates of primary production.

AIC models were developed separately for spring and summer; within each season, models for all lakes, as well as just the NGP lakes, were generated (Table 3). All of the models suggested multivariate control over primary production across these lakes. Each model also identified one or two of the strongest variables (with a predictor weight close to or equal to 1) correlated with rates of primary production. Looking across the variables with the highest predictor weights, the AIC approach identified dissolved Fe and NO_3^- as the best predictors of primary production in spring for all lakes, and calcium, dissolved Fe, and TP for the NGP lakes subset. In the summer, the best predictors for all lakes were C:P and ions (Cl^-, K^+, Na^+), and phosphorus parameters (TP, N:P, and SRP) for the NGP lakes. Thus, results indicated that the limiting factors for rates of primary production differed regionally as well as seasonally.

In the CART analyses, spring regression trees showed a split, with NO_3^- as the only branching variable (Fig. 2). This separation appeared to be related to geographic distribution, as high nitrate lakes ($[NO_3^-] > 17.5$ µg·L^{-1}) were located in the CGP and low nitrate lakes ($[NO_3^-] < 17.5$ µg·L^{-1}) were located in the NGP. Classification further split the NGP lakes by APA:Chl *a* ratio. Within the three groups delineated in Fig. 2, simple regressions did not yield any significant predictor variables for rates of primary production at the $\alpha = 0.05$ level. However, regressions for high NO_3^- lakes from the CGP showed a positive correlation between primary production and maximum depth ($R^2 = 0.5000$, $F = 4.01$, df = 1,4, $p = 0.12$), which may be a reflection of the very high turbidity and greater potential light limitation in the shallower lakes of the CGP. Low NO_3^-, low APA:Chl *a* lakes (designated SPR-N to reflect potential N limitation) showed a positive correlation between primary production and N:P ratios ($R^2 = 0.3623$, $F = 3.41$, df = 1,6, $p = 0.11$), and low NO_3^-, high APA:Chl *a* lakes (designated SPR-NP to reflect potential N and P co-limitation) showed a positive correlation between primary production and unfiltered APA rates ($R^2 = 0.3323$, $F = 3.98$, df = 1,8, $p = 0.08$) such that lakes in this subset with higher APA rates were more productive.

Summer regression trees showed a split with C:P seston ratios (Fig. 3). The high C:P group (C:P > 3591) contained most of the highly productive CGP lakes, whereas the group with lower C:P values (C:P < 3591) had lower rates of primary production on average and included NGP lakes and the remainder of the CGP lakes. The split was at an extremely high C:P ratio, outside of typical ranges for seston ratios for freshwater lakes (Elser et al. 2000; Sterner and Elser 2002), and generally follows geographic distribution as in the spring. When CGP lakes were excluded from the regression tree, there were no branches within the NGP lakes. These data suggested that phosphorus gradients were involved in controlling primary production during the summer, so APA:Chl *a* classification trees were used again for the NGP lakes alone. The main branching factor in this subset of lakes was soluble reactive P (SRP), with a branch point of 25 µg·L^{-1}. Simple regressions for the higher SRP group (designated SUM-N) showed a positive correlation between primary production rates and N:P ratios ($R^2 = 0.38$, $F = 5.55$, df = 1,9, $p = 0.043$). The regression for the lower SRP group (designated SUM-P) between rate of primary production and total P was significant ($R^2 = 0.78$, $F = 17.5$, df = 1,5, $p = 0.009$).

Spring experimental results

For the spring experiment, three lakes were selected from the SPR-NP group (Alkaline Lake, Coldwater Lake, and Free People Lake), as well as two from the SPR-N group (East Devils Lake and Stink Lake). The nutrient treatments affected primary production rates in four of the five lakes tested (Fig. 4; Table 4). Of the SPR-NP lakes predicted to respond to both N and P, rates in Alkaline Lake ($F = 30.6$, df = 4,10, $p < 0.001$) and Coldwater Lake ($F = 75.6$, df = 4,10, $p < 0.001$) increased in the N treatment, with additional increases in the N + P treatments. Free People Lake

Table 1. Summary of 2004 spring and summer survey data used in analyses.

Parameter	Units	All lakes	CGP only	NGP only
Spring				
Primary production rate	mg C·m^{-2}·h^{-1}	91 (4–452)	263 (138–452)	33 (4–102)
Chl *a*	μg·L^{-1}	76 (1–1066)	225 (2–1066)	10 (1–22)
Z_{max}	m	4.1 (1.0–13.0)	1.6 (1–2.5)	5.1 (1.0–13.0)
Temperature	°C	15 (9–22)	18 (16–22)	13 (9–17)
pH		9.04 (7.94–10.43)	9.61 (8.89–10.43)	8.79 (7.94–9.42)
Total alkalinity	mg $CaCO_3$·L^{-1}	4150 (200–54100)	11795 (300–54100)	752 (200–2030)
DOC	mg·L^{-1}	32 (18–82)	—	32 (18–82)
Total P	μg·L^{-1}	1269 (19–15860)	3863 (243–15860)	116 (19–273)
Total dissolved P	μg·L^{-1}	762 (14–10866)	2276 (47–10866)	89 (14–242)
Soluble reactive P	μg·L^{-1}	454 (3–5816)	1345 (18–5816)	57 (3–199)
Total N	μg·L^{-1}	5145 (587–23297)	12380 (997–23297)	1930 (587–4379)
Nitrate + nitrite	μg·L^{-1}	31 (1–147)	83 (69–147)	8 (1–18)
Dissolved Si	μg·L^{-1}	14 (0.2–93)	43 (7–93)	1 (0.2–2.5)
Total Fe	μg·L^{-1}	737 (39–8584)	2308 (141–8584)	126 (39–574)
Dissolved Fe	μg·L^{-1}	41 (3–289)	82 (13–289)	22 (4–88)
C:N		9.6 (6.1–15.1)	—	9.6 (6.1–15.1)
C:P		231 (79–579)	—	231 (79–579)
N:P		24 (11–41)	—	24 (11–41)
APA:Chl *a*		0.0484 (0.0000–0.8044)	—	0.0484 (0.0000–0.8044)
Conductivity	mS·cm^{-1}	9.86 (0.58–72.81)	18.24 (0.58–72.81)	6.13 (1.39–16.20)
Ca^{2+}	mg·L^{-1}	59 (4–338)	32 (4–127)	69 (7–338)
Mg^{2+}	mg·L^{-1}	179 (0–1729)	18 (0–65)	242 (31–1729)
Na^{+}	mg·L^{-1}	1657 (72–17569)	4123 (72–17569)	698 (101–2034)
K^{+}	mg·L^{-1}	567 (14–5528)	1842 (30–5528)	71 (14–188)
Cl^{-}	mg·L^{-1}	419 (11–4422)	788 (11–4422)	255 (18–931)
SO_4^{2-}	mg·L^{-1}	2017 (8–10842)	1186 (8–6138)	2386 (193–10842)
Filtered APA rate	nmol·L^{-1} MUP·h^{-1}	76.9 (0.0–417.0)	—	76.9 (0.0–278.0)
Unfiltered APA rate	nmol·L^{-1} MUP·h^{-1}	31.8 (17.6–82.2)	—	31.8 (17.6–82.2)
a_{350}	m^{-1}	23 (2–124)	69 (25–124)	8 (2–13)
a_{250}:a_{365}		24 (11–71)	30 (14–71)	22 (11–45)
Summer				
Primary production rate	mg C·m^{-2}·h^{-1}	286 (11–1747)	527 (11–1747)	125 (15–544)
Chl *a*	μg·L^{-1}	118 (3–1613)	237 (3–1613)	39 (6–197)
Z_{max}	m	3.7 (1.0–13.0)	1.6 (1.0–2.6)	5.1 (1.0–13.0)
Temperature	°C	19 (15–24)	20 (18–24)	18 (15–23)
pH		9.36 (8.41–10.66)	9.91 (8.88–10.66)	9.00 (8.41–10.14)
Total alkalinity	mg $CaCO_3$·L^{-1}	3725 (190–38000)	8121 (231–38000)	794 (190–2550)
DOC	mg·L^{-1}	161 (14–1512)	358 (48–1512)	29 (14–91)
Total P	μg·L^{-1}	4922 (25–71622)	12087 (89–71622)	145 (25–329)
Total dissolved P	μg·L^{-1}	810 (11–12328)	1873 (19–12328)	102 (11–315)
Soluble reactive P	μg·L^{-1}	475 (7–5874)	1085 (7–5874)	68 (7–271)
Total N	μg·L^{-1}	6042 (708–23020)	11246 (1689–23020)	2573 (708–3500)
Nitrate + nitrite	μg·L^{-1}	8 (0–55)	11 (0–55)	5 (1–18)
Dissolved Si	μg·L^{-1}	23 (1–156)	43 (2–156)	9 (1–26)
Total Fe	μg·L^{-1}	452 (24–4119)	925 (24–4119)	136 (24–516)
Dissolved Fe	μg·L^{-1}	31 (0–190)	26 (0–112)	34 (3–190)
C:N		12.2 (6.3–33.6)	17.2 (8.5–33.6)	8.9 (6.3–18.7)
C:P		2008 (131–8803)	4581 (432–8803)	292 (131–1000)
N:P		129 (16–705)	273 (52–705)	32 (16–53)
APA:Chl *a*		0.0761 (0.00002–0.9667)	0.1264 (0.00002–0.9667)	0.0426 (0.00002–0.3309)
Conductivity	mS·cm^{-1}	10.39 (0.53–82.10)	16.30 (0.53–82.10)	6.45 (1.51–16.60)
Ca^{2+}	mg·L^{-1}	45 (4–350)	11 (4–22.1)	67 (5–350)
Mg^{2+}	mg·L^{-1}	168 (0–1889)	20 (0–62)	266 (32–1889)
Na^{+}	mg·L^{-1}	1753 (74–21073)	3088 (74–21073)	862 (101–2716)
K^{+}	mg·L^{-1}	743 (15–7954)	1728 (35–7954)	86 (15–268)
Cl^{-}	mg·L^{-1}	473 (13–6394)	861 (13–6394)	235 (17–876)
SO_4^{2-}	mg·L^{-1}	2223 (5–12728)	1459 (5–9176)	2690 (231–12728)
Filtered APA rate	nmol·L^{-1} MUP·h^{-1}	2180.1 (2.5–58734.1)	5267.0 (2.5–58734.1)	122.1 (2.8–904.8)
Unfiltered APA rate	nmol·L^{-1} MUP·h^{-1}	4083.1 (5.8–98604.5)	8979.0 (6.8–98604.5)	819.1 (5.8–9848.1)
a_{350}	m^{-1}	20 (2–79)	38 (11–79)	8 (2–22)
a_{250}:a_{365}		26 (11–87)	37 (14–87)	20 (11–38)

Note: Values are expressed as mean with range in parentheses. Seston ratios are reported on a molar basis. CGP, central Great Plains; NGP, northern Great Plains; —, parameter not measured for these sites. APA, alkaline phosphatase activity; MUP, 4-methylumbelliferyl phosphate; a_{250}, a_{350}, and a_{365}, absorptivity at 250 , 350, and 365 nm, respectively.

Table 2. R^2 values for simple regressions of rates of primary productivity versus selected nutrient parameters.

	Spring		Summer	
Parameter	All lakes	NGP only	All lakes	NGP only
Total P	0.306*	0.034	0.316*	0.198
Dissolved P	0.072	0.095	0.011	0.099
SRP	0.030	0.150	0.062	0.055
Total N	0.202*	0.008	0.168*	0.238*
Nitrate + nitrite	0.561*	0.103	0.077	0.001

Note: NGP, northern Great Plains; SRP, soluble reactive phosphorus.

*$p < 0.05$

Table 3. ΔAIC_c values describe model fit, with smaller values indicating better fit: (*a*) summary of primary productivity models developed with Akaike's information criterion (AIC) for 2004 survey data; (*b*) summary of top predictor variables from AIC models of 2004 survey data.

(*a*) Summary of primary productivity models developed with AIC for 2004 survey data.

Model	Model predictors	ΔAIC_c	w	K	R^2
Spring – all lakes (44)*	log NO_3 (+), C:N (+), log DFE (–), log a_{750}/a_{665} (–)	0.00	0.086	4	0.795
	log NO_3 (+), C:N (+), log DFE (–)	0.72	0.060	3	0.756
Spring – NGP lakes only (3)*	log Ca (–), log SO_4 (–), log TN (+), log DFE (–)	1.01	0.052	4	0.786
	log Cond (–), log Ca (–), log TP (+), log DFE (–)	0.00	0.652	4	0.753
	log Alk (–), log Ca (–), log TP (+), log DFE (–)	2.40	0.196	4	0.717
Summer – all lakes (58)*	log Ca (–), log SO_4 (–), log TP (+), log DFE (–)	2.91	0.152	4	0.709
	log Na (–), log Cl (+), C:P (+), log DFE (+)	0.00	0.060	4	0.715
	Temp (–), log Na (–), log Cl (+), C:P (+)	0.03	0.059	4	0.714
	log K (–), log TP (+), C:P (+), log DFE (+)	0.17	0.055	4	0.713
Summer – NGP lakes only (17)*	log TP (+), log SRP (–), NP (+), log DFE (+)	0.00	0.202	4	0.730
	log TP (+), log SRP (–), NP (+), log TFE (+)	0.65	0.147	4	0.720
	log TP (+), log SRP (–), NP (+)	1.45	0.098	3	0.636

(*b*) Summary of top predictor variables from AIC models of 2004 survey data.

				95% CI	
Group	Predictor	Predictor weights	Model-averaged regression coefficient	Lower	Upper
Spring – all lakes	log DFE	0.94	–0.794	–1.239	–0.349
	log NO_3	0.81	0.916	0.444	1.387
	C:N	0.39	0.071	0.004	0.138
	log SO_4	0.25	–0.348	–0.708	0.012
Spring – NGP lakes only	log Ca	1.00	–1.318	–2.253	–0.382
	log DFE	1.00	–0.901	–1.283	–0.520
	log TP	1.00	1.699	0.916	2.482
	log Cond	0.65	–1.124	–1.628	–0.620
Summer – all lakes	C:P	1.00	0.00015	0.00009	0.00021
	log Cl	0.57	0.458	0.151	0.766
	log K	0.53	–0.485	–0.792	–0.178
	log Na	0.47	–0.604	–0.948	–0.261
Summer – NGP lakes only	log TP	0.69	2.440	1.216	3.665
	N:P	0.68	0.018	0.005	0.031
	log SRP	0.62	–1.338	–2.201	–0.476

Note: Akaike weights, denoted as w, describe the probability that the model is the best model generated, and K is the number of estimable parameters in the model. Predictor weights indicate the predictive strength of the variable, with values near 1 having the strongest predictive weight. Asterisk (*) indicates the number of models with $\Delta AIC_c < 4$, which were used to compute the Akaike weights. CI, confidence interval; DFE, dissolved Fe; TN, total N; Cond, conductivity; TP, total P; Alk, alkalinity; Temp, temperature; SRP, soluble reactive phosphorus; TFE, total Fe.

only responded to the N treatment ($F = 81.3$, df = 4,10, $p < 0.001$), with no additional increase in the combination treatment of N + P. It should be noted, however, that Free People Lake was classified as a SPR-NP lake based on 2004 data, but in 2006, the APA:Chl *a* ratio was below 0.005, moving it to the SPR-N group (Table 5). For the SPR-N group, predicted to respond to N alone, the rate of production only increased in East Devil's Lake in the N addition

Fig. 2. Lake classification for spring 2004 survey data. Nitrate, shown at the top of the figure, was identified as the main splitting variable based on an initial regression tree with primary production as the response metric. On the lower left portion of the figure, NGP lakes were further examined for P limitation with APA:Chl *a* ratios identified as the splitting variable based on a classification tree with P-limitation category (no P limitation or severe limitation) as the response variable. Simple regressions were performed within each subset of lakes, although no regressions were statistically significant ($\alpha = 0.05$). Abbreviations: CGP, central Great Plains; NGP, northern Great Plains; SPR-N, potentially N-limited lakes; SPR-NP, potentially N and P co-limited lakes.

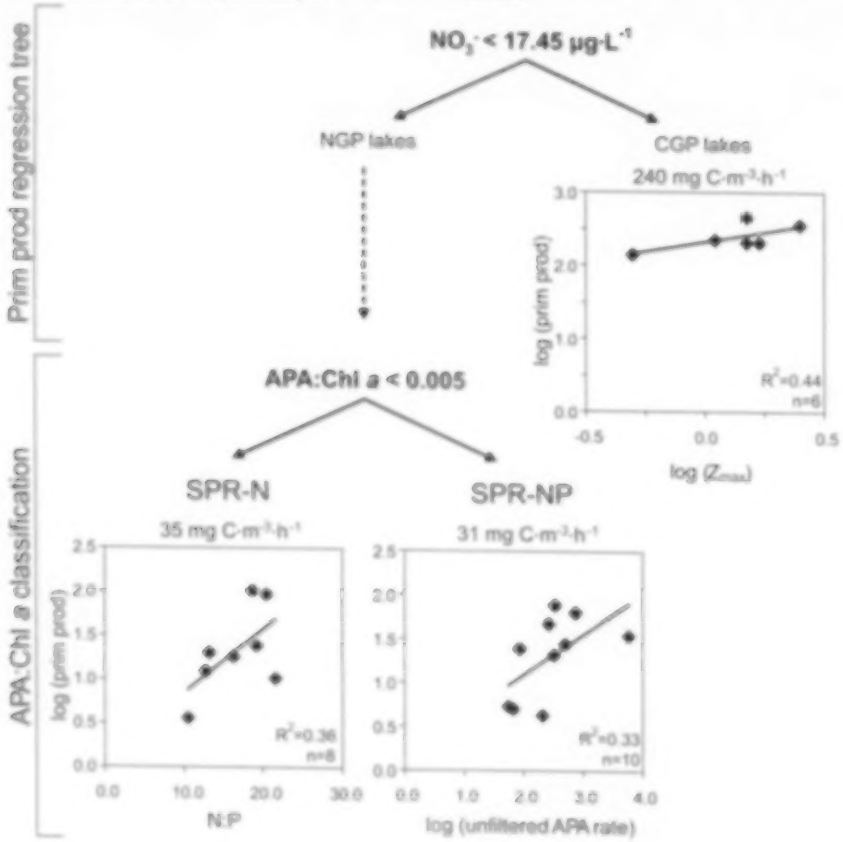

($F = 96.5$, df = 4,10, $p < 0.001$). Although there were significant differences across all treatments for Stink Lake ($F = 3.54$, df = 4,10, $p = 0.048$), differences were not large enough for Tukey's post-hoc test to identify homogeneous subsets. There appeared to be a bottle effect for this lake, with a substantial increase in production rates in all treatments compared with the initial values (for example, *669* mg C·m^{-3}·h^{-1} in the control compared with the initial value of 31.5 mg C·m^{-3}·h^{-1}).

Summer experimental results

For the summer experiment, three lakes were tested from each of the SUM-N (Alkaline Lake, East Devil's Lake, and Stink Lake) and SUM-P (Clear Lake, Coldwater Lake, and George Lake) groups. Rates of primary production differed among nutrient treatments in five of the six lakes (Fig. 5; Table 4). Of the SUM-N lakes predicted to respond to N, production rates in East Devil's Lake increased in response to the N addition ($F = 25.4$, df = 4,10, $p < 0.001$). In Alkaline Lake, rates increased in both the N treatment and the P treatment ($F = 80.9$, df = 4,10, $p < 0.001$), with even higher production rates in the N + P combination. Interannual differences may have also been important in Alkaline Lake, as this lake was originally classified in the SUM-N group based on 2004 data (Table 5). In the summer of 2006, however, the SRP concentration was undetectable (0.010 µg·L^{-1} detection limit), changing its classification to SUM-P. There were no significant differences in production rates for Stink Lake ($F = 1.329$, df = 4,10, $p = 0.325$) due to apparent bottle effects for this lake, as in the spring experiments. Control treatment production rates were elevated compared with the initial samples (167 mg C·m^{-3}·h^{-1} in the control versus an initial rate of 23.1 mg C·m^{-3}·h^{-1}). In the SUM-P lakes, predicted to be P-limited, Clear Lake had the highest production rates in the P treatment ($F = 26.3$, df = 4,10, $p < 0.001$), with no additional response to the N + P treatment. Production rates in Coldwater ($F = 195.9$, df = 4,10, $p < 0.001$) and George ($F = 92.0$, df = 4,10, $p < 0.001$) lakes both increased in the N addition, along with a significant increase in the N + P addition.

Fig. 3. Lake classification for summer 2004 survey data. C:P ratios, at the top of the figure, were identified as the main splitting variable based on an initial regression tree with primary production as the response metric. On the upper right, high C:P lakes from the CGP region showed a nonsignificant relationship between production and NO_3^- ($p = 0.073$, $y = 0.281x + 2.636$, df = 1,5, $F = 5.12$). On the lower left of the figure, lakes from the NGP region were further examined for P limitation with a classification tree with APA:Chl *a* class (no P limitation or severe limitation) as the response metric. Simple regressions were performed within each subset of lakes. The regressions were statistically significant for the SUM-N ($p = 0.043$, $y = 0.0246x + 1.219$, df = 1,9, $F = 5.55$) and SUM-P ($p = 0.009$, $y = 1.063x - 0.194$, df = 1,5, $F = 17.5$) groups. Abbreviations: CGP, central Great Plains; NGP, northern Great Plains; SUM-N, potentially N-limited lakes; SUM-P, potentially P-limited lakes.

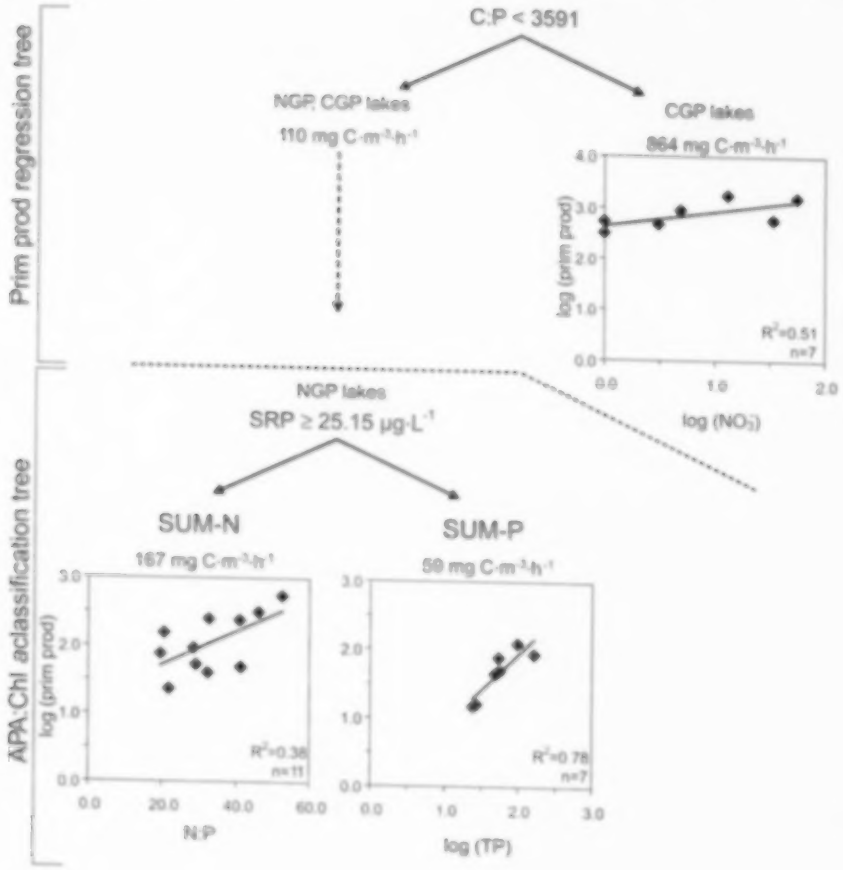

Discussion

Although previous studies of algal production in saline lakes have been able to identify limitation patterns within a few systems (Bierhuizen and Prepas 1985; Campbell and Prepas 1986; Waiser and Robarts 1995), our study investigated drivers of primary production by phytoplankton across a diverse set of saline lakes. The combination of predictive modeling and experimental tests allowed us to begin to delineate subsets of lakes and determine limitation patterns within them. The models and experiments presented here indicate that despite the high total nitrogen and phosphorus concentrations in these lakes, phytoplankton in these lakes are potentially nutrient-limited. Though many freshwater lakes are often phosphorus-limited (Dillon and Rigler 1974; Wetzel 2001), our results reveal widespread nitrogen limitation across these prairie saline lakes. A subset of these lakes is also secondarily limited by P, as indicated by high APA:Chl *a* ratios and large additional increases in algal production in the experimental N + P treatments. Although there is evidence for nitrogen limitation in single saline systems (Reuter et al. 1993), our study provides information on nutrient limitation patterns across a large region in central North America with a high density of subsaline and saline lakes. These data support observations that nitrogen may play a larger and more widespread role in nutrient limitation patterns in lake ecosystems than previously thought (Smith 1982; Elser et al. 1990; Lewis and Wurtsbaugh 2008).

Multiple statistical techniques enabled us to begin to discern these productivity patterns in prairie saline lakes, and results from these various methods were generally in agree-

Fig. 4. The results from a nutrient enrichment bioassay for spring rates of primary production that experimentally tested the lake classification groups: (*a*) SPR-NP and (*b*) SPR-N. Abbreviations: Alk, Alkaline Lake; CW, Coldwater Lake; FP, Free People Lake; ED, East Devil's Lake; Stk, Stink Lake; Prim prod, rate of primary production.

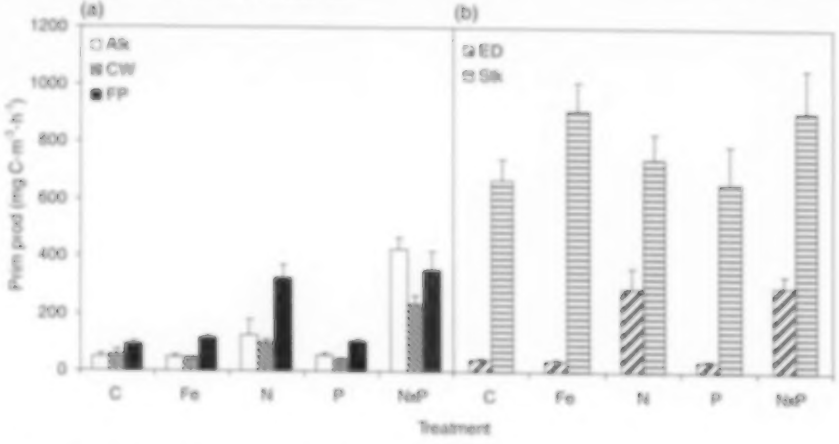

Table 4. Summary of Tukey's post-hoc analyses for spring and summer 2006 experiments.

	Spring					Summer					
Treatment	Alk*	CW*	FP*	ED*	Stk†	Alk*	ED*	Stk‡	Clear*	CW*	Grg*
C	1	1	1	1	—	1	1	—	1	1	1
Fe	1	1	1	1	—	1, 2	1	—	1	1	1
P	1, 2	1	1	1	—	2	1	—	2	1	1
N	2	2	2	2	—	2	2	—	1	2	2
N + P	3	3	2	2	—	3	2	—	2	3	3

Note: Numbers in columns indicate treatments within each lake with responses that are significantly different from each other ($\alpha = 0.05$). Nutrient treatments: C, control; Fe, Fe addition; P, P addition; N, N addition; N + P, combined N and P additions. Lake abbreviations: Alk, Alkaline Lake; CW, Coldwater Lake; FP, Free Peoples Lake; ED, East Devil's Lake; Stk, Stink Lake; Clear, Clear Lake; Grg, George Lake.

*$p < 0.001$ for analysis of variance.

†$p = 0.044$ for analysis of variance, but post-hoc analysis did not detect different subsets of lakes.

‡$p = 0.325$ for analysis of variance. Post-hoc analysis was not performed on these data.

Table 5. Summary of changes in classification groups from 2004 to 2006.

	Survey class	
Lake	2004	2006
Spring		
East Devil's	SPR-N	SPR-N
Stink	SPR-N	SPR-N
Free Peoples	SPR-NP	*SPR-N*
Alkaline	SPR-NP	SPR-NP
Coldwater	SPR-NP	SPR-NP
Summer		
East Devil's	SUM-N	SUM-N
Stink	SUM-N	SUM-N
Alkaline	SUM-N	*SUM-P*
Coldwater	SUM-P	SUM-P
George	SUM-P	SUM-P
Clear	SUM-P	SUM-P

Note: Lakes given in italic type indicate changed from predicted 2004 classification based on 2006 data.

ment. Simple and multiple regressions identified some potential limiting factors (such as NO_3^- in the spring for all lakes), but did not suggest singular seasonal controls across the entire suite of lakes. In addition, with covariation among some key parameters in these systems (e.g., correlations between log TN and log TP were $R^2 = 0.88$ in spring and $R^2 = 0.64$ in summer), it was not possible to identify whether one or both nutrients were actually limiting. Therefore, using additional statistical techniques, we developed more complex models to decipher drivers of productivity patterns across these diverse systems. AIC revealed a complex multivariate story of predictors of primary production, identifying several different predictive models and varying parameter weights. The CART analyses identified a similar group of variables to those from regressions and AIC but produced a simplified hierarchical ordering of these variables and thus served as a useful exploratory tool for examining broad trends across an ecologically complicated data set, as suggested by De'ath and Fabricius (2000). We recognize that the sample size for this study was relatively small, particularly after separating the lakes into subsets, and that more lakes would strengthen these models. However, even with a small sample size, the

Fig. 5. The results from a nutrient enrichment bioassay for summer rates of primary production that experimentally tested the lake classification groups: (*a*) SUM-N and (*b*) SUM-P. Abbreviations: Alk, Alkaline Lake; ED, East Devil's Lake; Stk, Stink Lake; Clear, Clear Lake; CW, Coldwater Lake; Grg, George Lake; Prim prod, rate of primary production.

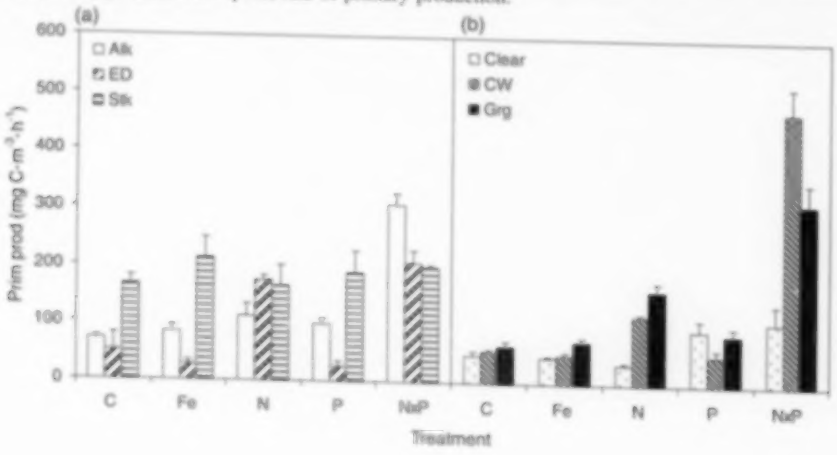

CART models helped to clarify trends within lake groups. Classifications developed from key variables identified with these techniques were easily tested via experiments in 2006. In the spring, the CART models correctly predicted N limitation in the SPR-N and SPR-NP lakes and secondary P limitation in the SPR-NP lakes. In the summer, lakes in the SUM-N group responded to N as predicted, except for one lake that changed classification groups in 2006 and was co-limited by N and P. We predicted an increase in production in P treatments in the SUM-P lakes, and although there was a response to P, two of the three lakes were mainly limited by N and secondarily by P. Despite this misidentification and generally small sample size, the CART models as a whole enabled us to identify limitation patterns across prairie saline lakes more clearly than in prior studies.

Although ambient nutrient concentrations were high, experimental nutrient additions stimulated primary production by phytoplankton. One explanation for this is the reduced bioavailability of nutrients in these lakes due to complexation with DOM (Hessen and Tranvik 1998; Findlay and Sinsabaugh 2003). As direct measurements of nutrient concentrations did not predict rates of primary production, physiological indicators of nutrient limitation were very important to the success of the lake classification system, with APA:Chl *a* serving as a reliable tool in discerning patterns of phosphorus limitation among the lakes. Unfortunately, a similarly reliable indicator of nitrogen limitation in these lakes is not apparent. Although N_2-fixation rates and heterocyst formation can indicate nitrogen limitation for cyanobacteria, few heterocysts were found in phytoplankton samples from the 2004 sampling (personal observation). C:N ratios of particulate material can be indicative of nitrogen limitation in other aquatic systems, with low C:N ratios suggesting that algae are nitrogen replete (Wetzel 2001); however, C:N ratios never emerged as significant in our analyses. Furthermore, in many lakes that responded positively to N additions, initial seston C:N values were low (many <9), which clearly did not reflect the physiological status of the algae. This observation, in conjunction with the extremely high seston C:P ratios in these lakes, raises the question of what these C ratios really reflect in these high DOM lakes. The development of additional physiological metrics would greatly improve our ability to assess N limitation patterns in these prairie lakes.

Our results indicate broad nitrogen limitation in lakes across this semi-arid region; other studies have also found N limitation in single saline lakes (Cloern et al. 1983; Herbst and Bradley 1989; Reuter et al. 1993). Terrestrial sources of nitrogen may be less abundant in grasslands than in forested areas, as humid grasslands tend to be nitrogen-limited with low soil N availability (Wedin 1995). These systems may be further driven to N limitation by various feedbacks, as dry conditions in grasslands slow N mineralization rates of already low quality (high C:N) litter (Wedin 1995). Other important feedbacks to consider in these prairie ecosystems include grazing and fire effects, as grazing tends to recycle N (Holland et al.1992) and fire tends to volatilize N (Ojima et al. 1994). In contrast to wetter temperate regions, reduced precipitation in grasslands can also decrease nutrient inputs from terrestrial runoff.

Nitrogen limitation in prairie saline lakes may also be caused by different physical and chemical conditions in these systems, which lead to N loss from the system and P release from sediments. Physically, lakes in the CGP and NGP tend to be shallow and turbulent, and the resulting variable mixing patterns could lead to alternating aerobic and anaerobic conditions at the lake bottom. These varying conditions allow for high rates of denitrification, a common pathway for nitrogen loss in shallow systems (Jensen and Andersen 1990). Though aerobic conditions typically cause P to precipitate out of the water column due to binding with Fe, turbulence also resuspends sediment and may cause overall P release if conditions vary between aerobic and anaerobic (Søndergaard et al. 1992). Chemically, Fe–P binding is reduced at high pH (Lijklema 1977), and all study lakes had pH greater than 8.3. There is also evidence for al-

tered P cycling under high sulfate concentrations, as the sulfate tends to bind Fe and thereby reduce Fe–P binding (Caraco et al. 1989; Curtis 1989). Saline lakes, particularly those in the NGP, can have high sulfate concentrations, and although ion concentrations did not directly correlate with primary production rates, sulfate may indirectly influence nutrient availability in these systems.

Although Fe was a top predictor variable for primary production in AIC and multiple regression models, the CART analyses did not identify Fe as important, and there was little evidence for Fe limitation in experimental results. In the spring experiments, a *Chroococcus* sp. in Stink Lake did increase substantially in biovolume in the Fe treatment (personal observation), suggesting that Fe was biologically available for uptake in this lake and season. Our results show that limitation by two or possibly more nutrients could be very important in controlling production in prairie lakes, and previous studies have indicated the potential of Fe and other trace metals (Marino et al. 1990; Evans and Prepas 1997) to act as limiting factors in prairie saline lakes. Future studies should consider the effects of not only single nutrient additions, but also those of combination treatments as well.

Lakes in the CGP were generally more productive than those of the NGP and, in the spring, had higher nitrate concentrations. Precipitation gradients are similar in both regions, but the higher N and hence productivity of the CGP lakes may be due to the higher temperatures in this region, which could increase terrestrial N mineralization rates, as well as N_2 fixation rates by cyanobacteria (Macarelli and Wurtsbaugh 2006; Scott et al. 2008). Land-use patterns also differ across these two regions, with the CGP serving as cattle rangeland and the NGP largely serving as arable agricultural land, some of which has been abandoned during recent decades. These differences in land use, as well as local geology as described above, may contribute to the higher productivity levels in the CGP lakes.

Shallow lakes and wetlands in prairie regions provide important ecosystem services, including carbon sequestration, wildlife habitat, and recreation (Batt et al. 1989; Euliss et al. 2006). These ecosystem services all involve algal production and standing crops, and hence a greater understanding of the factors that control primary production across these lakes is a critical aspect for ensuring the sustainability of these services. Our analyses suggest that patterns of primary production in prairie saline lakes of the central and northern Great Plains were complex. Although no trends were consistent across all saline lakes, likely due to geochemical and physical differences among these varied systems, exploratory classification models generally were successful in identifying productivity patterns within lake subsets. Nitrogen limitation was widespread in these systems, especially in spring, along with secondary limitation by phosphorus in some cases. The CART exploratory classification technique shows promise for determining primary production patterns across a complicated data set, and the resultant classification could be refined with a larger data set as well as with better physiological tools to assess limitation by nitrogen and possibly other nutrients. Prairie saline lakes are globally important systems, and thus, understanding the ecology of these complex systems is an essential component of a more comprehensive understanding of lake ecosystem function and structure.

Acknowledgements

We thank Danuta Bennett, Jessica Czubakowski, Carmen Daggett, Jarvis Erickson, Margaret Henke, Callie Martin, Brian McMullen, Caren Scott, Robert Toban, and Erin Wilcox for field and laboratory assistance. The Water Sciences Laboratory at the University of Nebraska – Lincoln conducted the iron, anion, and total nutrient analyses; we thank the director, Daniel D. Snow, for assistance with selection of appropriate analytical techniques. John Holz and Tad Barrow provided advice on lake selection in the CGP, as well as nutrient analyses and field assistance, and Leigh Stearns provided the map of study locations. We thank three anonymous reviewers for their helpful comments, which greatly improved this manuscript. This work was funded by the National Science Foundation (DEB-0315665). Additional funding was provided by a University of Wisconsin – La Crosse Graduate Research Grant and the River Studies Center (University of Wisconsin – La Crosse).

References

American Public Health Association. 1998. Standard methods for the examination of water and wastewater. 20th ed. APHA, Washington, D.C.

Anderson, G.C. 1958. Seasonal characteristics of two saline lakes in Washington. Limnol. Oceanogr. **3**: 51–68.

Armstrong, R., Anderson, D., and Callender, E. 1966. Primary productivity measurements at Devil's Lake, North Dakota. North Dakota Academy of Science, **20**: 136–149.

Arts, M.T., Roberts, R.D., Kasai, F., Waiser, M.J., Tumber, V.P., Plante, A.J., Rai, H., and de Lange, H.J. 2000. The attenuation of ultraviolet radiation in high dissolved organic carbon waters of wetlands and lakes on the northern Great Plains. Limnol. Oceanogr. **45**: 292–299.

Batt, B.D., Anderson, M.G., Anderson, C.D., and Caswell, F.D. 1989. The use of prairie potholes by North American ducks. *In* Northern prairie wetlands. *Edited by* A.G. van der Valk. Iowa State Press, Ames, Iowa. pp. 204–227.

Bierhuizen, J.F.H., and Prepas, E.E. 1985. Relationship between nutrients, dominant ions, and phytoplankton standing crop in prairie saline lakes. Can. J. Fish. Aquat. Sci. **42**: 1588–1594. doi:10.1139/f85-199.

Bluemle, J.P., and Clayton, L. 1984. Large-scale glacial thrusting and related processes in North Dakota. Boreas, **13**: 279–299.

Bulley, H.N.N., Merchant, J.W., Marx, D.B., Holz, J.C., and Holz, A.A. 2007. A GIS approach to watershed classification for Nebraska reservoirs. J. Am. Water Resour. Assoc. **43**(3): 605–621. doi:10.1111/j.1752-1688.2007.00048.x.

Burnham, K.P., and Anderson, D.R. 2002. Model selection and multimodel inference: a practical information-theoretic approach. Springer, New York.

Bushaw-Newton, K.L., and Moran, M.A. 1999. Photochemical formation of biologically available nitrogen from dissolved humic substances in coastal marine systems. Aquat. Microb. Ecol. **18**: 285–292. doi:10.3354/ame018285.

Campbell, C.E., and Prepas, E.E. 1986. Evaluation of factors related to the unusually low chlorophyll levels in prairie saline lakes. Can. J. Fish. Aquat. Sci. **43**: 846–854. doi:10.1139/f86-104.

Caraco, N.F., Cole, J.J., and Likens, G.E. 1989. Evidence for

sulphate-controlled phosphorus release from sediments of aquatic systems. Nature (London), **341**(6240): 316–318. doi:10.1038/341316a0.

Cloern, J.E., Cole, B.E., and Oremland, R.S. 1983. Seasonal changes in the chemistry and biology of a meromictic lake (Big Soda Lake, Nevada, U.S.A.). Hydrobiologia, **105**(1): 195–206. doi:10.1007/BF00025188.

Cole, J.J., Howarth, R.W., Nolan, S.S., and Marino, R. 1986. Sulfate inhibition of molybdate assimilation by planktonic algae and bacteria: some implications for the aquatic nitrogen cycle. Biogeochemistry, **2**(2): 179–196. doi:10.1007/BF02180194.

Cumming, B.F., and Smol, J.P. 1993. Development of diatom-based salinity models for paleoclimatic research from lakes in British Columbia (Canada). Hydrobiologia, **269/270**(1): 179–196. doi:10.1007/BF00028017.

Curtis, P.J. 1989. Effects of hydrogen ion and sulphate on the phosphorus cycle of a Precambrian Shield Lake. Nature (London), **337**(6203): 156–158. doi:10.1038/337156a0.

Curtis, P.J., and Adams, H.E. 1995. Dissolved organic matter quantity and quality from freshwater and saltwater lakes in east-central Alberta. Biogeochemistry, **30**(1): 59–76. doi:10.1007/BF02181040.

D'Elia, C.F., Studler, P.A., and Corwin, N. 1977. Determination of total nitrogen in aqueous samples using persulfate digestion. Limnol. Oceanogr. **22**: 760–764.

De Haan, H., and De Boer, T. 1987. Applicability of light absorbance and fluorescence as measures of concentration and molecular size of dissolved organic carbon in humic Lake Tjeukemeer. Water Res. **21**(6): 731–734. doi:10.1016/0043-1354(87)90086-8.

De'ath, G., and Fabricius, K.E. 2000. Classification and regression trees: a powerful yet simple technique for ecological data analysis. Ecology, **81**: 3178–3192.

Dillon, P.J., and Rigler, F.H. 1974. The phosphorus–chlorophyll relationship in lakes. Limnol. Oceanogr. **19**: 767–773.

Donovan, J.J. 1994. On the measurement of reactive mass fluxes in evaporative groundwater-source lakes. *In* Sedimentology and geochemistry of modern and ancient saline lakes. *Edited by* R.W. Renaut and W.M. Last. Society for Sedimentary Geology, Tulsa, Oklahoma. pp. 33–50.

Downes, M.T. 1978. An improved hydrazine reduction method for the automated determination of low nitrate levels in freshwater. Water Resour. **12**(9): 673–675. doi:10.1016/0043-1354(78)90177-X.

Elser, J.J., Marzolf, E.R., and Goldman, C.R. 1990. Phosphorus and nitrogen limitation of phytoplankton growth in freshwaters of North America: a review and critique of experimental enrichments. Can. J. Fish. Aquat. Sci. **47**: 1468–1477. doi:10.1139/f90-165.

Elser, J.J., Fagan, W.F., Denno, R.F., Dobberfuhl, D.R., Folarin, A., Huberty, A., Interlandi, S., Kilham, S.S., McCauley, E., Schulz, K.L., Siemann, E.H., and Sterner, R.W. 2000. Nutritional constraints in terrestrial and freshwater food webs. Nature (London), **408**(6812): 578–580. doi:10.1038/35046058. PMID: 11117743.

Emmons, E.E., Jennings, M.J., and Edwards, C. 1999. An alternative classification method for northern Wisconsin lakes. Can. J. Fish. Aquat. Sci. **56**(4): 661–669. doi:10.1139/cjfas-56-4-661.

Euliss, N.H., Jr., Gleason, R.A., Olness, A., McDougal, R.L., Murkin, H.R., Roberts, R.D., Bourbonniere, R.A., and Warner, B.G. 2006. North American prairie wetlands are important nonforested carbon storage sites. Sci. Total Environ. **369**: 179–188.

Evans, J.C., and Prepas, E.E. 1997. Relative importance of iron and molybdenum in restricting phytoplankton biomass in high phosphorus saline lakes. Limnol. Oceanogr. **42**: 461–472.

Findlay, S.E.G., and Sinsabaugh, R.L. (*Editors*). 2003. Aquatic ecosystems: interactivity of dissolved organic matter. Academic Press, San Diego, Calif.

Fritz, S.C., Juggins, S., and Battarbee, R.W. 1993. Diatom assemblages and ionic characterization of lakes of the northern Great Plains, North America: a tool for reconstructing past salinity and climate fluctuations. Can. J. Fish. Aquat. Sci. **50**(9): 1844–1856. doi:10.1139/f93-207.

Fritz, S.C., Ito, E., Yu, Z., Laird, K.R., and Engstrom, D.R. 2000. Hydrologic variation in the northern Great Plains during the last two millenia. Quat. Res. **53**(2): 175–184. doi:10.1006/qres.1999.2115.

Gosselin, D.C. 1997. Major-ion chemistry of compositionally diverse lakes, western Nebraska, U.S.A.: implications for paleoclimatic interpretations. J. Paleolimnol. **17**(1): 33–49. doi:10.1023/A:1007908909148.

Hammer, U.T. 1981. Primary production in saline lakes. Hydrobiologia, **81**(1): 47–57. doi:10.1007/BF00048705.

Healey, F.P., and Hendzel, L.L. 1980. Physiological indicators of nutrient deficiency in lake phytoplankton. Can. J. Fish. Aquat. Sci. **37**(3): 442–453. doi:10.1139/f80-058.

Herbst, D.B., and Bradley, T.J. 1989. Salinity and nutrient limitations on growth of benthic algae from two alkaline salt lakes of the western Great Basin (USA). J. Phycol. **25**(4): 673–678. doi:10.1111/j.0022-3646.1989.00673.x.

Hessen, D.O., and Tranvik, L.J. (*Editors*). 1998. Aquatic humic substances. Springer, Berlin, Germany.

Hill, H.D., Summer, G.K., and Waters, M.D. 1968. An automated fluorometric assay for alkaline phosphatase using 3-*O*-methylfluorescein phosphate. Anal. Biochem. **24**(1): 9–17. doi:10.1016/0003-2697(68)90054-7. PMID:5665203.

Holland, E.A., Parton, W.J., Detling, J.K., and Coppock, D.L. 1992. Physiological responses of plant populations to herbivory and their consequences for ecosystem nutrient flow. Am. Nat. **140**(4): 685–706. doi:10.1086/285435. PMID:19426039.

Jensen, H.S., and Andersen, F.Ø. 1990. Impact of nitrate and blue-green algae abundance on phosphorus cycling between sediment and water in two shallow eutrophic lakes. Verh. Int. Verein. Limnol. **24**: 224–230.

Kirk, J.T.O. 1994. Light and photosynthesis in aquatic ecosystems. 2nd ed. Cambridge University Press, Cambridge, UK.

LaBaugh, J.W. 1986. Limnological characteristics of selected lakes in the Nebraska Sandhills, U.S.A., and their relation to chemical characteristics of adjacent ground water. J. Hydrol. (Amst.), **86**(3–4): 279–298. doi:10.1016/0022-1694(86)90168-X.

Laird, K.R., Fritz, S.C., and Cumming, B.F. 1998. A diatom-based reconstruction of drought intensity, duration, and frequency from Moon Lake, North Dakota: a sub-decadal record of the last 2300 years. J. Paleolimnol. **19**(2): 161–179. doi:10.1023/A:1007929006001.

Lewis, W.M., Jr., and Wurtsbaugh, W.A. 2008. Control of lacustrine phytoplankton by nutrients: erosion of the phosphorus paradigm. Int. Rev. Hydrobiol. **93**(4–5): 446–465. doi:10.1002/iroh.200811065.

Lijklema, L. 1977. The role of iron in the exchange of phosphate between water and sediments. *In* Interactions between sediments and freshwater. *Edited by* H.L. Golterman. Dr W. Junk Publishers, New York. pp. 313–317.

Lind, O.T. 1985. Handbook of common methods in limnology. Kendall/Hall Publishing Company, Dubuque, Iowa.

Loope, D.B., Swinehart, J.B., and Mason, J.P. 1995. Dune-dammed paleovalleys of the Nebraska Sand Hills: intrinsic versus cli-

matic controls on the accumulation of lake and marsh sediments. Geol. Soc. Am. Bull. **107**(4): 396–406. doi:10.1130/0016-7606(1995)107<0396:DDPOTN>2.3.CO;2.

Macarelli, A.M., and Wurtsbaugh, W.A. 2006. Temperature and nutrient supply interact to control nitrogen fixation in oligotrophic streams: an experimental examination. Limnol. Oceanogr. **51**: 2278–2289.

Marino, R., Howarth, R.W., Shamess, J., and Prepas, E.E. 1990. Molybdenum and sulfate as controls on the abundance of nitrogen-fixing cyanobacteria in saline lakes in Alberta. Limnol. Oceanogr. **35**: 245–259.

Mason, J.P., Swinehart, J.B., and Loope, D.B. 1997. Holocene history of lacustrine and marsh sediments in a dune-blocked drainage, southwestern Nebraska Sand Hills, USA. J. Paleolimnol. **17**(1): 67–83. doi:10.1023/A:1007917110965.

Ojima, D.S., Schimel, D.S., Parton, W.J., and Owensby, C.E. 1994. Long- and short-term effects of fire on nitrogen cycling in tallgrass prairie. Biogeochemistry, **24**(2): 67–84. doi:10.1007/BF02390180.

Osburn, C.L., and St. Jean, G. 2007. The use of wet chemical oxidation with high-amplification isotope ratio mass spectrometry (WCO-IRMS) to measure stable isotope values of dissolved organic carbon in seawater. Limnol. Oceanogr. Methods, **5**: 296–308.

Reuter, J.E., Rhodes, C.L., Lebo, M.E., Kotzman, M., and Goldman, C.R. 1993. The importance of nitrogen in Pyramid Lake (Nevada, USA), a saline, desert lake. Hydrobiologia, **267**(1–3): 179–189. doi:10.1007/BF00018800.

Roberts, R.D., Evans, M.S., and Arts, M.T. 1992. Light, nutrients and water temperatures as determinants of phytoplankton production in two saline prairie lakes with high sulfate concentrations. Can. J. Fish. Aquat. Sci. **49**: 2281–2290. doi:10.1139/f92-250.

Salm, C.R., Saros, J.E., Martin, C.S., and Erickson, J.M. 2009. Patterns of seasonal phytoplankton distribution in prairie saline lakes of the northern Great Plains (U.S.A.). Saline Systems, **5**(1). doi:10.1186/1746-1448-5-1. PMID:19123939.

Saros, J.E., and Fritz, S.C. 2000. Nutrients as a link between ionic concentration/composition and diatom distributions in saline lakes. J. Paleolimnol. **23**(4): 449–453. doi:10.1023/A:1008186431492.

Scott, J.T., Doyle, R.D., Prochnow, S.J., and White, J.D. 2008. Are watershed and lacustrine controls on planktonic N_2 fixation hierarchically structured? Ecol. Appl. **18**(3): 805–819. doi:10.1890/07-0105.1. PMID:18488636.

Smith, V.H. 1979. Nutrient dependence of primary productivity in lakes. Limnol. Oceanogr. **24**: 1051–1064.

Smith, V.H. 1982. The nitrogen and phosphorus dependence of algal biomass in lakes: an empirical and theoretical analysis. Limnol. Oceanogr. **27**: 1101–1112.

Søndergaard, M., Kristensen, P., and Jeppesen, E. 1992. Phosphorus release from resuspended sediment in the shallow and wind-exposed Lake Arresø, Denmark. Hydrobiologia, **228**: 91–99. doi:10.1007/BF00006480.

Søndergaard, M., Jeppesen, E., Jensen, J.P., and Amsinck, S.L. 2005. Water Framework Directive: ecological classification of Danish lakes. J. Appl. Ecol. **42**(4): 616–629. doi:10.1111/j.1365-2664.2005.01040.x.

Sterner, R.W., and Elser, J.J. 2002. Ecological stoichiometry: the biology of elements from molecules to the biosphere. Princeton University Press, Princeton, N.J.

Waiser, M.J., and Roberts, R.D. 1995. Microbial nutrient limitation in prairie saline lakes with high sulfate concentration. Limnol. Oceanogr. **40**: 566–574.

Wedin, D.A. 1995. Species, nitrogen, and grassland dynamics: the constraints of stuff. *In* Linking species and ecosystems. *Edited by* C.G. Jones and J.H. Lawton. Chapman & Hall, New York. pp. 253–262.

Wetzel, R.G. 2001. Limnology: lake and river ecosystems. 3rd ed. Academic Press, San Diego, Calif.

Wetzel, R.G., and Likens, G.E. 1991. Limnological analyses. 2nd ed. Springer-Verlag, New York.

Williams, W.D. 1981. Inland salt lakes: an introduction. Hydrobiologia, **81–82**(1): 1–14. doi:10.1007/BF00048701.

Effects of temperature change on demersal fishes in the California Current: a bioenergetics approach

Chris J. Harvey

Abstract: Diverse fish assemblages should feature a range of biological and ecological responses to temperature change. Using preliminary bioenergetics models, I simulated growth and maturation of three California Current groundfish (yelloweye rockfish (*Sebastes ruberrimus*), sablefish (*Anoplopoma fimbria*), and spiny dogfish (*Squalus acanthias*)) at fixed temperatures ranging from 5 °C to 11 °C. I examined three response variables (size at age 1 (W_1), age at 50% maturity ($\tau_{50\%}$), and total prey consumption (C)). Yelloweye rockfish responded most strongly for W_1, which increased 496% as temperature increased from 5 °C to 11 °C. Spiny dogfish $\tau_{50\%}$ was highly sensitive, declining from >48 years at 5 °C to <13 years at 11 °C. Age-specific C was most responsive in yelloweye rockfish, increasing by more than fivefold over the range of temperatures, although sablefish likely have greater community-wide impact because their trophic level and absolute feeding rates are higher. Regime shifts, temperature anomalies, or global climate change may directly affect fish energy budgets, elicit range shifts, or produce complex ecological interactions. Studies like this will help managers to identify temperature-sensitive species and anticipate potential changes in populations and diverse communities.

Résumé : Les peuplements diversifiés de poissons devraient faire montre d'une gamme de réactions biologiques et écologiques variées au changement de température. Des modèles bioénergétiques préliminaires m'ont permis de simuler la croissance et la maturation chez trois poissons de fond du courant de la Californie (le sébaste à yeux jaunes (*Sebastes ruberrimus*), la morue charbonnière (*Anoplopoma fimbria*) et l'aiguillat commun (*Squalus acanthias*)) à des températures fixes entre 5 °C et 11 °C. Trois variables de réaction ont été examinées, la taille à l'âge 1 (W_1), l'âge à 50 % de maturité ($\tau_{50\%}$) et la consommation totale de proies (C). Les sébastes aux yeux jaunes réagissent le plus fortement en ce qui a trait à W_1 qui a augmenté de 496 % lorsque la température est passée de 5 °C à 11 °C. Le $\tau_{50\%}$ des aiguillats communs est très sensible, ayant diminué de >48 ans à 5 °C à <13 ans à 11 °C. La valeur de C spécifique à l'âge a réagi le plus fortement chez les sébastes à yeux jaunes, augmentant de >5 fois sur la gamme de températures, bien que les morues charbonnières aient vraisemblablement un plus grand impact au niveau de la communauté dans son ensemble à cause de leur niveau trophique et de leurs taux absolus d'alimentation plus élevés. Les changements de régime, les anomalies thermiques ou le changement climatique global peuvent affecter directement les bilans énergétiques des poissons, entraînant des changements de répartition ou produisant des interactions écologiques complexes. Des études comme celle-ci aideront les gestionnaires à identifier les espèces sensibles à la température et à anticiper les changements potentiels dans les populations et les communautés diversifiées.

[Traduit par la Rédaction]

Introduction

Temperature plays a central role in the biology of fishes. A considerable body of research has focused on the effect of temperature on fish feeding, growth, and reproductive rates and on the ways that fish behaviorally thermoregulate these rates (e.g., Magnuson et al. 1979; Crawshaw and O'Connor 1997; Jobling 2002). Temperature directly affects or is highly correlated with numerous key ecological and demographic variables, including swimming ability, spatial distribution, survival, recruitment, and population growth (Imsland et al. 1996; Hare and Able 2007; Hurst 2007). The central importance of these rates, behaviors, and variables underscores the influence of temperature in shaping not only the biology of individual fish species (e.g., Brett 1971), but also the structure and function of whole aquatic and marine communities (Magnuson et al. 1979; McGowan et al. 1998; Schiel et al. 2004).

In the California Current ecosystem along the west coast of North America, ocean temperatures vary on a number of scales. In spatial terms, temperatures vary in relation to many gradients and structuring forces (latitude, depth, zoogeographic boundaries, local or regional circulation, stratification patterns) that are also associated with changes in fish distribution, diversity, or assemblage structure (e.g., Allen and Smith 1988). In temporal terms, temperatures vary daily and seasonally due to patterns of solar irradiation, tides, winds, and circulation. At longer time scales, temperatures vary as a function of annual climate anomalies, such as the

Received 15 August 2008. Accepted 24 March 2009. Published on the NRC Research Press Web site at cjfas.nrc.ca on 21 August 2009. J20730

C.J. Harvey. Northwest Fisheries Science Center, NOAA Fisheries, 2725 Montlake Boulevard E, Seattle, WA 98112, USA (e-mail: Chris.Harvey@noaa.gov).

El Niño Southern Oscillation, or decadal regime shifts, such as variation in the position and strength of the Aleutian Low (McGowan et al. 1998). Climate variability at these scales has been linked to measurable changes in fish distribution, recruitment, diet, growth, and harvest (e.g., VenTresca et al. 1995; McGowan et al. 1998; Tolimieri and Levin 2005). Global climate change models predict further changes to come in the California Current (Auad et al. 2006).

It is unlikely that all species in a marine fish assemblage would respond to temperature variations in the same manner (e.g., Murawski 1993). This is an important consideration for managers of complex fish communities in dynamic ecosystems. The challenge of managing such communities includes understanding how different species compensate for environmental sensitivity via metabolic, behavioral, or other mechanisms, incorporating this information into stock assessments, and adjusting human activities (e.g., harvest) accordingly (King and McFarlane 2006). Bioenergetics models, which estimate growth, consumption, respiration, and other aspects of a fish's energy budget (Kitchell et al. 1977), are useful tools for intuiting the sensitivity of different fish species to temperature variability. Fish energy budgets are temperature-dependent, and their sensitivity to temperature changes as a function of fish size. Hence, bioenergetics models can estimate the ontogeny of temperature sensitivity throughout fish life histories (Harvey 2005). The direct link between fish growth and environmental variables like temperature makes bioenergetics modeling a potentially powerful analytical component of ecosystem approaches to fisheries management (Latour et al. 2003).

In this paper, I use bioenergetics models to compare the effects of temperature change on subadults of three taxonomically distinct species (yelloweye rockfish (*Sebastes ruberrimus*), sablefish (*Anoplopoma fimbria*), and spiny dogfish (*Squalus acanthias*)) from the California Current ecosystem. The rockfish model expands on a previously published *Sebastes* model (Harvey 2005), whereas models for the other two species are developed for the first time in the literature. My objective was to determine the magnitude and rank of species-specific responsiveness to temperature changes that are consistent with seasonal, annual, and decadal temperature variability in the California Current (e.g., Huyer et al. 2002; Palacios et al. 2004; Auad et al. 2006). I examined responsiveness to temperature change across three response variables: weight at age 1, age of maturation, and prey consumption. These variables are biologically and ecologically relevant: weight at age 1 is an indicator of first-year survival, based on the positive correlation between size and early survival in many fishes (Sogard 1997). Maturation rate is related to processes and parameters such as generation time, the rate at which a new year class recruits into a fishery, and the overall reproductive potential of a cohort (because delayed maturity means that fewer individuals survive to reproduce). Prey consumption is an indicator of individual energy requirements, as well as a species' impact on its prey resources and competitors. Finally, I speculate on how these and other California Current groundfish might plausibly express responses to temperature change in biological and ecological terms and how these responses might affect community structure and fisheries management in this complex system.

Materials and methods

Species descriptions

Yelloweye rockfish are among the largest and most long-lived and late-maturing of the *Sebastes*. They may reach sizes of >90 cm and ages of over 100 years and at some latitudes do not mature until they are over 20 years old (Wallace et al. 2006). Yelloweye rockfish dwell around high-relief rocky habitats on the continental shelf of western North America. They have fishery value, although their numbers have been severely depressed in recent decades. Sablefish live throughout much of the North Pacific Rim, with adults typically at the continental shelf–slope margin. They may reach 1 m in length (Schirripa and Colbert 2005), and maximum ages of over 100 years are reported (King and McFarlane 2003). They generally mature in 5–7 years. Sablefish support large, valuable commercial fisheries. Spiny dogfish are found in temperate and subarctic oceans from nearshore to shelf and slope waters (Love 1996). They rarely achieve lengths beyond about 1.5 m or ages beyond 75 years. They are notably slow to mature, with many females reaching first maturity at >20 years of age.

Model structure

Models for each species followed the general form of the fish bioenergetics model, which uses a core thermodynamic equation:

$$(1) \qquad C = R + S + F + U + \Delta B$$

where the rate of consumption (C, in units of weight or energy) is equal to the sum of respiration rate (R), specific dynamic action (S), egestion (F), excretion (U), and somatic growth (ΔB). Most of these terms represent functions (Table 1) that are dependent on fish weight (W, in grams) and temperature (T, in °C). Notably, the ambient temperature and estimates of optimal temperature, maximum temperature, and Q_{10} rates drive the temperature-dependence functions ($f(T)$) for both the consumption and respiration calculations (Table 1). The parameters that comprise the equations are listed and defined in Table 2. The derivation of these equations and parameters is described in detail by Kitchell et al. (1977).

The fraction of consumed energy not devoted to R, S, F, and U is dedicated to ΔB (or to gonadal development, which is not considered in this study). Energy allocation to ΔB was based on empirical observations of fish energy density, prey energy density, and growth, based on von Bertalanffy growth functions (VBGF) and length–weight (L–W) relationships. Length (cm) was converted to weight (g) using the allometric growth model $W = a \cdot L^b$; following the available demographic literature for each species, I used fork lengths (FL) for yelloweye rockfish and sablefish and total length (TL) for spiny dogfish (Table 3; Appendices A–C).

Bioenergetics parameters for each species (Table 2) largely came from published studies on feeding and respiration. Demographic parameters that describe growth and maturation (Table 3) were compiled from field studies and stock assessments; the models in this paper feature only demographic data for female fish because of their greater importance to population biology. Size-specific diets

Table 1. Equations used in bioenergetics models.

Metabolic function	Equations
Consumption	$C = CA \cdot W^{CB} \cdot P \cdot f_1(T)$, where
	$f_1(T) = V^X \cdot e^{(X(1-V))}$
	$V = (CTM - T) / (CTM - CTO)$
	$X = Z^2 \cdot (1 + (1 + 40/Y)^{0.5})^2/400$
	$Z = \ln(CQ) \cdot (CTM - CTO)$
	$Y = \ln(CQ) \cdot (CTM - CTO + 2)$
Respiration[a]	$R = RA \cdot W^{RB} \cdot f_2(T) \cdot ACT \cdot \alpha$, where
	$f_2(T) = RV^{RX} \cdot e^{(RX(1-RV))}$
	$RV = (RTM - T)/(RTM - RTO)$
	$RX = RZ^2 \cdot (1 + (1 + 40/RY)^{0.5})^2/400$
	$RZ = \ln(RQ) \cdot (RTM - RTO)$
	$RY = \ln(RQ) \cdot (RTM - RTO + 2)$
Specific dynamic action	$S = SDA \cdot (C - F)$
Egestion	$F = FA \cdot C$
Excretion	$U = UA \cdot (C - F)$

Note: Parameters are defined in Table 2.

[a]The constant α converts R from grams O_2 consumed to joules expended ($\alpha = 13560\ J \cdot g\ O_2^{-1}$).

Table 2. Parameters for yelloweye rockfish (*Sebastes ruberrimus*), sablefish (*Anoplopoma fimbria*), and spiny dogfish (*Squalus acanthias*) bioenergetics models.

Parameter	Description	Rockfish	Sablefish	Dogfish
CA	Intercept of the allometric consumption function ($g \cdot g^{-1} \cdot day^{-1}$)	0.1330	0.4200	0.1858
CB	Body mass scaling exponent for consumption	–0.3479	–0.3300	–0.2588
CQ	Q_{10} for consumption	2.80	2.20	2.465
CTO	Optimal temperature for consumption (°C)	17.83	18	19
CTM	Maximum temperature for consumption (°C)	23	23	25
RA	Intercept of the allometric respiration function ($g\ O_2 \cdot g^{-1} \cdot day^{-1}$)	0.0100	0.0198	0.0065
RB	Body mass scaling exponent for respiration	–0.2485	–0.2800	–0.1400
RQ	Q_{10} for respiration	2.50	1.90	2.124
ACT	Activity multiplier for respiration	1	1	1
RTO	Optimal temperature for respiration (°C)	23	23	25
RTM	Maximum temperature for respiration (°C)	28	26	28
SDA	Proportion of assimilated energy spent on digestion	0.163	0.163	0.100
FA	Proportion of consumed energy lost to egestion	0.104	0.104	0.18
UA	Proportion of assimilated energy lost to excretion	0.068	0.068	0.068
ED	Somatic energy density ($J \cdot g^{-1}$)	6120	5246	9400

Note: Derivations and literature sources of all parameters are described in Appendices A–C.

(Fig. 1) were taken from published studies. As often as possible, I used demographic and diet data collected in waters off of Oregon, Washington, and British Columbia, because these factors typically vary with latitude among groundfish in the California Current Ecosystem (e.g., Love 1996). Detailed derivations of the bioenergetic, demographic, and diet parameter values for each species are provided (Appendices A–C).

Baseline model conditions

I assumed a set of hypothetical conditions for a "baseline" scenario to describe the energy budget of typical females of each species, starting at birth and continuing until the age at 50% maturity (Table 3; Appendices A–C). The baseline conditions unquestionably simplify reality but are used as a means to judge the relative responsiveness of each species to temperature change. Baseline model temperature was fixed at 8 °C, which is similar to average bottom temperatures observed from 1961 to 1971 at depths of 100–200 m along the Newport oceanographic transect line (Huyer et al. 2002). Models were run at monthly time steps. I fitted individual weight at age t to expected size at age from each species' VBGF and L–W relationship (Table 3; Appendices A–C). I did this by iteratively changing P (the proportion of maximum C; see the consumption equation in Table 1) during each size-specific segment of a species' dietary ontogeny (Fig. 1) until the simulated growth trajectory best approximated (according to least squared residuals) the VBGF (size-specific, fitted P values are shown in Fig. 1).

Temperature perturbation scenarios

I next ran sets of models in which I changed temperatures from the baseline and tracked the resulting responses in each species. Temperatures were held constant for the duration of each model run. I ran six perturbation models at monthly time steps for each species, with lifetime temperature fixed

Table 3. Demographic parameters for the yelloweye rockfish (*Sebastes ruberrimus*), sablefish (*Anoplopoma fimbria*), and spiny dogfish (*Squalus acanthias*) models.

			Sablefish		
Parameter	Description	Rockfish	<38.4 cm	>38.4 cm	Dogfish
L_∞	VBGF theoretical maximum length (cm)	59.94	52.20	66.20	152.90
k	VBGF growth parameter (year^{-1})	0.083	0.070	0.246	0.036
t_0	VBGF theoretical age at length = 0 (years)	0	–0.24	n/a	–6.7
t_1	Initial age in alternate VBGF (years)	n/a	n/a	1.66	n/a
L_1	Initial length in alternate VBGF (cm)	n/a	n/a	38.40	n/a
a	Condition parameter of length–weight relationship	0.021	0.007	0.00244	0.00396
b	Curvature of length–weight relationship	2.9659	3.0619	3.3469	3.0040
$\tau_{50\%}$	Theoretical age of 50% maturity (years)	13.7	n/a	5.5	21.1

Note: Derivations and literature sources of all parameters are described in Appendices A–C.

at either 5, 6, 7, 9, 10, or 11 °C. The ±3 °C temperature range relative to the baseline was intended to span the range from extremely cool to extremely warm average conditions in the California Current, based on seasonal, annual, and decadal variation (McGowan et al. 1998; Huyer et al. 2002; Palacios et al. 2004). All other model functions remained unchanged from the baseline model: size-specific ontogenetic diet shifts were the same (Fig. 1), as were size-specific values of P (Table 1; Fig. 1), and the models ended when individuals reached the size at which the baseline models were ended (i.e., the size at which 50% of females are mature in the baseline scenario). Keeping these conditions unchanged was necessary to limit variability in model output to the effects of temperature variation.

In each simulation (including the baseline case), three outputs were monitored as indicators of the species' response to the temperature change: (*i*) W_1, the weight at the end of the first year; (*ii*) $\tau_{50\%}$, the time (in years) required to reach the currently observed size at 50% maturity among female fish in waters of Oregon, Washington, and southern British Columbia (Table 3); and (*iii*) C, the weight of prey consumed, both at specific ages (C_i, $i = 1, 2, \ldots$) and as cumulative prey consumption over the full model run, C_{total}. These variables were chosen for their association with key population and ecological parameters (see Introduction). Because the models were deterministic, all comparisons of response variables were strictly qualitative.

Model sensitivity

Sensitivity analysis is necessary because bioenergetics models use interacting parameters derived from multiple studies performed under a variety of conditions (and sometimes on related species). I used the Monte Carlo error analysis method of Bartell et al. (1986), in which model sensitivity to all model parameters is evaluated simultaneously. For each species, I used a Latin hypercube stratified random sampling method (McKay et al. 1979) to generate 1000 full parameter sets from normal distributions with means equal to parameter estimates (Table 1) and coefficients of variation (CV_{params}) of either 2%, 10%, or 20%. I ran models with each randomized parameter set ($n = 9000$) and temperature fixed at 8 °C. Sensitivity was judged according to each parameter's relative partial sum of squares (RPSS), derived from a multiple linear regression of $\log_{10}(W_1)$ against all parameters; RPSS quantifies the influence of a parameter after all other parameters have been accounted for (Bartell et al. 1986). The sum of the parameters' RPSS is equal to the R^2 of the multiple linear regression and indicates variation in $\log_{10}(W_1)$ explained by direct parameter effects.

Results

Baseline scenarios

In the baseline scenarios run at 8 °C, bioenergetics models closely reproduced weight-at-age based on VBGF expectations for all species (Fig. 2). Values of the P parameter used to fit model growth to VBGF expectations were generally less than 0.65 (Fig. 1), which is consistent with predicted and observed feeding rates of fishes (e.g., Kitchell et al. 1977; Essington et al. 2001); however, rockfish P values were clearly greater than those of sablefish and spiny dogfish. These scenarios also generated the baseline estimates for each of the three response variables. The baseline estimates are highlighted in the subsequent section as the basis for comparison with the temperature change scenarios (see data points set off by shaded areas in Fig. 3).

Responses to temperature changes

Each species experienced changes in the response variables as lifetime temperature was perturbed away from the baseline state. Response variables increased as a function of fixed lifetime temperature, and the changes were typically nonlinear over the range of temperatures examined. Interspecific differences for each response variable are detailed below.

Weight at the end of the first year, W_1, was highly temperature dependent for all species (Fig. 3*a*). As rearing temperatures increased, W_1 for all species experienced nonlinear increases. These increases were smooth for yelloweye rockfish and spiny dogfish. The trend for sablefish W_1 experienced abrupt plateaus and shifts as temperature increased, owing to a size-dependent diet shift at the 30 cm size threshold (Fig. 1*b*) that either promoted or mildly inhibited growth relative to the next highest or lowest temperature, depending on conditions. Sablefish achieved the largest W_1, regardless of temperature, whereas yelloweye rockfish were by far the smallest.

Yelloweye rockfish were clearly the most responsive of the three species in terms of temperature effects on W_1. I fit exponential functions to W_1–temperature relationships for each species, because those curves provided highly accurate

Fig. 1. Ontogenetic diet compositions used for bioenergetics modeling of subadult females of (*a*) yelloweye rockfish (*Sebastes ruberrimus*), (*b*) sablefish (*Anoplopoma fimbria*), and (*c*) spiny dogfish (*Squalus acanthias*). Energy density of prey (ED) and the proportion of maximum consumption (*P*) at which simulated fish fed are given for each ontogenetic stage.

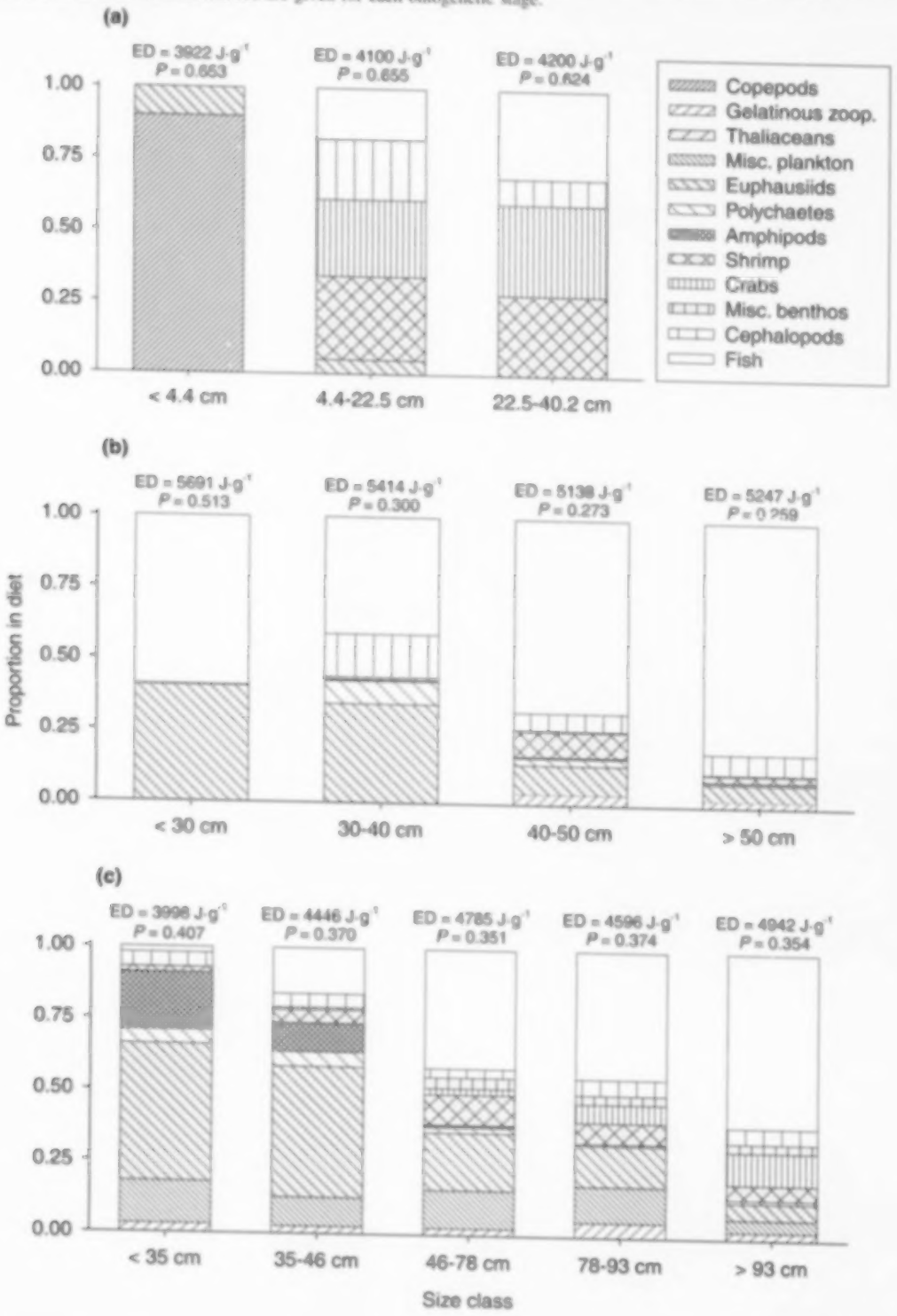

Fig. 2. Weight-at-age estimates for subadult females of yelloweye rockfish (*Sebastes ruberrimus*; solid circles), sablefish (*Anoplopoma fimbria*; open circles), and spiny dogfish (*Squalus acanthias*; solid triangles). Symbols indicate von Bertalanffy growth function estimates, and solid lines indicate estimates from bioenergetics models run under "baseline" conditions. The final symbol in each series represents the observed age at 50% maturity for that species.

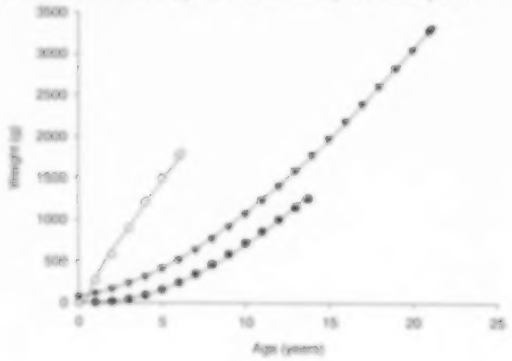

fits for yelloweye rockfish and spiny dogfish (Fig. 3*a*). The coefficient in the exponent was far greater for yelloweye rockfish (0.2674) than for either of the other species. Sablefish and spiny dogfish coefficients were similar, although the irregularities in the sablefish results make distinguishing the two coefficients difficult. Clearly, however, neither species experienced a response comparable in relative magnitude to that of yelloweye rockfish.

An alternative way to view the responsiveness of the three species to temperature is to examine the relative rate of change of W_1 around the 8 °C baseline scenario, where each magnitude of temperature change is analogous to annual climate anomalies of low (±1 °C), moderate (±2 °C), or severe (±3 °C) intensity. Over the range of low-intensity anomalies between 7 and 9 °C, W_1 of yelloweye rockfish ranged from 77% to 131% of baseline W_1 compared with 94% to 106% for spiny dogfish and essentially no change for sablefish. Over moderate anomalies from 6 to 10 °C, yelloweye rockfish W_1 ranged from 58% to 170% of baseline compared with 81% to 119% for sablefish and 89% to 114% for spiny dogfish. Over severe annual anomalies from 5 to 11 °C, yelloweye rockfish W_1 ranged from 44% to 218% of baseline (i.e., a fivefold change as temperature increased from 5 to 11 °C), followed by sablefish (66% to 114%) and spiny dogfish (84% to 121%).

Increasing temperature accelerated maturation in all three species. The responses of $\tau_{50\%}$, the age at which females reach the observed size at 50% maturity, followed decreasing power functions, driven by temperature (Fig. 3*b*). Spiny dogfish $\tau_{50\%}$ was the most sensitive to temperature, both in relative and absolute terms. The rate of change of the spiny dogfish $\tau_{50\%}$–temperature curve, represented by the scaling exponent (–1.6974), was greater than that of sablefish or yelloweye rockfish, the least sensitive species. In absolute terms, spiny dogfish experienced by far the broadest range of maturation times, spanning from over 48 years at 5 °C to just under 13 years at 11 °C. This 35-year difference contrasts with a total range of 10.25 years for yelloweye rockfish and 8.25 years for sablefish across the same range of temperatures.

Fig. 3. Changes in (*a*) weight at age 1 (W_1), (*b*) the time required to reach the observed size at 50% maturity ($\tau_{50\%}$), and (*c*) total cumulative prey consumption prior to maturation (C_{total}) as a function of temperature for yelloweye rockfish (*Sebastes ruberrimus*; solid circles), sablefish (*Anoplopoma fimbria*; open circles), and spiny dogfish (*Squalus acanthias*; solid triangles). Shaded areas indicate the baseline scenario (rearing temperature = 8 °C). Lines and equations represent best model fits based on least squares.

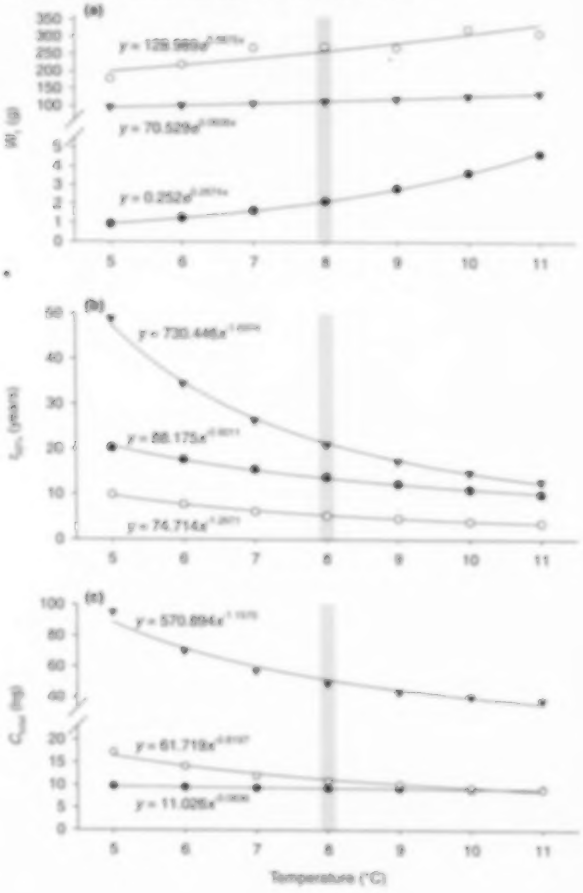

Temperature also had a pronounced effect on C_{total}, the total cumulative consumption over the course of the scenario, and this effect was strongest in spiny dogfish and sablefish (Fig. 3*c*). Though yelloweye rockfish C_{total} decreased only slightly over the range of temperatures, both sablefish and spiny dogfish required considerably less prey to reach maturity as temperature increased. The scaling constants in the exponents of the power functions were similar for sablefish and spiny dogfish, suggesting a comparable level of sensitivity to temperature for C_{total} among these two species. Spiny dogfish had the highest total energetic requirements to reach maturity, presumably because of their relatively slow maturation and large size at the observed age at 50% maturity (~3.3 kg compared with 1.8 kg for sablefish and 1.3 kg

for yelloweye rockfish). Yelloweye rockfish had the lowest energetic requirements, possibly due to their smaller size at maturity and also to their comparatively low mass-specific consumption rates. For example, their CA parameter, the theoretical maximum consumption rate of a 1 g individual at the optimal feeding temperature CTO, was the lowest of the three species (Table 2). This was also true of individuals at larger sizes: at the end of the baseline (8 °C) scenarios, the daily rate of mass-specific consumption by yelloweye rockfish (0.005 $g \cdot g^{-1} \cdot day^{-1}$) was lower than sablefish (0.021 $g \cdot g^{-1} \cdot day^{-1}$) or spiny dogfish (0.011 $g \cdot g^{-1} \cdot day^{-1}$) (data not shown).

The C_{total} outputs shown (Fig. 3c) represent a metric of individual energy requirements to reach maturity; however, energy consumption also places a demand on the prey community upon which these fish feed. When species-specific C_i estimates were plotted against temperature, sablefish had the greatest absolute impact on lower trophic levels in terms of the amount of prey consumed. However, the relative effect of temperature change was strongest for prey of yelloweye rockfish (Fig. 4; output from only 5, 8, and 11 °C shown for sake of clarity). In models for each species from age i = 0 to 4 years (i.e., ages prior to the age at which sablefish reach 50% maturity at 11 °C; see Fig. 4), yelloweye rockfish C_i varied by more than fivefold across the full range of temperatures examined (Fig. 4*a*); the median increase from the 5 °C scenario to the 11 °C scenario across $0 \leq i \leq 4$ was 553%. Spiny dogfish C_i was less variable (Fig. 4*b*; median increase = 262%) and was comparable to that of sablefish C_i (Fig. 4*c*; median increase = 234%). The trends for both sablefish and spiny dogfish (Figs. 4*b*, 4*c*) had occasional discontinuities that were related to ontogenetic prey shifts (see Fig. 1) that caused changes in the energy density of the diet and hence affected consumption rates in the bioenergetics modeling framework.

Sensitivity analyses

In the sensitivity analyses, R^2 values were high (0.761 to 0.998) for each species across all levels of CV_{param}. High R^2 values indicate that changes in the response variable ($\log_{10}W_f$)) were primarily due to direct parameter effects rather than to unexplainable, nonlinear interactions between parameters (Bartell et al. 1986). The amount of variability explained by direct parameter effects decreased as parameter uncertainty increased, particularly as CV_{param} increased from 10% to 20%. The relatively high RPSS values for consumption-related parameters, most notably CTO, CA, CB, CQ, and P, indicate not only that these parameters exert a high level of influence on model outputs, but also that these parameters are ones for which estimation uncertainty is most critical.

The parameter that explained the most variability was CTO, the optimal temperature for consumption (Fig. 5). If RPSS scores are ranked from 1 (highest) to 15 (lowest), CTO was ranked 1 for all species at all levels of CV_{param}. Although CTO was clearly the most influential parameter at CV_{param} = 2%, its RPSS dropped steeply as CV_{param} increased. Of the remaining parameters, the rankings of CA, CB, CQ, and P were almost always between 2 and 6. RTO, the optimal respiration temperature, was nearly always the most influential respiration-related parameter for all species, with rankings ranging from 4 to 6. The lowest-ranking, least influential parameters were generally the maximum temperatures of respiration and consumption and the coefficients for egestion, excretion, and specific dynamic action.

Fig. 4. Monthly prey consumption (C_i) by age-0 through age-4 (*a*) yelloweye rockfish (*Sebastes ruberrimus*), (*b*) sablefish (*Anoplopoma fimbria*), and (*c*) spiny dogfish (*Squalus acanthias*), at the minimum (5 °C, diamonds), baseline (8 °C, squares), and maximum (11 °C, triangles) temperatures simulated in bioenergetics models.

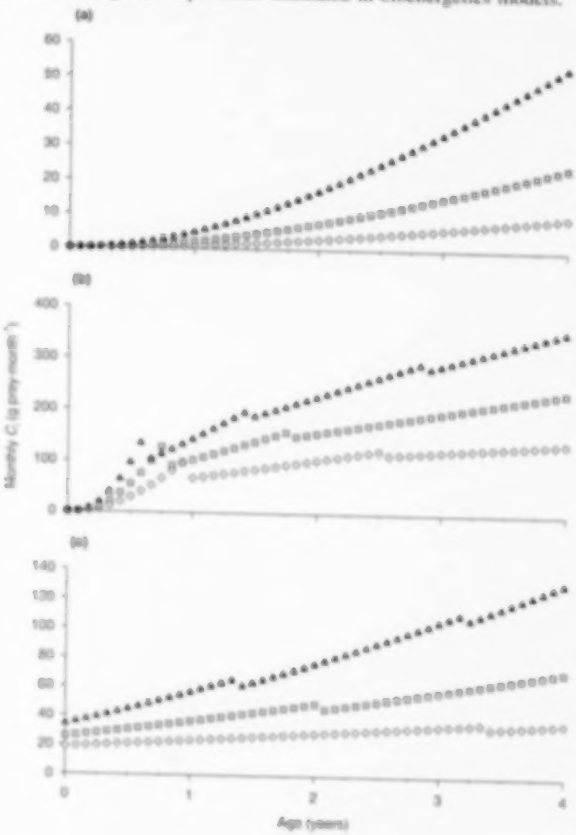

Discussion

Simulated long-term temperature changes elicited very different metabolic responses among the three species. Although that was to be expected, an important corollary is that the nature of the differences can be anticipated if basic information about the species' metabolism, life history, and trophic ecology is known. Bioenergetics models help us infer which species will be most responsive to temperature perturbations of different signs and intensities. Further, bioenergetics models allow us to determine if species that were relatively unresponsive at one life history stage become more responsive at another life history stage. Such information has great potential value to management of these species, provided that we also understand how temperature effects in a model translate into in situ changes in behavior, feeding rates, growth, and maturation.

Fig. 5. Sensitivity analysis of bioenergetics models for (*a*) yelloweye rockfish (*Sebastes ruberrimus*), (*b*) sablefish (*Anoplopoma fimbria*), and (*c*) spiny dogfish (*Squalus acanthias*), where parameters were drawn from distributions with means from Table 2 (except P; see Fig. 1) and coefficients of variation (CV) of 2%, 10%, or 20%. Residual partial sums of squares (RPSS) indicate parameter influence on output variability; the sum of the RPSS (R^2) indicates the total variability explained by linear parameter effects.

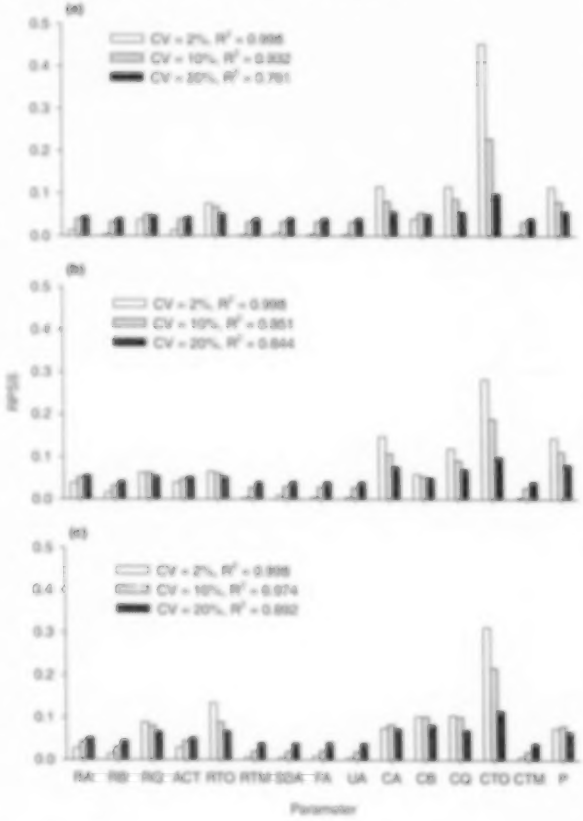
(a)
CV = 2%, R² = 0.998
CV = 10%, R² = 0.932
CV = 20%, R² = 0.781
(b)
CV = 2%, R² = 0.998
CV = 10%, R² = 0.851
CV = 20%, R² = 0.644
(c)
CV = 2%, R² = 0.998
CV = 10%, R² = 0.974
CV = 20%, R² = 0.892
RPSS
RA RB RQ ACT RTO RTM SDA FA UA CA CB CQ CTO CTM P
Parameter

Differences emerged among the three species despite the fact that the temperature perturbations were relatively small. However, the perturbations are relevant to recent conditions in the California Current. Since 1960, the North Pacific has experienced a mild warming signal (≤0.25 °C) in the upper 100 m and a cooling of similar magnitude at around 150 m (Barnett et al. 2005). An additional 0.3–0.8 °C of warming is expected in the upper 50 m of the water column, and slight cooling between 70 m and 300 m, between 1986–1996 and 2040–2050 (Auad et al. 2006). During strong El Niño events, bottom temperatures increase by 1–2 °C in shelf waters of the California Current (Huyer et al. 2002). Because many California Current groundfish use both pelagic and benthic habitats over the course of their lives (Love 1996), they likely experience cumulative thermal environments that span beyond the range depicted herein, particularly if temperature variability is factored in.

Temperature effects on size at age 1 and maturation rate

Size at age 1 (W_1) and age at 50% maturity ($\tau_{50\%}$) are of central importance in fish population biology. The three species' responses were distinct for these variables: W_1 was considerably more responsive to temperature change in yelloweye rockfish than in sablefish or spiny dogfish, whereas spiny dogfish were most responsive, both in relative and absolute terms, with respect to $\tau_{50\%}$. These differences may be related to differences in life history strategies. For example, rockfish generally have long life spans, slow growth, and high fecundity, traits that allow adults to endure years of suboptimal environmental conditions and take advantage of the occasional years in which conditions promote recruitment (King and McFarlane 2003; Tolimieri and Levin 2005). The sensitivity of yelloweye rockfish W_1 to temperature is consistent with high, environmentally driven variability in early juvenile survival, assuming a positive correlation between size and early survival (Sogard 1997). Because yelloweye rockfish are much smaller in their first year than the other species, size variation may have greater relative influence on their vulnerability to predation, starvation, or advection from nursery habitats.

The dramatic response of spiny dogfish $\tau_{50\%}$ was on the scale of extreme minimum and maximum ages of maturation observed in British Columbia female spiny dogfish (18 and 48 years; Jones and Geen 1977). This responsiveness seems counterintuitive: spiny dogfish are "equilibrium" life history strategists, characterized by slow population growth, long life span, late maturation, low fecundity, and very high parental care investment (King and McFarlane 2003). This life history, evolved to maximize population stability through time, seems incongruous with an energy budget that is sensitive to environmental perturbations such as temperature changes. Spiny dogfish may compensate for metabolic sensitivity by using a greater degree of behavioral thermoregulation than is used by the other species. For example, spiny dogfish in North Atlantic waters show preference for waters that are warm relative to the range of available temperatures (Shepherd et al. 2002; Methratta and Link 2007).

A species' $\tau_{50\%}$ is related not only to the maturation rate, but also to the size and long-term fecundity of adults. In many marine fishes, asymptotic length and age at maturity increase with latitude. This likely reflects a tradeoff between juvenile growth rate and asymptotic size (Berrigan and Charnov 1994), where slow-growing individuals mature later and larger, trading the relatively high survival derived from rapid growth for the increased fecundity of larger adult size. By contrast, rapidly growing juveniles mature earlier but smaller; after maturing, they quickly reach their asymptotic size and allocate much of their subsequent energy intake to reproduction. Thus, lowering $\tau_{50\%}$ may support faster population growth due to shortening generation times but may also produce smaller adults in fisheries.

Interpreting $\tau_{50\%}$ outputs requires caution: my assumption that maturity is a function of size is likely too simplistic and should be regarded as a first approximation. Size is certainly a major determinant of maturity (Jobling 2002), but maturity is also elicited by biological factors (hormonal cues, sex, age), condition, environmental cues, and evolved life history tradeoffs. This sophisticated relationship could be simulated in bioenergetics models, although functional relationships

relating these factors to a fish energy budget would need to be developed.

Temperature effects on consumption

Both sablefish and spiny dogfish experienced pronounced changes in the C_{total} required to reach a particular size. As temperatures increased, their growth efficiencies increased, enabling them to reach the size at 50% maturity more quickly and with less energy intake. This outcome is important because if an altered temperature regime affects a fish's energy budget, the fish may make different choices about the benefits and risks of active foraging in a space occupied by both prey and predators (Walters and Juanes 1993). In contrast to sablefish and spiny dogfish, the total prey intake that yelloweye rockfish required to reach maturity declined only slightly as temperature increased. This was in part a function of the parameter CQ, the Q_{10} of the consumption rate, which was greater for yelloweye rockfish than for the other species. The higher CQ caused greater increases in mass-specific consumption at age i as temperature increased, which offset the decrease in C_{total} related to accelerated maturation.

Consumption also relates to the impact that the fish has on the surrounding community, particularly its prey and the species that share the same prey resources. This impact depends not only on how sensitive C is to temperature change, but also on the predator's size, diet, trophic level, abundance, and age structure. Thus, although consumption rates of species such as yelloweye rockfish may respond strongly to temperature, the community may be most heavily affected by a moderately responsive species like sablefish, which is a large-bodied, widely distributed, abundant species that occupies a high trophic level (Schirripa and Colbert 2005).

Expressing responses to temperature

A major source of uncertainty is the matter of how groundfish behavior, biology, or ecology might actually change in response to temperature variation. That is, in the face of temperature changes, will groundfish (*i*) have simple positive or negative bioenergetic or demographic responses, (*ii*) change their behaviors or distributions to mitigate the temperature changes, or (*iii*) experience complex community interactions? The outcome will likely be some combination of these alternatives, although the relative strength of each is difficult to predict. Aspects of these changes are discussed below.

Bioenergetic or demographic responses will be a function of the sign, magnitude, and duration of a temperature change and the bioenergetics of the species. As shown in this study, fish may experience changes in size at age, condition, survival, feeding rate, and maturation rate as a direct result of temperature change. Any of these changes could affect their population biology. Behavioral thermoregulation may take the form of latitudinal range shifts, changes in preferred depths, or changes in foraging and habitat use (Crawshaw and O'Connor 1997). Several examples exist among Northeast Pacific groundfish. The northern extent of the annual Pacific hake (*Merluccius productus*) migration is correlated with temperature (Dorn 1995), and juvenile walleye pollock (*Theragra chalcogramma*) prefer cooler water (where respiratory costs are lower) when food is limited (Sogard and Olla 1996). Behavioral thermoregulation may be difficult for some species, however. Rockfish that strongly associate with fixed habitats like rocky reefs or kelp forests may be less likely to change depths or latitudes if their essential habitats are not readily available in those waters; they may remain on their preferred substrates despite unfavorable temperatures or declines in prey quality (e.g., VenTresca et al. 1995).

Complex community interactions include numerous possibilities. In particular, changes in temperature are generally associated with broader physical changes (e.g., in upwelling and stratification) that affect primary production (McGowan et al. 1998). Warming may also cause widespread changes in the composition and phenology of zooplankton (e.g., Mackas et al. 2007). These changes, in turn, affect food availability and quality. Changes in prey quality and quantity fundamentally affect model outputs; for example, an El Niño event might bring on warming coupled with a decrease in prey quality and quantity, resulting in poorer growing conditions than those implied herein. Additionally, a species may be insensitive to temperature change, but key predators or prey may be highly sensitive to it. Different members within a functional group may have different levels of temperature sensitivity, leading to shifts in competitive dominance, or new species may enter the California Current food web via range expansion (e.g., the jumbo squid (*Dosidicus gigas*); Zeidberg and Robison 2007). Understanding complex interactions requires empirical study and will benefit from scenario-driven food web models that incorporate environmental variability (Christensen and Walters 2004; Fulton et al. 2005; Werner et al. 2007).

Model sensitivity and caveats

These models were derived from many lab experiments, often involving related species, and were calibrated to hypothetical baseline growth, diet, and temperature conditions. Careful sensitivity analysis and consideration of caveats is warranted, particularly if the models are to be used in a predictive manner (e.g., Ney 1993). The sensitivity analysis demonstrated that the consumption-related parameters were the most important source of variation in model output. Future laboratory studies of these species' bioenergetics should thus examine consumption parameters over a broad range of temperatures, rations, and fish body sizes. When information was lacking, I made assumptions about parameters (e.g., optimal and maximum temperatures and Q_{10} values) based on general recommendations derived from other bioenergetics models (Hanson et al. 1997) or I "borrowed" parameters from related species. These parameter sets clearly need additional laboratory validation, and the extent of the simplifications that I made relegates these models to "preliminary" status. However, I submit that the conceptual exercise is important and necessary, given the potential effects of climate change and the value of ranking the responses of different species to climate variability.

To a great extent, the responses of the models were a function of fixing P (the proportion of the maximum consumption rate) and diet composition at baseline values. That assumption was likely unrealistic because prey quality and availability are also likely to change with varying temperatures and may decline at higher temperatures (e.g., Ven-

Tresca et al. 1995). However, fixing P at baseline levels was necessary to keep general model structure consistent across scenarios so that temperature was the main effect being tested. I emphasize that these model outputs are not "predictions" of what would actually occur as a result of temperature changes. Distinct responses in my model outputs primarily imply that the bioenergetic configuration of one species is relatively more sensitive to temperature change than other species. More realistic scenarios could certainly be devised but would first require further empirical observation of temperature effects on prey community structure and feeding behavior.

Future directions

Since the late 1990s, the California Current ecosystem has experienced strong El Niño and La Niña events, confusing patterns in basin-scale climate regime indices, and dramatic variability in the onset of spring production (Goericke et al. 2007). In the coming decades, climate models project increased surface temperatures, cooler deep shelf waters (Auad et al. 2006), and more frequent El Niño events (Timmermann et al. 1999). Bioenergetics modeling can help explain or predict fish responses to ecosystem-level changes (Latour et al. 2003), particularly in data-driven scenarios involving changes in temperature, prey quality or quantity, and feeding behavior. This field would benefit from further laboratory studies of metabolism, especially for ecologically important species that are poorly understood in bioenergetic terms (e.g., flatfish). Experiments that determine optimal temperatures and Q_{10} values for consumption and respiration would provide excellent diagnostics of metabolic sensitivity to temperature shifts. Because a diverse community most certainly has a diverse set of responses to temperature (e.g., Magnuson et al. 1979; McGowan et al. 1998), identifying sensitive species and life history stages is central to successful management during times of climate change.

Acknowledgements

Jim Kitchell, Phil Levin, Daniel Schindler, Tim Essington, Nick Tolimieri, Jameal Samhouri, Brian Beckman, Brian Burke, the NWFSC Brown Bag Seminar group, and two anonymous reviewers provided discussion and comments that greatly improved this study.

References

Allen, M.J., and Smith, G.B. 1988. Atlas and zoogeography of common fishes in the Bering Sea and Northeastern Pacific. NOAA Technical Report NMFS 66, National Oceanic and Atmospheric Administration, Seattle, Washington.

Auad, G., Miller, A., and Di Lorenzo, E. 2006. Long-term forecast of oceanic conditions off California and their biological implications. J. Geophys. Res. **111**(C9): C09008. doi:10.1029/2005JC003219.

Barnett, T.P., Pierce, D.W., Achutarao, K.M., Gleckler, P.J., Santer, B.D., Gregory, J.M., and Washington, W.M. 2005. Penetration of human-induced warming into the world's oceans. Science (Washington, D.C.), **309**(5732): 284–287. doi:10.1126/science.1112418. PMID:15933161.

Bartell, S.M., Breck, J.E., Gardner, R.H., and Brenkert, A.L. 1986. Individual parameter perturbation and error analysis of fish bioenergetics models. Can. J. Fish. Aquat. Sci. **43**(1): 160–168. doi:10.1139/f86-018.

Berrigan, D., and Charnov, E.L. 1994. Reaction norms for age and size at maturity in response to temperature: a puzzle for life historians. Oikos, **70**(3): 474–478. doi:10.2307/3545787.

Brett, J.R. 1971. Energetic responses of salmon to temperature: a study of some thermal relations in the physiology and freshwater ecology of sockeye salmon (*Oncorhynchus nerka*). Am. Zool. **11**: 99–113.

Christensen, V., and Walters, C.J. 2004. Ecopath with Ecosim: methods, capabilities and limitations. Ecol. Model. **172**(2–4): 109–139. doi:10.1016/j.ecolmodel.2003.09.003.

Crawshaw, L.I., and O'Connor, C.S. 1997. Behavioural compensation for long-term thermal change. *In* Global warming: implications for freshwater and marine fish. *Edited by* C.M. Wood and D.G. McDonald. Cambridge University Press, Cambridge, UK. pp. 351–376.

Dorn, M.W. 1995. The effects of age composition and oceanographic conditions on the annual migration of Pacific whiting, *Merluccius productus*. Calif. Coop. Ocean. Fish. Investig. Rep. **36**: 97–105.

Essington, T.E., Kitchell, J.F., and Walters, C.J. 2001. The von Bertalanffy growth function, bioenergetics, and the consumption rates of fish. Can. J. Fish. Aquat. Sci. **58**(11): 2129–2138. doi:10.1139/cjfas-58-11-2129.

Fulton, E.A., Smith, A.D.M., and Punt, A.E. 2005. Which ecological indicators can robustly detect effects of fishing? ICES J. Mar. Sci. **62**(3): 540–551. doi:10.1016/j.icesjms.2004.12.012.

Goericke, R., Venrick, E., Koslow, T., Sydeman, W.J., Schwing, F.B., Bograd, S.J., Peterson, W.T., Emmett, R., Lara Lara, J.R., Castro, G.G., Valdez, J.G., Hyrenbach, K.D., Bradley, R.W., Weise, M.J., Harvey, J.T., Collins, C., and Lo, N.C.H. 2007. The state of the California Current, 2006–2007: regional and local processes dominate. Calif. Coop. Fish. Ocean. Fish. Investig. Rep. **48**: 33–66.

Hanson, P.C., Johnson, T.B., Schindler, D.E., and Kitchell, J.F. 1997. Fish bioenergetics 3.0. University of Wisconsin Sea Grant Institute, Madison, Wisconsin.

Hare, J.A., and Able, K.W. 2007. Mechanistic links between climate and fisheries along the east coast of the United States: explaining population outbursts of Atlantic croaker (*Micropogonias undulatus*). Fish. Oceanogr. **16**(1): 31–45. doi:10.1111/j.1365-2419.2006.00407.x.

Harvey, C.J. 2005. Effects of El Niño events on energy demand and egg production of rockfish (Scorpaenidae: *Sebastes*): a bioenergetics approach. Fish. Bull. (Washington, D.C.), **103**: 71–83.

Hurst, T.P. 2007. Thermal effects on behavior of juvenile walleye pollock (*Theragra chalcogramma*): implications for energetics and food web models. Can. J. Fish. Aquat. Sci. **64**(3): 449–457. doi:10.1139/F07-025.

Huyer, A., Smith, R.L., and Fleischbein, J. 2002. The coastal ocean off Oregon and northern California during the 1997–8 El Niño. Prog. Oceanogr. **54**(1–4): 311–341. doi:10.1016/S0079-6611(02)00056-3.

Imsland, A.K., Sunde, L.M., Folkvord, A., and Stefansson, S.O. 1996. The interaction of temperature and fish size on growth of juvenile turbot. J. Fish Biol. **49**(5): 926–940. doi:10.1111/j.1095-8649.1996.tb00090.x.

Jobling, M. 2002. Environmental factors and rates of development and growth. *In* Handbook of fish biology and fisheries. Vol. 1. Fish biology. *Edited by* P.J.B. Hart and J.B. Reynolds. Blackwell Publishing, Malden, Massachusetts. pp. 97–122.

Jones, B.C., and Geen, G.H. 1977. Reproduction and embryonic development of spiny dogfish (*Squalus acanthias*) in the Strait

of Georgia, British Columbia. J. Fish. Res. Board Can. **34**: 1286–1292.

King, J.R., and McFarlane, G.A. 2003. Marine fish life history strategies: applications to fishery management. Fish. Manag. Ecol. **10**(4): 249–264. doi:10.1046/j.1365-2400.2003.00359.x.

King, J.R., and McFarlane, G.A. 2006. A framework for incorporating climate regime shifts into the management of marine resources. Fish. Manag. Ecol. **13**(2): 93–102. doi:10.1111/j.1365-2400.2006.00480.x.

Kitchell, J.F., Stewart, D.J., and Weininger, D. 1977. Applications of a bioenergetics model to yellow perch (*Perca flavescens*) and walleye (*Stizostedion vitreum vitreum*). J. Fish. Res. Board Can. **34**: 1922–1935.

Latour, R.J., Brush, M.J., and Bonzek, C.F. 2003. Toward ecosystem-based fisheries management: strategies for multispecies modeling and associated data requirements. Fisheries, **28**(9): 10–22. doi:10.1577/1548-8446(2003)28[10:TEFM]2.0.CO;2.

Love, M. 1996. Probably more than you want to know about the fishes of the Pacific coast. Really Big Press, Santa Barbara, California.

Mackas, D.L., Batten, S., and Trudel, M. 2007. Effects on zooplankton of a warmer ocean: recent evidence from the Northeast Pacific. Prog. Oceanogr. **75**(2): 223–252. doi:10.1016/j.pocean.2007.08.010.

Magnuson, J.J., Crowder, L.B., and Medvick, P.A. 1979. Temperature as an ecological resource. Am. Zool. **19**: 331–343.

McGowan, J.A., Cayan, D.R., and Dorman, L.M. 1998. Climate–ocean variability and ecosystem response in the Northeast Pacific. Science (Washington, D.C.), **281**: 210–217.

McKay, M.D., Conover, W.J., and Beckman, R.J. 1979. A comparison of three methods for selecting values of input variables in the analysis of output from a computer code. Technometrics, **21**(2): 239–245. doi:10.2307/1268522.

Methratta, E.T., and Link, J.S. 2007. Ontogenetic variation in habitat association for four groundfish species in the Gulf of Maine – Georges Bank region. Mar. Ecol. Prog. Ser. **338**: 169–181. doi:10.3354/meps338169.

Murawski, S.A. 1993. Climate change and marine fish distributions — forecasting from historical analogy. Trans. Am. Fish. Soc. **122**(5): 647–658. doi:10.1577/1548-8659(1993)122<0647:CCAMFD>2.3.CO;2.

Ney, J.J. 1993. Bioenergetics modeling today — growing pains on the cutting edge. Trans. Am. Fish. Soc. **122**(5): 736–748. doi:10.1577/1548-8659(1993)122<0736:BMTGPO>2.3.CO;2.

Palacios, D.M., Bograd, S.J., Mendelssohn, R., and Schwing, F.B. 2004. Long-term and seasonal trends in stratification in the California Current, 1950–1993. J. Geophys. Res. **109**(C10): C10016. doi:10.1029/2004JC002380.

Schiel, D.R., Steinbeck, J.R., and Foster, M.S. 2004. Ten years of induced ocean warming causes comprehensive changes in marine benthic communities. Ecology, **85**(7): 1833–1839. doi:10.1890/03-3107.

Schirripa, M.J., and Colbert, J.J. 2005. Status of the sablefish resource off the continental U.S. Pacific coasts in 2005. Pacific Fishery Management Council, Portland, Oregon. Available at www.pcouncil.org/groundfish/gfsafe0406/gfsafe0406.html.

Shepherd, T., Page, F., and Macdonald, B. 2002. Length and sex-specific associations between spiny dogfish (*Squalus acanthias*) and hydrographic variables in the Bay of Fundy and Scotian Shelf. Fish. Oceanogr. **11**(2): 78–89. doi:10.1046/j.1365-2419.2002.00191.x.

Sogard, S.M. 1997. Size-selective mortality in the juvenile stage of teleost fishes: a review. Bull. Mar. Sci. **60**: 1129–1157.

Sogard, S.M., and Olla, B.L. 1996. Food deprivation affects vertical distribution and activity of a marine fish in a thermal gradient: potential energy-conserving mechanisms. Mar. Ecol. Prog. Ser. **133**: 43–55. doi:10.3354/meps133043.

Timmermann, A., Oberhuber, J., Bacher, A., Esch, M., Latif, M., and Roeckner, E. 1999. Increased El Niño frequency in a climate model forced by future greenhouse warming. Nature (London), **398**(6729): 694–697. doi:10.1038/19505.

Tolimieri, N., and Levin, P.S. 2005. The roles of fishing and climate in the population dynamics of bocaccio rockfish. Ecol. Appl. **15**(2): 458–468. doi:10.1890/03-5376.

VenTresca, D.A., Parrish, R.H., Houk, J.L., Gingras, M.L., Short, S.D., and Crane, N.L. 1995. El Niño effects on the somatic and reproductive condition of blue rockfish, *Sebastes mystinus*. Calif. Coop. Ocean. Fish. Investig. Rep. **36**: 167–174.

Wallace, F.R., Tsou, T.S., Jagielo, T., and Cheng, Y.W. 2006. Status of yelloweye rockfish (*Sebastes ruberrimus*) off the U.S. West Coast in 2006. Pacific Fishery Management Council, Portland, Oregon. Available at www.pcouncil.org/groundfish/gfsafe0406/gfsafe0406.html.

Walters, C.J., and Juanes, F. 1993. Recruitment limitation as a consequence of natural selection for use of restricted feeding habitats and predation risk taking by juvenile fishes. Can. J. Fish. Aquat. Sci. **50**(10): 2058–2070. doi:10.1139/f93-229.

Werner, F.E., Ito, S.I., Megrey, B.A., and Kishi, M.J. 2007. Synthesis of the NEMURO model studies and future directions of marine ecosystem modeling. Ecol. Model. **202**(1-2): 211–223. doi:10.1016/j.ecolmodel.2006.08.019.

Zeidberg, L.D., and Robison, B.H. 2007. Invasive range expansion by the Humboldt squid, *Dosidicus gigas*, in the eastern North Pacific. Proc. Natl. Acad. Sci. U.S.A. **104**(31): 12948–12950. doi:10.1073/pnas.0702043104.

Appendix A. Model parameters for yelloweye rockfish

The bioenergetics parameters for yelloweye rockfish (Table 2) were mostly taken from a generic *Sebastes* bioenergetics model (Harvey 2005). Unlike the original *Sebastes* model, however, consumption is now modeled explicitly. The derivations of parameters concerning R, S, F, U, and rockfish energy density are described in detail by Harvey (2005). For consumption, I first assumed that CTM = RTO and CQ = RQ + 0.3, which follows conventions of bioenergetics modeling for data-poor species (Hanson et al. 1997). I then fit the consumption equation (Table 1) to mass-specific consumption rates of juvenile black rockfish (*S. melanops*; weight ≈ 7.5 g) at temperatures ranging from 7 to 18 °C (Boehlert and Yoklavich 1983). I used a fitting algorithm in which CA, CB, and CTO were unknowns and were fit according to least squares.

Yelloweye rockfish growth and length–weight (L–W) relationships (Table 3) were drawn from a recent stock assessment (Wallace et al. 2006). I used the length-at-age relationship of Wallace et al. (2006), who fit a growth function that assumes t_0 (the theoretical age at which fork length (FL) = 0 cm) is equal to 0. They did so because the standard VBGF produced unrealistic estimates for t_0 (–11.16 years) and FL at age 0 (25.5 cm). The alternative growth equation takes the form

(A1) $L_t = L_\infty(1 - e^{-kt})$

where L_∞ is the theoretical maximum FL and k is a growth rate parameter (Table 3). The size at 50% maturity (FL = 41 cm) was estimated by Barss (1989).

Diet data are scarce for yelloweye rockfish. Data were available for age-0 juveniles (Reilly et al. 1992) and for adults (average weight = 5.20 kg; Steiner 1979), but not for intermediate sizes and ages. I used the data from Reilly et al. (1992) for age-0 fish and the data of Steiner (1979) for fish greater than 1200 g (close to the weight at which females begin maturing); at intermediate ages, I assumed gradual shifts to a more energy-rich diet consistent with a transition from the zooplankton-rich diet observed by Reilly et al. (1992) to a diet dominated by fish and crabs as observed by Steiner (1979). The diet profile is shown in Fig. 1*a*. Energy densities for prey were taken from Thayer et al. (1973), Wacasey and Atkinson (1987), Brey et al. (1988), Perez (1994), and Foy and Norcross (1999).

References

Barss, W.H. 1989. Maturity and reproductive cycle for 35 species from the family Scorpaenidae found off Oregon. Oregon Department of Fish and Wildlife Information Report 89-7, Oregon Department of Fish and Wildlife, Portland, Oregon.

Boehlert, G.W., and Yoklavich, M.M. 1983. Effects of temperature, ration, and fish size on growth of juvenile black rockfish, *Sebastes melanops*. Environ. Biol. Fishes, **8**(1): 17–28. doi:10.1007/BF00004942.

Brey, T., Rumohr, H., and Ankar, S. 1988. Energy content of macrobenthic invertebrates — general conversion factors from weight to energy. J. Exp. Mar. Biol. Ecol. **117**(3): 271–278. doi:10.1016/0022-0981(88)90062-7.

Foy, R.J., and Norcross, B.L. 1999. Spatial and temporal variability in the diet of juvenile Pacific herring (*Clupea pallasi*) in Prince William Sound, Alaska. Can. J. Zool. **77**(5): 697–706. doi:10.1139/cjz-77-5-697.

Hanson, P.C., Johnson, T.B., Schindler, D.E., and Kitchell, J.F. 1997. Fish bioenergetics 3.0. University of Wisconsin Sea Grant Institute, Madison, Wisconsin.

Harvey, C.J. 2005. Effects of El Niño events on energy demand and egg production of rockfish (Scorpaenidae: *Sebastes*): a bioenergetics approach. Fish. Bull. (Washington, D.C.), **103**: 71–83.

Perez, M.A. 1994. Calorimetry measurements of energy value of some Alaskan fishes and squids. NOAA Technical Memorandum NMFS-AFSC-32, National Oceanic and Atmospheric Administration, Seattle, Washington.

Reilly, C.A., Wylie-Echeverria, T., and Ralston, S. 1992. Interannual variation and overlap in the diets of pelagic juvenile rockfish (genus *Sebastes*) off central California. Fish. Bull. (Washington, D.C.), **90**: 505–515.

Steiner, R.G. 1979. Food habits and species composition of neritic reef fishes off Depoe Bay, Oregon. M.S. thesis, Oregon State University, Corvallis, Oregon.

Thayer, G.W., Schaaf, W.E., Angelovic, J.W., and LaCroix, M.W. 1973. Caloric measurements of some estuarine organisms. Fish. Bull. (Washington, D.C.), **71**: 289–296.

Wacasey, J.W., and Atkinson, E.G. 1987. Energy values of marine benthic invertebrates from the Canadian Arctic. Mar. Ecol. Prog. Ser. **39**: 243–250. doi:10.3354/meps039243.

Wallace, F.R., Tsou, T.S., Jagielo, T., and Cheng, Y.W. 2006. Status of yelloweye rockfish (*Sebastes ruberrimus*) off the U.S. West Coast in 2006. Pacific Fishery Management Council, Portland, Oregon. Available at www.pcouncil.org/groundfish/gfsafe0406/gfsafe0406.html.

Appendix B. Model parameters for sablefish

The bioenergetics parameters for sablefish (Table 2) come from laboratory and field studies, although some parameters were assumed, due to lack of data. I derived the allometric consumption term CB from a study by Sullivan and Smith (1982), who examined feeding of sablefish ranging from 250 to 2780 g. The temperature-dependence term CQ was estimated from consumption by young-of-year sablefish across a range of temperatures in feeding experiments conducted by Sogard and Olla (2001). I then solved the consumption equation (Table 1) for CA, using the CB and CQ estimates and fitting to consumption data from Sullivan and Smith (1982). Optimal and maximum consumption temperatures CTO and CTM were derived from the study by Sogard and Olla (2001). Following fish bioenergetics modeling conventions (Hanson et al. 1997), the optimal respiration temperature RTO was assumed to equal CTM, and RTM was assumed to be 3 °C greater than RTO. The RB parameter was based on oxygen consumption estimates taken by Sullivan and Smith (1982) on sablefish ranging from 250 to 3000 g. I solved the respiration equation (Table 1) for RA by fitting to Sullivan and Smith's data for oxygen consumption, assuming that RQ = 1.9; due to a lack of data in the literature on sablefish RQ, I assumed that RQ = CQ – 0.3, an approximation based on other fish bioenergetics models (Hanson et al. 1997). I set ACT = 1 because Sullivan and Smith (1982) studied routine respiration rates, not resting rates. The SDA, FA, and UA values were drawn from the general fish bioenergetics literature (Hanson et al. 1997). Sablefish energy density was reported by Perez (1994) and Sullivan and Smith (1982) for fish spanning 180–2200 g.

Growth and maturation parameters (Table 3) were drawn from a recent stock assessment by Schirripa and Colbert (2005). I used their female VBGF and maturation schedules, as well as their general length–weight (L–W) relationship, calculated for both sexes. Schirripa and Colbert (2005) used an alternate form of the VBGF:

(B1) $L_t = L_\infty + (L_1 - L_\infty) \cdot e^{(k \cdot (t_1 - t))}$

where L_t, L_∞, and k are as before, L_1 is an initial FL, and t_1 is the age at which the initial FL was measured (see Table 3). For sablefish with FL < 38.4 cm (i.e., smaller than the theoretical size at age t_1), I used VBGF and L–W parameters for age-0 sablefish in British Columbia waters as determined by McFarlane and Beamish (1983); their VBGF parameters use the standard form of the VBGF (Table 3).

Diet data for sablefish were derived from an extensive stomach content data set amassed during bottom trawl surveys on the US West Coast in the 1980s and 1990s (Kerim Aydin, Alaska Fisheries Science Center, NOAA Fisheries, 7600 Sand Point Way NE, Seattle, WA 98115, USA, unpublished data). Stomach contents were measured from 62 sablefish ranging in FL from 20 to 70 cm and pooled in 10 cm length bins. Energy densities for prey are from the same references as with yelloweye rockfish. Sablefish diet ontogeny is presented in Fig. 1*b*.

References

Hanson, P.C., Johnson, T.B., Schindler, D.E., and Kitchell, J.F. 1997. Fish bioenergetics 3.0. University of Wisconsin Sea Grant Institute, Madison, Wisconsin.

McFarlane, G.A., and Beamish, R.J. 1983. Preliminary observations on the juvenile biology of sablefish (*Anoplopoma fimbria*) in waters off the west coast of Canada. *In* Proceedings of the International Sablefish Symposium, Anchorage, Alaska, 29–31 March 1983. Alaska Sea Grant Report 83-8. University of Alaska, Fairbanks, Alaska. pp. 237–249.

Perez, M.A. 1994. Calorimetry measurements of energy value of some Alaskan fishes and squids. NOAA Technical Memorandum NMFS-AFSC-32, National Oceanic and Atmospheric Administration, Seattle, Washington.

Schirripa, M.J., and Colbert, J.J. 2005. Status of the sablefish resource off the continental U.S. Pacific coasts in 2005. Pacific Fishery Management Council, Portland, Oregon. Available at www.pcouncil.org/groundfish/gfsafe0406/gfsafe0406.html.

Sogard, S.M., and Olla, B.L. 2001. Growth and behavioral responses to elevated temperatures by juvenile sablefish *Anoplopoma fimbria* and the interactive role of food availability. Mar. Ecol. Prog. Ser. **217**: 121–134. doi:10.3354/meps217121.

Sullivan, K.M., and Smith, K.L., Jr. 1982. Energetics of sablefish, *Anoplopoma fimbria*, under laboratory conditions. Can. J. Fish. Aquat. Sci. **39**(7): 1012–1020. doi:10.1139/f82-136.

Appendix C. Model parameters for spiny dogfish

Bioenergetics parameters for spiny dogfish (Table 2) were largely drawn from field and laboratory studies but in some cases were derived iteratively. I estimated CB based on annual intake estimates from Jones and Geen (1977*a*) for spiny dogfish ranging from <40 cm to >90 cm (a range of ~400 to ~3500 g). I again set CTM equal to RTO and CQ at 0.3 greater than RQ (see below). The estimate for RTM is from observations by Huntsman and Sparks (1924), and RTO was assumed to be 3 °C less than RTM. I derived RA and RB values from shark oxygen consumption estimates from Sims (2000), who compiled these parameters for sharks ranging from 0.35 to 3.51 kg. I used the RQ value measured in 0.56 to 1.05 kg rough hound shark, *Scyliorhinus canicula*, held at temperatures between 7 and 17 °C (Butler and Taylor 1975); that value was conservative relative to other shark Q_{10} estimates (Sims 2000). I set ACT to 1 because the O_2 consumption study by Sims (2000) assumed routine activity levels. I used the ED estimate of Gunderson and Dygert (1988). After these values were set, I iteratively estimated CA and CTO. When CTO < 19 °C, growth of mature spiny dogfish tended to be exponential rather than asymptotic. Thus, I set CTO = 19 °C, entered the other consumption parameters (see above) into the consumption equation (Table 1), and solved for CA. I estimated CA last because that parameter (the consumption rate of a 1 g spiny dogfish at CTO) is highly theoretical, given that newborn pups are approximately 70 g (Jones and Geen 1977*b*).

Size at age was derived from the VBGF for female dogfish off the coast of Washington state (Ketchen 1975) and a length–weight (*L*–*W*) relationship described by Gunderson and Dygert (1988) (Table 3). The maturation schedule was derived from Ketchen (1972). All length measurements and length-based conversions for spiny dogfish use total length (Ketchen 1972, 1975).

Size-specific spiny dogfish diets were taken from Jones and Geen (1977*a*). Diet energy density estimates were derived from the same references as for yelloweye rockfish and sablefish. The spiny dogfish diet profile used in the model is summarized in Fig. 1*c*.

References

Butler, P.J., and Taylor, E.W. 1975. The effect of progressive hypoxia on respiration in the dogfish (*Scyliorhinus canicula*) at different seasonal temperatures. J. Exp. Biol. **63**(1): 117–130. PMID:1159356.

Gunderson, D.R., and Dygert, P.H. 1988. Reproductive effort as a predictor of natural mortality rate. J. Cons. Int. Expl. Mer, **44**: 200–209.

Huntsman, A.G., and Sparks, M.I. 1924. Limiting factors for marine animals. 3. Relative resistance to high temperatures. Contrib. Can. Biol. **2**: 97–114.

Jones, B.C., and Geen, G.H. 1977*a*. Food and feeding of spiny dogfish (*Squalus acanthias*) in British Columbia waters. J. Fish. Res. Board Can. **34**: 2067–2078.

Jones, B.C., and Geen, G.H. 1977*b*. Reproduction and embryonic development of spiny dogfish (*Squalus acanthias*) in the Strait of Georgia, British Columbia. J. Fish. Res. Board Can. **34**: 1286–1292.

Ketchen, K.S. 1972. Size at maturity, fecundity, and embryonic growth of the spiny dogfish (*Squalus acanthias*) in British Columbia waters. J. Fish. Res. Board Can. **29**: 1717–1723.

Ketchen, K.S. 1975. Age and growth of dogfish *Squalus acanthias* in British Columbia waters. J. Fish. Res. Board Can. **32**: 43–59.

Sims, D.W. 2000. Can threshold foraging responses of basking sharks be used to estimate their metabolic rate? Mar. Ecol. Prog. Ser. **200**: 289–296. doi:10.3354/meps200289.

Influence of oceanographic variability on recruitment of yellowfin tuna (*Thunnus albacares*) in the western and central Pacific Ocean

Adam Langley, Karine Briand, David Seán Kirby, and Raghu Murtugudde

Abstract: Recruitment estimates for yellowfin tuna (*Thunnus albacares*) in the western and central Pacific Ocean (WCPO), derived from a stock assessment model, are highly variable seasonally, interannually, and over decadal periods. A generalized linear model (GLM) was developed that predicts the variation in yellowfin tuna recruitment in response to a range of oceanographic variables. The GLM model accounted for 54% of the variation in quarterly recruitment for the period 1980–2003, with the inclusion of seven different oceanographic variables derived from a zone within the northwestern equatorial region of the WCPO. The robustness of the recruitment model was investigated by cross-validation. The GLM was complemented by a cluster analysis approach that identified five principal oceanographic states within the northwestern zone selected by the GLM. Incorporation of the recent GLM recruitment indices in the yellowfin tuna stock assessment model is likely to improve the precision of estimates of current and projected (next 1–2 years) biomass and exploitation rates. In a broader context, the recruitment model provides a tool to investigate how yellowfin tuna recruitment might vary in response to short- and long-term variation in the oceanographic conditions of the WCPO.

Résumé : Les estimations du recrutement de l'albacore à nageoires jaunes (*Thunnus albacares*) dans l'ouest et le centre du Pacifique (WCPO), obtenues à l'aide d'un modèle d'évaluation des stocks, varient fortement en fonction de la saison et de l'année et au cours des différentes décennies. Nous mettons au point un modèle linéaire généralisé (GLM) qui prédit la variation du recrutement de l'albacore à nageoires jaunes en réaction à une gamme de variables océanographiques. Le modèle GLM explique 54 % de la variation trimestrielle du recrutement pour la période 1980–2003 avec l'inclusion de sept variables océanographiques différentes mesurées dans une zone du nord-ouest de la région équatoriale de WCPO. Nous avons étudié la robustesse du modèle de recrutement par validation croisée. Le GLM est complété par une méthode d'analyse de groupement qui identifie cinq états océanographiques principaux dans la zone du nord-ouest retenue par le GLM. L'incorporation des indices récents de recrutement provenant du GLM dans le modèle d'évaluation des stocks des albacores à nageoires jaunes va vraisemblablement améliorer la précision des estimations de la biomasse et des taux d'exploitation courants et projetés (sur les prochaines 1–2 années). Dans un contexte élargi, le modèle fournit un outil pour déterminer de quelle manière le recrutement de l'albacore à nageoires jaunes peut changer en réaction aux variations à court et à long termes des conditions océanographiques de WCPO.

[Traduit par la Rédaction]

Introduction

Yellowfin tuna (*Thunnus albacares*) is a dominant pelagic species in equatorial waters of the world's oceans. The species is principally distributed in the epipelagic zone in areas where sea surface temperature exceeds 26 °C, with the distribution centered on tropical waters and extending to temperate waters (Suzuki et al. 1978; Maury et al. 2001). Yellowfin tuna are multiple spawners, and a reproductive behaviour appears to be related to water temperature, with the onset of spawning triggered above 24–26 °C (Ueyanagi 1969; Suzuki 1994; Wild 1994).

Yellowfin tuna in the western and central tropical Pacific Ocean (WCPO) support a large fishery that yields an annual catch of ~400 000 tonnes (Fig. 1*a*; Langley et al. 2006). Historically, yellowfin tuna were principally caught by domestic and distant-water longline vessels. Since the early 1980s, the fishery has become increasingly dominated by the purse seine method and small-scale domestic fisheries operating within the national waters of Indonesia and the Philippines (Langley et al. 2006).

In the WCPO, most of the yellowfin tuna catch is taken within the western Pacific warm pool (Fig. 1*a*), a relatively deep (~150 m depth) surface layer of warm (>28 °C) water usually confined to the western side of the ocean basin (Fig. 1*b*). The warm pool is formed by converging upper ocean currents (Fig. 1*c*) forced by the northeast trade winds in the Northern Hemisphere and the southeast trade winds in the Southern Hemisphere (McPhaden and Picaut 1990). Variability in the spatial extent of the warm pool on interannual time scales is described by the El Niño – Southern Oscillation (ENSO), with the warm pool extending into the eastern

Received 10 September 2008. Accepted 30 March 2009. Published on the NRC Research Press Web site at cjfas.nrc.ca on 25 August 2009.
J20769

Paper handled by Associate Editor Ray Hilborn.

A. Langley,[1] K. Briand, and D.S. Kirby. Oceanic Fisheries Programme, Secretariat of the Pacific Community, BP D5, 98848 Nouméa, New Caledonia.
R. Murtugudde. Earth System Science Interdisciplinary Center, University of Maryland, College Park, MD 20742-2465, USA.

[1]Corresponding author (e-mail: adam_langley@xtra.co.nz).

Fig. 1. Spatial distribution of (*a*) yellowfin tuna (*Thunnus albacares*) catch in the western and central Pacific Ocean (WCPO), (*b*) average sea surface temperature (SST), (*c*) average current flow, and (*d*) spatial stratification used in the generalized linear model (GLM) model. Yellowfin tuna catch is aggregated for 1980–2003; catches are in 10^3 tonnes. The broken line in panel (*a*) represents spatial domain of MULTIFAN-CL (MFCL) stock assessment model. SST and current are averaged over 1980–2003: SST is represented by 28 and 29 °C isotherms; current is represented by vectors. Major currents are labeled: NEC, North Equatorial Current; NECC, North Equatorial Countercurrent; SEC, South Equatorial Current. Panel (*d*) presents the finest scale spatial resolution used to aggregate oceanographic data (small boxes) and the larger area used in the final GLM (bold broken lines).

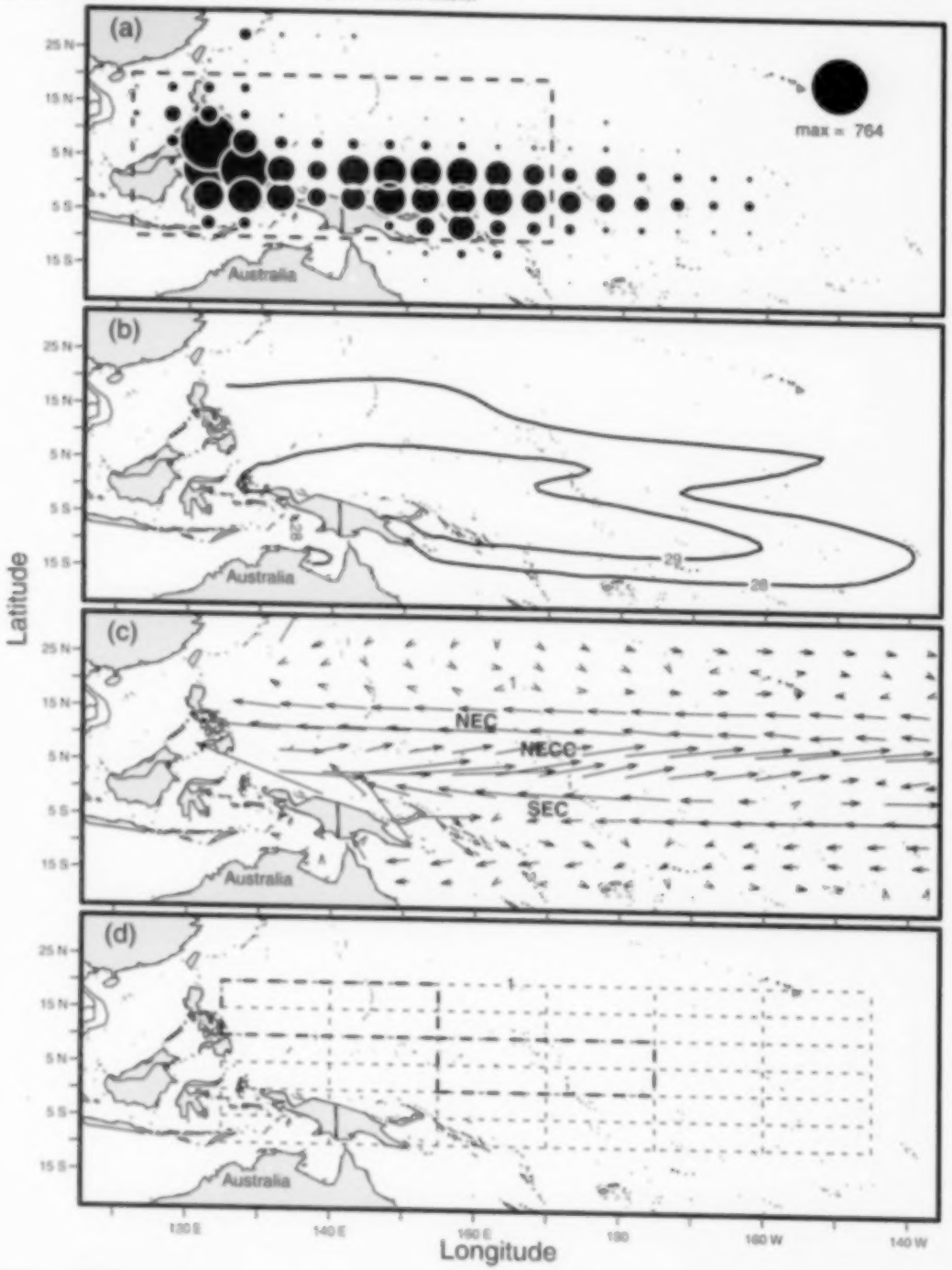

Pacific during the El Niño phase and contracting back to the western Pacific during La Niña (Picaut et al. 1996 and 2001). The longitudinal distribution of the equatorial tuna purse seine fishery also follows this pattern (Lehodey et al. 1997).

Variability of the pelagic environment at seasonal to decadal scales is likely to contribute directly to the observed variation in yellowfin tuna recruitment. The availability of oceanographic data at appropriate spatial and temporal resolution provides the opportunity to identify those variables that are most correlated with yellowfin tuna recruitment and, thereby, determine the relevance of oceanic variability to tuna recruitment at different spatio-temporal scales.

There are no direct measurements of recruitment strength for yellowfin tuna. However, estimates of recruitment strength at quarterly or annual time intervals are available from assessment models for each of the main yellowfin tuna stocks: eastern Pacific Ocean (EPO) (Hoyle and Maunder 2006), WCPO (Langley et al. 2007), Atlantic Ocean (International Commission for the Conservation of Atlantic Tunas 2004), and Indian Ocean (Indian Ocean Tuna Commission 2006). The recruitment estimates are derived as parameter estimates from the statistical population models, which integrate the available biological and fisheries data, including catch, fishing effort, and the size composition of catch. For each of these stocks, recruitment is highly variable over short and long time periods, with models for some stocks (especially in the EPO) revealing decadal shifts in recruitment (Hoyle and Maunder 2006).

For the WCPO fishery, estimates of quarterly recruitment are considered to be more reliable from the early 1980s onwards (i.e., the period for which length frequency data is available from the fisheries that predominantly catch small yellowfin tuna). These data provide the stock assessment model with sufficient information to link the individual length modes to the respective quarter when spawning occurred via the estimated growth function. Conversely, quarterly recruitment estimates from the earlier period of the model (before 1980) are likely to be less precise. Size data for this period are only available from the longline fisheries, which predominantly catch large (adult) yellowfin tuna. The modal structure of these size data represents the amalgamation of many quarterly age classes, and consequently, the model has limited information with which to resolve individual age classes.

The apparent high variation in yellowfin tuna recruitment over the short- and long-term may provide sufficient contrast to link the trends in recruitment with key oceanographic indicators and, thereby, formulate a predictive model for yellowfin tuna recruitment in the WCPO. A predictive model for yellowfin tuna recruitment would have direct application in future stock assessments for yellowfin in the WCPO and the application of the assessment model in the provision of management advice.

As in most stock assessment models, the most recent estimates of recruitment are frequently the least precise, and consequently, there is a high level of uncertainty regarding current biomass levels and fishing mortality rates, particularly for those fisheries targeting smaller fish. Unfortunately, it is this information that is most crucial to fishery managers. A reliable, predictive model would considerably improve estimates of recent and current recruitment, thereby improving estimates of current biomass and increasing the accuracy of forward projections of the stock assessment model (see Langley et al. 2007).

A predictive model may also provide greater insights into trends in recruitment for the period predating the development of the fisheries whose catch is dominated by juvenile yellowfin tuna. This may assist in resolving whether historical trends in recruitment represent genuine phase changes in productivity of the stock or, rather, are due to a misspecification of the assessment model. Lastly, the development of such a predictive model may increase the understanding of the inherent relationship between yellowfin tuna recruitment and the environment and improve our ability to interpret future trends in recruitment from the stock.

Materials and methods

Overview

A series of "observed" recruitment values were derived from a stock assessment model that encompasses the core distribution of yellowfin tuna within the WCPO. Oceanographic data were obtained and configured in such a way that a generalized linear model (GLM) could be developed, relating oceanographic variability to yellowfin tuna recruitment for the period 1980–2003. This model was then hindcast to predict yellowfin tuna recruitment for the period 1948–2003. A cluster analysis was also applied to the oceanographic data set included in the GLM to discriminate the predominate categories of prevailing oceanographic conditions occurring in the study area.

Observed recruitment

The observed recruitment values for yellowfin tuna were estimated from a stock assessment conducted using MULTIFAN-CL (MFCL; Hampton and Fournier 2001). MFCL implements a statistical, size-based, age- and spatially structured model developed and used for stock assessments of Pacific tuna and other highly migratory fish species (www.multifan-cl.org). MFCL provides estimates of population parameters, including recruitment, biomass, and fishing mortality, based on observed size frequency, catch, effort, and tagging data from the fisheries. For this study, the MFCL model was configured for yellowfin tuna in a similar manner to the model formulated for the 2007 stock assessment of yellowfin in WCPO (Langley et al. 2007); however, the spatial extent of the current model was restricted to the main area of the yellowfin tuna fishery — the western equatorial region, which accounts for 80% of the total yellowfin tuna catch from the WCPO (see Fig. 1*a*) and approximately 65% of the total WCPO recruitment (Langley et al. 2007). The single region model is described in detail in Langley et al. (2007).

The population model incorporates catch, effort, and size (length and weight frequency) data from 10 fisheries: three longline fisheries, two purse seine fisheries (associated and unassociated set types), a distant-water pole-and-line fishery, the Philippine handline fishery, and the domestic fisheries in Indonesia and Philippines waters. More details on these fisheries and the associated data are given in Langley et al. (2007).

The model encompasses the 1952–2006 period, divided into quarterly time intervals. Recruitment estimates are derived for each quarter of the model period. The recruitment estimates are computed as deviates from the estimated

Table 1. Summary of oceanographic data, sources, and a description of composite variables used in the statistical approach.

Attribute	Description	Unit	Source
tempavg	Mean sea temperature within 0–100 m depth (for spatial–temporal stratum z, β_p)	°C	ESSIC
temprange	Range in sea temperature within 0–100 m depth	°C	
currentuavg	Mean zonal (E–W) current velocity within 0–100 m depth	$m \cdot s^{-1}$	ESSIC
currentrange	Range in zonal current velocity within 0–100 m depth	$m \cdot s^{-1}$	
currentvavg	Mean meridional (N–S) current velocity within 0–100 m depth	$m \cdot s^{-1}$	ESSIC
currentvrange	Range in meridional current velocity within 0–100 m depth	$m \cdot s^{-1}$	
currentdir	Current direction	quadrant	ESSIC
ppavg	Mean primary production within 0–400 m depth	$mmol\ m^{-2} \cdot day^{-1}$	ESSIC
winduavg	Mean zonal (E–W) wind speed at 10 m altitude	$m \cdot s^{-1}$	NCEP
windvavg	Mean meridional (N–S) wind speed at 10 m altitude	$m \cdot s^{-1}$	NCEP
turbulence	Index of turbulent kinetic energy (wind speed cubed)	$m^3 \cdot s^{-3}$	NCEP

Note: ESSIC, Earth System Science Interdisciplinary Center; NCEP, National Centers for Environmental Prediction.

Fig. 2. (*a*) Quarterly estimates of yellowfin tuna (*Thunnus albacares*) recruitment (millions of fish) and (*b*) juvenile (light grey fill) and adult (dark grey fill) yellowfin tuna biomass for 1952–2004 from the MULTIFAN-CL (MFCL) stock assessment undertaken for western subequatorial region of the western and central Pacific Ocean (WCPO). Grey line in panel (*a*) represents the smoothed trend in recruitment estimates.

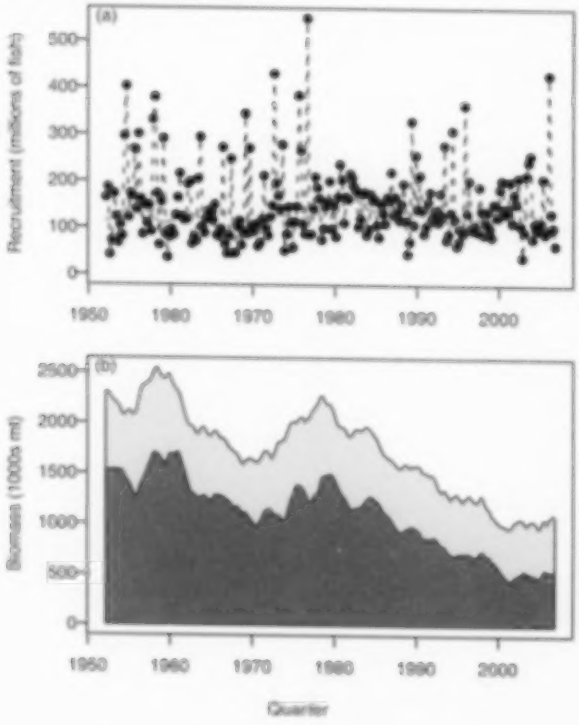

Beverton–Holt stock–recruitment relationship (SRR). The model assumes an uninformative prior for the value of steepness of the stock recruitment relationship and a very low penalty for recruitment deviations from the SRR. Growth is considered to be constant for the entire model period. The model estimate of steepness, a value of 0.865, indicates a weak relationship between recruitment and spawning biomass (i.e., a reduction in spawning biomass to 20% of the unexploited equilibrium level is predicted to result in a 13.5% reduction in equilibrium recruitment).

Only recruitment estimates from 1980 to 2003 (96 quarters) were included in the subsequent analysis. Recruitment estimates from the last 12 quarters included in the model (2004–2006) were also excluded from the subsequent analysis. Recruitment estimates were expressed as numbers of fish in the first quarterly age class included in the model (3–6 months). The distribution of the recruitment estimates closely approximated a lognormal distribution (mean = 18.74, SD = 0.40).

Oceanographic data

The analysis incorporated oceanographic data from two different sources. Most of the data, including sea surface temperature (averaged over 0–100 m depth), east–west (zonal, *u*) current component, north–south (meridional, *v*) current component (averaged over 0–100 m depth), and primary production (averaged over 0–400 m depth), were derived from a physical–biogeochemical model for the Pacific Ocean, developed at the Earth System Science Interdisciplinary Center (ESSIC), University of Maryland (Christian et al. 2002*a*, 2002*b*; Christian and Murtugudde 2003). In addition, *u* and *v* wind components at 10 m altitude were obtained from the National Centers for Environmental Prediction – National Center for Atmospheric Research (NCEP–NCAR) reanalysis provided by NOAA Earth System Research Laboratory from their web site (www.cdc.noaa.gov/cdc/data.ncep.reanalysis.derived.surface.html; Kalnay et al. 1996). All data were available for 1948–2004 and the spatial and temporal resolution was $1^\circ \times 1^\circ$ (latitude, longitude) and 30 days for ESSIC data and $2.5^\circ \times 2.5^\circ$ and 30 days for NCEP data, respectively. For each $2.5^\circ \times 2.5^\circ$ and 30-day period, an index of turbulence was calculated from *u* and *v* wind components based on the fact that turbulent kinetic energy is proportional to the third power or cube of absolute wind speed (Niller and Kraus 1977).

Generalized linear model

A two-phase approach was developed to investigate the relationship between the range of available oceanographic variables and the yellowfin tuna recruitment indices for 1980–2003. The first phase involved the identification of key zones within the western equatorial Pacific Ocean for which the oceanographic data were most highly correlated with the yellowfin tuna recruitment indices.

Fig. 3. Akaike's information criteria (AIC) values from generalized linear models (GLMs) incorporating oceanographic data from 15° latitude, 15° longitude spatial strata for the three different temporal strata (*a*: quarter prior to spawning; *b*: quarter of spawning; *c*: quarter after spawning). The asterisk (*) in panel (*b*) shows the spatial cell used to define oceanographic data sets included in the final GLM.

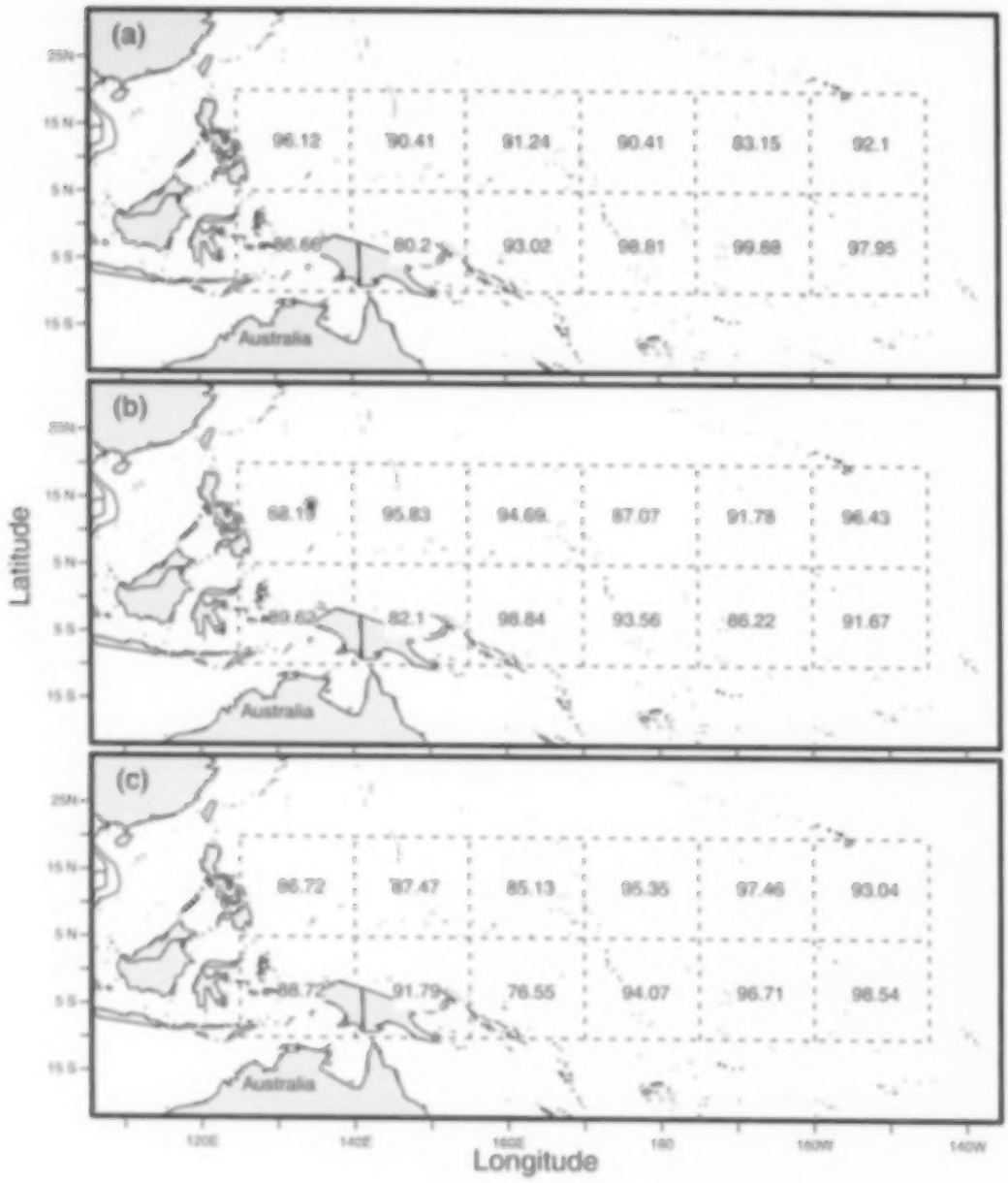

The location and spatial extent of these zones were assessed using a GLM approach with the natural logarithm of the observed recruitment values (numbers of fish) as the dependent variable with a normally distributed error structure. The oceanographic variables were included in the model in a stepwise fitting procedure. The resulting additive model incorporates the significant oceanographic variables to explain the variation in the natural logarithm of the observed recruitment values.

The western equatorial region of the Pacific Ocean (latitude 10° S to 20° N, longitude 125° E to 140° W) was divided into zones configured at six different spatial resolutions (r), resulting in 99 different spatial zones (z): 5° latitude × 15° longitude (36 zones), 10° × 15° (18 zones), 15° × 15° (12

Table 2. Proportion of the variation in observed recruitment explained by the inclusion of successive environmental variables to the final generalized linear model (GLM) (R^2) and corresponding Akaike's information criteria (AIC) value.

Variable	R^2	AIC
windsavg	0.1814	86.69
+ ppavg	0.2564	83.47
+ temprange	0.3434	77.52
+ currentvrange	0.3815	77.79
+ windvavg	0.4263	76.57
+ turbulence	0.4805	73.03
+ currentuvrange	0.5360	68.19

Fig. 4. A comparison of the natural logarithm of the observed recruitment indices (millions of fish) and predicted recruitment estimates from the final generalized linear model (GLM) model and associated 95% confidence interval. The broken line represents unity.

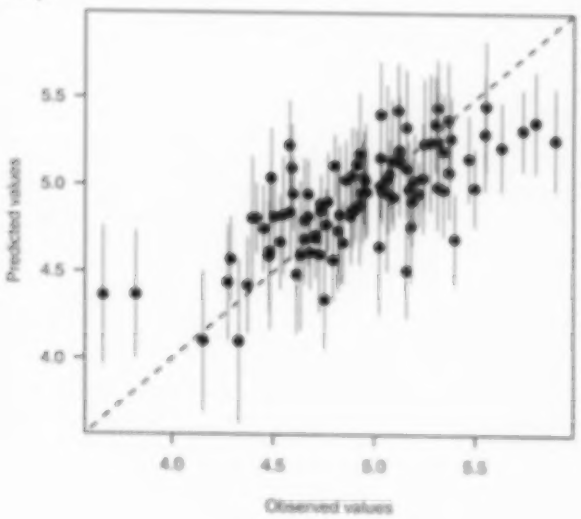

zones), 5° × 30° (18 zones), 10° × 30° (9 zones), 15° × 30° (6 zones) (see Fig. 1*d*).

For each zone, the oceanographic data included within the zone were aggregated over the spatial extent of the zone and by quarterly time period (t), and summary statistics were computed, principally the mean value and the range. The resulting list of oceanographic variables is described (Table 1). For example, for a given spatial zone of resolution r indexed by location i ($z_{r,i}$) and temporal interval t_j, the mean value of sea surface temperature was computed from the 1° × 1° latitude–longitude cells within the boundaries of the spatial zone and three monthly periods that comprised the quarterly time strata (i.e., the value of the tempavg variable, see Table 1). Similarly, the range (maximum – minimum) of sea surface temperature data from the same spatial–temporal stratum was used to calculate the value of the temprange variable. In addition, the average u and v current components (currentuavg and currentvavg, respectively) were used to derive the current direction (currentdir; in quadrants). Comparable variables were derived from the aggregated east–west and north–south current flow data (average and range) and the primary production and zonal and meridional wind components (average).

To examine the temporal influence of oceanographic conditions on recruitment, the oceanographic data for each zone were considered at three time intervals (t): the quarter prior to the quarter when spawning occurred, the quarter when spawning occurred, and the quarter following the spawning period.

In total, 297 different configurations of the oceanographic data were investigated: 99 different spatial zones (z) at the six different levels of spatial resolution (r) and the three different temporal intervals (t). For each configuration (z,t), the oceanographic variables were included as potential explanatory variables in the GLM fitting procedure. The explanatory variables were represented in the form of third-order polynomial functions, with the exception of current direction, which was categorical. The stepwise GLM was implemented using the stepAIC function in the statistical software R (Venables and Ripley 2002; R Development Core Team 2006). The forward and backward selection of significant variables was undertaken based on the Akaike's information criteria (AIC).

The initial model selection procedure can be summarized as follows. For each spatial zone (i = 1 to n), within each spatial resolution (r = 1 to 6) and each temporal interval (j = 1 to 3), (1) select spatial zone $z_{r,i}$ and temporal interval t_j; (2) determine oceanographic summary statistics for $z_{r,i}t_j$; (3) construct GLM with potential predictor variables from (2) using stepwise fitting procedure; (4) report AIC.

The spatial–temporal stratum with the lowest AIC ($z_{r^*,i^*}t_{j^*}$) was then selected as the base stratum for the final GLM model. The next phase of the model fitting involved testing the explanatory power of the model with the inclusion of oceanographic data from different areas (of the same spatial resolution (r^*) and temporal interval (j^*).

The second phase of the model building process is summarized as follows. Select initial model (lowest AIC) derived from $z_{r^*,i^*}t_{j^*}$ oceanographic data. For the other spatial zones with an equivalent spatial resolution to the initial model ($r = r^*$; i = 1 to n; $i \neq i^*$) and the temporal interval equivalent to the initial model ($j = j^*$), (1) select spatial zone $z_{r,i}$; (2) determine oceanographic summary statistics for $z_{r,i}t_{j^*}$; (3) construct GLM using stepwise fitting procedure with potential predictor variables from initial model zone–time $z_{r^*,i^*}t_{j^*}$ and second zone $z_{r,i}t_{j^*}$ (2); (4) report model and AIC.

The iterative fitting procedure minimized the simultaneous fitting of potentially hundreds of different oceanographic variables (11 variables compiled for each time–area stratum). It may also have made the resulting model easier to interpret, as it was based on oceanographic variables derived from a relatively limited spatial range. The parameterization of the individual variables included in the final GLM was examined using the "predict" function in R. For the main oceanographic variables included in the final GLM, the influence of the individual variables was investigated by examining the fitted values for each of the individual variables included within the additive model.

Table 3. Correlation matrix for the variables included in the final generalized linear model (GLM).

	winduavg	ppavg	temprange	currentvrange	windvavg	turbulence	currenturange
winduavg	1.0000	–0.5288	–0.5013	0.4056	0.8641	–0.7640	0.2358
ppavg		1.0000	0.4540	0.0128	–0.7613	0.7677	0.0150
temprange			1.0000	0.0167	–0.5747	0.4713	0.1115
currentvrange				1.0000	0.3205	–0.1784	0.4795
windvavg					1.0000	–0.8296	0.1702
turbulence						1.0000	–0.1985
currenturange							1.0000

The robustness of the final GLM was assessed following the cross-validation approach of Francis (2006). This approach involves refitting the model iteratively, successively excluding each recruitment observation (r_i). For each iteration (i), the percentage of the variation explained (PVE) by the model is calculated as the difference between the deviation between the mean of the recruitment series (excluding r_i) and the observed value (r_i) and the deviation between the estimated recruitment value (from the refitted model) and the observed value (r_i). A PVE of zero means that the model does not perform any better than the assumption of average recruitment, while a PVE of 1.0 means that the model estimates the recruitment index without error (see Francis 2006 for further details).

Hindcasting

The final GLM was employed for a hindcast by applying the predictive model to historical oceanographic data to predict recruitment for the entire period of the oceanographic model run (1948–2003). The recruitment predictions were compared with the observed recruitment estimates from the yellowfin tuna stock assessment model. Further, for each of the main oceanographic variables included within the model, the relative influence of the variables on the short- and long-term trends in predicted recruitment was examined.

Cluster analysis

For an individual spatial zone, many of the oceanographic variables included in the model data set are likely to be highly correlated. A clustering approach was applied to the oceanographic variables included in the final GLM to attempt to discriminate predominate oceanographic conditions within the study area. The resulting categories of oceanographic conditions were then compared with the observed recruitment indices (1980–2003) from the corresponding period.

The cluster analysis was undertaken using the "clara" function in the cluster package of R. The number of specified clusters was assessed by comparing the improvement in the objective function with increasing numbers of clusters.

Results

MFCL stock assessment for yellowfin tuna

There is considerable short- and long-term variation in the quarterly yellowfin tuna recruitment estimates derived from the stock assessment model (Fig. 2). Over the longer term, the stock assessment model estimates that recruitment declined during the 1950s and 1960s, increased during the late 1960s and 1970s, and remained stable at a relatively high level in the late 1970s and 1980s. Recruitment was estimated to be relatively low during the mid 1990s and high during the early 2000s. Total yellowfin tuna biomass is predicted to have declined sharply during the 1960s, increased through the 1970s, and declined sharply over the subsequent period (Fig. 2). Recent adult biomass levels are estimated to be approximately one-third of the biomass levels in the 1950s.

GLMs

The initial GLMs, derived from oceanographic data compiled for individual spatial and temporal strata, accounted for between 4% and 54% of the observed variation in the natural logarithm of the recruitment indices (1980–2003). In general, the highest explanatory power was obtained from models comprising oceanographic data from the northwestern spatial zones. For the range of spatial resolutions investigated, higher explanatory power was generally obtained from models with a relatively coarse spatial resolution (i.e., 15° latitude, 15° longitude). In relation to the temporal stratification, the highest explanatory power (lowest AIC) was generally obtained from models comprising oceanographic variables derived from the quarterly data from the period corresponding to when the fish were spawning (rather than the quarter prior to or after spawning) (Fig. 3).

The model building process first selected a 15° latitude, 15° longitude zone in the northwest of the study area (Fig. 3) for the period corresponding to the quarter of spawning. The model was then offered each of the remaining 15° × 15° zones and selected an additional zone in the southeast. The inclusion of the second zone resulted in a considerable improvement in the AIC; however, the two zone models included a total of 15 explanatory variables of the 22 potential explanatory variables (11 from each zone). It was considered that the added complexity of the two region models (an additional eight variables) outweighed the improvement in the explanatory power of the model.

The final GLM was restricted to the oceanographic data set from the northwestern zone and included 7 of the 11 potential explanatory variables: winduavg, ppavg, temprange, currentvrange, windvavg, turbulence, and currenturange (Table 2). The final GLM model has the following structure:

$$\begin{aligned}\log(\text{recruit}_i) = {} & \text{mean} + \text{poly}(\text{winduavg}, 3) \\ & + \text{poly}(\text{ppavg}, 3) \\ & + \text{poly}(\text{temprange}, 3) \\ & + \text{poly}(\text{currentvrange}, 3) \\ & + \text{poly}(\text{winduavg}, 3) \\ & + \text{poly}(\text{turbulence}, 3) \\ & + \text{poly}(\text{currenturange}, 3) \\ & + \text{error}\end{aligned}$$

Fig. 5. Predicted relationship between yellowfin tuna recruitment (natural logarithm of number of fish, in millions) and oceanographic variables included in the final generalized linear model (GLM). Broken lines represent approximate 95% confidence interval of model prediction. Distribution of data included in the model for the individual variable is presented as tick marks along the *x* axis.

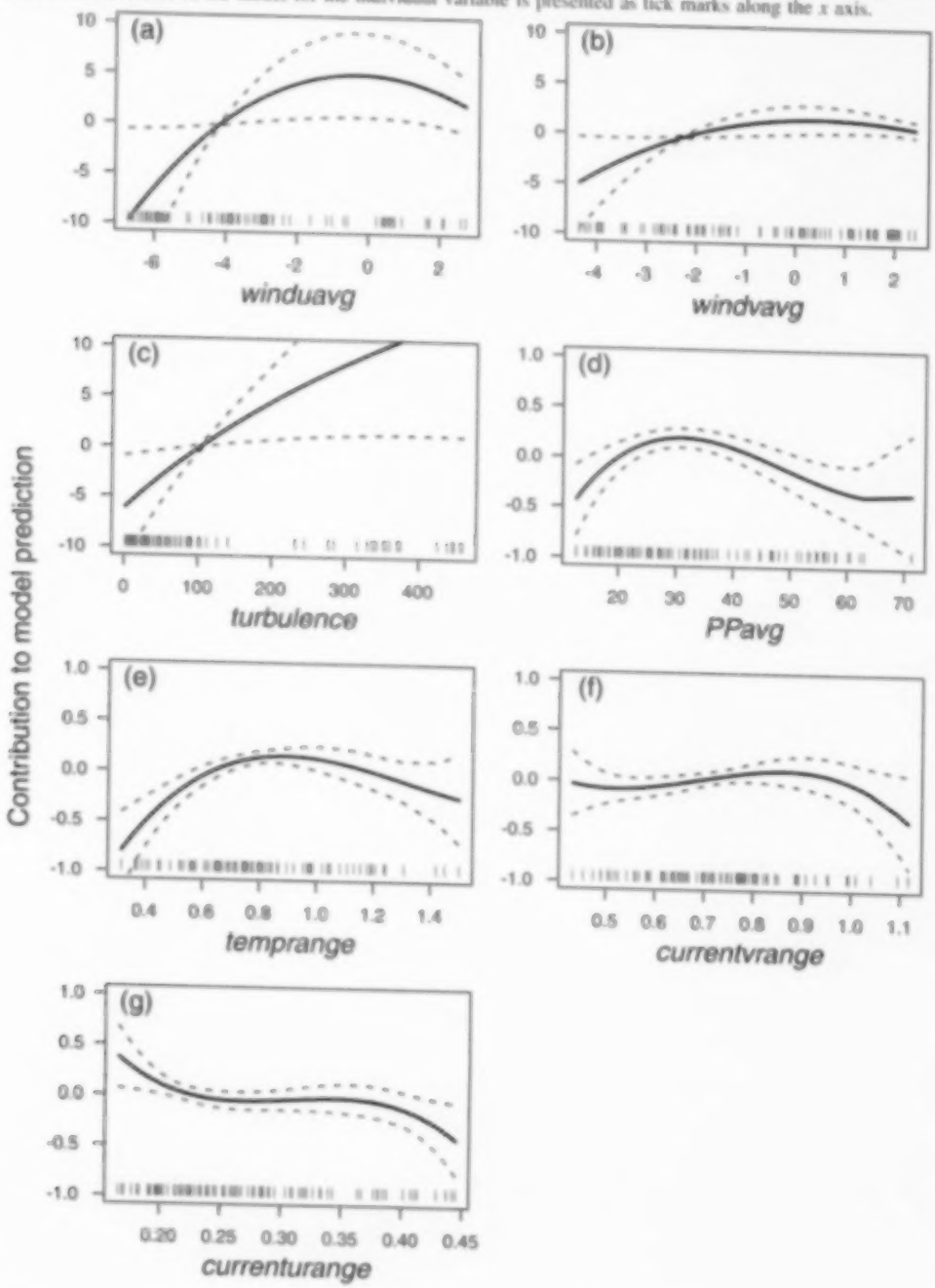

The final GLM accounts for 54% of the observed variation in the recruitment time series. The GLM approximates the observed values over the main range of the recruitment series data, although there is considerable deviation between individual observed and predicted values, and many of the predicted values are not well estimated (i.e., relatively high standard error) (Fig. 4). Further, the GLM performs poorly in predicting recruitment values at the extremes of the range; low recruitment observations are generally overestimated by the GLM and vice versa.

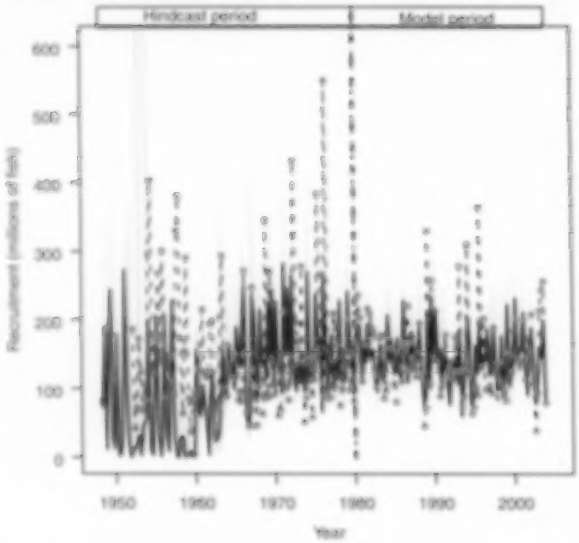

Fig. 6. "Observed" quarterly estimates of yellowfin tuna recruitment from MULTIFAN-CL (MFCL) assessment model (broken line with points) and "predicted" recruitment from final generalized linear model (GLM) for 1948–2003 (solid black line). Broken vertical line indicates the start of the period used to construct predictive model. Shaded area shows 95% confidence interval of individual recruitment prediction.

A comparison of the model residuals with the MFCL estimates of adult biomass at the time of spawning revealed no trend in the residuals. This observation is consistent with the high value of steepness of the SRR estimated by the MFCL stock assessment model.

The PVE statistics calculated from the cross-validation of the final GLM indicate that the model has moderate predictive power (median value: 0.48; range: 0.45–0.51). Essentially, the model is able to account for 48% of the observed variation in the recruitment index from the long-term mean of the series. This indicates that the final GLM is capable of providing a reasonably reliable estimate of recruitment over the range of observed oceanographic conditions.

Many of the variables included in the final GLM are highly correlated (Table 3). Consequently, it is not possible to make definitive conclusions regarding the causal affect on yellowfin tuna recruitment of the specific oceanographic variables included in the model. Instead, the variables included in the model should be considered as representing a series of indices of the prevailing oceanographic conditions that are directly or indirectly influential in determining yellowfin tuna recruitment in the region. Nonetheless, an examination of the parameterization of these variables in the final GLM is likely to be informative regarding the key variables influencing yellowfin tuna recruitment (Fig. 5).

Of the seven variables included in the model, the u and v wind component variables (windvavg and windvavg) are highly correlated (Table 3) and reveal that either southwesterly (positive windvavg and negative windvavg) or northeasterly winds prevail in the northwestern zone. The parameterization of the wind variables in the GLM indicates that higher or lower recruitment occurs during southwesterly or northeasterly conditions, respectively (Fig. 5). However, this is mediated by the parameterization of the turbulence variable (calculated from u and v wind components), which predicts recruitment increases strongly with increasing values of turbulence; turbulence is highest during period of strong southwesterly winds (Fig. 5).

Primary production (ppavg) is the second most influential variable included in the GLM. Recruitment is predicted to peak at moderate values of this variable, with lower recruitment predicted at the extremes of the range (Fig. 5). The variable defining the range in the sea surface temperature (temprange) is essentially an index of the latitudinal contrast in the sea surface temperature within the spatial strata. The final GLM predicts increasing recruitment with increased values of temprange up to a threshold level.

The variables currenturange and currentvrange are relatively uninformative in the final GLM; recruitment is predicted to remain relatively constant over the range of two variables, except for the extremities of the range where the relationship is poorly determined (Fig. 5).

Model prediction

For the model building period (1980–2003), the time series of predicted recruitment from the final GLM approximates the fluctuations in the recruitment estimates from the stock assessment model (Fig. 6). Overall, 67% of the recruitment predictions from the final GLM are within ±25% of the observed recruitment estimates from the assessment model. The recruitment predictions from the final GLM have a coefficient of variation of approximately 15%, and most of the observed recruitment estimates are within the confidence interval of the recruitment predictions from the final GLM. However, the final GLM underestimates the magnitude of some of the higher observed recruitment estimates, particularly in the early 1990s (Fig. 6).

The GLM recruitment predictions are driven by strong seasonal trends in the windvavg, turbulence, and windvavg variables (Fig. 7). The deviation of the recruitment indices from these seasonal processes is largely explained by the deviations in the ppavg and temprange variables. For example, the predictions of low recruitment in the middle and late 1990s are largely attributed to low values of the temprange variable during those periods (Fig. 7). The inclusion of these additional variables contributes to the substantial improvement in the fit of the final GLM relative to a simple GLM including season (quarter) as the sole predictive variable (14.3% compared with 54% of the observed variation in recruitment).

The final GLM was also applied to predict quarterly yellowfin tuna recruitment for 1948–1979, the hindcast period for which oceanographic data were available. For the 1950s and early 1960s, there is a divergence between recruitment predicted by the GLM and the MFCL recruitment estimates (Fig. 6). For this period, the GLM predictions are highly variable; a high proportion of the predictions are very low and most are poorly determined. For a number of the oceanographic variables (temprange, currentvrange, and currenturange), the observed values from the 1950s to early 1960s are beyond the range observed during the model building period (1980–2003), and on that basis, the GLM re-

Fig. 7. Quarterly trends for each of the key environmental variables included in the final generalized linear model (GLM) model for 1948–2003 (points and grey line) and the partition of the total recruitment prediction associated with each variable presented in each panel (black line). The summation of the recruitment predictions from each variable equals the prediction of total recruitment (expressed as the natural logarithm of the number of fish, in millions).

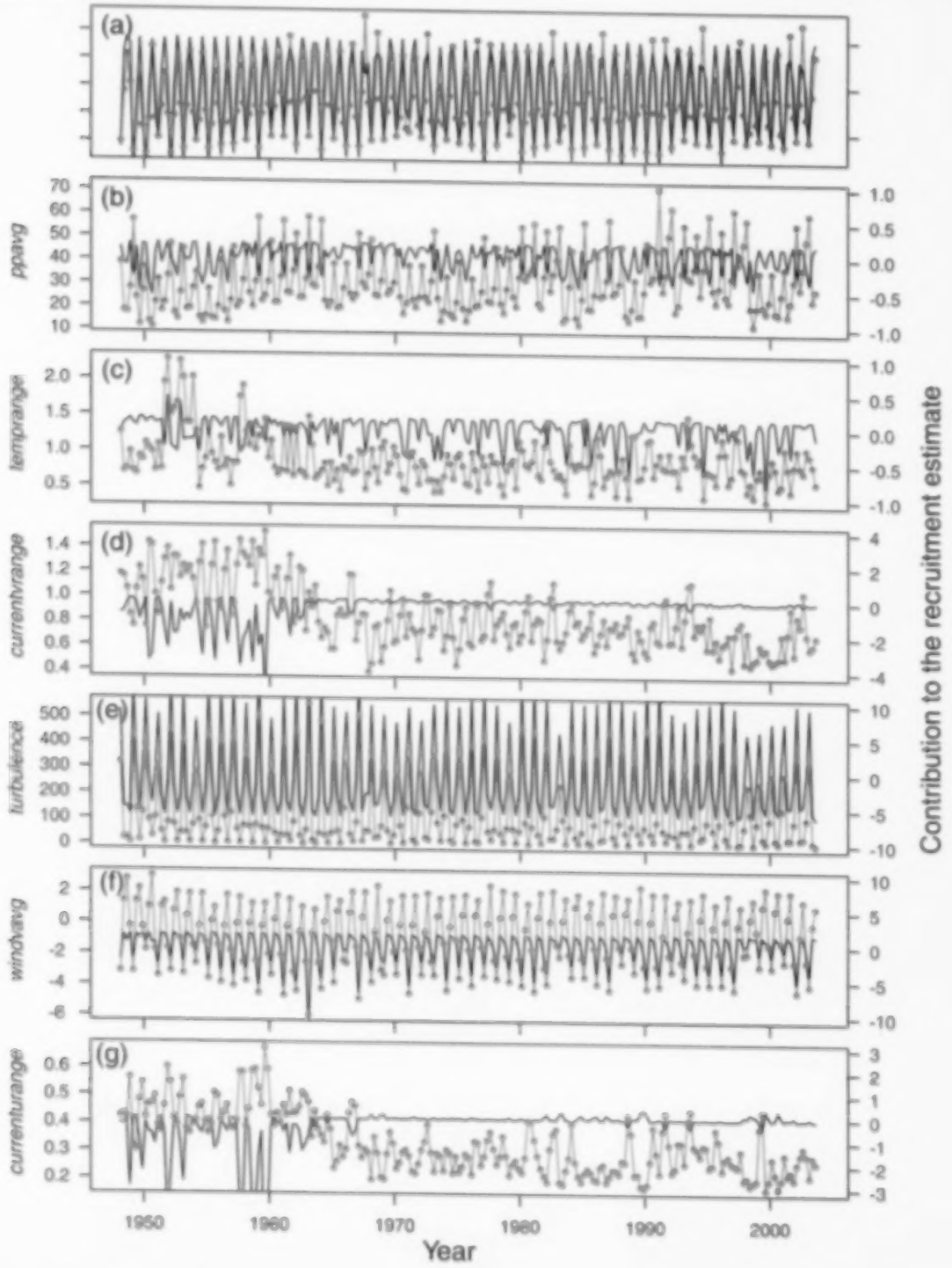

Fig. 8. A comparison of the key oceanographic variables (from the northwestern zone) included in the cluster analysis. The cluster assigned to each data point is denoted by the number (1 to 5).

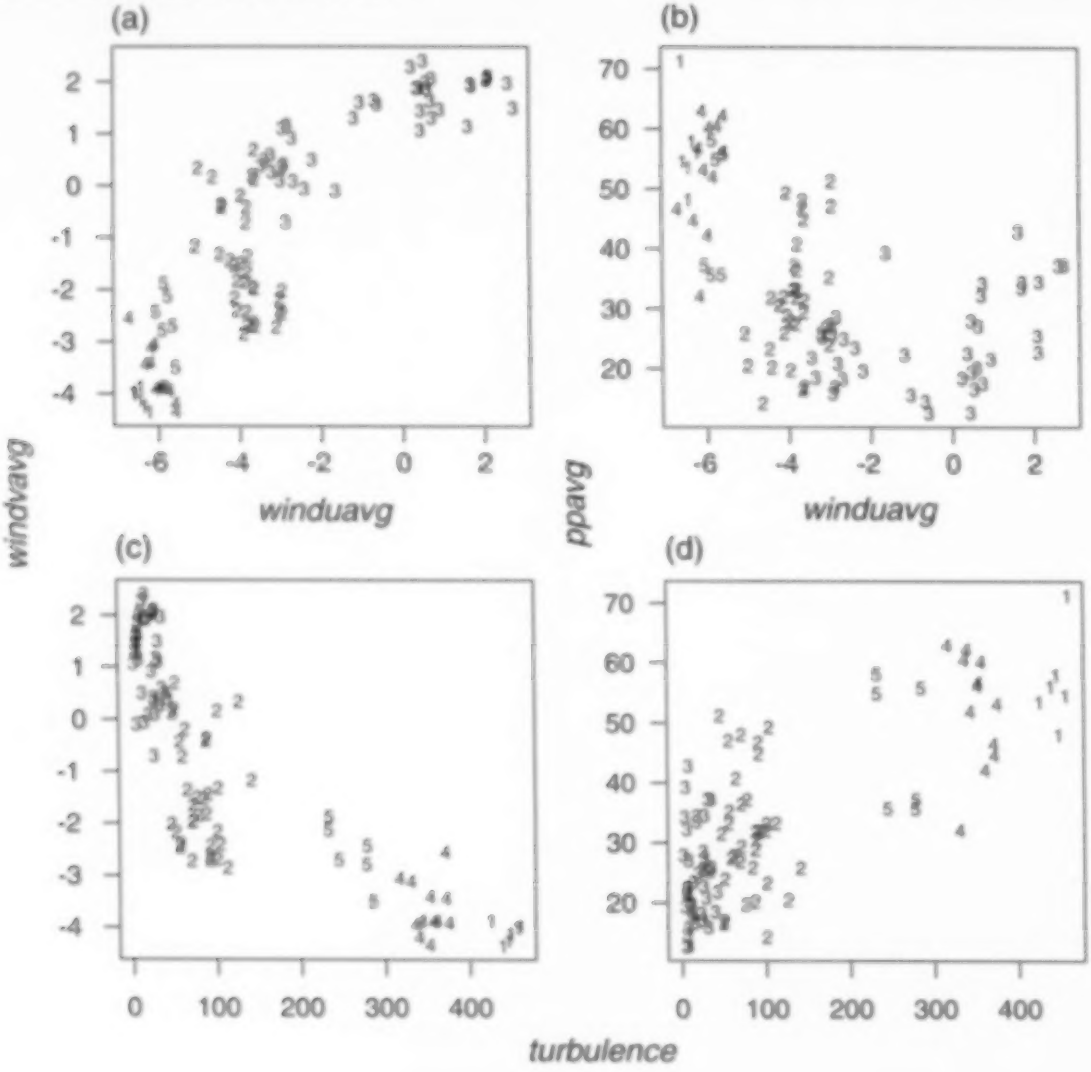

cruitment estimates from the early period should be disregarded (Fig. 7).

From the mid-1960s to 1980, the overall magnitude of the recruitment estimates predicted from the final GLM (mean value 144 million fish) is comparable to the average of the observed recruitment values for the same period (143 million fish) (Fig. 6). The predicted recruitment also appears to reflect some of the short-term variation in observed recruitment; for example, during the mid-1960s the sequences of observed and predicted recruitments are similar. However, the recruitment series are poorly correlated (correlation coefficient = 0.189); there are significant deviations between individual recruitment observations and predictions. Most notably, the GLM consistently underestimates the very high recruitments observed during the mid-1970s. Partly for this reason, the GLM does not capture the overall trend of increasing recruitment observed during the late 1960s and 1970s.

Cluster analysis

The cluster analysis of the seven oceanographic variables included in the final GLM identified five clusters. A qualitative examination of the results from the cluster analysis revealed that clusters are principally defined by four key variables: winduavg, ppavg, windvavg, and turbulence (Fig. 8, Table 4). For example, cluster 1 is characterized by year or quarters with low values for the winduavg and windvavg variables and high values for ppavg and turbulence, while the opposite is the case for cluster 3.

The MFCL recruitment observations from each year or

Table 4. Median values of the principal environmental variables for each of the five clusters defined in cluster analysis.

	Cluster				
Variable	1	2	3	4	5
windsavg	−6.45	−3.81	0.23	−6.02	−5.81
ppavg (median)	55.35	31.53	22.81	54.67	46.07
temprange	1.09	0.78	0.72	1.00	0.78
currentvrange	0.65	0.63	0.76	0.68	0.58
windvavg	−4.06	−1.65	1.45	−3.87	−2.56
turbulence	446.75	77.78	14.97	352.71	261.10
currenturange	0.22	0.26	0.26	0.24	0.27
Median recruitment	168	117	136	181.5	187.5
Mean recruitment	179.4	125.3	147.5	183.7	187.2
SD recruitment	22.8	39.4	63.9	78.1	56.1
No. of records	6	33	39	12	6

Note: The number of records (recruitment observations) and the median, mean, and standard deviation (SD) of the recruitment observations that correspond to each cluster are also presented.

quarter were grouped into the corresponding clusters. In general, observed recruitment was higher in clusters 1 and 5 and lower in cluster 2 (Table 4, Fig. 9). Observed recruitment was more variable for clusters 3 and 4, although recruitment was generally below average in the former and above average in the latter.

The oceanographic conditions corresponding to high recruitment (clusters 1 and 5) are typically characterized by strong northeasterly winds, a moderate northwestward current, and a relatively strong latitudinal gradient in sea surface temperature (compressed isotherms) within the northwestern area — the area used to derive the oceanographic variables included in the final GLM and cluster analysis (Fig. 10). Over the broader equatorial region, the oceanographic conditions corresponding to high recruitment are typically characterized by the presence of waters exceeding 30 °C in the proximity of northern Papua New Guinea and the location of the 28 °C isotherm west of 180° along the equator. These conditions occur more frequently during the first quarter of the year.

In contrast, lower recruitment generally corresponds to comparatively weaker winds, limited variation in sea surface temperature, and either westerly or southwesterly current flows within the northwestern area (clusters 2 and 3; Fig. 10). These conditions tend to occur in either the second and third quarters of the year (cluster 2) or third and fourth quarters (cluster 3).

Discussion

The spatial extent and variability of the spawning habitat of yellowfin tuna in the western tropical Pacific Ocean preclude the direct measurement of recruitment strength of yellowfin tuna cohorts. Recruitment estimates for yellowfin tuna are available as an output of an age-structured population model that integrates catch, effort data, and fish (length and weight) size data from the principal fisheries operating in the area. However, recruitment estimates may be biased because of incorrect specification of the assessment model or imprecise because of data limitations. More critically, from a management perspective, the most recent estimates

Fig. 9. Box plot of recruitment observations (1980–2003) grouped by the five clusters defined in the cluster analysis of the principal environmental variables. The box represents the interquantile range of the recruitment observations in each cluster, and the solid line represents the median value. The whiskers represent 1.5 times the interquantile range, and the points represent outliers in the data. The broken horizontal line represents the average of all the recruitment observations.

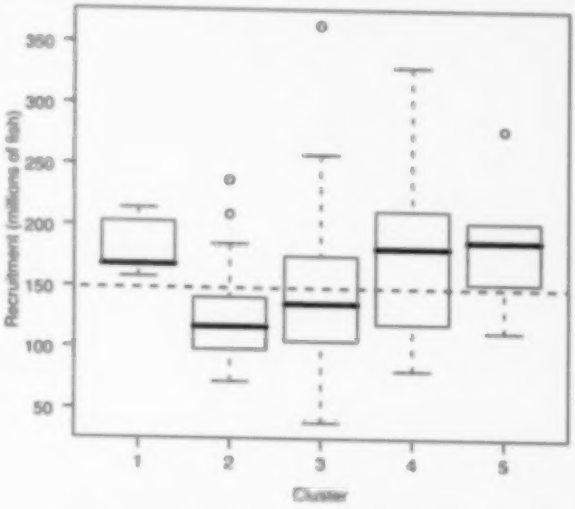

of recruitment from the assessment model tend to be the most uncertain, as there are few observations of the cohort in the fishery. Consequently, for a relatively short-lived species such as yellowfin tuna, estimates of current levels of stock biomass are also highly uncertain, as the population is dominated by a small number of cohorts. Therefore, the development of a predictive model for this species has the potential to increase the precision of the model estimates of current biomass and also improve the ability to forecast trends in biomass over the short term (1–2 years).

A moderate proportion of the variation in yellowfin tuna recruitment in the WCPO can be explained by a suite of metrics that describe the oceanographic conditions in the northwestern tropical Pacific. The results from the GLM model were also complemented by the results from the cluster analysis of the environmental data; this analysis identified five principal ocean states, and of these, higher levels of recruitment were associated with two ocean states and weaker recruitment generally corresponding to another two ocean states.

The process that links the environmental conditions in the northwestern zone with the regional variation in yellowfin tuna recruitment is unclear. There are two main hypotheses that in fact are likely to represent the extremes of a continuum. Firstly, the northwestern zone represents a major source of the total recruitment to the entire equatorial region of the western Pacific. Alternatively, the oceanography in the northwestern zone represents an indicator of the broader scale regional oceanographic conditions that influence yellowfin tuna recruitment throughout the equatorial region.

Plankton surveys have revealed that yellowfin tuna larvae are abundant throughout the western tropical region of the

Fig. 10. Examples of the prevailing oceanographic conditions from the two high recruitment clusters determined from the cluster analysis of environmental data (*a*: first quarter of 1996, cluster 1; *b*: first quarter 1999, cluster 5) and two low recruitment clusters (*c*: second quarter of 1995, cluster 2; *d*: third quarter 1996, cluster 3). The isotherms of the quarterly average sea surface temperature are plotted (solid lines). The arrows represent relative average current flow (black) and average wind flow (grey) for the zone included in the final generalized linear model (GLM) model.

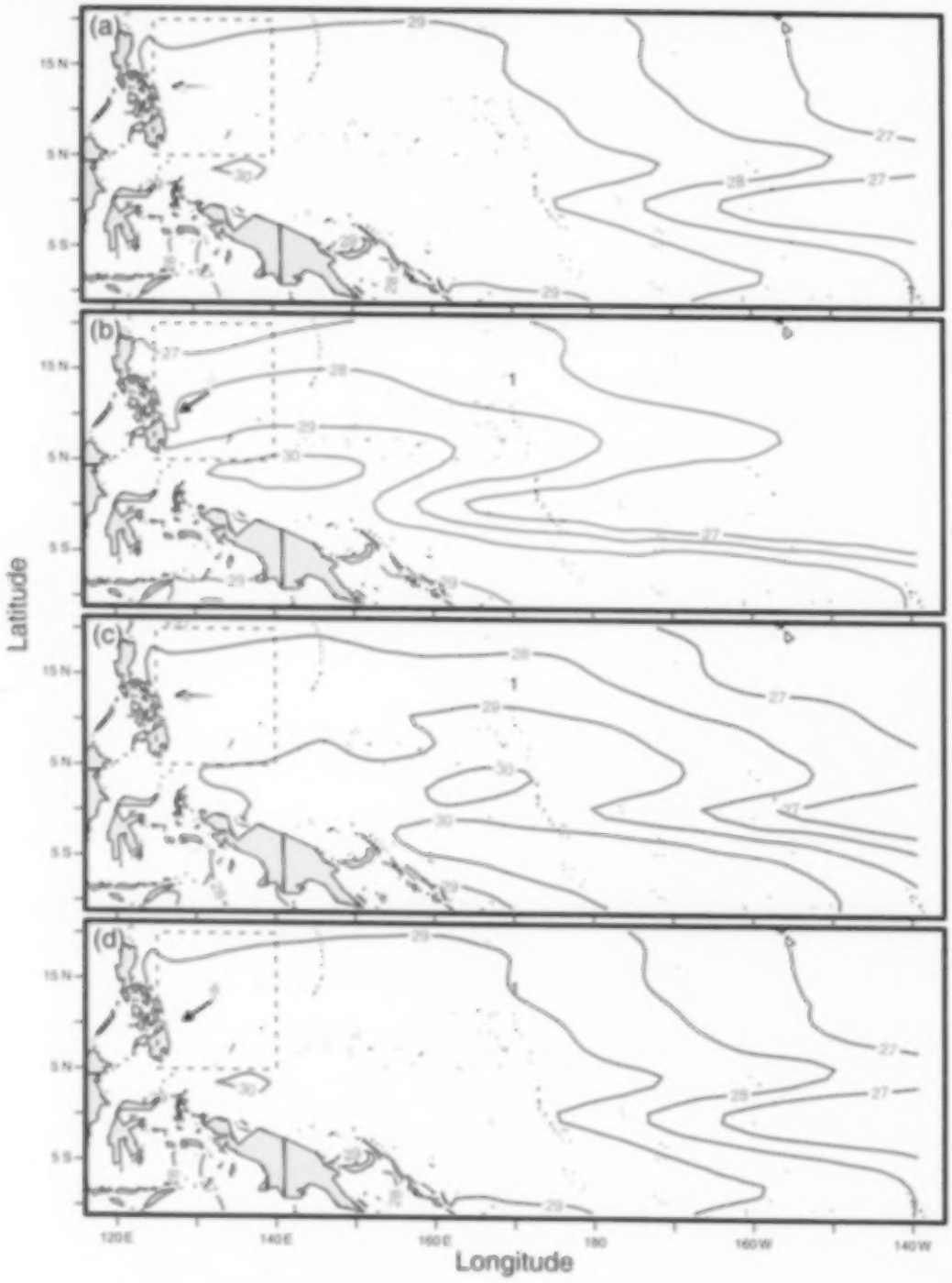

Pacific Ocean, including the northwestern zone selected in the GLM analysis (Nishikawa et al. 1985). While the northwestern zone is likely to contribute to the overall level of yellowfin tuna recruitment, it appears more plausible that the oceanographic conditions observed in this area provide a broader scale index of the oceanography of the wider area crucial for yellowfin tuna spawning and the survival of early life stages.

The predictive model does not provide a direct, mechanistic link between the prevailing oceanographic conditions and yellowfin tuna recruitment, although the statistical models do provide some insights into the broader–scale oceanographic conditions that may influence recruitment strength. For example, a recent study linked yellowfin tuna larval survivorship to water turbulence — experimentally determining the optimal turbulence intensity that enhances larval survival (Kimura et al. 2004). Turbulence was included as a variable in the final GLM model, although given the direct interaction between the two wind component variables, there is a high degree of confounding in the parameterization of these three variables. Nevertheless, the cluster analysis reveals that higher recruitment of yellowfin tuna is associated with stronger northwesterly winds, which are likely to increase turbulence of the surface layer.

The oceanographic conditions prevailing at the mesoscale (i.e., in the northwestern zone) are, in turn, likely to be broadly correlated with the oceanographic conditions at the regional scale. Lehodey et al. (2003) asserted that yellowfin tuna recruitment in the WCPO is driven by the variability in the spatial extent of the warm pool, which tends to occur when the North Equatorial Countercurrent becomes more dominant than the South Equatorial Current (El Niño conditions), allowing the warm pool to extend further east (Lehodey et al. 1997; Picaut et al. 2001). This assertion is consistent with the observation from many studies that relate yellowfin tuna spawning and larval survivorship to sea surface temperature (summarized in Suzuki 1994 and Wild 1994), with spawning occurring at water temperatures above 26 °C and optimal larval survivorship at 26–28 °C.

The present study reveals a more complex set of oceanographic conditions that are associated with variations in the level of yellowfin tuna recruitment. High recruitment tends to occur during periods of strong westward flow of the South Equatorial Current, dominating the North Equatorial Countercurrent, and a weak North Equatorial Current. These conditions coincide with northwestward currents and northeasterly winds in the northwestern zone, resulting in a strong latitudinal gradient in sea surface temperature in that area and a concentration of waters exceeding 30 °C in the western equatorial region. Conversely, this study reveals that low recruitment tends to occur during periods of lower flow of the South Equatorial Current and increased strength of the North Equatorial Countercurrent. These results somewhat contradict the general conclusions of Lehodey et al. (2003).

The statistical modeling approach attempts to provide a method of predicting the overall level of recruitment across a wide range of observed oceanographic conditions. For the model building period (1980–2003), the GLM appears to be capable of providing relatively good predictions of recruitment in the equatorial region of the WCPO; the cross-validation study indicates the model is capable of predicting almost 50% of the variation in future recruitment. Certainly, the potential to predict for the short term represents a substantial improvement over the previous assumption that recruitment would default to the long-term average recruitment for short-term projections of the yellowfin tuna stock assessment model (see Langley et al. 2007). However, for the earlier period (1962–1979), the model estimates are poorly correlated with the recruitment observations, suggesting (*i*) a departure from the modeled relationship between oceanographic conditions and recruitment, (*ii*) lower accuracy of the recruitment observations derived from the stock assessment for this period, and (or) (*iii*) lower reliability of the environmental variables derived from the ESSIC and NCEP–NCAR models during the earlier period.

The first explanation is plausible if the final GLM has failed to include key variables that over the long term are more crucial in determining yellowfin tuna recruitment or if the parameterization of the relationships between key oceanographic variables and recruitment are poorly determined for the model building period. The second explanation is also plausible. The higher level of statistical uncertainty associated with recruitment observations prior to 1980 (see Langley et al. 2007) is largely due to the lack of size frequency data from the fisheries catching small yellowfin tuna within the earlier period of the MFCL stock assessment model.

The statistical modeling has also assumed that the output from the ESSIC physical–biogeochemical model is without error or, at least, without major temporal biases in the key model outputs used in the final GLM model. Because of a lack of observational data, only limited validation of the output from the physical–biogeochemical model has been undertaken, and these assessments have been limited to the latter period included in the model (1990s) (Christian et al. 2002*a*). Christian and Murtugudde (2003) concluded that there was a general consistency between the modeled results and the range of observations available, although there are some important processes that the model represents imperfectly; for example, the model produces excessively high rates of primary production, especially under strong upwelling conditions.

Christian and Murtugudde (2003) also noted that the performance of the physical–biogeochemical model is quite sensitive to errors in the NCEP monthly mean wind stress data — the principally forcing data set included in the physical–biogeochemical model. The authors of this paper were unable to source published information regarding the relative accuracy of the NCEP data over the timeframe of the physical–biogeochemical model, although it is assumed that NCEP data is more accurate since the advent of global operational satellite observing systems starting in 1979 (Kalnay et al. 1996).

Overall, it is reasonable to conclude that the precision of both the recruitment observations (from the stock assessment model) and the key oceanographic variables (from the ESSIC model) are likely to be less well determined prior to 1980, and both sources of error are likely to be contributing to the discrepancy between the observed and predicted recruitments before 1980. Further refinement of the yellowfin tuna recruitment model is envisaged with the extension of

the recruitment time series as additional observations are available from future stock assessments and improved oceanographic data are available from future refinements to the physical–biogeochemical model.

The GLM includes no information regarding the magnitude of the spawning biomass of yellowfin tuna in the WCPO; essentially the model attributes all the short- and long-term variation in recruitment to the prevailing oceanographic conditions and assumes there is no relationship between recruitment and adult biomass, at least at the levels of stock biomass observed within the model domain. This is consistent with various stock assessments for yellowfin tuna that have tended to assume high values of steepness for the spawning stock–recruitment relationship (SRR); (i.e., there is no decline in recruitment until spawning biomass falls to very low levels; Hoyle and Maunder 2006). Hilborn and Walters (1992), in summarizing available information on SRRs, noted that tuna species are one of the major species groups where good relationships between stock abundance and recruitment have failed to appear and concluded that this is almost certainly due to the fact that the stocks are generally not fished sufficiently hard for an SRR to be evident.

There is also a circularity in the estimation of SRR for species such as yellowfin tuna that are relatively short-lived and have a short generation time, particularly when recruitment and, therefore, spawning biomass are highly autocorrelated with prevailing oceanographic conditions. For example, a period of favourable oceanographic conditions will result in high recruitment followed (within a generation) by an increase in spawning biomass. Conversely, a period of less favourable conditions will result in lower recruitment and, therefore, lower spawning biomass. If the periods of more or less favourable oceanographic conditions persist for considerably longer than the generation time of the species, then the resulting observations of recruitment and spawning biomass may be misconstrued as a strong SRR. The premise of this paper is that at the range of biomass levels observed over the history of the fishery, the variation in recruitment is essentially attributable to variation in oceanographic conditions. Nevertheless, this relationship may erode at lower biomass levels, as recruitment may become more strongly influenced by the level of spawning biomass.

The development of a reliable predictive model for yellowfin tuna recruitment has direct application to the ongoing stock assessment of yellowfin tuna in the WCPO. There is also potential to apply a similar approach to the stock assessment of yellowfin tuna and other pelagic species in other oceans, particularly for short-lived species such as skipjack tuna (*Katsuwonus pelamis*). Principally, the predictive model enables recent (last 1–2 years) recruitments to be estimated more precisely, thereby increasing the precision of estimates of current biomass and exploitation rates. The increased precision of the current age structure of the population also improves the accuracy of any short-term (next 1–2 years) stock projections from the assessment model. In a broader ecological context, the recruitment model provides a tool to investigate how yellowfin tuna recruitment may vary in response to short- and long-term variation in the oceanographic conditions in the WCPO.

Acknowledgements

This work was carried out as part of the project "Regime shifts and recruitment in western and central Pacific Ocean tuna fisheries" funded by the Pelagic Fisheries Research Program, University of Hawai'i, with additional support from the European Community funded Pacific Regional Oceanic and Coastal Fisheries (PROCFish) Project and with AusAID and NZAID programme funding to Oceanic Fisheries Programme, Secretariat of the Pacific Community. The authors acknowledge John Hampton for his guidance in the use of the MFCL software and comments on the manuscript. Keith Bigelow and two anonymous reviewers provided useful comments on a draft version of the paper.

References

Christian, J.R., and Murtugudde, R. 2003. Tropical Atlantic climate variability in a coupled physical–biogeochemical ocean model. Deep Sea Res. Part II Top. Stud. Oceanogr. **50**(22-26): 2947–2969. doi:10.1016/j.dsr2.2003.07.005.

Christian, J., Verschell, M., Murtugudde, R., Busalacchi, A., and McClain, C. 2002*a*. Biogeochemical modeling of the tropical Pacific Ocean I: Seasonal and interannual variability. Deep Sea Res. Part II Top. Stud. Oceanogr. **49**(1-3): 509–543. doi:10.1016/S0967-0645(01)00110-2.

Christian, J., Verschell, M., Murtugudde, R., Busalacchi, A., and McClain, C. 2002*b*. Biogeochemical modeling of the tropical Pacific Ocean II: Iron biogeochemistry. Deep Sea Res. Part II Top. Stud. Oceanogr. **49**(1-3): 545–565. doi:10.1016/S0967-0645(01)00111-4.

Francis, R.I.C.C. 2006. Measuring the strength of environment recruitment relationships: the importance of including predictor screening within cross-validations. ICES J. Mar. Sci. **63**(4): 594–599. doi:10.1016/j.icesjms.2006.01.001.

Hampton, J., and Fournier, D.A. 2001. A spatially-disaggregated, length-based, age-structured population model of yellowfin tuna (*Thunnus albacares*) in the western and central Pacific Ocean. Mar. Freshw. Res. **52**(7): 937–963. doi:10.1071/MF01049.

Hilborn, R., and Walters, C.J. 1992. Quantitative fisheries stock assessment. Chapman and Hall, London, UK.

Hoyle, S., and Maunder, M. 2006. Status of yellowfin tuna in the eastern Pacific Ocean in 2004 and outlook for 2005. Inter-American Tropical Tuna Commission, San Diego, Calif. Stock Assess. Rep. 6.

Indian Ocean Tuna Commission. 2006. Report of the ninth session of the Scientific Committee, Victoria, Seychelles, 6–10 November 2006 [online]. Indian Ocean Tuna Commission, Victoria, Seychelles. IOTC-2006-SC-R[EN]. Available from www.iotc.org/files/proceedings/2006/sc/IOTC-2006-SC-R[EN].pdf.

International Commission for the Conservation of Atlantic Tunas. 2004. 2003 ICCAT Atlantic yellowfin stock assessment session. SCRS/2003/016 Col. Vol. Sci. Pap. ICCAT 56. pp. 443–527.

Kalnay, E., Kanamitsu, M., Kistler, R., Collins, W., Deaven, D., Gandin, L., Iredell, M., Saha, S., White, G., Woollen, J., Zhu, Y., Leetmaa, A., Reynolds, R., Chelliah, M., Ebisuzaki, W., Higgins, W., Janowiak, J., Mo, K.C., Ropelewski, C., Wang, J., Jenne, R., and Joseph, D. 1996. The NCEP/NCAR 40-year reanalysis project. Bull. Am. Meteorol. Soc. **77**(3): 437–471. doi:10.1175/1520-0477(1996)077<0437:TNYRP>2.0.CO;2.

Kimura, S., Nakata, H., Margulies, D., Suter, J., and Hunt, S.L. 2004. Effect of oceanic turbulence on the survival of yellowfin tuna larvae. Nippon Suisan Gakkai Shi, **70**(2): 175–178 . [In Japanese with English abstract.] doi:10.2331/suisan.70.175.

Langley, A., Williams, P., and Hampton, J. 2006. The western and

central Pacific tuna fishery: 2005 overview and status of stocks. Tuna Fisheries Assessment Report 7. Secretariat of the Pacific Community, Noumea, New Caledonia.

Langley, A., Hampton, J., Kleiber, P., and Hoyle, S. 2007. Stock assessment of yellowfin tuna in the western and central Pacific Ocean, including an analysis of management options. Honolulu, Hawai'i, 13–24 August 2007. WCPFC-SC3-SA SWG/WP-1. Available from www.wcpfc.int/system/files/documents/meetings/scientific-committee/3rd-regular-session/stock-assessment-swg-working-papers/WCPFC-SC3%20SA-SWG%20WP-01.pdf.

Lehodey, P., Bertignac, M., Hampton, J., Lewis, A., and Picaut, J. 1997. El Niño Southern Oscillation and tuna in the western Pacific. Nature (London), **389**(6652): 715–718. doi:10.1038/39575.

Lehodey, P., Chai, F., and Hampton, J. 2003. Modelling climate-related variability of tuna populations from a coupled ocean–biogeochemical–populations dynamics model. Fish. Oceanogr. **12**(4-5): 483–494. doi:10.1046/j.1365-2419.2003.00244.x.

Maury, O., Gascuel, D., Marsac, F., Fonteneau, A., and De Rosa, A. 2001. Hierarchical interpretation of nonlinear relationships linking yellowfin tuna (*Thunnus albacares*) distribution to the environment in the Atlantic Ocean. Can. J. Fish. Aquat. Sci. **58**(3): 458–469. doi:10.1139/cjfas-58-3-458.

McPhaden, M.J., and Picaut, J. 1990. El Nino–Southern Oscillation displacements of the western equatorial Pacific warm pool. Science (Washington, D.C.), **250**(4986): 1385–1388. doi:10.1126/science.250.4986.1385. PMID:17754983.

Niller, P.P., and Kraus, E.B. 1977. One-dimensional models of the upper ocean. *In* Modelling and prediction of the upper layers of the ocean. *Edited by* E.B. Kraus. Pergamon Press, New York. pp. 143–172.

Nishikawa, Y., Honma, M., Ueyanagi, S., and Kikawa, S. 1985. Average distribution of larvae of oceanic species of scombroid fishes, 1956–1981. Far Seas Fish. Res. Lab, Shimizu, Japan.

Picaut, J., Ioualalen, M., Menkes, C., Delcroix, T., and McPhaden, M.J. 1996. Mechanism of the zonal displacement of the Pacific warm pool: implications for ENSO. Science (Washington, D.C.), **274**(5292): 1486–1489. doi:10.1126/science.274.5292.1486. PMID:8929400.

Picaut, J., Ioualalen, M., Delcroix, T., Masia, F., Murtugudde, R., and Vialard, J. 2001. The oceanic zone of convergence on the eastern edge of the Pacific warm pool: a synthesis of results and implications for El Niño–Southern Oscillation and biogeochemical phenomena. J. Geophys. Res. **106**(C2): 2363–2386. doi:10.1029/2000JC900141.

R Development Core Team. 2006. R: a language and environment for statistical computing [online]. R Foundation for Statistical Computing, Vienna, Austria. ISBN 3-900051-07-0. Available from www.R-project.org.

Suzuki, Z. 1994. A review of the biology and fisheries for yellowfin tuna, *Thunnus albacares*, in the western and central Pacific Ocean. *In* Proceedings of the FAO Expert Consultation on Interactions of Pacific Tuna Fisheries, 3–11 December 1991, Noumea, New Caledonia.. *Edited by* R.S. Shomura, J. Majkowski, and S. Langi. FAO Fish. Tech. Pap. 336/2. pp. 108–137.

Suzuki, Z., Tomlinson, P.K., and Honma, M. 1978. Population structure of Pacific yellowfin tuna. Bull. I-ATTC, **17**(5): 273–441.

Ueyanagi, S. 1969. Observations on the distribution of tuna larvae in the Indo-Pacific Ocean with emphasis on the delineation of the spawning areas of albacore, *Thunnus alalunga*. Bull. Far Seas Fish. Res. Lab, **2**: 177–256.

Venables, W.N., and Ripley, B.D. 2002. Modern applied statistics with S. 4th ed. Springer, New York. ISBN 0-387-95457-0.

Wild, A. 1994. A review of the biology and fisheries for yellowfin tuna, *Thunnus albacares*, in the eastern Pacific Ocean. *In* Proceedings of the FAO Expert Consultation on Interactions of Pacific Tuna Fisheries, 3–11 December 1991, Noumea, New Caledonia.. *Edited by* R.S. Shomura, J. Majkowski, and S. Langi. FAO Fish. Tech. Pap. 336/2. pp. 52–107.

Patterns of genetic differentiation between two co-occurring demersal species: the red mullet (*Mullus barbatus*) and the striped red mullet (*Mullus surmuletus*)

J.A. Galarza, G.F. Turner, E. Macpherson, and C. Rico

Abstract: The accurate identification of genetic partitioning is of primarily importance when devising conservation management strategies for today's marine resources. The great variety of genetic structure displayed by demersal species underscores the need for the identification of common patterns that can be found across species. Here, we analyse allele frequency variation at 10 microsatellite loci of two congener demersal fish, the red mullet (*Mullus barbatus*) and the striped red mullet (*Mullus surmuletus*), from the Atlantic Ocean and the Mediterranean Sea. The results indicate that two different gene flow patterns exist between these species. The red mullet's genetic distribution was found to be highly structured, resembling that of a metapopulation composed by independent, self-recruiting subpopulations with some connections between them. The striped red mullet displayed less genetic heterogeneity within the Mediterranean Sea and a substantial gene flow reduction between the Atlantic Ocean and Mediterranean Sea. Our results indicate that gene flow patterns in the demersal environment can be substantially different between closely related species with highly comparable biology, suggesting that biogeographic boundaries can affect demersal species in a different way despite common ecological features and spatial overlap. We conclude that the delimitation of such boundaries could be determined by the fine differences in life history traits between species.

Résumé : L'identification précise du partionnement génétique est d'importance considérable lorsqu'on met au point des stratégies de conservation-gestion des ressources marines actuelles. La grande variété de structures génétiques retrouvées chez les espèces démersales souligne le besoin d'identification de patrons communs qui peuvent s'appliquer à l'ensemble des espèces. Nous analysons ici la variation de la fréquence des allèles à 10 locus microsatellites chez deux poissons démersaux de même genre, le rouget de vase (*Mullus barbatus*) et le rouget de roche (*Mullus surmuletus*) de l'Atlantique et de la Méditerranée. Les résultats révèlent deux patrons de flux génique différents chez ces espèces. La distribution génétique du rouget de vase est fortement structurée ressemblant à celle d'une métapopulation composée de sous-populations indépendantes à recrutement autonome avec certaines connections entre elles. Le rouget de roche montre moins d'hétérogénéité génétique dans la Méditerranée et une réduction significative du flux génique entre l'Atlantique et la Méditerranée. Nos résultats démontrent que les patrons de flux génique dans le milieu démersal peuvent être très différents entre des espèces fortement apparentées possédant des biologies très semblables; cela laisse croire que les frontières biogéographiques peuvent affecter les poissons démersaux de façon différente malgré leurs caractéristiques écologiques communes et leur chevauchement spatial. Nous conclusons que la délimitation de telles frontières pourrait se baser sur des différences mineures de traits du cycle biologique entre les espèces.

[Traduit par la Rédaction]

Introduction

The accurate identification of population genetic subdivision is of primarily importance when devising conservation management strategies for today's marine resources. Population genetic studies are increasingly being used for population structure assessment of economically important species, providing valuable information towards their management and conservation (Cimmaruta et al. 2005). However, obtaining an accurate assessment of genetic structure patterns in the marine environment remains a difficult task. For marine species, the absence of obvious barriers to adult dispersal

Received 27 July 2008. Accepted 28 April 2009. Published on the NRC Research Press Web site at cjfas.nrc.ca on 26 August 2009. J20690

Paper handled by Associate Editor Michael Hansen.

J.A. Galarza.[1,2] Department of Biological Sciences, University of Hull, HU6 7RX, United Kingdom.
G.F. Turner. School of Biological Sciences, University of Wales, Bangor, Gwynedd LL57 2UW, United Kingdom.
E. Macpherson. Centre d'Estudis Avançats de Blanes (CSIC), Carrer d'accés a la Cala Sant Francesc, núm.14, 17300 Blanes, Spain.
C. Rico. Estación Biológica Doñana (CSIC), Av. Americo Vespucio S/N 41092, Seville, Spain.

[1]Corresponding author (e-mail: j.a.galarza@ebd.csic.es).
[2]Present address: Department of Biological and Environmental Science, University of Jyväskylä, FIN-40014, Jyväskylä, Finland.

Fig. 1. Sampling locations of *Mullus* spp. from the Atlantic Ocean and the Mediterranean Sea: CA, Canary Islands; CO, Conil; CG, Cabo de Gata; HE, Herradura; MA, Mallorca; BL, Blanes; IT, Italy; PO, Porticello; SI, Syracuse; GR, Greece; TR, Turkey. Stars indicate striped red mullet (*Mullus surmuletus*) samples; open circles indicate red mullet (*Mullus barbatus*) samples; crosses indicate both species. Mediterranean major surface current patterns and eddies are represented by solid and broken lines, respectively. Figure is modified from Alhammoud et al. (2005) and Millot (1999).

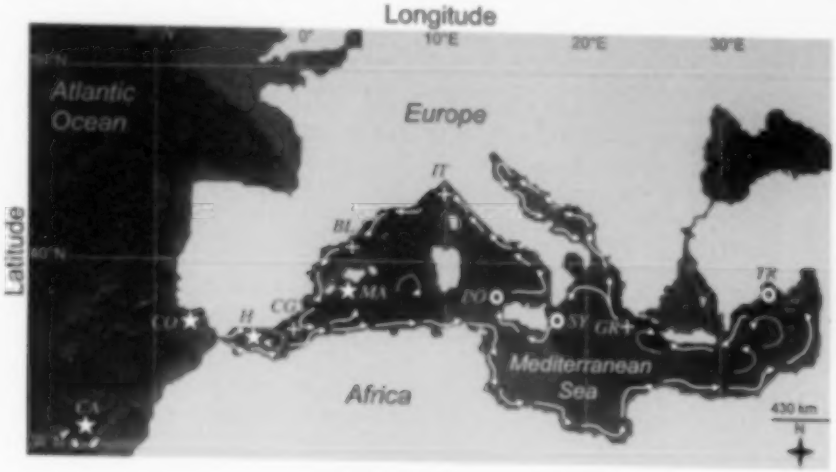

commonly allows individuals to intermix throughout the species range. In addition, physical processes such as winds and currents may favour passive transport of early-life stages, such as eggs and larvae, away from their spawning location (Botsford et al. 2001; Richards et al. 2007; Underwood et al. 2007). These possibilities of high connectivity among marine populations may greatly reduce structuring by homogenizing gene pools within relatively large areas. However, mounting evidence shows that small-scale genetic structuring is a common phenomenon even for highly mobile species with long larval phases, such as Atlantic cod (*Gadus morhua*) and Atlantic herring (*Clupea harengus*) (Knutsen et al. 2003; Jørgensen et al. 2005). Structured populations within a particular area may possess independent demographic parameters such as recruitment, mortalities, and abundances. Hence, they should be monitored as independent breeding units or stocks towards conservation management purposes.

Genetic subdivision of a particular species results from a substantial reduction of gene flow. The Mediterranean Sea consists of two partly isolated basins (western and eastern) connected by the Strait of Sicily and the narrow Strait of Messina (Cuttitta et al. 2004). The two basins differ in their oceanography, particularly in their thermal structures, salinity profiles, and circulation regimes (Millot 1999). The western Mediterranean Sea is an interesting geographical area characterized by a particular geomorphology and associated oceanography, mostly conditioned by the inflow of the North Atlantic Central Water (NACW) through the Strait of Gibraltar (Fig. 1) (Salat 1996; Millot 2005). The NACW enters continuously near the surface, and its encounter with higher density Mediterranean water generates two oceanographic fronts, separated by ~600 km. The first front (Almeria–Oran Front, AOF), situated ~400 km east from the Strait of Gibraltar, is very strong, being nearly permanent through the year, and with differences in density of 1.5 σ_t between water masses (Tintoré et al. 1988). After this first front, the original characteristics of the NACW are progressively modified, increasing its salinity, into a mass usually called modified Atlantic waters (MAW). These waters reach the northwestern Mediterranean basin through the Spanish coast and are deflected eastward by the cyclonic circulation around the Balearic Islands, forming a well-defined second density front. This second front (Balearic Front, BF) is weaker, with only differences of 0.5 σ_t between water masses and where dynamic processes are not constant through the year (Fig. 1). The MAW also reaches the islands of Corse and Sardinia. The overall MAW is also distributed along the Algerian coast, closely linked to the topography, crossing the Channel of Sicily to the Gulf of Sirta, the Italian peninsula, and around the whole eastern basin (Millot 2005). Before the entry of the Atlantic waters throughout the Strait of Gibraltar, the NACW recirculates near the Strait, in front of Cape Trafalgar, towards the northwest along the coast of Cadiz (Garcia-Lafuente et al. 2006). This area is also influenced by the intense tidal current regime of the Strait of Gibraltar and the strong topographic interaction between the swift alongshore tidal flow and a submerged ridge running perpendicular to the shoreline (Garcia-Lafuente et al. 2006; Ruiz and Garcia-Lafuente 2006). These processes originate persistently as a patch of cold water that can also affect the connectivity between populations at both sides of the Strait of Gibraltar. However, this relationship is not well studied.

Within the Mediterranean Sea, genetic differentiation at the geographical level has been reported for several taxa at particular areas. Numerous studies based on genetic markers have provided evidence for a genetic break between the Mediterranean and the Atlantic Ocean for marine species such as swordfish (*Xiphias gladius*; Kotoulas et al. 1995),

European hake (*Merluccius merluccius*; Lo Brutto et al. 2004), triplefin fish (*Tripterygion delaisi*; Carreras-Carbonell et al. 2006), pelagic crustaceans (*Meganyctiphanes norvegica*; Zane et al. 2000), marine sponges (*Crambe crambe*; Duran et al. 2004), and sea stars (*Asterina gibbosa*, *Astropecten aranciacus*) (Bazs et al. 2005). The AOF has been identified as the phylogeographical break between the Mediterranean Sea and the Atlantic Ocean associated with this front rather than with the Strait of Gibraltar mentioned above (Patarnello et al. 2007). Furthermore, the BF is also the origin of genetic subdivision in fish populations (Galarza et al. 2009). Regions such as the Sardinian channel and the Aegean Sea are also suggested as biogeographic boundaries for European anchovy (*Engraulis encrasicolus*) and gilthead seabream (*Sparus aurata*) populations (Borsa 2002; De Innocentiis et al. 2004). The Siculo–Tunisian strait has been reported to be the cause of genetic subdivision for poor cod (*Trisopterus minutus capelanus*) and Atlantic mackerel (*Scomber scombrus*) populations form eastern and western Mediterranean basins (Mattiangeli et al. 2004). However, some studies have also provided evidence of extensive gene flow occurring between Mediterranean and Atlantic basins for loggerhead sea turtle (*Caretta caretta*), Pacific chub mackerel (*Scomber japonicus*), and Norway lobster (*Nephrops norvegicus*) populations (Stamatis et al. 2004; Zardoya et al. 2004). In addition, contradictory results have also been reported for closely related species within this area by Bargelloni et al. (2003), who analysed genetic variation at nuclear and mitochondrial loci in five species belonging to the Sparidae family. The results provided evidence for a genetic break between the Mediterranean Sea and the Atlantic Ocean for only two species of the five investigated. Furthermore, intense debate still exists about genetic differences in populations of bluefin tuna (*Thunnus thynnus thynnus*) between these two basins (e.g., Broughton and Gold 1997; Pujolar et al. 2003; Viñas et al. 2003).

These discrepancies, as well as the limited understanding about (*i*) the role of the two oceanographic fronts (AOF and BF), (*ii*) the recirculation processes before the entry of the Atlantic waters throughout the Strait of Gibraltar, and (*iii*) the oceanographic differences between eastern and western Mediterranean basins, on the connectivity among populations strongly recommend additional studies on the population structure of the Mediterranean species. The Mediterranean Sea is considered as one "hot spot" in marine biodiversity (Macpherson 2002), with many fish populations close to collapse (Lleonart and Maynou 2003). Therefore, the great variety of population structure patterns displayed by demersal fish underscores the need for the identification of common gene flow patterns that can be found at the largest possible geographical extent. Common structuring patterns can be expected between closely related, ecologically similar, and co-occurring species. Here we compare spatial allele–genotype frequency variation at 10 microsatellite loci of two co-occurring demersal fish, the red mullet (*Mullus barbatus*) and its congener, the striped red mullet (*Mullus surmuletus*), from the Atlantic Ocean and the Mediterranean Sea.

The red mullet and striped red mullet are two of the main targets of the bottom trawl multispecies fishery in the Mediterranean Sea (Stergiou et al. 1997). Both species are frequently fished simultaneously with European hake (*Merluccius merluccius*) by trawlers and a range of other small-scale fishing vessels using a variety of gears (Martin et al. 1999). The red mullet is now considered as overexploited or fully exploited throughout the Mediterranean, but no reliable assessments are currently available for the striped red mullet (Food and Agriculture Organisation of the United Nations 2005). Because of their highly similar morphology (particularly during the juvenile stages), both species are frequently sold as a single species in local markets throughout the Mediterranean. The adults of the two species are, however, clearly differentiated by the profile of the head and the length of the barbels (Hureau 1986). Despite their high economic value, most genetic studies have focused on taxonomical and intraspecific relationships (Mamuris et al. 1998*a*, 1999*a*, 1999*b*), whereas only a few population genetic studies have been performed within a small portion of their distribution ranges showing the existence of structured populations of both species along some localities of the coasts of France and Greece (Mamuris et al. 1998*b*; Garoia et al. 2004). The small portion of the geographic distribution considered in these studies avoids the comparison of the population structure of these species and the oceanographic processes occurring in the Mediterranean Sea and adjacent Atlantic waters that might influence their genetic structure. Both mullets co-occur over muddy and rocky substrates along the littoral zone and display pelagic eggs and larvae (Hureau 1986; Sabatés 1990). The duration of the pelagic stage has only been documented for the striped red mullet (approximately 25–35 days; Macpherson and Raventos 2006). Nonetheless, the pelagic stage duration of the red mullet has been observed to be approximately the same length as that of the striped red mullet (E. Macpherson, personal observation). Both species are found at depths of less than 100 m and there is no evidence of adult migratory behaviour in any of the species (Hureau 1986; Özbilgin et al. 2004). However, this last point is not well studied. Our general objective is to compare the genetic structuring of these closely related and ecologically similar species across a range of common environmental conditions. Our specific aims are to (*i*) test if different structuring patterns exist within the Mediterranean Sea between the two species and (*ii*) test for differences between Atlantic and Mediterranean striped red mullet samples. The results are discussed in relation to environmental features of the Mediterranean Sea and in terms of conservation and management of the current stocks of these species.

Materials and methods

Sample collection

During the period of 2003–2005, a total of 222 red mullet (*M. barbatus*) and 212 striped red mullet (*M. surmuletus*) adult individuals were collected in nine locations within the Mediterranean Sea. An additional 78 striped red mullet adult individuals were obtained from two locations from the Atlantic Ocean in the same period (Fig. 1). No Atlantic samples could be collected for red mullet. Numbers of individuals per sampling location and species are listed (Table 1). Individuals were obtained from commercial trawls as well as through local fisherman and by scuba diving.

Table 1. Summary statistics of 10 microsatellite loci among sampling collections of red mullet (*Mullus barbatus*) and striped red mullet (*Mullus surmuletus*).

	Locus										
	Mb3	Mb11	Mb14	Mb28	Mb46	Mb55	Mb63	Mb130	Mb132	Mb133	Overall loci
***M. barbatus*, Cabo de Gata (MbCG)**											
n	48	46	44	48	45	48	48	48	48	48	47.1
a	17	9	31	2	7	12	11	11	10	12	12.2
R_s	12.823	6.254	19.014	1.699	6.41	9.715	8.919	7.259	8.223	8.557	8.887
H_e	0.909	0.600	0.953	0.063	0.815	0.867	0.852	0.714	0.808	0.796	
H_o	0.883	0.580	0.411	0.065	0.763	0.833	0.779	0.647	0.787	0.779	
F_{IS}	0.086	0.013	**0.563***	–0.023	0.081	0.033	0.091	0.112*	0.024	0.095	0.107
***M. barbatus*, Blanes (MbBL)**											
n	37	35	33	37	34	37	37	37	37	37	36.1
a	15	11	16	3	6	15	11	7	11	10	10.5
R_s	13.457	9.463	14.996	2.845	5.776	13.063	9.916	5.987	10.472	8.755	9.473
H_e	0.916	0.826	0.915	0.332	0.734	0.893	0.845	0.723	0.856	0.813	
H_o	0.875	0.810	0.157	0.400	0.681	0.860	0.830	0.698	0.841	0795	
F_{IS}	0.102	0.004	**0.336***	–0.192	0.095	0.101	0.036	0.097	0.003	0.025	0.06
***M. barbatus*, Italy (MbIT)**											
n	46	47	44	48	42	48	48	48	48	48	46.7
a	19	8	27	4	7	13	14	14	8	16	13
R_s	13.792	5.902	16.499	2.401	6.661	11.383	9.554	10.204	6.988	9.798	9.318
H_e	0.914	0.585	0.934	0.109	0.743	0.894	0.849	0.845	0.722	0.817	
H_o	0.954	0.570	0.795	0.113	0.711	0.744	0.814	0.822	0.750	0.781	
F_{IS}	–0.033	0.003	**0.360***	–0.031	0.106	0.124*	0.089	0.051	–0.027	0.108	0.075
***M. barbatus*, Porticello (MbPO)**											
n	15	15	13	15	13	15	15	15	15	15	14.6
a	10	5	8	3	6	5	7	3	6	8	6
R_s	12.194	5.925	13.362	1.748	4.295	10.467	7.891	7.465	4.297	8.437	7.608
H_e	0.875	0.656	0.836	0.225	0.723	0.653	0.704	0.375	0.777	0.820	
H_o	0.853	0.576	0.428	0.193	0.697	0.645	0.714	0.359	0.888	0.790	
F_{IS}	0.091	0.165*	**0.544***	0.096	0.042	0.013	–0.063	0.07	–0.085	0.097	0.089
***M. barbatus*, Syracuse (MbSY)**											
n	15	15	14	15	12	15	15	15	15	15	14.6
a	8	3	5	2	4	3	2	4	2	3	3.3
R_s	12.253	4.734	13.785	1.948	4.729	10.634	6.925	7.552	4.893	8.681	7.613
H_e	0.846	0.611	0.777	0.218	0.533	0.682	0.632	0.726	0.593	0.625	
H_o	0.8571	0.583	0.665	0.173	0.482	0.674	0.593	0.705	0.579	0.593	
F_{IS}	–0.065	0.087	**0.333***	0.097	0.102	0.048	0.02	0.092	0.078	0.083	0.087
***M. barbatus*, Greece (MbGR)**											
n	48	48	45	47	39	48	48	48	45	48	14.6
a	20	12	27	3	7	10	9	9	7	12	11.6
R_s	13.2	4.307	17.909	2.756	6.826	8.061	7.859	6.707	4.127	11.017	8.391
H_e	0.926	0.782	0.942	0.043	0.682	0.877	0.822	0.832	0.727	0.850	
H_o	0.914	0.750	0.761	0.044	0.679	0.817	0.803	0.814	0.742	0.836	
F_{IS}	0.028	0.085	**0.360***	–0.006	0.008	0.127*	0.019	0.047	–0.007	0.046	0.07
***M. barbatus*, Turkey (MbTR)**											
n	48	43	48	48	41	48	48	48	48	48	46.4
a	16	5	22	3	8	9	9	9	5	13	9.9
R_s	15.039	7.548	19.263	2.619	7.486	11.225	9.801	8.389	8.77	10.095	10.023
H_e	0.904	0.531	0.939	0.178	0.825	0.829	0.837	0.687	0.477	0.788	
H_o	0.887	0.500	0.770	0.192	0.800	0.792	0.710	0.661	0.615	0.751	
F_{IS}	0.021	0.077	**0.222***	–0.059	0.051	0.035	0.115*	0.067	–0.272	0.078	0.033

Table 1 (*continued*).

	Locus										
	Mb3	Mb11	Mb14	Mb28	Mb46	Mb55	Mb63	Mb130	Mb132	Mb133	Overall loci
***M. surmuletus*, Canary Islands (MsCA)**											
n	48	48	48	48	45	47	48	48	48	48	46.8
a	5	12	20	3	6	8	14	16	10	10	10.4
R_s	2.078	4.619	5.865	2.26	2.579	3.777	5.793	4.874	5.041	4.78	4.166
H_e	0.287	0.761	0.881	0.390	0.526	0.737	0.891	0.737	0.839	0.805	
H_o	0.253	0.757	0.533	0.386	0.521	0.688	0.874	0.714	0.818	0.780	
F_{IS}	0.071	0.012	**0.167***	0.013	0.002	0.077	0.054	0.048	0.017	0.025	0.048
***M. surmuletus*, Conil (MsCO)**											
n	30	30	30	30	27	30	30	29	30	30	29.7
a	7	11	16	3	6	6	13	10	11	14	9.7
R_s	2.79	4.862	5.729	2.107	3.284	3.606	4.527	4.707	5.181	5.511	4.230
H_e	0.478	0.880	0.877	0.509	0.873	0.718	0.734	0.78	0.846	0.867	
H_o	0.452	0.862	0.676	0.484	0.869	0.683	0.625	0.776	0.825	0.842	
F_{IS}	0.097	0.078	**0.243***	0.064	0.033	0.084	0.164*	0.009	0.046	0.061	0.087
***M. surmuletus*, Herradura (MsHE)**											
n	48	45	47	48	48	48	46	48	45	48	47.1
a	6	11	16	2	6	7	14	10	10	11	9.7
R_s	5.677	4.862	5.729	2	3.284	6.323	13.381	4.707	9.745	10.416	4.230
H_e	0.419	0.880	0.877	0.189	0.873	0.704	0.893	0.785	0.833	0.848	
H_o	0.444	0.868	0.743	0.182	0.765	0.653	0.815	0.760	0.846	0.793	
F_{IS}	−0.060	0.178	**0.243***	0.113	0.033	0.121	0.088	0.043	−0.015	0.122*	0.086
***M. surmuletus*, Cabo de Gata (MsCG)**											
n	46	45	48	48	44	48	48	48	48	48	47.1
a	7	18	17	2	5	7	16	15	10	17	11.4
R_s	2.963	6.029	5.923	1.251	2.424	3.434	5.481	5.219	4.712	5.749	4.318
H_e	0.560	0.901	0.892	0.065	0.524	0.703	0.868	0.834	0.816	0.881	
H_o	0.540	0.889	0.681	0.068	0.492	0.685	0.850	0.814	0.790	0.868	
F_{IS}	0.094	0.071	**0.246***	−0.024	0.101	0.078	0.007	0.032	0.066	0.022	0.069
***M. surmuletus*, Blanes (MsBL)**											
n	48	48	48	48	44	48	48	48	47	48	47.5
a	8	21	17	3	4	9	17	13	9	11	11.2
R_s	2.711	6.371	6.087	1.57	2.611	3.903	5.583	4.928	4.179	5.338	4.328
H_e	0.4933	0.919	0.905	0.160	0.579	0.748	0.868	0.799	0.7401	0.861	
H_o	0.4667	0.882	0.711	0.173	0.533	0.760	0.841	0.768	0.8261	0.848	
F_{IS}	0.065	0.075	**0.326***	−0.073	0.091	−0.006	0.097	0.048	−0.105	0.071	0.058
***M. surmuletus*, Mallorca (MsMA)**											
n	48	48	48	48	42	48	48	48	48	41	46.7
a	8	11	17	3	5	10	18	14	12	21	11.9
R_s	2.733	4.517	6.114	1.756	2.373	3.731	6.423	4.727	5.416	6.502	4.429
H_e	0.458	0.744	0.908	0.219	0.501	0.706	0.924	0.783	0.868	0.925	
H_o	0.426	0.713	0.466	0.187	0.489	0.698	0.909	0.728	0.806	0.895	
F_{IS}	0.059	0.064	**0.495***	0.081	0.058	0.002	0.011	0.127*	0.138*	0.093	0.112
***M. surmuletus*, Italy (MsIT)**											
n	48	48	45	48	46	48	48	48	48	48	47.5
a	8	17	19	4	4	6	15	8	9	13	10.3
R_s	2.415	5.935	6.207	1.899	2.418	3.601	5.657	6.522	4.585	7.444	4.268
H_e	0.3833	0.887	0.910	0.266	0.481	0.725	0.877	0.79	0.797	0.865	
H_o	0.428	0.878	0.780	0.277	0.533	0.698	0.864	0.761	0.774	0.851	
F_{IS}	−0.104	0.005	**0.193***	−0.029	−0.09	0.073	0.028	0.079	0.043	0.071	0.026

Table 1 (*concluded*).

	Locus										
	Mb3	Mb11	Mb14	Mb28	Mb46	Mb55	Mb63	Mb130	Mb132	Mb133	Overall loci
***M. surmuletus*, Greece (MsGR)**											
n	48	41	48	48	47	48	48	48	48	48	47.2
a	5	21	3	2	4	6	17	19	9	13	9.9
R_s	2.156	6.385	2.079	1.59	2.454	3.679	5.483	5.874	4.073	9.974	3.974
H_e	0.3435	0.917	0.510	0.18	0.507	0.729	0.864	0.883	0.727	0.891	
H_o	0.3590	0.882	0.278	0.200	0.484	0.714	0.832	0.869	0.714	0.879	
F_{IS}	–0.032	0.071	**0.216***	–0.097	0.065	0.013	0.089	0.067	0.032	0.021	0.044

Note: n, number of individuals, a, number of alleles; R_s, allelic richness; H_e, expected heterozygosity; H_o, observed heterozygosity; F_{IS}, inbreeding coefficient (Weir and Cockerham 1984). Asterisks represent significant F_{IS} at $\alpha = 0.05$. Significant values after false discovery rate (FDR) correction are presented in bold.

Microsatellite data analysis

DNA extractions were performed from pectoral fin and barbel tissue following HotSHOT protocol (Truett et al. 2000). Ten dinucleotide microsatellite loci originally isolated from the red mullet were successfully amplified by polymerase chain reaction as described in (Galarza et al. 2007). Amplified products were resolved on an ABI3100 Genetic Analyzer (Applied Biosystems). Allele scoring was carried out using GeneMapper v. 3.5 software (Applied Biosystems, Foster City, California). The total number of alleles per locus and sample was obtained using GENETIX v. 4.01 (Belkhir et al. 1997). The program FSTAT v. 2.9.3 (Goudet 1995) was used to determine allelic richness, which quantifies the number of alleles independently of sample size. Observed and expected heterozygosities were calculated using the software package Arlequin v. 2.0 (Schneider et al. 2000). Deviations from Hardy–Weinberg expectations (HWE) were estimated according to the level of significance determined by means of 10 000 Markov chain Monte Carlo (MCMC) iterations using GENEPOP v. 3.4 (Raymond and Rousset 1995). To correct for possible type I errors when performing multiple tests, we employed a false discovery rate (FDR) approach (Benjamini and Hochberg 1995; Verhoeven et al. 2005). The FDR can be viewed as the fraction of false positives among all tests that are declared significant. For example, setting an FDR of 5% means that (on average) 5% of the tests declared significant are actually false positives.

Within-species population structure

For each species, the null hypothesis of nondifferentiation of allelic and genotypic distributions across all sample pairs (geographic locations) within the sampling area was tested. Significance of both tests was obtained by 10 000 iterations executed in GENEPOP v. 3.4 (Raymond and Rousset 1995). To estimate the overall effects of gene flow among samples, pairwise F_{ST} values and their estimated probabilities were calculated by 10 000 permutations using GENETIX v. 4.01 according to Weir and Cockerham (1984). The alternative hypothesis of significant genetic differentiation was accepted if the probability was equal or less than 0.05. FDR corrections were applied for multiple tests (Verhoeven et al. 2005). Finally, the software MSAnalyzer v. 2.39 (Dieringer and Schlötterer 2003) was used to compute Nei's standard genetic distance (D) among population samples. A multidimensional scaling (MDS) analysis of D was performed to examine the population's genetic relationships on a two-dimensional plane using MATLAB v. 7.0 (The MathWorks Inc., Natick, Massachusetts).

M. barbatus vs. *M. surmuletus* population structure

We compared the genetic distribution patterns of both species by two different approaches. For these tests, only Mediterranean populations were included. First, we compared the pattern of genetic divergence over geographical distance of both species through a genetic spatial autocorrelation analysis using GENALEX v. 6 (Peakall and Smouse 2006). The autocorrelation coefficient (r) provides a measure of the genetic similarity between pairs of individuals whose geographic separation falls within a given distance class (Smouse and Peakall 1999). We set an increment of 500 km for each class and included only those individuals of both species sampled at the same geographic locations. Thus, comparisons between species over the same geographical distance are examined. Statistical significance for the null hypothesis of no significant autocorrelation was determined by creating 95% confidence intervals around r values through 999 random permutations. If the calculated r value falls outside these confidence intervals, then individuals in that class are more similar than would be expected by chance. Likewise, the first intercept of the r value with the x axis represents the largest geographic distance at which individuals become genetically independent. This distance has been interpreted as the average distance of gene flow per generation (Sokal and Wartenberg 1983), often referred to as neighborhood or genetic patch size (Peakall et al. 2003; Palumbi 2004; Laikre et al. 2005; but see below). Second, we compared the overall level of structuring between the species by analyzing the number of significant F_{ST} pairwise comparisons across all loci. Here, we tested for differences in the distribution of significant pairwise F_{ST} counts displayed by each species at each locus. Statistical significance for the differences between count's distributions was attained through a Wilcoxon t test.

Results

Microsatellite variability

The total number of alleles per locus ranged from 2 to 27 in red mullet (*M. barbatus*) and from 2 to 21 in striped red mullet (*M. surmuletus*) (Table 1). Expected heterozygosity and overall genetic variability as judged by allelic richness

Table 2. Population pairwise F_{ST} values (above diagonal) and geographic distances given in kilometres (below diagonal) among samples of *Mullus barbatus* (Mb, *a*) and *Mullus surmuletus* (Ms, *b*).

(*a*) *Mullus barbatus*.

	MbCG	MbBL	MbIT	MbGR	MbTR
MbCG		0.022*	0.015*	0.021*	0.068*
MbBL	1086		0.031*	0.034*	0.079*
MbIT	1776	689		−0.006	0.080*
MbGR	3965	2879	2189		0.082*
MbTR	4998	3911	3222	1032	

(*b*) *Mullus surmuletus*.

	MsCA	MsCO	MsHE	MsCG	MsBL	MsMA	MsIT	MsGR
MsCA		0.0161	0.216*	0.150*	0.153*	0.180*	0.152*	0.216*
MsCO	1175		0.137*	0.086*	0.090*	0.140*	0.088*	0.156*
MsHE	1350	174		0.021*	0.033*	0.137*	0.020*	0.042*
MsCG	1544	368	194		0.001	0.127*	0.017*	0.066*
MsBL	2630	1455	1280	1086		0.134*	0.019*	0.067*
MsMA	2059	1069	894	700	385		0.105*	0.146*
MsIT	3320	2145	1970	1776	689	1075		0.070*
MsGR	5510	4334	4159	3965	2879	3264	2189	

Note: CA, Canary Islands; CO, Conil; CG, Cabo de Gata; HE, Herradura; MA, Mallorca; BL, Blanes; IT, Italy; GR, Greece; TR, Turkey.

*Significant at $\alpha = 0.05$ after false discovery rate (FDR) correction.

were slightly higher in red mullet than in striped red mullet (Table 1). We found no evidence of linkage disequilibrium between locus pairs. Significant deviations from HWE within sampling locations were observed in both species. Out of 140 tests performed across species, 14 remained significant after FDR correction. For both species, the totality of significant departures occurred in locus Mb14 across all sampling locations (Table 1). This is most likely due to technical causes such as mis-scoring or poor amplification. Therefore, locus Mb14 was removed from subsequent analysis. Finally, because of the relatively low number of individuals and to avoid statistical sample-size artefacts, the two red mullet samples from Sicily (MbPO and MbSY, $n = 15$ for each) were not included in further analyses. However, F_{ST} value for this population pair was highly significant (data not shown).

Within-species population structure

The exact tests for homogeneity of allelic and genotypic frequency distributions indicated that single discrete populations exist within the sampling area for both species. Both exact tests showed significant differences between all sample pairs (significant at $P < 0.0001$ after FDR correction), except for the Italian and Greek red mullet samples and for the Italian and the Spanish samples of Blanes and Cabo de Gata of the striped red mullet. Population pairwise F_{ST} values were congruent with both exact tests. For the red mullet, differentiation was observed between all population pairwise comparisons performed except for the Italian and Greek samples (Table 2). The majority of comparisons among the striped red mullet populations were also significantly different, the exceptions being those between the Spanish samples from Cabo de Gata and Blanes, but more surprisingly between those two samples and the sample from northwestern Italy (Table 2). Furthermore, no significant differentiation was observed between the Atlantic striped red mullet samples form the Canary Islands and Conil (Table 2).

MDS analysis showed a clear genetic grouping for striped red mullet, with the Atlantic populations of the Canary Islands and Conil forming one group and the majority of the Mediterranean population samples (Italy, Blanes, and Cabo de Gata) forming another. Interestingly, the population from Herradura clustered between these two groups. The Balearic population from Mallorca and the Greek population clustered separately from these groups as well as from each other (Fig. 2*b*). A more complex pattern was observed for the red mullet, with high genetic similarity displayed between the geographically distant Italian and Greek populations. Unsurprisingly, the Turkish population was the most distinct, while Spanish populations of Blanes and Cabo de Gata clustered separately (Fig. 2*a*).

M. barbatus vs. *M. surmuletus* population structure

Spatial autocorrelation analysis between pairs of individuals revealed a significant positive genetic autocorrelation at the 500 km distance class for red mullet and at the 500, 1000, 1500 km distance classes for the striped red mullet ($P < 0.05$). No other significant autocorrelation was found for the rest of spatial distance classes in either species (Fig. 3). The level of genetic autocorrelation decreased sharply for the red mullet populations and more continuously for the striped red mullet as geographical distance increased. The correlogram curve first intercepted the x axis at 842 km for the red mullet, whereas for the striped red mullet it intercepted at 1723 km (Figs. 3*a*, 3*b*). This suggests a genetic patch size of 500–1000 km for the red mullet and 1500–2000 km for the striped red mullet. It is important to note, however, that caution should be taken when interpreting this result. A single correlogram may not reflect accurately the true nonrandom spatial genetic pattern. The

Fig. 2. Multidimensional scaling plot of population's genetic distance for red mullet (*Mullus barbatus*) (*a*) and striped red mullet (*Mullus surmuletus*) (*b*). CA, Canary Islands; CO, Conil; CG, Cabo de Gata; HE, Herradura; MA, Mallorca; BL, Blanes; IT, Italy; GR, Greece; TR, Turkey.

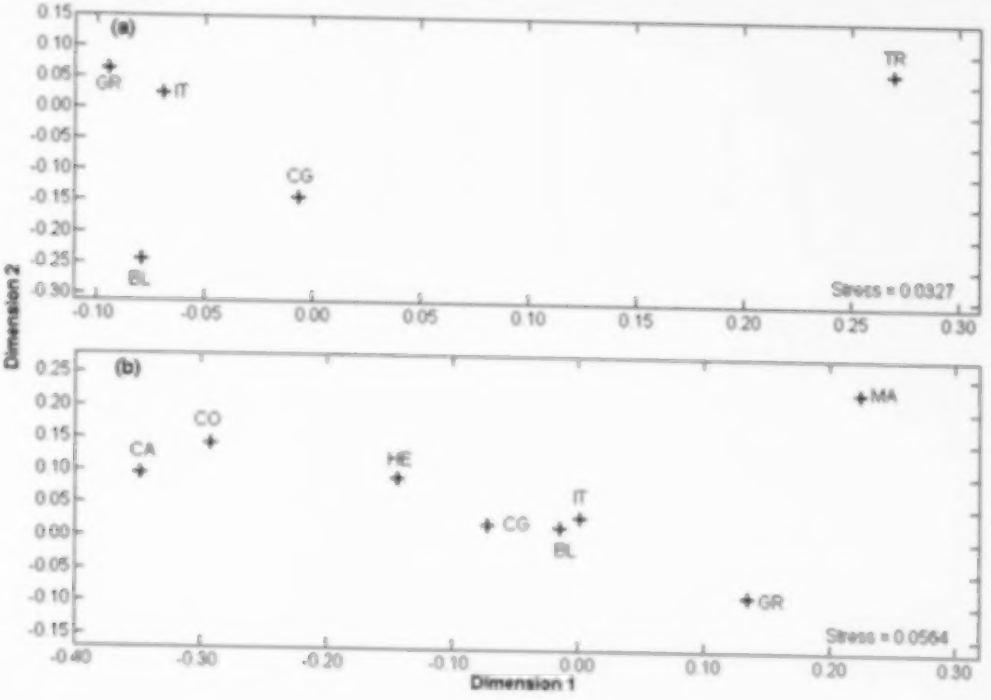

Fig. 3. Genetic autocorrelation (*r*) for red mullet (*Mullus barbatus*) (*a*) and striped red mullet (*Mullus surmuletus*) (*b*) individuals as a function of distinct geographic distance classes. The first intercept of the *r* value with the *x* axis (horizontal line at zero) represents the largest geographic distance at which populations become genetically independent. Broken lines indicate upper and lower 95% confidence intervals about the null hypothesis of no significant ($P < 0.05$) autocorrelation as determined by bootstrapping.

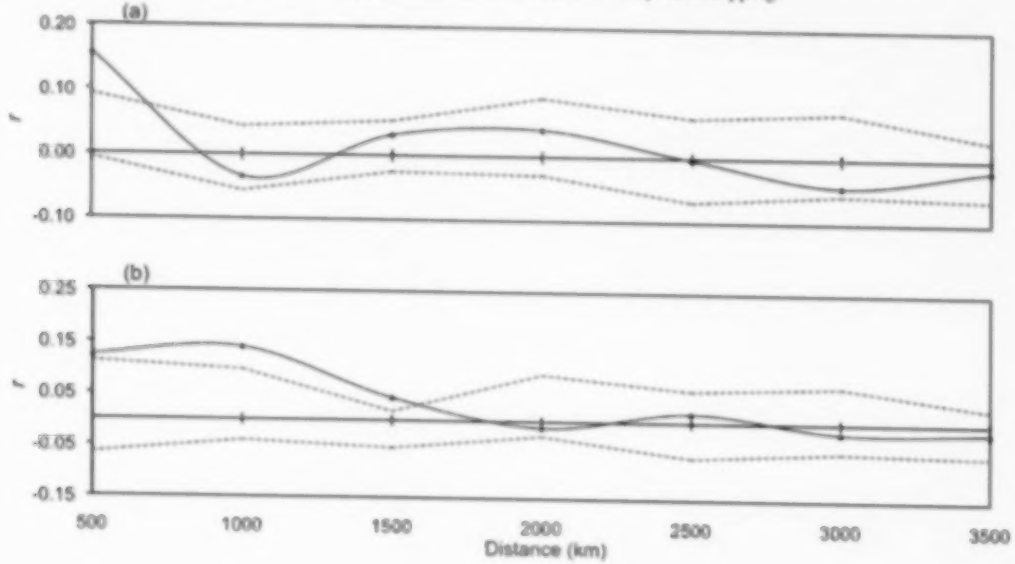

Fig. 4. Significant ($P < 0.05$) pairwise F_{ST} counts in each locus for the red mullet (*Mullus barbatus*) (solid bars) and the striped red mullet (*Mullus surmuletus*) (open bars).

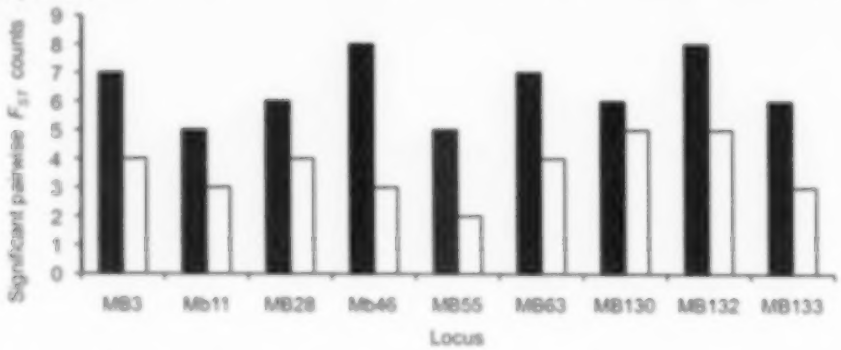

geographic distance at which the r value intercepts with the x axis largely depends on the extent of the genetic structure, the size of the distance class chosen, and the associated number of samples per distance class (Peakall and Smouse 2006). However, in our case, it may be appropriate to interpret these results as evidence that gene flow primarily occurs over shorter geographical distances for the red mullet relative to the striped red mullet. Congruently, the t test revealed that significant differences exist between the species' distributions of significant pairwise F_{ST} counts ($P < 0.05$). Out of the 90 pairwise tests performed in each species across all loci, 58 were significant for the red mullet, whereas only 33 showed significant differences in the striped red mullet (Fig. 4).

Discussion

Overall genetic diversity

In this study, a comprehensive genetic evaluation of the Mediterranean populations of red mullet (*M. barbatus*) and striped red mullet (*M. surmuletus*) was carried out covering a large fraction of the distribution ranges of these species. Our results showed high genetic variability in both species. These results are in line with previous genetic studies where large numbers of alleles per locus and high heterozygosity values have been found in both species using allozymes (Mamuris et al. 1998*b*; Mamuris et al. 1999*b*), as well as using microsatellites in the red mullet (Garoia et al. 2004). No previous microsatellite studies are available for the striped red mullet. Nonetheless, overall genetic variability values were nearly as high as those of red mullet, although this could also be due to the hypervariability of the loci analysed.

Within Mediterranean analysis

Our results showed two distinct patterns of genetic distribution within the Mediterranean, as well as a greater level of structuring in the red mullet. The spatial genetic autocorrelation analysis revealed a much shorter genetic patch size for the red mullet relative to the striped red mullet. Likewise, the red mullet displayed almost twice the number of significant F_{ST} counts across loci over the same area. The differences in genetic distribution among the species can be easily illustrated by direct comparison of samples taken at the same localities. For example, the red mullet showed significant genetic differentiation across Cabo de Gata – Blanes–Italy comparisons, whereas the striped red mullet display genetic homogeny for the same comparisons. Furthermore, striped red mullet samples from Greece and Italy showed significant genetic differences, whereas the opposite was true for the red mullet. Below, we discuss possible causes and propose different hypotheses for such discordant genetic distribution patterns between these species.

The Cabo de Gata – Blanes–Italy samples are located along the Liguro–Provençal–Catalan (LPC) current, which follows a quasipermanent southwestern trajectory alongside the coasts of Italy, France, and Spain at a mean surface velocity of 0.35 m·s^{-1} (Mounier et al. 2005). The LPC is one of the major current systems in the Mediterranean Sea. The core of the current extends from 25 to 45 km from the coast to a depth range between 400 and 650 m. (Conan and Millot 1995; Mounier et al. 2005). The spawning area of both mullets lies well within such a current system. Therefore, considering the long pelagic stages of the species, it can be suggested that drifting eggs and larvae could potentially be transported along this current system, homogenizing neutral allele frequencies into a single gene pool within this region. This notion could help explain the lack of genetic differentiation observed for the striped red mullet. However, as mentioned above, direct observation has shown that early-life history traits are highly similar in both species. Thus, the same pattern would be expected for the red mullet. This discordant result suggests that the species may differ in some trenchant, perhaps yet undetected life history trait(s) presumably developed at the juvenile or adult stage.

On the other hand, the finding that red mullet populations from Greece and Italy did not show any apparent differences between them (as opposite to striped red mullet) is puzzling considering that these locations are separated by more than 2100 km with no apparent surface circulation pattern interconnecting them. The Mediterranean's eastern and western basins are separated by the Strait of Sicily, also referred to as the Siculo–Tunisian Strait. Hydrographic measurements show that surface Atlantic water follows the African coast eastwards, entering the western basin through this strait to balance the water mass deficit due to evaporation (Alhammoud et al. 2005). This phenomenon is commonly identified as subsurface minimum of salinity between 30 and 200 m

depth (Ozsoy et al. 1989). Various studies have pointed at these peculiar oceanographic conditions taking place at the Siculo–Tunisian Strait as the main cause of limited gene flow between eastern and western Mediterranean basins. Populations of species such as sea bass (*Dicentrarchus labrax*), poor cod (*Trisopterus minutus capelanus*), Atlantic bluefin tuna (*Thunnus thynnus thynnus*), and Atlantic mackerel (*Scomber scombrus*) have all showed a clear genetic discontinuity between eastern and western basins (Bahri-Sfar et al. 2000; Carlsson et al. 2004; Zardoya et al. 2004). These genetic differences, however, are not observed in other species such as European hake (*Merluccius merluccius*) and swordfish (*Xiphias gladius*) (Lundy et al. 1999; Pujolar et al. 2002). Direct comparisons, however, cannot be precisely established with the above studies because of the use of different molecular markers and (or) sampling schemes. Furthermore, there are differences in life history traits between red mullet and those species, which include pelagic forms with schooling and homing behaviour. Nevertheless, Mamuris et al. (1998*b*, 1999*b*) found a clear genetic subdivision pattern for red mullet populations between the eastern and western Mediterranean basins using enzyme-coding loci and random amplified polymorphic DNA (RAPD). Two main hypotheses may be established to explain the results obtained in the present study. (*i*) The existence of nonsampled populations occurring along the Mediterranean coast of Italy assists in the exchange of migrants between these populations, thereby maintaining similar frequencies of neutral alleles. (*ii*) The populations were historically linked but currently are in the process of splitting. In any event, the fact that the transition zone reported at the Siculo–Tunisian Strait does not seem to be effective for red mullet, whereas apparently it holds true for striped red mullet, warrants further investigation.

The Atlantic–Mediterranean transition

A sharp genetic divide was detected when comparing striped red mullet samples originating from the Atlantic Ocean and samples originating from the Mediterranean Sea. This same pattern has been previously observed for other demersal species with Atlanto-Mediterranean distributions (Patarnello et al. 2007; Galarza et al. 2009). The Mediterranean Sea is connected to the Atlantic Ocean through the Strait of Gibraltar. As mentioned above, this strait has been hypothesized to represent the division between two biogeographic regions: the Northeast Atlantic and the Mediterranean (Quignard 1978). In this area, a strong inflow transports less saline surface Atlantic waters into the Alboran Sea, creating an Atlantic domain within the Mediterranean and partially isolating the Alboran Sea from the other Mediterranean basins (Tintoré et al. 1988). However, it is still uncertain whether this transition zone extends homogeneously throughout the Alboran Sea until the well-identified biogeographic barrier at the AOF or if further subdivision occurs. Our sampling scheme for the striped red mullet included one location (Herradura) between the Strait of Gibraltar and the AOF and another (Conil) in Atlantic waters, near the Strait and separated by ~170 km. The results show a clear genetic differentiation between the two localities, suggesting that the oceanographic processes occurring before the entry of the Atlantic waters throughout the Strait of Gibraltar also play an important role in the genetic structure of this species. The lack of structure between the two Atlantic localities (Canary Islands and Conil, separated by more than 1000 km) reinforces the relevance of the oceanographic dynamism around the Strait of Gibraltar.

At the Alboran Sea, the main circulation is characterized by two semipermanent, anticyclonic vortices that give rise to the western and eastern Alboran gyres (Viúdez et al. 1998). Here, nutrient-enriched water produced by upwelling and Atlantic inflow is recirculated before it propagates eastwards along the African coast (Béranger et al. 2005). This flow pattern may induce retention–concentration mechanisms of pelagic larvae within this enriched water. Hence, favorable conditions for eggs and larval development arise, promoting nearby recruitment by potentially retaining early life stages long enough to develop. Likewise, juvenile and adult individuals may also benefit from these retention–concentration mechanisms by encountering favorable foraging conditions in these highly productive waters, thus remaining within the area. Occasional adult dispersal and passive transport may occur from adjacent Atlantic and Mediterranean samples, although this may not be enough to prevent short-term genetic drift between Atlantic and Mediterranean populations. Furthermore, the present pattern of marine currents in the area seems to assist in maintaining this differentiation.

The Balearic Islands have also been considered as a breakpoint delimiting the distribution boundaries for Atlanto-Mediterranean fauna (Abelló et al. 2002). In this study, significant differences were observed between the sample from the Balearic Islands (Mallorca) and the rest. However, the magnitude of differentiation was smaller between the Mediterranean samples than that of the Atlantic samples. These differences are originated by the BF that reduces the gene flow between these islands and other localities (i.e., Blanes and Italy) (Galarza et al. 2009). Although some passive dispersal could potentially occur between the islands and the mainland, levels of genetic exchange may be too low to prevent drift, perhaps allowing local adaptation and enhancing recruitment of locally produced larvae, as suggested by the relatively large F_{IS} values found at this sampling site.

This study complements previous genetic studies performed on the red mullet across the eastern Mediterranean Sea (Mamuris et al. 1998*a*; Garoia et al. 2004). Here, we provide data from a large fraction of the Mediterranean distribution of both mullets. More sampling is needed along the Mediterranean coast of Italy as well as from the North Atlantic and Mediterranean African coast to have representative samples from the complete distribution range of the species and elucidate management conservation strategies accordingly. However, to date, all red mullet studies coincide in the existence of different subpopulations or stocks across relatively small areas, an indication that effective dispersal is limited in this demersal species. Within the Mediterranean Sea, red mullet's genetic distribution resembles that of a metapopulation structure composed of largely independent, self-recruiting subpopulations, with some connections between them. Each of these subpopulations can have a different response to environmental variables and human-induced activities (i.e., fishing pressure), and consequently,

all should be monitored independently and considered as separate management units.

On the other hand, this is the first microsatellite-based study of striped red mullet populations. Our results coincide with the bulk of studies that have found a reduction of gene flow between the Atlantic Ocean and Mediterranean Sea for other demersal species. This is consistent with the current management policy for these species, in which Atlantic and Mediterranean stocks are considered separate stocks. Nonetheless, within the Mediterranean Sea, the genetically homogeneous populations from the Northwest Mediterranean ought to be considered as a shared stock between countries or regions for conservation management purposes, whereas populations originating from the Balearic Islands and Greece should be managed as regionally segregated populations that have little or no intermixing with their respective surrounding populations.

Overall, both species showed different genetic patterns, neither of which was similar to those of other commercially exploited demersal fish species in the area. These results can have relevant implications particularly for multispecies fisheries where each species has a different level of genetic structure. We show that the patterns of genetic distribution in the demersal environment can be substantially different even between closely related species with highly comparable ecologies. This indicates that marine biogeographical boundaries can affect in a different way species sharing many ecological features with spatial overlap. Furthermore, the delimitation of such boundaries could be largely influenced by fine differences in life history traits between species. This emphasizes the importance of understanding the basic biology of species that are fished simultaneously. A reasonable strategy would be to regulate multispecies fisheries according to the most finely grained structure found. However, in view of the international context of this fishery, this appears as a difficult task. Repeated sampling is needed to ensure temporal stability of the genetic differences observed. Nonetheless, the overall pattern of spatial variation in allele–genotype distribution is unlikely to change substantially between species based on the congruency of previous and current genetic evidence. More research is needed to obtain an accurate characterization of life history traits of both species, particularly during the juvenile–adult stages.

Acknowledgements

The authors thank Josep Carreras, Ettore Randi, Costas Triantaphyllidis, Alexander Triantaphyllidis, Paola Laiolo, Ma. Carmen Argüello, and H. Tuncay for their help in collecting and providing samples. The authors are also grateful to Pilar Bazaga for her valuable help in extracting DNA. This work was funded in part by the Mexican Council for Science and Technology (CONACyT) and Junta de Andalucia Ref. 2003X880_1.

References

Abelló, P., Carbonell, A., and Torres, P. 2002. Biogeography of epibenthic crustaceans on the shelf an upper slope off the Iberian Peninsula Mediterranean coasts: implications for the establishment of natural management areas. Sci. Mar. **66**: 183–193.

Alhammoud, B., Béranger, K., Mortier, L., Crépon, M., and Dekeyser, I. 2005. Surface circulation of the Levantine Basin: comparison of model results with observations. Prog. Oceanogr. **66**(2–4): 299–320. doi:10.1016/j.pocean.2004.07.015.

Bahri-Sfar, L., Lemaire, C., Ben Hassine, O.K., and Bonhomme, F. 2000. Fragmentation of sea bass populations in the western and eastern Mediterranean as revealed by microsatellite polymorphism. Proc. R. Soc. B Biol. Sci. **267**: 929–935. doi:10.1098/rspb.2000.1092.

Bargelloni, L., Alarcon, J.A., Alvarez, M.C., Penzo, E., Magoulas, A., Reis, C., and Patarnello, T. 2003. Discord in the family Sparidae (Teleostei): divergent phylogeographical patterns across the Atlantic–Mediterranean divide. J. Evol. Biol. **16**(6): 1149–1158. doi:10.1046/j.1420-9101.2003.00620.x. PMID: 14640406.

Baus, E., Darrock, D.J., and Bruford, M.W. 2005. Gene-flow patterns in Atlantic and Mediterranean populations of the Lusitanian sea star *Asterina gibbosa*. Mol. Ecol. **14**(11): 3373–3382. doi:10.1111/j.1365-294X.2005.02681.x. PMID:16156809.

Belkhir, K., Borsa, P., Goudet, J., Chikhi, L., and Bonhomme, F. 1997. Genetix v.4.01 logiciel sous Windows TM pour la génétique des populations. Laboratoire Génome, Populations, Interactions, Montpellier, France.

Benjamini, Y., and Hochberg, Y. 1995. Controlling the false discovery rate: a practical and powerful approach to multiple testing. J. R. Stat. Soc. B. **57**: 289–300.

Béranger, K., Mortier, L., and Crépon, M. 2005. Seasonal variability of water transport through the Straits of Gibraltar, Sicily and Corsica, derived from a high-resolution model of the Mediterranean circulation. Prog. Oceanogr. **66**(2-4): 341–364. doi:10.1016/j.pocean.2004.07.013.

Borsa, P. 2002. Allozyme, mitochondrial-DNA, and morphometric variability indicate cryptic species of anchovy (*Engraulis encrasicolus*). Biol. J. Linn. Soc. **75**: 261–269.

Botsford, L.W., Hastings, A., and Gaines, S.D. 2001. Dependence of sustainability on the configuration of marine reserves and larval dispersal distance. Ecol. Lett. **4**(2): 144–150. doi:10.1046/j.1461-0248.2001.00208.x.

Broughton, R.E., and Gold, J.R. 1997. Microsatellite development and survey of variation in northern bluefin tuna (*Thunnus thynnus*). Mol. Mar. Biol. Biotechnol. **6**: 308–314.

Carlsson, J., McDowell, J.R., Díaz-Jaimes, P., Carlsson, J.E., Boles, S.B., Gold, J.R., and Graves, J.E. 2004. Microsatellite and mitochondrial DNA analyses of Atlantic bluefin tuna (*Thunnus thynnus thynnus*) population structure in the Mediterranean Sea. Mol. Ecol. **13**(11): 3345–3356. doi:10.1111/j.1365-294X.2004.02336.x. PMID:15487994.

Carreras-Carbonell, J., Macpherson, E., and Pascual, M. 2006. Population structure within and between subspecies of the Mediterranean triplefin fish *Tripterygion delaisi* revealed by highly polymorphic microsatellite loci. Mol. Ecol. **15**(12): 3527–3539. doi:10.1111/j.1365-294X.2006.03003.x. PMID:17032255.

Cimmaruta, R., Bondanelli, P., and Nascetti, G. 2005. Genetic structure and environmental heterogeneity in the European hake (*Merluccius merluccius*). Mol. Ecol. **14**(8): 2577–2591. doi:10.1111/j.1365-294X.2005.02595.x. PMID:15969736.

Conan, P., and Millot, C. 1995. Variability of the northern current off Marseilles, western Mediterranean Sea, from February to June. Oceanol. Acta, **18**(2): 193–205.

Cuttitta, A., Arigo, A., Basilone, G., Bonanno, A., Buscaino, G., Rollandi, L., Garcia Lafuente, J., Garcia, A., Mazzola, S., and Patti, B. 2004. Mesopelagic fish larvae species in the Strait of Sicily and their relationships to main oceanographic events. Hydrobiologia, **527**(1): 177–182. doi:10.1023/B:HYDR.0000043299.65829.2f.

De Innocentiis, S., Lesti, A., Livi, S., Rossi, A.R., Crosetti, D., and

Sola, L. 2004. Microsatellite markers reveal population structure in gilthead sea bream *Sparus auratus* from the Atlantic Ocean and Mediterranean Sea. Fish. Sci. **70**(5): 852–859. doi:10.1111/j.1444-2906.2004.00879.x.

Dieringer, D., and Schlötterer, C. 2003. Microsatellite analyser (MSA): a platform independent analysis tool for large microsatellite data sets. Mol. Ecol. Notes, **3**(1): 167–169. doi:10.1046/j.1471-8286.2003.00351.x.

Duran, S., Pascual, M., Estoup, A., and Turon, X. 2004. Strong population structure in the marine sponge *Crambe crambe* (Poecilosclerida) as revealed by microsatellite markers. Mol. Ecol. **13**(3): 511–522. doi:10.1046/j.1365-294X.2004.2080.x. PMID: 14871357.

Food and Agriculture Organisation of the United Nations. 2005. Review of the state of world marine fishery resources. FAO, Rome, Italy. Fish. Tech. Pap. 457.

Galarza, J.A., Turner, G.F., Macpherson, E., Carreras-Carbonell, J., and Rico, C. 2007. Cross-amplification of 10 new isolated polymorphic microsatellite loci for red mullet (*Mullus barbatus*) in striped red mullet (*Mullus surmuletus*). Mol. Ecol. Notes, **7**(2): 230–232. doi:10.1111/j.1471-8286.2006.01551.x.

Galarza, J.A., Carreras-Carbonell, J., Macpherson, E., Pascual, M., Roques, S., Turner, G.F., and Rico, C. 2009. The influence of oceanographic fronts and early-life-history traits on connectivity among littoral fish species. Proc. Natl. Acad. Sci. U.S.A. **106**(5): 1473–1478. doi:10.1073/pnas.0806804106. PMID:19164518.

Garcia-Lafuente, J., Delgado, J., Criado-Aldeanueva, B.M., Del Rio, J., and Vargas, J.M. 2006. Water mass circulation on the continental shelf of the Gulf of Cadiz. Deep Sea Res. Part I Oceanogr. Res. Pap. **53**(11-13): 1182–1197. doi:10.1016/j.dsr2.2006.04.011.

Garoia, F., Guarniero, I., Piccinetti, C., and Tinti, F. 2004. First microsatellite loci of red mullet (*Mullus barbatus*) and their application to genetic structure analysis of Adriatic shared stock. Mar. Biotechnol. **6**(5): 446–452. doi:10.1007/s10126-004-3045-x. PMID:15791489.

Goudet, J. 1995. FSTAT (Version 1.2): a computer program to calculate F-statistics. J. Hered. **86**: 485–486.

Hureau, J.C. 1986. Mullidae. *In* Fishes of the north-eastern Atlantic and the Mediterranean. *Edited by* P.J.P. Whitehead, M.L. Bauchot, J.C. Hureau, J. Nielsen, and E. Tortonese. UNESCO, Paris, France. pp. 877–882.

Jorgensen, H.B.H., Hansen, M.M., Bekkevold, D., Ruzzante, D.E., and Loeschcke, V. 2005. Marine landscapes and population genetic structure of herring (*Clupea harengus* L.) in the Baltic Sea. Mol. Ecol. **14**(10): 3219–3234. doi:10.1111/j.1365-294X.2005.02658.x. PMID:16101787.

Knutsen, H., Jorde, P.E., André, C., and Stenseth, N.C. 2003. Fine-scaled geographical population structuring in a highly mobile marine species: the Atlantic cod. Mol. Ecol. **12**(2): 385–394. doi:10.1046/j.1365-294X.2003.01750.x. PMID:12535089.

Kotoulas, G., Magoulas, A., Tsimenides, N., and Zouros, E. 1995. Marked mitochondrial DNA differences between Mediterranean and Atlantic populations of the swordfish, *Xiphias gladius*. Mol. Ecol. **4**(4): 473–481. doi:10.1111/j.1365-294X.1995.tb00241.x.

Laikre, L., Miller, L.M., Palmé, A., Palm, S., Kapuscinski, A.R., Thoresson, G., and Ryman, N. 2005. Spatial genetic structure of northern pike (*Esox lucius*) in the Baltic Sea. Mol. Ecol. **14**(7): 1955–1964. doi:10.1111/j.1365-294X.2005.02570.x. PMID: 15910318.

Lleonart, J., and Maynou, F. 2003. Fish stock assessments in the Mediterranean: state of the art. Sci. Mar. **67**: 37–49.

Lo Brutto, S., Arculeo, M., and Parrinello, N. 2004. Congruence in genetic markers used to describe Mediterranean and Atlantic populations of European hake (*Merluccius merluccius* L. 1758). J. Appl. Ichthyology, **20**(2): 81–86. doi:10.1046/j.1439-0426.2003.00514.x.

Lundy, C.J., Moran, P., Rico, C., Milner, R.S., and Hewitt, G.M. 1999. Macrogeographical population differentiation in oceanic environments: a case study of European hake (*Merluccius merluccius*), a commercially important fish. Mol. Ecol. **8**(11): 1889–1898. doi:10.1046/j.1365-294x.1999.00789.x. PMID: 10620232.

Macpherson, E. 2002. Large-scale species-richness gradients in the Atlantic Ocean. Proc. R. Soc. Lond. B Biol. Sci. **269**(1501): 1715–1720. doi:10.1098/rspb.2002.2091.

Macpherson, E., and Raventos, N. 2006. Relationship between pelagic larval duration and geographic distribution of Mediterranean littoral fishes. Mar. Ecol. Prog. Ser. **327**: 257–265. doi:10.3354/meps327257.

Mamuris, Z., Apostolidis, A.P., Theodorou, A.J., and Triantaphyllidis, C. 1998*a*. Application of random amplified polymorphic DNA (RAPD) markers to evaluate intraspecific genetic variation in red mullet (*Mullus barbatus*). Mar. Biol. (Berlin), **132**(2): 171–178. doi:10.1007/s002270050383.

Mamuris, Z., Apostolidis, A.P., and Triantaphyllidis, C. 1998*b*. Genetic protein variation in red mullet (*Mullus barbatus*) and striped red mullet (*M. surmuletus*) populations from the Mediterranean Sea. Mar. Biol. (Berlin), **130**(3): 353–360. doi:10.1007/s002270050255.

Mamuris, Z., Stamatis, C., Bani, M., and Triantaphyllidis, C. 1999*a*. Taxonomic relationships between four species of the Mullidae family revealed by three genetic methods: allozymes, random amplified polymorphic DNA and mitochondrial DNA. J. Fish Biol. **55**(3): 572–587. doi:10.1111/j.1095-8649.1999.tb00700.x.

Mamuris, Z., Stamatis, C., and Triantaphyllidis, C. 1999*b*. Intraspecific genetic variation of striped red mullet (*Mullus surmuletus* L.) in the Mediterranean Sea assessed by allozyme and random amplified polymorphic DNA (RAPD) analysis. Heredity, **83**(1): 30–38. doi:10.1038/sj.hdy.6885400. PMID:10447700.

Martin, P., Sartor, P., and Garcia-Rodriguez, M. 1999. Exploitation patterns of European hake *Merluccius merluccius*, red mullet *Mullus barbatus* and striped red mullet *Mullus surmuletus* in the western Mediterranean. J. Appl. Ichthyology, **15**(1): 24–28. doi:10.1046/j.1439-0426.1999.00125.x.

Mattiangeli, V., Ryan, A.W., Paul Galvin, P., Mork, J., and Cross, T.F. 2004. Populations in the Mediterranean Sea: evidence from allozyme and minisatellite loci. Mar. Ecol. (Berlin), **24**(4): 247–258.

Millot, C. 1999. Circulation in the western Mediterranean Sea. J. Mar. Syst. **20**(1-4): 423–442. doi:10.1016/S0924-7963(98)00078-5.

Millot, C. 2005. Circulation in the Mediterranean Sea: evidences, debates and unanswered questions. Sci. Mar. **69**: 5–21.

Mounier, F., Echevin, V., Mortier, L., and Crepon, M. 2005. Analysis of the mesoscale circulation in the occidental Mediterranean Sea during winter 1999–2000 given by a regional circulation model. Prog. Oceanogr. **66**(2-4): 251–269. doi:10.1016/j.pocean.2004.11.003.

Öztilgin, H., Tosunoglu, Z., Bilecenoglu, M., and Tokaç, A. 2004. Population parameters of *Mullus barbatus* in Izmir Bay (Aegean Sea), using length frequency analysis. J. Appl. Ichthyology, **20**(3): 231–233. doi:10.1111/j.1439-0426.2004.00555.x.

Ozsoy, E., Hecht, A., and Ünlüata, Ü. 1989. Circulation and hydrography of the Levantine Basin — results of POEM co-ordinated experiments 1985–1986. Prog. Oceanogr. **22**(2): 125–170. doi:10.1016/0079-6611(89)90004-9.

Palumbi, S.R. 2004. Marine reserves and ocean neighborhoods: the spatial scale of marine populations and their management. Annu. Rev. Environ. Resour. **29**(1): 31–68. doi:10.1146/annurev.energy.29.062403.102254.

Patarnello, T., Volckaert, F.A.M.J., and Castilho, R. 2007. Pillars of Hercules: is the Atlantic–Mediterranean transition a phylogeographical break? Mol. Ecol. **16**(21): 4426–4444. doi:10.1111/j.1365-294X.2007.03477.x. PMID:17908222.

Peakall, R., and Smouse, P.E. 2006. GENALEX 6: genetic analysis in Excel. Population genetic software for teaching and research. Mol. Ecol. Notes, **6**(1): 288–295. doi:10.1111/j.1471-8286.2005.01155.x.

Peakall, R., Ruibal, M., and Lindenmayer, D.B. 2003. Spatial autocorrelation analysis offers new insights into gene flow in the Australian bush rat, *Rattus fuscipes*. Evolution, **57**(5): 1182–1195. PMID:12836834.

Pujolar, J.M., Roldán, M.I., and Pla, C. 2002. A genetic assessment of the population structure of swordfish (*Xiphias gladius*) in the Mediterranean Sea. J. Exp. Mar. Biol. Ecol. **276**(1-2): 19–29. doi:10.1016/S0022-0981(02)00245-9.

Pujolar, J.M., Roldán, M.I., and Pla, C. 2003. Genetic analysis of tuna populations, *Thunnus thynnus thynnus* and *T. alalunga*. Mar. Biol. (Berlin), **143**: 613–621. doi:10.1007/s00227-003-1080-1.

Quignard, J.-P. 1978. La Mediterranee, creuset ichthyologique. Boll. Zool. **45**(suppl): 23–26.

Raymond, M., and Rousset, F. 1995. GENEPOP (Version 3.4) population genetics software for exact tests and ecumenicism. J. Hered. **86**: 248–249.

Richards, V.P., Thomas, J.D., Stanhope, M.J., and Shivji, M.S. 2007. Genetic connectivity in the Florida reef system: comparative phylogeography of commensal invertebrates with contrasting reproductive strategies. Mol. Ecol. **16**(1): 139–157. doi:10.1111/j.1365-294X.2006.03145.x. PMID:17181727.

Ruiz, J., and Garcia-Lafuente, J. 2006. The Gulf of Cadiz oceanography: a multidisciplinary view. Deep-Sea Res. Part II Top. Stud. Oceanogr. **53**(11–13): 1141–1143. doi:10.1016/j.dsr2.2006.06.001.

Sabatés, A. 1990. Distribution pattern of larval fish populations in the northwestern Mediterranean. Mar. Ecol. Prog. Ser. **59**: 75–82. doi:10.3354/meps059075.

Salat, J. 1996. Review of hydrographic environmental factors that may influence anchovy habitats in northwestern Mediterranean. Sci. Mar. **60**(Suppl. 2): 21–32.

Schneider, S., Roessli, D., and Excoffier, L. 2000. Arlequin ver. 2.0: a software for population genetics data analysis. Genetics and Biometry Laboratory, University of Geneva, Switzerland.

Smouse, P.E., and Peakall, R. 1999. Spatial autocorrelation analysis of individual multiallele and multilocus genetic structure. Heredity, **82**(5): 561–573. doi:10.1038/sj.hdy.6885180. PMID:10383677.

Sokal, R.R., and Wartenberg, D.E. 1983. A test of spatial autocorrelation analysis using an isolation-by-distance model. Genetics, **105**(1): 219–237. PMID:17246154.

Stamatis, C., Triantafyllidis, A., Moutou, K.A., and Mamuris, Z. 2004. Mitochondrial DNA variation in Northeast Atlantic and Mediterranean populations of Norway lobster, *Nephrops norvegicus*. Mol. Ecol. **13**(6): 1377–1390. doi:10.1111/j.1365-294X.2004.02165.x. PMID:15140084.

Stergiou, K.I., Christou, E.D., Georgopoulos, D., Zenetos, A., and Souvermezoglou, C. 1997. The Hellenic seas: physics, chemistry, biology and fisheries. Oceanogr. Mar. Biol. Annu. Rev. **35**: 415–538.

Tintoré, J., LaViolette, P.E., Blade, I., and Cruzado, A. 1988. A study of an intense density front in the eastern Alboran Sea: the Almeria–Oran front. J. Phys. Oceanogr. **18**(10): 1384–1397. doi:10.1175/1520-0485(1988)018<1384:ASOAID>2.0.CO;2.

Truett, G.E., Heeger, P., Mynatt, R.L., Truett, A.A., Walker, J.A., and Warman, M.L. 2000. Preparation of PCR-quality mouse genomic DNA with hot sodium hydroxide and tris (HotSHOT). BioTechniques, **29**(1): 52–54. PMID:10907076.

Underwood, J.N., Smith, L.D., Van Oppen, M.J.H., and Gilmour, J.P. 2007. Multiple scales of genetic connectivity in a brooding coral on isolated reefs following catastrophic bleaching. Mol. Ecol. **16**(4): 771–784. doi:10.1111/j.1365-294X.2006.03187.x. PMID:17284210.

Verboeven, K.J.F., Simonsen, K.L., and McIntyre, L.M. 2005. Implementing false discovery rate control: increasing your power. Oikos, **108**(3): 643–647. doi:10.1111/j.0030-1299.2005.13727.x.

Viñas, J., Pla, C., Tawil, N.Y., Hattour, A., Farrugia, A.F., and de la Serna, J.M. 2003. Mitochondrial genetic characterization of bluefin tuna (*Thunnus thynnus*) from three Mediterranean (Libya, Malta, Tunisia); and one Atlantic locations (Gulf of Cadiz). International Commission for the Conservation of Atlantic Tunas (ICCAT) Col. Vol. Sci. Pap. **55**(3): 1282–1288. SCRS/2002/172. Available from www.iccat.int/Documents/CVSP/CV055_2003/no_3/CV055031282.pdf.

Vúdez, A., Pinot, J.M., and Haney, R.L. 1998. On the upper layer circulation in the Alborán Sea. J. Geophys. Res. **103**(C10): 21653–21666. doi:10.1029/98JC01082.

Weir, B.S., and Cockerham, C.C. 1984. Estimating F-statistics for the analysis of population structure. Evolution, **38**(6): 1358–1370. doi:10.2307/2408641.

Zane, L., Ostellari, L., Maccatrozzo, L., Bargelloni, L., Cuzin-Roudy, J., Buchholz, F., and Patarnello, T. 2000. Genetic differentiation in a pelagic crustacean (*Meganyctiphanes norvegica*: Euphausiacea) from the North East Atlantic and the Mediterranean Sea. Mar. Biol. (Berlin), **136**(2): 191–199. doi:10.1007/s002270050676.

Zardoya, R., Castilho, R., Grande, C., Favre-Krey, L., Caetano, S., Marcato, S., Krey, G., and Patarnello, T. 2004. Differential population structuring of two closely related fish species, the mackerel (*Scomber scombrus*) and the chub mackerel (*Scomber japonicus*), in the Mediterranean Sea. Mol. Ecol. **13**(7): 1785–1798. doi:10.1111/j.1365-294X.2004.02198.x. PMID:15189203.

Polyploid microsatellite data reveal stock complexity among estuarine North American green sturgeon (*Acipenser medirostris*)

Joshua A. Israel, K. Jun Bando, Eric C. Anderson, and Bernie May

Abstract: North American green sturgeon (*Acipenser medirostris*) display the distinctive behavior of long ocean migrations along the west coast punctuated by summer residence in estuaries; however, little is known about stock composition in these tidal environments. Pairwise comparisons and genetic clustering analysis were used to characterize the two green sturgeon Distinct Population Segments (DPSs) from 20 collections using eight tetrasomic and two disomic microsatellite loci. The observed pattern of green sturgeon DPS composition among five estuaries in California, Oregon, and Washington was supported with assignment testing approaches utilizing the same genotypic data in codominant polysomic and pseudodominant allele phenotype formats. The majority of individuals in northern DPS estuaries originated from the threatened Southern DPS, except in Winchester Bay and Grays Harbor. We detected few Northern DPS green sturgeon in San Pablo Bay, the principal Southern DPS estuary, supporting that green sturgeon preferentially disperse north once they enter their coastal migration. Our genetic findings suggest that stock complexity in green sturgeon is pervasive and support precautionary, interjurisdictional approaches for managing green sturgeon beyond rigid, regulatory boundaries.

Résumé : L'esturgeon vert (*Acipenser medirostris*) d'Amérique du Nord possède un comportement particulier qui comprend de longues migrations en mer le long de la côte ouest interrompues par des séjours d'été dans les estuaires; on connaît cependant peu la composition des stocks dans ces milieux sous influence de la marée. Des comparaisons appariées et une analyse de groupement génétique nous ont servi à caractériser deux segments distincts de population (DPS) d'esturgeons verts à partir de 20 échantillons et à l'étude de huit locus microsatellites tétrasomiques et deux disomiques. Le patron obtenu de composition des DPS dans cinq estuaires de Californie, d'Oregon et du Washington est confirmé par des méthodes d'essais d'attribution d'après les mêmes données génotypiques dans des formats de phénotypes d'allèles polysomiques codominants et pseudodominants. La plupart des individus des estuaires du DPS du nord proviennent du DPS menacé du sud, à l'exception de ceux de la baie Winchester et de Grays Harbor. Nous avons décelé peu d'esturgeons verts du DPS du nord dans la baie de San Pablo, l'estuaire principal du DPS du sud, ce qui appuie l'hypothèse qui veut que les esturgeons verts se dispersent de préférence vers le nord une fois qu'ils commencent leur migration côtière. Nos observations génétiques indiquent que la complexité du stock est générale et elles nous amènent à recommander des approches prudentes couvrant les diverses juridictions et dépassant les frontières rigides de la règlementation pour la gestion de l'esturgeon vert.

[Traduit par la Rédaction]

Introduction

Information about the stock composition of anadromous sturgeon aggregating in coastal bays and estuaries is very limited, yet essential for reducing risks associated with port dredging and development, coastal and estuarine fisheries, and habitat modification impacting sturgeon species in these waters. Adult North American green sturgeon (*Acipenser medirostris*) spawn in deep, cool, swift freshwater habitats and juveniles rear in natal rivers and estuaries before emigrating to the ocean in their second or third year (Allen and Cech 2007). Subadult green sturgeon make extensive oceanic migration along the Pacific coastal shelf (Erickson and Hightower 2007) northward in the fall and aggregate in bays and estuaries in the summer and fall (Moser and Lindley 2007). These estuarine aggregations do not seem related to spawning migration, since most aggregations do not occur in estuaries of spawning rivers, and green sturgeon appear to return south in the spring to enter spawning rivers (Lindley et al. 2008). Recent studies have suggested that de-

Received 12 September 2008. Accepted 30 March 2009. Published on the NRC Research Press Web site at cjfas.nrc.ca on 27 August 2009.
J20774

Paper handled by Associate Editor Michael Hansen.

J.A. Israel,[1] **K.J. Bando, and B. May.** Genomic Variation Laboratory, Department of Animal Science, 1 Shields Avenue, University of California, Davis, CA 95616, USA.
E.C. Anderson.[2] Southwest Fisheries Science Center, 110 Shaffer Road, Santa Cruz, CA 95060, USA.

[1]Corresponding author (e-mail: jaisrael@ucdavis.edu).
[2]Present address: Department of Applied Mathematics and Statistics, University of California, Santa Cruz, CA 95064, USA.

Fig. 1. Location of green sturgeon collection sites from spawning rivers and estuarine aggregation sites along the Pacific coast.

spite extensive marine migrations, anadromous sturgeon exhibit notable patterns of possibly stock-specific movement and aggregation (Waldman et al. 1996; Dugo et al. 2004). Thus, it is possible that green sturgeon migration patterns are distinct among estuaries and the relationship of these migratory patterns to the individuals' population of origin remains unknown. Recognition of stock complexity at local scale is essential for effective fisheries management, stock assessment, and recovery planning (Stephenson 1999; Cadrin et al. 2005).

North American green sturgeon range from Ensenada, Mexico, to the Bering Sea, Alaska (Moyle 2002; Colway and Stevenson 2007). Green sturgeon are currently known to spawn in two large California basins in the Sacramento and Klamath rivers and the Rogue River in Oregon. Late sexual maturity (approximately 15 years of age; Van Eenennaam et al. 2006), iteroparity, and extensive marine migrations expose green sturgeon to numerous threats throughout their life history. Aquatic ecosystems are strained by water management, and similar to other diadromous fish populations, green sturgeon have been impacted by flow and temperature alterations in spawning habitats caused by the construction of dams, degradation of estuarine rearing and foraging habitats by levee construction, dredging, and invasive species, and trawl fishing on migratory routes along the western coast of North America (Adams et al. 2007; Erickson and Webb 2007; Lackey 2009). The Sakhalin sturgeon, a sibling species in the Asian Pacific, has been extirpated from multiple spawning rivers and only persists at extremely low abundances (Shmigirilov et al. 2007).

Table 1. Location, sampling dates, collecting organization, sample size (*n*), collection site (measured in river kilometre distance (rkm) from the mouth), and fish size range (total length) for 1196 green sturgeon samples.

Collection location	Code	Dates	Organization	*n*	Collection site	Total length range (mm)
Sacramento River, California	**SAC**	June–July 2002	USFWS	18	rkm 388.8	26–52
		June–July 2003	USFWS	43	rkm 388.8	23–30
		May–July 2004	USFWS	24	rkm 388.8	24–41
		June–July 2005	USFWS	89	rkm 388.8	25–41
		June–July 2006	USFWS	92	rkm 388.8	25–42
San Pablo Bay, California	SPB	August–September 2001	CDFG	114	Estuary	600–1830
		April–May and August–September 2004	UCD	105	Estuary	690–2030
Klamath River, California	**KLA**	April–June 1998	YTFP	60	rkm 0.0–80.0	1550–2110
		April–June 2001	YTFP	29	rkm 0.0–80.0	1450–2400
		April–May 2003	YTFP	35	rkm 0.0–80.0	1460–2230
Rogue River, Oregon	**ROG**	May–July 2000	ODFW	34	rkm 1.8–104.6	1470–2250
		April–September 2002	ODFW	45	rkm 12.0–39.2	1530–2160
		April 2003	ODFW	34	rkm 13.6–39.2	1450–2130
Winchester Bay, Oregon	WIN	August 2000	ODFW	97	rkm 14.4–19.2	760–2110
		June–July 2002	ODFW	22	rkm 14.4–20.8	660–2080
Columbia River, Washington	COL	October 1995	WDFW	32	rkm 0.0–32.0	1190–1590
		1999	ODFW	49	Lower Columbia River	na
		July–August 2004	WDFW	94	rkm 18.8–35.2	980–2220
Willapa Bay, Washington	WIL	July–September 2003	WDFW	98	Areas WF2GW, WF2GE, and WF02J	1050–1950
Grays Harbor, Washington	GHR	June–July 2005	WDFW	82	Areas WFO2B and WFO2D	990–2400

Note: Population codes for spawning rivers are in bold type. USFWS, US Fish and Wildlife Service; CDFG, California Department of Fish and Game; UCD, University of California, Davis; YTFP, Yurok Tribal Fisheries Program; ODFW, Oregon Department of Fish and Wildlife; WDFW, Washington Department of Fish and Wildlife. na, not available.

Table 2. PCR conditions, genotyping dilutions optimized for electrophoresis, and PCR success rate for each locus.

Locus	Primer source(s)	PCR profile	Optimized conditions	PCR dilution	Ladder (bp)	PCR success rate (%)
Spl120b	McQuown et al. 2000; Israel et al. 2004	Fastart	2.0 mmol/L MgCl[a]	1 to 2	400	95.9
Aox27	King et al. 2001	Touchdown	1.25 mmol/L MgCl[b]	1 to 8	400	89.3
AfuG43	Welsh et al. 2003	Promega	1.75 mmol/L MgCl,[c] T_A = 59 °C	1 to 2	400	98.8
Spl106	McQuown et al. 2000	Touchdown	2.0 mmol/L MgCl[b]	1 to 2	400	98.0
AfuG135	Welsh et al. 2003	Promega	2.0 mmol/L MgCl,[c] T_A = 52 °C	1 to 8	400	94.5
Spl101b	Israel et al. 2004	Promega	T_A = 54 °C[c]	1 to 8	400	95.6
AfuG41	Welsh et al. 2003	Touchdown	2.0 mmol/L MgCl[b]	1 to 8	400	95.7
AfuG247	Welsh et al. 2003	Fastart	2.0 mmol/L MgCl[a]	1 to 2	400	94.7
An76	Zane et al. 2002	Fastart	T_A = 50 °C[a]	No dilution	400	90.0
As007	Zhu et al. 2005	Promega	2.5 mmol/L MgCl[c]	1 to 4	500	94.3

[a]95 °C for 4 min; 30 cycles of 95 °C for 30 s, 56 °C for 30 s, and 72 °C for 1 min; 72 °C for 5 min.

[b]95 °C for 1 min; 15 cycles of 95 °C for 30 s, 65 °C for 1min (–1 °C per cycle), and 72 °C for 1 min; 15 cycles of 95 °C for 30 s, 50 °C for 1 min, and 72 °C for 1 min.

[c]95 °C for 1 min 30 s; 40 cycles of 95 °C for 30 s, 56 °C for 30 s, and 72 °C for 1 min; 72 °C for 5 min.

In response to population declines, the National Marine Fisheries Service conducted a biological review of green sturgeon. One of the review's most important findings was that there are two spawning populations that appear to be reproductively isolated (Israel et al. 2004; Adams et al. 2007). The southern group, called the Southern Distinct Population Segment (DPS), consists of fish that spawn only in the Sacramento River. It was listed in 2006 as threatened under the *Endangered Species Act*. The Northern DPS, a National Marine Fisheries Service Species of Concern, consists of green sturgeon that spawn in rivers north of and including the Eel River in California. It is believed that fish in the Southern DPS are considerably less abundant than in the Northern DPS rivers, where more spawning habitat is available, harvest monitoring indicates hundreds of annual adult spawners, and there is minimal loss to entrainment (Adams et al. 2007).

Understanding how the behavior and population structure of green sturgeon influence the species' responses to impacts in diverse riverine, estuarine, and ocean habitats is challenging. Recent ultrasonic tagging studies have been successful in illuminating migration patterns of the species, although these studies alone cannot answer questions about the impacts of fishing or environmental alterations upon

Table 3. Estimates of observed (H_o) and expected heterozygosity (H_e) and number of alleles per locus (A) in each collection.

	Double reduction observed									Tetrasomic					
	AfaG41			*Aa76*			*AfaG135*			*AfaG43*			*Spl106*		
Collection	H_o	H_e	A	H_o	H_e	A	H_o	H_e	A	H_o	H_e	A	H_o	H_e	A
SAC 2002	0.59	0.64	9	0.32	0.75	12	0.41	0.55	6	0.75	0.64	6	0.19	0.25	3
SAC 2003	0.61	0.70	11	0.30	0.73	12	0.39	0.49	6	0.67	0.62	7	0.16	0.24	6
SAC 2004	0.69	0.74	9	0.46	0.73	11	0.22	0.32	5	0.51	0.56	4	0.06	0.06	3
SAC 2005	0.57	0.68	9	0.33	0.69	14	0.31	0.42	9	0.57	0.61	6	0.10	0.11	4
SAC 2006	0.62	0.68	11	0.30	0.75	16	0.32	0.46	10	0.68	0.69	7	0.19	0.26	6
SPB 2001	0.59	0.71	13	0.28	0.75	16	0.38	0.51	14	0.63	0.64	7	0.19	0.25	10
SPB 2004	0.66	0.71	10	0.28	0.69	13	0.36	0.46	9	0.63	0.62	6	0.14	0.15	6
KLA 1998	0.64	0.80	13	0.51	0.80	17	0.53	0.82	13	0.76	0.74	9	0.48	0.46	6
KLA 2001	0.78	0.80	13	0.43	0.71	13	0.62	0.77	11	0.47	0.50	6	0.64	0.62	7
KLA 2003	0.63	0.79	12	0.38	0.78	13	0.55	0.82	12	0.75	0.72	7	0.37	0.36	3
ROG 2000	0.76	0.80	13	0.30	0.80	15	0.60	0.82	13	0.72	0.71	8	0.53	0.57	5
ROG 2002	0.79	0.79	12	0.41	0.82	18	0.60	0.80	12	0.69	0.76	9	0.40	0.38	4
ROG 2003	0.61	0.82	12	0.63	0.79	9	0.54	0.81	11	0.75	0.73	8	0.27	0.32	3
WIN 2002	0.76	0.77	10	0.41	0.81	13	0.61	0.80	10	0.71	0.75	7	0.45	0.49	6
WIN 2000	0.64	0.76	17	0.31	0.75	20	0.44	0.65	13	0.68	0.70	9	0.23	0.24	8
COL 1995	0.64	0.72	11	0.23	0.69	11	0.31	0.54	9	0.65	0.65	6	0.15	0.15	4
COL 1999	0.67	0.78	13	0.43	0.77	21	0.32	0.54	10	0.65	0.65	7	0.15	0.14	5
COL 2004	0.63	0.74	14	0.30	0.79	19	0.40	0.60	11	0.63	0.62	7	0.10	0.10	4
WIL 2003	0.60	0.75	14	0.46	0.80	19	0.41	0.57	10	0.68	0.68	8	0.13	0.15	4
GHR 2005	0.63	0.80	14	0.37	0.81	19	0.57	0.77	14	0.69	0.70	11	0.12	0.12	5

Southern and Northern DPS green sturgeon in specific areas (Lindley et al. 2008). Typically, green sturgeon have been tagged in estuaries, where they are easy to capture. A number of recaptures and acoustic detections of green sturgeon tagged in Northern DPS estuaries and Southern DPS rivers and these locations indicate migration by individuals between the two DPSs (Miller 1972; Lindley et al. 2008). However, information derived from the tagging effort is limited by not knowing the population of origin for a majority of these fish and the rates of marking and recapture or detection, in the case of ultrasonic tagging studies.

Genetic stock identification (GSI) studies can provide information about the origin of green sturgeon in aggregations and only require a single contact with the sample. However, green sturgeon population studies are complicated by their degenerating tetraploid genome. Most microsatellite markers used in this study carry four copies of most genes, although some seem to have decayed to amplify two copies of a gene. Tetrasomy makes it very difficult to verify that the assumptions underlying standard statistical genetic methods are satisfied; however, these methods can still yield accurate results. Salmonid genomes are also tetraploid derivatives (Wright et al. 1983), and the treatment and assumptions surrounding the use of isolocus allozyme frequency data for population differentiation and GSI studies were often different among studies (Marsden et al. 1989; Scribner et al. 1998; Seeb et al. 2000). Applications of GSI (Beacham et al. 1987; Smouse et al. 1990) and other methods of genetic assignment testing (Paetkau et al. 1995) are now commonplace with diploid microsatellite data. In diploid species, interpreting microsatellite data and applying the statistical models underlying GSI follow the relatively simple and well-understood laws of Mendelian inheritance. This simplicity is lost in polyploid organisms such as green sturgeon, and without careful multigenerational studies, the statistical model describing how tetrasomic genes are inherited cannot be known with confidence. Accordingly, the application of GSI to polysomic microsatellite data has been somewhat restricted.

The objectives of this study were to (*i*) test the use of genetic assignment testing programs suitable for tetrasomic microsatellite data and (*ii*) evaluate the stock composition of green sturgeon in estuarine aggregations. Genetic assignment testing methods were examined using two different scoring models (a dominant versus a fully-resolved codominant model). Further, we assessed the accuracy of these GSI estimates by resampling entire individuals into simulated baselines and mixtures. This procedure allowed us to challenge our methods with simulated data that were faithful to the tetrasomic inheritance mechanism of each locus, without that mechanism being exactly known.

Green sturgeon in the Southern and Northern DPSs were previously shown to be genetically differentiated at six microsatellite DNA loci (Israel et al. 2004). In this study, we used these microsatellite markers along with four others to identify Northern and Southern DPS green sturgeon individuals in nine collections of green sturgeon taken from five estuaries in California, Oregon, and Washington to evaluate two estuarine aggregation hypotheses. The null hypothesis that green sturgeon in estuaries originated primarily from their most proximal geographic population was examined. Alternatively, the possibility that estuarine green sturgeon were observed in proportion to the purported abundance of the two DPSs was also evaluated.

Materials and methods

Collection of DNA samples, polymerase chain reaction (PCR), and gel electrophoresis

Green sturgeon samples were collected from eight west coast locations in the United States (Fig. 1). Collections of freshwater samples were assumed to represent spawning

Spl101b			*AfiuG247*			*As007*			Disomic *Aox27*			*Spl120*		
H_o	H_e	A	H_o	H_e	A	H_o	H_e	A	H_o	H_e	A	H_o	H_e	A
0.68	0.72	9	0.46	0.53	4	0.71	0.76	8	0.46	0.37	4	0.68	0.67	6
0.66	0.67	12	0.59	0.67	9	0.76	0.78	8	0.41	0.54	4	0.61	0.78	8
0.75	0.77	12	0.51	0.64	6	0.65	0.77	8	0.44	0.36	4	0.67	0.70	7
0.84	0.82	15	0.59	0.68	9	0.70	0.77	13	0.67	0.51	4	0.33	0.71	5
0.72	0.80	16	0.55	0.68	10	0.75	0.83	9	0.44	0.46	5	0.64	0.69	8
0.80	0.83	22	0.48	0.61	10	0.74	0.82	12	0.46	0.48	4	0.64	0.73	8
0.79	0.80	20	0.57	0.64	8	0.76	0.80	10	0.60	0.68	4	0.84	0.83	9
0.83	0.83	13	0.49	0.68	13	0.69	0.77	12	0.62	0.65	5	0.86	0.84	13
0.78	0.82	9	0.50	0.60	8	0.72	0.74	8	0.57	0.62	4	0.61	0.83	8
0.79	0.78	10	0.50	0.64	8	0.77	0.80	11	0.74	0.65	3	0.76	0.84	11
0.82	0.82	12	0.48	0.65	11	0.65	0.83	13	0.71	0.63	4	0.76	0.81	12
0.84	0.82	10	0.60	0.66	9	0.79	0.83	10	0.73	0.67	4	0.47	0.79	11
0.73	0.76	10	0.43	0.70	9	0.79	0.79	9	0.58	0.66	4	0.82	0.85	11
0.88	0.84	10	0.55	0.71	8	0.74	0.75	8	0.53	0.55	4	0.50	0.79	12
0.75	0.81	17	0.53	0.65	12	0.77	0.82	11	0.55	0.54	6	0.90	0.83	11
0.87	0.85	16	0.59	0.64	8	0.70	0.82	8	0.45	0.39	3	0.79	0.79	9
0.65	0.70	17	0.46	0.70	6	0.74	0.77	9	0.42	0.47	3	0.68	0.80	11
0.77	0.78	19	0.55	0.60	9	0.72	0.77	10	0.56	0.52	3	0.76	0.73	8
0.82	0.83	20	0.58	0.61	10	0.72	0.79	12	0.47	0.44	5	0.73	0.78	10
0.73	0.84	15	0.54	0.71	13	0.74	0.80	12	0.49	0.52	4	0.73	0.79	9

populations, while estuarine collections were of unknown origin. Spawning populations were represented by larvae and fry (age 0+) samples from the Sacramento River and adult samples (unknown ages) from the Klamath and Rogue rivers (Table 1). Green sturgeon occupying fresh and estuarine waters before the onset of maturation are referred to as juveniles, while fish between the onset of maturation and full maturity that have entered coastal and estuarine waters are called subadults (Klimley et al. 2007). Adult sturgeon are reproductively mature fish and can be found in all aquatic environments. Fin clips of individuals were either dried or preserved in 95% ethanol and stored at room temperature. DNA was isolated using the Wizard SV DNA extraction kit (Promega). Because green sturgeon may be misidentified as white sturgeon, the taxonomic identity of all samples was verified using a green sturgeon specific restriction fragment length polymorphism (Israel et al. 2004).

In addition to the six microsatellite DNA loci previously described in Israel et al. (2004), we used four additional loci: *AfiuG41* and *AfiuG247* (Welsh et al. 2003), *An76* (Zane et al. 2002), and *As007* (Zhu et al. 2005). These 10 loci (Table 2) were amplified by PCR in each of the samples and genotyping dilutions optimized for electrophoresis on the BaseStation DNA fragment analyzer (MJ Research/Bio-Rad, Inc.). PCR success rates for each locus are reported in Table 2. A 0.5 μmol/L solution containing the forward primer end-labeled with one of three PRISM fluorophores, NED, VIC, or 6-FAM (Applied Biosystems Inc.), was included in each primer set. One microlitre of diluted PCR product for each locus was pooled with products from two other labeled primers and combined with 2 μL of water, 1.45 μL of 100% deionized formamide (Sigma), 0.5 μL of blue dextran loading dye, and 0.05 μL of ABI GeneScan-400 Rox internal size standard. Samples were denatured at 95 °C for 3 min and chilled on ice. One microlitre aliquots of PCR product and size standard mixtures were loaded manually into a 48-well, 75 μm, 5.5% denaturing polyacrylamide gel and size fractionated by electrophoresis in 1× TBE running buffer with a 2 min prerun at 1900 V, a 30 s constant injection at 4000 V, and a 6000 scan collection run at 2600 V. PCR products were analyzed and genotypic data were generated using Cartographer (version 1.2.6g) DNA fragment analysis software. Multiple individuals were rerun on each gel to standardize intergel allele size and and validate gene dosage scoring.

Gene dosages for the eight tetrasomic microsatellite DNA markers were interpreted by analysis of relative peak intensity from the genotyping electropherograms, similar to other sturgeon studies with polysomic markers (McQuown et al. 2000; Pyatskowit et al. 2001; Welsh et al. 2003). If three peaks were present, the largest peak was assigned two doses. If two peaks were present and equal in size, each peak was scored as representing two doses. When two peaks were present but not equal in size, the largest peak was interpreted as presumably three doses of its corresponding allele. A single electrophoretic peak or four peaks were assigned as either four doses of a single allele or one dose of each of four alleles, respectively. Since scoring gene dosage of tetrasomic loci may not be 100% accurate for estimating allele and genotype frequencies (De Silva et al. 2005; Luo et al. 2005), we also conducted analyses based merely on the presence or absence of different alleles. For these analyses, genotypic data were transformed into pseudodominant "allele phenotypes" (Becher et al. 2000; Rodzen and May 2002) by scoring an allele as present or absent, regardless of dosage. This presence–absence matrix combined all of the alleles at the 10 loci to represent 204 pseudodominant markers.

Genetic diversity and population structure

Green sturgeon is a functional tetraploid (Ludwig et al. 2001) and contains 249 ± 8 chromosomes (Van Eenennaam

Table 4. Pairwise F_{ST} estimates for spawning population and summer aggregation collections used in this study.

	SAC 2002	SAC 2003	SAC 2004	SAC 2005	SAC 2006	SPB 2004	SPB 2001	KLA 1998	KLA 2001	KLA 2003	ROG 2002
SAC 2002		0.008	0.023	**0.013**	**0.013**	**0.011**	0.006	**0.059**	**0.043**	**0.054**	**0.044**
SAC 2003	**0.007**		**0.015**	**0.006**	**0.010**	**0.002**	0.003	**0.067**	**0.046**	**0.059**	**0.053**
SAC 2004	0.015	**0.012**		**0.022**	**0.015**	**0.018**	**0.014**	**0.085**	**0.067**	**0.078**	**0.071**
SAC 2005	**0.011**	**0.004**	**0.017**		**0.010**	**0.003**	**0.006**	**0.075**	**0.052**	**0.069**	**0.059**
SAC 2006	**0.014**	**0.012**	**0.016**	**0.014**		**0.008**	**0.006**	**0.071**	**0.053**	**0.066**	**0.054**
SPB 2004	**0.009**	0.001	**0.014**	**0.002**	**0.011**		0.001	**0.070**	**0.046**	**0.062**	**0.053**
SPB 2001	**0.003**	0.003	**0.010**	**0.005**	**0.008**	0.001		**0.062**	**0.039**	**0.057**	**0.045**
KLA 1998	**0.053**	**0.074**	**0.080**	**0.079**	**0.072**	**0.075**	**0.064**		**0.015**	**0.009**	**0.012**
KLA 2001	**0.045**	**0.066**	**0.073**	**0.069**	**0.062**	**0.063**	**0.053**	**0.011**		**0.011**	**0.011**
KLA 2003	**0.057**	**0.081**	**0.084**	**0.088**	**0.079**	**0.080**	**0.071**	**0.010**	**0.011**		**0.005**
ROG 2002	**0.043**	**0.065**	**0.071**	**0.069**	**0.061**	**0.064**	**0.053**	**0.010**	**0.009**	**0.006**	
ROG 2000	**0.057**	**0.080**	**0.082**	**0.089**	**0.075**	**0.081**	**0.066**	0.004	**0.014**	**0.015**	**0.010**
ROG 2003	0.056	**0.072**	**0.079**	**0.084**	**0.077**	**0.077**	**0.063**	**0.016**	0.024	**0.013**	0.007
WIN 2002	0.031	**0.056**	**0.060**	**0.056**	**0.047**	**0.053**	**0.041**	**0.008**	**0.007**	**0.008**	0.001
WIN 2000	0.005	**0.011**	**0.019**	**0.014**	**0.015**	**0.010**	**0.006**	**0.037**	**0.029**	**0.038**	**0.025**
COL 1995	**0.011**	**0.008**	0.017	**0.008**	**0.008**	**0.004**	**0.003**	**0.055**	**0.050**	**0.068**	**0.050**
COL 2004	0.004	0.005	0.012	**0.007**	**0.016**	**0.005**	0.002	**0.054**	**0.048**	**0.059**	**0.047**
COL 1999	0.008	**0.009**	**0.020**	**0.012**	**0.014**	**0.009**	**0.010**	**0.045**	**0.038**	**0.046**	**0.037**
WIL 2003	0.005	**0.009**	0.010	**0.011**	**0.011**	**0.009**	**0.004**	**0.048**	**0.043**	**0.055**	**0.039**
GHR 2005	0.018	**0.027**	**0.030**	**0.033**	**0.029**	**0.026**	**0.021**	**0.022**	**0.020**	**0.023**	**0.015**

Note: Above the diagonal are F_{ST} estimates for only the eight tetrasomic loci, while below is the entire 10-loci data set. Bold values indicate significant

et al. 1999). Based on inheritance data (J.A. Israel, unpublished data), we assumed that tetrasomic and disomic loci in green sturgeon were under random assortment of chromosomes from a quadrivalent or bivalent parent without double reduction (Bever and Felber 1992) in all loci except *AfuG41*, *An76*, and *AfuG135*. In these loci, double reduction may be caused by sister chromatids segregating into the same gamete resulting in heterozygote deficiency, which could lead to miscalculation of observed and expected heterozygosity. Observed and Hardy–Weinberg expected heterozygosities at the five tetrasomic loci showed no evidence of double reduction and the two disomic loci were estimated with the programs AUTOTET (Thrall and Young 2000) and GDA (Lewis and Zaykin 2001), respectively. Expected heterozygosity for the tetrasomic loci appearing to undergo double reduction was computed in AUTOTET assuming random chromatid separation with maximum double reduction ($\alpha = 0.142$). To consider the utility of the codominant markers as dominant markers, we calculated the average number of alleles per individual at a locus for the two types of tetrasomic loci in AUTOTET. The number of alleles observed in a collection was calculated using AUTOTET and FSTAT (Goudet 2001).

Pairwise F_{ST} values between collections were calculated in FSTAT to evaluate possible differentiation with 1000 bootstrapped permutations completed to assess significance (Weir and Cockerham 1984). The effect of potentially different rates of mutation and genetic drift among the disomic and tetrasomic markers was considered by calculating F_{ST} values separately for three data sets. The first contained the eight tetrasomic loci, which were transformed by doubling the number of individuals in each collection with pseudogenotypes containing the second half of alleles at these four-dose loci. The second data set contained only the two disomic loci; the third contained all 10 loci. For the 10-loci data set, half of the disomic data were scored as missing, so an equivalent number of individuals could be included for the transformed tetrasomic loci data. These approaches permitted all alleles at a locus to be included in calculating allele frequencies at both tetrasomic and disomic loci. The two data sets including the three loci undergoing double reduction violated assumptions in the calculation of expected heterozygosities for each collection, which may have influenced pairwise F_{ST} calculation.

A neighbor-joining dendrogram of the Cavalli-Sforza–Edwards chord measure (Cavalli-Sforza and Edwards 1967) was created with PHYLIP 3.66 (Felsenstein 2005) with each data set to graphically represent the genetic relationships between all collections. To determine the significance of the neighbor-joining tree's nodes, 1000 bootstrap replicates were completed. The potential number of subpopulations in the entire data set was evaluated with 10 iterations of *structure* 2.2 (Pritchard et al. 2000) with K, the number of populations, between 1 and 10 using the no-admixture model with uncorrelated allele frequencies. The PLOIDY parameter was set to 4 and the two disomic loci scored with two missing alleles each, while burn-in and run lengths of 100 000 and 200 000, respectively, provided Markov chain convergence and consistency in α and q values.

Estimation of DPS contributions to estuarine aggregations

The proportion of fish from each green sturgeon DPS in the estuarine aggregations was determined using three different approaches. First, we applied the likelihood-based mixed stock analysis program *gsi_sim* (Anderson et al. 2008), which assumes a codominant phenotype model. Second, we used the program AFLPOP (Duchesne and Bernatchez 2002), a likelihood-based method for population assignment, which uses a dominant model of allelic expression. Third, we used the Bayesian clustering method of

ROG 2000	ROG 2003	WIN 2002	WIN 2000	COL 1995	COL 2004	COL 1999	WIL 2003	GHR 2005
0.059	**0.063**	**0.028**	**0.011**	**0.013**	**0.007**	0.014	0.009	**0.024**
0.066	**0.062**	**0.035**	**0.010**	**0.008**	**0.004**	**0.008**	**0.011**	**0.026**
0.081	**0.084**	**0.052**	**0.025**	0.018	0.016	**0.025**	0.014	**0.033**
0.078	**0.079**	**0.039**	**0.014**	**0.007**	**0.007**	**0.010**	**0.011**	**0.031**
0.068	**0.073**	**0.034**	**0.013**	**0.010**	**0.013**	**0.015**	**0.010**	**0.029**
0.069	**0.072**	**0.036**	**0.009**	**0.004**	**0.006**	**0.008**	**0.010**	**0.025**
0.058	**0.060**	**0.026**	**0.006**	**0.002**	**0.004**	**0.011**	**0.005**	**0.020**
0.006	**0.018**	**0.010**	**0.038**	**0.050**	**0.053**	**0.046**	**0.044**	**0.021**
0.018	**0.027**	**0.010**	**0.022**	**0.036**	**0.037**	**0.032**	**0.031**	**0.017**
0.018	**0.014**	**0.009**	**0.031**	**0.050**	**0.047**	**0.037**	**0.039**	**0.015**
0.014	0.008	0.001	**0.021**	**0.038**	**0.041**	**0.034**	**0.031**	**0.014**
	0.023	0.008	**0.037**	**0.051**	**0.055**	**0.050**	**0.048**	**0.026**
0.019		**0.016**	**0.034**	**0.054**	**0.048**	**0.045**	**0.043**	**0.018**
0.007	0.015		0.009	**0.019**	**0.023**	0.019	**0.015**	0.006
0.039	**0.034**	0.018		**0.002**	**0.006**	**0.007**	**0.004**	**0.008**
0.063	**0.063**	**0.034**	**0.005**		**0.003**	**0.009**	0.001	**0.015**
0.060	**0.051**	**0.035**	0.005	**0.005**		0.007	0.003	**0.014**
0.051	**0.045**	0.027	0.005	**0.009**	0.007		**0.009**	**0.015**
0.056	**0.049**	**0.031**	**0.004**	**0.002**	0.003	**0.006**		**0.011**
0.027	0.019	0.011	**0.008**	**0.017**	**0.015**	**0.012**	**0.011**	

values at the 5% level corrected for multiple comparisons.

Fig. 2. Neighbor joining tree of Cavalli-Sforza–Edwards unbiased minimum genetic distance of spawning river collections used in the study constructed with data from (*a*) two disomic loci, (*b*) eight tetrasomic loci, and (*c*) all 10 loci. Node support corresponds to proportion of 1000 bootstrapped permutations yielding similar topologies. Collection codes are listed in Table 1.

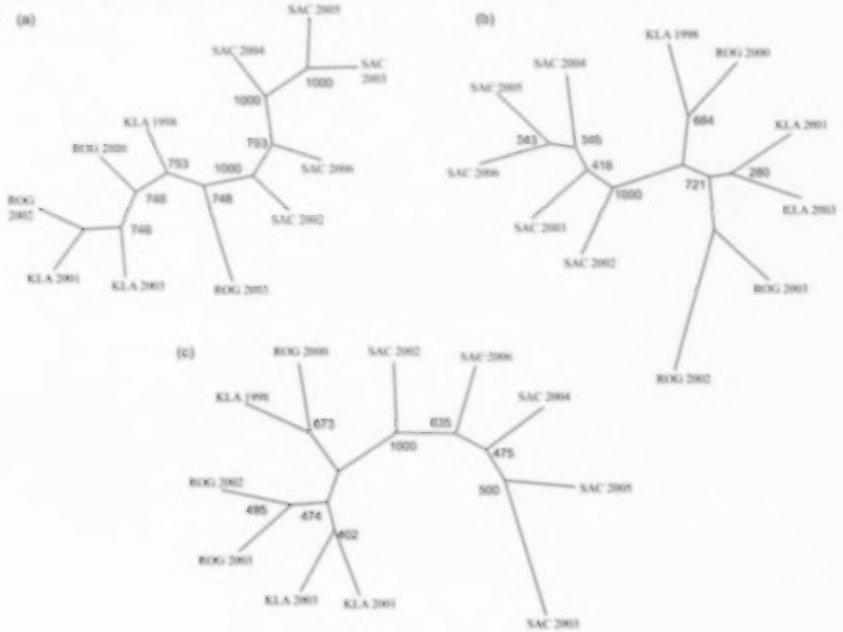

structure 2.2. In the two likelihood-based analyses, fish of known origin were included as baseline data (also known as "reference individuals"). The Southern DPS was represented in the baseline by pooling the 5 years of fry samples in the Sacramento River (n = 266). The Northern DPS baseline included samples from two populations: 125 adults taken over 3 years from the Klamath represented one source population and 113 adults sampled over 3 years in the Rogue River represented the second. The fraction of fish estimated from the Northern DPS was the sum of the fraction estimated from

Fig. 3. Plots of expected (true, *x*-axis) and observed (model output, *y*-axis) proportions of Southern DPS demonstrate mixture estimation accuracy. (*a*) Each point represents an estimate obtained with one of 5000 training and test set pairs. Training and test sets were obtained by sampling from baseline samples without replacement. (*b*) Number of Southern DPS fish in a test sample ($n = 50$) on the *x*-axis. This displays the variance due solely to inaccuracy in genetic assignment, while Fig. 3*a* includes variance due to binomial sampling of mixture proportion and a finite test sample size of 50.

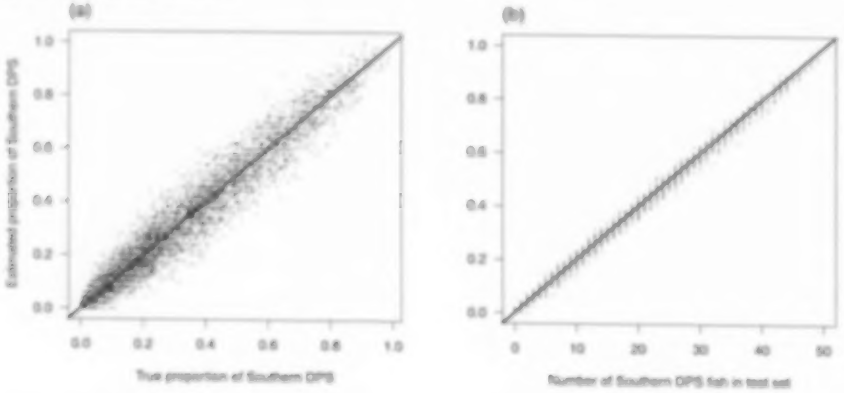

Fig. 4. Log-likelihood values from self-assigned baseline individuals with AFLPOP showing correctly and "misassigned" allelic phenotypes. Small triangles represent correct Northern DPS reallocation and diamonds represent correct Southern DPS reallocations. Large triangles represent incorrectly reallocated Northern DPS individuals and squares represent incorrectly reallocated Southern DPS individuals. The line represents values of equal probability.

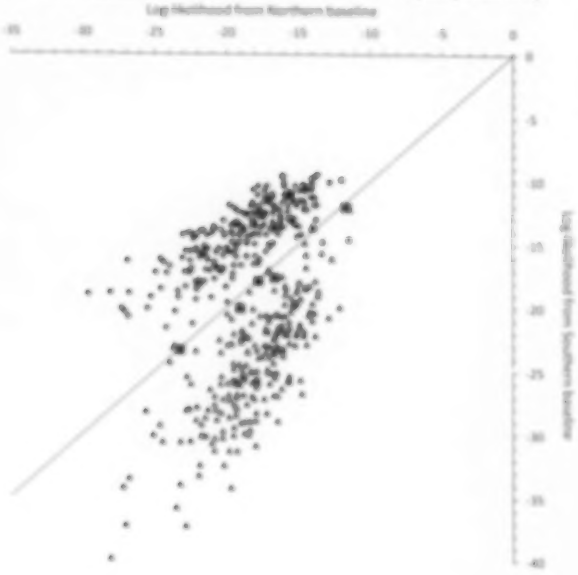

discrete Klamath and Rogue baselines. Reference samples were not used with *structure* because that feature is not available with polyploid data.

The method implemented in *gsi_sim* extends the likelihood model of GMA (Kalinowski 2003) to polysomic data by assuming that the allelic types of all four gene copies are known at each tetrasomic locus. This requires assuming that allelic dosages can be inferred from the electrophoretic data. In the model, the probability of a fish's genotype at any locus follows that of a sample of four from a compound Dirichlet multinomial distribution with parameters determined by the frequency of different alleles in the baselines and a Dirichlet prior of 1/(number of alleles) for each allele in each locus (Rannala and Mountain 1997). The loci are assumed to be in linkage equilibrium, so the multilocus genotype probability is just the product over loci of the single-locus probabilities. The expectation–maximization algorithm (Dempster et al. 1977) is used to find the maximum likelihood estimate of the mixture proportions in an estuary. The estimates of the mixture proportions can then be combined, using Bayes' rule, with a fish's genotype probability to estimate the posterior probability that the fish originated from a given source population. The posterior probability that a fish was from the Northern DPS was calculated as the sum of posterior probabilities that it was from the Klamath or Rogue population. Because the *gsi_sim* method assumes a simple model for tetrasomic inheritance and phenotypic expression that might be violated, we assessed the potential for bias with numerous simulations (see below).

The software AFLPOP (Duchesne and Bernatchez 2002) assumes a dominant model for the data: each allele is counted as either observed or unobserved in an individual. Hence, it does not require assuming that the allelic types of all four gene copies are known or that they are in Hardy–Weinberg equilibrium, alleviating potential problems associated with gene dosage scoring and double reduction. This method assumes that each population's dominant band frequencies are accurate and there is no significant disequilibrium among loci. AFLPOP's likelihood-based method was applied to two different data sets, one with just the eight tetrasomic loci and another with all 10 loci. Because the number of reference individuals allowed in AFLPOP is limited to 254, 12 reference individuals were randomly removed from the 266-fish Southern DPS baseline. The codominant microsatellite data were transformed into pseudodominant allele phenotypes by recording each allele at every locus as present (1) or absent (0), creating a presence–absence matrix

Fig. 5. Proportion of Southern DPS fish in collections of estuarine green sturgeon. Codes as given in Table 1. Standard errors are represented by bars. Shaded bars are *gsi_sim* proportions, solid columns are *structure* proportions, and open bars are AFLPOP proportions.

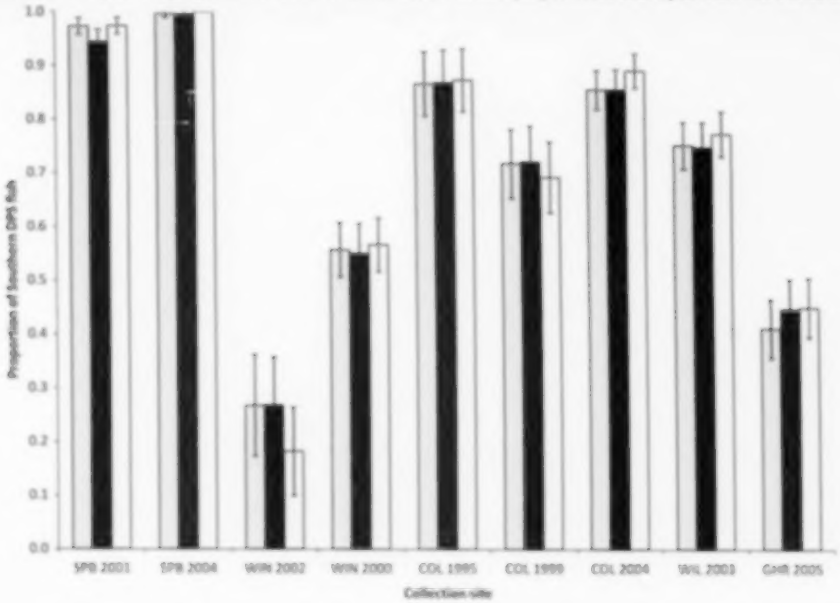

in which the rows represent alleles and the columns individuals. In the absence of a dominant band in a candidate population, AFLPOP's default frequency correction value of $1/(n + 1)$ was used, where n is the number of samples. AFLPOP computes the log-likelihood of an unknown individual's allele phenotype in each baseline population based on the frequency of the dominant (present) bands at each locus using a variation of the method of Paetkau et al. (1995) and then allocates it into the candidate population with the greatest log-likelihood value.

Like *gsi_sim*, the Bayesian cluster algorithm in *structure* assumes that the allelic types of all four gene copies are known and that population allele frequencies are in Hardy–Weinberg equilibrium with minimal linkage disequilibrium. Results from 10 iterations of *structure* with $K = 2$ were averaged and individuals assigned to the DPS from which they had the highest proportion of ancestry ($q > 0.5$) to obtain the fraction of a collection originating from either DPS.

Assessment of GSI accuracy

To evaluate *gsi_sim*'s performance at estimating mixture proportions and assigning individuals to each DPS, two approaches were taken. The first assessed the self-assignment accuracy of individuals in the baseline (using a leave-one-out procedure). In the second method, we used a cross-validation scheme (Efron and Gong 1983), creating multiple "training" and "test" data sets by sampling individual fish from the baseline randomly and without replacement. The true baseline was sampled with replacement to create a training set containing 216 individuals from the Sacramento collections, 75 individuals from the Klamath collections, and 63 from the Rogue collections. This was done to allow for a consistent baseline sample size and to reserve enough individuals from the baselines to be randomly sampled without replacement into test sets of simulated mixtures ($n = 50$). Training and test sets were replicated 5000 times with mixing proportions of the three baseline populations drawn from a uniform Dirichlet distribution. The proportion of Northern and Southern DPS fish in each simulated mixture was estimated using the training set as the reference sample.

Allocation success rate in AFLPOP was evaluated by removing individual allele phenotypes from the known baseline collections and reallocating them to the baseline population with the highest log-likelihood value. This method of reallocation was compared with AFLPOP's procedure of simulating allelic phenotypes from the allele frequencies of the baseline populations and calculating their log-likelihood values of origin to the baseline populations to assess bias and incorrect assignment.

The accuracy of the assignments made with *structure* was evaluated using the q values for individuals of known origin (Manel et al. 2002; Latch et al. 2006). Since we used no reference sets in the *structure* runs, we first had to decide which of the two clusters corresponded to each DPS. This decision was easily made based on the average q value of reference individuals. We then quantified the rates of correct and incorrect misassignment by designating known-origin individuals with $q > 0.5$ as being correctly assigned and those with $q < 0.5$ as incorrectly assigned.

Identifying cryptic populations in mixed aggregations

The possibility that green sturgeon in estuarine collections may have originated from populations not included in the baseline was evaluated using individuals' negative log-likelihood values from *gsi_sim*. Empirical cumulative density functions (ECDFs) of values from unknown individuals assigned to the Sacramento, Klamath, or Rogue River baselines were compared with the ECDFs of values from

reference individuals, computed using the leave-one-out procedure from the Sacramento, Klamath, and Rogue baselines. Data for multiple years were combined into composite ECDFs for each geographically sampled location using fish that had no more than one locus of missing data. These ECDFs from the unknown and reference individuals were plotted and compared visually and tested for differences using a Kolmogorov–Smirnov (K–S) two-sample test (Sokal and Rohlf 1995).

Results

Genetic diversity and population structure

A total of 1197 green sturgeon samples were genotyped in 20 collections from eight locations (Table 1). Observed heterozygosity among these 20 collections ranged from 0.41 to 0.84 for disomic loci, from 0.22 to 0.79 for doubly reduced tetrasomic loci, and from 0.06 to 0.88 for randomly inherited tetrasomic loci (Table 3). The average number of alleles per individual at a locus ranged between 1.5 and 2.9 for the doubly reduced tetrasomic loci and 1.1 and 3.1 for the randomly inherited tetrasomic loci.

Moderate levels of genetic differentiation were observed among geographically distinct collections of green sturgeon, while low levels of statistically significant temporal differentiation seemed to exist between annual collections from spawning populations regardless of the number of loci in the analyzed dataset. Pairwise F_{ST} values from the 10-locus data set indicated low and moderate levels of genetic differentiation ranging from 0.001 to 0.085 (Table 4). The largest pairwise F_{ST} values (0.043–0.085) were between spawning populations from the Southern and Northern DPSs and almost all inter-DPS pairwise values were significant (85 out of 90). Neighbor-joining dendrograms of the spawning collections demonstrated strong support for the distinctiveness of the DPSs but not for temporal structuring within populations or between the Rogue and Klamath rivers in the Northern DPS, regardless of the number of loci in the analyzed data set (Fig. 2).

The clustering method in *structure* (Pritchard et al. 2000) was run with values of K up to 10 and did not find a minimum likelihood value, although a plot of negative log-likelihood values did appear to reach its asymptote after $K = 8$ (data not shown). Since no value of $\ln \Pr(X|K)$ could be reliably called a maximum, it was not possible to infer a value of K using $\ln \Pr(X|K)$ alone. As K increased to greater than 2, individuals did not show a high fraction of ancestry from any one cluster, and q values for individuals to each inferred cluster became increasingly equal, implying that these solutions for population structure were poor choices (Pritchard et al. 2007). Using 10 runs of *structure* for K between 1 and 10, the mean of the absolute value of the second-order rate of change was calculated and compared with $\ln \Pr(X|K)$ for each K value (Evanno et al. 2005) that showed a single, clear mode for $K = 2$.

Assessment of GSI accuracy with polysomic data

The self-assignment of reference samples showed that individuals from the Southern and Northern DPSs can be distinguished with great accuracy. In *gsi_sim*, 263 of 266 Southern DPS fish (98.8%) were correctly assigned to the Southern DPS. Likewise, 236 (99.2%) of the 238 Northern DPS fish were correctly assigned to the Northern DPS. The self-assignment tests also showed that fish from the two populations within the Northern DPS could not be accurately distinguished: 54.9% and 75.2% of Rogue and Klamath fishes, respectively, were correctly assigned back to their spawning populations. The accuracy of estimates of DPS mixing proportions was confirmed by creating 5000 training and test data sets by permutation (Fig. 3). The fraction of fish from the Southern DPS in the test sets estimated from the Southern DPS are evenly spread about their true value throughout the mixture range from 0 to 1 (Fig. 3*a*), indicating that the mixing proportion can be estimated with little bias. The variance in the estimates due solely to inaccuracy in genetic assignment of individuals within the test set is shown in Fig. 3*b*.

Accuracy in assignment with AFLPOP's dominant expression model where original genotypes from the 10-loci data set were assigned back to one of the two DPSs was also quite high. Using the leave-one-out procedure, 98.7% of the Northern DPS individuals were correctly assigned back to one of the two Northern DPS populations, while 97.2% of the Southern DPS individuals were correctly assigned. Among the two Northern DPS reference groups, 73.2% and 70.6% of Klamath and Rogue individuals, respectively, were correctly assigned back to their original population. The log-likelihood values of individual allelic phenotypes removed and reallocated to the Northern or Southern DPS baseline allelic phenotype frequencies are displayed in Fig. 4. Additionally, AFLPOP simulated 25, 100, and 250 individual allelic phenotypes 100 times from the baseline allelic phenotype frequencies and allocated these phenotypes into the two possible DPSs to test the allocation success rate. Across iterations, simulated allelic phenotypes were correctly assigned to the original DPSs' allelic phenotype frequencies from which they were simulated greater than 99.5% of the time.

Finally, using *structure*, 97.9% of individuals in the Klamath River baseline collection were assigned ($q > 0.5$) to the correct Northern DPS cluster. Likewise, 99.5% of the fish from the Rogue River collection were also assigned to the Northern DPS cluster, and 97.2% of the Sacramento River collection were assigned to the Southern DPS cluster. Ninety-five percent of the reference samples from the Klamath and Rogue rivers had $q \geq 0.98$ estimated to be from the Northern DPS cluster, while 95% of the fish in the Sacramento River baseline had $q \geq 0.94$ from the Southern DPS cluster.

Estimation of estuarine aggregation stock composition

Estuarine aggregations of green sturgeon were determined to originate from both DPSs, although not necessarily reflecting their proximity to spawning populations. The three assignment testing programs yielded very similar estimates of estuarine stock composition (Fig. 5). The Southern DPS was the principal contributor to mixed collections found in San Pablo Bay, the Columbia River, and Willapa Bay. All three methods characterized both of the San Pablo Bay collections as being composed almost exclusively of green sturgeon from the Southern DPS. The estuary collections from the Columbia River and Willapa Bay contained larger pro-

portions (0.69–0.88) of Southern DPS green sturgeon than Northern DPS green sturgeon. The collection from Grays Harbor was estimated to have nearly equal proportions of Northern and Southern DPS green sturgeon, although all three analytical methods estimated slightly more Northern DPS (0.54–0.59) than Southern DPS green sturgeon. The Winchester Bay collections showed the largest range of stock composition variation (0.16–0.55 originating from the Southern DPS) between years and methods, and it could not be explained by the sample size difference alone.

Identifying cryptic populations in mixed aggregations

The negative log-likelihood ECDFs for fish assigned to the Southern DPS from any of the estuaries were all very similar in shape to the ECDF from the Southern DPS baseline (result not shown). In all estuary collections, it was impossible to reject the hypothesis that the distribution of negative log-likelihoods of the Southern DPS assigned fish differed from those of known Southern DPS fish (K–S test, $p > 0.26$ in all cases). The ECDFs of fish in the Willapa and Winchester estuary collections assigned to either the Rogue or Klamath River overlapped well with the ECDFs from the Rogue and Klamath baseline samples, respectively, and were, in fact, statistically indistinguishable (K–S test, $p > 0.21$ in all cases). However, in the Columbia River estuary sample, Rogue-assigned fish had negative log-likelihood values that differed significantly from the Rogue baseline (K–S test, $p = 0.049$), as did their Klamath-assigned counterparts (K–S test, $p = 0.009$). Similarly, in the collections from Grays Harbor, the ECDF of Rogue-assigned fish differed from the baseline (K–S test, $p = 0.01$), as did the ECDF of the Klamath-assigned fish (K–S test, $p = 0.005$). These results could indicate that in the two northernmost estuaries sampled, there were Northern DPS contributions from populations genetically distinguishable from either the Rogue or the Klamath. However, such a conclusion would merit caution, as none of the K–S tests remain statistically significant at the 0.05 level following Bonferroni correction for multiple tests.

Discussion

Comparison of methodological approaches

Polysomic microsatellites have been used in the literature for population structure analyses but have been possibly underutilized in assignment testing due to their perceived problems. The observed heterozygosity and number of alleles per individual per locus were similar among the microsatellite loci regardless of their gene dosage and inheritance pattern, suggesting that combining these data for pairwise population comparisons is a reasonable procedure that does not bias population structure analysis. Observed heterozygosities are likely influenced by relatedness among individuals in spawning collections and admixture of spawning populations in some estuarine collections. Since the number of loci inherited either disomically or tetrasomically under double reduction or independently is restricted, any calculations of linkage disequilibrium and Hardy–Weinberg proportions are similarly limited.

The highly variable nature of the polysomic microsatellite data provided an opportunity for comparing the relative utility of dominant and codominant data for individual assignment. The polymorphism at individual loci was great enough to permit algorithms using frequency data to characterize population identity as Northern and Southern DPSs based on this genetic variation. Moderate levels of genetic variation, supported by F_{ST} and neighbor-joining networks, between spawning populations were large enough to effectively assign unknown green sturgeon individuals into a genetic baseline representative of the principal green sturgeon lineages. The assignment testing procedures used demonstrated that the fractions of Southern DPS fish estimated in west coast estuaries were most likely accurate and reliable, despite the uncertainty in genetic scoring and inheritance of these tetrasomic markers. These results are encouraging and suggest that these assignment testing programs may be useful with other polyploid fish taxa of management interest such as sharks and carp (Leggatt and Iwama 2003).

All three individual assignment methods seemed quite accurate with low bias, and allelic phenotype and genotypic frequency data sets yielded very similar results when tested for accurate self-assignment and allocation of unknown individuals. With *gsi_sim*, much of the variance in test set estimates of Southern DPS composition can be attributed to simple binomial sampling error caused by the fact that each test set contains a random, discrete number of Southern DPS fish. This fraction of simulated fishes assigned to baselines with AFLPOP was likely greater than the ones obtained by self-assignment of reference individuals because the phenotypes of the simulated individuals were simulated according to the inference model AFLPOP used, while the phenotypes of the self-assigned individuals from the reference samples are generated according to the correct, but unknown, natural process.

A better understanding of the inheritance of the tetrasomic markers would assist in adequately characterizing the rate of double reduction and describing the expected heterozygosity of these markers. Also, collections characterizing spawning populations constituted individual and multiple brood years in the cases of the Southern and Northern DPSs, respectively. Inheritance and sampling may influence the assignment of unknown fish to DPSs, although the similar observed heterogeneity and polymorphic content among collections and loci support the use of these collections and makers for individual assignment testing. It appears that genetic differentiation (allelic variation) among DPSs in the baseline is large enough that any unrecognized misinterpretation of genotype variation (allelic frequency) does not affect our results. This was supported by the high success rate of self-assignment and consensus between the methods used for assigning individuals from highly skewed and equally proportioned mixtures.

Stock composition of aggregations

The persistence of genetic differentiation among spawning populations of North American green sturgeon despite significant coastal movement suggests that migration is not a homogenizing force in this broadly distributed species and spawning fidelity has likely generated moderate genetic differences between Northern and Southern DPSs. Although low genetic differentiation among annual collections from spawning rivers was observed, these were grouped into two

baseline groups reflecting both DPSs for the likelihood-based individual assignment testing, since spawning cohorts are overlapping and intergenerational.

These data do not support the hypothesis that all green sturgeon aggregations are composed of the spawning populations that they are closest to and demonstrate a population-scale pattern of Southern DPS specific green sturgeon presence in Northern DPS estuaries. Except for a very small number of Northern DPS green sturgeon in the most southern summer aggregation, estuaries sampled in this study contained both population segments. Our results found very few Northern DPS green sturgeon in the San Pablo Bay collections, supporting the observation that green sturgeon migrate north preferentially once they enter their coastal migration (Lindley et al. 2008). In Winchester Bay, the proportions of green sturgeon from the two DPSs are distinct between the years sampled, although the small sample size of the 2002 collection does not appear to influence the relatively small proportion of Southern DPS fish in that collection. Southern DPS green sturgeon were present in the Columbia River, Willapa Bay, and Grays Harbor collections in greater propotion than expected based on the proximity of these collections to Northern DPS spawning rivers.

This study's results do not support aggregation mixture proportions reflecting the purported abundance of green sturgeon in spawning rivers. Hundreds of adult green sturgeon in the Klamath River are annually harvested, while considerably fewer adult green sturgeon are observed annually in the Sacramento River spawning areas (Adams et al. 2007; M. Gingras, California Department of Fish and Game, Bay Delta Region, 4001 North Wilson Way, Stockton, CA 95205, USA, personal communication (2008); J.A. Israel, unpublished data). Given these limited data, subadult and adult Northern DPS green sturgeon should be more frequently encountered in Northern DPS estuaries than Southern DPS green sturgeon. However, Southern DPS green sturgeon were observed in greater numbers in the majority of estuaries sampled within and outside their DPS boundary and formed the majority of aggregations in the Columbia River, and Willapa Bay and in one Winchester Bay collection. Winchester Bay is the first estuary north of Northern DPS spawning rivers and the variable composition of aggregations may possibly be influenced by nonsynchronous DPS subadult abundances, although no data exist to explore this hypothesis. This study's results suggest that neither spawning river proximity nor adult abundance explains aggregation composition patterns in green sturgeon, and other population-specific processes may contribute to stock composition patterns. It is possible that the southerly sampling on green sturgeon's distribution has biased the apparent dissimilarity between presumed abundance and proportion of occurrence in estuarine collections. Additional collection of green sturgeon from northern Pacific rivers and estuaries would allow for a closer examination of Northern DPS fishes' presence in estuaries.

Green sturgeon migration patterns appear to not be limited to spawning river fidelity, and they may be similar to other sturgeon that use known locations to enhance their fitness and chances for survival (Bemis and Kynard 1997). Southern DPS green sturgeon may demonstrate preferences for estuarine habitat distinct from Northern DPS fishes, and aggregation into preferred estuarine habitats has been demonstrated in other anadromous and marine fishes (Kallio-Nyberg et al. 1999; Corten 2002). The occupation of estuaries by Southern DPS green sturgeon far from their spawning river is similar to the pattern of estuarine occupancy observed for anadromous Gulf sturgeon (*Acipenser oxyrinchus desotoi*) (Sulak and Randall 2002). It is also similar to the Hudson River Atlantic sturgeon's (*Acipenser oxyrinchus oxyrinchus*) propensity for coastal migration into the distant Delaware River and aggregation with sturgeon from other spawning rivers (Waldman et al. 1996). Investigation into mechanisms of habit formation and migratory tradition in green sturgeon and other anadromous sturgeon could provide insight into nongenetic determinants of fidelity and migration behavior.

Efforts to continue interjurisdictional studies to evaluate distribution and abundance of each green sturgeon DPS are critical to the recovery of Southern DPS green sturgeon and the conservation of this species. Recognizing each green sturgeon DPS's complex migratory patterns is necessary for effectively monitoring and minimizing negative impacts on each population segment. Recent closures of estuarine bycatch and sport fisheries involving green sturgeon in California, Oregon, and Washington will benefit the Southern green sturgeon DPS by decreasing the potential for overexploitation of this threatened stock where it occurs in Northern DPS estuaries. In locations such as Winchester Bay and Grays Harbor, where mixing occurs between DPSs, the collection and analysis of additional ecological data on aggregation and capture locations will be useful for identifying each DPS's preferred habitat during estuarine occupancy and migration. Due to stock complexity, the management of green sturgeon will require more focused, intensive interdisciplinary research and monitoring to reduce the uncertainties of alternate restoration and recovery actions for the species.

Acknowledgements

This study was made possible through the collaboration of D. Hillemeier and associates of the Yurok Tribal Fisheries Program, N. Kogut and M. Gingras and associates of the California Department of Fish and Game, B. Poytress and associates of the Red Bluff Fish and Wildlife Service Office, T. Rien, R. Farr, and associates of the Oregon Department of Fish and Wildlife, and O. Langness and associates of the Washington Department of Fish and Wildlife, who all collected and provided samples for this study. Ethan Mora provided the map. Earlier drafts of this manuscript benefited from constructive comments from P. Moyle, B. Ardren, and M. Chilcote as well as three anonymous reviewers. This study has been supported by funds from CALFED (Nos. ERP-02D-P57, 98-C15, and 99-F105), Anadromous Fish Restoration Program (11332-1-G005), Washington Department of Fish and Wildlife, and University of California, Davis, Ecology Graduate Group Block Grants, Hart, Cole, Goss Summer Research Fellowships, and Butler and Walker University Fellowships to J.A.I.

References

Adams, P.B., Grime, C., Hightower, J.E., Lindley, S.T., Moser, M.L., and Parsley, M.J. 2007. Population status of North Amer-

ican green sturgeon, *Acipenser medirostris*. Environ. Biol. Fishes, **79**(3–4): 339–356. doi:10.1007/s10641-006-9062-z.

Allen, P.J., and Cech, J.J., Jr. 2007. Age/size effects on juvenile green sturgeon, *Acipenser medirostris*, oxygen consumption, growth, and osmoregulation in saline environments. Environ. Biol. Fishes, **79**(3–4): 211–229. doi:10.1007/s10641-006-9049-9.

Anderson, E.C., Waples, R.S., and Kalinowski, S.T. 2008. An improved method for predicting the accuracy of genetic stock identification. Can. J. Fish. Aquat. Sci. **65**(7): 1475–1486. doi:10.1139/F08-049.

Beacham, T.D., Gould, A.P., Withler, R.E., Murray, C.B., and Barner, L.W. 1987. Biochemical genetic survey and stock identification of chum salmon (*Oncorhynchus keta*) in British Columbia. Can. J. Fish. Aquat. Sci. **44**(10): 1702–1713. doi:10.1139/f87-209.

Becher, S.A., Steinmetz, K., Weising, K., Boury, S., Peltier, D., Renou, J.-P., Kahl, G., and Wolff, K. 2000. Microsatellites for cultivar identification in *Pelargonium*. Theor. Appl. Genet. **101**(4): 643–651. doi:10.1007/s001220051526.

Bemis, W.E., and Kynard, B. 1997. Sturgeon rivers: an introduction to acipenseriform biogeography and life history. Environ. Biol. Fishes, **48**(1–4): 167–183. doi:10.1023/A:1007312524792.

Bever, J.D., and Felber, F. 1992. The theoretical population genetics of autoploidy. *In* Oxford surveys in evolutionary biology. Oxford University Press, Oxford, U.K. pp. 185–217.

Cadrin, S.X., Friedland, K.D., and Waldman, J.R. 2005. Stock identification methods — an overview. *In* Stock identification methods. *Edited by* S.X. Cadrin, K.D. Friedland, and J.R. Waldman. Elsevier, Burlington, Mass. pp. 3–6.

Cavalli-Sforza, L.L., and Edwards, A.W.F. 1967. Phylogenetic analysis. Models and estimation procedures. Am. J. Hum. Genet. **19**(3 Pt. 1): 233–257. PMID:6026583.

Cosway, C., and Stevenson, D.E. 2007. Confirmed records of two green sturgeon from the Bering Sea and Gulf of Alaska. Northwest. Nat. **88**(3): 188–192. doi:10.1898/1051-1733(2007)88[188:CROTGS]2.0.CO;2.

Corten, A. 2002. The role of "conservatism" in herring migrations. Rev. Fish Biol. Fish. **11**(4): 339–361. doi:10.1023/A:1021347630813.

De Silva, H.N., Hall, A.J., Rikkerink, E., McNeilage, M.A., and Fraser, L.G. 2005. Estimation of allele frequencies in polyploids under certain patterns of inheritance. Heredity, **95**(4): 327–334. doi:10.1038/sj.hdy.6800728. PMID:16094298.

Dempster, A.P., Laird, N.M., and Rubin, D.B. 1977. Maximum likelihood from incomplete data via the EM algorithm (with discussion). J. R. Stat. Soc. B, **39**: 1–38.

Duchesne, P., and Bernatchez, L. 2002. AFLPOP: a computer program for simulated and real population allocation, based on AFLP data. Mol. Ecol. Notes, **2**(3): 380–383. doi:10.1046/j.1471-8286.2002.00251.x.

Dugo, M.A., Kreiser, B.R., Ross, S.T., Slack, W.T., Heise, R.J., and Bowen, B.R. 2004. Conservation and management implications of fine-scale genetic structure of Gulf sturgeon in the Pascagoula River, Mississippi. J. Appl. Ichthyol. **20**(4): 243–251. doi:10.1111/j.1439-0426.2004.00572.x.

Efron, B., and Gong, G. 1983. A leisurely look at the bootstrap, the jackknife, and cross-validation. Am. Stat. **37**(1): 36–48. doi:10.2307/2685844.

Erickson, D.L., and Hightower, J.E. 2007. Oceanic distribution and behavior of green sturgeon. *In* Anadromous sturgeons: habitats, threats, and management. *Edited by* J. Munro, D. Hatin, K. McKown, J. Hightower, K.J. Sulak, A.W. Kahnle, and F. Caron. American Fisheries Society Symposium No. 56. American Fisheries Society, Bethesda, Md. pp. 197–211.

Erickson, D.L., and Webb, M.A.H. 2007. Spawning periodicity, spawning migration, and size at maturity of green sturgeon, *Acipenser medirostris*, in the Rogue River, Oregon. Environ. Biol. Fishes, **79**(3–4): 255–268. doi:10.1007/s10641-006-9072-x.

Evanno, G., Regnaut, S., and Goudet, J. 2005. Detecting the number of clusters of individuals using the software STRUCTURE: a simulation study. Mol. Ecol. **14**(8): 2611–2620. doi:10.1111/j.1365-294X.2005.02553.x. PMID:15969739.

Felsenstein, J. 2005. PHYLIP (Phylogeny Inference Package) version 3.6.6. Available from evolution.genetics.washington.edu/phylip.html [accessed 20 September 2006].

Goudet, J. 2001. FSTAT, a program to estimate and test gene diversities and fixation indices (version 2.9.3). Available from www2.unil.ch/popgen/softwares/fstat.htm.

Israel, J.A., Cordes, J.F., Blumberg, M.A., and May, B. 2004. Geographic patterns of genetic differentiation among collections of green sturgeon. N. Am. J. Fish. Manag. **24**(3): 922–931. doi:10.1577/M03-085.1.

Kalinowski, S.T. 2003. Genetic Mixture Analysis 1.0. Department of Ecology, Montana State University, Bozeman, MT 59717, USA. Available for download from www.montana.edu/kalinowski.

Kallio-Nyberg, I., Peltonen, H., and Rita, H. 1999. Effects of stock-specific and environmental factors on the feeding migration of Atlantic salmon (*Salmo salar*) in the Baltic Sea. Can. J. Fish. Aquat. Sci. **56**(5): 853–861. doi:10.1139/cjfas-56-5-853.

King, T.L., Lubinski, B.A., and Spidle, A.P. 2001. Microsatellite DNA variation in Atlantic sturgeon (*Acipenser oxyrinchus oxyrinchus*) and cross-species amplification in the Acipenseridae. Conserv. Genet. **2**(2): 103–119. doi:10.1023/A:1011895429669.

Klimley, A.P., Allen, P.J., Israel, J.A., and Kelly, J.T. 2007. Green sturgeon and its environment: past, present, and future. Environ. Biol. Fishes, **79**(3–4): 415–421. doi:10.1007/s10641-006-9177-2.

Lackey, R.T. 2009. Challenges to sustaining diadromous fishes through 2100: lessons learned from western North America. *In* Challenges for diadromous fishes in a dynamic global environment. *Edited by* A. Haro, K.L. Smith, R.A. Rulifson, C.M. Moffitt, R.J. Klauda, M.J. Dadswell, R.A. Cunjak, J.A. Cooper, K.L. Beal, and T.S. Avery. American Fisheries Society Symposium No. 69, American Fisheries Society Symposium, Bethesda, Md. In press.

Latch, E.K., Dharmarajan, G., Glaubitz, J.C., and Rhodes, O.E., Jr. 2006. Relative performance of Bayesian clustering software for inferring population substructuring and individual assignment at low levels of population differentiation. Conserv. Genet. **7**(2): 295–302. doi:10.1007/s10592-005-9098-1.

Leggatt, R.A., and Iwama, G.K. 2003. Occurrence of polyploidy in the fishes. Rev. Fish Biol. Fish. **13**(3): 237–246. doi:10.1023/B:RFBF.0000033049.00668.fe.

Lewis, P.O., and Zaykin, D. 2001. Genetic Data Analysis: computer program for the analysis of allelic data. Version 1.0 (d16c). Available from lewis.eeb.uconn.edu/lewishome/software.html [accessed 15 September 2006].

Lindley, S.T., Moser, M.L., Erickson, D.L., Belchik, M., Welch, D.W., Rechisky, E.L., Kelly, J.T., Heublein, J.C., and Klimley, A.P. 2008. Marine migration of North American green sturgeon. Trans. Am. Fish. Soc. **137**(1): 182–194. doi:10.1577/T07-055.1.

Ludwig, A., Belfiore, N.M., Pitra, C., Svirsky, V., and Jenneckens, I. 2001. Genome duplication events and functional reduction of ploidy levels in sturgeon (*Acipenser*, *Huso* and *Scaphirhynchus*). Genetics, **158**(3): 1203–1215. PMID:11454768.

Luo, Z.W., Zhang, Z., Zhang, R.M., Pandey, M., Gailing, O., Hattemer, H.H., and Finkeldey, R. 2005. Modeling population ge-

netic data in autotetraploid species. Genetics, **172**(1): 639–646. doi:10.1534/genetics.105.044974. PMID:16172506.

Manel, S., Berthier, P., and Luikart, G. 2002. Detecting wildlife poaching: identifying the origin of individuals with Bayesian assignment tests and multilocus genotypes. Conserv. Biol. **16**(3): 650–659. doi:10.1046/j.1523-1739.2002.00576.x.

Marsden, J.E., Krueger, C.C., and May, B. 1989. Identification of parental origin of naturally produced lake trout in Lake Ontario: application of mixed stock analysis to a second generation. N. Am. J. Fish. Manag. **9**(3): 257–268. doi:10.1577/1548-8675(1989)009<0257:IOPOOL>2.3.CO;2.

McQuown, E.C., Sloss, B.L., Sheehan, R.J., Rodzen, J., Tranah, G.J., and May, B. 2000. Microsatellite analysis of genetic variation in sturgeon: new primer sequences for *Scaphirhynchus* and *Acipenser*. Trans. Am. Fish. Soc. **129**(6): 1380–1388. doi:10.1577/1548-8659(2000)129<1380:MAOGVI>2.0.CO;2.

Miller, L.W. 1972. Migrations of sturgeon tagged in the Sacramento – San Joaquin Estuary. Calif. Fish Game, **58**: 102–106.

Moser, M.M., and Lindley, S.T. 2007. Use of Washington estuaries by subadult and adult green sturgeon. Environ. Biol. Fishes, **79**(3–4): 243–253. doi:10.1007/s10641-006-9028-1.

Moyle, P. 2002. Inland fishes of California. University of California Press, Berkeley, Calif.

Paetkau, D., Calvert, W., Stirling, I., and Strobeck, C. 1995. Microsatellite analysis of population structure in Canadian polar bears. Mol. Ecol. **10**: 2375–2388.

Pritchard, J.K., Stephens, M., and Donnelly, P. 2000. Inference of population structure using multilocus genotype data. Genetics, **155**(2): 945–959. PMID:10835412.

Pritchard, J.K., Wen, X., and Falush, D. 2007. Documentation for structure software. Version 2.2. University of Chicago, Chicago, Ill.

Pyatskowit, J.D., Krueger, C.C., Kincaid, H.L., and May, B. 2001. Inheritance of microsatellite loci in the polyploid lake sturgeon (*Acipenser fulvescens*). Genome, **44**(2): 185–191. doi:10.1139/gen-44-2-185. PMID:11341728.

Rannala, B., and Mountain, J.L. 1997. Detecting immigration by using multilocus genotypes. Proc. Natl. Acad. Sci. U.S.A. **94**(17): 9197–9201. doi:10.1073/pnas.94.17.9197. PMID:9256459.

Rodzen, J.A., and May, B. 2002. Inheritance of microsatellite loci in the white sturgeon (*Acipenser transmontanus*). Genome, **45**(6): 1064–1076. doi:10.1139/g02-083. PMID:12502251.

Scribner, K.T., Crane, P.A., Spearman, W.J., and Seeb, L.W. 1998. DNA and allozyme markers provide concordant estimates of population differentiation: analyses of U.S. and Canadian populations of Yukon River fall-run chum salmon (*Oncorhynchus keta*). Can. J. Fish. Aquat. Sci. **55**(7): 1748–1758. doi:10.1139/cjfas-55-7-1748.

Seeb, L.W., Habicht, C., Templin, W.D., Tarbox, K.E., Davis, R.Z., Brannian, L.K., and Seeb, J.E. 2000. Genetic diversity of sockeye salmon of Cook Inlet, Alaska, and its application to management of populations affected by the *Exxon Valdez* oil spill. Trans. Am. Fish. Soc. **129**(6): 1223–1249. doi:10.1577/1548-8659(2000)129<1223:GDOSSO>2.0.CO;2.

Shmigirilov, A.P., Mednikova, A.A., and Israel, J.A. 2007. Comparison of biology of the Sakhalin sturgeon, Amur sturgeon, and kaluga from the Amur River, Sea of Okhotsk, and Sea of Japan biogeographic Province. Environ. Biol. Fishes, **79**(3–4): 383–395. doi:10.1007/s10641-006-9050-3.

Smouse, P.E., Waples, R.S., and Tworek, J.A. 1990. A genetic mixture analysis for use with incomplete source population data. Can. J. Fish. Aquat. Sci. **47**(3): 620–634. doi:10.1139/f90-070.

Sokal, R.R., and Rohlf, F.T. 1995. Biometry. W.H. Freeman and Company, New York.

Stephenson, R.L. 1999. Stock complexity in fisheries management: a perspective of emerging issues related to population sub-units. Fish. Res. **43**(1–3): 247–249. doi:10.1016/S0165-7836(99)00076-4.

Sulak, K.J., and Randall, M. 2002. Understanding sturgeon life history: enigmas, myths, and insights from scientific studies. J. Appl. Ichthyol **18**(4–6): 519–528. doi:10.1046/j.1439-0426.2002.00413.x.

Thrall, P.H., and Young, A. 2000. AUTOTET: a program for analysis of autotetraploid genotypic data. J. Hered. **91**(4): 348–349. doi:10.1093/jhered/91.4.348. PMID:10912686.

Van Eenennaam, A.L., Murray, J.D., and Medrano, J.F. 1999. Karotype of the American green sturgeon. Trans. Am. Fish. Soc. **128**(1): 175–177. doi:10.1577/1548-8659(1999)128<0175:KOTAGS>2.0.CO;2.

Van Eenennaam, J.P., Linares, J., Doroshov, S.I., Hillemeier, D.C., Willson, T.E., and Nova, A.A. 2006. Reproductive conditions of the Klamath River green sturgeon. Trans. Am. Fish. Soc. **135**(1): 151–163. doi:10.1577/T05-030.1.

Waldman, J.R., Hart, J.T., and Wirgin, I.I. 1996. Stock composition of the New York Bight Atlantic sturgeon fishery based on analysis of mitochondrial DNA. Trans. Am. Fish. Soc. **125**(3): 364–371. doi:10.1577/1548-8659(1996)125<0364:SCOTNY>2.3.CO;2.

Weir, B., and Cockerham, C.C. 1984. Estimating *F*-statistics for the analysis of population structure. Evolution, **38**(6): 1358–1370. doi:10.2307/2408641.

Welsh, A.B., Blumberg, M.A., and May, B. 2003. Identification of microsatellite loci in lake sturgeon, *Acipenser fulvescens*, and their variability in green sturgeon, *A. medirostris*. Mol. Ecol. Notes, **3**(1): 47–55. doi:10.1046/j.1471-8286.2003.00346.x.

Wright, J.E., Jr., Johnson, K., Hollister, A., and May, B. 1983. Meiotic models to explain classical linkage, pseudolinkage, and chromosome pairing in tetraploid derivative salmonid genomes. Isozymes: Curr. Top. Biol. Med. Res. **10**: 239–260. PMID:6354984.

Zane, L., Patarnello, T., Ludwig, A., Fontana, F., and Congiu, L. 2002. Isolation and characterization of microsatellites in the Adriatic sturgeon (*Acipenser naccarii*). Mol. Ecol. Notes, **2**(4): 586–588. doi:10.1046/j.1471-8286.2002.00328.x.

Zhu, B., Liao, X., Shao, Z., Rosenthal, H., and Chang, J. 2005. Isolation and characterization of microsatellites in Chinese sturgeon, *Acipenser sinensis*. Mol. Ecol. Notes, **5**(4): 888–892. doi:10.1111/j.1471-8286.2005.01100.x.

Unnatural random mating policies select for younger age at maturity in hatchery Chinook salmon (*Oncorhynchus tshawytscha*) populations

David G. Hankin, Jacqueline Fitzgibbons, and Yaming Chen

Abstract: We explored the long-term consequences of three mating regimes ((1) completely random, (2) completely random but excluding jacks (age 2 males), and (3) male length ≥ female length) on age and sex structure of wild and hatchery populations of Chinook salmon (*Oncorhynchus tshawytscha*). Regimes similar to regimes 1 or 2 are used at most salmon hatcheries, whereas regime 3 emulates the outcomes of natural spawning behaviors that favor larger males. Inheritance of age at maturity is captured in age- and sex-structured models via matrices of age- and sex-specific conditional maturation probabilities that depend on age and sex of parents. In unexploited populations, regime 1 leads to substantial long-term selection for younger age at maturity, an effect that is somewhat reduced by regime 2, but greatly reduced under regime 3. Equilibrium age and sex structures for wild and hatchery populations under regime 3 are similar to those of natural populations, whereas mating regime 1 generates age structure that is greatly shifted toward younger ages and jacks. To prevent unintentional selection for younger age at maturity, we recommend that large-scale hatcheries replace unnatural completely random mating regimes with mating regimes that emulate the outcomes of natural spawning behaviors.

Résumé : Nous explorons les conséquences à long terme de trois régimes d'appariement ((1) complètement aléatoire, (2) complètement aléatoire à l'exception des madeleineaux (mâles d'âge 2) et (3) la longueur des mâles ≥ celle des femelles) sur la structure d'âge et de sexe de populations sauvages et de populations de pisciculture de saumons chinook (*Oncorhynchus tshwawytscha*). La plupart des pisciculture de saumons utilisent des régimes semblables à 1 ou 2, alors que le régime 3 simule les résultats des comportements naturels de fraie qui favorisent les mâles plus grands. L'héritabilité de l'âge à la maturité est saisie dans les modèles structurés d'après l'âge et le sexe à travers des matrices de probabilités conditionnelles de maturation spécifiques à l'âge et au sexe qui dépendent de l'âge et du sexe des parents. Dans les populations inexploitées, le régime 1 conduit à une importante sélection à long terme d'une réduction de l'âge à la maturité; cet effet est moins marqué avec le régime 2 et fortement réduit par le régime 3. L'âge à l'équilibre et la structure sexuelle des populations sauvages et élevées sous le régime 3 sont semblables à ceux des populations naturelles, alors que le régime d'appariement 1 produit une structure d'âge qui favorise fortement les âges moins élevés et les madeleineaux. Afin d'éviter une sélection involontaire d'une réduction de l'âge à la maturité, nous recommandons que les grandes piscicultures remplacent les régimes d'appariement complètement aléatoires qui ne sont pas naturels par des régimes qui simulent les résultats des comportements naturels de fraie.

[Traduit par la Rédaction]

Introduction

Of the semelparous Pacific salmon (*Oncorhynchus*) species, the Chinook salmon, *Oncorhynchus tshawytscha*, has perhaps the greatest variation in size and age at maturity. Female Chinook salmon typically return to freshwater as mature adults at ages 3 through 6, at sizes ranging from 4 to 40 kg; female maturation at age 2 is rare. Male Chinook salmon typically mature at ages 2 (as precocious males hereafter referred to as "jacks") through 6 at sizes ranging from 1 to 50 kg; male maturation as jacks is common in many stocks (Healey 1991). Nicholas and Hankin (1988) classified Oregon coastal Chinook salmon populations into three categories (early-, mid-, and late-maturing) based on the dominant age of females among returning spawners. In early-maturing Oregon stock types, most females mature at age 3, whereas in mid- and late-maturing populations, most females mature at ages 4 and 5, respectively. Male age at maturity is not always closely tied to female age at maturity. Most late-maturing populations have a low incidence of jacks (e.g., Trask River, Oregon, fall Chinook salmon), but some late-maturing populations (e.g., Salmon River, Oregon, fall Chinook salmon) have a high incidence of jacks (Nicholas and Hankin 1988, their table I.2).

The possibility of fishery-induced long-term decreases in the average size and age at maturity of Chinook salmon has been of concern for more than 100 years (Rutter 1904; Hard et al. 2008), but it is only relatively recently that fishery scientists have begun to appreciate and quantify the extent to which age at maturity is inherited in this species. Based on hatchery age-at-maturity experiments carried out at the Uni-

Received 17 July 2008. Accepted 20 April 2009. Published on the NRC Research Press Web site at cjfas.nrc.ca on 2 September 2009. J20674

D.G. Hankin,[1] J. Fitzgibbons, and Y. Chen. Department of Fisheries Biology, Humboldt State University, Arcata, CA 95521, USA.

[1]Corresponding author (e-mail: dgh1@humboldt.edu).

versity of Washington in the 1960s, Ricker (1972) estimated heritabilities for age at maturity of 0.22 for males and 0.19 for females. Based on returns from more extensive age-at-maturity experiments carried out at Oregon's Elk River Hatchery during the 1970s, Hankin et al. (1993) calculated substantially higher heritabilities for age at maturity: 0.49–0.57 for males and 0.39–0.41 for females. Elk River Hatchery experiments also showed that male parental age had much more effect on age at maturity of male than female progeny (Hankin et al. 1993). Using more sophisticated methods, Hard's (1995) recalculated heritabilities for the Elk River Hatchery experiments were 0.81 for male parent on male offspring, 0.67 for male parent on female offspring, 0.39 for female parent on male offspring, and 0.59 for female parent on female offspring. Hard (2004) reported model-based maximum likelihood estimates of heritability for age at maturity in Chinook salmon that ranged from 0.35 to 0.52.

Size-selective ocean fishery harvest of immature Chinook salmon shifts the age structure of spawning runs toward younger ages, the result of a classic "fishing-down" process (see Ricker 1976; Hankin and Healey 1986). A fishery-induced shift toward younger-aged spawners, coupled with strong inheritance of age at maturity, can theoretically cause additional long-term genetic changes in the average size and age at which fish mature (Ricker 1980; Hard 2004; Hard et al. 2008). In naturally spawning populations, such fishery-induced long-term genetic shifts toward younger ages may be partially offset by natural spawning behaviors that favor spawning success of older and larger fish, particularly males (Baxter 1991; Berejikian et al. 2000). Jacks usually spawn as sneaker males (Gross 1991; Fleming and Gross 1994; Fleming and Reynolds 2004) and are often driven off by females and larger males (Baxter 1991). Among adult males that directly compete for females, the largest and oldest males spawn more frequently in dominant status and with a greater number of females (Baxter 1991). Female behaviors may also reduce the spawning success of jacks and smaller males through at least two mechanisms: females may delay successive spawning events when only smaller males are present (Berejikian et al. 2000), and they exhibit agnostic behaviors toward males smaller than their size (Baxter 1991).

At most salmon hatcheries, larger and older males do not enjoy greater reproductive success than smaller and younger males because mating regimes are often deliberately "completely random" (or nearly so) as a device to maximize genetic diversity and effective population size of hatchery populations (Flagg et al. 2004; Hatchery Scientific Review Group (HSRG) 2004; US Fish and Wildlife Service 2005). (Note, however, that actual spawnings in a real hatchery setting may not be "completely random", even when hatchery guidelines call for that result. See McLean et al. 2005.) Under a completely random mating policy, a small jack has the same probability of successful mating as a large age 5 or age 6 male. Such unnatural random mating protocols should cause unintended and possibly strong genetic selection for younger age at maturity. A reduction in mean age at maturity may contribute to a reduction in spawning success of hatchery fish (as compared with wild fish) spawning in natural habitats, may have a negative effect on productivity of wild populations due to interbreeding between stray hatchery fish and wild fish (Waples 1991; Araki et al. 2007), and may thereby reduce long-term fishery yields from naturally spawning populations.

In this paper, we develop age- and sex-structured models of hatchery and wild (naturally spawning) populations of Chinook salmon that explicitly incorporate mating regimes (mating behaviors) and size-selective ocean fishing. Model performance is driven primarily by age- and sex-specific conditional maturation probabilities that depend on the ages of male and female parents. These parental age- and sex-dependent maturation probabilities reflect the underlying maturity schedule of a given natural population and allow our models to incorporate inheritance of age at maturity. We used these models to study the potential long-term effects of (*i*) alternative mating regimes and (*ii*) size-selective ocean fishing on the age and sex composition of an example early- to mid-maturing stock type for hatchery and wild populations of Chinook salmon.

Materials and methods

Our models for both hatchery and wild populations of Chinook salmon assume the following annual sequence of events for a fish alive in the ocean at age k ($k = 2, \ldots, 6$): ocean harvest, followed by potential maturation and return to a hatchery or natural spawning grounds for spawning, followed by ocean natural mortality (for fish that remain immature at age k). Males mature at ages 2 through 6, and females mature at ages 3 through 6, with ages of males and females distinguished by subscripts "M" and "F", respectively. Both models incorporate size-selective ocean fishing that targets both maturing and immature fish prior to potential maturation and return to freshwater for spawning. Given that a fish is alive and is not caught at age k, the probability that an individual will mature at age k is based on age- and sex-specific conditional maturation probabilities, $\sigma_{kM}(i,j)$ or $\sigma_{kF}(i,j)$, where i denotes age of male parent and j denotes age of female parent. For each mating type (i,j), there are five possible ages at maturity for males and four possible ages at maturity for females. There are a total of 20 possible mating types (i,j); hence, there are a total of 100 $\sigma_{kM}(i,j)$ for males and 80 $\sigma_{kF}(i,j)$ for females. Specification of these $\sigma_{kM}(i,j)$ and $\sigma_{kF}(i,j)$ is somewhat analogous to a specification of heritability of age at maturity in this species.

A listing of model variables and parameters that are shared by both hatchery and wild population models is provided (Table 1). Model components that are specific to hatchery or wild population models are presented separately in following sections. Below we provide a summary of model assumptions and basic model components.

Model assumptions

Our models invoke a considerable number of assumptions about (*a*) mating and rearing procedures for hatchery populations or mating behaviors of wild populations, (*b*) ocean and freshwater fisheries, and (*c*) length at age. These assumptions are invoked to simplify development, analysis, and interpretation of the models presented in this paper, but many could be relaxed in future modeling research. Assumptions include (*i*) all matings are 1:1 and there is no

Table 1. Definitions of model variables (upper case) and parameters (lower case) that are shared by wild and hatchery models.

$\sigma_{kF}(i,j)$	Conditional probability of maturing at age k for an age k female with age i male parent and age j female parent (given alive at age k)
$\sigma_{kM}(i,j)$	Conditional probability of maturing at age k for an age k male with age i male parent and age j female parent (given alive at age k)
$N_{kF}(t)$	Number of age k females returning to spawn in year t
$N_{kM}(t)$	Number of age k males returning to spawn in year t
$R(t)$	Total ocean recruits at age 2 in year t, prior to fishing, produced by parental spawners in year $t-2$
$R_{ij}(t)$	Total number of age 2 recruits produced by matings of age i males with age j females in year $t-2$
$X_{ij}(t)$	Expected number of matings of age i males with age j females
$\Theta_{ij}(t)$	Expected total number of eggs generated from matings of age i males with age j females
p_2	Probability of survival from egg to age 2
p_k	Probability of survival from age k to age $k+1$ given that a fish is (a) alive at age k, (b) not caught in the ocean fishery at age k, and (c) does not mature at age k
u_k	Ocean exploitation rate at age k (probability of capture in ocean fishery at age k, given alive at age k)

Note: Lower-case t refers to year of recruitment, spawning, or adult return.

pooling of eggs or sperm; (*ii*) $\sigma_{2F}(i,j) = 0$ for all (i,j) (i.e., no females mature at age 2); (*iii*) all eggs, regardless of parental ages, are equally likely to hatch and survive to age 2; (*iv*) size at age k is independent of parental mating type (i,j); (*v*) male : female sex ratio at age 2 in the ocean, prior to possible maturation, is 50:50; (*vi*) age-specific ocean fishery exploitation rates are independent of parental mating type (i,j) and fish sex and are constant from year to year; (*vii*) there is no noncatch mortality in ocean fisheries; and (*viii*) there is no freshwater fishery harvest.

Basic model development and structure

Basic model structure

Given the above definitions and simplifying assumptions, the total number of fish returning to spawn by age and sex in year t are calculated from age 2 recruitments, $R_{ij}(t)$, for both hatchery and wild populations according to the following equations:

$$(1)\quad N_{2M}(t) = [0.5(1-u_2)]\sum_{i=2}^{6}\sum_{j=3}^{6}[\sigma_{2M}(i,j)R_{ij}(t)]$$

$$(2)\quad N_{3M}(t) = [0.5p_2(1-u_2)(1-u_3)]\sum_{i=2}^{6}\sum_{j=3}^{6}[\sigma_{3M}(i,j)(1-\sigma_{2M}(i,j))R_{ij}(t-1)]$$

$$(3)\quad N_{3F}(t) = [0.5p_2(1-u_2)(1-u_3)]\sum_{i=2}^{6}\sum_{j=3}^{6}[\sigma_{3F}(i,j)R_{ij}(t-1)]$$

$$(4)\quad N_{4M}(t) = [0.5p_2p_3(1-u_2)(1-u_3)(1-u_4)]\sum_{i=2}^{6}\sum_{j=3}^{6}[\sigma_{4M}(i,j)(1-\sigma_{2M}(i,j))(1-\sigma_{3M}(i,j))R_{ij}(t-2)]$$

$$(5)\quad N_{4F}(t) = [0.5p_2p_3(1-u_2)(1-u_3)(1-u_4)]\sum_{i=2}^{6}\sum_{j=3}^{6}[\sigma_{4F}(i,j)(1-\sigma_{3F}(i,j))R_{ij}(t-2)]$$

$$(6)\quad N_{5M}(t) = [0.5p_2p_3p_4(1-u_2)(1-u_3)(1-u_4)(1-u_5)]\sum_{i=2}^{6}\sum_{j=3}^{6}[\sigma_{5M}(i,j)(1-\sigma_{2M}(i,j))(1-\sigma_{3M}(i,j))\times(1-\sigma_{4M}(i,j))R_{ij}(t-3)]$$

$$(7)\quad N_{5F}(t) = [0.5p_2p_3p_4(1-u_2)(1-u_3)(1-u_4)(1-u_5)]\sum_{i=2}^{6}\sum_{j=3}^{6}[\sigma_{5F}(i,j)(1-\sigma_{3F}(i,j))(1-\sigma_{4F}(i,j))R_{ij}(t-3)]$$

$$(8)\quad N_{6SM}(t) = [0.5p_2p_3p_4p_5(1-u_2)(1-u_3)(1-u_4)(1-u_5)(1-u_6)]\sum_{i=2}^{6}\sum_{j=3}^{6}[\sigma_{6SM}(i,j)(1-\sigma_{2SM}(i,j))(1-\sigma_{3SM}(i,j))\times(1-\sigma_{4SM}(i,j))(1-\sigma_{5SM}(i,j))R_{ij}(t-4)]$$

$$(9)\quad N_{6F}(t) = [0.5p_2p_3p_4p_5(1-u_2)(1-u_3)(1-u_4)(1-u_5)(1-u_6)]\sum_{i=2}^{6}\sum_{j=3}^{6}[\sigma_{6F}(i,j)(1-\sigma_{3F}(i,j))(1-\sigma_{4F}(i,j))\times(1-\sigma_{5F}(i,j))R_{ij}(t-4)]$$

Models for hatchery populations

We present our evaluation of model performance for three alternative hatchery mating regimes: (1) completely random mating; (2) completely random mating, but excluding jacks as parents; and (3) male length ≥ female length.

Alternative mating regimes

Mating regime 1 — completely random mating

Under a completely random mating regime, all males are equally likely to serve as parents, regardless of their age or size, and the expected numbers of matings between age j females and age i males are

$$(10)\quad X_{ij}(t) = N_{jF}(t)\left[\frac{N_{iM}(t)}{N_{2M}(t)+N_{3M}(t)+N_{4M}(t)+N_{5M}(t)+N_{6M}(t)}\right]$$

Mating regime 2 — completely random mating, but jacks excluded

If no jacks are used as male parents, but hatchery matings are otherwise completely at random, then $X_{2j}(t) = 0$ for all j, and for $i \geq 3$, the expected numbers of matings between age j females and age i males are

$$(11)\quad X_{ij}(t) = N_{jF}(t)\left[\frac{N_{iM}(t)}{N_{3M}(t)+N_{4M}(t)+N_{5M}(t)+N_{6M}(t)}\right]$$

Mating regime 3 — male parent length ≥ female parent length

For this model, we separate male and female spawners into 27 grouping intervals, each 2 cm wide. We let l_n denote the upper limit of these intervals and we set $l_1 = 50$ and $l_{26} = 100$, roughly bracketing the smallest and largest lengths (MEPS (mid-eye to posterior scale) lengths, in cm) at maturity of age 3 and older adults in most Chinook salmon stocks. Assuming normal distributions of length at a given age, we used sex-specific means and standard deviations of lengths at age (see below) to calculate the expected proportions of fish that would have a size less than or equal to the upper limit of a length interval. Letting n denote grouping interval and $p(l_{iMn})$ and $p(l_{iFn})$ denote the probability that a male or female spawner, respectively, in a given age group would have length $\leq l_n$, the expected number of male and females parents of age k in each grouping interval would be

$$(12)\quad N_{kMn} = \begin{cases} N_{kM}\cdot p(l_{kM1}) & n=1 \\ N_{kM}\cdot[p(l_{kMn}) - p(l_{kM(n-1)})] & 2\leq n\leq 26 \\ N_{kM}\cdot[1-p(l_{kM26})] & n=27 \end{cases}$$

$$(13)\quad N_{kFn} = \begin{cases} N_{kF}\cdot p(l_{kF1}) & n=1 \\ N_{kF}\cdot[p(l_{kFn}) - p(l_{kF(n-1)})] & 2\leq n\leq 26 \\ N_{kF}\cdot[1-p(l_{kF26})] & n=27 \end{cases}$$

Under a mating regime for which male length ≥ female length, the corresponding expected numbers of matings between age j females and age i males are

$$(14)\quad X_{ij}(t) = \sum_{n=1}^{27}\left\{N_{jFn}(t)\left[\frac{\sum_{m\geq n}N_{iMm}(t)}{\sum_{k=2}^{6}\sum_{m\geq n}N_{kMm}(t)}\right]\right\}$$

(Note that because each length interval is 2 cm wide, it is possible that length of a male parent may actually be as much as 2 cm less than that of a female parent.)

Eggs to recruitment

For all three mating protocols, the expected number of eggs produced by each mating type, $\Theta_{ij}(t)$, was calculated from mean age-specific fecundities, f_j, as $\Theta_{ij}(t) = X_{ij}(t)f_j$. We assumed that a hatchery has a maximum egg rearing capacity, Θ_{max}, and that equal proportions of "excess" eggs were culled from each mating type (i,j) whenever

$$(15)\quad \sum_{i=2}^{6}\sum_{j=3}^{6}\Theta_{ij}(t) > \Theta_{max}$$

in which case the number of eggs retained for each mating type (i,j), $\Theta'_{ij}(t)$, was

$$(16)\qquad \Theta^{*}_{ij}(t) = \frac{\Theta_{ij}(t)\Theta_{\max}}{\sum_{i=2}^{6}\sum_{j=3}^{6}\Theta_{ij}(t)}$$

After culling, the total number of retained eggs equals $\Theta_{\max}$, which we set at 8 000 000, consistent with the capacity of a large-scale hatchery. For hatchery populations, the expected numbers of age 2 recruits originating from each mating type (i, j) are

$$(17)\qquad R_{ij}(t) = \begin{cases} p_1\Theta^{*}_{ij}(t-2) & \sum_{i=2}^{6}\sum_{j=3}^{6}\Theta_{ij}(t) > \Theta_{\max} \\ p_1 X_{ij}(t-2)f_j & \sum_{i=2}^{6}\sum_{j=3}^{6}\Theta_{ij}(t) \le \Theta_{\max} \end{cases}$$

Wild population models

Our models for naturally spawning populations of Chinook salmon share the same basic model structure sketched in eqs. 1–9 but also incorporate a Ricker (1954) stock–recruitment relation (to ensure a stable population size of moderate size) and stochastic rather than deterministic submodels for mate selection. (The performance of our wild population models with alternative stock–recruitment models has not been explored.) One submodel for mate selection is designed to emulate the outcomes of natural spawning behaviors and incorporates size- and frequency-dependent mate selection; a second submodel allows simulation of completely random mating.

Size- and frequency-dependent mate selection

Our model for natural mate selection in Chinook salmon was required to have two key features. First, for a female of a given length, the relative probability that a male would mate with this female must be a function of the relative size of the male compared with the size of particular female, with males (much) larger than this female having (much) greater relative probability of mating than males smaller than this female. Second, the actual probability that a given male might mate with a particular female must also be frequency-dependent, taking into account the size frequency distribution of all other males in the spawning population. Our simulations of matings in a wild Chinook population therefore incorporated a two-step process for mate selection, as described below.

Calculation of relative mating probability

We used cumulative logistic distribution functions with location parameters μ (mean) and s (scale) to generate relative mating probabilities, P_M, for males of length l_M to spawn with a particular female of length $l_F = \mu$:

$$(18)\qquad P_M = \frac{1}{1 + e^{-(l_M - \mu)/s}}$$

Equation 18 implies that $P_M = 0.5$ whenever $l_M = l_F$. P_M was set equal to 0.98 when $l_M = 110$ (maximum male length), allowing solution for s in terms of l_F:

$$(19)\qquad s = 0.2569 \cdot (110 - l_F)$$

An illustrative family of relative mating probability curves generated by the above procedures shows that relative mating probabilities for a male of MEPS length 80 cm would range from about 0.85 to less than 0.05 as female size ranged from 65 cm to 95 cm (Fig. 1).

Frequency-dependent mate selection

All females were assumed to spawn successfully, and individual females were selected randomly (equal probability without replacement) for selection of male mates. For a particular selected female of length l_F, relative mating probabilities for individual males (calculated using eqs. 18 and 19, with $\mu = l_F$) were summed over all males, producing a total value Z. (Note that the value of Z reflects the length frequency distribution and associated P_M values for all males in the population.) A male mate for this female was then selected by generating a uniform random variate on the interval $(0, Z)$ and finding the male for which the cumulative sum of the P_M corresponded to this random choice. These procedures generated mate selection probabilities with values P_M/Z for individual males; these probabilities sum to one. We allowed individual males to mate with multiple females via a parameter η that controlled the maximum number of matings for a given male. We let $\eta = 2$, 5, or 10 to assess sensitivity of our results to specification of η. If a particular male was selected as a successful mate on η occasions, it was removed from the population of potential male mates, thereby reducing the sum Z.

Completely random mate selection

For this submodel, individual males were selected as mates with equal probability with replacement, thereby allowing individual males to mate with more than one distinct female, with $\eta = 2$, 5, or 10.

Ricker stock–recruitment model

For both mate selection submodels, we tabulated the simulated number of matings of age i males with age j females, $X_{ij}(t)$. We calculated the corresponding total number of eggs produced by these matings, $\Theta_{ij}(t)$, by summing the length-specific expected fecundities (see below) for all of the age j females that had mated with age i males.

We used a Ricker (1954) stock–recruitment model to relate spawning stock, $S(t)$, to recruitment, $R(t + 2)$: $R(t + 2) = \alpha S(t)e^{-\beta S(t)}$. We measured $S(t)$ as the total number of eggs deposited by spawning females (i.e., $S(t) = \sum_{i=2}^{6}\sum_{j=3}^{6}\Theta_{ij}(t)$). Because all eggs were assumed equally likely to hatch and survive to age 2, the number of age 2 ocean recruits originating from each mating type (i, j), $R_{ij}(t + 2)$, was calculated as

$$(20)\qquad R_{ij}(t+2) = R(t+2)\frac{\Theta_{ij}(t)}{S(t)}$$

We set $\alpha = 0.0035$ and $\beta = 0.0000005$ so as to produce a (computationally tractable) unexploited equilibrium spawning population size of about 1000 adults (age 3 and older males and females combined) for both submodels of mate selection.

Specification of model parameter values

The performance of hatchery and wild population models was explored for an early- to mid-maturing stock type intended to mimic Oregon's Elk River fall Chinook salmon population for which there are extensive data concerning hatchery and natural spawners. In this section, we describe the basis for our specifications of model parameter values.

Age- and sex-specific conditional maturation probabilities

The most critical model parameters are the age- and sex-specific conditional maturation probabilities, calculated from analysis of returns from age- and sex-specific mating experiments carried out at Oregon's Elk River Hatchery (Hankin et al. 1993). We summarized these age- and sex-specific conditional maturation probabilities as a series of matrices (five for age 2 to age 6 males, four for age 3 to age 6 females), denoted by Φ_{aM} for males and Φ_{aF} for females, with (column, row) entries equal to the conditional maturation probabilities, $\sigma_{aM}(i,j)$ or $\sigma_{aM}(i,j)$, corresponding to a mating type of an age i male (ages 2–6, columns 1–5) with an age j female (ages 3–6, rows 1–4). For example, for age 3 males, we used

$$\Phi_{3M} = \begin{bmatrix} 0.7210 & 0.7004 & 0.4818 & 0.2633 & 0.1317 \\ 0.6730 & 0.6538 & 0.4497 & 0.2458 & 0.1229 \\ 0.6249 & 0.6070 & 0.4176 & 0.2282 & 0.1141 \\ 0.5768 & 0.5603 & 0.3855 & 0.2106 & 0.1053 \end{bmatrix}$$

From Φ_{3M}, if a male fish has reached age 3, the probability of maturing at age 3 is 0.7210 if the male parent were age 2 and female parent were age 3, compared with 0.2106 if the male and female parents were ages 5 and 6, respectively. The remaining Φ_{aM} and Φ_{aF} matrices are presented in Appendix A.

Fecundities

Mean age-specific fecundities (used for the hatchery population models) were based on the average fecundities of fish returning to Elk River Hatchery from 1971 through 1986 (D.G. Hankin, unpublished data). Average fecundities at age were $f_3 = 3850$, $f_4 = 4667$, and $f_5 = 5056$. Few age 6 fish were spawned, and when they were, mean fecundities were similar to those for age 5 fish. Therefore, we assumed that mean fecundities of age 6 fish were the same as those of age 5 fish (5056).

Expected length-specific fecundities (used for the wild population models) were based on records of individual fecundities (f_i) and lengths (l_i) for females returning to Elk River Hatchery in 1974–1975, 1977–1981, and 1986–1992. We fit a linear regression of $\ln(f_i)$ against $\ln(l_i)$ to estimate the parameters of an allometric length–fecundity relation: $f_i = 4.309 \cdot l_i^{4.202}$ ($n = 2335$, $P < 0.00005$, $R^2 = 0.4916$ for ln–ln fit).

Survival rates

Following Hankin et al. (1993), survival rates were set at $p_2 = 0.5$ and $p_3 = p_4 = p_5 = 0.8$ (values used for modeling Klamath River Chinook salmon by the Pacific Fishery Management Council). Survival rate from release to ocean age 2, p_1, was set equal to 0.01, a value consistent with a rough estimate of mean survival rate for fingerling releases of hatchery fall Chinook salmon (Hankin 1990).

Fig. 1. Example family of four cumulative logistic functions used to generate relative mating probabilities, P_M, for males of length l_M to mate with individual females of length l_F, here specified as l_F = 65, 75, 85, 95. $P_M = 0.50$ when $l_M = l_F$, and $P_M = 0.98$ at $l_M = 110$ for all l_F.

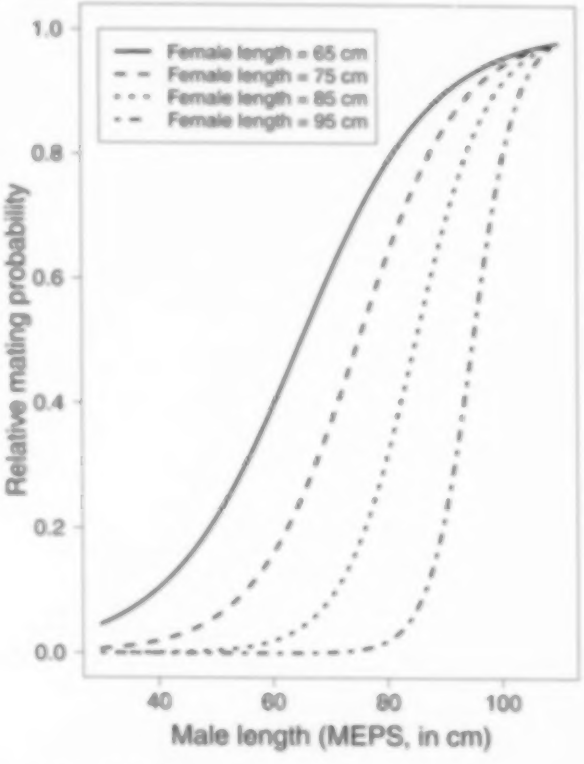

Ocean exploitation rates

Age-specific ocean exploitation rates, u_a, were allowed to take on three sets of levels (unexploited, moderately exploited, and heavily exploited) based on Hankin (1990) and Hankin et al. (1993). Age 2 Chinook are typically all below legal size limits, and only a fraction of age 3 Chinook salmon typically exceed minimum size limits in ocean fisheries, whereas virtually all age 4 and older Chinook salmon exceed minimum size limits. Therefore, we assumed generally that $u_2 = 0$ and that $u_3 < u_4 = u_5 = u_6$. Sets of exploitation rates used in model analysis were as follows:

Exploitation	u_2	u_3	u_4	u_5	u_6
None	0	0	0	0	0
Moderate	0	0.200	0.350	0.350	0.350
Heavy	0	0.250	0.438	0.438	0.438

Means and standard deviations of lengths at age

Means and standard deviations of MEPS lengths at ages 2 through 5 for males and females were based on returns from 1974 brood-year experimental releases of progeny with known-age parents from Elk River Hatchery, Oregon (table 4 in Hankin et al. 1993). We averaged mean lengths and standard deviations in lengths at age for male and female

progeny returning from age 3 × age 3 matings and from age 5 × age 5 matings. Mean length and standard deviation of length at age 6 for females were calculated from lengths of all age 6 females spawned at Elk River Hatchery in the 1974–1975, 1977–1981, and 1986–1992 spawning seasons (mean = 844.27, standard deviation = 47.77, n = 55). To obtain mean length of males at age 6, the ratios of mean lengths at age 6 compared with age 5 were assumed the same for males and females, and we assumed that standard deviation in length at age 6 for males was the same as that for males at age 5. Mean lengths of males and females were similar at ages 3 and 4, but mean male lengths were slightly larger than mean female lengths at ages 5 and 6 (Table 2).

Table 2. Mean and standard deviations of length of adult Elk River Hatchery Chinook salmon (*Oncorhynchus tshawytscha*) by age and sex.

	Male		Female	
Age	Mean length	Standard deviation	Mean length	Standard deviation
2	401.00	28.10	NA	NA
3	629.45	52.35	636.40	34.05
4	734.05	44.35	739.00	39.15
5	818.55	50.50	798.40	50.10
6	865.58	50.50	844.27	47.77

Model analysis

Initialization of models

For both hatchery and wild models, initialization of model calculations required specification of some or all age- and sex-specific returns for the first 6 years. Numbers at age by sex were specified for all ages in the first 2 years, for ages 3 through 6 in the 3rd year, for ages 4 through 6 in the 4th year, for ages 5 and 6 in the 5th year, and for age 6 in the 6th year. Thereafter, all returns were model-generated.

Assessment and characterization of long-term equilibria

Hatchery population models

Equations 1–9 are intended to capture the dynamics of a hatchery population of Chinook salmon which may be subjected to a size-selective ocean fishery and mated according to one of the three alternative regimes that are defined in eqs. 10–14. Specification of model parameter values will ordinarily determine a unique long-term equilibrium age and sex structure. We used computer calculations (S-PLUS 2000; Insightful Corporation, Seattle, Washington) to determine these long-term equilibrium states because no analytic solutions for these equilibria are available (see Carroll et al. 2005). Fixed parameter values in these computer calculations included the $\sigma_{kM}(i,j)$ and $\sigma_{kF}(i,j)$, Θ_{max}, p_k, f_k, and age- and sex-specific mean lengths and corresponding standard deviations. Long-term equilibrium age structure was considered reached when the calculated proportions at age did not vary between years at the sixth decimal place (Table 3). Specified returns to the hatchery for the first 6 years were varied to verify that apparent long-term equilibria were independent of initial conditions. Calculations of long-term equilibria were made for each of the three alternative mating regimes at each of the three levels of ocean fishery exploitation (none, moderate, high).

Wild population models

For the wild population models, a unique long-term stable equilibrium age and sex structure or unique age frequency distribution was not achieved exactly because mate selection is an inherently stochastic process. Nevertheless, the long-term age and sex structure fell within a certain narrow range of values (Table 4). We therefore characterized long-term equilibria by the calculated means and standard deviations of age- and sex-specific proportions in the simulated spawning populations during modeled years 50–100, well after apparent approximate equilibrium had clearly been reached.

Fixed parameters for model runs included those for the hatchery population models as well as the Ricker α and β parameters and the length-specific fecundities, f_k.

Effects of exploitation: fishing down vs. fishery-induced selection

Under size-selective fishing, the fishing-down process can lead to dramatic shifts in the age structure of fish populations, even if the maturity schedule of a fish population is fixed. We wished to distinguish such direct fishing-down effects from additional shifts due to interaction between size-selective fishing and inheritance of age at maturity. To do so, we calculated the equilibrium age and sex structures that would result under moderate and heavy exploitation when age- and sex-specific maturation probabilities, σ_{kM} and σ_{kF}, were assumed independent of the age and sex of parents. We then compared these long-term equilibria with those achieved under our inheritance models (i.e., using $\sigma_{kM}(i,j)$ and $\sigma_{kF}(i,j)$). We attributed the differences between exploited equilibria, for model runs with and without inheritance of age at maturity, to the additional shifts in age and sex structure of the populations that were due to interaction between size-selective fishing and inheritance of age at maturity. Key for such comparisons is specification of the appropriate values for σ_{kM} and σ_{kF}.

We calculated σ_{kM} and σ_{kF} using the methods of Hankin and Healey (1986). Hankin and Healey (1986) showed that equilibrium proportions in the escapement, by age and by sex (ω_{kF}, ω_{kM}, $\sum_{k=2}^{6}(\omega_{kF}+\omega_{kM})=1$), are related to one another, via maturation probabilities and exploitation rates, by

$$(21)\qquad \frac{\omega_{kF}p_k(1-u_{k+1,F})\sigma_{k+1,F}}{\omega_{k+1,F}}=\frac{\sigma_{kF}}{1-\sigma_{k+1,F}} \qquad \text{for } 2\le k\le 5$$

$$(22)\qquad \frac{\omega_{kM}p_k(1-u_{k+1,M})\sigma_{k+1,M}}{\omega_{k+1,M}}=\frac{\sigma_{kM}}{1-\sigma_{k+1,M}} \qquad \text{for } 2\le k\le 5$$

If one assumes that $\sigma_{6F}=\sigma_{6M}=1$, then the above equations can be solved by iteration to give estimates of σ_{5F} and σ_{5M}. The resulting estimates for σ_{5F} and σ_{5M} can then be used to generate estimates of σ_{4F} and σ_{4M} and so on.

We used these methods to estimate σ_{kM} and σ_{kF} from two different kinds of data. First, we estimated σ_{kM} and σ_{kF} from empirical observations of age and sex structure of 1968–1977 brood-year natural spawners from Elk River (Nicholas

Table 3. Example of approximate equilibrium proportions of females by age (reached by year 38 for this example) achieved by an unexploited hatchery population with completely random mating (early- to mid-maturing stock type).

Year	Age 3	Age 4	Age 5	Age 6
25	11.833603	23.471998	2.295369	0.09648178
26	11.858550	23.468037	2.272982	0.09424013
27	11.872279	23.466320	2.257326	0.09199838
28	11.882699	23.462496	2.245956	0.09199219
29	11.893650	23.459726	2.239174	0.08974647
30	11.900381	23.459726	2.232443	0.08974647
31	11.904602	23.456956	2.227906	0.08974445
32	11.908287	23.455378	2.223269	0.08973841
33	11.912774	23.455378	2.221026	0.08973841
34	11.912774	23.455378	2.218782	0.08973841
35	11.914750	23.454851	2.216489	0.08973640
36	11.916459	23.453799	2.216390	0.08973237
37	11.918970	23.454325	2.216439	0.08973439
38	11.918970	23.454325	2.214196	0.08973439
39	11.918970	23.454325	2.214196	0.08973439
40	11.918970	23.454325	2.214196	0.08973439
41	11.918970	23.454325	2.214196	0.08973439
42	11.918970	23.454325	2.214196	0.08973439
43	11.918970	23.454325	2.214196	0.08973439
44	11.918970	23.454325	2.214196	0.08973439
45	11.918970	23.454325	2.214196	0.08973439

Note: Year denotes number of years from initiation of model calculations, beginning with specified initial conditions for years 1–6. Proportions are expressed in terms of the total number of returning males and females of all ages, including jacks.

Table 4. Example of approximate equilibrium proportions of females by age achieved by an unexploited wild population with completely random mating (early- to mid-maturing stock type).

Year	Age 3	Age 4	Age 5	Age 6
25	11.6197	23.5915	2.3239	0.0704
26	11.8728	23.6042	2.1908	0.0707
27	11.8861	23.8434	2.2776	0.0712
28	11.6328	23.3357	2.1023	0.0701
29	11.8596	23.2982	2.2456	0.0702
30	11.8930	23.5046	2.3927	0.0704
31	11.8310	23.5915	2.1127	0.0704
32	11.8728	23.6042	2.1201	0.0707
33	11.7523	23.5749	2.2519	0.0704
34	11.8930	23.4342	2.1816	0.0704
35	11.9014	23.5211	2.2535	0.0704
36	11.9713	24.0143	2.2222	0.0717
37	11.5871	23.4551	2.1067	0.0702
38	11.8763	23.1904	2.1785	0.0703
39	11.8138	23.2801	2.5017	0.0695
40	12.1515	23.8742	2.1444	0.1430
41	11.5627	23.5459	2.1023	0.0701
42	11.9435	23.3922	2.0495	0.0707
43	11.9182	23.5543	2.5388	0.0705
44	11.8477	23.4838	2.0451	0.1410
45	11.7361	23.1944	2.1528	0.0694

Note: Year denotes number of years from initiation of model calculations, beginning with specified initial conditions for years 1–6. Proportions are expressed in terms of the total number of returning males and females of all ages, including jacks.

and Hankin 1988, their table II.25), assuming exploitation rates of $u_2 = 0$, $u_3 = 0.2$, and $u_4 = u_5 = u_6 = 0.35$, roughly consistent with exploitation rates estimated from CWT recovery data for that period of years (Hankin et al. 1993, their table 3). Derived values of σ_{AM} and σ_{AF} were then used to calculate the expected equilibrium age and sex composition in spawning escapement consistent with no exploitation and with the fishing-down effects that one would expect at moderate and high levels of exploitation. Second, we estimated σ_{AM} and σ_{AF} from the modeled long-term equilibrium age and sex structures in the unexploited case for the completely random and length-based hatchery mating regimes. (For the unexploited case, equilibria will be the same for σ_{AM} and σ_{AF} and $\sigma_{AM}(i,j)$ and $\sigma_{AF}(i,j)$.) We then generated equilibrium exploited (moderate and high) age and sex compositions for each of these sets of fixed maturation probabilities and compared the resulting age and sex compositions with those achieved under our inheritance models.

Results

Hatchery population models

Model stability and equilibrium

Given the fixed parameter values previously identified, our hatchery population models generated unique stable equilibria for all mating regimes at all three levels of exploitation. Equilibria were typically reached within 20–50 years (Table 3). Specification of initial age and sex composition of spawners affected the number of years to reach equilibrium

Fig. 2. Modeled long-term equilibrium percentage of total returns by age and sex for (*a*) males and (*b*) females for an unexploited early- to mid-maturing hatchery population of Chinook salmon (*Oncorhynchus tshawytscha*) for which matings are completely random (open bars), completely random but excluding jacks (solid bars), or the mating regime guarantees that male length ≥ female length (hatched bars).

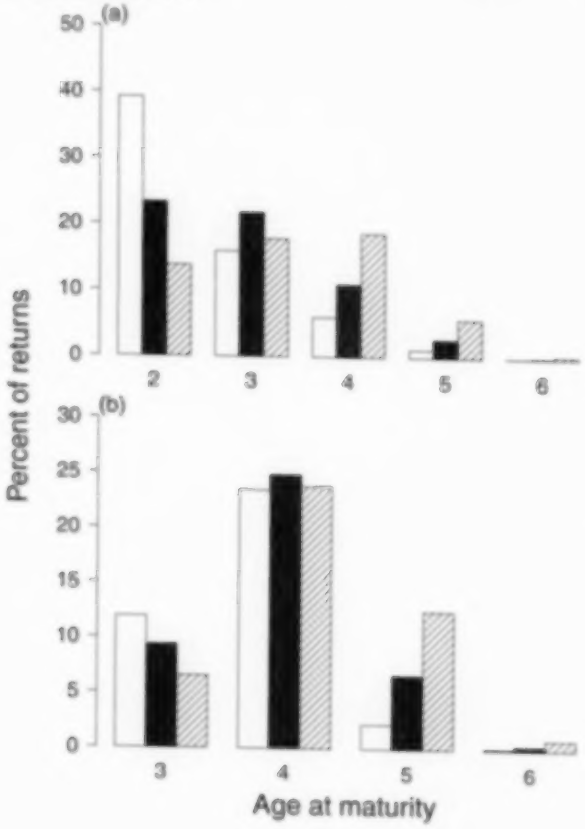

Fig. 3. Modeled long-term equilibrium percentage of total returns by age in an early- to mid-maturing hatchery population of Chinook salmon (*Oncorhynchus tshawytscha*) mated according to three alternative mating regimes (*a*) completely random, (*b*) completely random but excluding jacks, or (*c*) a regime that guarantees that male length ≥ female length) at three levels (unexploited, open bars; moderately exploited, solid bars; heavily exploited, hatched bars) of ocean fishery exploitation.

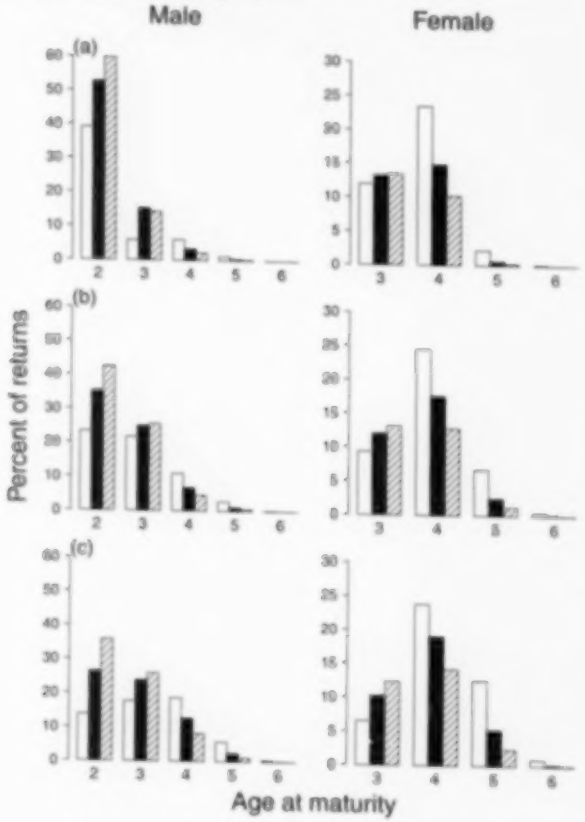

(more years required when initial specifications were further from eventual equilibrium) but did not affect the long-term equilibrium proportions.

Effects of alternative mating regimes on unexploited equilibria

Alternative mating regimes had a substantial impact on the long-term unexploited equilibrium age and sex structure of hatchery populations, particularly for males (Fig. 2). For example, percentages of jacks among all returns were 39.25, 23.36, and 13.80 for the completely random, completely random excluding jacks, and male length ≥ female length regimes, respectively. Analogous percentages of age 4 and age 5 males (combined) were 7.15, 13.65, and 24.43, respectively. For females, the most obvious effects were on ages 3 and 5, with more age 3 and fewer age 5 returns for the completely random mating regime, and fewer age 3 but more age 5 returns for the male length ≥ female length mating regime.

The striking differences in long-term equilibria among alternative mating regimes reflected the impacts of the $\sigma_{MS}(i,j)$ and $\sigma_{MS}(i,j)$ on distributions of mating types at equilibrium. For example, for the completely random mating regime, the most common matings (divisors are total number of matings at equilibrium) were between jacks and age 4 females (6585/16 855 = 0.391) and between jacks and age 3 females (3346/16 855 = 0.199), whereas for the male length ≥ female length mating regime, the most common matings were between age 4 males and age 4 females (4584/15 072 = 0.304) and between age 5 males and age 4 females (3068/15 072 = 0.204).

Effects of exploitation

For all three alternative mating regimes, exploitation produced a strong shift toward younger ages among hatchery returns. At heavy levels of exploitation, males were dominated by jacks and age 3 adults for all mating regimes, although degree of dominance by these ages was much greater for the completely random mating regime (73.93% of returns) than for the male length ≥ female length mating regime (61.78%;

Table 5. Calculated fixed age- and sex-specific maturation probabilities, independent of the age and sex of parents, based on unexploited equilibria for three alternative mating regimes (completely random, completely random but excluding jacks, male length ≥ female length) and based on empirical observations of age and sex structure in wild Elk River spawning runs.

Age and sex	Completely random	Random, but jacks excluded	Male length ≥ female length	Elk River wild
σ_{2M}	0.4375	0.2269	0.1198	0.1824
σ_{3M}	0.6296	0.5454	0.3490	0.2340
σ_{4M}	0.8015	0.7562	0.7074	0.5085
σ_{5M}	0.9787	0.9608	0.9321	0.7340
σ_{6M}	1.0000	1.0000	1.0000	1.0000
σ_{2F}	0.2656	0.1821	0.1140	0.0452
σ_{3F}	0.8898	0.7373	0.5826	0.5079
σ_{4F}	0.9530	0.9415	0.9168	0.8987
σ_{5F}	1.0000	1.0000	1.0000	1.0000

Fig. 3). The shift toward younger age was less striking for females (Fig. 3), but at heavy levels of exploitation, the most abundant female age was age 3 for the completely random mating regime (13.35%) compared with age 4 for the male length ≥ female length mating regime (14.18%). At heavy exploitation, age 5 females were essentially absent for the completely random mating regime (0.23%) but were present at a greater rate for the male length ≥ female length mating regime (2.42%). Exploitation also produced substantial shifts in the sex ratios of adults spawners. For example, for the completely random regime, adult sex ratios (age 3 and older males:females) for unexploited and heavily exploited populations were 0.61:1 and 0.69:1, respectively, compared with 0.97:1 and 1.21:1, respectively, for the male length ≥ female length mating regime.

Fishing-down effects vs. selective effects of size-selective fisheries

Based on long-term modeled equilibrium age and sex structures, calculated values of fixed conditional maturation probabilities for the male length ≥ female length mating regime were much more similar to those estimated from spawning escapements of Elk River fall Chinook salmon than were values calculated from equilibria resulting from the completely random and completely random excluding jacks mating regimes (Table 5). When exploited equilibrium age and sex structures for populations with fixed maturation probabilities (σ_{iF}, σ_{iM}) were compared with those for populations with age- and sex-dependent maturation probabilities ($\sigma_{iF}(i,j)$, $\sigma_{iM}(i,j)$), it was apparent that there was a modest interaction between size-selective fishing and inheritance of age at maturity, over and above the basic fishing-down process (Table 6). For example, for the male length ≥ female length mating regime, the percentages of jacks among returns increased from 13.8% for unexploited populations to 28.83% and 35.87% for fixed and (i,j)-dependent maturation probabilities, respectively, under heavy exploitation. Similarly, the proportions of age 4 and older females decreased from 37.2% (unexploited) to 20.8% and 16.7%, respectively, under heavy exploitation for the male length ≥ female length mating regime. We interpret these differences as reflecting the long-term genetic impacts of size-selective fishing as distinguished from the expected demographic effects of the fishing-down process.

Wild population models

Model stability and equilibrium

Our wild population models generated apparent approximate stable equilibria for both mating submodels at all three levels of exploitation. Approximate equilibrium proportions were typically reached within 25–50 years (Table 4) and were not affected by specification of initial age and sex composition of spawners.

Effects of alternative mating regimes and exploitation on wild populations

Qualitative effects of mating behaviors and fishery exploitation were similar to those noted for hatchery populations. Age distribution of male spawners was substantially shifted toward younger ages, especially jacks, under completely random matings compared with size- and frequency-dependent matings, and exploitation shifted age distributions toward younger ages for both mating submodels (Fig. 4). For females, differences were most apparent for unexploited populations (fewer age 3 females and more age 5 females for size- and frequency-dependent matings), and exploitation again shifted female spawners toward younger ages (Fig. 4). Variation in the η parameter had little effect on equilibrium age and sex structure. Equilibrium proportions were essentially the same for $\eta = 10$ and $\eta = 5$, with a slight shift toward a younger age structure for $\eta = 2$ (Table 7).

Although equilibrium unexploited and exploited proportions of males and females were nearly identical for hatchery and wild populations when matings were completely at random, equilibrium proportions were divergent for wild and hatchery populations under length-based mating regimes or behaviors (Table 8). When matings were length- and frequency-dependent, age composition for the wild population model was slightly shifted toward younger ages, for both unexploited and heavily exploited populations, when compared with the hatchery population model.

Comparison of modeled populations with wild Elk River fall Chinook salmon

Extensive spawning escapement data were available for Elk River fall Chinook salmon from the 1968–1977 brood

Table 6. Comparison of equilibrium percentages of total returns by age and sex between models with fixed maturation probabilities (fixed σ_{iAM}, σ_{iAF}) and maturation probabilities based on age and sex of parents ($\sigma_{iAM}(i,j)$, $\sigma_{iAF}(i,j)$), under two alternative hatchery mating regimes (completely random mating (including jacks), and male length ≥ female length) and under three levels of ocean fishery exploitation (unexploited, moderately exploited, and heavily exploited (unexploited, moderate, and high, respectively).

	Fixed σ_{iAM}, σ_{iAF}			$\sigma_{iAM}(i,j)$, $\sigma_{iAF}(i,j)$		
	Unexploited	Moderate	High	Unexploited	Moderate	High
Completely random mating						
Age 2 males	39.25	50.34	56.84	39.25	52.69	59.72
Age 3 males	15.89	16.30	16.11	15.89	15.13	14.21
Age 4 males	5.99	4.00	2.88	5.99	3.27	2.13
Age 5 males	1.16	0.50	0.27	1.16	0.36	0.16
Age 6 males	0.02	0.01	0.00	0.02	0.00	0.00
Age 3 females	11.92	12.23	12.08	11.92	13.17	13.36
Age 4 females	23.45	15.64	11.29	23.45	14.78	10.19
Age 5 females	2.21	0.96	0.51	2.21	0.59	0.23
Age 6 females	0.09	0.03	0.01	0.09	0.01	0.00
Male length ≥ female length						
Age 2 males	13.80	22.36	28.83	13.80	26.43	35.87
Age 3 males	17.69	22.93	25.87	17.69	23.80	25.91
Age 4 males	18.67	15.73	12.97	18.67	12.61	8.17
Age 5 males	5.76	3.15	1.90	5.76	2.34	1.04
Age 6 males	0.34	0.12	0.05	0.34	0.08	0.02
Age 3 females	6.56	8.51	9.60	6.56	10.27	12.32
Age 4 females	23.78	20.03	16.52	23.78	18.97	14.18
Age 5 females	12.49	6.84	4.12	12.49	5.28	2.42
Age 6 females	0.91	0.32	0.14	0.91	0.21	0.06

years (Nicholas and Hankin 1988). Estimated ocean fishery exploitation rates for a 1974 brood-year release of coded wire tagged fall Chinook salmon released from Elk River Hatchery were $\tilde{u}_2 = 0.0045$, $\tilde{u}_3 = 0.2131$, $\tilde{u}_4 = 0.3757$, and $\tilde{u}_5 = 0.3022$ (Hankin et al. 1993, their table 3). We therefore concluded that these spawning escapement data were collected during a period of "moderate" ocean fishery exploitation rates. Agreement between Elk River wild escapement data and model predictions of equilibrium age and sex composition based on length-based matings (male length ≥ female length) was imperfect but clearly superior to that for models assuming completely random mating (Table 9). Equilibrium proportions of jacks and age 3 females were much larger, and proportions of age 5 males and females were much smaller than Elk River observed proportions for both hatchery and wild population models under completely random mating.

Discussion

According to Falconer and Mackay (1996, chapter 12), experimental studies of deliberate directional selection for specific traits (e.g., mean weight of mice at 6 weeks of age) have shown that the consequences of directional selection can usually be reliably predicted for at least 20 generations based on an assumption of fixed heritability for the trait in question. Assuming a mean generation time of 4 years for an unexploited early- to mid-maturing Chinook salmon stock, 20 generations would translate into approximately 80 years. Thus, the duration of time that our models required for exact or approximate equilibrium to become established (about 25–50 years for hatchery and wild population models) seems well within the range of years for which an assumption of essentially fixed heritabilities (i.e., fixed $\mathbf{\Theta}_{\mathbf{AM}}$ and $\mathbf{\Theta}_{\mathbf{AF}}$) would be valid. Thus, we believe that our models should provide reasonable predictions of the long-term consequences of alternative mating regimes in hatchery and wild populations of Chinook salmon.

Model results presented in this paper provide a sound theoretical basis for serious concern regarding the potential long-term consequences of completely random, or nearly so, mating regimes at Chinook salmon hatcheries. Completely random mating will produce a substantial long-term shift toward younger age at maturity. In an early- to mid-maturing stock type such as Elk River fall Chinook salmon, use of jacks as male parents in a completely random mating regime can lead to especially striking increases in the proportion of returns that are jacks. The shift toward younger age at maturity can be modestly reduced by excluding jacks as parents (this paper) or by strong selection against jacks as parents (e.g., spawning only 1 in 20 jacks; Fitzgibbons 2004). Adoption of a hatchery mating regime that emulates the outcomes of natural spawning behaviors of Chinook salmon (e.g., male parent length ≥ female parent length) will lead instead to a long-term equilibrium age and sex structure that is shifted toward older ages and females and more closely matches apparent long-term equilibrium in a natural early- to mid-maturing population of Chinook salmon. In our models for naturally spawning populations of Chinook salmon, we found that a very similar but stochastic and size- and frequency-dependent mating regime produced a long-term equilibrium age and sex structure that is much more similar

Table 7. Mean wild population equilibrium percentages by age and sex (from years 50 to 100) for three values of η (maximum number of matings per male) given size- and frequency-dependent mating success (male length ≥ female length).

	Unexploited			Moderately exploited			Heavily exploited		
Age and sex	$\eta = 10$	$\eta = 5$	$\eta = 2$	$\eta = 10$	$\eta = 5$	$\eta = 2$	$\eta = 10$	$\eta = 5$	$\eta = 2$
Age 2 males	20.66	20.45	22.82	36.97	37.46	38.51	46.93	46.92	47.97
Age 3 males	19.68	19.72	20.06	22.70	22.55	22.22	22.01	22.09	21.48
Age 4 males	13.73	13.83	12.31	7.23	7.06	6.63	4.27	4.23	4.01
Age 5 males	3.80	3.82	3.27	1.14	1.10	1.00	0.47	0.47	0.45
Age 6 males	0.17	0.17	0.16	0.00	0.00	0.00	0.00	0.00	0.00
Age 3 females	8.29	8.25	8.86	11.79	11.83	12.01	13.06	13.08	13.11
Age 4 females	24.45	24.47	24.48	17.34	17.25	17.10	12.18	12.15	12.00
Age 5 females	8.70	8.76	7.61	2.70	2.63	2.41	1.06	1.06	0.98
Age 6 females	0.52	0.54	0.43	0.13	0.12	0.12	0.00	0.00	0.00

Fig. 4. Modeled long-term approximate equilibrium percentage of total returns by age and sex in an early- to mid-maturing naturally spawning population of Chinook salmon (*Oncorhynchus tshawytscha*) for which a stochastic mating submodel is completely random (open bars) or follows a length-based, frequency-dependent algorithm (solid bars), at three levels of ocean fishery exploitation (*a*) unexploited, (*b*) moderately exploited, (*c*) heavily exploited).

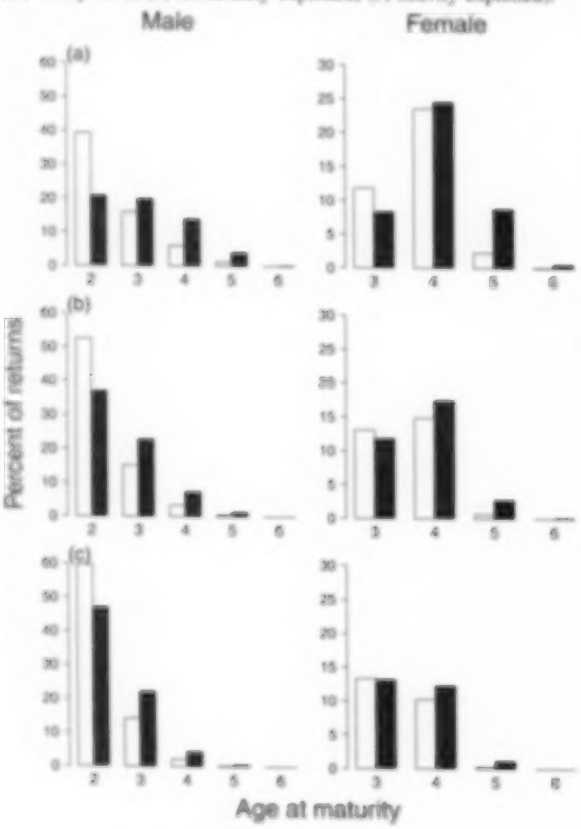

to that for the wild Elk River fall Chinook salmon population than an alternative model assuming that all natural matings are completely at random. Thus, we feel that our model results, together with behavioral observations of Chinook salmon spawning (Baxter 1991; Berejikian et al. 2000; Berejikian and Tezak 2001), provide compelling support for our contention that completely random mating regimes are "unnatural" for Chinook salmon and will produce "unnatural" long-term age and sex structure in hatchery Chinook salmon populations. In a similar vein, we note that McLean et al. (2005) recently stated that "to improve the fitness of ... hatchery fish ..., a better understanding of factors associated with the range of reproductive success and mate-choice mechanisms in the wild is vital. This knowledge may then be applied to artificial propagation programs designed for conservation or enhancement." We believe that our proposed male length ≥ female length mating regime represents such an application.

There is also some substantial circumstantial, empirical evidence that random mating policies can cause selection for younger age at maturity in Chinook salmon. First, Carmichael et al. (1998) and R. Carmichael (Oregon Department of Fish and Wildlife, 1410 L Avenue, La Grande, OR 97850, personal communication, 2003) have found that the age structure of the hatchery population of Imnaha River, Oregon, Chinook salmon has become shifted toward younger ages than the corresponding wild population as an apparent consequence of hatchery practices (see their fig. 13). Imnaha River Chinook salmon were listed as threatened under the US Endangered Species Act in 1992, and a conservation hatchery was developed in an attempt to prevent extinction of this population of Chinook. The hatchery population was started with wild Imnaha River brood stock and every attempt was made to cause as little shift as possible in distributions of phenotypic traits. Hatchery mating policies called for completely random, complex matrix pairings of males and females.

Second, Knudsen et al. (2006) found that the age composition of Yakima River hatchery spring Chinook salmon was rapidly shifted toward younger age 3 males (analogous to jacks in an ocean-type fall Chinook population) when compared with the wild population from which the hatchery population was derived. For at least the first 2 years of this program, an essentially completely random mating policy was used (C. Knudsen, Oncorh Consulting, 2623 Galloway SE, Olympia, WA 98501, personal communication, 2008).

Current specifications of "best management practices" for hatchery populations of Chinook salmon consistently recommend completely random mating, sometimes with some slight modifications concerning usage of jacks as male parents (Flagg et al. 2004; HSRG 2004; US Fish and Wildlife

Table 8. Modeled equilibrium age and sex composition of returns to hatchery or to spawning grounds for hatchery and wild population models for completely random matings and for length-based matings (male length ≥ female length hatchery mating regime and size- and frequency-dependent wild mating behaviors).

	Unexploited		Heavily exploited	
Age and sex	Hatchery	Wild	Hatchery	Wild
Completely random matings				
Age 2 males	39.25	39.28	59.72	59.72
Age 3 males	15.89	15.90	14.21	14.23
Age 4 males	5.99	6.00	2.13	2.13
Age 5 males	1.16	1.16	0.16	0.14
Age 6 males	0.02	0.00	0.00	0.00
Age 3 females	11.92	11.85	13.36	13.29
Age 4 females	23.45	23.52	10.19	10.23
Age 5 females	2.21	2.21	0.23	0.26
Age 6 females	0.09	0.07	0.00	0.00
Length-based matings				
Age 2 males	13.80	20.66	35.87	46.94
Age 3 males	17.69	19.68	25.91	22.01
Age 4 males	18.67	13.73	8.17	4.27
Age 5 males	5.76	3.80	1.04	0.47
Age 6 males	0.34	0.17	0.02	0.00
Age 3 females	6.56	8.29	12.32	13.06
Age 4 females	23.78	24.45	14.18	12.18
Age 5 females	12.49	8.70	2.42	1.06
Age 6 females	0.91	0.52	0.06	0.00

Table 9. Modeled equilibrium age and sex composition of returns to hatchery or to spawning grounds for hatchery and wild models of an early- to mid-maturing Chinook salmon (*Oncorhynchus tshawytscha*) population at moderate levels of exploitation compared with observed age and sex composition among returns of wild fall Chinook salmon spawners to Elk River, Oregon, 1968–1977 brood years.

	Hatchery model		Wild model		
Age and sex	Completely random	Male length ≥ female length	Completely random	Male length ≥ female length	Elk River wild
Males					
Age 2	52.90	26.43	52.60	36.97	34.83
Age 3	15.13	23.80	15.19	22.70	14.61
Age 4	3.27	12.61	3.30	7.23	12.65
Age 5	0.36	2.34	0.37	1.14	4.67
Age 6	0.00	0.08	0.00	0.00	0.01
Females					
Age 3	13.17	10.27	13.10	11.79	3.50
Age 4	14.78	18.97	14.84	17.34	19.52
Age 5	0.59	5.28	0.60	2.70	8.84
Age 6	0.01	0.21	0.00	0.13	0.52

Note: Elk River wild age composition is from table II.25 in Nicholas and Hankin (1988) and is believed to reflect a period with "moderate" levels of ocean fishery exploitation.

Service 2005). Completely random mating, including at least some use of jacks as parents, is typically recommended for three reasons: (*i*) to maximize genetic diversity and effective population size; (*ii*) to prevent directed selection for life history traits; and (*iii*) to insure that the jack life history type is maintained. As shown in this paper, however, completely random mating is in fact a form of unintentional directed selection for younger age at maturity, and exclusion of jacks from matings does not imply loss of jacks as a life history type. As long as $\sigma_2(i, j)$ exceeds zero for male parental ages greater than 2, some jacks will always be produced.

Maximizing genetic diversity may be a critical consideration for very small hatchery populations (e.g., number of female spawners per year ≤ 100), but it is a much less

important objective for large populations (e.g., number of female spawners per year ≥ 1000) and, in any event, must be weighed against the long-term consequences of unintentional selection for younger age at maturity that results from completely random mating. Also, the loss of genetic diversity and (or) effective population size that might result from the male length ≥ female length mating protocol, as compared with completely random mating, may not be large. For example, by this proposed mating strategy, a small age 3 female might be mated with virtually any age 3 to age 5 adult male or possibly with an exceptionally large jack. Of course, the spectrum of possible male mates becomes progressively smaller among older and larger females, but there is still a very substantial amount of "randomness" in pairings of individual males and females. Theoretical calculations of the effects of a male length ≥ female length mating regime on genetic diversity and effective population size should certainly be made before a male length ≥ female length mating policy should be considered wise for small hatchery populations. However, we believe that there is already persuasive logic for such a policy to be adopted for large hatchery populations.

The modeling results presented in this paper should be regarded as preliminary in nature, and it is important to recognize that the specific results that we obtained strictly apply only to an early- to mid-maturing stock type, like Elk River fall Chinook, with a substantial natural tendency to produce jacks. Although our general model structure is broadly applicable (for related modeling results for a hypothetical late-maturing stock type, see Fitzgibbons (2004) and Chen (2007)), additional age-at-maturity experiments are needed to provide a better quantitative basis for the maturation probabilities specified in the $\boldsymbol{\Theta}_{\mathbf{kM}}$ and $\boldsymbol{\Theta}_{\mathbf{kF}}$. Also, improved statistical methods are needed for imputing $\sigma_{kM}(i,j)$ or $\sigma_{kF}(i,j)$ when there have been no matching parental mating types (see Appendix A and Supplementary Appendix S1[2]). Notably absent for the Elk River stock were experimental matings specifically designed to assess the effect of female parent age on male offspring age (e.g., age 3 males × age 3 females vs. age 3 males × age 5 females). Better specification of the $\sigma_{kM}(i,j)$ and $\sigma_{kF}(i,j)$ would no doubt provide more accurate predictions of probable long-term equilibria under alternative hatchery mating regimes. Unfortunately, because the $\boldsymbol{\Theta}_{\mathbf{kM}}$ and $\boldsymbol{\Theta}_{\mathbf{kF}}$ are stock-specific and reflect the natural tendencies of particular stocks to mature at particular ages, a set of $\boldsymbol{\Theta}_{\mathbf{kM}}$ and $\boldsymbol{\Theta}_{\mathbf{kF}}$ for an early- to mid-maturing fall Chinook stock, such as Elk River, cannot be directly used to model a late-maturing stock type in which almost no males would return as jacks even if matings were completely at random.

Based on the very limited number of known-age mating experiments that have been carried out with Chinook salmon, despite the striking evidence concerning inheritance of age at maturity in this species (Hankin et al. 1993; Hard 2004), it seems unlikely to expect that much more about inheritance of age at maturity in this species will be learned through conventional age- and sex-specific mating experiments. Instead, we suspect that techniques like parental-based tagging (Anderson and Garza 2006) will provide a much more elegant means to achieve the same purpose. With parental-based tagging, all (or a substantial fraction) of hatchery parents are aged and genotyped at numerous loci so that on return of progeny to a hatchery facility, it is possible to genotype progeny and associate them with the most likely parental pairs. Because ages of these parental pairs are known, the average sequence of age-specific returns for parental matings of type (i,j) could, along with some ancillary coded wire tag recovery data for hatchery fish with identical or very similar release size and timing (see Hankin 1990), provide an empirical basis for estimating all entries in the $\boldsymbol{\Phi}_{\mathbf{kM}}$ and $\boldsymbol{\Phi}_{\mathbf{kF}}$ matrices. Inheritance of a large number of other traits could also theoretically be assessed using this same technology.

We have strong confidence in the validity of our modeling conclusions with respect to unexploited populations, particularly for hatcheries that employ 1:1 mating protocols as assumed by our models. Campton (2004), however, noted that many hatcheries instead mix eggs and sperm from multiple females and males (often five males and five females). The long-term consequences of such gamete pooling would be difficult to model, as experimental studies (summarized in Campton 2004) have consistently shown that pooling typically leads to highly unequal contributions from male spawners. Thus, pooling of eggs and sperm could lead, according to Campton (2004), to undesirable artificial selection for life history traits associated with sperm potency and fertilization success. On the natural spawning grounds, similar pooling of sperm may take place when multiple males successfully spawn, nearly simultaneously, with a single female, with resulting unequal fertilization success by competing males. It would be challenging to construct a model for natural spawning behaviors that could adequately capture the consequences of multiple male mates and unequal fertilization success.

We have less confidence in the validity of our results concerning the potential long-term impacts of size-selective fishing and our attempts to separate classic fishing-down effects from additional shifts in age structure due to inheritance of age at maturity. One of the important simplifying assumptions made in our model is that size at age is unaffected by parental age. (This assumption is not critical to our modeling results for unexploited populations. Chen (2007) found that the male length ≥ female length mating regime gave results very similar to a male age ≥ female age mating regime that does not invoke this assumption.) In Chinook salmon, it is known that size at age and maturation must be, to some degree, correlated traits (see references in Hankin et al. 1993). For example, Hankin et al. (1993) noted that there was evidence that faster-growing fish, within a known-age-specific mating type, matured at earlier ages than slower-growing fish, and more recently Wells et al. (2007) concluded that "faster growth during the year before

[2] Supplementary data for this article are available on the journal Web site (http://cjfas.nrc.ca) or may be purchased from the Depository of Unpublished Data, Document Delivery, CISTI, National Research Council Canada, Building M-55, 1200 Montreal Road, Ottawa, ON K1A 0R6, Canada. DUD 3986. For more information on obtaining material refer to http://cisti-icist.nrc-cnrc.gc.ca/eng/ibp/cisti/collection/unpublished-data.html.

return led to earlier maturation". Recently, Hard (2004) has been modeling the co-evolution of correlated traits in Chinook salmon populations subjected to size-selective fishing. To the degree that ocean fishing selectively removes faster-growing fish (at age), leaving the slower-growing members as more probable parents for future generations, the effects of size-selective fishing on age at maturity may be somewhat less than those modeled in this paper. Much more work needs to be done in this area. We note, however, that under heavy exploitation, the demographic fishing-down effects of size-selective ocean exploitation on Chinook salmon appear to dwarf the additional effects due to inheritance of age at maturity in this species. We suspect that this result would also be obtained for a model in which size at age and age at maturity were modeled as correlated traits.

In conclusion, we believe that the widespread recommendation to employ completely random, or nearly so, mating regimes at Chinook salmon hatcheries should be reconsidered. At large-scale facilities, we believe that mating regimes that better emulate the outcomes of natural mating behaviors should instead be adopted. We suspect that institution of such more natural mating regimes would also be wise for other large hatchery populations of *Oncorhynchus* species. Implementation of a feasible scheme that roughly emulates the outcomes of natural spawning behaviors, such as our proposed male length ≥ female length scheme, should prevent a long-term shift toward younger-aged spawners and should produce an age structure that is more similar to that in the wild population from which a hatchery population is derived. We recognize that a shift to a male length ≥ female length mating regime would, through correlations among genetic traits, no doubt produce other long-term effects. We question, however, that such unknown impacts should be assumed a priori to be negative. Instead, we believe that the "null" mating regime should be a regime that emulates the outcomes of natural spawning behaviors and that the wisdom of completely random mating should be evaluated against this null mating regime. Indeed, we suspect that reduction in mean age and size of hatchery spawners may be an important determinant of the relatively poor reproductive success of hatchery fish in natural environments as noted in some recent publications (e.g., Araki et al. 2007).

Acknowledgments

We thank Ken Currens, Jeff Hard, and Eric Loudenslager for discussions that encouraged us to attempt explicit modeling of inheritance of age at maturity in exploited populations of Chinook salmon. Ron Olson provided much useful guidance concerning current "best management practices" and directed us to several useful references. We also thank the Yurok Tribe and Dave Hillemeier, Fisheries Program Leader, for their generous financial support of the modeling research described in this paper.

References

Anderson, E.C., and Garza, J.C. 2006. The power of single-nucleotide polymorphisms for large-scale parentage inference. Genetics, **172**(4): 2567–2582. doi:10.1534/genetics.105.048074. PMID: 16387880.

Araki, H., Cooper, B., and Blouin, M.S. 2007. Genetic effects of captive breeding cause a rapid, cumulative fitness decline in the wild. Science (Washington, D.C.), **318**(5847): 100–103. doi:10.1126/science.1145621. PMID:17916734.

Baxter, R.D. 1991. Chinook salmon spawning behavior: evidence for size-dependent male spawning success and female mate choice. Unpublished M.S. thesis, Natural Resources Graduate Program, Humboldt State University, Arcata, Calif.

Berejikian, B.A., and Tezak, E.P. 2001. Reproductive behavior and breeding success of captively reared Chinook salmon. N. Am. J. Fish. Manage. **21**(1): 255–260.

Berejikian, B.A., Tezak, E.P., and LaRae, A.L. 2000. Female mate choice and spawning behavior of Chinook salmon under experimental conditions. J. Fish Biol. **57**(3): 647–661. doi:10.1111/j.1095-8649.2000.tb00266.x.

Campton, D.E. 2004. Sperm competition in salmon hatcheries: the need to institutionalize genetically benign spawning protocols. Trans. Am. Fish. Soc. **133**(5): 1277–1289. doi:10.1577/T03-200.1.

Carmichael, R.W., Parker, S.J., and Whitesel, T.A. 1998. Status review of the chinook salmon hatchery program in the Imnaha River Basin, Oregon. *In* Lower Snake River compensation plan status review symposium. US Fish and Wildlife Service, Boise, Idaho. pp. 119–139.

Carroll, J.E., Lauck, T., and Lamberson, R.H. 2005. A Perron Theorem for positive componentwise bilinear maps. Linear Algebra Appl. **396**: 259–272. doi:10.1016/j.laa.2004.09.021.

Chen, Y. 2007. Long-term effects of alternative hatchery matings practices and size-selective fishing on age and sex composition of Chinook salmon populations returning to hatcheries. M.S. thesis, Humboldt State University, Arcata, Calif.

Falconer, D.S., and Mackay, T.F.C. 1996. Introduction to quantitative genetics. 4th ed. Prentice Hall, Essex, UK.

Fitzgibbons, J. 2004. Effects of hatchery mating practices and ocean fisheries on the age and sex structure of hatchery populations of Chinook salmon (*Oncorhynchus tshawytscha*). M.S. thesis, Humboldt State University, Arcata, Calif.

Flagg, T.A., Mahnken, C.V.W., and Iwamoto, R.N. 2004. Conservation hatchery protocols for Pacific salmon. Am. Fish. Soc. Symp. **44**: 603–619.

Fleming, I.A., and Gross, M.R. 1994. Breeding competition in a Pacific salmon (Coho: *Oncorhynchus kisutch*): measures of natural and sexual selection. Evolution, **48**(3): 637–665. doi:10.2307/2410475.

Fleming, I.A., and Reynolds, J.D. 2004. Salmonid breeding systems. *In* Evolution illuminated: salmon and their relatives. *Edited by* A. Hendry and S. Stearns. Oxford University Press, Oxford, UK. pp. 264–294.

Gross, M.R. 1991. Salmon breeding behavior and life history evolution in changing environments. Ecology, **72**(4): 1180–1186. doi:10.2307/1941091.

Hankin, D.G. 1990. Effects of month of release of hatchery-reared Chinook salmon on size at age, maturation schedule, and fishery contribution. Information Report No. 90-4, Oregon Department of Fish and Wildlife, Portland, Oregon.

Hankin, D.G., and Healey, M.C. 1986. Dependence of exploitation rates for maximum yield and stock collapse on age and sex structure of chinook salmon (*Oncorhynchus tshawytscha*) stocks. Can. J. Fish. Aquat. Sci. **43**: 1746–1759. doi:10.1139/f86-219.

Hankin, D.G., Nicholas, J.W., and Downey, T.W. 1993. Evidence for inheritance of age of maturity in chinook salmon, *Oncorhynchus tshawytscha*. Can. J. Fish. Aquat. Sci. **50**(2): 347–358. doi:10.1139/f93-040.

Hard, J.J. 1995. Genetic monitoring of life history characters in salmon supplementation: problems and opportunities. Am. Fish. Soc. Symp. **15**: 212–225.

Hard, J.J. 2004. Evolution of chinook salmon life history under

size-selective harvest. *In* Evolution illuminated: salmon and their relatives. *Edited by* A. Hendry and S. Stearns. Oxford University Press, Oxford, UK. pp. 315–337.

Hard, J.J., Gross, M.R., Heino, M., Hilborn, R., Kope, R.G., Law, R., and Reynolds, J.D. 2008. Evolutionary consequences of fishing and their implications for salmon. Evol. Appl. **1**(2): 388–408. doi:10.1111/j.1752-4571.2008.00020.x.

Hatchery Scientific Review Group. 2004. Mobrand, L., Barr, J., Blankenship, L., Campton, D., Evelyn, T., Flagg, T., Mahnken, C., Piper, R., Seidel, P., Seeb, L., and Smoker, B. 2004. Hatchery reform: principles and recommendations of the HSRG. Long Live the Kings, Seattle, Wash.

Healey, M.C. 1991. Life history of chinook salmon (*Oncorhynchus tshawytscha*). *In* Pacific salmon life histories. *Edited by* C. Groot and L. Margolis. UBC Press, Vancouver, B.C. pp. 311–394.

Knudsen, C.M., Schroder, S.L., Busack, C.A., Johnston, M.V., Pearsons, T.N., Bosch, W.J., and Fast, D.E. 2006. Comparison of life history traits between first-generation hatchery and wild upper Yakima River spring Chinook salmon. Trans. Am. Fish. Soc. **135**(4): 1130–1144. doi:10.1577/T05-121.1.

McLean, J.E., Bentzen, P., and Quinn, T.P. 2005. Nonrandom, size- and timing-biased breeding in a hatchery population of steelhead trout. Conserv. Biol. **19**(2): 446–454. doi:10.1111/j.1523-1739.2005.00515.x.

Nicholas, J.W., and Hankin, D.G. 1988. Chinook salmon populations in Oregon coastal river basins: description of life histories and assessment of recent trends in run strengths. Oregon Department of Fish and Wildlife, Information Report No. 88-1.

Ricker, W.E. 1954. Stock and recruitment. J. Fish. Res. Board Can. **11**: 559–623.

Ricker, W.E. 1972. Hereditary and environmental factors affecting certain salmonid populations. *In* The stock concept in Pacific salmon. *Edited by* R.C. Simon and P. Larkin. Mitchell Press Limited, Vancouver, B.C. pp. 19–160.

Ricker, W.E. 1976. Computation and interpretation of biological statistics of fish populations. Bulletin No. 191, Department of the Environment, Fisheries and Marine Service, Ottawa.

Ricker, W.E. 1980. Causes of the decrease in age and size of chinook salmon (*Oncorhynchus tshawytscha*). Can. Tech. Rep. Fish. Aquat. Sci. No. 944.

Rutter, C. 1904. Natural history of the quinnat salmon. A report of investigations in the Sacramento River, 1986–1901. Bull. U.S. Fish. Comm. **1902**: 65–141.

US Fish and Wildlife Service. 2005. Columbia River Basin Hatchery Review Team: principles. US Fish and Wildlife Service, Pacific Region Federal Hatchery Review, Portland, Oregon.

Waples, R.S. 1991. Genetic interactions between hatchery and wild salmonids: lessons from the Pacific Northwest. Can. J. Fish. Aquat. Sci. **48**(Suppl. 1): 124–133. doi:10.1139/f91-311.

Wells, B.K., Grimes, C.B., and Waldvogel, J.B. 2007. Quantifying the effects of wind, upwelling, curl, sea surface temperature and sea level height on growth and maturation of a California Chinook salmon (*Oncorhynchus tshawytscha*) populations. Fish. Oceanogr. **16**(4): 363–382. doi:10.1111/j.1365-2419.2007.00437.x.

Appendix A. Calculation of age- and sex-specific conditional maturation probabilities, $\sigma_{aSM}(j,j)$ and $\sigma_{aSF}(j,j)$

In this Appendix, we provide a brief sketch of the procedures that we used to specify entries in the maturation probability matrices Φ_{aM} for males and Φ_{aF} for females. Because the performance of our models is highly sensitive to specification of these values, we provide a more detailed explanation of the procedures that we used in an online Supplementary Appendix S1.[2]

Generation of the values in the maturation probability matrices relied first on cohort analyses of estimated river returns from age-at-maturity experiments carried out at Oregon's Elk River Hatchery (Hankin et al. 1993). Specifically, we relied upon age- and sex-specific returns from 1974 brood-year matings of age 3 males with age 3 females (3 × 3) and age 5 males with age 5 females (5 × 5) and 1980 matings of jacks with ages 4, 5, and 6 females (2 × 4+), and ages 4, 5, and 6 males with ages 4, 5, and 6 females (4+ × 4+). Ages 4 to 6 parents used in the 1980 brood-year 2 × 4+ and 4+ × 4+ matings were dominated by age 5 individuals, with mean female age of 4.81 for the 2 × 4+ matings and mean male and female ages of 4.78 and 4.89, respectively, for the 4+ × 4+ matings. Therefore, we treated these matings as if they had been 2 × 5 and 5 × 5 matings. In cohort analyses, we assumed conditional ocean survival rates of 0.50 between ages 2 and 3 and 0.80 between older ages, and we assumed that exploitation rates experienced by progeny from the 1980 and 1974 brood-year experimental matings (0.00, 0.20, 0.35, 0.35, and 0.35 at ages 2 to 6, respectively) were the same as those for the previously noted 1974 release of coded wire tagged Elk River Hatchery fall Chinook salmon.

The Elk River Hatchery mating experiments allowed direct estimation of $\sigma_{aSF}(2,5)$, $\sigma_{aF}(2,5)$, $\sigma_{aSF}(3,3)$, $\sigma_{aF}(3,3)$, $\sigma_{aSF}(5,5)$, and $\sigma_{aF}(5,5)$. Thus, for each of the Φ_{aM} and Φ_{aF} matrices, 3 of the 20 entries had solid empirical origins and provided a basis for specification of the full set of maturation probabilities. Supplementary Appendix S1[2] provides full details of the sequence of steps that we took to generate remaining maturation probabilities for each matrix. The fully specified set of matrices used in our modeling are listed below (with the exception of the previously listed Φ_{SM}).

$$\Phi_{2M} = \begin{bmatrix} 0.5810 & 0.2997 & 0.1786 & 0.0574 & 0.0287 \\ 0.5428 & 0.2800 & 0.1668 & 0.0536 & 0.0268 \\ 0.5280 & 0.2600 & 0.1549 & 0.0498 & 0.0249 \\ 0.4652 & 0.2400 & 0.1430 & 0.0460 & 0.0223 \end{bmatrix}$$

$$\Phi_{4M} = \begin{bmatrix} 0.8649 & 0.8125 & 0.7621 & 0.7107 & 0.6592 \\ 0.8444 & 0.7933 & 0.7441 & 0.6939 & 0.6437 \\ 0.8239 & 0.7740 & 0.7260 & 0.6770 & 0.6280 \\ 0.8035 & 0.7548 & 0.7080 & 0.6602 & 0.6124 \end{bmatrix}$$

$$\Phi_{SM} = \begin{bmatrix} 1.0000 & 1.0000 & 0.9710 & 0.9418 & 0.9126 \\ 1.0000 & 0.9855 & 0.9570 & 0.9281 & 0.8994 \\ 1.0000 & 0.9717 & 0.9435 & 0.9151 & 0.8868 \\ 0.9851 & 0.9572 & 0.9294 & 0.9014 & 0.8736 \end{bmatrix}$$

$$\Phi_{3F} = \begin{bmatrix} 0.4026 & 0.3103 & 0.2182 & 0.1280 & 0.0604 \\ 0.2740 & 0.2112 & 0.1484 & 0.0856 & 0.0429 \\ 0.1456 & 0.1122 & 0.0789 & 0.0455 & 0.0228 \\ 0.0726 & 0.0567 & 0.0394 & 0.0228 & 0.0140 \end{bmatrix}$$

$$\Phi_{4F} = \begin{bmatrix} 1.0000 & 0.8410 & 0.6804 & 0.5199 & 0.3595 \\ 0.9730 & 0.8166 & 0.6607 & 0.5048 & 0.3490 \\ 0.9440 & 0.7922 & 0.6410 & 0.4898 & 0.3386 \\ 0.9149 & 0.7678 & 0.6212 & 0.4747 & 0.3282 \end{bmatrix}$$

$$\Phi_{4\bar{F}} = \begin{bmatrix} 1.0000 & 0.9793 & 0.9578 & 0.9362 & 0.8955 \\ 0.9804 & 0.9593 & 0.9382 & 0.9171 & 0.8772 \\ 0.9600 & 0.9393 & 0.9186 & 0.8980 & 0.8589 \\ 0.9396 & 0.9193 & 0.8991 & 0.8788 & 0.8406 \end{bmatrix}$$

Reference

Hankin, D.G., Nicholas, J.W., and Downey, T.W. 1993. Evidence for inheritance of age of maturity in chinook salmon, *Oncorhynchus tshawytscha*. Can. J. Fish. Aquat. Sci. **50**(2): 347–358. doi:10.1139/f93-040.

In situ dissolved organic carbon (DOC) release by submerged macrophyte–epiphyte communities in southern Quebec lakes

M. Demarty and Y.T. Prairie

Abstract: We studied the in situ release of dissolved organic carbon (DOC) by growing a submerged freshwater macrophyte–epiphyte complex. Incubations with benthic chambers in five southeastern Quebec lakes show a net DOC production for different communities of *Myriophyllum spicatum* and *Potamogeton* spp. Daytime DOC release rates range from undetectable to 9.7 mg C·m^{-2}·h^{-1}. Although DOC release was restricted to daylight hours and thus suggestive of a photosynthesis-related process, we found no strong link between DOC release rates and concurrent illumination or temperature. We found no difference in DOC release rates between the three main colonizing species of the studied region. The overall mean DOC release rate was 4.57 mg C·m^{-2}·h^{-1} (standard deviation (SD), ±0.65) or 56 µg C·g dry weight^{-1}·h^{-1} (SD, ±8), which we suggest can be used for extrapolations at the lake scale.

Résumé : Nous étudions la libération in situ de carbone organique dissous (DOC) par un complexe submergé de macrophytes et d'épiphytes d'eau douce en croissance. Des incubations dans des enceintes benthiques dans cinq lacs du sud-est du Québec indiquent des productions nettes de DOC dans différentes communautés de *Myriophyllum spicatum* et de *Potamogeton* spp. Les taux de libération de DOC durant le jour varient de valeurs indécelables à 9,7 mg C·m^{-2}·h^{-1}. Bien que la libération de DOC soit restreinte aux heures d'éclairement et donc probablement un processus relié à la photosynthèse, il n'existe pas de lien solide entre les taux de libération de DOC et la température et l'éclairement concomitants. Il n'y a pas de différence entre les taux de libération de DOC des trois principales espèces colonisatrices de la région étudiée. Le taux global moyen de libération de DOC est de 4,57 C·m^{-2}·h^{-1} (écart type (ET), ±0,65) ou 56 µg C·g masse sèche^{-1}·h^{-1} (ET, ±8), valeurs que nous croyons pouvoir être utilisées pour des extrapolations à l'échelle du lac tout entier.

[Traduit par la Rédaction]

Introduction

The loading of terrestrial dissolved organic carbon (DOC) can contribute significantly to the energy pathways of lake ecosystems (Pace et al. 2004; Carpenter et al. 2005; Kritzberg et al. 2006). The concept of net heterotrophy in lakes whereby ecosystem respiration exceeds gross primary production has considerably changed our view of how lakes support their living biota. This pattern of excess respiration is believed to be found mostly in oligotrophic systems with DOC concentrations > 5–6 mg·L^{-1} (del Giorgio et al. 1997; Prairie et al. 2002; Hanson et al. 2003) and is believed to be largely responsible for the CO_2 supersaturation observed in most lakes of the world (Cole et al. 1994; del Giorgio et al. 1999; Duarte and Prairie 2005). However, recent studies have also shown that in some lakes at least, pelagic net heterotrophic metabolism can be observed simultaneously with CO_2 undersaturation, i.e., with a net CO_2 influx from the atmosphere (Prairie et al. 2002). Such discrepant properties would occur if a source of organic carbon metabolized in epilimnetic waters originated from elsewhere within the ecosystem. In such cases, net heterotrophy of the water column would not necessarily reflect the metabolic status of the whole ecosystem. Freshwater systems are among the ecosystems in which this situation is most likely to occur because benthic primary production often dominates the overall productivity of the system, particularly in shallow oligotrophic lakes (Vadeboncoeur et al. 2003). Indeed, studies of lake metabolism that do not consider the potential role of the benthic zone are likely to yield a biased assessment of the overall metabolic balance. In particular, if benthic organic matter production is translocated in some way to the water column and respired there, it could lead to a net heterotrophy of the pelagic zone but not necessarily of the whole ecosystem. To our knowledge, this hypothesis seldom has been explored in freshwater systems, largely because of the common misconception that the benthic zone is not often quantitatively significant (Vadeboncoeur et al. 2002). Yet, this situation has been described in marine systems by Gazeau et al. (2005), who argued that a benthic community dominated by macrophytes (*Posidonia oceanica*) could partly balance the net heterotrophy of the planktonic compartment, an idea sup-

Received 3 August 2008. Accepted 11 May 2009. Published on the NRC Research Press Web site at cjfas.nrc.ca on 3 September 2009. J20701

Paper handled by Associate Editor Charles Ramcharan.

M. Demarty[1] and Y. Prairie. Département des Sciences Biologiques, Université du Québec à Montréal, Case Postale 8888, Succursale Centre-ville, Montréal, QC H3C 3P8, Canada.

[1]Corresponding author (e-mail: maud.demarty@gmail.com).

ported by other studies as well (Duarte and Cebrian 1996; Wetzel and Søndergaard 1998; Ziegler and Benner 1999).

Macrophyte beds represent a potential DOC source to the open water from both plant decay (Otsuki et Wetzel 1974; Mann 1988; Alber et Valiela 1994) and DOC release by living plants and their epiphytes. Dissolved organic matter release by macrophytes was demonstrated several decades ago by Khailov and Burlakova (1969), who worked with five marine species of macroalgae. Further studies confirmed the release of DOC on both marine (Brylinsky 1977) and freshwater (Wetzel and Manny 1972; Godmaire and Nalewajko 1989) species. Reported rates of DOC vary enormously, ranging from 0.006 to 9.1 mg C·g(dry weight)$^{-1}$·h^{-1}, and this release can represent a non-negligible part of aquatic plant production (1.1% to 67%). Some studies described higher levels of DOC release in the light than in the dark (Sieburth 1969; Pregnall 1983; Nalewajko et Godmaire 1993), thus underlying a possible link between the release and the photoperiod. Similarly, DOC release has been described in marine phytoplankton and was viewed as an overflow mechanism linked to the photosynthesis in nutrient-limiting conditions (Jensen 1984). It therefore seems that DOC release is a phenomenon shared by aquatic photosynthetic organisms. In vivo, macrophytes are closely linked with epiphytic algae (hereafter referred as epiphytes), which also potentially release DOC. However, removing epiphytes from macrophytes to study the process on separate organisms is known to modify the response (Godmaire and Nalewajko 1986). In this in situ study, we therefore consider the macrophyte–epiphyte complex as one photosynthetic unit. Our main objective was to quantify DOC release by the macrophyte–epiphyte complex in a series of natural lakes to explore whether DOC release is as an overflow mechanism for photosynthate in nutrient-limiting conditions. This hypothesis supposes that when CO_2 and light are not limiting factors, photosynthesis of the macrophyte–epiphyte complex will produce carbohydrates even if nutrient-limiting conditions prevent the production of biomass from these simple molecules. According to this hypothesis, DOC release occurs only during photosynthesis and the rate of DOC release should be related to factors such as light and temperature, which are known to influence positively macrophyte and epiphyte photosynthetic rates (Kirk 1994; Madsen and Brix 1997). We assume that both macrophytes and epiphytes behave in the same way (i.e., they release DOC) and that the processes occurring by both of them are added, thus leading to the observation of the release. The effect of epiphytic bacteria cannot be tested and is therefore assumed to be part of the unexplained variance of the responses observed. As photosynthetic capacity differs among macrophyte species (Nielsen and Sand-Jensen 1989), we also tested whether DOC release rates vary consistently among four different species (*Myriophyllum spicatum*, *Potamogeton amplifolius*, *Potamogeton richardsonii*, *Potamogeton robinsii*). The hypotheses were tested both as rates per unit area (in milligrams of carbon per square metre per hour, mg C·m^{-2}·h^{-1}) and as per unit plant biomass (in milligrams of carbon per gram of dry weight per hour, mg C·g dw^{-1}·h^{-1}), respectively, representing responses at the community and plant levels. Finally, we examined the temporal variability in DOC release over the growing season.

Materials and methods

Study site and experimental design

The measurements were undertaken during the summers of 2004, 2005, and 2006 in six lakes of the Eastern Township region ~100 km east of Montréal, Québec (Table 1). These lakes are of glacial origin and are influenced by the alluvial sedimentary geology of the Saint Lawrence River.

To test our hypothesis, we used in situ benthic chambers inserted in the sediments. Chambers were made with a polyvinyl chloride (PVC) cylinder (height, 20 cm; diameter, 20 cm) covered hermetically with a polyethylene transparent plastic bag equipped with a sampling port (Barrón et al. 2003). At each study site, we randomly selected monospecific macrophyte beds coupled with a nearby unvegetated sediment location as control (except in shallow lac Trois Lacs where *Potamogeton richardsonii* covered the entire benthic surface). A list of the macrophyte species studied is provided (Table 2). Depending on the experiment, two, three, or four replicate transparent benthic chambers were placed on macrophytes (TM) and two were placed on unvegetated sediments (TS). Testing the effect of light on DOC release first implied a comparison between daily and nightly rates. Therefore, all in situ incubations lasted 24 or 36 h from sunrise or sunset (T0). Water samples from chambers were taken in duplicates for DOC at the beginning (T0), then just before sunset (or just after sunrise; T1), and finally just after the following sunrise (or just before sunset; T2) for the 24 h incubations; one more sampling was made 12 h after (before sunset or just after sunrise; T3) for the 36 h incubations made in lac Stukely. Samples were kept refrigerated in the dark at 4 °C until analysis in the following week.

We also tested the effect of mean light and temperature received during the daytime on concurrent DOC release rates. To obtain a wider and more continuous range in light and temperature conditions, we carried out additional experiments with transparent benthic chambers containing macrophytes covered with one or two neutral screens (noted TM + screen). Daytime averaged temperature in TM chambers ranged between 17.09 and 28.01 °C, and daytime averaged light received ranged between 612 and 19 523 lux. Taking TM + screen chambers into account, the lowest temperature and the lowest light received became 16.68 °C and 78 lux, respectively.

According to our hypothesis, we should observe the maximum release at the highest photosynthesis, i.e., at maximum light and temperature. To further explore this prediction, we followed DOC concentrations over a 24 h cycle at a much higher time resolution by taking samples every 1 or 2 h during the day for 2 TM chambers in lac Stukely. Light intensity and temperature were measured in each transparent benthic chamber with HOBO Temperature/Light Pendant Data Logger (Onset Computer Corp., Bourne, Mass.) every 10 s but averaged for every minute.

Water samples for DOC measurements were drawn through the sampling ports with 60 mL (polyethylene) acid-washed (HCl 10%) syringes, filtered on 0.45 µm Filtropur filters (Starstedt, Nümbrecht, Germany), and kept refrigerated (4 °C) in 40 mL acid-washed tubes with silicone–Teflon caps to prevent gas exchange during analysis. The sampling led to a volume reduction inside the

Table 1. Summertime characteristics of studied lakes.

Lake	Longitude (W)	Latitude (N)	Surface (km^2)	Mean depth (m)	Mean Secchi depth (m)	TP ($\mu g \cdot L^{-1}$) (SD)	TN ($mg \cdot L^{-1}$) (SD)	Chl *a* ($\mu g \cdot L^{-1}$) (SD)	DOC ($mg \cdot L^{-1}$) (SD)	MB ($g\ dw \cdot m^{-2}$)		
										2004	2005	2006
D'Argent	72°18′	45°18′	0.96	4.6	2.5	12.4 (4.4)	0.4 (0.1)	3.4 (1.6)	7.7 (1.5)	24	4.4	ND
Booker	72°12′	45°25′	2.3	25.9	7.9	4.9 (3.0)	0.2 (0.0)	0.9 (0.3)	2.6 (0.3)	0	—	—
Peasley	72°16′	45°16′	0.23	10.5	2.9	10.5 (6.4)	0.3 (0.0)	3.2 (1.5)	6.9 (1.0)	—	—	27
Stukely	72°15′	45°21′	3.86	13.6	5.4	7.4 (6.2)	0.3 (0.0)	1.7 (0.6)	4.6 (0.3)	17	0	0
Trois Lacs	71°53′	45°48′	2.85	1.26	1.5	30.9 (17.4)	0.7 (0.1)	4.4 (2.4)	9.9 (1.8)	68	90	ND
Waterloo	72°31′	45°20′	1.15	2.9	0.9	34.1 (14.4)	0.6 (0.2)	16.8 (10.4)	7.3 (1.4)	10	15	—

Note: MB, macrophyte biomass; dw, dry weight; TP, total phosphorus; TN, total nitrogen; Chl *a*, chlorophyll *a*; DOC, dissolved organic carbon; SD, standard deviation; ND, not determined.

chambers of around 1%. DOC analysis were made with a 1010 TIC–TOC analyser (O.I. Analytical, College Station, Texas) by high temperature wet oxidation (sodium persulfate; 100 $g \cdot L^{-1}$) after dissolved inorganic carbon (DIC) elimination by acidification (sulphuric acid 5%) and sparging; analytical samples were taken in triplicate in 2004 but only in duplicate in 2005 and 2006, given the high reproducibility observed. Analytical replicates had a coefficient of variation of 0.7%, and sample replicates had a coefficient of variation of 1%.

At the end of the 24 h incubation, the water volume within each benthic chamber was estimated by injecting a 10 mL weak fluorescein solution (absorption peak at 552 nm) and drawing two samples after mixing for 5 min. Calculated volumes ranged between 4 and 11 L. At the end of each experiment, macrophyte shoots within the PVC ring were harvested to measure their aboveground biomass after rinsing and drying at 55 °C for 24 h to 36 h.

Macrophyte biomass was also quantified at the whole-lake scale. Random quadrat samples were taken during the second week of August in 2004 and the first week of August in 2005 and 2006 within the zone confined by the maximum depth for macrophytes colonization estimated from the Secchi depth (Chambers and Kalff 1985). For each lake except lac Trois Lacs, where macrophytes colonized the entire benthic surface, we randomly choose sampling points in the colonization zone from digital bathymetric map; in the field, these sampling points were reached with a GPS. We used a 25 × 25 cm quadrat and estimated the number of replicates needed after Downing and Anderson (1985). Between 10 and 22 replicates were taken in each lake. Macrophyte shoots inside the quadrat were harvested to measure their aboveground biomass after rinsing and drying at 55 °C for 24 h to 36 h.

DOC release by macrophyte–epiphyte communities

Diurnal and nocturnal DOC variations were calculated as the simple difference in DOC concentrations between sunrise and sunset (photoperiod) and sunset and sunrise, respectively, in both TM and TS chambers. DOC changes with time within each chamber were expressed both per unit area ($mg\ C \cdot m^{-2} \cdot h^{-1}$) and per unit plant biomass ($mg\ C \cdot g\ dw^{-1} \cdot h^{-1}$), hereafter referred as DOC release rates. Standard error of each calculated rate was estimated. For each sampling date, rates obtained for the same incubations (TM for example) were compiled to obtain mean rates and standard errors (see Table 2).

The presence of macrophytes is known to alter their own environments by increasing the sedimentation rate (Barko and James 1998; Rooney and Kalff 2003; Schulz and Köhler 2006) and the nature of the sedimenting material (Duarte and Chiscano 1999; Barrón et al. 2006) and by providing efficient mechanisms for solute transport within the sediment or at the interface (Carpenter and Lodge 1986). Thus, basic calculations of DOC production or consumption from DOC concentration changes in chambers containing both water and sediments provide estimates of the net effect of the presence of macrophytes on DOC release patterns (termed net bulk DOC release). Indeed, daily and nightly DOC variations measured in transparent chambers containing macrophytes (TM) are the sum of several processes occurring

Table 2. Mean daily and nightly dissolved organic carbon release rates (DOCr) for five studied lakes with corresponding daily temperature and received light inside the benthic chamber.

				Day		Night			
Lake	Sampling date	Species	*n*	Mean DOCr ($mg \cdot m^{-2} \cdot h^{-1}$) (SE)	Mean DOCr ($\mu g \cdot g\ dw^{-1} \cdot h^{-1}$) (SE)	Mean DOCr ($mg \cdot m^{-2} \cdot h^{-1}$) (SE)	Mean DOCr ($\mu g \cdot g\ dw^{-1} \cdot h^{-1}$) (SE)	Temperature (°C) (SE)	Light (lux) (SE)
Bowker	7 July 2004	P. rob	2	**9.7** (1.1)	92 (7)	–0.8 (0.1)	–8 (1)		
D'Argent	28 June 2004	P. amp	2	3.2 (0.9)	49 (12)	–2.1 (0.5)	–33 (10)		
	6 June 2005	Myrio	4	0.4 (0.2)	4 (3)	0.6 (0.3)	6 (4)	21.11 (0.05)	10 673 (2352)
	8 June 2005	P. amp	4	0.4 (0.3)	22 (20)	–0.7 (0.3)	–74 (51)	21.00 (0.07)	3 090 (57)
	27 June 2006	Myrio	3	3.8 (1.7)	50 (32)	–3.3 (0.8)	–26 (3)	22.04 (0.05)	7 000 (350)
	28 June 2006	Myrio	3	4.5 (1.3)	36 (10)	1.5 (0.9)	10 (6)	21.58 (0.11)	3 140 (1087)
	3 August 2006	P. amp	3	1.0 (1.4)	6 (12)	–1.5 (2.2)	–10 (19)	22.49 (0.07)	1 746 (263)
	5 September 2006	P. amp	3	–0.4 (1.4)	–6 (23)	–0.4 (0.2)	–6 (3)	18.27 (0.05)	1 076 (233)
Peasley	11 July 2006	P. amp	3	5.5 (2.0)	47 (17)	–0.6 (0.2)	–5 (1)	24.72 (0.04)	5 578 (589)
	7 August 2006	P. amp	3	0.1 (2.0)	7 (19)	–0.8 (1.2)	–8 (15)	24.85 (0.06)	9 731 (1694)
Stukely	22 June 2005	Myrio	4	1.7 (0.5)	48 (11)	–1.7 (0.3)	**–63** (23)	19.00 (0.10)	9 412 (1670)
	28 June 2005	P. amp	3	8.1 (1.0)	**157** (32)	–2.3 (0.8)	–46 (19)	27.93 (0.04)	17 528 (658)
	6 July 2005	Myrio	2	3.4 (0.6)	75 (36)	–0.1 (2.0)	–15 (41)	21.44 (0.01)	11 322 (1146)
	9 August 2005	P. amp	3	5.8 (1.7)	75 (24)	–0.3 (0.6)	–4 (8)		
	12 June 2006	P. amp	3	2.6 (1.3)	47 (23)	–2.2 (0.9)	–42 (19)	17.16 (0.07)	12 312 (182)
	21 June 2006	P. amp	3	9.1 (0.9)	75 (11)	0.1 (2.7)	–2 (18)	21.62 (0.07)	2 661 (377)
	17 July 2006	P. amp	3	7.8 (0.4)	68 (8)	**1.5** (0.8)	**12** (5)	27.24 (0.05)	14 830 (1486)
	20 July 2006	Myrio	2	8.0 (0.6)	79 (13)	–2.8 (3.4)	–36 (41)	26.69 (0.06)	19 446 (77)
	18 August 2006	P. amp	3	3.6 (0.4)	43 (9)	1.5 (1.6)	13 (16)	22.47 (0.03)	16 198 (776)
Trois Lacs	19 July 2005	P. rich	2	5.3 (1.1)	87 (32)	–1.9 (1.5)	–33 (28)	27.16 (0.08)	7 791 (1598)
	28 July 2005	P. rich	3	2.8 (0.4)	25 (2)	–1.9 (0.5)	–18 (5)	24.82 (0.04)	5 079 (1609)
	20 June 2006	P. rich	3	8.1 (0.3)	47 (3)	**–3.8** (1.4)	–20 (7)	22.89 (0.01)	2 899 (213)
	1 August 2006	P. rich	3	2.1 (0.8)	16 (11)	0.6 (1.3)	9 (11)	24.41 (0.04)	3 339 (664)
Waterloo	6 July 2004	Myrio	2	**9.7** (2.6)	112 (56)	–0.6 (1.8)	–26 (32)		
	15 June 2005	Myrio	3	8.0 (3.2)	141 (54)	–0.5 (0.3)	–16 (14)	20.81 (0.04)	5 021 (362)

Note: Myrio, P. amp, P. rich, and P. rob represent *Myriophyllum spicatum*, *Potamogeton amplifolius*, *Potamogeton richardsonii*, and *Potamogeton robinsii*, respectively.

Published by NRC Research Press

Fig. 1. Trends in dissolved organic carbon (DOC) concentration (left axis; dotted lines) and light intensity (right axis; shaded lines) during 36 h in two transparent chambers (● and ▲, respectively) containing *P. amplifolius* in lac Stukely in 2005. Bars represent standard error ($n = 4$).

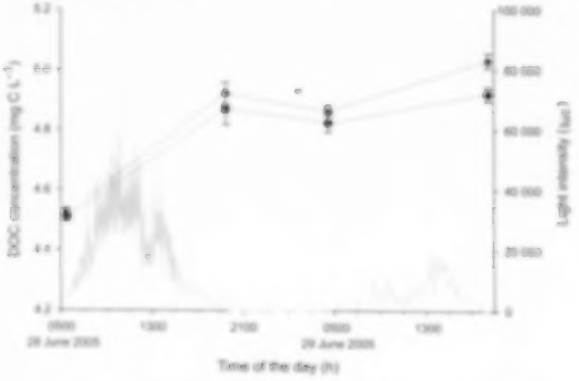

simultaneously. In an attempt to further disentangle these processes, we made additional measurements with benthic chambers on bare sediments near the macrophyte bed, thus providing the closest control in terms of sediments, as well as phytoplanktonic and heterotrophic communities of the surrounding water. The production and consumption of DOC can be derived from several potential compartments: macrophyte–epiphyte complex (me), phytoplankton (Ψ), heterotrophic community (h), and the sediments (sed). In transparent chambers placed on sediments (TS), the same processes are present except for the contribution of the macrophyte–epiphyte complex. Although an imperfect control, these experiments provide valuable clues by estimating, by subtraction, the net DOC release attributable to the macrophyte–epiphyte complex itself (termed DOC_{me}). Equations 1 to 4 describe the processes occurring in transparent macrophytes (TM) and sediments (TS) chambers:

$$(1)\quad \Delta DOC(TM)day = DOC_{me}(d) + DOC_{\Psi}(d) + DOC_{h}(d) + DOC_{sed}(d) - R$$

$$(2)\quad \Delta DOC(TM)night = DOC_{me}(n) + DOC_{\Psi}(n) + DOC_{h}(n) + DOC_{sed}(n) - R$$

$$(3)\quad \Delta DOC(TS)day = DOC_{\Psi}(d) + DOC_{h}(d) + DOC_{sed}(d) - R'$$

$$(4)\quad \Delta DOC(TS)night = DOC_{\Psi}(n) + DOC_{h}(n) + DOC_{sed}(n) - R'$$

where R is the DOC respired in TM chambers, R' is the DOC respired in TS chambers, and d and n refer to day and night, respectively. By successive subtractions, we obtained net DOCme:

$$(5)\quad \Delta DOC(TM)day - \Delta DOC(TM)night - \Delta DOC(TS)day + \Delta DOC(TS)night = DOC_{me}(d) - DOC_{me}(n)$$

and

Fig. 2. Daytime and nighttime general mean dissolved organic carbon (DOC) rates (with data from all years, in mg C·m^{-2}·h^{-1}) for transparent chambers containing macrophytes at lac d'Argent (*P. amplifolius* and *M. spicatum*), lac Bowker (*P. robinsii*), lac Peasley (*P. amplifolius*), lac Stukely (*P. amplifolius* and *M. spicatum*), lac Trois Lacs (*P. richardsonii*; *, lac Trois Lacs data for 20 June 2005 are presented separately), and lac Waterloo (*M. spicatum*). Bars represent standard error.

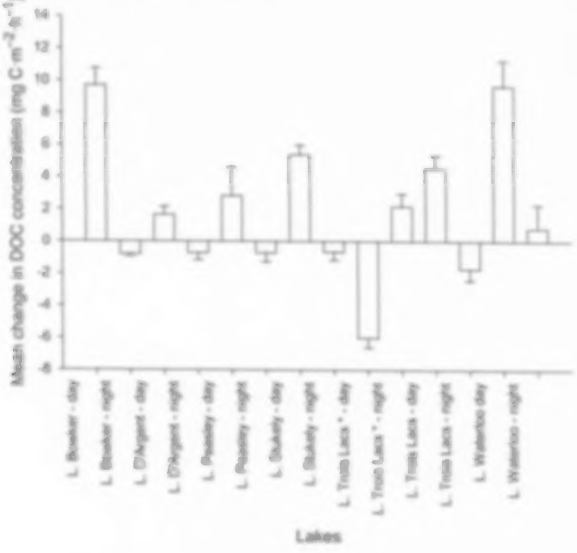
Mean change in DOC concentration (mg C·m⁻²·h⁻¹)
L. Bowker - day
L. Bowker - night
L. D'Argent - day
L. D'Argent - night
L. Peasley - day
L. Peasley - night
L. Stukely - day
L. Stukely - night
L. Trois Lacs * - day
L. Trois Lacs * - night
L. Trois Lacs - day
L. Trois Lacs - night
L. Waterloo day
L. Waterloo - night
Lakes

$$(6)\quad DOC_{me}(d) - DOC_{me}(n) = DOC_{me}$$

both expressed in mg C·m^{-2}·h^{-1} and in mg C·g dw^{-1}·h^{-1}. Uncertainty estimates for these compound calculations were derived from classical error propagation formulas.

Results

Macrophyte biomass data

In the benthic chambers, areal macrophytes biomass varied between 6 and 336 g dw·m^{-2}, with a mean of 95 g dw·m^{-2} (standard error (SE), ±3.4; $n = 246$), which is in the same range as other reported macrophyte biomasses in southeastern Quebec lakes (Chambers and Kalff 1985; Rooney and Kalff 2000; Duarte and Kalff 1990). We naturally observed significant increases in mean biomass through the summertime (analysis of variance (ANOVA), $p < 0.05$), with average growth rates of 37 g dw·month^{-1} in June–July and 10 g dw·month^{-1} in July–August. Estimated macrophytes biomasses at the whole-lake scale for the sampling period are given for each lake (Table 1).

Day–night comparison in DOC release rates

Our macrophyte incubations clearly showed that the DOC release is linked to the photoperiod as it occurred during day but stopped at night (Fig. 1; Table 2). This was the case whether experiments were begun in the evening or in the morning, showing that the observed DOC release was tied to the photoperiod and not to the initiation time of the incubations. In all cases, we observed an increase in DOC con-

centration during the day but not during the night in benthic chambers containing macrophyte (Fig. 2; one-way ANOVA for each lake, $p < 0.05$), except for one of the sampling dates in lac Trois Lacs (20 June 2005) where DOC was apparently consumed faster than it was produced. Considering different TM chambers used for each experiment (per date and lake) as replicates, we obtained mean daily DOC accumulation rates (considered as release rates by macrophyte–epiphyte complex) varying from undetectable to 9.7 mg $C \cdot m^{-2} \cdot h^{-1}$ (SE, ±1.1; $n = 2$) in lac Waterloo or from undetectable to 157 µg $C \cdot g\ dw^{-1} \cdot h^{-1}$ (SE, ±32; $n = 3$) in lac Stukely. Nightly variations in DOC were mostly negative, thus representing DOC consumption. They varied from –3.8 mg $C \cdot m^{-2} \cdot h^{-1}$ (SE, ±1.4; $n = 3$) in lac Trois Lacs to 1.5 mg $C \cdot m^{-2} \cdot h^{-1}$ (SE, ±0.8; $n = 3$) or from –63 µg $C \cdot g\ dw^{-1} \cdot h^{-1}$ (SE, ±23; $n = 4$) to 12 µg $C \cdot g\ dw^{-1} \cdot h^{-1}$ (SE, ±5; $n = 3$) both in lac Stukely. In chambers without macrophyte (TS), we observed no significant DOC changes in all our experiments (ANOVA, $p > 0.05$), meaning that the planktonic community of the benthic zone and naked sediments do not release DOC and therefore changes in DOC concentration observed in TM chambers are attributable to the presence of the macrophyte–epiphyte community.

Estimation of net DOC release rates by the macrophyte–epiphyte communities (DOC_{mc})

As we explained earlier, daytime DOC rates obtained from direct measurements in chambers containing macrophytes take into account not only the effect of the macrophyte–epiphyte complex, but also the effect of the overall metabolic activity occurring within the chamber, including DOC consumption occurring simultaneously with the release. In some cases (e.g., lac Trois Lacs, 20 June 2005), this consumption can be strong enough to totally mask the diurnal DOC release. Equation 5, developed earlier, allows the estimation of the DOC release rate more closely attributable to the macrophyte–epiphyte complex itself, rather than by the entire community found in the benthic chambers. Because there were no significant DOC variations in the chambers devoid of macrophytes (TS, results not shown), we considered the DOC release by phytoplankton and (or) sediments to be quantitatively negligible. As a result, calculation of the net DOC release from macrophytes (DOC_{mc}, eq. 6) can be simplified to

$$(7) \qquad DOC_{mc} = \Delta DOC(TM)day - \Delta DOC(TM)night$$

From individual DOC release rates, we calculated corrected rates of DOC release by the macrophyte–epiphyte complex (DOC_{mc}) using eq. 7. Uncertainty estimates for these compound calculations were derived from classical error propagation formulas.

Once averaged (per date and lake), obtained rates varied from undetectable to 11.9 mg $C \cdot m^{-2} \cdot h^{-1}$ (SE, ±1.72; $n = 3$) for lac Trois Lacs and from undetectable to 203 µg $C \cdot g\ dw^{-1} \cdot h^{-1}$ (SE, ±50; $n = 3$) for lac Stukely. For the following analysis, we excluded the data obtained on 20 June 2005 in lac Trois Lacs, which still pointed to a strong net consumption even after correction (mean DOC_{mc} of –8.7 mg $C \cdot m^{-2} \cdot h^{-1}$ (SD, ±2.5) or –218 µg $C \cdot g\ dw^{-1} \cdot h^{-1}$ (SD, ±154)). In all cases, these corrections (from subtractions) compounded the uncertainty of our measurements and therefore decreased the statistical power of our analysis. Nevertheless, we performed the two sets of calculations to examine both the robustness of our conclusions and the potential importance of these corrections. We therefore will be able to conclude on the implication of the pelagic and sedimentary community versus the macrophyte–epiphyte complex on the DOC release.

Fig. 3. Trends in dissolved organic carbon (DOC) concentration (left axis; dotted lines) and light intensity (right axis; shaded lines) for benthic chambers containing macrophytes during time course experiments in lac Stukely in (*a*) 2005 and (*b*) 2006. Bars represent standard error.

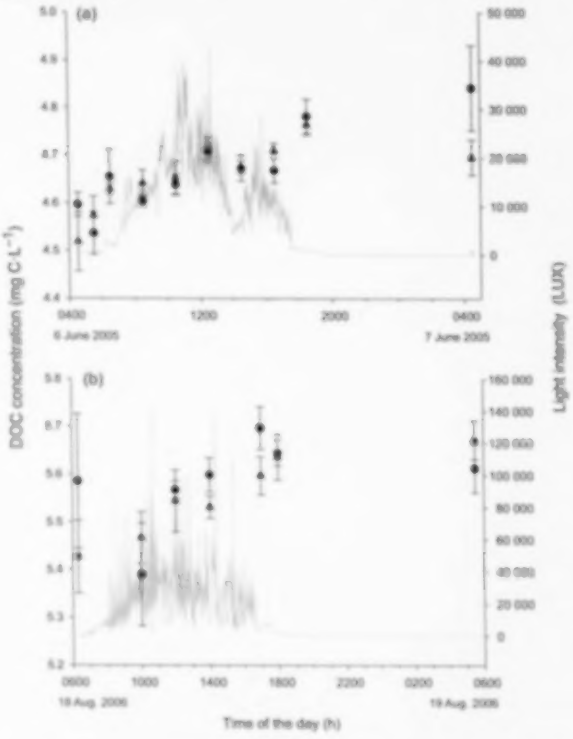

Short-term daytime evolution of DOC concentration in macrophyte–epiphyte communities

In 2005 and 2006, we followed diurnal DOC concentrations more intensively in lac Stukely on *P. amplifolius* incubations: DOC measurements were taken at sunrise and then every 2.5 h on average. We observed an increase in DOC from the first hours and occurring all day through (Figs. 3*a* and 3*b* for 2005 and 2006, respectively). In each replicate benthic chamber, rates of DOC changes were not statistically different between sampling steps (analysis of covariance (ANCOVA) time × step: $p > 0.05$, data not shown). It therefore suggests that DOC release is a continuous process that begins at sunrise but is not clearly related to the rate of photosynthesis. Taking the two sampling years separately, we found no relationship between the increase in DOC concentration for each step and temperature or the amount of light received during that same period. Thus, at this short temporal scale, DOC release is independent of temperature

and light, pointing to a decoupling between the rates of release and the main factors regulating photosynthesis.

Influence of light and temperature and temporal patterns in DOC release rates

Combining all our measurements (2004, 2005, 2006; TM and TM + screen, $n = 108$), we found no temporal pattern through summertime in the mean daily illumination in the benthic chambers, whereas temperature clearly increased from early June to the middle of July and then decreased until the end of our experiments at the beginning of September. Similarly, it was clear that DOC release rates were not constant over the growing season (ANOVA, $p < 0.05$): for temperature, rates reached a peak in late June – early July and declined to minimal values in late August. Once the seasonality effect was extracted using sampling day as a fixed factor, we found that temperature had a weak positive effect on DOC release rates (when expressed per unit plant biomass), explaining 7% of the variation, whereas light did not (ANCOVA: sampling time × mean daily temperature × mean illumination; model $R^2 = 0.56$, $p < 0.05$). Expressed on areal basis, neither light nor temperature had a significant effect on DOC release rates. Seasonality in corrected DOC release rates was less clear, and tests showed no effect of combined sampling time, mean daily temperature, and mean illumination (ANCOVA, $p > 0.05$). The weak association between release rates and physical factors does not point to a strong coupling between photosynthesis and release rates.

Variation in release rates among macrophyte species

According to our hypothesis and because photosynthetic capacity differs among macrophyte species, mean DOC release rate should also differ among species. Given the temporal trend noted above, we tested a possible difference among species by using the residuals of the polynomial function. An ANOVA detected no difference in the temporally detrended mean DOC rates (with uncorrected or corrected rates) between species ($p > 0.05$, $n = 25$). DOC release measurements grouped by genera instead of species also showed no difference in mean DOC release rates (ANOVA $p > 0.05$).

Based on this lack of difference from results presented in Table 2, the overall mean DOC release rates of 4.57 mg $C \cdot m^{-2} \cdot h^{-1}$ (SD, ±0.65) or 56 µg $C \cdot g\ dw^{-1} \cdot h^{-1}$ (SD, ±8) can be used as a general estimate of DOC release, which may be useful for extrapolations to the lake scale.

Discussion

Relevance of correcting rates

Water column heterotrophic organisms can be efficient at controlling the pool of DOC compounds and therefore may obscure actual rates of DOC release by the macrophyte–epiphyte complex. The corrections increased or reduced the observed DOC released rates ranging from undetectable to 9.7 mg $C \cdot m^{-2} \cdot h^{-1}$ before corrections to ranging from undetectable to 11.9 mg $C \cdot m^{-2} \cdot h^{-1}$ after corrections. Although the correction rate was 2.55 on average (i.e., corrected rates are on average 2.55 higher than uncorrected), it was highly variable (SD, ±12.67), suggesting that it was quite important in individual measurements.

These corrections make several assumptions regarding the metabolism of the heterotrophic community, e.g., the similarity between daytime and nighttime respiration, both in water column and sediments. It also assumes that the presence of macrophytes does not alter the rates of these background metabolic processes. Naturally, respiration is enhanced by warmer temperature in these compartments (see review in Pace and Prairie 2005) and can therefore be higher during the day than at night. Thus, the amount of DOC consumed by the heterotrophic community during the day may be higher than we assumed, leading to conservative DOC_{nr} rates. However, we observed that the corrections did not lead to changes in relationships between release rate and light or temperature. As well, the global release rates proposed to upscale our result at the lake scale were not statistically different with or without correction. Finally, this exercise allowed us to underline the dominant role of the macrophyte–epiphyte complex in DOC release and the fact that variations in environmental factors do not induce a shift from DOC production by the macrophyte–epiphyte complex to production by the rest of the community (planktonic and (or) heterotrophic communities or sediments).

Patterns in DOC release by the macrophyte–epiphyte complex

To our knowledge, this study is the first to provide in situ evidence of a substantial DOC release by living freshwater macrophytes together with their epiphytes. DOC release has been reported for macrophytes and epiphytes separately in laboratory experiments (e.g., Penhale and Smith 1977), but these results have been discussed later because of the effect of removing epiphytes from their substrate (Godmaire and Nalewajko 1986). However, because we were more interested in quantifying this release in natural conditions, we could not separate these two components and therefore attribute the release to the macrophyte–epiphyte complex. Because we did not measure epiphyte biomass or diversity, it is hazardous to conclude on the possible different impacts of epiphytic communities. The studied macrophyte communities presented weak visible epiphytes, so our conclusions could be questionable in case of high epiphyte density.

As previously shown in laboratory experiments for macrophytes (Nalewajko and Godmaire 1993) and for marine phytoplankton (Marañón et al. 2004), DOC release occurred during the daytime only and is thus closely associated with the photosynthetic process. As the same patterns were observed for incubations beginning at sunset or sunrise, it rules out the possibility that the release was due to the initial experimental stress associated with plant manipulation.

The DOC release rates that we measured (from undetectable to 9.7 mg $C \cdot m^{-2} \cdot h^{-1}$ or from undetectable to 157 µg $C \cdot g\ dw^{-1} \cdot h^{-1}$ for macrophyte biomass varying between 6 and 336 g $dw \cdot m^{-2}$) are lower to those of Barrón et al. (2003) for marine macrophyte–epiphyte communities. This is likely attributable to the much higher macrophyte biomass in their systems (0.14 to 0.6 g $C \cdot m^{-2} \cdot day^{-1}$ for macrophyte biomass varying between 242 and 4841 g $dw \cdot m^{-2}$). Ziegler and Benner (1999) also found net daily DOC flux from seagrass higher than our DOC release rates. Qualitatively, these comparisons show that freshwater macrophyte–epiphyte communities act as their marine equivalent and that the release

is likely not associated with osmotic stresses induced by the environment. However, to allow future comparisons of DOC release rates from various ecosystems and species, we clearly see the importance of expressing DOC release rate not only as a function of the colonized surface (per square metre, reflecting the phenomenon at the community scale), but also per unit of macrophyte biomass (per gram dry weight, reflecting the role of the organism itself).

To examine the relative importance of macrophyte DOC release to other internal DOC sources to the ecosystem, we compared our rates with those obtained for phytoplankton DOC release. Because phytoplankton and macrophyte processes operate in different dimensional setting, we integrated our observed areal rates over the water column above the macrophyte to yield commensurable volumetric rates. For marine phytoplankton, Marañón et al. (2005) obtained DOC production rates varying between 1 and 3 $mg \cdot m^{-3} \cdot day^{-1}$ in an oligotrophic environment. From rates obtained in our benthic chambers and the water column depth at the sampling site, we calculated volumetric DOC production rates by the macrophyte–epiphyte complex ranging between 0.4 and 98 $mg\ C \cdot m^{-3} \cdot day^{-1}$ in the oligotrophic lac Stukely. Thus, a living macrophyte–epiphyte complex can constitute a major internal source of organic carbon, even in oligotrophic systems. Therefore, we can hypothesize that the proportion of DOC contributed by a macrophyte–epiphyte complex in relation to that released by phytoplankton should vary, along a trophic gradient, simply as a function of the predictable switch of the major source of primary production from the benthic to the pelagic zone (Vadeboncoeur et al. 2003).

Light and temperature effects: do they confirm our hypothesis?

Because both light and temperature are known to universally affect photosynthetic rates, we expected that if DOC release can be viewed as an overflow mechanism when an important element is limiting (such as nutrients), DOC release rates should increase with both light intensity and temperature. We conducted two follow-up experiments to test the effects of light and temperature on DOC release rates, one at a short time scale in one chosen lake (lac Stukely) with samples taken every 2.5 h and the other at the summertime scale in the six studied lakes, using rates calculated on a daily basis. Neither showed a strong relationship between mean light received and concurrent DOC release rates. This leads to a rejection of the link between DOC release and photosynthesis because release rates would have increased with increasing light if it was the case. Moreover, we observed that DOC release began with sunrise, which means that according to the overflow mechanism hypothesis, nutrients are limiting to biomass production even at low light. This observation therefore supports the critique of this hypothesis as it would not be evolutionary advantageous for a macrophyte–epiphyte complex to maintain high photosynthetic capacity in an environment that cannot lead to maximum growth efficiency (the DOC release being a loss for the macrophyte–epiphyte complex).

For temperature effect, even if the short time scale study concludes that there was no relationship between temperature and DOC release, the longer time scale study showed a general weak positive effect of temperature, stronger at lake scale, particularly for lac Stukely. Two explanations can be proposed for this relationship. Firstly and according to the hypothesis of an overflow mechanism, higher temperature could induce a higher DOC release because of a higher photosynthesis efficacy (light being constant; Madsen and Brix 1997) leading to higher accumulation of photosynthates, considering that environment could be nutrient-limiting. This explanation is acceptable but we do not support it as our study of light effect just rejected the hypothesis of an overflow mechanism. The second explanation is suggested by the work of Madsen and Brix (1997), who observed that in inorganic-carbon-limiting conditions, *E. canadensis* and *R. aquatilis* increased their carboxylation efficiency when temperature increased (higher Q_{10} than if CO_2 diffusion rate was the only implicated factor). To increase this carboxylation efficiency, enzymatic, morphologic, or anatomic changes could be implied. Therefore, we can suggest that DOC release could be partly implied in increasing carboxylation efficiency of the macrophyte–epiphyte complex in response to increased temperature in inorganic-carbon-limiting conditions, as would an increase in extracellular carbonic anhydrase. This hypothesis therefore implies that in nonlimiting inorganic carbon conditions, DOC release rates would be lower. This proposition, as well as the link between nutrient availability and DOC release, has to be tested to surely reject the hypothesis viewing the DOC release as an overflow mechanism.

Implication to the whole ecosystem

To our knowledge, our study is the first one comparing in situ DOC release rates, and we found no differences between species or among lakes. Perhaps such differences exist but are too weak to be measured with our technique. However, until these estimates can be further refined, we suggest that the use of our overall average DOC release rate ($4.57\ mg\ C \cdot m^{-2} \cdot h^{-1}$ (SD, ±0.65) or $56\ \mu g\ C \cdot g\ dw^{-1} \cdot h^{-1}$ (SD, ±8)) constitutes the best approximation to estimate the ecosystem implication of a submerged macrophyte–epiphyte complex in lake DOC dynamics. Estimation of the potential contribution of a macrophyte–epiphyte complex to the DOC budget of the whole ecosystem can thus be calculated as the simple product of the average release rate and the average macrophyte biomass in the colonisable zone of lakes.

In conclusion, we demonstrated the occurrence of daytime DOC release by a macrophyte–epiphyte complex in southeastern Quebec lakes. We reject the hypothesis presenting DOC release as an overflow mechanism for recent photosynthates produced in limited environments as we demonstrated no link between physical factors influencing photosynthesis and DOC release rates. Finally, because we observed no difference in averaged DOC release rates between the three main colonizing macrophyte–epiphyte complexes of our lakes, we proposed a mean DOC release rate useful for quantitative extrapolation of the process at the whole-lake scale.

Acknowledgements

We thank R. Gravel, V. Gauvin, and C. Blain for field assistance and C. Beauchemin for DOC analysis. This project was funded by the Natural Sciences and Engineering Re-

search Council of Canada (NSERC) in the form of a Discovery grant to Y.T. Prairie. This study is a contribution to the GRIL (Groupe de Recherche Interuniversitaire en Limnologie).

References

Alber, M., and Valiela, I. 1994. Production of microbial organic aggregates from macrophyte-derived dissolved organic material. Limnol. Oceanogr. **39**: 37–50.

Barko, J.W., and James, W.F. 1998. Effects of submerged aquatic macrophytes on nutrient dynamics, sedimentation, and resuspension. *In* The structuring role of aquatic macrophytes in lakes. *Edited by* E. Jeppesen, M. Søndergaard, M. Søndergaard, and K. Christoffersen. Springer, New York. pp. 197–214.

Barrón, C., Marbà, N., Duarte, C.M., Pedersen, M.F., Lindblad, C., Kersting, K., Moy, F., and Bokn, T. 2003. High organic carbon export precludes eutrophication responses in experimental rocky shore communities. Ecosystems (N.Y., Print), **6**: 144–153. doi:10.1007/s10021-002-0402-3.

Barrón, C., Middelburg, J.J., and Duarte, C.M. 2006. Phytoplankton trapped within seagrass (*Posidonia oceanica*) sediments are a nitrogen source: an in situ isotope labeling experiment. Limnol. Oceanogr. **51**: 1648–1653.

Brylinsky, M. 1977. Release of dissolved organic matter by some marine macrophytes. Mar. Biol. (Berl.), **39**(3): 213–220. doi:10.1007/BF00390995.

Carpenter, S.R., and Lodge, D.M. 1986. Effects of submersed macrophytes on ecosystem processes. Aquat. Bot. **26**: 341–370. doi:10.1016/0304-3770(86)90031-8.

Carpenter, S.R., Cole, J.J., Pace, M.L., Van De Bogert, M., Bade, D.L., Bastviken, D., Gille, C.M., Hodgson, J.R., Kitchell, J.F., and Kritzberg, E.S. 2005. Ecosystem subsidies: terrestrial support of aquatic food webs from C-13 addition to contrasting lakes. Ecology, **86**(10): 2737–2750. doi:10.1890/04-1282.

Chambers, P.A., and Kalff, J. 1985. Depth distribution and biomass of submerged aquatic macrophyte communities in relation to Secchi depth. Can. J. Fish. Aquat. Sci. **42**(4): 701–709. doi:10.1139/f85-090.

Cole, J.J., Caraco, N.F., Kling, G.W., and Kratz, T.K. 1994. Carbon dioxide supersaturation in the surface waters of lakes. Science (Washington, D.C.), **265**(5178): 1568–1570. doi:10.1126/science.265.5178.1568. PMID:17801536.

del Giorgio, P.A., Cole, J.J., and Cimbleris, A. 1997. Respiration rates in bacteria exceed phytoplankton production in unproductive aquatic systems. Nature (London), **385**(6612): 148–151. doi:10.1038/385148a0.

del Giorgio, P.A., Cole, J.J., Caraco, N.F., and Peters, R.H. 1999. Linking planktonic biomass and metabolism to net gas fluxes in northern temperate lakes. Ecology, **80**(4): 1422–1431. doi:10.1890/0012-9658(1999)080[1422:LPBAMT]2.0.CO;2.

Downing, J.A., and Anderson, M.R. 1985. Estimating the standing biomass of aquatic macrophytes. Can. J. Fish. Aquat. Sci. **42**: 1860–1869. doi:10.1139/f85-234.

Duarte, C.M., and Cebrian, J. 1996. The fate of marine autotrophic production. Limnol. Oceanogr. **41**: 1758–1766.

Duarte, C.M., and Chiscano, C.L. 1999. Seagrass biomass and production: a reassessment. Aquat. Bot. **65**(1–4): 159–174. doi:10.1016/S0304-3770(99)00038-8.

Duarte, C.M., and Kalff, J. 1990. Biomass density and the relationship between submerged macrophyte biomass and plant growth form. Hydrobiologia, **196**(1): 17–23. doi:10.1007/BF00008889.

Duarte, C.M., and Prairie, Y.T. 2005. Prevalence of heterotrophy and atmospheric CO_2 emissions from aquatic ecosystems. Ecosystems (N.Y., Print), **8**(7): 862–870. doi:10.1007/s10021-005-0177-4.

Gazeau, F., Duarte, C.M., Gattuso, J.P., Barrón, C., Navarro, N., Ruiz, S., Prairie, Y.T., Calleja, M., Delille, B., Frankignoulle, M., and Borges, A.V. 2005. Whole-system metabolism and CO_2 fluxes in a Mediterranean bay dominated by seagrass beds (Palma Bay, NW Mediterranean). Biogeosciences, **2**: 43–60.

Godmaire, H., and Nalewajko, C. 1986. Axenic culture of *Myriophyllum spicatum* L.: importance to extracellular product estimates. Aquat. Bot. **26**: 385–392. doi:10.1016/0304-3770(86)90034-3.

Godmaire, H., and Nalewajko, C. 1989. Growth, photosynthesis, and extracellular organic release in colonized and axenic *Myriophyllum spicatum*. Can. J. Bot. **67**(12): 3429–3438. doi:10.1139/b89-419.

Hanson, P.C., Bade, D.L., Carpenter, S.R., and Kratz, T.K. 2003. Lake metabolism: relationships with dissolved organic carbon and phosphorus. Limnol. Oceanogr. **48**: 1112–1119.

Jensen, A. 1984. Excretion of organic carbon as a function of nutrient stress. *In* Marine phytoplankton and productivity. *Edited by* O. Holm-Hansen, L. Bolis, and R. Gilles. Springer, New York. pp. 61–72.

Khailov, K.M., and Burlakova, Z.P. 1969. Release of dissolved organic matter by marine seaweeds and distribution of their total organic production to inshore communities. Limnol. Oceanogr. **14**: 521–532.

Kirk, J.T.O. (*Editor*). 1994. Photosynthesis in the aquatic environment. *In* Light and photosynthesis in aquatic ecosystems. Cambridge University Press, Cambridge, UK. pp. 314–359.

Kritzberg, E.S., Cole, J.J., Pace, M.M., and Granéli, W. 2006. Bacterial growth on allochtonous carbon in humic and nutrient-enriched lakes: results from whole-lake C-13 addition experiments. Ecosystems (N.Y., Print), **9**(3): 489–499. doi:10.1007/s10021-005-0115-5.

Madsen, T.V., and Brix, H. 1997. Growth, photosynthesis and acclimation by two submerged macrophytes in relation to temperature. Oecologia (Berl.), **110**(3): 320–327. doi:10.1007/s004420050165.

Mann, K.H. 1988. Production and use of detritus in various freshwater, estuarine, and coastal marine ecosystems. Limnol. Oceanogr. **33**: 910–930.

Marañón, E., Cermeno, P., Fernanadez, E., Rodriguez, J., and Zabala, L. 2004. Significance and mechanisms of photosynthetic production of dissolved organic carbon in a coastal eutrophic ecosystem. Limnol. Oceanogr. **49**: 1652–1666.

Marañón, E., Cermeno, P., and Perez, V. 2005. Continuity in the photosynthetic production of dissolved organic carbon from eutrophic to oligotrophic waters. Mar. Ecol. Prog. Ser. **299**: 7–17. doi:10.3354/meps299007.

Nalewajko, C., and Godmaire, H. 1993. Extracellular products of *Myriophyllum spicatum* L. as a function of growth phase and diel cycle. Arch. Hydrobiol. **127**: 345–356.

Nielsen, S.L., and Sand Jensen, K. 1989. Regulation of photosynthetic rates of submerged rooted macrophytes. Oecologia (Berl.), **81**: 364–368.

Otsuki, A., and Wetzel, R.G. 1974. Release of dissolved organic matter by autolysis of a sumerged macrophyte, *Scirpus subterminalis*. Limnol. Oceanogr. **19**: 842–845.

Pace, M.L., and Prairie, Y.T. 2005. Respiration in lakes. *In* Respiration in aquatic ecosystems. *Edited by* P.A. del Giorgio and P.J. le B. Williams. Oxford University Press, Oxford, UK. pp. 103–121.

Pace, M.L., Cole, J.J., Carpenter, S.R., Kitchell, J.F., Hodgson, J.R., Van De Bogert, M.C., Bade, D.L., Kritzberg, E.S., and Bastviken, D. 2004. Whole-lake carbon-13 additions reveal ter-

restrial support of aquatic food webs. Nature (London), **427**(6971): 240–243. doi:10.1038/nature02227. PMID:14724637.

Penhale, P.A., and Smith, W.O. 1977. Excretion of dissolved organic carbon by eelgrass (*Zostera marina*) and its epiphytes. Limnol. Oceanogr. **22**: 400–407.

Prairie, Y.T., Bird, D.F., and Cole, J.J. 2002. The summer metabolic balance in the epilimnion of southeastern Quebec lakes. Limnol. Oceanogr. **47**: 316–321.

Pregnall, A.M. 1983. Release of dissolved organic carbon from estuarine intertidal macroalga *Enteromorpha prolifera*. Mar. Biol. (Berl.), **73**(1): 37–42. doi:10.1007/BF00396283.

Rooney, N., and Kalff, J. 2000. Inter-annual variation in submerged macrophyte community biomass and distribution: the influence of temperature and lake morphometry. Aquat. Bot. **68**(4): 321–335. doi:10.1016/S0304-3770(00)00126-1.

Rooney, N., and Kalff, J. 2003. Submerged macrophyte-bed effects on water-column phosphorus, chlorophyll *a*, and bacterial production. Ecosystems (N.Y., Print), **6**(8): 797–807. doi:10.1007/s10021-003-0184-2.

Schulz, M., and Köhler, J. 2006. A simple model of phosphorus retention evoked by submerged macrophytes in lowland rivers. Hydrobiologia, **563**(1): 521–525. doi:10.1007/s10750-006-0027-1.

Sieburth, J.M. 1969. Studies on algal substances in the sea. III. The production of extracellular organic matter by littoral marine algae. J. Exp. Mar. Biol. Ecol. **3**(3): 290–309. doi:10.1016/0022-0981(69)90052-5.

Vadeboncoeur, Y., Vander Zanden, M.J., and Lodge, D.M. 2002. Putting the lake back together: reintegrating benthic pathways into lake food web models. Bioscience, **52**(1): 44–54. doi:10.1641/0006-3568(2002)052[0044:PTLBTR]2.0.CO;2.

Vadeboncoeur, Y., Jeppesen, E., Vander Zanden, M.J., Schierup, H.H., Christoffersen, K., and Lodge, D.M. 2003. From Greenland to green lakes: cultural eutrophication and the loss of benthic pathways in lakes. Limnol. Oceanogr. **48**: 1408–1418.

Wetzel, R.G., and Manny, B.A. 1972. Secretion of dissolved organic carbon and nitrogen by aquatic macrophytes. Verh. Int. Verein. Limnol. **18**: 162–170.

Wetzel, R.G., and Søndergaard, M. 1998. Role of submerged macrophytes for the microbial community and dynamics of dissolved organic carbon in aquatic ecosystems. *In* The structuring role of aquatic macrophytes in lakes. *Edited by* E. Jeppesen, M. Søndergaard, M. Søndergaard, and K. Christoffersen. Springer, New York. pp. 133–148.

Ziegler, S., and Benner, R. 1999. Dissolved organic carbon cycling in a subtropical seagrass-dominated lagoon. Mar. Ecol. Prog. Ser. **180**: 149–160. doi:10.3354/meps180149.

Mercury biomagnification in the food webs of acidic lakes in Kejimkujik National Park and National Historic Site, Nova Scotia

Brianna Wyn, Karen A. Kidd, Neil M. Burgess, and R. Allen Curry

Abstract: Mercury (Hg) concentrations in fish from acidic lakes (pH < 6.0) are typically elevated above those from near-neutral systems. It is unknown whether high biomagnification rates through the supporting food web can explain elevated Hg concentrations in top predators from low pH lakes. To investigate this, we collected yellow perch (*Perca flavescens*), brown bullhead (*Ameiurus nebulosus*), banded killifish (*Fundulus diaphanous*), golden shiner (*Notemigonus crysoleucas*), and littoral and pelagic invertebrates from four acidic lakes in Kejimkujik National Park and Historic Site (KNPNHS), Nova Scotia, Canada, and analyzed them for total Hg and methyl Hg (MeHg), and $\delta^{13}C$ and $\delta^{15}N$ to determine sources of energy and trophic position, respectively. Mercury biomagnification rates (slopes of log Hg versus $\delta^{15}N$) varied significantly among the four lakes but did not explain the among-lake differences in perch Hg; these slopes were also within the range published for near-neutral systems. Rather, Hg concentrations in yellow perch (i.e., predatory fish) in KNPNHS were higher in lakes with higher MeHg in lower-trophic-level organisms and suggest that processes influencing Hg uptake at the base of the food web are more important than rates of food web biomagnification for understanding the variation in concentrations of this contaminant among top predators.

Résumé : Les concentrations de mercure (Hg) dans les poissons des lacs acides (pH < 6,0) sont typiquement plus élevées que celles des poissons de systèmes près de la neutralité. On ne sait pas si ce sont des taux élevés de bioamplification à travers le réseau alimentaire de support qui peuvent expliquer les concentrations élevées de Hg dans les prédateurs supérieurs des lacs à pH bas. Pour étudier la question, nous avons prélevé des perchaudes (*Perca flavescens*), des barbottes brunes (*Ameiurus nebulosus*), des fondules barrés (*Fundulus diaphanus*), des chattes de l'est (*Notemigonus crysoleucas*), ainsi que des invertébrés littoraux et pélagiques dans quatre lacs acides du parc national et lieu historique national de Kejimkujik (KNPNHS), Nouvelle-Écosse, Canada, et nous avons dosé le Hg total et le méthylmercure (MeHg) et calculé les valeurs de $\delta^{13}C$ et de $\delta^{15}N$ afin de déterminer respectivement les sources d'énergie et la position trophique. Les taux de bioamplification du mercure (pentes de log Hg sur $\delta^{15}N$) varient significativement entre les quatre lacs, mais n'expliquent pas les différences de Hg chez les perchaudes dans ces différents lacs; ces pentes se retrouvent aussi dans la gamme des pentes publiées pour les lacs près de la neutralité. Au contraire, les concentrations de Hg chez les perchaudes (des poissons prédateurs) dans le KNPNHS sont plus fortes dans les lacs qui ont plus de MeHg dans les organismes de niveau trophique inférieur; cela laisse croire que les processus qui influencent l'incorporation de Hg à la base du réseau alimentaire sont plus importants que les taux de bioamplification dans le réseau alimentaire pour expliquer la variation des concentrations de ce contaminant chez les prédateurs de niveau supérieur.

[Traduit par la Rédaction]

Introduction

Mercury (Hg) contamination of freshwater ecosystems became a widespread issue decades ago, yet the variation in Hg concentrations among top predators from different lakes still has not been completely explained (Watras et al. 1998; Kamman et al. 2005). Hg contamination of lakes remains of concern because organic forms of mercury, particularly methyl mercury (MeHg), biomagnify up freshwater food webs to concentrations that can cause sublethal reproductive and behavioural effects in predatory fishes and their consumers (Burgess 2005). Total Hg (THg) concentrations in freshwater fishes vary because of differences in trophic level, growth rates, and habitat use and surface water pH and dissolved organic carbon (DOC) concentrations (Chen et al. 2005; Drysdale et al. 2005; Kamman et al. 2005). It is

Received 14 July 2008. Accepted 28 April 2009. Published on the NRC Research Press Web site at cjfas.nrc.ca on 5 September 2009. J20668

Paper handled by Associate Editor Ralph Smith.

B. Wyn[1] and K.A. Kidd.[2] Canadian Rivers Institute and Department of Biology, University of New Brunswick, Saint John, NB E2L 4L5, Canada.
N.M. Burgess. Canadian Wildlife Service, Environment Canada, Mount Pearl, NL A1N 4T3, Canada.
R.A. Curry. Canadian Rivers Institute, University of New Brunswick, Fredericton, NB E3B 6E1, Canada.

[1]Present address: North/South Consultants Inc., Winnipeg, MB R3Y 1G4, Canada.
[2]Corresponding author (e-mail: kiddk@unbsj.ca).

well understood that concentrations of Hg increase from one trophic level to the next in aquatic food webs, and this has traditionally been examined using biomagnification factors (ratios of Hg in predator to that in prey; e.g., Herrin et al. 1998). Whereas trophic level was traditionally determined using gut contents and based on discrete integer assignments, more studies are using stable isotopes to provide a continuous measure of the dietary habits of organisms and to quantify biomagnification of Hg through food webs (e.g., Kidd et al. 2003; McIntyre and Beauchamp 2007).

The use of stable isotopes to examine trophic transfer of Hg through aquatic food webs shows considerable promise for making broader comparisons of this process across systems (Jardine et al. 2006). Stable isotope ratios of carbon and nitrogen (expressed as $\delta^{13}C$ and $\delta^{15}N$, respectively) measure the use of different energy sources and trophic positioning, respectively, because an animal's isotopic content reflects that of its diet (Deniro and Epstein 1978; Minagawa and Wada 1984; Cabana and Rasmussen 1994). The heavier isotope of C (^{13}C) is only slightly enriched (0.4‰ ± 1.3‰; Deniro and Epstein 1978) between prey and predator, and as a result, an organism's $\delta^{13}C$ signature can be traced back to the base of the food web (Doucett et al. 1996; Vander Zanden and Rasmussen 1999). In contrast, the heavier isotope of nitrogen (^{15}N) increases an average of 3.4‰ with each trophic transfer, providing a means by which relative position within the food web can be determined (Minagawa and Wada 1984). Because both Hg and $\delta^{15}N$ increase from prey to predator, the slope of the relationship between these two variables is being used to quantify Hg biomagnification through food webs (Cabana and Rasmussen 1994; Kidd et al. 1995). Studies that have used $\delta^{15}N$ to quantify Hg biomagnification through food webs have been conducted on near-neutral lakes (pH 7.0–9.0), including a lake in Papua New Guinea (Bowles et al. 2001), Lake Malawi (Kidd et al. 2003), Lake Washington (McIntyre and Beauchamp 2007), Lake Tanganyika (Campbell et al. 2008), and Clear Lake, California (Eagles-Smith et al. 2008), and it was not known whether this approach could be used in acidic systems and, ultimately, for broader geographic comparisons across lakes that differ in their chemical, physical, and biological characteristics.

Herein, we examine whether $\delta^{15}N$ is a significant predictor of Hg concentrations through food webs of acidic lakes, if these relationships are comparable with those observed for near-neutral systems, and whether higher Hg concentrations in fishes from acidic lakes (Watras et al. 1998; Kamman et al. 2005) may be explained, in part, by greater trophic transfer of this contaminant. Kejimkujik National Park and National Historic Site (KNPNHS), Nova Scotia, Canada, was chosen as the study site because all the lakes are acidic and it is characterized as a "hotspot" because of the high Hg in top predators (O'Driscoll et al. 2005; Evers et al. 2007). We collected yellow perch (*Perca flavescens*), brown bullhead (*Ameiurus nebulosus*), banded killifish (*Fundulus diaphanous*), golden shiner (*Notemigonus crysoleucas*), littoral and profundal invertebrates, and bulk zooplankton from four acidic lakes to characterize the food web structure (using $\delta^{13}C$ and $\delta^{15}N$) in these systems and Hg concentrations in the organisms. One objective was to examine factors affecting Hg in predatory fish (i.e., yellow perch) from acidic lakes, including carbon source, trophic level, biomagnification rates (using Hg versus $\delta^{15}N$), and concentrations of MeHg in lower-trophic-level organisms. The second objective was to compare the rates of Hg biomagnification (i.e., slope of Hg versus $\delta^{15}N$) in these four lakes with those in the literature for near-neutral systems to determine whether elevated Hg concentrations in top predators from acidic systems may be caused by enhanced biomagnification of Hg through these food webs.

Materials and methods

Study site

KNPNHS is in southwestern Nova Scotia, Canada (Fig. 1), and is not impacted by local industrial developments or other point sources of pollutants (O'Driscoll et al. 2005). The park is downwind of major North American urban and industrial centres (e.g., New York, Chicago, and southern Ontario and Quebec), and Hg and acidifying substances originating from these areas are transported to and deposited in the region (Drysdale et al. 2005; Temme et al. 2007). Despite these influxes, atmospheric concentrations of Hg in the park are lower than those reported for other rural and urban sites in North America (Temme et al. 2007). Logging and tourism are the main industries for this part of the province, but no development is permitted within park boundaries.

The four study lakes are all small, oligotrophic, acidic, and polymictic (Table 1). Water chemistry data are from routine monitoring performed by Environment Canada in the spring and fall of each year during lake turnover. Surface water samples were collected from the middle of each lake by helicopter and kept on ice until they were returned to the lab for processing using the techniques described in Vaiyda et al. (2000). Lakes in KNPNHS are naturally acidic (mean pH 5.8, range 5.4–6.2) and have moderate total organic carbon (TOC) because of the low buffering capacity of the soils and abundance of bogs and fens (which export organic acids) in the watersheds (Ginn et al. 2007). Additionally, like lakes in many other regions, they have also acidified (mean decrease of 0.31–0.38 pH units) due to the deposition of industrially derived sulphate (Clair et al. 2007; Ginn et al. 2007). No improvements in chemical characteristics of the lakes have been recorded over the last ~25 years (Whitfield et al. 2006).

Sample collection

Pelagic, profundal, and littoral invertebrates were sampled from the four lakes (Beaverskin, North Cranberry, Pebbleloggitch, and Puzzle) in May, July, and August 2006 with Wisconsin nets (153 µm mesh), Ekman dredges (6" × 6"), and sweep nets (750 µm mesh), respectively. Zooplankton (n = 3 per lake per date) and profundal samples were collected from the deepest site in each lake. Samples were collected on several dates because isotopic signatures and Hg concentrations are known to be more variable over time for short-lived organisms compared with long-lived biota (Cabana and Rasmussen 1996; Herrin et al. 1998). These are shallow lakes (mean depths of 1.4–2.7 m; Table 1) with littoral zones (<2 m depth) extending ~50 m offshore. On each sampling date, littoral samples were collected from the surface sediments and cobbles at one or two sites per lake, with each site encompassing ~200–400 m of shoreline. Im-

Fig. 1. Four study lakes in Kejimkujik National Park and National Historic Site, Nova Scotia, Canada. Inset shows location in Eastern Canada.

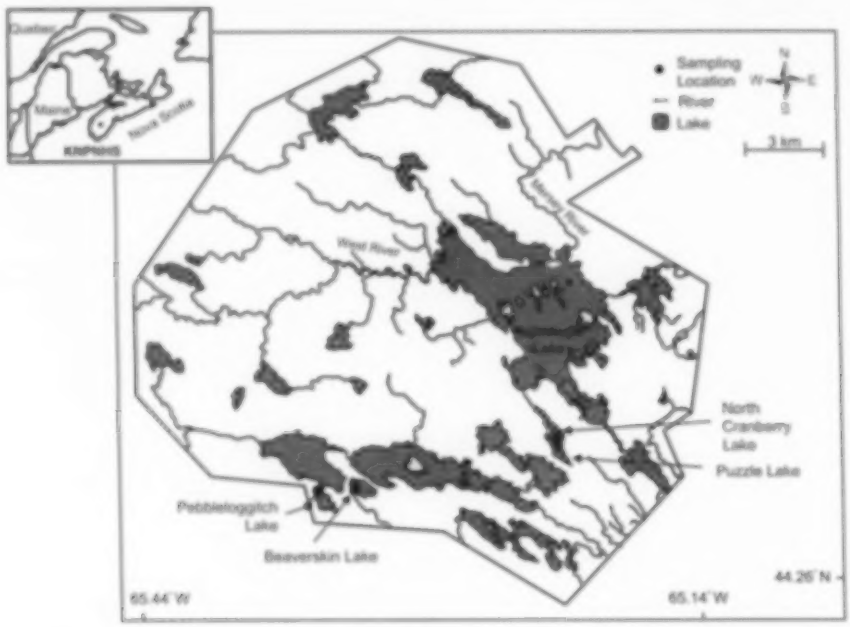

Table 1. Mean physical and chemical[a] (2000–2007) characteristics of Beaverskin, North Cranberry, Pebbleloggitch, and Puzzle lakes in Kejimkujik National Park and National Historic Site (Kerekes and Schwinghamer 1973; Tom Clair, Environment Canada, Atlantic Region, P.O. Box 6227, Sackville, NB E4L 1G6, Canada, unpublished data).

Parameter	Units	Beaverskin	North Cranberry	Pebbleloggitch	Puzzle
Latitude	°N	65.33	65.23	65.35	65.23
Longitude	°W	44.31	44.33	44.30	44.33
Surface area	ha	41.8	34.4	33.4	33.7
Maximum depth	m	6.25	5	2.5	6.1
Mean depth	m	2.19	1.45	1.42	2.7
Volume	10^3 m^3	864	498	474	911
Drainage basin area	km^2	4.8	4.6	2	4.6
Wetland	%	0	21.3	17.6	35.3
Flushing rate	year^{-1}	0.98	6.12	2.87	1.95
pH		5.5±0.03	4.88/5.41	4.5±0.02	5.48/5.68
TOC	mg·L^{-1}	2.4±0.13	4.4/5.9	10.5±1.23	3.0/3.5
Total P	μg·L^{-1}	6±<1	8/9	15±1	6/7

[a]Water chemistry at Beaverskin and Pebbleloggitch lakes was measured semi-annually (spring and fall 2000–2007, n = 15). North Cranberry and Puzzle lakes were sampled in fall 2006 and spring 2007 (n = 2). Values are given as mean ± standard error, SE, for Beaverskin and Pebbleloggitch lakes and fall 2006/spring 2007 for North Cranberry and Puzzle lakes.

mediately after collection, invertebrates were live-sorted to major taxa (except zooplankton), pooled across sites, and frozen in Whirlpacs™.

Fishes were collected from each lake in August and September 2006 using a fyke net set overnight in the littoral zone of each lake. Nets were set in a low slope area near macrophyte beds, if present. Fish species composition was known for each lake (Chris McCarthy, Parks Canada, Mainland Nova Scotia Field Unit, Kejimkujik National Park and National Historic Site of Canada, P.O. Box 236, Maitland Bridge, NS B0T 1B0, unpublished data). We netted >400 fish per lake and captured all known species. A subset of individuals was randomly chosen for analysis. These fishes included nine yellow perch from each of three size classes (5–10 cm, 10–15 cm, and 15–23 cm), 15 golden shiner, 15 banded killifish, and 10 brown bullhead (when present). All fish handling procedures were approved by the Animal Care Committee at the University of New Brunswick (UNB). Weight (±0.01 g) and length (±1 mm; fork length for yellow perch and golden shiner; total length for banded killifish and brown bullhead) were measured for each fish, and scales were obtained from yellow perch for ageing. Fish condition

was calculated as 100 × weight (g)/length (cm)^3. After sampling, fish were euthanized and frozen in individual Whirlpac™ or Ziploc™ bags.

In the laboratory, macroinvertebrate samples were thawed and identified to the lowest possible taxa using Merritt and Cummins (1996), Thorp and Covich (2001), and Needham and Westfall (1955) and removed from their cases when present. Teflon Petri dishes and stainless-steel forceps were soaked in a 5% HCl bath between samples. Zooplankton were not sorted to the major taxa because preliminary analyses showed that they did not compose a major portion of fish diets (see Results). Composite macroinvertebrate samples (each ≥ three individuals per date for total n = 2–3 per taxa; Table 2), bulk zooplankton (n = 3 per date for stable isotope analysis; pooled to n = 1 per date for MeHg), skinless dorsal muscle from individual fish (for stable isotopes), and whole bodies of fish (for THg analyses of all species except brown bullhead) were freeze-dried and then homogenized. Stainless-steel and glass tools used during dissection and homogenization were washed with soapy water and rinsed with excess amounts of distilled water to minimize cross contamination. Fish tissues were weighed before and after freeze-drying to obtain moisture content.

Stable isotope analyses

Preparation and analysis of composite invertebrate samples and individual fish muscle for stable isotopes analyses were performed according to the methods described by Jardine et al. (2005); the exception was that the current samples were prepared by freeze-drying rather than oven-drying. Laboratory isotopic standards were sucrose (International Atomic Energy Agency (IAEA); $\delta^{13}C$ = –10.4‰) and ammonium sulfate (IAEA; $\delta^{15}N$ = 20.3‰) and had an absolute deviation from the accepted values of less than 0.1‰ (n = 10 per standard). Replicate analysis of every 10th sample revealed that precision for both $\delta^{13}C$ and $\delta^{15}N$ was within 0.1‰ (one standard deviation, SD; n = 51). Gut contents of the fishes were not analysed (i.e., to verify the stable isotope analyses) because previous studies have shown that $\delta^{13}C$ and $\delta^{15}N$ ratios in tissues are more accurate representations of the long-term feeding habits of individuals, whereas gut content analyses represent a snapshot of recently ingested items (Vander Zanden et al. 1997; Clarke et al. 2005).

Mercury analyses

Subsamples of whole-body homogenates of fish were analyzed for THg using atomic absorption spectrometry on a Milestone DMA-80 Direct Mercury Analyzer at UNB, Fredericton. Whole fish were analysed instead of fillets because of ongoing concerns about the effects of Hg on the health of the common loon, a main predator of yellow perch, in KNPNHS. However, THg concentrations in fillets are significantly related to those in whole-body samples ($THg_{whole\ body} = 0.6THg_{fillet}$, r^2 = 0.902, $p < 0.001$, n = 21; B. Wyn, unpublished data). For quality assurance, samples from whole bodies of 31 yellow perch and 19 golden shiner were also analyzed by National Wildlife Research Centre (NWRC) of Environment Canada using atomic absorption spectrometry. Recoveries of standard reference materials (SRM) were 94.6% ± 2.0% (range 90.3% – 101.2%, n = 60) for DORM-2 (dogfish muscle, National Research Council of Canada, NRCC) at UNB and 111.3% ± 7.0% (range unavailable, n = 8) for DOLT-3 (dogfish liver, NRCC) and Oyster Tissue 1566 b (National Institute of Standards and Technology) at NWRC. Precision of the laboratory working standard (yellow perch) at UNB was 11.8% (n = 16). Triplicate samples had precision within 13.5% (n = 85) at UNB and within 5.9% (n = 10) at NWRC. Blanks were never more than 1.6% of sample values; therefore the values presented herein were not corrected for the blanks. Of the samples analysed at both labs, yellow perch THg results were highly correlated between labs (slope = 0.95, r^2 = 0.95, $p < 0.001$, n = 31), whereas golden shiner THg had a weaker correlation (NWRC > UNB, slope = 0.82, r^2 = 0.59, p = 0.02, n = 19). Only data from UNB were used in the subsequent analyses, and all are presented as SRM-corrected dry weight (dw) concentrations unless otherwise stated.

MeHg analyses of fish and invertebrate samples were performed at three laboratories: NWRC, Flett Research Ltd. (Winnipeg, Manitoba), and the University of Ottawa (U Ottawa). Thirty-one yellow perch and 19 golden shiner representing a range of THg concentrations were sent to NWRC for MeHg analysis using atomic absorption spectrometry (method MET-CHEM-AA-04E; National Wildlife Research Centre (NWRC) 2007). Low mass invertebrate samples (<30 mg, n = 20) were analysed by fluorescence following EPA method 1630 at Flett Research Ltd. All other invertebrate samples (mass > 30 mg, n = 50) were extracted at UNB and then analysed for MeHg content at U Ottawa via atomic fluorescence spectrometry using the methods in Cai et al. (1997). SRM recoveries were 94.3% ± 5.7% (DORM-2 and DOLT-3, n = 9) at NWRC. Within-run DORM-2 recoveries were 88.2% and 94.6% (n = 2 each) at Flett Research Ltd., and 106.9% ± 10.9% and 97.8% ± 5.5% (n = 6 each) at U Ottawa. Precision of samples was within 15.3% (n = 8) at NWRC, 7.3% (n = 10) at Flett Research Ltd., and 15.6% (n = 29) at U Ottawa. All MeHg data are presented as SRM-corrected dry weight (dw) concentrations unless otherwise stated.

Data transformations

Because these fish relied mainly on littoral carbon sources (see Results), a littoral primary consumer (caddisfly, Family Limnephilidae) common to all lakes was chosen to standardize the $\delta^{15}N$ of the other food web organisms. Limnephilidae in Puzzle Lake had significantly (analysis of variance, ANOVA, $p < 0.04$) higher $\delta^{15}N$ ratios than those in the other lakes (Table 2); therefore, trophic position (TP) of the fishes was calculated using the approach of Cabana and Rasmussen (1996):

$$(\delta^{15}N_{sample} - \delta^{15}N_{limnephilid})/3.4 + 2$$

The C–N ratios (C:N; a surrogate of lipid content) were significantly (ANOVA, $p < 0.05$) different among the species within each lake; therefore, $\delta^{13}C$ data were corrected for lipid content using

$$\delta^{13}C_{lipid} = 3.32 + 0.99 \times C:N$$

(Post et al. 2007). The IsoError mixing model (Phillips and Gregg 2001) was then used to estimate the proportion of lit-

Table 2. Mean (± standard deviation, SD) MeHg, $\delta^{13}C$, lipid-corrected $\delta^{13}C$, $\delta^{15}N$, and trophic position of select invertebrates collected in 2006 from Beaverskin, North Cranberry, Pebbleloggitch, and Puzzle lakes in Kejimkujik National Park and National Historic Site.

Invertebrates	*n*	MeHg (μg·g^{-1} dw)	*n*	$\delta^{13}C$ (‰)	$\delta^{13}C_{lipid}$ (‰)	$\delta^{15}N$ (‰)	Trophic position
Beaverskin							
Limnephilidae	3	0.03±0.01	3	−29.40±1.22	−26.55±1.27	1.00±0.35	2.00±0.10
Heptageniidae	1	0.07	2	−27.94	−26.82	1.47	2.14
Chironomidae – littoral	3	0.07±0.02	3	−26.96±2.02	−25.77±2.10	2.73±0.34	2.51±0.10
Aeshna umbrosa	3	0.25±0.05	3	−27.88±0.67	−26.99±0.95	3.88±0.40	2.85±0.12
Zooplankton	2	0.11	9	−32.51±1.09	−30.89	4.39	3.00
Amphipoda	3	0.14±0.06	3	−27.27±0.46	−26.21±0.42	4.41±0.87	3.01±0.26
Chironomidae – profundal		—	3	−30.12±1.04	−28.95±1.39	4.46±0.57	3.02±0.17
North Cranberry							
Limnephilidae	3	0.09±0.02	3	−31.64±1.48	−28.55±1.47	1.45±0.43	2.00±0.13
Amphipoda	3	0.17±0.05	3	−29.14±0.37	−27.74±0.40	1.91±0.27	2.13±0.09
Chironomidae – profundal		—	3	−39.53±1.01	−38.45±0.97	2.11±1.83	2.19±0.54
Heptageniidae	3	0.18±0.08	3	−28.54±0.25	−27.69±0.31	2.26±0.78	2.24±0.23
Chironomidae – littoral	3	0.19±0.04	3	−30.23±0.76	−29.10±0.79	3.51±0.51	2.61±0.15
Aeshna umbrosa	3	0.44±0.17	3	−29.43±1.74	−28.74±1.92	4.32±0.12	2.84±0.04
Zooplankton	3	0.23±0.12	9	−35.20±1.53	−34.08±1.45	4.51±0.90	2.90±0.27
Pebbleloggitch							
Limnephilidae	3	0.05±0.02	3	−31.13±1.26	−27.63±0.78	0.82±0.11	2.00±0.03
Heptageniidae	3	0.07±0.03	3	−29.36±0.15	−28.23±0.63	1.10±0.51	2.08±0.15
Amphipoda	3	0.09±0.04	3	−29.39±1.74	−28.09±1.71	2.46±1.09	2.48±0.32
Chironomidae – littoral	3	0.08±0.02	3	−29.30±0.64	−28.20±0.58	2.66±0.39	2.54±0.11
Zooplankton	3	0.09±0.04	9	−35.81±1.43	−34.78±1.39	3.10±0.97	2.67±0.29
Aeshna umbrosa	3	0.17±0.03	3	−28.79±0.56	−28.01±0.29	3.27±0.53	2.72±0.15
Chironomidae – profundal		—	3	−35.02±1.69	−33.92±1.49	4.78±0.18	3.16±0.05
Puzzle							
Heptageniidae	2	0.11	3	−28.94±0.85	−28.63	1.79	1.86
Limnephilidae	3	0.15±0.07	3	−31.59±0.77	−28.65±0.62	2.27±0.20	2.00±0.56
Chironomidae – littoral	3	0.14±0.04	3	−32.26±1.18	−31.19±1.27	3.27±0.38	2.29±0.11
Amphipoda	3	0.18±0.03	3	−29.15±0.43	−27.92±0.22	4.05±0.66	2.52±0.19
Aeshna umbrosa	3	0.35±0.03	3	−30.79±1.91	−29.99±1.66	4.28±0.25	2.59±0.08
Zooplankton	3	0.16±0.07	9	−34.69±1.82	−33.60±1.67	4.31±0.58	2.60±0.17
Chironomidae – profundal		—	2	−34.99±1.45	−33.98±1.47	5.30±0.63	2.89±0.18

Note: Invertebrates are arranged from lowest to highest trophic position (TP) within each lake. dw, dry weight; —, not measured.

toral carbon in fish diets using the seasonal mean $\delta^{13}C_{lipid}$ of all littoral invertebrates and mean $\delta^{13}C_{lipid}$ of zooplankton as the littoral and pelagic end-members, respectively. Diet–tissue fractionation of $\delta^{13}C$ was considered to be negligible for this model.

We evaluated different methods of calculating Hg biomagnification rates within lakes prior to comparing the results among lakes. Two types of Hg data (THg_{fish} or $MeHg_{fish}$ either as dw or wet weight (ww)) were contrasted to examine their impact on Hg biomagnification rates (slope of log Hg versus $\delta^{15}N$ regression; Kidd et al. 1995). THg_{fish} concentrations were measured directly, whereas the $MeHg_{fish}$ concentrations were calculated using the within-species and within-lake MeHg–THg ratios (MeHg:THg) of yellow perch and golden shiner. Banded killifish were assumed to have the same percent MeHg as golden shiner. Percent moisture was determined for individual fish; wet weight concentrations of MeHg in invertebrates were calculated assuming 80% water content (Hall et al. 1998).

Data analysis

Prior to any statistical analyses, data were inspected for normality and homoscedasticity using Kolmogorov–Smirnov's test and *F* ratio, respectively. Fish lengths and weights and all Hg data were $\log_{10}$-transformed to approximate the normal distribution. Studentized residuals were examined to identify outlying data points, and outliers were removed when residuals exceeded an absolute value of 3.0.

Within each lake, log THg concentrations of each fish species were regressed against their log(length) or log(weight), condition, age (yellow perch only), or $\delta^{15}N$. In addition, backward stepwise linear regressions, removing parameters with $p > 0.05$, were used to determine the statistical importance of log(length), age, TP, and $\delta^{13}C$ in determining THg concentrations in yellow perch. To determine the factors influencing differences in perch THg among lakes, mean THg in this species were regressed (simple generalized linear model, GLM) against the biomagnification rates (slope of log Hg versus $\delta^{15}N$), MeHg at the base of the food webs (intercept of log Hg versus $\delta^{15}N$), mean MeHg in each invertebrate taxa, mean perch lengths, mean weights, mean $\delta^{13}C$, mean TP, or length-at-age (slope of log(length) versus age) or the mean physical or chemical characteristics listed for these lakes (Table 1).

Across lakes, differences in condition of each fish species or length-at-age of perch were evaluated using the intercepts of analysis of covariance (ANCOVA; log(length) as the dependent variable and log(weight) or age as the covariate). Log(lengths), log(weights), and TP of fishes, ages of perch, and log Hg of all organisms were compared among the lakes using ANOVA and Tukey's multiple comparison tests for each species. Among-lake comparisons of THg concentrations in fishes could not be done using ANCOVA (with length, weight, or age as a covariate) because THg was not significantly related to any of these parameters (GLM, $p > 0.12$) for banded killifish and golden shiner in any lake or yellow perch in Beaverskin Lake.

Linear regression analyses were used to determine the relationship between log Hg and $\delta^{15}N$ for each food web. Regression slopes (i.e., food web biomagnification rates) were compared among lakes and for dry versus wet weight or THg_{fish} versus $MeHg_{fish}$ within lakes using ANCOVA with log Hg as the dependent variable and $\delta^{15}N$ as the covariate. Alpha was adjusted to 0.008 using the Bonferroni correction for multiple pairwise analyses. When the slopes were not significantly different across lakes, the intercepts were compared using a Tukey's multiple comparison test. All analyses were performed on SYSTAT 10 for Windows (Systat Software Inc., Chicago, Illinois) with $\alpha = 0.05$, unless otherwise indicated. All results are presented as mean ± standard deviation (SD) unless stated otherwise.

Results

Food web structure

The $\delta^{13}C$ analyses revealed that all four food webs in KNPNHS were similar with respect to the relative importance of benthic versus pelagic carbon sources for consumers (Fig. 2). In each lake, zooplankton and profundal chironomids were consistently depleted in $\delta^{13}C$ when compared with the littoral macroinvertebrates, mean $\delta^{13}C$ of fishes were similar to the $\delta^{13}C$ of littoral invertebrates, and golden shiner and 5–10 cm yellow perch typically had the most depleted $\delta^{13}C$ of any of the fishes (Fig. 2; Tables 2 and 3). Across lakes, mean use of littoral carbon ranged from 46.8% ± 9.8% to 100% for golden shiner, 68.7% ± 4.6% to 100% for brown bullhead, 84.7% ± 6.6% to 100% for banded killfish, and 85.2% ± 4.8% to 100% for yellow perch (Table 3).

In all four lakes in this study, $\delta^{15}N$ was lowest in collector–gatherers (Limnephilidae and Heptageniidae), moderate in predaceous macroinvertebrates (Aeshnidae), and highest in fishes (Fig. 2). Limnephilids and heptagenids typically had the lowest mean $\delta^{15}N$, suggesting that that these invertebrates were primary consumers (Fig. 2; Table 2). The predaceous dragonfly nymph, *Aeshna umbrosa*, had $\delta^{15}N$ between 2‰ and 3‰ higher than the limnephilids, whereas the littoral chironomids and amphipods typically had mean $\delta^{15}N$ that fell between the values measured for the limnephilids and aeshnids (Fig. 2; Table 2). $\delta^{15}N$ of profundal chironomids and zooplankton were generally similar to those of the most trophically elevated littoral invertebrates, with the exception of profundal chironomids in North Cranberry Lake, where the $\delta^{15}N$ of this taxon spanned the range of ratios measured for all littoral invertebrates (Fig. 2). All fish in these lakes had $\delta^{15}N$ values that were 3‰–6‰ higher than any littoral invertebrate, indicating that these fishes were insectivorous on predatory invertebrates such as *Aeshna umbrosa* or that they fed on a combination of invertebrates and fish (i.e., forage fishes or juveniles). Within lakes, fish species were all at a similar TP (means within 0.21). Across lakes within species, mean TP was lowest in Puzzle Lake (by up to 0.5 TP), moderate in Pebbleloggitch Lake, and highest across the other two lakes (Table 3; Fig. 2). Trophic positions of the large yellow perch were typically between 0.03 and 0.31 levels higher than those of the smaller individuals (Fig. 2).

Hg concentrations and influential factors

MeHg concentrations in the macroinvertebrates were significantly different across lakes and were higher in those taxa occupying a higher trophic level. Of the invertebrate taxa analyzed, concentrations of MeHg were lowest in the primary consumer limnephilids and highest, between three- and eight-fold higher, in predatory aeshnids from the same lake (Table 2). Mean MeHg of limnephilids, chironomids, or aeshnids were significantly higher in Puzzle and North Cranberry lakes than in Pebbleloggitch and Beaverskin lakes (ANOVA, $p < 0.03$). There were no differences among lakes for each of the other invertebrate taxa ($p > 0.19$).

Mean THg, size, and trophic position of the fishes were significantly different among the four lakes. Mean THg concentrations in golden shiner, banded killifish, and yellow perch from North Cranberry Lake were, with one exception, significantly (50%–135%; ANOVA, $p < 0.03$) higher than those measured in the respective species from the other lakes (Table 4). The exception was that mean THg in banded killifish from Beaverskin Lake was not significantly ($p = 0.86$) different from the mean concentration in the same species from North Cranberry Lake (Table 4). Golden shiner and banded killifish from North Cranberry Lake were significantly ($p < 0.012$) shorter (8%–18%) than those from Beaverskin and Puzzle lakes (Table 4). There were no significant (ANOVA, $p > 0.86$) differences in length or weight of yellow perch collected in the different lakes, but length-at-age was significantly (ANCOVA intercept, $p < 0.004$) higher in perch from Beaverskin and Pebbleloggitch lakes compared with those from Puzzle and North Cranberry lakes. Perch were older, though not significantly ($p = 0.19$), in North Cranberry and Puzzle lakes (5.6 ± 2.5 years and 5.3 ± 2.4 years, respectively) compared with Beaverskin and Pebbleloggitch lakes (4.6 ± 2.2 years and 4.5 ± 1.6 years, respectively). For all species, fish from North Cranberry and Beaverskin lakes were trophically elevated (using TP) above those from Puzzle Lake (ANOVA, $p < 0.02$), and yellow perch from Pebbleloggitch Lake had significantly ($p < 0.001$) lower TP than those in North Cranberry and Beaverskin lakes, but higher TP than the same species from Puzzle Lake ($p < 0.001$). With the exception of golden shiner in Beaverskin Lake (47% littoral carbon in their diets), all other species collected in these lakes obtained the majority of their carbon from the littoral zone (Table 3).

The predictors of THg in fish were different for each species and each lake (Table 5). Within each lake, $\delta^{15}N$ was generally the best predictor of THg as it significantly (GLM, $p < 0.046$) predicted 16%–83% of THg in both the

Fig. 2. Mean (± standard deviation, SD) $\delta^{15}N$ and $\delta^{13}C$ (‰) of fish and pelagic, profundal, and littoral invertebrates from (*a*) Beaverskin, (*b*) North Cranberry, (*c*) Pebbleloggitch, and (*d*) Puzzle lakes, 2006. Abbreviations: au, Aeshnidae; am, Amphipoda, c-p, profundal chironomids; c-l, littoral chironomids; hp, Heptageniidae; ld, Limnephilidae; lp, Lepidoptera; z, pelagic zooplankton; yp, yellow perch (*Perca flavescens*); gs, golden shiner (*Notemigonus crysoleucas*); bb, brown bullhead (*Ameiurus nebulosus*). Yellow perch are from three different size classes: yp1, 5–10 cm; yp2, 10–15 cm; yp3, 15–23 cm.

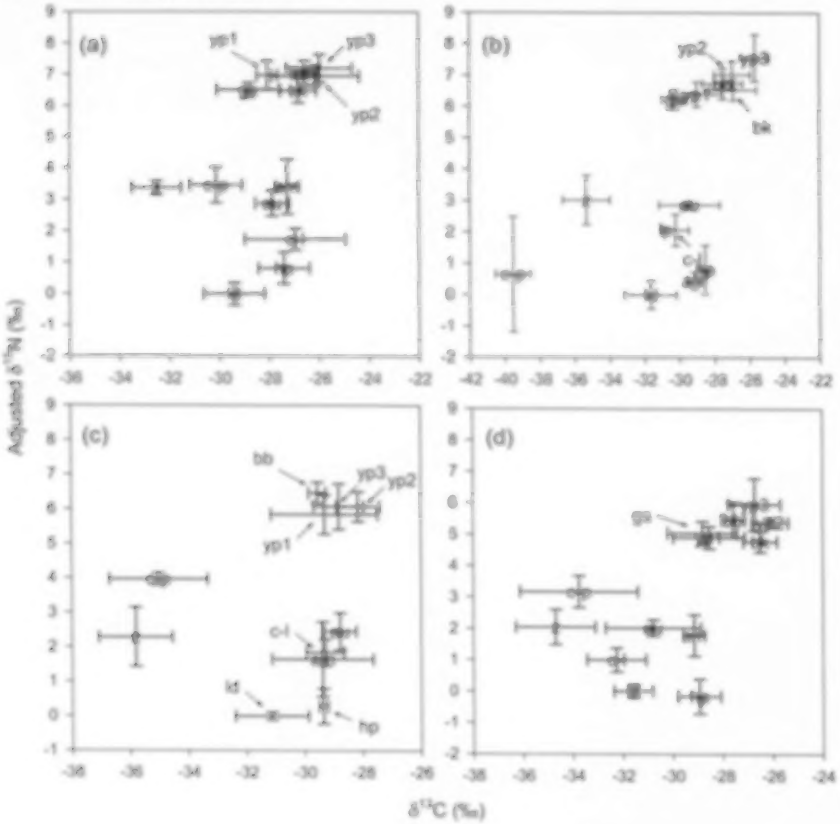

banded killifish and yellow perch from every lake (Table 5). For the golden shiner, the only significant ($p < 0.03$, $r^2 > 0.90$) predictors of THg were log(length) and log(weight), and these relationships were only significant in Beaverskin Lake (Table 5). Significant and positive relationships between $\delta^{15}N$ and length were also observed for yellow perch in North Cranberry ($p < 0.001$, $r^2 = 0.56$) and Puzzle ($p < 0.001$, $r^2 = 0.48$) lakes but not for those in Beaverskin ($p = 0.25$, $r^2 = 0.05$) or Pebbleloggitch ($p = 0.21$, $r^2 = 0.06$) lakes. Trophic position of perch was also significantly ($p < 0.001$, $r^2 > 0.38$) predicted by length or age in North Cranberry and Puzzle lakes. When stepwise regression was used with log(length), age, $\delta^{13}C$, and TP as factors, log THg in perch was significantly predicted by length and age ($p = 0.01$, $r^2 = 0.30$) in Beaverskin Lake, length only in North Cranberry and Puzzle lakes ($p < 0.001$ and $r^2 = 0.46$ and $p < 0.001$ and $r^2 = 0.81$, respectively), and length and TP in Pebbleloggitch Lake ($p = 0.005$, $r^2 = 0.34$).

Biomagnification of Hg through food webs

Within each lake, the food web biomagnification of Hg was similar regardless of the data used in the regression between Hg and $\delta^{15}N$. The slopes of the log Hg versus $\delta^{15}N$ regressions were not significantly (ANCOVA interaction, $p > 0.62$) different within lakes when either dry or wet weight Hg data were considered and when either THg or MeHg data were used for fish (Table 6). The intercepts of $MeHg_{invertebrate}$–THg_{fish} and $MeHg_{invertebrate}$–$MeHg_{fish}$ were not significantly (ANCOVA, $p > 0.22$) different within lakes for either the dry or wet weight data, but the intercepts for the regressions using wet weight Hg data were significantly ($p < 0.001$) lower than those of the dry weight data (Table 6).

Food web biomagnification rates of Hg and MeHg concentrations at the base of the food web (intercept) were significantly different among the lakes in KNPNHS. The slopes of log Hg versus $\delta^{15}N$ were 0.19, 0.20, 0.21, and 0.23 in North Cranberry, Puzzle, Pebbleloggitch, and Beaverskin lakes, respectively, and varied significantly (ANCOVA interaction, $p = 0.01$) among the systems (Fig. 3; Table 6). Pairwise comparisons using $MeHg_{invertebrate}$–THg_{fish} (dw) versus $\delta^{15}N$ showed that the regression slope was significantly (ANCOVA interaction, $p = 0.001$, Bonferroni corrected $\alpha = 0.008$) lower in the North Cranberry Lake food web than in the Beaverskin Lake food web, but that other

Table 3. Mean (± standard deviation, SD) $\delta^{13}C$, lipid-corrected $\delta^{13}C$, proportion of C derived from littoral sources, $\delta^{15}N$, and trophic positions of golden shiner (*Notemigonus crysoleucas*), banded killifish (*Fundulus diaphanous*), yellow perch (*Perca flavescens*), and brown bullhead (*Ameirurus nebulosus*) in Beaverskin, North Cranberry, Pebbleloggitch, and Puzzle lakes, Kejimkujik National Park and National Historic Site.

	n	$\delta^{13}C$	$\delta^{13}C_{lipid}$ (‰)	Proportion littoral C (%)	$\delta^{15}N$ (‰)	Trophic position
Beaverskin						
Golden shiner	15	−28.83±1.26	−29.07±1.25	46.79±9.80	7.50±0.23	3.91±0.07 a
Banded killifish	15	−26.82±0.73	−27.07±0.72	84.74±6.56	7.48±0.39	3.91±0.11 a
Yellow perch	27	−26.74±1.55	−27.10±1.54	85.54±8.05	8.00±0.36	4.06±0.10 a
Brown bullhead	10	−26.50±0.60	−26.77±0.62	92.17±6.88	7.96±0.31	4.05±0.09
North Cranberry						
Golden shiner	15	−30.26±0.71	−30.56±0.70	61.97±7.12	7.68±0.30	3.83±0.09 a
Banded killifish	15	−26.92±1.33	−27.15±1.30	122.01±9.00	7.99±0.33	3.92±0.10 a
Yellow perch	27	−27.23±1.75	−27.42±1.69	117.25±8.49	8.40±0.62	4.04±0.18 a
Brown bullhead	10	−27.55±1.14	−27.91±1.14	108.63±8.35	8.14±0.36	3.97±0.11
Pebbleloggitch						
Golden shiner	2	−28.47 / −28.14	−28.65 / −28.33	87.0 / 92.4	6.23 / 6.62	3.59 / 3.71
Banded killifish	0					
Yellow perch	28	−28.77±1.27	−29.03±1.26	85.19±4.76	6.84±0.56	3.77±0.17 b
Brown bullhead	10	−29.85±0.30	−30.14±0.36	68.74±4.62	6.88±0.29	3.78±0.08
Puzzle						
Golden shiner	15	−28.80±1.39	−29.11±1.39	102.05±12.30	7.31±0.37	3.48±0.11 b
Banded killifish	15	−26.49±0.67	−26.80±0.66	154.54±18.80	7.04±0.34	3.40±0.10 b
Yellow perch	26	−27.15±1.52	−27.48±1.50	139.09±16.57	7.60±0.51	3.57±0.15 c
Brown bullhead	10	−27.62±0.42	−27.96±0.41	128.18±13.46	7.64±0.50	3.58±0.15

Note: Different letters following trophic position values represent significant differences within a species among lakes. Golden shiner values for Pebbleloggitch are minimums/maximums because $n = 2$.

among-lake comparisons were not significantly different ($p > 0.02$; Table 6). Differences in the intercept of the regression were evaluated only among lakes with similar slopes. The Hg concentrations at the base of the food webs (i.e., $MeHg_{invertebrate}$–THg_{fish} (dw) versus $\delta^{15}N$ ANCOVA intercept) were significantly (Tukey's test; $p < 0.005$) different, with North Cranberry Lake > Puzzle Lake > Pebbleloggitch Lake (Table 6). MeHg at the base of the Beaverskin Lake food web was significantly ($p = 0.001$) lower than that for Puzzle and Pebbleloggitch lakes (Table 6).

Hg biomagnification rates can also be calculated as the slope of the log Hg versus TP regression to examine an average trophic transfer (per 3.4‰ $\delta^{15}N$) rather than as increases per unit $\delta^{15}N$. Relative slopes and intercepts derived from log Hg versus TP were similar to those of the log Hg versus $\delta^{15}N$ relationships. Regressions of dry weight $MeHg_{invertebrate}$–THg_{fish} versus TP in each lake were

$$\text{Beaverskin: } Hg = 0.79 \pm 0.03(TP) - 3.06 \pm 0.12,\ p < 0.001,\ r^2 = 0.92$$
$$\text{North Cranberry: } Hg = 0.64 \pm 0.03(TP) - 2.29 \pm 0.11,\ p < 0.001,\ r^2 = 0.90$$
$$\text{Pebbleloggitch: } Hg = 0.72 \pm 0.04(TP) - 2.77 \pm 0.12,\ p < 0.001,\ r^2 = 0.89$$
$$\text{Puzzle: } Hg = 0.69 \pm 0.03(TP) - 2.34 \pm 0.10,\ p < 0.001,\ r^2 = 0.91$$

The variability in THg concentrations in top predators (i.e., yellow perch) among the four lakes in KNPNHS was significantly related to only a few biological or physical parameters. Across lakes, mean THg concentrations in yellow perch were negatively related to the slope of log $MeHg_{invertebrate}$–THg_{fish} (dw) versus $\delta^{15}N$ (GLM, $p = 0.03$, $r^2 = 0.997$) and positively related to mean MeHg in aeshnids (GLM, $p = 0.03$, $r^2 = 0.998$); no relationship was found between mean THg in perch and the intercepts of log Hg versus $\delta^{15}N$ (GLM, $p = 0.08$). Mean THg in yellow perch was also marginally significantly (simple GLM, mean THg = 7.46 ± 0.48 – 95.06 ± 7.74 (length-at-age), $p = 0.051$, $r^2 = 0.993$) negatively related to length-at-age (slope of log(length) versus age regression) of fish and positively related to flushing rate of the lake ($p = 0.03$) but not to other biological, physical, or chemical characteristics in Tables 1, 3, or 4 (simple GLM, $p > 0.09$).

Discussion

Food web structure and the dietary habits of fishes were similar across the four acidic lakes in KNPNHS, with more reliance on nearshore than offshore carbon. The trophic position of the fishes and invertebrates (determined using $\delta^{15}N$) was a significant predictor of their MeHg or THg concentrations within each lake, and the slopes of the log Hg versus $\delta^{15}N$ relationships were comparable in three of the four lakes. Within the lakes, log THg concentrations were higher

Table 4. Mean (± standard deviation, SD) length, weight, condition, THg, and percent MeHg of golden shiner (*Notemigonus crysoleucas*), banded killifish (*Fundulus diaphanous*), yellow perch (*Perca flavescens*), and brown bullhead (*Ameiurus nebulosus*) collected in 2006 from Beaverskin, North Cranberry, Pebbleloggitch, and Puzzle lakes in Kejimkujik National Park and National Historic Site.

	n	Length (cm)	Weight (g)	Condition (10^2 g·cm^{-3})	*n*	Hg (μg·g^{-1} dw)	MeHg/THg (%)
Beaverskin							
Golden shiner	15	7.8±1.5 b	6.04±4.26 ab	1.13±0.05 a	6	1.00±0.43 b	90.16±5.07
Banded killifish	15	8.6±0.7 a	5.16±1.20 a	0.79±0.04 a	6	1.86±0.65 a	—
Yellow perch	27	13.3±4.6 a	37.03±36.51 a	1.11±0.07*	27	1.36±0.43 b	94.72±11.62
Brown bullhead	10	15.1±3.6	49.38±34.79	1.23±0.08	—	—	—
North Cranberry							
Golden shiner	15	7.4±0.6 b	4.22±1.05 b	1.03±0.04 b	6	1.81±0.67 a	86.21±8.51
Banded killifish	15	7.2±0.7 c	3.18±0.92 b	0.85±0.04 a	6	1.65±0.57 a	—
Yellow perch	27	13.1±4.0 a	33.31±30.33 a	1.10±0.12*	27	2.26±1.34 a	95.17±2.54
Brown bullhead	10	16.2±1.2	56.29±16.49	1.30±0.13	—	—	—
Pebbleloggitch							
Golden shiner	2	12.1 / 15.2	24.38 / 49.80	1.38 / 1.42	—	—	—
Banded killifish	0	—	—	—	—	—	—
Yellow perch	28	12.6±3.7 a	29.27±24.54 a	1.14±0.08*	28	0.96±0.35 c	98.14±16.23
Brown bullhead	10	21.2±1.9	140.33±34.31	1.46±0.11	—	—	—
Puzzle							
Golden shiner	15	9.0±1.7 a	9.05±6.22 a	1.10±0.11 a	6	0.95±0.23 b	93.98±4.09
Banded killifish	15	7.8±0.5 b	3.83±0.73 b	0.80±0.07 a	5	0.81±0.19 b	—
Yellow perch	26	12.5±3.9 a	28.42±24.09 a	1.08±0.11*	26	1.51±0.56 b	99.05±17.54
Brown bullhead	10	15.9±2.4	59.89±33.95	1.37±0.18	—	—	—

Note: —, not measured; dw, dry weight; different letters following values represent significant differences within a species among lakes. Golden shiner values for Pebbleloggitch are minimums/maximums because $n = 2$.

*Significant interaction in ANCOVA, therefore cannot test for significant differences in condition of yellow perch among lakes.

in larger or trophically elevated (δ^{15}N) yellow perch when individual variables were examined, or combinations of length and age or TP for multiple regressions. Elevated THg concentrations in yellow perch from the KNPNHS lakes could not be explained by atypical food web structure or enhanced biomagnification rates but were higher in fish with lower growth rates and for those from lakes with longer flushing rates. In addition, mean THg in yellow perch was positively related to MeHg in one of their potential invertebrate prey items (*Aeshna umbrosa*), indicating that the concentrations of THg in lower-trophic-level organisms were important in determining THg in this fish species.

Food web structure

Differences in δ^{13}C of zooplankton, profundal and littoral invertebrates, and the dietary habits of fishes (inferred from the δ^{13}C of prey) in the acidic lakes in KNPNHS were similar to those reported in the literature (Vander Zanden and Rasmussen 1999; Gorski et al. 2003; Barry Hanson 2004). As expected, δ^{13}C of littoral macroinvertebrates was enriched, whereas profundal and pelagic invertebrates had depleted δ^{13}C; this difference in δ^{13}C of invertebrates collected from these different habitats has been previously attributed to differential fractionation of dissolved inorganic carbon (DIC) by littoral or pelagic primary producers (Hecky and Hesslein 1995). Fishes from the KNPNHS lakes relied mainly on littoral carbon sources, although there were minor deviations in dietary habits of species and size classes from lake to lake. Similar to our findings, the δ^{13}C of banded killifish and golden shiner in lakes in southern New Brunswick also reflected diets consisting mainly of littoral carbon (Barry Hanson 2004). In a study of Ritchie Lake, Michigan, yellow perch also relied heavily on nearshore carbon: their δ^{13}C ranged between approximately –24.0‰ and –25.5‰, whereas the δ^{13}C of limnephilids and zooplankton ranged from approximately –25.5‰ to –24.0‰ and –33.5‰ to –29.0‰, respectively (Gorski et al. 2003). Although yellow perch inhabit open waters, they primarily eat littoral macroinvertebrates and some small benthic fishes, as evidenced by gut content and stable isotope analyses in this and other studies (Vander Zanden et al. 1997; Scott and Crossman 1998).

The δ^{15}N analyses of macroinvertebrates and fishes from KNPNHS lakes supported our general understanding of the dietary habits and relative trophic positions of these organisms. Trichopteran larvae are known to be primary consumers (Merritt and Cummins 1996) and had the lowest δ^{15}N of any macroinvertebrate in this study. In contrast, aeshnids in the KNPNHS lakes were enriched in their δ^{15}N by 2‰–3‰ above those of other littoral invertebrates, supporting that dragonfly nymphs are carnivorous (Merritt and Cummins 1996). Littoral chironomids and amphipods typically had mean δ^{15}N that fell between the values measured for the limnephilids and aeshnids, suggesting either a more omnivorous diet for chironomids and amphipods or that bacterial processing of detrital matter (with an elevated δ^{15}N signature) was an important food source for these organisms (Fisher Wold and Hershey 1999). Within each of the four KNPNHS lakes, all fishes were at a similar TP (within 0.21) and were consistently about 1 TP higher than the aeshnids, indicating that the fishes fed mainly on predaceous in-

Table 5. Results of simple linear regressions between log THg and log(length), log(weight), condition, or $\delta^{15}N$ for each fish species in Beaverskin, North Cranberry, Pebbleloggitch, and Puzzle lakes.

	Log(length)	Log(weight)	Condition	$\delta^{15}N$
Golden shiner				
Beaverskin	**$p = 0.002$**	**$p = 0.03$**	$p = 0.28$	$p = 0.21$
	$r^2 = 0.93$	**$r^2 = 0.91$**	$r^2 = 0.28$	$r^2 = 0.35$
North Cranberry	$p = 0.35$	$p = 0.46$	$p = 0.26$	$p = 0.61$
	$r^2 = 0.22$	$r^2 = 0.14$	$r^2 = 0.30$	$r^2 = 0.07$
Pebbleloggitch	—	—	—	—
Puzzle	$p = 0.91$	$p = 0.83$	$p = 0.33$	$p = 0.36$
	$r^2 = 0.004$	$r^2 = 0.01$	$r^2 = 0.23$	$r^2 = 0.21$
Banded killifish				
Beaverskin	$p = 0.07$	**$p = 0.04$**	$p = 0.50$	**$p = 0.01$**
	$r^2 = 0.59$	**$r^2 = 0.70$**	$r^2 = 0.12$	**$r^2 = 0.83$**
North Cranberry	$p = 0.88$	$p = 0.94$	$p = 0.59$	**$p = 0.046$**
	$r^2 = 0.007$	$r^2 = 0.001$	$r^2 = 0.08$	**$r^2 = 0.67$**
Pebbleloggitch	—	—	—	—
Puzzle	$p = 0.21$	$p = 0.19$	$p = 0.52$	**$p = 0.02$**
	$r^2 = 0.46$	$r^2 = 0.49$	$r^2 = 0.15$	**$r^2 = 0.87$**
Yellow perch				
Beaverskin	$p = 0.12$	$p = 0.11$	$p = 0.11$	**$p = 0.04$**
	$r^2 = 0.09$	$r^2 = 0.10$	$r^2 = 0.10$	**$r^2 = 0.16$**
North Cranberry	**$p < 0.001$**	**$p < 0.001$**	With outlier: $p = 0.05$	**$p < 0.001$**
	$r^2 = 0.46$	**$r^2 = 0.44$**	$r^2 = 0.59$	**$r^2 = 0.40$**
			Without outlier: **$p = 0.007$**	
			$r^2 = 0.27$	
Pebbleloggitch	**$p = 0.01$**	**$p = 0.01$**	$p = 0.70$	**$p = 0.02$**
	$r^2 = 0.23$	**$r^2 = 0.22$**	$r^2 = 0.006$	**$r^2 = 0.19$**
Puzzle	**$p < 0.001$**	**$p < 0.001$**	**$p = 0.003$**	**$p < 0.001$**
	$r^2 = 0.81$	**$r^2 = 0.79$**	**$r^2 = 0.31$**	**$r^2 = 0.55$**

Note: Significant results are shown in bold. Species: golden shiner, *Notemigonus crysoleucas*; banded killifish, *Fundulus diaphanous*; yellow perch, *Perca flavescens*; brown bullhead, *Ameiurus nebulosus*.

vertebrates or a combination of herbivorous invertebrates and fishes (forage fishes and juveniles). Golden shiner in KNPNHS lakes had mean TPs that ranged from 3.48 to 3.91, which was higher than those for red shiner from the San Juan River, New Mexico (TP of 2.6; Gido et al. 2006) but similar to golden shiner from Trout Lake, New Brunswick (TP of approximately 3.5; Barry Hanson 2004). Yellow perch consume different food sources depending on their life stage, time of year, and prey abundance (Scott and Crossman 1998; Kövecses et al. 2005; Rennie et al. 2005). This plasticity in dietary habits results in TP for this species that range from 3.45 to 4.47 (Vander Zanden et al. 1997; Gorski et al. 2003; McIntyre and Beauchamp 2007), similar to the range found at KNPNHS (3.28–4.46). As such, it does not appear that the positioning of organisms were atypical in the acidic food webs of KNPNHS when compared with near-neutral systems and cannot explain the elevated THg in yellow perch in KNPNHS.

Among-lake differences were observed in the relative importance of pelagic versus littoral carbon and trophic positions for some fish species collected from KNPNHS. Golden shiner typically consume zooplankton and macroinvertebrates (Scott and Crossman 1998). Isotope mixing models with the $\delta^{13}C$ data showed that golden shiner in Beaverskin and North Cranberry lakes were more zooplanktivorous (53% and 38%, respectively) than those in the Pebbleloggitch and Puzzle lakes (7% and 0%, respectively). Golden shiner from Beaverskin and North Cranberry lakes also had higher TPs, which may be due to the fact that pelagic invertebrates tend to have elevated $\delta^{15}N$ when compared with littoral invertebrates (Kidd et al. 1999). Small yellow perch initially feed upon zooplankton and, by the end of their first summer, shift to diets consisting of odonates and other littoral invertebrates (Scott and Crossman 1998). Although small perch (5–10 cm) in this study were consistently lighter in their $\delta^{13}C$ when compared with perch >10 cm, littoral carbon formed a majority of the diet across all sizes collected. Trophic positions were similar among all size classes of yellow perch in Beaverskin and Pebbleloggitch lakes, but large yellow perch in North Cranberry and Puzzle lakes were trophically elevated above the smaller fish in these lakes, suggesting that the large fish were more piscivorous than the smaller fish.

Hg in biota

Invertebrates from lakes in KNPNHS had higher MeHg concentrations when compared with other freshwater systems without point sources of THg. Mean MeHg concentrations in zooplankton at KNPNHS ranged from 0.09 ± 0.04 μg·g dw^{-1} to 0.23 ± 0.12 μg·g dw^{-1} and were higher than the mean concentrations in zooplankton from two lakes in Isle Royale National Park, Michigan (0.049 μg·g dw^{-1}

Table 6. Slopes and intercepts (± standard deviation, SD) of log Hg versus $\delta^{15}N$ regressions for Beaverskin (n = 54), North Cranberry (n = 56), Pebbleloggitch (n = 46), and Puzzle (n = 54) lakes.

		Beaverskin		North Cranberry		Pebbleloggitch		Puzzle	
Method		Slope	Intercept	Slope	Intercept	Slope	Intercept	Slope	Intercept
$MeHg_{dw}$–THg_{dw}	dw	0.23±0.01 a	−1.71±0.07	0.19±0.01 b	−1.25±0.06	0.21±0.01 ab	−1.51±0.06	0.20±0.01 ab	−1.44±0.06
		p<0.001, r^2 = 0.92		p<0.001, r^2 = 0.91		p<0.001, r^2 = 0.89		p<0.001, r^2 = 0.91	
$MeHg_{dw}$–$MeHg_{dw}$	dw	0.23±0.01	−1.70±0.06	0.18±0.01	−1.27±0.06	0.21±0.01	−1.50±0.06	0.20±0.01	−1.44±0.06
		p<0.001, r^2 = 0.92		p<0.001, r^2 = 0.89		p<0.001, r^2 = 0.89		p<0.001, r^2 = 0.90	
$MeHg_{ww}$–THg_{ww}	ww	0.25±0.01	−2.45±0.06	0.19±0.01	−1.97±0.06	0.22±0.01	−2.22±0.06	0.21±0.01	−2.17±0.06
		p<0.001, r^2 = 0.92		p<0.001, r^2 = 0.91		p<0.001, r^2 = 0.90		p<0.001, r^2 = 0.91	
$MeHg_{ww}$–$MeHg_{ww}$	ww	0.24±0.01	−2.46±0.06	0.19±0.01	−1.96±0.06	0.22±0.01	−2.22±0.06	0.21±0.01	−2.16±0.06
		p<0.001, r^2 = 0.93		p<0.001, r^2 = 0.91		p<0.001, r^2 = 0.89		p<0.001, r^2 = 0.90	

Note: Different letters represent significant differences for regressions using $MeHg_{dw}$–THg_{dw}.

Fig. 3. Regressions of log Hg (μg·g dry weight (dw)$^{-1}$) versus $\delta^{15}N$ (‰) for fish and littoral invertebrates collected from Beaverskin (solid line, shaded circles), North Cranberry (long-dashed line, ×), Pebbleloggitch (short-dashed line, ◇), and Puzzle (dotted line, △) lakes at Kejimkujik National Park and National Historic Site, 2006. Slopes from Beaverskin and North Cranberry lakes were significantly different.

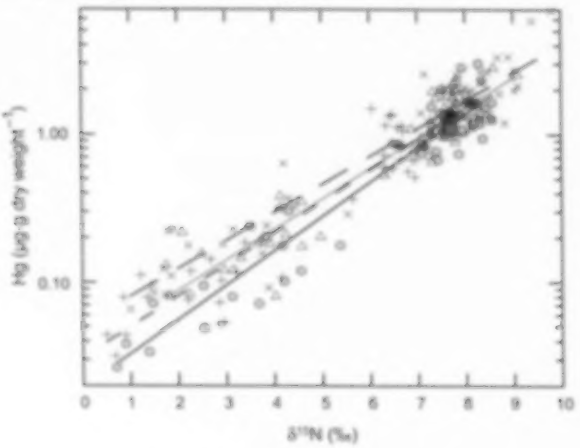

and 0.074 μg·g dw^{-1}; Gorski et al. 2003) and from 15 natural lakes in northern Wisconsin (0.053 μg·g dw^{-1}; Watras et al. 1998). Amphipods, like most of the other littoral primary consumers in KNPNHS, had MeHg concentrations (0.09 ± 0.04 – 0.18 ± 0.03 μg·g dw^{-1}) that were 2.5–7.5 times higher than the same taxon from a reference lake (L632) at the Experimental Lakes Area (ELA; 0.018–0.057 μg·g dw^{-1}; Hall et al. 1998). Predatory aeshnids (Merritt and Cummins 1996) in the KNPNHS lakes had MeHg concentrations (0.17 ± 0.03 – 0.44 ± 0.17 μg·g^{-1}) that were 2–10 times higher than those in related species from uncontaminated lakes (Tremblay et al. 1996; Hall et al. 1998; Gorski et al. 2003).

As was found for the invertebrates, THg concentrations in fishes from KNPNHS were higher than those from uncontaminated regions. Mean THg concentrations for golden shiner and banded killifish in KNPNHS were 0.27 ± 0.12 μg·g ww^{-1} and 0.32 ± 0.15 μg·g ww^{-1}, respectively, whereas THg concentrations of these species collected from acidic lakes in New Brunswick in 1996 and 1997 were 0.11 ± 0.05 μg·g ww^{-1} and 0.08 ± 0.04 μg·g ww^{-1}, respectively (Barry Hanson 2004). Mean concentrations of THg in these two species from KNPNHS were also higher than those of northern redbelly dace (*Phoxinus eos*) or fathead minnow (*Pimephales promelas*) from reference lakes at the ELA (approximately 0.15 μg·g ww^{-1} and 0.25 μg·g ww^{-1}, respectively; Kidd et al. 1999), and they were two to three times higher than those reported in pumpkinseed (*Lepomis gibbosus*) and spottail shiner (*Notropis hudsonius*) from various lakes in northwestern Ontario (Swanson et al. 2003). Mean THg concentration of yellow perch from KNPNHS (0.36 ± 0.21 μg·g ww^{-1}) was more than double that of the mean concentration for the same species from Lake Washington (0.127 ± 0.013 μg·g ww^{-1}; calculated from table 1 in McIntyre and Beauchamp (2007)), although this was partly because the mean fish length (22.8 ± 1.5 cm) was much longer than that in KNPNHS (13.8 ± 5.2 cm). These findings and those

of the invertebrates described above support the characterization of KNPNHS as a "hotspot" of biological Hg concentrations in northeastern North America (Evers et al. 2007).

The predictors of THg concentrations in perch from KNPNHS were similar to those reported for fish in other studies. Within each lake at KNPNHS, THg concentrations in the predatory yellow perch were significantly predicted by length, weight, or $\delta^{15}N$ (simple GLM) or length, age, or TP (stepwise GLM). It has often been shown that THg concentrations in fish increase with length, weight, or age because THg is depurated at a slower rate than it is taken up and the organism consequently accumulates this pollutant in its tissues (Huckabee et al. 1979; Watras et al. 1998; Kamman et al. 2005). However, increases in THg with size do not occur for all fishes in all lakes (e.g., Kidd et al. 1995) because of differences in ontogeny and growth rates among species and locations (Trudel and Rasmussen 2006). In particular, the negative relationship between THg and length-at-age observed among the KNPNHS lakes illustrates that lakes with faster-growing perch had diluted concentrations of THg, as has been shown in other systems (Greenfield et al. 2001; Essington and Houser 2003). The influence of $\delta^{15}N$ or TP on THg has been shown repeatedly because animals generally increase their trophic position and bioaccumulate THg as they grow (Kidd et al. 2003; McIntyre and Beauchamp 2007). Although both age and TP could be used to separate the effects of length of exposure from those of trophic enrichment (McIntyre and Beauchamp 2007), simple regressions in the current study showed that TP was significantly related to age or length in fish from two lakes, and stepwise regressions showed that TP and age were not the most important predictors of THg in all lakes. As such, age and TP can be collinear and should not automatically be included in all multiple regressions examining the factors influencing THg in fishes.

As has been seen in previous studies of freshwater lakes, Hg biomagnification through the food webs of KNPNHS was significantly predicted by $\delta^{15}N$; when compared across all four lakes, the slope of this relationship was significantly higher in Beaverskin Lake (0.23) than in North Cranberry Lake (0.19). Although previous studies focused on differences in fish THg concentrations to explain among-lake variability in these slopes (Bowles et al. 2001; McIntyre and Beauchamp 2007), we found that mean THg concentrations in perch were negatively related to the Hg versus $\delta^{15}N$ slopes. More specifically, biomagnification of Hg was significantly higher through the food web in Beaverskin Lake when compared with North Cranberry Lake, although the top consumers (i.e., yellow perch) were similar in size, age, and TP, and THg concentrations in perch from the latter lake were significantly higher. However, length-at-age was greater for perch from Beaverskin Lake, which suggests that these fish may have lower THg concentrations due to growth dilution (Trudel and Rasmussen 2006). Higher THg in perch was also related to longer flushing rates, and North Cranberry Lake had the highest flushing rate and lowest biomagnification rate, whereas Beaverskin Lake had the lowest flushing rate and highest biomagnification rate; however, factors influencing this cannot currently be explained. Food web structure and the dietary habits of fishes were similar among these lakes and cannot explain the differences in biomagnification rates. Further, the chemistries of the four lakes were not related to the biomagnification rates: Beaverskin Lake had the highest pH and lowest TOC, but Pebbleloggitch Lake did not have the lowest slope, despite having the lowest pH and highest TOC. Finally, the lower-trophic-level organisms in Beaverskin and North Cranberry lakes were at similar trophic positions, but limnephilids, chironomids, and aeshnids in North Cranberry Lake had higher MeHg. It is interesting to note that for these two lakes, Hg biomagnification is lowest in the lake with the highest concentrations of MeHg in invertebrates and THg in perch and highest in the lake with the lowest concentrations of MeHg in invertebrates and THg in perch. This cannot be explained and warrants further research into whether the absolute concentration of MeHg in lower trophic levels affects its transfer to upper level consumers.

Mercury concentrations in yellow perch in KNPNHS were not highest in lakes with the highest food web biomagnification of this pollutant. Rather, MeHg in the predaceous dragonfly, which was likely prey for the perch (as determined by $\delta^{13}C$ and $\delta^{15}N$), was a better predictor of the THg concentration in this fish species. Variation in MeHg of lower trophic organisms is known to be an important predictor of THg in fish (Watras et al. 1998; Trudel and Rasmussen 2006), and results from our study concur and show that this was a more useful predictor of THg in yellow perch than the rate at which THg is transferred from prey to predator.

Food web biomagnification rates calculated for the four acidic lakes in KNPNHS were similar to those reported in other studies. Although we observed significant differences in the slopes of the log Hg versus $\delta^{15}N$ (and log Hg versus TP) relationships within KNPNHS (Table 6), the slopes of these regressions (0.19–0.23) fell within the range of those reported in temperate lake food webs of Canada and the US (0.17–0.29; McIntyre and Beauchamp 2007; Eagles-Smith et al. 2008; K. Kidd, unpublished data) and in tropical systems (0.16, 0.20, and 0.28; Bowles et al. 2001; Kidd et al. 2003; Campbell et al. 2008). We originally predicted that Hg biomagnification rates in acidic ecosystems, such as those of KNPNHS, would exceed those of other regions because THg concentrations in fish tend to be higher in acidic conditions (Chen et al. 2005); however, our results do not support this hypothesis. This study did not find enhanced biomagnification rates in acidic lakes compared with near-neutral ones; therefore, at this time, differences in Hg biomagnification cannot explain the higher contaminant concentrations in top predators from acidic ecosystems. Considering that the biomagnification rates in this study and in the literature were quantified in lakes across a gradient of climate, pH, lake trophies (eutrophic through oligotrophic), and different fish communities, it appears that Hg biomagnification rates through entire food webs are similar across lacustrine systems, despite their variable physical, chemical, or biological characteristics.

In conclusion, we found that Hg biomagnifies through food webs of low pH lakes at rates similar to those found in near-neutral systems, and that within the acidic lakes of this study, concentrations of THg in perch were better predicted by MeHg in their prey and by perch growth rates than by differences in the trophic transfer of this pollutant. Because trophic positioning of yellow perch in this study was similar to what has been found in other lakes, the ele-

vated THg concentrations in fish and loons from KNPNHS appear to be caused by the elevated THg concentrations in the lower trophic organisms and not by atypical food web structures or biomagnification rates.

Acknowledgements

The authors gratefully acknowledge T. Barrett, A. Hicks, H. Loomer, M. Dobrin, S. Kidd, K. Munkittrick, and M. Gautreau for assistance with field sampling and E. Bellyea, L. Baker, and T. Jardine for Hg analyses. Funding for this project was provided by the Natural Sciences and Engineering Research Council of Canada (NSERC) Discovery, Canada Graduate Scholarship, and Canada Research Chair programmes, Parks Canada, and Environment Canada.

References

Barry Hanson, E. 2004. Mercury concentrations and trophic interactions of fish species in southwestern New Brunswick lakes. M.Sc. thesis, Department of Biology, University of New Brunswick, Fredericton, N.B.

Bowles, K.C., Apte, S.C., Maher, W.A., Kawei, M., and Smith, R. 2001. Bioaccumulation and biomagnification of mercury in Lake Murray, Papua New Guinea. Can. J. Fish. Aquat. Sci. **58**(5): 888–897. doi:10.1139/cjfas-58-5-888.

Burgess, N.M. 2005. Mercury in biota and its effects. *In* Mercury: sources, measurements, cycles and effects. *Edited by* M.B. Parsons and J.B. Percival. Mineral Association of Canada, Ottawa, Ont. pp. 235–258.

Cabana, G., and Rasmussen, J.B. 1994. Modeling food-chain structure and contaminant bioaccumulation using stable nitrogen isotopes. Nature (London), **372**(6503): 255–257. doi:10.1038/372255a0.

Cabana, G., and Rasmussen, J.B. 1996. Comparison of aquatic food chains using nitrogen isotopes. Proc. Natl. Acad. Sci. U.S.A. **93**(20): 10844–10847. doi:10.1073/pnas.93.20.10844. PMID:8855268.

Cai, Y., Tang, G., Jaffe, R., and Jones, R. 1997. Evaluation of some isolation methods for organomercury determination in soil and fish samples by capillary gas chromatography – atomic fluorescence spectrometry. Int. J. Environ. Anal. Chem. **68**(3): 331–345. doi:10.1080/03067319708030499.

Campbell, L., Verburg, P., Dixon, D.G., and Hecky, R.E. 2008. Mercury biomagnification in the food web of Lake Tanganyika (Tanzania, East Africa). Sci. Total Environ. **402**(2–3): 184–191. doi:10.1016/j.scitotenv.2008.04.017. PMID:18559282.

Chen, C.Y., Stemberger, R.S., Kamman, N.C., Mayes, B.M., and Folt, C.L. 2005. Patterns of Hg bioaccumulation and transfer in aquatic food webs across multi-lake studies in the northeast US. Ecotoxicology, **14**(1–2): 135–147. doi:10.1007/s10646-004-6265-y. PMID:15934168.

Clair, T.A., Aherne, J., Dennis, I.F., Gilliss, M., Couture, S., McNicol, D., Weeber, R., Dillon, P.J., Keller, W., Jeffries, D.S., Page, S., Timoffee, K., and Cosby, B.J. 2007. Past and future changes to acidified eastern Canadian lakes: a geochemical modeling approach. Appl. Geochem. **22**(6): 1189–1195. doi:10.1016/j.apgeochem.2007.03.010.

Clarke, L.R., Vidergar, D.T., and Bennett, D.H. 2005. Stable isotopes and gut content show diet overlap among native and introduced piscivores in a large oligotrophic lake. Ecol. Freshwat. Fish, **14**(3): 267–277. doi:10.1111/j.1600-0633.2005.00103.x.

Deniro, M.J., and Epstein, S. 1978. Influence of diet on distribution of carbon isotopes in animals. Geochim. Cosmochim. Acta, **42**(5): 495–506. doi:10.1016/0016-7037(78)90199-0.

Doucett, R.R., Barton, D.R., Guiguer, K.R.A., Power, G., and Drimmie, R.J. 1996. Comment: Critical examination of stable isotope analysis as a means for tracing carbon pathways in stream ecosystems. Can. J. Fish. Aquat. Sci. **53**(8): 1913–1915. doi:10.1139/cjfas-53-8-1913.

Drysdale, C., Burgess, N.M., d'Entremont, A., Carter, J., and Brun, G. 2005. Mercury in brook trout, white perch, and yellow perch in Kejimkujik National Park. *In* Mercury cycling in a wetland dominated ecosystem: a multidisciplinary study. *Edited by* N.J. O'Driscoll, A.N. Rencz, and D.R.S. Lean. Society of Environmental Toxicology and Chemistry (SETAC), Pensacola, Fla. pp. 323–348.

Eagles-Smith, C.A., Suchanek, T.H., Colwell, A.E., and Anderson, N.L. 2008. Mercury trophic transfer in a eutrophic lake: the importance of habitat-specific foraging. Ecol. Appl. **18**(8, Suppl): A196–A212. doi:10.1890/06-1476.1. PMID:19475925.

Essington, T.E., and Houser, J.N. 2003. The effect of whole-lake nutrient enrichment on mercury concentration in age-1 yellow perch. Trans. Am. Fish. Soc. **132**(1): 57–68. doi:10.1577/1548-8659(2003)132<0057:TEOWLN>2.0.CO;2.

Evers, D.C., Han, Y.J., Driscoll, C.T., Kamman, N.C., Goodale, M.W., Lambert, K.F., Holsen, T.M., Chen, C.Y., Clair, T.A., and Butler, T. 2007. Biological mercury hotspots in the northeastern United States and southeastern Canada. Bioscience, **57**(1): 29–43. doi:10.1641/B570107.

Fisher Wold, A.K., and Hershey, A.E. 1999. Effects of salmon carcass decomposition on biofilm growth and wood decomposition. Can. J. Fish. Aquat. Sci. **56**(5): 767–773. doi:10.1139/cjfas-56-5-767.

Gido, K.B., Franssen, N.R., and Propst, D.L. 2006. Spatial variation in $\delta^{15}N$ and $\delta^{13}C$ isotopes in the San Juan River, New Mexico and Utah: implications for the conservation of native fishes. Environ. Biol. Fishes, **75**(2): 197–207. doi:10.1007/s10641-006-0009-1.

Ginn, B.K., Cumming, B.F., and Smol, J.P. 2007. Assessing pH changes since pre-industrial times in 51 low-alkalinity lakes in Nova Scotia, Canada. Can. J. Fish. Aquat. Sci. **64**(8): 1043–1054. doi:10.1139/F07-078.

Gorski, P.R., Cleckner, L.B., Hurley, J.P., Sierszen, M.E., and Armstrong, D.E. 2003. Factors affecting enhanced mercury bioaccumulation in inland lakes of Isle Royale National Park, USA. Sci. Total Environ. **304**(1–3): 327–348. doi:10.1016/S0048-9697(02)00579-X. PMID:12663194.

Greenfield, B.K., Hrabik, T.R., Harvey, C.J., and Carpenter, S.R. 2001. Predicting mercury levels in yellow perch: use of water chemistry, trophic ecology, and spatial traits. Can. J. Fish. Aquat. Sci. **58**(7): 1419–1429. doi:10.1139/cjfas-58-7-1419.

Hall, B.D., Rosenberg, D.M., and Wiens, A.P. 1998. Methyl mercury in aquatic insects from an experimental reservoir. Can. J. Fish. Aquat. Sci. **55**(9): 2036–2047. doi.10.1139/cjfas-55-9-2036.

Hecky, R.E., and Hesslein, R.H. 1995. Contributions of benthic algae to lake food webs as revealed by stable isotope analysis. J. N. Am. Benthol. Soc. **14**(4): 631–653. doi:10.2307/1467546.

Herrin, R.T., Lathrop, R.C., Gorski, P.R., and Andren, A.W. 1998. Hypolimnetic methylmercury and its uptake by plankton during fall destratification: a key point of mercury into lake food chains. Limnol. Oceanogr. **43**: 1476–1486.

Huckabee, J.W., Elwood, J.W., and Hildebrand, S.G. 1979. Accumulation of mercury in freshwater biota. *In* The biogeochemistry of mercury in the environment. *Edited by* J.O. Nriagu. Elsevier/North Holland Biomedical Press, New York. pp. 277–302.

Jardine, T.D., Cartwright, D.F., Dietrich, J.P., and Cunjak, R.A. 2005. Resource use by salmonids in riverine, lacustrine and mar-

ine environments: evidence from stable isotope analysis. Environ. Biol. Fishes, **73**(3): 309–319. doi:10.1007/s10641-005-2259-8.

Jardine, T.D., Kidd, K.A., and Fisk, A.T. 2006. Applications and assumptions of stable isotope analysis in ecotoxicology. Environ. Sci. Technol. **40**(24): 7501–7511.

Kamman, N.C., Burgess, N.M., Driscoll, C.T., Simonin, H.A., Goodale, W., Linehan, J., Estabrook, R., Hutcheson, M., Major, A., Scheuhammer, A.M., and Scruton, D.A. 2005. Mercury in freshwater fish of northeast North America — a geographic perspective based on fish tissue monitoring databases. Ecotoxicology, **14**(1–2): 163–180. doi:10.1007/s10646-004-6267-9. PMID: 15931965.

Kerekes, J., and Schwinghamer, P. 1973. Aquatic resources inventory, Kejimkujik National Park. Part 2: Lake drainage and morphometry. Canadian Wildlife Service, Halifax, N.S.

Kidd, K.A., Hesslein, R.H., Fudge, R.J.P., and Hallard, K.A. 1995. The influence of trophic level as measured by $\delta^{15}N$ on mercury concentrations in freshwater organisms. Water Air Soil Pollut. **80**(1–4): 1011–1015. doi:10.1007/BF01189756.

Kidd, K.A., Paterson, M.J., Hesslein, R.H., Muir, D.C.G., and Hecky, R.E. 1999. Effects of northern pike (*Esox lucius*) additions on pollutant accumulation and food web structure, as determined by $\delta^{13}C$ and $\delta^{15}N$, in a eutrophic and an oligotrophic lake. Can. J. Fish. Aquat. Sci. **56**(11): 2193–2202. doi:10.1139/cjfas-56-11-2193.

Kidd, K.A., Bootsma, H.A., Hesslein, R.H., Lockhart, W.L., and Hecky, R.E. 2003. Mercury concentrations in the food web of Lake Malawi, East Africa. J. Great Lakes Res. **29**: 258–266.

Kövecses, J., Sherwood, G.D., and Rasmussen, J.B. 2005. Impacts of altered benthic invertebrate communities on the feeding ecology of yellow perch (*Perca flavescens*) in metal-contaminated lakes. Can. J. Fish. Aquat. Sci. **62**(1): 153–162. doi:10.1139/f04-181.

McIntyre, J.K., and Beauchamp, D.A. 2007. Age and trophic position dominate bioaccumulation of mercury and organochlorines in the food web of Lake Washington. Sci. Total Environ. **372**(2–3): 571–584. doi:10.1016/j.scitotenv.2006.10.035. PMID: 17157357.

Merritt, R.W., and Cummins, K.W. 1996. An introduction to the aquatic insects of North America. 3rd ed. Kendall/Hunt Publishing Company, Dubuque, Iowa.

Minagawa, M., and Wada, E. 1984. Stepwise enrichment of ^{15}N along food chains: further evidence and the relation between $\delta^{15}N$ and animal age. Geochim. Cosmochim. Acta, **48**(5): 1135–1140. doi:10.1016/0016-7037(84)90204-7.

National Wildlife Research Centre. 2007. Method for determining the organic mercury concentration in wildlife tissues using the AMA 254 Advanced Mercury Analyser. Laboratory Services Section, National Wildlife Research Centre (NWRC), Ottawa, Ont.

Needham, J.G., and Westfall, M.J., Jr. 1955. A manual of the dragonflies of North America (Anisoptera). University of California Press, Berkeley, California.

O'Driscoll, N.J., Rencz, A.N., and Lean, D.R.S. 2005. Review of factors affecting mercury fate in Kejimkujik Park, Nova Scotia. *In* Mercury cycling in a wetland-dominated ecosystem: a multidisciplinary study. *Edited by* N.J. O'Driscoll, A.N. Rencz, and D.R.S. Lean. Society of Environmental Toxicology and Chemistry (SETAC), Pensacola, Fla. pp. 5–13.

Phillips, D.L., and Gregg, J.W. 2001. Uncertainty in source partitioning using stable isotopes. Oecologia (Berl.), **127**(2): 171–179. doi:10.1007/s004420000578.

Post, D.M., Layman, C.A., Arrington, D.A., Takimoto, G., Quattrochi, J., and Montana, C.G. 2007. Getting to the fat of the matter: models, methods and assumptions for dealing with lipids in stable isotope analyses. Oecologia (Berl.), **152**(1): 179–189. doi:10.1007/s00442-006-0630-x.

Rennie, M.D., Collins, N.C., Shuter, B.J., Rajotte, J.W., and Couture, P. 2005. A comparison of methods for estimating activity costs of wild fish populations: more active fish observed to grow slower. Can. J. Fish. Aquat. Sci. **62**(4): 767–780. doi:10.1139/f05-052.

Scott, W.B., and Crossman, E.J. 1998. Freshwater fishes of Canada. Galt House Publications Ltd., Oakville, Ontario.

Swanson, H.K., Johnston, T.A., Leggett, W.C., Bodaly, R.A., Doucett, R.R., and Cunjak, R.A. 2003. Trophic positions and mercury bioaccumulation in rainbow smelt (*Osmerus mordax*) and native forage fishes in northwestern Ontario lakes. Ecosystems (N.Y., Print), **6**(3): 289–299. doi:10.1007/s10021-002-0205-6.

Temme, C., Blanchard, P., Steffen, A., Banic, C., Beauchamp, S., Poissant, L., Tordon, R., and Wiens, B. 2007. Trend, seasonal and multivariate analysis study of total gaseous mercury data from the Canadian atmospheric mercury measurement network (CAMNet). Atmos. Environ. **41**(26): 5423–5441. doi:10.1016/j.atmosenv.2007.02.021.

Thorp, J.H., and Covich, A.P. 2001. Ecology and classification of North American freshwater invertebrates. 2nd ed. Academic Press, San Diego, California.

Tremblay, A., Lucotte, M., and Rheault, I. 1996. Methylmercury in a benthic food web of two hydroelectric reservoirs and a natural lake of Northern Quebec (Canada). Water Air Soil Pollut. **91**(3-4): 255–269. doi:10.1007/BF00666262.

Trudel, M., and Rasmussen, J.B. 2006. Bioenergetics and mercury dynamics in fish: a modelling perspective. Can. J. Fish. Aquat. Sci. **63**(8): 1890–1902. doi:10.1139/F06-081.

Vaidya, O.C., Howell, G.D., and Leger, D.A. 2000. Evaluation of the distribution of mercury in lakes in Nova Scotia and Newfoundland (Canada). Water Air Soil Pollut. **117**(1/4): 353–369. doi:10.1023/A:1005190429095.

Vander Zanden, M.J., and Rasmussen, J.B. 1999. Primary consumer $\delta^{13}C$ and $\delta^{15}N$ and the trophic position of aquatic consumers. Ecology, **80**(4): 1395–1404. doi:10.1890/0012-9658(1999)080[1395:PCCANA]2.0.CO;2.

Vander Zanden, M.J., Cabana, G., and Rasmussen, J.B. 1997. Comparing trophic position of freshwater fish calculated using stable nitrogen isotope ratios ($\delta^{15}N$) and literature dietary data. Can. J. Fish. Aquat. Sci. **54**(5): 1142–1158. doi:10.1139/cjfas-54-5-1142.

Watras, C.J., Back, R.C., Halvorsen, S., Hudson, R.J.M., Morrison, K.A., and Wente, S.P. 1998. Bioaccumulation of mercury in pelagic freshwater food webs. Sci. Total Environ. **219**(2-3): 183–208. doi:10.1016/S0048-9697(98)00228-9. PMID:9802248.

Whitfield, C.J., Aherne, J., Watmough, S.A., Dillon, P.J., and Clair, T.A. 2006. Recovery from acidification in Nova Scotia: temporal trends and critical loads for 20 headwater lakes. Can. J. Fish. Aquat. Sci. **63**(7): 1504–1514. doi:10.1139/F06-053.

Egg consumption in mature Pacific salmon (*Oncorhynchus* spp.)

Shawn R. Garner, John W. Heath, and Bryan D. Neff

Abstract: For over a century, conventional wisdom has maintained that Pacific salmon (*Oncorhynchus* spp.) cease feeding when they return to freshwater rivers to spawn. Here, we overturn this belief by showing that multiple species of Pacific salmon consume eggs during spawning. Overall, 13% of stomachs contained eggs, and feeding rates were estimated at up to 14 eggs or 52 kJ per day. Feeding experiments revealed that mature salmon could digest eggs, as fed salmon maintained significantly higher body mass than unfed salmon. Such egg consumption presents a fundamental shift in our understanding of Pacific salmon ecology that may have important implications for migration and management models. Indeed, the energy from consumed eggs could allow salmon to migrate up to an additional 3.8 km upstream per day of feeding, or extend the duration of spawning activity by up to 12%. Furthermore, salmon stocks may have evolved local adaptations to their specific migration and spawning requirements that include nutrients from salmon eggs. Thus, successful salmon management efforts may need to preserve not only spawning habitat and migration corridors, but also feeding opportunities.

Résumé : Depuis plus d'un siècle, il est généralement convenu que les saumons du Pacifique (*Oncorhynchus* spp.) cessent de se nourrir lorsqu'ils retournent dans les rivières d'eau douce pour frayer. Nous infirmons cette croyance en montrant que plusieurs espèces de saumons du Pacifique consomment des œufs durant la fraie. Globalement, 13 % des estomacs contiennent des œufs et nous estimons les taux de consommation à 14 œufs ou 52 kJ par jour. Des expériences alimentaires montrent que les saumons matures sont capables de digérer les œufs, puisque les saumons alimentés maintiennent une masse corporelle significativement supérieure à celles des saumons qui jeûnent. Une telle consommation des œufs représente un changement fondamental dans notre compréhension de l'écologie des saumons du Pacifique, ce qui peut avoir des conséquences sur les modèles de migration et de gestion. En effet, l'énergie provenant de la consommation des œufs pourrait permettre aux saumons de migrer jusqu'à 3,8 km plus en amont par jour d'alimentation ou de prolonger leurs activités de fraie de jusqu'à 12 %. De plus, les stocks de saumons peuvent avoir développé des adaptations locales pour satisfaire leurs besoins spécifiques de migration et de fraie, ce qui inclut l'obtention de nutriments à partir des œufs de saumons. Ainsi, les efforts fructueux de gestion des saumons doivent peut-être préserver non seulement les habitats de fraie et les corridors de migration, mais aussi les occasions d'alimentation.

[Traduit par la Rédaction]

Introduction

Despite the enormous economic and cultural significance of anadromous salmonids, many stocks are suffering from dwindling returns or have been entirely extirpated (Parrish et al. 1998; Kareiva et al. 2000; Gustafson et al. 2007). These declines have been largely attributed to anthropogenic disturbances such as dams that prevent access to spawning areas (Levin and Tolimieri 2001) and commercial fisheries that harvest a million tonnes of salmonids annually (Food and Agriculture Organisation of the United Nations (FAO) 2007). These fisheries consist almost entirely of Pacific salmon (*Oncorhynchus* spp.), and as such, managing Pacific salmon stocks has become a key conservation priority. However, despite the clear importance of incorporating biological information into recovery planning, perhaps surprisingly, some fundamental aspects of their ecology remain poorly understood.

Pacific salmon, like many other salmonids, are typically anadromous and therefore migrate between fresh and salt waters during their life span. These fishes begin life as eggs in the gravel of freshwater streams, which then emerge to feed for a few weeks to several years in the fresh water (Quinn 2005). The juveniles subsequently migrate to the ocean where they may continue to feed and grow for several years until they mature and return to their natal streams to spawn. The spawning migration is a period of extraordinary energetic requirement — salmon travel hundreds of kilometres in the ocean to reach their natal rivers and may then spend months in fresh water. Indeed, some stocks travel over 1000 km upstream and reach elevations that are 1000 m above sea level before they spawn (Quinn 2005).

Received 27 November 2008. Accepted 29 April 2009. Published on the NRC Research Press Web site at cjfas.nrc.ca on 5 September 2009.
J20896

Paper handled by Associate Editor Bror Jonsson.

S.R. Garner and B.D. Neff.[1] Department of Biology, University of Western Ontario, London, ON N6A 5B7, Canada.
J.W. Heath. Yellow Island Aquaculture Limited, 1681 Brook Crescent, Campbell River, BC V9W 6K9, Canada.

[1]Corresponding author (e-mail: bneff@uwo.ca).

Salmon must survive this costly spawning migration, while simultaneously completing development of sexual characters and maintaining sufficient energy stores to complete spawning once they finish their migration.

Analyses of other anadromous salmonids suggest that feeding rates are significantly reduced when the adults return to freshwater rivers to spawn. For example, brown trout (*Salmo trutta*; Jonsson and Gravem 1985; Elliott 1997), white-spotted char (*Salvelinus leucomaenis*; Takami et al. 1996), Arctic char (*Salvelinus alpinus*; Rikardsen et al. 2003), and Atlantic salmon (*Salmo salar*; Johansen 2001) all feed less after returning to fresh water than they do in the ocean. The Pacific salmon are believed to show a similar pattern, and indeed for over 100 years, conventional wisdom has held that Pacific salmon cease feeding entirely when they return to freshwater rivers to spawn (Rutter 1903; Greene 1926). This belief persists despite a 50-year-old report indicating that limited feeding occurs in mature nonanadromous Chinook salmon (*Oncorhynchus tshawytscha*) (Bullivant 1959) and evidence that returning Masu salmon adults (*Oncorhynchus masou*) feed occasionally during migration (Higgs et al. 1995). Indeed, the belief that Pacific salmon cease feeding in fresh water has remained so deeply ingrained that it is frequently presented with no reference to supporting evidence (e.g., Brett 1995; Mesa and Magie 2006). The belief persists in part because the cessation of feeding is also thought to be associated with atrophy of the digestive tract, such that any ingested food would provide no nourishment (Rutter 1903). However, if these assumptions prove to be false and mature salmon do continue to feed in fresh water, then the ecology of Pacific salmon at this critical life stage will have been fundamentally misunderstood.

The return to fresh water is a critical period for anadromous salmon management programs because of the high energetic requirements of migration and the heightened vulnerability to anthropogenic disturbances. For example, hydroelectric dams and climate change have considerably altered the conditions experienced by migrating fishes (Rand et al. 2006; Battin et al. 2007; Waples et al. 2008). Consequently, modeling the bioenergetics of migration and spawning has received considerable attention (Gilhousen 1980; Crossin et al. 2004; Mesa and Magie 2006). In Pacific salmon, these models unequivocally assume that feeding stops when the fishes enter fresh water and thus that they have a fixed energy budget. Importantly, if Pacific salmon are not operating on a fixed energy budget, then these models may underestimate migration cost and overestimate the resilience of stocks to additional energetic stressors.

Here we document egg consumption in three species of Pacific salmon, thus overturning the conventional wisdom that feeding stops when these salmon mature. We provide four lines of evidence to document feeding behaviour in spawning Pacific salmon. First, we surveyed stomach contents of Pacific salmon from three rivers on eastern Vancouver Island, British Columbia. Second, detailed behavioural observations were taken during the breeding season on captive Chinook salmon in freshwater spawning channels. Third, feeding trials in Chinook salmon assessed the ability of mature fish to make use of energy from ingested eggs. Fourth, the stomach contents of fed salmon were sampled over time to measure the clearance times for ingested eggs and to estimate feeding rates. We discuss the consequences of these results for salmon management programs.

Materials and methods

Fish survey

Feeding behaviour was examined in three species of Pacific salmon collected from four locations (Fig. 1). These rivers represent important native habitat for salmon, with each river home to Chinook salmon, chum salmon (*Oncorhynchus keta*), coho salmon (*Oncorhynchus kisutch*), and pink salmon (*Oncorhynchus gorbuscha*), as well as steelhead (*Oncorhynchus mykiss*) and cutthroat trout (*Oncorhynchus clarkii*). Our fourth sampling location was Yellow Island Aquaculture Ltd. (YIAL), which maintains a population of Chinook salmon and an experimental spawning channel facility that allowed us to perform detailed behavioural studies and to investigate egg metabolism. The YIAL population was founded with gametes from the Robertson Creek Hatchery on Vancouver Island and has been maintained since 1986.

Stomach content in wild salmon was examined during 9 October to 6 November 2007. The salmon were collected either after they had returned to the hatchery (residing on the natal rivers) or were collected directly from the river shortly after they had died. Body mass of each fish was measured with a hand scale (female body mass excluded the mass of her eggs). The stomachs were then dissected and the numbers of eggs or whole-egg casings in the stomach were counted, and any other items were noted. Prevalence of egg consumption was compared between species, sites, and sexes using a loglinear model, with partial chi-square values used to test the associations between all combinations of individual factors. The loglinear model was analyzed using an iterative backward elimination algorithm implemented in the model selection function of SPSS (ver. 17.0; SPSS Inc., Chicago, Illinois). Body mass was compared between fish that consumed or did not consume eggs using an analysis of variance (ANOVA) that also included species and sex as factors.

Genetic analysis was used to identify the species origin for a subset of the recovered eggs. DNA was extracted from the eggs using a proteinase K digestion followed by ethanol precipitation (Neff et al. 2000). To ensure there was no cross contamination of DNA from the eggs and the host stomach, the eggs were first washed with distilled water, and the outer membrane was excised and discarded. In addition, microsatellite genotypes of a subset of eggs ($n = 6$) were compared with the genotype of the individual that consumed them to confirm that the eggs were not being contaminated with host DNA. Species were identified by amplifying the major histocompatibility complex class II gene and using restriction enzymes to identify unique digestion patterns as described by Withler et al. (1997).

During 5 October to 15 November 2006, an examination of spawning behaviour was conducted using Chinook salmon at YIAL. Mature males ($n = 110$, age = 2–4 years, mass = 0.17–5.23 kg) and mature females ($n = 81$, age = 3–5 years, mass = 1.03–4.90 kg) were transferred from sea water to six freshwater spawning channels, each 15 × 3.5 m in area with

Fig. 1. Sampling locations in British Columbia, Canada, used for stomach content analysis of three species of Pacific salmon (*Oncorhynchus* spp.). Locations: BQ, Big Qualicum River; PR, Puntledge River; QR, Quinsam River; YI, Yellow Island Aquaculture.

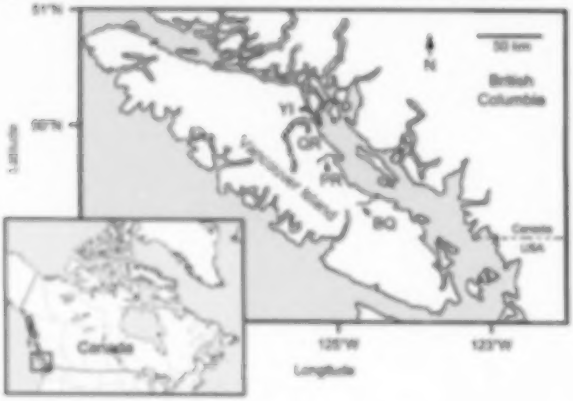

a water depth of 1 m. Behaviour was then observed continuously during daylight by two observers stationed in 5 m high towers overlooking the channels. A previous study of this population has shown typical patterns of sexual selection, with both competition and mate choice operating (Neff et al. 2008). When each fish died, it was collected from the channels and the mass and stomach content were examined as described above.

Feeding trials

Trials were conducted from 17 October to 16 November 2007 to determine if mature fish could successfully digest eggs and if energy from eggs contributed to spermatogenesis or body condition. Thirty-two mature male Chinook salmon from YIAL (mean mass = 0.57 kg, range = 0.44–0.76 kg) were transferred to four outdoor freshwater tanks (3000 L), with each tank divided evenly into two sections by a rigid screen (four fish per section, eight fish per tank). These tanks were covered by netting to exclude predators but were otherwise subject to natural patterns of light and precipitation. Tanks received a freshwater flow of approximately 10 L·min^{-1}, with a temperature of 7.5 ± 2.0 °C. Fish were allowed two days to acclimate and then were anaesthetized with buffered MS-222 (tricaine methanesulfonate) so that they could be uniquely marked by clipping the adipose or left pelvic fin, mass and fork length could be measured, and milt could be collected before returning them to the divided tanks. To avoid diluting milt with water, the area around the genital pore was dried prior to milt collection, and care was taken to avoid expressing milt accidentally during handling. Milt was collected by applying pressure to the abdomen until it was no longer readily expressed, with all collections performed by the same individual to ensure consistency. Milt samples were collected in a preweighed Styrofoam cup to measure the total mass of available milt. Spermatocrit was determined as the percentage by volume of sperm cells in the homogenized milt and was measured in triplicate using a standard protocol (Liljedal et al. 1999); approximately 60 μL of milt was drawn into a capillary tube and then centrifuged for 5 min before measuring the percentage of packed cells. Following these initial measurements, half of each tank was fed unfertilized Chinook salmon eggs twice daily (approximately 50 eggs per fish per day), whereas the other half received no eggs. At the start of the trials, fed and unfed fish did not differ in body mass, fork length, milt mass, or spermatocrit (*t* tests, all $P > 0.62$). Every seven days, fish were anaesthetized to measure body mass and collect milt. Dead fish were removed daily and noted to compare survival between groups. After 28 days, feeding was stopped and measurements were concluded, although surviving fish were maintained in fresh water for an additional two days to quantify survival.

Daily change in body mass was calculated as the natural log of final body mass (the mass on day 28 or the mass at death for fish that lived less than 28 days) minus the natural log of body mass at the start of the trials, then divided by the number of days in fresh water, and expressed as a percentage. The daily change in body mass was compared between fed and unfed fish using an ANOVA that included diet and tank as factors. To control for differences in milt production between fed and unfed fish, we also calculated daily change in body mass after adding the mass of milt collected from each fish back to their final body masses and analyzed these data as described above. Differences in spermatocrit and the mass of milt were compared between fed and unfed fish using an ANOVA that included diet, tank, and sampling date (7, 14, 21, 28 days) as factors. A log-rank survival analysis was used to compare survival between fed and unfed fish.

Egg retention

To evaluate gastric evacuation rate, force-feeding trials were performed using YIAL Chinook salmon from 10 to 17 November 2007. Mature fish (n = 108, mean mass = 1.49 kg, range = 0.26–4.00 kg) were transferred to fresh water for at least 24 h and then anaesthetized with buffered MS-222 so that 10 unfertilized, water-hardened eggs could be fed to each fish. Eggs were fed by using a rubber tube to bypass the throat sphincter, with a piston inside the tube injecting the eggs into the stomach. Fed fish were subsequently held in groups of 20 or fewer in 3000 L tanks. Tanks were located indoors with a 16 h light – 8 h dark cycle, freshwater flow of approximately 10 L·min^{-1}, and a temperature of 7.5 ± 1.0 °C. Fish were sacrificed at 0, 8, 24, 48, 96, or 168 h after the force feeding, and the stomach was removed to count the number of eggs and egg casings. Five fish were excluded from these analyses because their stomachs still contained food pellets from saltwater feeding, which could increase the retention time of fed eggs. The percentage of eggs remaining at each sampling period were fit to an exponential model of gastric evacuation (Elliott 1972). The instantaneous rate of gastric evacuation derived from this equation was then used to estimate the daily feeding rate for individuals collected in the survey of spawning fish, using daily feeding rate = 24 × stomach content × rate of gastric evacuation (Eggers 1979; Bromley 1994). We converted these estimates to energy consumption rates assuming an average egg mass of 0.29 g, which was an average of the values for Chinook, chum, and coho salmon native to Vancouver Island (Beacham and Murray 1993). For these estimates, we used a previously reported energy

density of salmon eggs (18.7 kJ·g^{-1}; 95% digestible) (Meka and Margraf 2007) and assumed that 30% of the available energy was lost through faeces (Brett 1995). Energy consumption rates were converted into a river migration distance and a duration of spawning activity using an average of the previously presented migration costs (4.56 kJ·kg^{-1}·km^{-1}) and spawning costs (145 kJ·kg^{-1}·day^{-1}) for Pacific salmon (Brett 1995). The average mass of feeding fish used in this calculation came from the individuals collected in our study and ranged from 2.18 kg in female coho salmon from the Puntledge River to 9.48 kg in male Chinook salmon from the Quinsam River.

Results

Body mass in wild fish was highest in Chinook salmon (males, 0.9–14.2 kg; females, 3.9–11.1 kg), followed by chum salmon (males, 2.3–8.4 kg; females, 2.5–4.9 kg) and coho salmon (males, 0.3–6.7 kg; females, 1.1–3.9 kg). The surveys of stomach contents showed that egg consumption occurred in all three rivers in British Columbia, but the proportion of fish that fed on eggs differed significantly among rivers (loglinear model: $\chi^2 = 34.3$, df = 2, $P < 0.001$; Table 1), as well as among species ($\chi^2 = 21.0$, df = 2, $P < 0.001$), with the highest frequency in coho salmon (21.2%) and lower levels in chum (7.1%) and Chinook (9.8%) salmon. There was, however, no difference in the prevalence of egg consumption between live fish collected at the hatcheries (16%) and dead fish collected directly from the rivers (10%) ($\chi^2 = 1.98$, df = 1, $P = 0.16$). Although occurring in both sexes, egg consumption was more frequent in females (20.7%) than in males (11.8%) ($\chi^2 = 8.50$, df = 1, $P = 0.004$). All higher-order interactions included in the model had no significant effect on the frequency of egg consumption (all $P > 0.77$). There was no significant difference in body mass between salmon that consumed eggs (mean = 4.2 kg, range = 0.3–12.9 kg) and salmon that did not consume eggs (mean = 4.7 kg, range = 0.3–14.2 kg) after controlling for differences based on sex and species (ANOVA, $F_{[1,863]} = 2.75$, $P = 0.098$). Qualitative observations during sampling suggested that digestive atrophy (thickening and hardening of the stomach) was uncommon in salmon from these rivers, as most salmon had non-occluded stomachs with thin, flexible walls.

Genetic identification determined the species origin for a subset of the recovered eggs. For 12 eggs recovered from five Chinook salmon stomachs, all of the eggs were identified as being from Chinook salmon. For 20 eggs recovered from 11 coho salmon stomachs, 18 coho salmon eggs and two Chinook salmon eggs were identified. Alternative food items were not observed in the stomach of any fish, although a small percentage of the sampled stomachs did contain stones (1.1%), wood or leaves (1.1%), plastic (0.2%), or tapeworms (1.3%).

Stomach content analysis of Chinook salmon in freshwater spawning channels similarly identified egg consumption (Table 1), whereas the behavioural observations of these fish revealed a typical feeding pattern. Egg cannibalism was observed a combined six times in two males and one female. For each observed incidence of egg cannibalism, a female was digging in an area of previous egg deposition and forced eggs upwards into the water column, at which point another fish ate them. The cannibal was always close (less than 3 m) to the area where the digging occurred and responded rapidly to the sight of the egg, capturing it before the egg settled back to the gravel. For the single female that we observed cannibalizing an egg, the event occurred in the territory of a female who was immediately adjacent and upstream to her own territory, several days after the cannibal had deposited eggs in her own nest. Although a similar pattern was seen for each of the six observed feeding events, these events account for only a small proportion of the 128 eggs recovered from the stomachs of channel fish. Thus, egg consumption may also involve other less conspicuous behaviours.

Feeding trials in Chinook salmon showed that mature fish could make use of energy from ingested eggs. Average body mass remained close to constant, with only a modest 0.8% decline in fish fed eggs for four weeks, whereas body mass declined by a more significant 19.3% in unfed fish (ANOVA, $F_{[1,27]} = 24.8$, $P < 0.001$; Fig. 2*a*). The change in mass did not differ among tanks (ANOVA, $F_{[3,27]} = 0.98$, $P = 0.42$). Spermatocrit declined significantly over time (ANOVA, $F_{[3,85]} = 3.84$, $P = 0.012$) but did not differ between fed and unfed fish (ANOVA, $F_{[1,85]} = 1.34$, $P = 0.25$; Fig. 2*b*) or between tanks (ANOVA, $F_{[3,85]} = 1.39$, $P = 0.25$). Significantly more milt was collected from unfed fish than from fed fish (ANOVA, $F_{[3,84]} = 19.5$, $P < 0.001$; Fig. 2*c*). The mass of milt that was collected increased significantly over time (ANOVA, $F_{[3,84]} = 5.32$, $P = 0.002$) and also differed among tanks (ANOVA, $F_{[3,84]} = 2.86$, $P = 0.042$). The difference in body mass was not driven by these differences in milt retention, as unfed fish still lost significantly more mass than fed fish (ANOVA, $F_{[1,28]} = 18.5$, $P < 0.001$) when the mass of expelled milt was added to final body mass. The fed fish had a longer median survival in fresh water compared with the unfed fish (29.0 days vs. 21.5 days), but the difference was not significant (survival analysis, $\chi^2 = 0.48$, df = 1, $P = 0.49$; Fig. 2*d*).

These feeding trials were also used to estimate feeding rates by comparing the change in mass between the fed and unfed fish. Unfed fish lost an average of 0.763% body mass per day, whereas fed fish lost an average of 0.029% body mass per day, indicating that feeding provided a daily benefit equivalent to 0.734% body mass to the fed fish. Assuming a standard energy content for body mass of 6 kJ·g wet mass^{-1} as in other salmonids (Meka and Margraf 2007) and an average observed mass of 565 g for fed fish, this represents an average energy gain of 25 kJ·day^{-1} in the fed fish. As salmon eggs contain approximately 18.7 kJ·g wet mass^{-1}, with 95% of that energy digestible (Meka and Margraf 2007), and assuming that 30% of the available energy is lost through faeces (Brett 1995), this suggests that the fed fish were consuming on average 2.0 g of eggs per day, which at an average egg mass of 0.27 g measured at YIAL, represents an average feeding rate of 7 eggs·day^{-1}. This estimate is consistent with estimates from feeding fish derived from the natural-stream stomach surveys (see below).

Measuring the clearance time for ingested eggs revealed that 85% of the eggs were cleared within two days of ingestion (Fig. 3). Based on these data, we calculated the rate of gastric evacuation and, as in Eggers (1979), used this rate in

Table 1. Numbers of Pacific salmon (*Oncorhynchus* spp.) consuming eggs and the estimated mean feeding rates for these fish.

			Stomach content			Feeding rate (eggs·day^{-1})	
Species	Location	Sex	Present	Absent	%	All fish	Feeding fish
Chum	Big Qualicum River	Female	0	11	0.0	0.00	—
		Male	3	28	9.7	0.13	1.37
Coho	Puntledge River	Female	1	38	2.6	0.03	1.03
		Male	1	31	3.1	0.03	1.03
	Quinsam River	Female	25	37	40.3	1.69	4.19
		Male	24	84	22.2	3.20	14.38
Chinook	Big Qualicum River	Male	0	26	0.0	0.00	—
	Quinsam River	Female	13	63	17.1	0.36	2.13
		Male	5	77	6.1	0.11	1.85
	Yellow Island channels	Female	0	76	0.0	0.00	—
		Male	14	93	13.1	1.21	9.24
Total			86	564	13.2	0.96	7.24

Fig. 2. Changes in (*a*) body mass, (*b*) spermatocrit, (*c*) total milt mass, and (*d*) survival in fed and unfed Chinook salmon (*Oncorhynchus tshawytscha*). Fish were repeatedly sampled every 7 days during the 28-day feeding period, with survival measurements continuing for an additional 2 days after feeding stopped. Changes in body mass were calculated on day 28, or at the time of death for fish that survived less than 28 days. Spermatocrit was measured as the percentage of sperm cells by volume in the milt. Means are presented with ± 1 standard error (SE) for fed fish (solid symbols and solid bars) and unfed fish (open symbols and open bars). Survival is reported as the proportion of fed fish (broken line) and unfed fish (solid line) that were alive on each day. Significant differences between fed and unfed fish are indicated with asterisks.

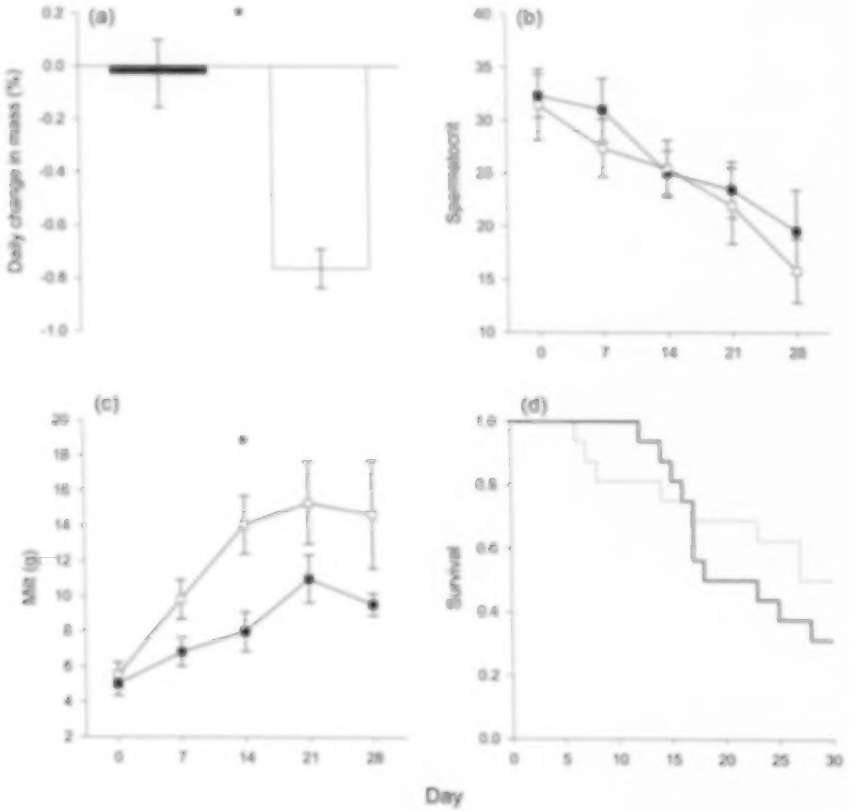

Fig. 3. Proportion of a standard meal remaining over time in Chinook salmon (*Oncorhynchus tshawytscha*) that were force-fed 10 eggs. Mean proportions of eggs remaining in the stomach are reported with ± 1 standard error (SE). The line is from a regression modelling exponential evacuation of stomach contents and has the equation: stomach content = $94.22 \cdot e^{-0.042(\text{time})}$ ($r^2 = 0.59$, $n = 108$, $P < 0.001$).

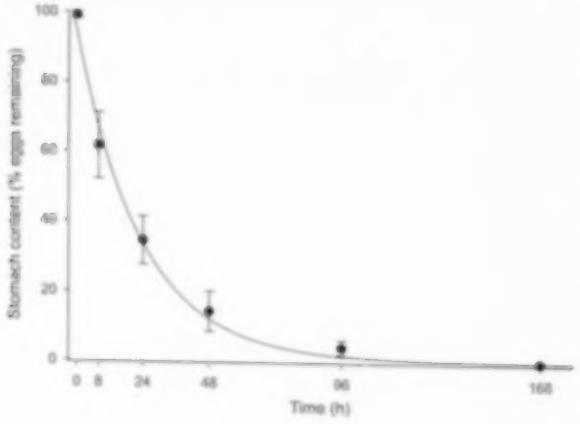

combination with the number of eggs recovered in the survey of spawning fish to estimate daily feeding rates (Table 1). Mean feeding rates ranged from 0 to 1.7 eggs·day^{-1} in female salmon and from 1 to 4 eggs·day^{-1} in females that were observed feeding. These feeding rates correspond to a mean energy gain of 0–6.1 kJ·day^{-1} in female salmon and 3.7–15.1 kJ·day^{-1} in females that were observed feeding. Mean feeding rates ranged from 0 to 3.2 eggs·day^{-1} in male salmon and from 1 to 14 eggs·day^{-1} in males that were observed feeding. These feeding rates correspond to a mean energy gain of 0–11.5 kJ·day^{-1} in male salmon and 3.7–51.9 kJ·day^{-1} in males that were observed feeding.

Discussion

Egg consumption appears to be common in spawning Pacific salmon. Pacific salmon are thus consistent with a number of other salmonids that also consume eggs during spawning, including brook trout (*Salvelinus fontinalis*) (White 1930; Greeley 1932; Blanchfield and Ridgway 1999), Miyabe char (*Salvelinus malma miyabei*) (Maekawa and Hino 1987), Atlantic salmon (Jones and King 1950), and rainbow trout (Greeley 1932). In our study, we identified egg consumption in all three rivers and in each of the three species that we examined. Overall, we recovered eggs in 13% of the stomachs that we sampled, and prevalence was highest in coho salmon from the Quinsam River at 27%. These estimates are conservative as force-feeding experiments in Chinook salmon revealed that 85% of ingested eggs were cleared from the stomach within two days. Thus, we would detect only eggs consumed within about two days and may miss eggs consumed more sporadically during the spawning season. Therefore, the prevalence of egg consumption is likely a minimum estimate for our sample populations.

Mature salmon can benefit from consuming eggs. We showed that fed salmon could use the energy from ingested eggs to maintain higher body mass than unfed fish. This increased mass may enable feeding fish to maintain high levels of activity associated with spawning behaviour (Brett 1995). Surprisingly, fed fish produced less milt than unfed fish, which suggests that feeding did not contribute to sperm production. Survival was also not significantly higher in fed fish than unfed fish, but our study maintained fish in a benign environment relative to spawning grounds where energetic limitations may have a greater impact on survival. Regardless of the exact benefits of egg consumption, the reduced rate of body mass loss in the fed fish clearly supports the ability of mature salmon to digest eggs.

Here we have demonstrated a serious error in the understanding of Pacific salmon breeding ecology — feeding does not stop upon the return to fresh water. Thus, the ubiquitous assumption of a fixed energy budget is false and may result in an underestimate of the actual cost of migration and spawning. Given that Pacific salmon stocks show high natal philopatry, it is also possible that many stocks have evolved local adaptations to their specific migration and spawning requirements that include nutrients from salmon eggs. Such a dependence on supplemental energy from freshwater feeding could explain why some stocks fail to recover even when released from fishing pressure, as lower abundances of salmon may remove feeding opportunities that some stocks depend on to successfully complete migration and spawning. Indeed, using the energy gains that we estimated for feeding salmon and previous estimates of the energetic costs of migration and spawning in Pacific salmon (Brett 1995), the females that we examined could migrate an additional 0.25–1.15 km per day of feeding or extend the duration of spawning activity by 0.7%–3.6%. Similarly, the males that we examined could migrate an additional 0.15–3.83 km per day of feeding or extend the duration of spawning activity by 0.4%–12%. Pacific salmon may require this supplemental energy for successful migration and spawning.

Pacific salmon stocks may need to be managed within an integrated framework. We found that 10% of the ingested eggs in coho salmon, which typically migrate and spawn shortly after the other salmon (Quinn 2005), were from Chinook salmon. This 10% represents about 5 kJ·day^{-1} and suggests that some species may depend on nutrients acquired from the eggs of previously arriving fish to complete their own maturation. Thus, salmon conservation efforts may need to preserve not only spawning habitat and migration corridors, but also feeding opportunities.

In conclusion, our observations of egg consumption provide a novel insight into the freshwater ecology of the Pacific salmon. These data are in direct contradiction to the fixed energy budget universally assumed for spawning Pacific salmon. These findings also suggest interesting new directions for study, as the benefits of feeding for spawning fish, the prevalence of egg consumption prior to reaching the spawning grounds, and the temporal and geographic patterns of egg consumption remain to be determined.

Acknowledgements

We thank A. Heath, G. Heath, K. Beauchamp, K. Jones, and the staff of the Big Qualicum, Quinsam, and Puntledge

hatcheries for assistance with experiments. D. Heath, T. Pitcher, H. Suk, T. Hain, R. Breckels, M. Evans, and two anonymous reviewers provided valuable comments on the manuscript. Yellow Island Aquaculture Limited and the Natural Sciences and Engineering Research Council of Canada provided funding.

References

Battin, J., Wiley, M.W., Ruckelshaus, M.H., Palmer, R.N., Korb, E., Bartz, K.K., and Imaki, H. 2007. Projected impacts of climate change on salmon habitat restoration. Proc. Natl. Acad. Sci. U.S.A. **104**(16): 6720–6725. doi:10.1073/pnas.0701685104. PMID:17412830.

Beacham, T.D., and Murray, C.B. 1993. Fecundity and egg size variation in North American Pacific salmon (*Oncorhynchus*). J. Fish Biol. **42**(4): 485–508. doi:10.1111/j.1095-8649.1993.tb00354.x.

Blanchfield, P.J., and Ridgway, M.S. 1999. The cost of peripheral males in a brook trout mating system. Anim. Behav. **57**(3): 537–544. doi:10.1006/anbe.1998.1014. PMID:10196043.

Brett, J.R. 1995. Energetics. *In* Physiological ecology of Pacific salmon. *Edited by* C. Groot, L. Margolis, and W.C. Clarke. University of British Columbia Press, Vancouver, B.C. pp. 3–68.

Bromley, P.J. 1994. The role of gastric evacuation experiments in quantifying the feeding rates of predatory fish. Rev. Fish Biol. Fish. **4**(1): 36–66. doi:10.1007/BF00043260.

Bullivant, J.S. 1959. Stomach contents of spawning quinnat salmon. Nature (London), **184**: 71. doi:10.1038/184071a0.

Crossin, G.T., Hinch, S.G., Farrell, A.P., Higgs, D.A., Lotto, A.G., Oakes, J.D., and Healey, M.C. 2004. Energetics and morphology of sockeye salmon: effects of upriver migratory distance and elevation. J. Fish Biol. **65**(3): 788–810. doi:10.1111/j.0022-1112.2004.00486.x.

Eggers, D.M. 1979. Comment on some recent methods for estimating food consumption by fish. J. Fish. Res. Board Can. **36**: 1018–1019.

Elliott, J.M. 1972. Rates of gastric evacuation in brown trout, *Salmo trutta* L. Freshw. Biol. **2**(1): 1–18. doi:10.1111/j.1365-2427.1972.tb01575.x.

Elliott, J.M. 1997. Stomach contents of adult sea trout caught in six English rivers. J. Fish Biol. **50**: 1129–1132. doi:10.1111/j.1095-8649.1997.tb01638.x.

Food and Agriculture Organisation of the United Nations. 2007. Capture production 1950–2005. FAO Fisheries Information and Statistics Service, Rome, Italy.

Gilhousen, P. 1980. Energy sources and expenditures in Fraser river sockeye salmon during their spawning migration. International Pacific Salmon Fisheries Commission, Bulletin XXII, New Westminster, B.C.

Greeley, J.R. 1932. The spawning habits of brook, brown and rainbow trout and the problem of egg predators. Trans. Am. Fish. Soc. **62**(1): 239–248. doi:10.1577/1548-8659(1932)62[239:TSHOBB]2.0.CO;2.

Greene, C.W. 1926. The physiology of the spawning migration. Physiol. Rev. **6**: 201–241.

Gustafson, R.G., Waples, R.S., Myers, J.M., Weitkamp, L.A., Bryant, G.J., Johnson, O.W., and Hard, J.J. 2007. Pacific salmon extinctions: quantifying lost and remaining diversity. Conserv. Biol. **21**(4): 1009–1020. doi:10.1111/j.1523-1739.2007.00693.x. PMID:17650251.

Higgs, D.A., MacDonald, J.S., Levings, C.D., and Dosanjh, B.S. 1995. Nutrition and feeding habits in relation to life history stage. *In* Physiological ecology of Pacific salmon. *Edited by* C. Groot, L. Margolis, and W.C. Clarke. UBC Press, Vancouver, British Columbia. pp. 159–315.

Johansen, M. 2001. Evidence of freshwater feeding by adult salmon in the Tana River, northern Norway. J. Fish Biol. **59**(5): 1405–1407. doi:10.1111/j.1095-8649.2001.tb00201.x.

Jones, J.W., and King, G.M. 1950. Further experimental observations on the spawning behaviour of the Atlantic salmon (*Salmo salar* Linn.). Proc. Zool. Soc. Lond. **120**: 217–223.

Jonsson, B., and Gravem, F.R. 1985. Use of space and food by resident and migrant brown trout, *Salmo trutta*. Environ. Biol. Fishes, **14**(4): 281–293. doi:10.1007/BF00002633.

Kareiva, P., Marvier, M., and McClure, M. 2000. Recovery and management options for spring/summer chinook salmon in the Columbia River basin. Science (Washington, D.C.), **290**(5493): 977–979. doi:10.1126/science.290.5493.977. PMID:11062128.

Levin, P.S., and Tolimieri, N. 2001. Differences in the impacts of dams on the dynamics of salmon populations. Anim. Conserv. **4**: 291–299. doi:10.1017/S1367943001001342.

Liljedal, S., Folstad, I., and Skarstein, F. 1999. Secondary sex traits, parasites, immunity and ejaculate quality in the Arctic charr. Proc. R. Soc. B Biol. Sci. **266**: 1893–1898. doi:10.1098/rspb.1999.0863.

Maekawa, K., and Hino, T. 1987. Effect of cannibalism on alternative life histories in charr. Evolution, **41**(5): 1120–1123. doi:10.2307/2409196.

Meka, J.M., and Margraf, F.J. 2007. Using a bioenergetic model to assess growth reduction from catch-and-release fishing and hooking injury in rainbow trout, *Oncorhynchus mykiss*. Fish. Manag. Ecol. **14**(2): 131–139. doi:10.1111/j.1365-2400.2007.00533.x.

Mesa, M.G., and Magie, C.D. 2006. Evaluation of energy expenditure in adult spring Chinook salmon migrating upstream in the Columbia River Basin: an assessment based on sequential proximate analysis. River Res. Appl. **22**(10): 1085–1095. doi:10.1002/rra.955.

Neff, B.D., Fu, P., and Gross, M.R. 2000. Microsatellite multiplexing in fish. Trans. Am. Fish. Soc. **129**(2): 584–593. doi:10.1577/1548-8659(2000)129<0584:MMIF>2.0.CO;2.

Neff, B.D., Garner, S.R., Heath, J.W., and Heath, D.D. 2008. The MHC and non-random mating in a captive population of Chinook salmon. Heredity, **101**(2): 175–185. doi:10.1038/hdy.2008.43. PMID:18506203.

Parrish, D.L., Behnke, R.J., Gephard, S.R., McCormick, S.D., and Reeves, G.H. 1998. Why aren't there more Atlantic salmon (*Salmo salar*)? Can. J. Fish. Aquat. Sci. **55**(Suppl. 1): s281–s287. doi:10.1139/cjfas-55-S1-281.

Quinn, T.P. 2005. The behaviour and ecology of Pacific salmon and trout. University of Washington Press, Seattle, Washington.

Rand, P.S., Hinch, S.G., Morrison, J., Foreman, M.G.G., MacNutt, M.J., Macdonald, J.S., Healey, M.C., Farrell, A.P., and Higgs, D.A. 2006. Effects of river discharge, temperature, and future climates on energetics and mortality of adult migrating Fraser River sockeye salmon. Trans. Am. Fish. Soc. **135**(3): 655–667. doi:10.1577/T05-023.1.

Rikardsen, A.H., Amundsen, P.A., and Bodin, P.J. 2003. Growth and diet of anadromous Arctic charr after their return to freshwater. Ecol. Freshwat. Fish, **12**(1): 74–80. doi:10.1034/j.1600-0633.2003.00001.x.

Rutter, C. 1903. Natural history of the Quinnat salmon. A report of investigations in the Sacramento River, 1896–1901. Bull. U.S. Fish. Comm. **22**: 65–141.

Takami, T., Murakami, Y., and Mori, M. 1996. Growth and feeding habits of anadromous white-spotted charr (*Salvelinus leucomae-*

nis) in southwestern Hokkaido, Japan. Sci. Rep. Hokkaido Fish Hatchery, **50**: 37–44.

Waples, R.S., Zabel, R.W., Scheuerell, M.D., and Sanderson, B.L. 2008. Evolutionary responses by native species to major anthropogenic changes to their ecosystems: Pacific salmon in the Columbia River hydropower system. Mol. Ecol. **17**(1): 84–96. doi:10.1111/j.1365-294X.2007.03510.x. PMID:18268786.

White, H.C. 1930. Some observations on the eastern brook trout (*S. fontinalis*) of Prince Edward Island. Trans. Am. Fish. Soc. **60**(1): 101–108. doi:10.1577/1548-8659(1930)60[101:SOOTEB]2.0.CO;2.

Withler, R.E., Beacham, T.D., Ming, T.J., and Miller, K.M. 1997. Species identification of Pacific salmon by means of a major histocompatibility complex gene. N. Am. J. Fish. Manage. **17**(4): 929–938. doi:10.1577/1548-8675(1997)017<0929:SIOPSB>2.3.CO;2.

A Bayesian mark–recapture model for multiple-recapture data in a catch-and-release fishery

Rebecca Whitlock and Murdoch McAllister

Abstract: This paper extends a state–space Bayesian mark–recapture framework to multiple-recapture data to estimate fishery-specific capture and mortality rates and seasonal movement rates for fish in different length classes. The methodology is applied to tag recapture data for white sturgeon (*Acipenser transmontanus*) collected in the recreational fishery and the Canadian Department of Fisheries and Ocean's test fishery at Albion in the lower Fraser River. Significant differences were found between some estimated movement rates by season and length class, supporting the notion of there being marked differences in seasonal movement patterns between different life history stages of *A. transmontanus* in the lower Fraser River. Uncertainty in the tag reporting rate parameter, quantified using a recreational creel sampling program, is summarized by a prior distribution. The utility of recreational fishing effort as a model covariate in accounting for seasonal and spatial variation in recapture rates is addressed using Bayesian model evaluation criteria. The data provide strong support in favour of models that include fishing effort as a covariate. The appropriate level of stratification for the recreational catchability parameter q is assessed using Bayesian model evaluation criteria; models in which q is estimated by season and length class have the highest posterior probabilities.

Résumé : Notre travail élargit le cadre état–espace bayésien de marquage–recapture aux données de recaptures multiples afin d'estimer les taux de capture et de mortalité spécifiques à une pêche donnée, ainsi que les taux de déplacements saisonniers des poissons des différentes classes de longueur. Nous appliquons la méthodologie à des données de récupération des étiquettes de l'esturgeon blanc (*Acipenser transmontanus*) obtenues lors de la pêche sportive, de même que lors de la pêche expérimentale du ministère canadien des Pêches et Océans, à Albion sur le cours inférieur du fleuve Fraser. Il existe des différences significatives entre certains taux estimés de déplacements en fonction de la saison et de la classe de longueur, ce qui appuie l'idée qu'il y a des différences importantes dans les patrons de déplacements saisonniers au cours des différents stades du cycle biologique d'*A. transmontanus* dans le Fraser inférieur. L'incertitude reliée au paramètre du taux de retour des étiquettes, calculé d'après un programme d'enquêtes auprès des pêcheurs, est résumée par une distribution a priori. L'utilité de l'effort de pêche sportive comme covariable du modèle pour tenir compte de la variation saisonnière et spatiale des taux de recapture est déterminée à l'aide de critères bayésiens d'évaluation des modèles. Les données appuient fortement les modèles qui incluent l'effort de pêche comme l'une des covariables. Le niveau approprié de stratification du paramètre de capturabilité à la pêche sportive q est estimé à l'aide de critères bayésiens d'évaluation des modèles; les modèles dans lesquels q est estimé en fonction de la saison et de la classe de longueur possèdent les probabilités a posteriori les plus élevées.

[Traduit par la Rédaction]

Introduction

Variation in the spatial distribution and seasonal migration patterns of anadromous fish stocks resulting from life history stage specific patterns of habitat utilization may be an important feature of their population dynamics. Fishing effort is usually spatially heterogeneous and may be directed at aggregations of migratory fish that are predictable in space and time (Neis et al. 1999; Stöcker 1999). While there have been a growing number of applications of spatially structured stock assessment models (e.g., International Commission for the Conservation of Atlantic Tunas 2003; Inter-American Tropical Tuna Commission 2008), their application is still far from common practice owing to limitations in data to support such modelling efforts and relatively few available methodologies. The development and application of models that account for spatial heterogeneities in habitat use and fisheries targeting offer to provide more accurate estimates of exploitation rates (Die et al. 1990) and more useful advice for the management of highly migratory stocks.

Received 29 September 2008. Accepted 29 April 2009. Published on the NRC Research Press Web site at cjfas.nrc.ca on 2 September 2009.
J20798

Paper handled by Associate Editor Ray Hilborn.

R. Whitlock.[1,2] Division of Biology, Imperial College London, South Kensington Campus, London SW7 2AZ, UK.
M. McAllister. Fisheries Centre, Aquatic Ecosystems Research Laboratory, 2202 Main Mall, The University of British Columbia, Vancouver, BC V6T 1Z4, Canada.

[1]Corresponding author (e-mail: whitlock@iiasa.ac.at).
[2]Present address: International Institute for Applied Systems Analysis, Schlossplatz 1, Laxenburg, Austria A-2361.

Information on demographic parameters, including spatially related ones, such as seasonal- and (or) age-specific migration rates, is a requisite for the assessment and management of human activities impacting highly migratory fish and wildlife populations (Pine et al. 2003; Brooks et al. 2004). Mark–recapture methods provide a concise framework for estimation of survival rates, population abundance, and, depending on tagging study design, movement rates (Otis et al. 1978; Seber 1982; Pine et al. 2003). Where there is large uncertainty in population status and demographic parameters, the Bayesian approach allows incorporation of additional qualitative and quantitative data elicited from experts or taken from other populations, stocks, or species (Punt and Hilborn 1997; Malakoff 1999; Michielsens et al. 2008). For this reason, it may be a suitable methodology for stock assessments of populations of conservation concern for which commercial fishery or survey data are often unavailable and whose abundance and productivity are often highly uncertain.

The importance of accounting for uncertainty in the structural formulation of stock assessment models has gained increasing recognition among fisheries scientists, as the management policy identified as the "best" in simulation evaluations often depends on the model structure assumed (Patterson 1999; Parma 2001; McAllister and Kirchner 2002). Identifying the appropriate level of stratification for estimation of model parameters is important to account for the main sources of variation in recapture data and avoid parameter redundancy. Model selection methods have been used to compare hypotheses regarding the seasonal and annual dependency of movement rates estimated using mark–recapture data (Sibert et al. 1999). Anganuzzi et al. (1994) used Akaike's information criterion (Akaike 1974) to compare models with one-time or annual movement and those in which selectivity was estimated or fixed. Akaike's information criterion may be interpreted as a measure of a model's ability to predict a replicate data set with the structure of that observed. However, it does not provide a measure of the relative credibilities of alternative model structures. Bayesian mark–recapture modelling permits computation of Bayes' posterior probability for each alternative model, a summary of the empirical support for each alternative hypothesis about model structure. It therefore offers a conceptually intuitive way of testing for dependency of estimates of key population parameters including mortality rates and movement rates for tagged cohorts on covariates such as fish length, season, and fishing effort.

This paper extends the state–space Bayesian mark–recapture framework (Michielsens et al. 2006, 2008) to multiple-recapture data to estimate seasonal movement rates for two size classes of tagged white sturgeon (*Acipenser transmontanus*) between three serial sections of the lower Fraser River, British Columbia. The Bayesian modelling framework also facilitates incorporation of a prior probability density function (pdf) (or "prior") for the tag reporting rate based on sampling of recreational catches in the Fraser River sport fishery (Whitlock 2007). Process error in survival rates is incorporated through the use of an error term with a variance dependent on the length of the model time step (Michielsens 2003). Observation error is incorporated through the use of a negative binomial probability model. The potential accuracy of the model under a variety of conditions is evaluated using data simulated from a model with known structure and parameter values. Model structural uncertainty in the level of aggregation for recreational catchability parameters is explored by calculating Bayes' factors, which summarize the weight of evidence for alternative statistical models. Bayesian model evaluation criteria are also applied to evaluate the utility of recreational fishing effort as a covariate for seasonal catchabilities in the recreational fishery.

Materials and methods

Fraser River sturgeon fishery and data collection

Data for mark–recapture analyses were obtained from the Fraser River Sturgeon Conservation Society, whose passive integrated transponder (PIT) tagging programme supplies volunteering recreational anglers and angling guides with tags and hand-held scanners as well as data sheets to record tagging events. At the time of writing, over 30 000 tags had been applied within a study area spanning about 185 km of the river from the Fraser River estuary (at the Strait of Georgia) to the Fraser Canyon (at Yale). Of these, more than 8600 had been recaptured.

The Canadian Department of Fisheries and Oceans' salmon test fishery at Albion also participates in the programme, tagging and recording recapture information for sturgeon incidentally captured in its daily drift net sets. Recapture covariates recorded under the Fraser River Sturgeon Conservation Society's programme include the date, river kilometre, length at capture/recapture, and a condition code based on the fish's appearance and behaviour at release. Thus, it is possible to construct a seasonally and spatially structured model that tracks released cohorts of sturgeon of a certain length class over the duration of the tagging programme. Fishing effort is also recorded by most anglers participating in the PIT tagging programme in units of rod hours (number of fishing rods multiplied by hours fished). The quality of all field and data collection activities was regularly monitored to ensure that programme integrity and data reliability were maintained at a high level (Nelson et al. 2004).

Owing to the voluntary participation in the tagging programme, sampling is concentrated in areas of high fishing effort, which results in a strong seasonal and spatial pattern in sampling intensity within a year (Fig. 1). Multiple-recapture data can be used to estimate size- and season-specific movement rates based on subsequent recapture locations of individuals from each cohort of tagged fish released. Fork lengths of fish captured in the recreational fishery between 2000 and 2004 ranged from 24 to 343 cm (Fig. 2) with a modal length of 78 cm. Times to recapture over the same period were distributed between 1 day and 4 years and 10 months with a mean time to recapture of 9.5 months. Times at large display a strongly cyclical pattern (Fig. 3) with a period of 1 year, which is consistent with the seasonal pattern in fishing effort.

Bayesian mark–recapture models

The stage-structured Bayesian mark–recapture models describe the seasonal movement, mortality, growth, and capture of tagged fish in the recreational fishery. The estimated

Fig. 1. Yearly distribution of fishing effort in model areas 1 (downstream) to 3 (upstream). Solid line, area 1; dashed line, area 2; dotted line, area 3.

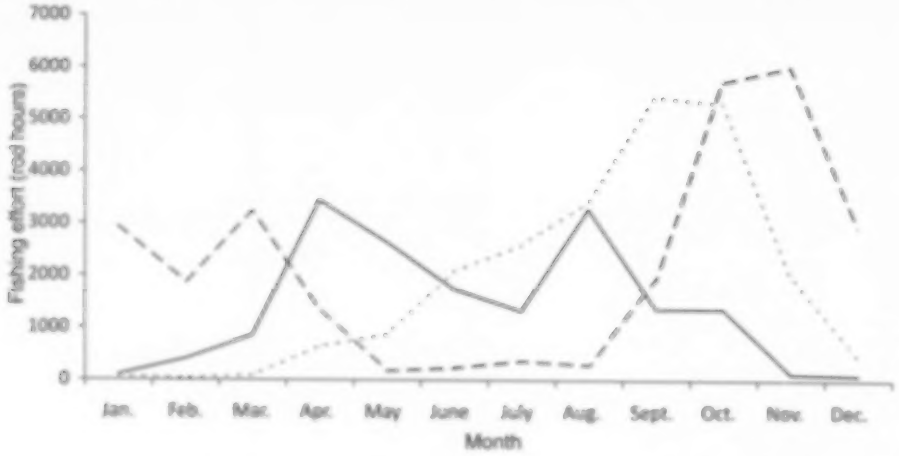

Fig. 2. Length-frequency distribution of white sturgeon captured in the recreational fishery.

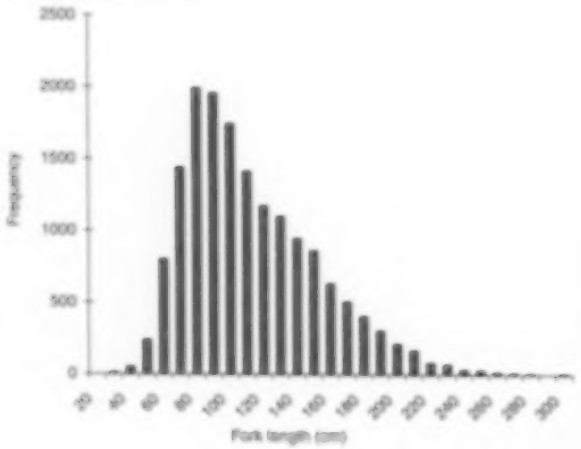

mortality rate term (β) is a composite of several sources of mortality or apparent mortality, including tag loss or malfunction, natural mortality, permanent emigration from the study area where tagging is conducted, and residual fishing mortality (i.e., for fisheries for which a mortality rate is not estimated in the model such as bycatch mortality in First Nations fisheries and illegal harvest). Each cohort of fish released in a given year, season, and area, and at a given length class at release is modelled discretely and independently of other release cohorts. Movement in any time step is assumed to be independent of all prior locations except that in the previous time step, i.e., first-order Markovian. It is assumed that there is no permanent emigration from the study site for the duration of the mark–recapture experiment; telemetry studies have reported low rates of emigration from the lower Fraser River (RL&L Environmental Services Ltd. 2000). No assumptions are made about the way an animal moves from area i at time t to area j at time $t + 1$. Direct movement between strata is thus not identifiable from a movement vector with a number of intermediate movements that ends in area j at $t + 1$. Growth between length classes is modelled as a Bernoulli process. Mark–recapture models had two length classes (length class 1, <110 cm fork length; length class 2, ≥110 cm fork length), two seasons (season 1, January–June; season 2, July–December), and three areas, with area 1 corresponding to the downstream area and area 3 to the upstream area. The test fishery at Albion is located in downstream area 1.

The number of reported recaptured tags in each time, area, and size stratum from releases in a given time, area, and size stratum is assumed to follow a negative binomial distribution. The negative binomial distribution has a variance no less than its mean and can describe the overdispersion or clustering of recapture events. It can therefore be suitable for situations where random mixing of fish in space does not occur so that recapture events are not independent. The overdispersion parameter used in the mark–recapture model has a direct biological interpretation as a measure of the tendency for schooling in tagged white sturgeon. A parameterization of the negative binomial pdf for the number of recaptures r given parameter vector θ in terms of the mean m and overdispersion parameter τ was used (Hilborn and Mangel 1997):

$$(1) \qquad p(r|\theta) = \frac{\Gamma(\tau + r)}{\Gamma(\tau) r!} \left(\frac{\tau}{\tau + m}\right)^{\tau} \left(\frac{m}{m + \tau}\right)^{r}$$

The larger the value of the overdispersion parameter, the more closely the negative binomial distribution approximates the Poisson distribution. The m and τ parameterization of the negative binomial distribution used for WinBUGS mark–recapture models was provided by Samu Mäntyniemi (Department of Biological and Environmental Sciences, University of Helsinki, FIN-00014 Helsinki, Finland).

For notational simplicity, year, season, area, and length class subscripts for individual release cohorts are omitted from the following equations. The number of tagged fish in length class b in area k at the beginning of season w in year y is given by

Fig. 3. Frequency distribution of days at large for tagged fish.

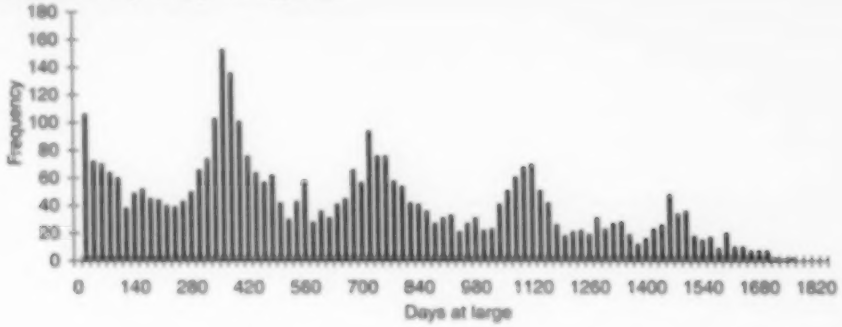

$$(2) \quad N_{y,w,k,b} = \sum_{j=1}^{J} N_{y,w-1,j,b} p_{w,j,k,b} V_b$$

where $N_{y,w-1,j,b}$ is the number of tagged fish after fishing and mortality in season $w - 1$, area j, and length class b, $p_{w,j,k,b}$ is the probability of movement from area j to area k in season w for tagged fish in length class b, and V_b is a correction factor for the increase in the mean vulnerability of closed cohorts of tagged fish over time, necessary because of the coarse length classes used in the model. It is equal to 1 plus the estimated average increase in vulnerability at length in one model time step for length class b.

The number of tagged fish in length class c surviving after incidental fishing mortality and nontagging-related mortality in season w and area k is given by

$$(3) \quad N_{y,w,k,c} = \sum_{b=1}^{B} N_{y,w,k,b}(1 - \psi_b) e^{-F_{R,y,w,k}} e^{-F_{A,y,w,k}} e^{-\beta_b/s} \varepsilon_b$$

where $e^{-F_{R,y,w,k}}$ is the survival rate in the recreational fishery, $e^{-F_{A,y,w,k}}$ is the survival rate in the Albion test fishery, $e^{-\beta_b/s}$ is the survival rate from nontagging-related mortality for length class b, and the denominator s scales annual mortality to its seasonal equivalent. For example, for a 6 month time step, $s = 2$. The term $1 - \psi_b$ is the probability of growing out of length class b to the next length class (ψ_b is the residency probability for length class b). The total number of length classes, B, is equal to 2. ε_b is the process error term with variance dependent on the length of the time step and the mortality rate β. The prior distribution for process error in survival rates has a uniform distribution around 1 (Michielsens 2003).

Recreational and Albion test fishery mortality rates $F_{R,y,w,k,b}$ and $F_{A,y,w,b}$ are given by

$$(4) \quad F_{R,y,w,k,b} = \rho_R q_{R,w,b} E_{R,y,w,k}$$

$$(5) \quad F_{A,y,w,b} = \rho_A q_{A,w,b}{}^{\Delta} E_{A,y,w}$$

where ρ_R and ρ_A are rates of capture-induced mortality in the recreational and Albion test fisheries, respectively, expressed as a proportion of the harvest rate in each fishery.

Recaptures in the recreational fishery

The reported catch in the recreational fishery of tagged fish in release season w, area k, and length class c is given by

$$(6) \quad C_{R,y,w,k,c} = N_{y,w,k,c} H_{R,y,w,k,c} \lambda_R$$

where λ_R is the PIT tag detection and reporting rate for the recreational fishery. $H_{R,y,w,k,c}$ is the harvest rate for the recreational fishery in year y and season w and area k for tagged fish in length class c:

$$(7) \quad H_{R,y,w,k,c} = 1 - e^{-q_{R,w,c} E_{R,y,w,k}}$$

where $q_{R,w,c} E_{R,y,w,k}$ is the fishery capture rate in year y, season w, and area k for length class c, $q_{R,w,c}$ is the catchability coefficient of tagged fish in length class c and season w, and $E_{R,y,w,k}$ is the recreational fishing effort in year y, season w, and area k in rod hours. For models that did not use fishing effort as a covariate, $H_{R,y,w,k,c}$ was replaced by capture probability $\varphi_{R,y,w,k,c}$.

Recaptures in the Albion test fishery

The reported catch in the Albion test fishery of tagged fish in release year y, season w, and length class c is given by

$$(8) \quad C_{A,y,w,c} = N_{y,w,1,c} H_{A,y,w,c} \lambda_A$$

where λ_A is the detection or reporting rate for tags captured in the Albion test fishery. $H_{A,y,w,c}$ is the Albion test fishery harvest rate in year y and season w for length class c:

$$(9) \quad H_{A,y,w,c} = 1 - e^{-q_{A,w,c} E_{A,y,w}}$$

where $q_{A,w,c} E_{A,y,w}$ is the capture rate of tagged fish in the Albion test fishery in year y and season w for length class c, $q_{A,w,c}$ is the Albion specific catchability coefficient of tagged fish in length class c in season w, and $E_{A,y,w}$ is the test fishery fishing effort in year y and season w.

Growth parameters were calculated using age–length data in conjunction with mark–recapture data. Age–length data were available for 282 sturgeon sampled from the lower Fraser River stock group (RL&L Environmental Services Ltd. 2000) in addition to data for 958 juvenile sturgeon (Lane and Rosenau 1995). Priors for von Bertalanffy growth coefficient (κ) and asymptotic length (L_∞) parameters were based on estimates of these parameters and their associated variances for other *A. transmontanus* stocks (Semakula and Larkin 1968; Beamesderfer et al. 1995; DeVore et al. 1995).

Priors were first updated with the age–length data and the resulting posteriors used as prior pdfs in a time at large model for the PIT tagging mark–recapture data (Fig. 4), where the length of fish captured at time t is given by

$$(10) \qquad L_t = L_R + (L_\infty - L_R)(1 - e^{-k\Delta t})$$

where L_t is length at time t, L_R is length at release, and Δt is time at large. Posterior means and standard deviations for age–length and PIT tagging data are provided in Table 1.

Bayesian mark–recapture model priors

Prior probability distributions are assigned to population dynamics parameters (survival rates, length class transition rates, and seasonal movement coefficients between three reaches of the lower Fraser) and parameters related to the recreational fishery and tagging process (catchabilities in the recreational fishery, PIT tag reporting rates for the recreational fishery and Albion test fishery, capture/handling mortality rates, and negative binomial distribution overdispersion parameters for both fisheries) (Table 2). Where no additional data were available, priors were specified to be relatively uninformative with respect to estimated quantities of interest, reflecting a high degree of uncertainty in their true value. This approach has been recommended (Punt and Hilborn 1997) where there is no information (e.g., expert judgement or data from other stocks or species) available to support the use of informative priors. Priors based on additional data included the PIT tag reporting rate, length class transition probabilities, and angling mortality rate. A prior was formulated for the PIT tag reporting rate using data collected during a sampling programme of recreational catches (Whitlock 2007). This study involved duplicate scanning of captured fish by an observer aboard recreational fishing vessels during two seasons (May–July 2004 and October–November 2006) where fishers were not aware of the observer's data collection purpose. To formulate the prior, a vague beta distribution was updated with the observer study tag reporting data; hence, the precision of the posterior for the reporting rate is empirically based. The resulting beta distribution had 2.5th and 97.5th percentiles of 0.77 and 0.98, respectively.

The rate of tagging-induced mortality has not been reported for the Fraser River programme; it is likely to be low, since tagging is a fairly brief process and PIT tags are very small relative to the body size of most fish captured in the recreational fishery. Tagging mortality is treated as a component of capture-induced mortality in the recreational fishery. The tag shedding rate is also unquantified, although it is thought to be negligible over the short term owing to the fact that PIT tags are implanted well beneath the skin. Tag malfunction and expiry are likely to be more important considerations for this tagging programme.

The prior for growth from the first to the second length class was based on the average expected proportion of individuals that would move into the larger length class per model time step. This proportion was estimated by simulating the growth of a cohort with a length-frequency distribution given by the length-frequency distribution of released fish, sampling the von Bertalanffy parameters from their estimated posterior distributions. The resulting frequency distribution of length after 6 months of simulated growth was used to determine the mean value for the length class transition probability.

The prior for the capture mortality rate in the sport fishery was centred at the estimated proportion of fish that were recorded as either dead or "lethargic and bleeding". This estimate is considered conservative, since there is likely to be a downward bias in the reporting rate of fish that died as a result of the capture and tagging process in the recreational fishery.

Priors for the negative binomial likelihood function overdispersal parameters were specified to be uninformative (Table 2).

The numbers of tags from a tagged cohort released in area j in time step w in areas $k = 1$ to K in time step $w + 1$ can be viewed as multinomial coefficients conditioned on the number released in area j at time w. Movement probabilities from area j to $k = 1$ to K were estimated as a complete matrix, i.e., summing to 1 for all j. This condition was satisfied by using an uninformative Dirichlet prior for movement probabilities, the conjugate prior for the multinomial distribution (Table 2).

Model implementation and convergence diagnostics

Bayesian mark–recapture models were implemented using WinBUGS (Bayesian inference using Gibbs sampling) software version 1.4 (http://www.mrc-bsu.cam.ac.uk/bugs). The WinBUGS programme samples the posterior probability distribution using Markov chain Monte Carlo (MCMC) methods. MCMC refers to a general method of drawing values of a parameter vector from a proposal distribution and then correcting those draws to better approximate the target distribution (Gelman et al. 1995). Sequential draws form a Markov chain; that is, each draw of θ depends only on the value of the previous draw. The simulated draws from $p(\theta|y)$ are used to summarize the posterior density and compute probability intervals, moments, and other quantities of interest. The Gibbs sampler is an MCMC algorithm that samples from full conditional posterior distributions (Gelfand and Smith 1990; Gelman et al. 1995; Gilks et al. 1996).

It is common for the marginal and joint density functions obtained from values in the initial sequence of a Markov chain to deviate considerably from the target distribution and for values in the chain to more closely approach the target distribution as the number of iterations increases. To avoid basing inference on early draws, which are still influenced by the starting values that may not conform closely to the target posterior density function, the initial sequence of draws is usually discarded (commonly referred to as the "burn-in") with the length of the initial sequence to discard being based on the inspection of several different diagnostics. The burn-in point and convergence to the target posterior distribution (assumed to have occurred when the Gibbs sampler has reached apparent stationarity) were evaluated by applying the Gelman–Rubin diagnostic (Gelman and Rubin 1992), the Geweke time series diagnostic (Geweke 1992), and the Monte Carlo error statistic (Spiegelhalter et al. 2003).

Bayesian p values offer a comparison of model predicted quantities with the observed data (Meng 1994). A Bayesian p value is defined as the probability that a discrepancy statistic for a model predicted value is as or more extreme than

Fig. 4. Prior and posterior probability distributions for κ updated with age–length and mark–recapture data. Dashed line, prior; solid line, age–length data; dotted line, PIT tagging data.

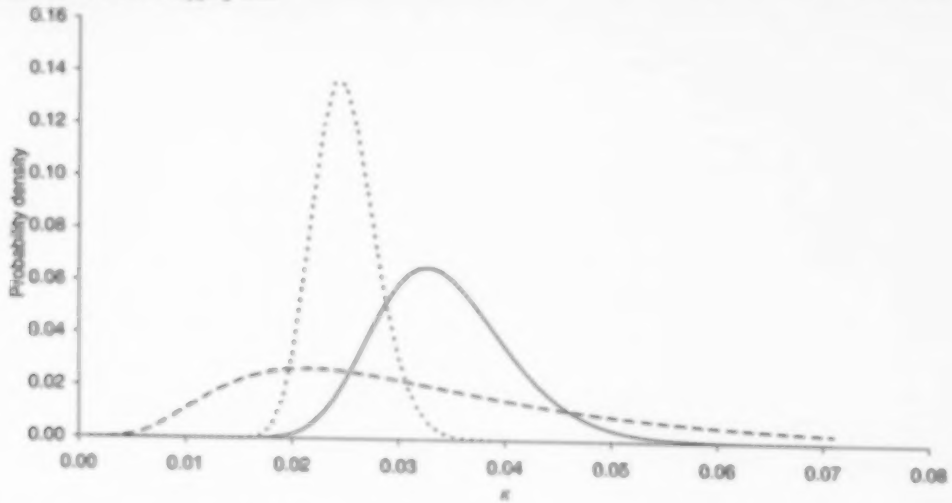

Table 1. Prior and posterior means (standard deviations in parentheses) for von Bertalanffy κ and L_∞ parameters.

	Prior	Posterior	
		Age–length data	PIT tagging data
κ	0.019 (0.006)	0.034 (0.003)	0.024 (0.003)
L_∞	471.3 (154.1)	304.3 (23.2)	421.2 (39.7)

that for the observed value; extreme p values reflect the implausibility of the data given a particular model. In this application, empirical p values were used to assess how well the posterior predictive distribution replicated the observed recapture data based on the mean ranking of paired simulated and observed data points over many samples from the posterior distribution. Thus, p values close to 0.5 represent a good fit of the model to the data, since on average the replicated values are less than or greater than the observed value with equal frequency.

Evaluation of mark–recapture model structural uncertainty

Using the general model structure described above, and with the available data, length-specific catchabilities, mortality rates (β), and tag reporting rates are confounded, i.e., it is not possible to estimate them simultaneously without auxiliary data. This is because fewer recaptures in a given length class could be equally well explained by a higher β, lower q, or lower λ. Support for values of the tag reporting rate was limited to the range of plausible values resulting from a field study designed to estimate this parameter. Inclusion of fishing effort data should reduce the negative correlation between β and q, since the harvest rate is a product of q and the fishing effort in a particular time/area cell. For evaluations of alternative model structures, the value for β at length was fixed, since when q varies by length and season, q at length and β at length values are not estimable without additional independent data on either. Stage-structured Bayesian mark–recapture models were developed according to the equations above, but differing in the level of aggregation of the catchability coefficient q, which was estimated either by length class (c) only or by length class and season (c, w) (Table 3). Catchability might also be expected to vary by area; however, area was not included as a covariate for catchability because estimates of area-specific catchabilities would be confounded with estimated movement rates.

In addition, for both of these configurations, four scenarios for the length class specific mortality rate were applied (Table 3). In three of these, β was assumed to be equal for both length classes; in the fourth, a higher β was applied for the smaller length class. This latter scenario might represent a biologically realistic situation, for example, if predation rates and density-dependent effects lead to a higher mortality rate for younger sturgeon. Plausible values for β were set according to the range indicated for the rate of natural mortality M by estimates derived from life history invariants and their associated variances. Estimates of the von Bertalanffy κ parameter (in addition to that from this study) and maximum longevity were collated in a literature review for the Fraser River and other *A. transmontanus* populations and used to formulate a prior for M (Scott and Crossman 1973; DeVore et al. 1995; RL&L. Environmental Services Ltd. 2000).

The predictive efficacy of fishing effort as a covariate was also investigated using different model configurations. A previous mark–recapture analysis of these data (Walters et al. 2005) omitted effort data. This omission was made owing to concerns about the consistency of the unit of effort (rod hour) as a measure of fishing intensity or capture rate in the Fraser River. For example, when abundance is low, many anglers, particularly guides, may fish more intently per hour fished than when abundance is high. If catchability varies inversely with fish density (e.g., Peterman and Steer 1981; Hilborn and Walters 1992; Arreguin-Sanchez 1996), one might also expect that fishing effort may not covary linearly with the recreational capture rate. In addition, there is a possibility that capture rate per unit of fishing effort may

Table 2. Mark–recapture model parameter prior distributions.

Parameter	Description	Prior	Median	95% probability interval
β	Nontagging-related mortality rate	log $N(-3.3,0.6^2)$	0.037	0.011–0.121
ρ_R	Recreational fishing mortality coefficient	Beta(3,115)	0.023	0.005–0.060
ρ_A	Albion test fishery mortality coefficient	Beta(1.6,30)	0.041	0.004–0.150
λ_A	Albion test fishery tag reporting rate	Beta(10,2)	0.852	0.586–0.976
λ_R	Recreational fishery tag reporting rate	Beta(26,3)	0.906	0.764–0.977
q_R	Catchability in the recreational fishery	log $N(-11,0.6^2)$	1.657×10^{-5}	$2.329 \times 10^{-6} - 1.172 \times 10^{-4}$
q_A	Catchability in the Albion test fishery	log $N(-12.5,0.6^2)$	3.701×10^{-6}	$2.966 \times 10^{-7} - 4.768 \times 10^{-5}$
p_M	Movement rate	Dirichlet(0.5[ ])	0.25	0.0004–0.96
ψ_c	Length class residency rate	Beta(50,2)	0.967	0.895–0.995
τ_R	Recreational catch overdispersion parameter	log $N(0,1.3^2)$	1.00	0.078–12.6
τ_A	Test fishery catch overdispersion parameter	Unif(0,10)	5	0.25–9.75

Table 3. Mark–recapture model structures (β_i, mortality rate for length class i; q, catchability in the recreational fishery; c and w, length class and season (level of stratification for q).

β_1	β_2	q	Effort data
0.025	0.025	c	+
		c, w	+/–
0.05	0.05	c	+
		c, w	
0.075	0.075	c	+
		c, w	
0.075	0.025	c	+
		c, w	

be limited by handling time constraints in peak-fishing seasons such that capture rates become invariant to fish density at intermediate to high fish densities. A further possibility is that the spatial allocation of fishing effort may deviate considerably from a random sample of the fish population and apparent temporal variation in capture rates may simply reflect to a large extent interannual variability in the spatial distribution of the fish population rather than variation in population abundance. Given these various caveats, interpretation of results obtained from the use of recreational fishing effort as a covariate for capture rate warrants caution. The posterior probability of a mark–recapture model that included effort data as a covariate was compared with that from a model that did not make use of covariate effort data. For models that did not use fishing effort as a covariate, harvest rate $H_{R,i,w,k,c}$ was replaced by $\varphi_{i,w,k,c}$, the capture probability for tagged fish in year i, season w, area k, and length class c.

It was assumed that the principal causes of variation in catchability in the Fraser River recreational fishery are the size of fish and the time of year/season. Fish in different length classes would be expected to show varying catchabilities because of length-dependent differences in vulnerability to the recreational fishing gear (rod and line). Vulnerability is very low for fishes of 40 cm length and below, which are very rarely captured by the recreational gear used, while it is probable that vulnerability decreases for larger fish. For larger-sized fish, gear breakage and higher escapement rates could cause declining vulnerability, although without auxiliary data, it is not possible to assess the inflection point or rate of decline.

Formulating problems within a Bayesian framework allows direct comparison of models with differing structures that do not necessarily have to be hierarchically nested, as is the case with frequentist likelihood ratio tests (Mood et al. 1974; Huelsenbeck and Rannala 1997). Standard Bayesian inference involves the computation of the marginal probability of the data given the model $p(D|M)$, which is the integral of the product of the prior and probability of the data given a parameter value over the parameter space. This integral is the quantity that is required for comparison of different hypotheses about model structure. The posterior probability $p(M_i|D)$ (Bayes' posterior) for model i is proportional to its prior probability times the marginal probability of the data given a particular model structure $p(D|M_i)$. $p(M_i|D)$ can be interpreted as a numerical summary of the evidence in favour of model M_i. The modeller can then elect to use the structure and parameter estimates from the most probable model or to assign weights to different model structures according to their respective posterior probabilities (Wasserman 2000).

The posterior odds of one model versus another model are computed as $p(M_1|D)/p(M_2|D)$ and can be interpreted as a measure of the evidence provided by the data in favour of one scientific hypothesis (statistical model) over another. The Bayes' factor is an alternative measure of evidence that removes the influence of the prior probabilities for each model $p(M_i)$:

$$(11) \qquad B_{12} = \frac{p(M_1|D)/p(M_2|D)}{p(M_1)/p(M_2)}$$

The Bayes' factor is thus the ratio of the posterior odds of M_1 to its prior odds (Kass and Raftery 1995) and reflects the ratio of the marginal probability of the data for two alternative models. The reciprocal of the marginal probability of the data $p(D|M)$ can be approximated by the harmonic mean of the probability of the data given the value of a parameter or vector for a sample approximately drawn from the posterior density (Newton and Raftery 1994). The marginal probability of the data for each alternative model considered was estimated using WinBUGS14 software. WinBUGS allows a deviance (–2 log probability of the data) node to be monitored so that once the burn-in phase has been completed, a record of the value of the probability of the data at each draw in the simulation can be obtained. The harmonic mean of the probability of the data (HMPD) is then estimated as follows:

$$\text{HMPD} = \frac{m}{\sum_{k=1}^{m} \frac{1}{p(D|\theta_k, M_i)}} \quad (12)$$

i.e., the average of the inverse probability of the data taken over m MCMC iterations.

A potential problem with this method is that the HMPD is known to be a computationally unstable estimate of $p(D|M)$ (i.e., it is consistent but may have infinite variance across simulations; Raftery et al. 2006). Raftery et al. (2006) noted that if the HMPD after m draws is plotted against m, the plot can show large jumps as the number of iterations increases. To investigate the stability of the HMPD in this study, the cumulative HMPD was computed for multiple overdispersed chains in a Bayesian mark–recapture model at intervals of a fixed number of iterations after the burn-in phase.

An alternative way to approximate the posterior probability of each model is provided by the Bayes' information criterion (BIC) (Schwarz 1978). The BIC approximation for Bayes' factors was computed to assess consistency with the HMPD approximation. BIC provides a large sample estimator of a transformation of the Bayesian posterior probability for a given model and can be regarded as an approximation to the logarithm of the Bayes' factor (Kass and Raftery 1995; Wasserman 2000). It is equal to –2 times the natural logarithm of the posterior mean of the probability of the data (i.e., the posterior mean deviance) for model i plus the product of the estimated number of parameters in model i and the natural logarithm of the sample size:

$$\text{BIC} = -2 \ln f(D|\theta_i) + k \ln n \quad (13)$$

where $f(D|\theta_i)$ is the posterior mean deviance of model i, k_i is the number of parameters in model i, and n is the sample size (which is the same for all models). The BIC for comparison of two alternative model structures is given by

$$\text{BIC}_{12} = -2 \ln[f(D|\theta_1, M_1) - f(D|\theta_2, M_2)] + (k_1 - k_2)\ln n \quad (14)$$

Models with a large number of parameters are penalized by the BIC, accounting for the trade-off between parsimony and complexity. BIC can be calculated using the estimated posterior mean deviance and effective number of parameters obtainable in the output that is provided for the deviance information criterion (DIC) in WinBUGS.

Results

Model fit

Bayesian p values based on a comparison of a set of replicated data (i.e., the posterior predictive distribution) with the observed data show that the fit of the model was reasonably good (Fig. 5). Bayesian p values were obtained for nonzero recapture data only, since zero data points give a p value of 1 (simulated recaptures from a negative binomial distribution take nonnegative integer values); 0.7% of p values were less than 0.025 and 1.3% were greater than 0.975.

Posterior pdfs for estimated parameters

The prior mean for the recreational fishery PIT tag reporting rate obtained from sampling recreational fishery catches was updated slightly by the mark–recapture data. The posterior mean shows a slightly lower PIT tag reporting rate than that observed in the sampling programme (Fig. 6; Table 4). The posterior precision of the estimated tag reporting rate was only slightly higher than the prior precision. The posterior mean was very similar to the prior mean for the Albion test fishery tag reporting rate and there was a small increase in the posterior precision for this parameter (Table 4).

Estimates of the catchability coefficients for both fisheries were markedly updated by the PIT tag recapture data (Figs. 7 and 8). Seasonal and length-specific variation in catchabilities is also evident in the posteriors for these parameters, whereas specification of priors made no assumptions about the pattern of seasonal variations and differences in catchabilities by length.

Posterior mean catchability coefficients for capture in the Albion test fishery were considerably lower than the prior means placed on these parameters (Fig. 7). The catchability coefficients for capture in the second half of the year were updated more than those for the first half, as can be seen from their peaked posterior pdfs. The median catchability was lower in the second season for both length classes. There was also a difference by length class in the posterior medians for season 1, with smaller fish having a higher catchability.

The posterior mean catchability of smaller sturgeon in the recreational fishery was greater than that for the larger length class during the first season (January–June) as was observed for recaptures in the Albion test fishery (Fig. 8). In contrast with the seasonal pattern in catchabilities in the test fishery, estimated catchabilities between July and December for both length classes were also higher relative to the catchability of large fish in the first season in the recreational fishery.

The posterior means for recreational and Albion test fishery mortality rates were slightly lower than the prior means (Table 4). The precision of the estimate of the Albion test fishery incidental catch-and-release mortality rate was improved slightly when updated with the mark–recapture data, whereas the precision of the estimate for the recreational fishery remained unchanged.

The prior pdf for the length class transition probability ($1 - \psi_1$) was updated by using mark–recapture data for two length classes (Table 4). Under the current model structure, growth out of the second length class is confounded with the nontagging related mortality term (β) for this length class; therefore, this parameter was not estimated in mark–recapture models.

Residency probabilities (i.e., indicating that fish remain in the area in which they were last captured) were higher than coefficients for movements to other areas for both seasons and length classes, with the highest level of residency for both length classes occurring in the upstream model area between January and June. Rates of residency were generally lower for the larger length class, with the exception of area 3 (upstream).

There were significant differences between movement coefficients for the two length classes for fish either remaining in the downstream area or making an upstream movement in season 2 (between July and December). A significantly higher residency rate was observed for the smaller length

Table 4. Prior and posterior median and standard deviation for parameters estimated in the Bayesian mark–recapture model.

	Prior		Posterior	
	Median	SD	Median	SD
λ_A	0.852	0.104	0.818	0.093
λ_B	0.906	0.056	0.873	0.055
ρ_A	0.041	0.039	0.036	0.034
ρ_B	0.023	0.014	0.020	0.013
$\beta[1]$	0.037	0.029	0.041	0.023
$\beta[2]$	0.037	0.030	0.025	0.015
$\phi[1]$	0.967	0.026	0.941	<0.01
$\varphi_A[1,1]$	3.70×10^{-6}	1.74×10^{-5}	1.10×10^{-6}	3.10×10^{-7}
$\varphi_A[1,2]$	3.70×10^{-6}	1.74×10^{-5}	7.27×10^{-7}	2.34×10^{-7}
$\varphi_A[2,1]$	3.70×10^{-6}	1.74×10^{-5}	7.33×10^{-7}	2.28×10^{-7}
$\varphi_A[2,2]$	3.70×10^{-6}	1.74×10^{-5}	6.55×10^{-7}	2.24×10^{-7}
$\varphi_B[1,1]$	1.66×10^{-5}	7.15×10^{-5}	9.38×10^{-6}	3.10×10^{-6}
$\varphi_B[1,2]$	1.66×10^{-5}	7.15×10^{-5}	6.97×10^{-6}	2.34×10^{-6}
$\varphi_B[2,1]$	1.66×10^{-5}	7.15×10^{-5}	9.99×10^{-6}	3.28×10^{-6}
$\varphi_B[2,2]$	1.66×10^{-5}	7.15×10^{-5}	9.11×10^{-6}	3.04×10^{-6}
τ_A	4.996	2.901	1.013	0.358
τ_B	1.000	4.842	0.724	0.081
ε	1.000	0.014	1.013	0.008

class, and a significantly higher upstream movement rate to adjacent area 2 was observed for the larger length class (Fig. 9). There were also significant differences by length class for coefficients for fish residing in upstream area 3 or moving downstream to area 2 between July and December. A higher proportion of larger fish remained in area 3, while there was a higher rate of movement downstream for smaller fish.

There were significant differences by season for movements from area 3 to all areas for the smaller length class, with a significantly lower residency rate and higher downstream movement rates to areas 1 and 2 in the second half of the year relative to the first half. The same pattern was observed for the larger length class, although differences were only significant for the residency rate and movement to the adjacent downstream area (2).

Posterior correlations between length class specific mortality rates and catchabilities were low; however, there were large negative correlations between the reporting rate parameter and catchability coefficients (Table 5). Posterior correlations between the reporting rate and length class specific mortality rates were low (less than 0.05), as were posterior correlations between movement parameters and total mortality (not less than –0.05 or greater than 0.04). Posterior correlations between the movement parameters and growth rate parameters were also fairly low (not less than –0.05 or greater than 0.372).

Evaluation of alternative model structure probabilities

The HMPD was shown to provide a reasonable approximation of $p(DM)$ for this application. Bayes' factors computed using the HMPD were similar to BICs for most model structures and showed the same pattern of relative support for alternative model structures.

Jeffreys (1961) recommended a scale of evidence for interpreting Bayes' factors (Table 6). Kass and Raftery (1995) suggested interpreting Bayes' factors as twice the natural logarithm of Jeffreys' scale to provide a measure of evidence that is on the same scale as deviance and likelihood ratio statistics. This scale of evidence may also be used to interpret BIC, which is an approximation to twice the logarithm of Bayes' factor. The estimated Bayes' factors for the range of scenarios evaluated indicate that the mark–recapture data provide more support for models with a lower mortality rate. Bayes' factors are highest (strongest evidence) for a mortality rate of 0.025 for both length classes relative to a mortality rate of 0.075 for both classes (38.8). The data do not provide any evidence in favour of a higher mortality rate ($\beta = 0.075$) for smaller individuals in the first length class compared with lower mortality rates of 0.025 and 0.05 for both length classes, although there is more support provided by the data for this scenario relative to $\beta = 0.075$ for both length classes (Table 7). This comparison corroborates mortality rate estimates from the state–space Bayesian mark–recapture model (Table 4).

The computed Bayes' factor and BIC for alternative levels of aggregation for the catchability coefficient (q) in the recreational fishery indicate that the data provide strong evidence for estimation of q by length class and season in comparison with by length class only (Bayes' factor = 11.7, BIC = 6.4). The estimated Bayes' factors and BIC for mark–recapture models including/omitting covariate effort data provided strong support according to Jeffreys' scale in favour of inclusion of effort data (Bayes' factor = 57.1, BIC = 98.9).

Discussion

Incorporating a prior for the tag reporting rate

Confounding between model parameters is a key issue in fitting complex nonlinear models (Dorazio and Rago 1991; Anganuzzi et al. 1994) and is often an important question in the context of mark–recapture-type models where length

Fig. 5. Frequency distribution of Bayesian p values for the mark–recapture model.

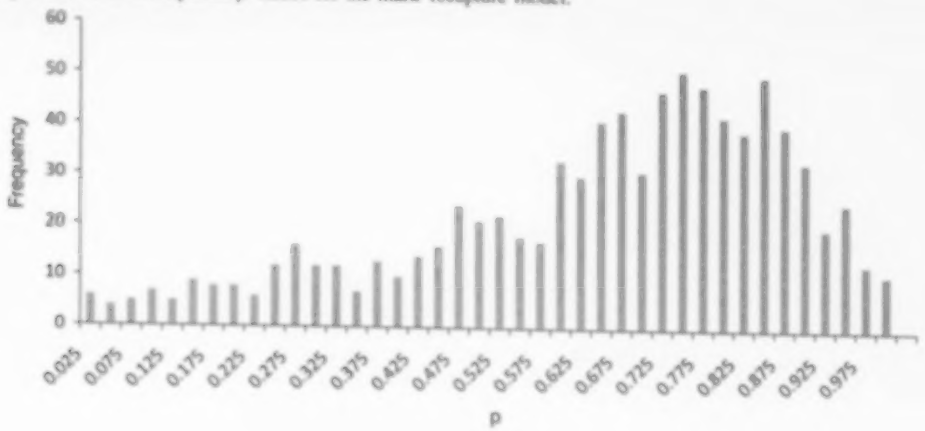

Fig. 6. Prior (dotted line) and posterior (solid line) for the recreational fishery tag reporting rate.

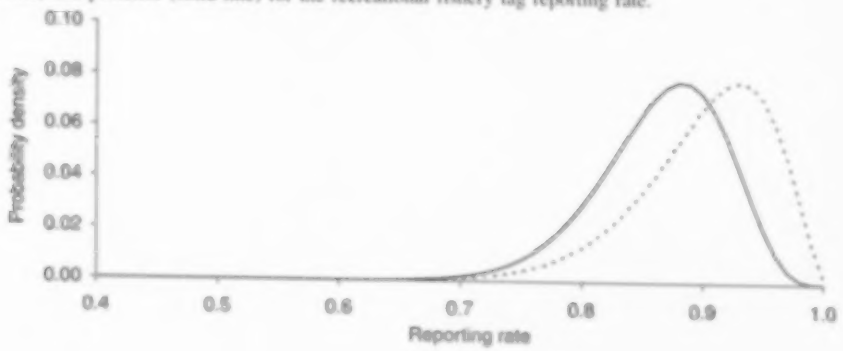

class or age class specific mortality rates, catchabilities, and reporting rates are estimated. Large negative posterior correlations were obtained for the tag reporting rates and catchability parameters. This phenomenon arises because the observed recaptures could be equally well explained by a low reporting rate and high catchability or vice versa. This demonstrates the importance of using a relatively precise prior distribution for the tag reporting rate (Whitlock 2007), which effectively limits the plausible range of values that the reporting rate and catchability coefficients can take as well as giving higher prior probability to values of the reporting rate that were most likely given data collected during an observer study to estimate the reporting rate. That the analysis of tagging data did not result in any gains in precision to the prior pdfs for the reporting rates is expected. This is due to the fact that the priors were already quite informative, so that the available information in the tagging data was limited relative to that summarized in the priors. Furthermore, the strong negative posterior correlations between the tag reporting rate and catchability coefficients indicate that the posterior probability density is fairly flat across a range of combinations of the reporting rate and catchabilities. The high precision of the priors for tag reporting rates thus provided important information in terms of more precise estimation of other model parameters.

Comparison of results with other studies

The natural mortality rate M is one of the most important parameters in fisheries stock assessment and management, as it has been shown to be correlated with the potential maximum yield as a proportion of the unexploited fishable stock size (Beddington and Cooke 1983; Kirkwood et al. 1994). The low posterior medians obtained (0.041 and 0.025·year^{-1}) for the length class specific mortality rates (excluding capture mortalities) thus suggest that the lower Fraser River white sturgeon population is capable of sustaining only low exploitation rates. Comparison of the total mortality rates (i.e., inclusive of capture-induced mortalities in the recreational and Albion fisheries) yields similar estimates (0.097 and 0.081 for length classes 1 and 2, respectively) to those from other studies for *A. transmontanus*. Walters et al. (2005) concluded that total mortality Z was in the range 0.07–0.14 from spatially aggregated and disaggregated maximum-likelihood mark–recapture analyses of the Fraser River PIT tagging data, with lower estimates obtained using spatially disaggregated models. Catch-curve analyses for white sturgeon also indicate higher levels of total mortality (e.g., $Z = 0.10$, Beamesderfer et al. 1995; $Z = 0.19$–0.21, Walters et al. 2005). The values obtained using the Bayesian mark–recapture model fall within the lower end of this spectrum; this may result from the fact that estimates of mortality from

Fig. 7. Prior (dotted line) and posterior probability density functions for the Albion test fishery catchability coefficients. Dashed black line, $q[1,1]$; solid black line, $q[1,2]$; dashed grey line, $q[2,1]$; solid grey line, $q[2,2]$.

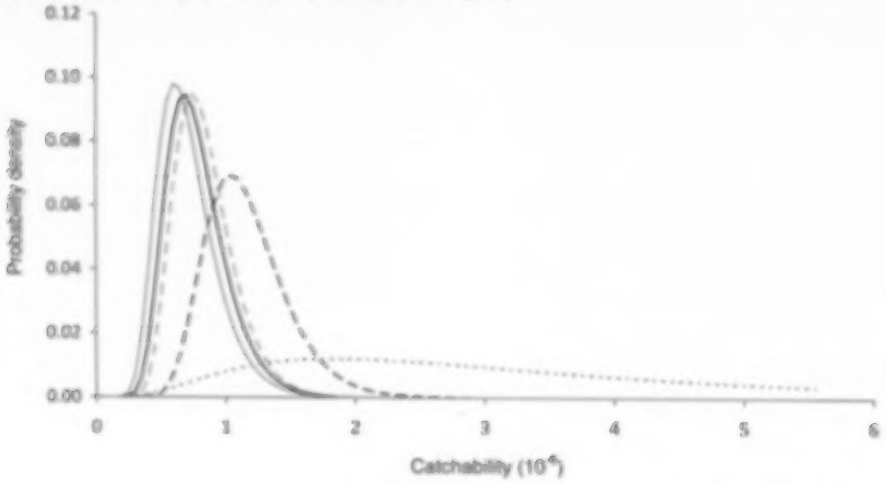

Fig. 8. Prior (dotted line) and posterior probability density functions for the recreational fishery catchability coefficients. Dashed black line, $q[1,1]$; solid black line, $q[1,2]$; dashed grey line, $q[2,1]$; solid grey line, $q[2,2]$.

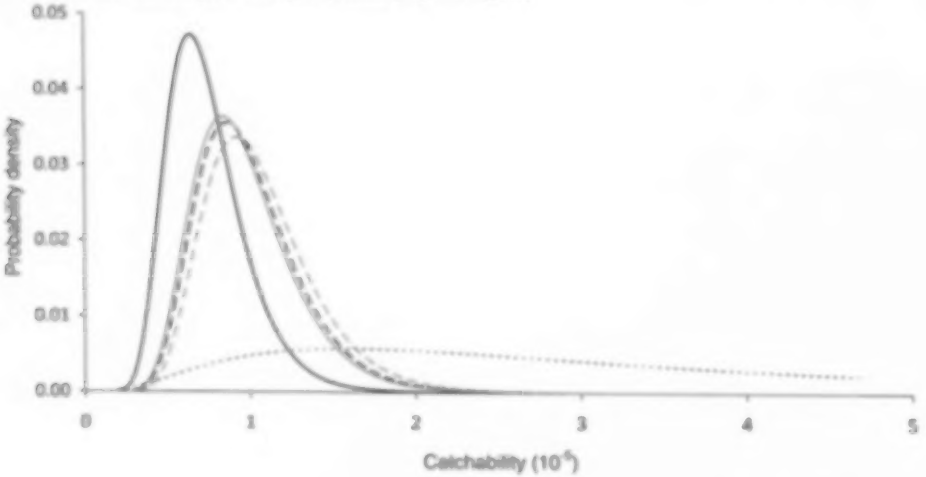

Table 5. Posterior correlations for mortality and the recreational tag reporting rate with catchabilities by length and season in the recreational fishery.

	$qu[1,1]$	$qu[1,2]$	$qu[2,1]$	$qu[2,2]$
$\beta[1]$	0.04	–0.05	0.04	–0.05
$\beta[2]$	–0.11	–0.09	–0.10	–0.09
λ_R	–0.77	–0.73	–0.84	–0.86

spatially disaggregated models can be significantly lower than those from spatially aggregated models. This is often caused by poorer definition of model domain in spatially aggregated models combined with emigration out of fishing grounds appearing as a major component of natural mortality (Sibert et al. 1999). However, life history invariants ($M = 1.7\kappa$, Pauly 1980; $M = 1.5\kappa$, Jensen 1996) suggest that the natural mortality rate for *A. transmontanus* is in the range 0.023–0.045 based on the estimated 95% Bayesian probability interval for the von Bertalanffy κ growth coefficient, which concurs with results from the mark–recapture model.

When evaluating alternative management strategies for the lower Fraser sturgeon population, it is important to consider the cumulative effects of different sources of fishing mortality. Given recent annual catch rates in the recreational fishery, the mortality rate estimated in the Bayesian mark–recapture model equates to 100–200 mortalities from fishing for fish in the recruited size range annually. Estimates of capture-induced mortalities in the recreational and Albion test fisheries are in accord with estimates from a recent study of tagging mortality (as a direct result of tagging, stress caused by handling, etc.) conducted for the PIT tagging programme for Fraser River white sturgeon (Robichaud et al. 2006). The authors reported a direct angling mortality

Fig. 9. Schematic diagram of posterior mean movement coefficients between three sections of the lower Fraser River in (*a*) season 1 and (*b*) season 2. In each diagram, the solid arrows and adjacent figures indicate rates of movement for fish in length class 1 and dashed arrows show movement rates for length class 2. Large type font figures (centrally positioned within each area) indicate residency probabilities. Asterisks indicate significant differences (overlap $p \leq 0.05$) in movement coefficients by length class and daggers indicate significant differences by season.

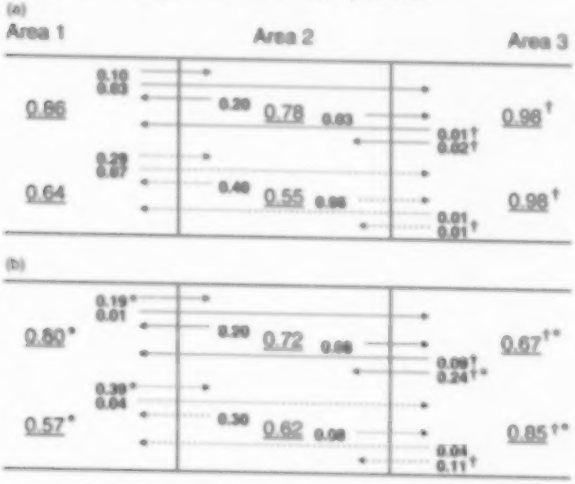

rate of less than 0.012% and a postrelease mortality rate of 2.6% based on a 3 day holding study of fish captured by angling and PIT tagged, which is comparable with the recreational capture-induced mortality rate estimated in the Bayesian mark–recapture models. Robichaud et al. (2006) estimated a direct drift net mortality rate of 4.8% for the First Nations sockeye salmon (*Oncorhynchus nerka*) food, social, and ceremonial fishery. This estimate is slightly higher than the posterior median for the Albion test fishery (3.6%); it seems likely that this difference could be attributed to a shorter soak time in the Albion fishery (usually around 30 min). These mortality rates are fairly low, although it seems likely that mortality rates in set net fisheries will be higher. Given the large number of tags applied and recaptured in this fishery, it may be possible to estimate separate tagging- and capture-induced mortality rates as the difference between a composite tagging and capture mortality rate for untagged fish and a capture mortality rate for recaptures.

Estimated movement rates show that the population of white sturgeon in the lower Fraser River is fairly mobile, with characteristic annual movement patterns for fish belonging to different length classes. Lower levels of residency associated with the larger length class indicate that these fish make more frequent longer range movements than the smaller fish. Differences in annual movement patterns between the length classes are probably due to differential exploitation of seasonally available food resources. In addition, fish belonging to the smaller length class are unlikely to be reproductively mature and would not be expected to make upstream movements for spawning made by fish in the larger length class. The higher rates of upstream movements

Table 6. Jeffreys' scale of evidence for Bayes' factors.

Bayes' factor	2 ln Bayes' factor	Interpretation
$B_{ij} < 1/10$	$B_{ij} < -4.6$	Strong evidence for j
$1/10 < B_{ij} < 1/3$	$-4.6 < B_{ij} < -2.2$	Positive evidence for j
$1/3 < B_{ij} < 1$	$-2.2 < B_{ij} < 0$	Weak evidence for j
$1 < B_{ij} < 3$	$0 < B_{ij} < 2.2$	Weak evidence for i
$3 < B_{ij} < 10$	$2.2 < B_{ij} < 4.6$	Positive evidence for i
$B_{ij} > 10$	$B_{ij} > 4.6$	Strong evidence for i

Table 7. 2 ln Bayes' factors (BIC in parentheses) for β.

β	0.05	0.075	0.075, 0.025
0.025	18.9 (18.2)	38.8 (38.5)	24.4 (29.4)
0.05		20.3 (21.0)	11.3 (12.5)
0.075			−14.4 (−9.0)
0.075, 0.025			

Note: The strength of support for models in row i relative to those in column j is indicated by estimated Bayes' factors and BIC in parentheses.

for larger fish compared with smaller fish during the second half of the year could be due to movements to spawning sites as well as the use of overwintering holes located upstream of feeding grounds used in spring and summer. The higher rates of downstream movement for fish in both length classes in autumn–winter compared with spring–summer might be related to anticipation of the spring eulachon (*Thaleichthys pacificus*) run, which offers an abundant source of food in the estuarine and downstream areas of the river.

The pattern of movement estimated by the Bayesian mark–recapture model is consistent with other observations and estimates of the timing and direction of movements in the lower Fraser River. Results from previous studies indicate that individuals remain on summer feeding grounds with localized movements before migrating in autumn or winter followed by a period of relative inactivity over winter (RL&L Environmental Services Ltd. 2000; Nelson et al. 2004). In the lower Fraser, extensive movements of tagged fish have been associated with seasonal availability of food resources such as eulachon, salmon, and salmon roe. Nelson et al. (2004) reported a downstream migration prior to and during the eulachon migration in April and May, a decrease in movement in June and July, and upstream migration coinciding with spawning runs of salmon between August and December.

Evaluation of model structural alternatives

The support provided by the data for mark–recapture models with a fixed low rate of nontagging-related mortality (β) is consistent with the posterior pdfs for the mortality rates β from the state–space model. Bayes' factors for alternative model structures strongly supported models that included covariate effort data. This suggests that in light of the uneven spatial and temporal distribution of fishing effort in the lower Fraser recreational fishery, it has utility as a covariate in accounting for seasonal and spatial variation in recapture rates. Since effort data are informative with respect to the recapture rate, they should not be omitted in future analyses of these data. In addition, the data provided support for stratification of the catchability coefficient q by length

class and season rather than by length class only. This seasonal variation in the catchability coefficient may be the result of seasonal changes in the feeding habits of fish as well as changes in their activity levels in response to fluctuations in water temperature. Catchability was assumed to be the same in all areas and potential spatial differences in catchability could not be estimated owing to confounding with the movement rate parameters. It is likely that catchability could vary substantially between the areas and that the currently estimated movement rates between particular areas could be biased if catchability in fact varies by area. The deployment of large numbers of radiotelemetry tags would be required to disentangle estimates of movement rates from potential differences in catchability between areas.

Limitations to the methodology and potential improvements

Using a deterministic correction factor for the vulnerability of cohorts of tagged fish over time (V_h) may cause bias in estimates of survival and capture-induced mortality rates if there is misspecification of the growth and (or) selectivity functions used for its calculation. For example, if estimates of growth rates or the gradient of the ascending part of the selectivity curve are too high, the correction factor may overcompensate for increasing vulnerability leading to positively biased estimates of nontagging-related and capture mortality rates. This problem could be addressed by sampling the length-frequency distribution of sturgeon in the Fraser for better estimation of selectivity for fish of different lengths. Development of a model with less coarse length classes would also reduce potential bias in estimated parameters resulting from increases in mean cohort vulnerability over time.

There are currently insufficient data for estimation of emigration rates from the lower Fraser River statistical area, and estimates of length class specific and season-specific movement rates as well as mortality rates could be improved by additional information on emigration rates; this could be addressed by undertaking a long-term radio or acoustic tagging programme to quantify the frequency of long-distance movements out of the statistical area. One telemetry study conducted to date (RL&L Environmental Services Ltd. 2000) and an analysis of the strontium concentration in pectoral fin rays (Veinott et al. 1999) have indicated that the rate of movement out of the lower Fraser River is fairly low. However, recent recoveries of tags from other rivers such as the Columbia (Troy Nelson, Fraser River Sturgeon Conservation Society, 520 West 6th Avenue, Vancouver, British Columbia, personal communication) demonstrate that long-range movements of *A. transmontanus* do occur.

Estimation of movement rates using a method independent of the spatiotemporal distribution of fishing effort in the recreational fishery (e.g., a random or stratified random sampling design with a standardized effort across seasons) may help to eliminate or reduce bias in parameter estimates arising from the current recreational fishing effort driven sampling pattern.

Additional limitations relating to the structure of the mark–recapture model include the assumptions that recreational fishing effort is known without error and that catchability in the recreational fishery remains constant over time and space, when plausible alternative structural hypotheses might be that catchability is some increasing function of time, or varies spatially. The latter might occur if fish show life history stage and (or) season-dependent residency of estuarine and lower river areas. Since these fish are spread throughout a larger area, they would be expected to have lower catchability than fish upstream (Carl Walters, Fisheries Centre, University of British Columbia, Vancouver, British Columbia, personal communication). The hypothesis of a differing catchability in area 1 was investigated by running Bayesian mark–recapture models with a fixed quotient for q in the lower river area versus the middle and upstream areas. The results from these models (not shown) indicated that unaccounted for spatial variability in q may lead to severely biased estimates of movement probabilities; these models, however, had lower model posterior probabilities than a model in which q was assumed to be equal in all areas.

Further, this model assumes that the catchability of tagged fish varies only by season and fish size, whereas it has been hypothesized that recreational catchability may vary with fish density (Troy Nelson, Fraser River Sturgeon Conservation Society, 520 West 6th Avenue, Vancouver, British Columbia, and Carl Walters, Fisheries Centre, University of British Columbia, Vancouver, British Columbia, personal communications). However, evaluations of models with or without fishing effort demonstrate that there is strong evidence supporting the use of fishing effort as a covariate for probability of capture. However, the strong covariation of recaptures with recreational fishing effort does not exclude the possibility that density-dependent variation in catchability and other above-mentioned issues with the use of effort data may cause problems for estimation.

Although auxiliary data on length-specific selectivities and emigration rates would lead to improved estimates of mortality rates for the lower Fraser River population of white sturgeon, the mark–recapture model presented here can be used to estimate aggregate (natural mortality, emigration, unaccounted for fishing mortality) mortality rates and season-specific and length class specific movement rates. These estimates can be used within a population dynamics modelling framework to aid the evaluation of alternative area-based fishery management strategies for long-lived migratory species. Estimation of capture-induced fishing mortalities and seasonal movement rates should allow evaluation of area-based management strategies for the lower Fraser white sturgeon population.

Acknowledgements

Thanks to Troy Nelson, Rick Hansen, and the Fraser River Sturgeon Conservation Society for enabling this research to be carried out and for their support of collection of field data in British Columbia. Thanks also to Fred Helmer, Marc Laynes, and all of the other angling guides who contributed boat time to make possible data collection in the recreational fishery and to Jim Rissling, Marvin Rosenau, Alan Baker, Kevin Buxton, and Ted Down for their

help. Geoff Kirkwood, Carl Walters, and Sieve McAdam provided helpful insights during the preparation of this manuscript for which we are grateful. R. Whitlock was funded by a UK Natural Environment Research Council Ph.D. studentship.

References

Akaike, H. 1974. A new look at the statistical model identification. IEEE Trans. Automat. Contr. **19**(6): 716–723. doi:10.1109/TAC.1974.1100705.

Anganuzzi, A., Hilborn, R., and Skalski, J.R. 1994. Estimating size selectivity and movement rates from mark–recovery data. Can. J. Fish. Aquat. Sci. **51**(3): 734–742. doi:10.1139/f94-073.

Arreguin-Sanchez, F. 1996. Catchability, a key parameter for fish stock assessment. Rev. Fish Biol. Fish. **6**: 221–242.

Beamesderfer, R.C.P., Rien, T.A., and Nigro, A.A. 1995. Differences in the dynamics and potential production of impounded and unimpounded white sturgeon populations in the Lower Columbia River. Trans. Am. Fish. Soc. **124**(6): 857–872. doi:10.1577/1548-8659(1995)124<0857:DITDAP>2.3.CO;2.

Beddington, J.R., and Cooke, J.G. 1983. On the potential yield of fish stocks. FAO Fish. Tech. Pap. 242. FAO, Rome, Italy.

Brooks, S.P., Catchpole, E.A., and Coulson, T., Lebreton, J.D., and Morgan, B.J.T. 2004. Recent Progress in using marked individuals to understand animal population biology. Rep UKC/IMS/04/26. Institute of Mathematics, Statistics, and Actuarial Science, University of Kent, Canterbury, Kent, U.K.

DeVore, J.D., James, B.W., Tracy, C.A., and Hale, D.A. 1995. Dynamics and potential production of white sturgeon in the unimpounded Lower Columbia River. Trans. Am. Fish. Soc. **124**(6): 845–856. doi:10.1577/1548-8659(1995)124<0845:DAPPOW>2.3.CO;2.

Die, D.J., Restrepo, V.R., and Fox, W.W. 1990. Equilibrium production models that incorporate fished area. Trans. Am. Fish. Soc. **119**(3): 445–454. doi:10.1577/1548-8659(1990)119<0445:EPMTIF>2.3.CO;2.

Dorazio, R.M., and Rago, P.J. 1991. Evaluation of a mark–recapture method for estimating mortality and migration rates of stratified populations. Can. J. Fish. Aquat. Sci. **48**(2): 254–260. doi:10.1139/f91-035.

Gelfand, A.E., and Smith, A.F.M. 1990. Sampling-based approaches to calculating marginal densities. J. Am. Stat. Assoc. **85**(410): 398–409. doi:10.2307/2289776.

Gelman, A., and Rubin, D.R. 1992. A single series from the Gibbs sampler provides a false sense of security. *In* Bayesian statistics 4. *Edited by* J.M. Bernardo, J.O. Berger, A.P. Dawid, and A.F.M. Smith. Oxford University Press, Oxford, U.K. pp. 625–631.

Gelman, A., Carlin, J., Stern, H., and Rubin, D. 1995. Bayesian data analysis. Chapman and Hall, New York.

Geweke, J. 1992. Evaluating the accuracy of sampling-based approaches to the calculation of posterior moments (with discussion). *In* Bayesian statistics 4. *Edited by* J.M. Bernardo, J.O. Berger, A.P. Dawid, and A.F.M. Smith. Oxford University Press, Oxford, U.K. pp. 169–194.

Gilks, W.R., Richardson, S., and Spiegelhalter, D.J. 1996. Markov chain Monte Carlo in practice. Chapman and Hall/CRC, London, U.K.

Hilborn, R., and Mangel, M. 1997. The ecological detective: confronting models with data. Monographs in Population Biology 28. Princeton University Press, Princeton, N.J.

Hilborn, R., and Walters, C.J. 1992. Quantitative fisheries stock assessment: choice, dynamics and uncertainty. Chapman and Hall, New York.

Huelsenbeck, J.P., and Rannala, B. 1997. Phylogenetic methods come of age: testing hypotheses in an evolutionary context. Science, **276**(5310): 227–232. doi:10.1126/science.276.5310.227. PMID:9092465.

Inter-American Tropical Tuna Commission. 2008. Fishery Status Report No. 5. Tunas and billfishes in the eastern Pacific Ocean in 2006. Inter-American Tropical Tuna Commission, La Jolla, Calif.

International Commission for the Conservation of Atlantic Tunas. 2003. Report of the 2002 Atlantic bluefin tuna stock assessment session. SCRS/2002/012. Collective Volume of Scientific Papers, ICCAT, Vol. 55(3). pp. 710–937. Available online: www.iccat.int/Documents/CVSP/CV055_2003/no_3/CV055030710.pdf

Jeffreys, H. 1961. Theory of probability. 3rd ed. Oxford University Press, Oxford, U.K.

Jensen, A.L. 1996. Beverton and Holt life history invariants result from optimal trade-off of reproduction and survival. Can. J. Fish. Aquat. Sci. **53**(4): 820–822. doi:10.1139/cjfas-53-4-820.

Kass, R.E., and Raftery, A.E. 1995. Bayes factors. J. Am. Stat. Assoc. **90**(430): 773–795. doi:10.2307/2291091.

Kirkwood, G.P., Beddington, J.R., and Rossouw, J.R. 1994. Harvesting species of different lifespans. *In* Large-scale ecology and conservation biology. *Edited by* P.J. Edwards, R. May, and N.R. Webb. Blackwell Scientific, Oxford, U.K. pp. 199–227.

Lane, E.D., and Rosenau, M. 1995. The conservation of sturgeon stocks in the Lower Fraser Watershed. A baseline investigation of habitat, distribution, age and population of juvenile white sturgeon (*Acipenser transmontanus*) in the Lower Fraser River, downstream of Hope, B.C. Final Report. Habitat Conservation Trust Fund, P.O. Box 9354, Stn. Prov. Govt., Victoria, BC V8W 9M1, Canada.

Malakoff, D. 1999. Bayes offers a 'new' way to make sense of numbers. Science, **286**(5444): 1460–1464. doi:10.1126/science.286.5444.1460. PMID:10610542.

McAllister, M.K., and Kirchner, C. 2002. Accounting for structural uncertainty to facilitate precautionary fishery management: illustration with Namibian orange roughy. Bull. Mar. Sci. **70**(2): 499–540.

Meng, X.I. 1994. Posterior predictive *p*-values. Ann. Stat. **22**(3): 1142–1160. doi:10.1214/aos/1176325622.

Michielsens, C.G.J. 2003. Bayesian decision theory for fisheries management of migratory species with multiple life histories. Ph.D. thesis, Imperial College, University of London, London, U.K.

Michielsens, C.G.J., McAllister, M.K., Kuikka, S., Pakarinen, T., Karlsson, L., Romakkaniemi, A., Perä, I., and Mäntyniemi, S. 2006. A Bayesian state–space mark–recapture model to estimate exploitation rates in mixed-stock fisheries. Can. J. Fish. Aquat. Sci. **63**(2): 321–334. doi:10.1139/f05-215.

Michielsens, C.G.J., McAllister, M.K., Kuikka, S., Mäntyniemi, S., Romakkaniemi, A., Pakarinen, T., Karlsson, L., and Uusitalo, L. 2008. Combining multiple Bayesian data analyses in a sequential framework for quantitative fisheries stock assessment. Can. J. Fish. Aquat. Sci. **65**(5): 962–974. doi:10.1139/F08-015.

Mood, A.M., Graybill, F.A., and Boes, D.C. 1974. Introduction to the theory of statistics. 3rd ed. McGraw-Hill, New York.

Neis, B., Schneider, D.C., Felt, L., Haedrich, R.L., Fischer, J., and Hutchings, J.A. 1999. Fisheries assessment: what can be learned from interviewing resource users? Can. J. Fish. Aquat. Sci. **56**(10): 1949–1963. doi:10.1139/cjfas-56-10-1949.

Nelson, T.C., Gazey, W.J., English, K.K., and Rosenau, M.L. 2004. Status of white sturgeon in the lower Fraser River: report on findings of the lower Fraser River white sturgeon monitoring and assessment program, 2000–2004. Draft Report EA 1613.

Fraser River Sturgeon Conservation Society, Vancouver, B.C. Available online: www.fraserstурgeon.com/pdf/2_StatusofWhiteSturgeonintheLowerFraserRiver1999-2004.pdf

Newton, M.A., and Raftery, A.E. 1994. Approximate Bayesian inference by the weighted likelihood bootstrap (with discussion). J. R. Stat. Soc. B, **56**: 3–48.

Otis, D.L., Burnham, K.P., White, G.C., and Anderson, G.R. 1978. Statistical inference for capture data on closed animal populations. Wildl. Monogr. **62**.

Parma, A.M. 2001. Bayesian approaches to the analysis of uncertainty in the stock assessment of Pacific halibut. Am. Fish. Soc. Symp. **27**: 113–136.

Patterson, K.R. 1999. Evaluating uncertainty in harvest control law catches using Bayesian Markov chain Monte Carlo virtual population analysis with adaptive rejection sampling and including structural uncertainty. Can. J. Fish. Aquat. Sci. **56**(2): 208–221. doi:10.1139/cjfas-56-2-208.

Pauly, D. 1980. On the interrelationships between natural mortality, growth parameters and mean environmental temperature in 175 fish stocks. J. Cons. Int. Explor. Mer. **39**(2): 175–192.

Peterman, R., and Steer, G.J. 1981. Relation between sport-fishing catchability coefficients and salmon abundance. Trans. Am. Fish. Soc. **110**(5): 585–593. doi:10.1577/1548-8659(1981)110<585:RBSCCA>2.0.CO;2.

Pine, W.E., Pollock, K.H., Hightower, J.E., Kwak, T.J., and Rice, J.A. 2003. A review of tagging methods for estimating fish population size and components of mortality. Fish. Res. **28**: 10–23.

Punt, A.E., and Hilborn, R. 1997. Fisheries stock assessment and decision analysis: the Bayesian approach. Rev. Fish Biol. Fish. **7**(1): 35–63. doi:10.1023/A:1018419207494.

Raftery, A.E., Newton, M.A., Satagopan, J.M., and Krivitsky, P.N. 2006. Estimating the integrated likelihood via posterior simulation using the harmonic mean identity. Working Pap. No. 60. Working Centre for Statistics and the Social Sciences, University of Washington, Seattle, Wash.

RL&L Environmental Services Ltd. 2000. Fraser River White Sturgeon Monitoring Program — Comprehensive Report (1995 to 1999). RL&L Rep. No. 815F. Final report prepared for B.C. Fisheries, Victoria, B.C.

Robichaud, D., English, K.K., Bocking, R.C., and Nelson, T.C. 2006. Direct and delayed mortality of white sturgeon caught in three gear types in the lower Fraser River. Report prepared by LGL Limited, Sydney, B.C., for Tsawwassen First Nation Fisheries, Delta, B.C. Available online: www.fraserstурgeon.com/reports.html

Schwarz, G. 1978. Estimating the dimension of a model. Ann. Stat. **6**(2): 461–464. doi:10.1214/aos/1176344136.

Scott, W. B., and Crossman, E. J. 1973. Freshwater fishes of Canada. Fish. Res. Board Can. Bull. 184.

Seber, G.A.F. 1982. The estimation of animal abundance. 2nd ed. Blackburn Press, Caldwell, N.J.

Semakula, S.N., and Larkin, P.A. 1968. Age, growth, food and yield of the white sturgeon (*Acipenser transmontanus*) of the Fraser River, British Columbia. J. Fish. Res. Board Can. **25**(12): 2589–2602.

Sibert, J.R., Hampton, J., Fournier, D.A., and Bills, P.J. 1999. An advection–diffusion–reaction model for the estimation of fish movement parameters from tagging data, with application to skipjack tuna (*Katsuwonus pelamis*). Can. J. Fish. Aquat. Sci. **56**(6): 925–938. doi:10.1139/cjfas-56-6-925.

Spiegelhalter, D., Thomas, A., Best, N., and Lunn, D. 2003. WinBUGS user manual. Version 1.4. January 2003. Available online: www.mrc-bsu.cam.ac.uk/bugs/winbugs/manual14.pdf.

Stöcker, S. 1999. Models for tuna school formation. Math. Biosci. **156**(1-2): 167–190. doi:10.1016/S0025-5564(98)10065-2. PMID: 10204392.

Veinott, G., Northcote, T., Rosenau, M., and Evans, R.D. 1999. Concentrations of strontium in the pectoral fin rays of the white sturgeon (*Acipenser transmontanus*) by laser ablation sampling – inductively coupled plasma – mass spectrometry as an indicator of marine migrations. Can. J. Fish. Aquat. Sci. **56**(11): 1981–1990. doi:10.1139/cjfas-56-11-1981.

Walters, C.J., Korman, J., and McAdam, S. 2005. An assessment of white sturgeon stock status and trends in the lower Fraser River. Canadian Science Advisory Secretariat Res. Doc. 2005/066. Canadian Science Advisory Secretariat, Vancouver, B.C.

Wasserman, L. 2000. Asymptotic inference for mixture models using data dependent priors. J. R. Stat. Soc. B, **62**(1): 159–180. doi:10.1111/1467-9868.00226.

Whitlock, R.E. 2007. Applying Bayesian mark–recapture and decision analysis methods to evaluate fisheries management options for Fraser River white sturgeon. Ph.D. thesis, Imperial College, University of London, London, U.K.

Population genetic structure in the redefined vermilion rockfish (*Sebastes miniatus*) indicates limited larval dispersal and reveals natural management units

John R. Hyde and Russell D. Vetter

Abstract: Recent studies have revealed that the vermilion rockfish *Sebastes miniatus* is a cryptic species pair. The splitting of this species impacts stock size estimates and draws attention to the unintended consequences of current management policies. Differences in exploitation level between the species necessitated an evaluation of population structure and connectivity among regional management segments of the fishery. Analysis of gene flow and calculations of larval dispersal values were accomplished using 782 bp of DNA sequence data from the mitochondrial cytochrome *b* gene of 684 vermilion rockfish sampled from 16 sites between Kyuquot Sound, Canada, and San Quintin, Mexico. Significant genetic heterogeneity was found among sample sites (Φ_{ST} = 0.0742, $p < 0.001$ and F_{ST} = 0.0899, $p < 0.001$). Isolation by distance analysis produced a significant correlation, suggesting low average larval dispersal distance. Analysis of molecular variance showed significant partitioning of genetic variance across the biogeographic boundary at Point Conception (Φ_{CT} = 0.0923, $p < 0.001$ and F_{CT} = 0.0135, $p < 0.001$) with additional genetic barriers found at Cape Mendocino, Punta Colnett, Santa Monica Bay, and along the coast of Washington. These genetic barriers conform to oceanographic compartments previously proposed for the California Current Ecological Province and suggest natural management units for this species.

Résumé : Des études récentes ont montré que le sébaste vermillon *Sebastes miniatus* représente en fait une paire d'espèces cryptiques. La séparation de cette espèce a des répercussions sur les estimations de taille des stocks et souligne les conséquences imprévues des politiques actuelles de gestion. Des différences de niveaux d'exploitation entre les deux espèces nécessitent une évaluation de la structure de population et de la connectivité entre les secteurs régionaux de gestion de cette pêche. L'analyse du flux génique et le calcul des taux de dispersion larvaire se sont faits à partir des données de séquençage de 782 pb d'ADN du gène mitochondrial du cytochrome *b* chez 684 sébastes vermillons provenant de 16 sites entre le détroit de Kyuquot, Canada, et San Quintin, Mexique. Il existe une hétérogénéité génétique significative entre les sites d'échantillonnage (Φ_{ST} = 0,0742, $p < 0,001$ et F_{ST} = 0,0899, $p < 0,001$). Une analyse d'isolement par la distance produit une corrélation significative, ce qui laisse croire à une faible distance moyenne de dispersion larvaire. L'analyse de la variance moléculaire montre un partionnement significatif de la variance génétique à travers la frontière biogéographique de Point Conception (Φ_{CT} = 0,0923, $p < 0,001$ et F_{CT} = 0,0135, $p < 0,001$) avec des barrières génétiques additionnelles au cap Mendocino, à Punta Colnett, dans la baie de Santa Monica et le long de la côte de l'état de Washington. Ces barrières génétiques correspondent aux compartiments océaniques proposés antérieurement pour la province écologique du courant de Californie et indiquent des unités naturelles de gestion pour cette espèce.

[Traduit par la Rédaction]

Introduction

A long-term goal of fisheries genetics is to discover natural management units that may replace fish stock definitions based on nonbiological considerations. Nowhere is this need more urgent than with the approximately 65 rockfish species (genus *Sebastes*) that constitute the bulk of US and Canadian west coast demersal fisheries. Using a suite of nuclear and mitochondrial markers, Hyde et al. (2008) showed that the vermilion rockfish (*Sebastes miniatus*) (Jordan and Gilbert 1880) was actually a complex of two cryptic species.

Received 14 October 2008. Accepted 29 April 2009. Published on the NRC Research Press Web site at cjfas.nrc.ca on 9 September 2009.
J20819

Paper handled by Associate Editor Anti Vasemgi.

J.R. Hyde.[1,2] Scripps Institution of Oceanography, University of California, San Diego, 9500 Gilman Drive, La Jolla, CA 92093-0203, USA.
R.D. Vetter. Southwest Fisheries Science Center, National Marine Fisheries Service, National Oceanic and Atmospheric Administration, 8604 La Jolla Shores Drive, La Jolla, CA 92037, USA.

[1]Corresponding author (e-mail: John.Hyde@noaa.gov).
[2]Present address: Southwest Fisheries Science Center, National Marine Fisheries Service, National Oceanic and Atmospheric Administration, 8604 La Jolla Shores Drive, La Jolla, CA 92037, USA.

The two species are separated primarily by depth of adult occurrence, with the "true" vermilion rockfish (*S. miniatus*) found at shallower depths (typically <100 m) than the sunset rockfish (*Sebastes crocotulus*) (typically >100 m) (Hyde et al. 2008). The discovery of this cryptic species pair, segregated by depth of adult occurrence, will eventually clarify many life history discrepancies, but in the short term, it complicates the assessment and management of both species.

The bulk of the sunset rockfish population occurs south of Point Conception at depths >100 m (Hyde et al. 2008) whereas the "true" vermilion rockfish are abundant from central Oregon to at least Punta Baja, Mexico, and typically occur in kelp forests (*Macrocystis pyrifera* and *Nereocystis luetkeana*) and nearshore rocky reefs at shallower depths than 100 m. Tagging (Miller and Geibel 1973; Hartmann 1987; Lea et al. 1999) and acoustic tracking studies (e.g., Starr et al. 2002; Jorgensen et al. 2006; Parker et al. 2007) of several *Sebastes* species have shown remarkable site fidelity and homing behavior, suggesting that the majority of geographic dispersal is accomplished during larval and pelagic juvenile stages. While few studies have focused directly on vermilion rockfish, the available data suggest that vermilion rockfish also display high site fidelity (Hartmann 1987; Lea et al. 1999). The locations and depths investigated in these studies strongly suggest that they refer only to the "true" vermilion rockfish. Such limited adult dispersal suggests that gene flow is primarily accomplished by dispersal of pelagic larval and juvenile life stages.

Fishes such as the live-bearing *Sebastes* species with both high fecundity and lengthy periods of larval dispersal are expected to show a high degree of gene flow with little or no genetic differentiation between populations. Despite these life history traits, there seems to be overwhelming evidence for genetic heterogeneity among populations of most *Sebastes* species studied to date (e.g., Rocha-Olivares and Vetter 1999; Buonaccorsi et al. 2005; Gomez-Uchida and Banks 2005). This may be due to multiple factors including timing of larval release, elimination of a drifting egg stage, precocious swimming capability, and directed homing behaviors.

To the extent that pelagic dispersal is driven by oceanography and not behavior, spawning season can have a profound effect on the degree and direction of dispersal and hence the connectivity and demographics of metapopulations located along the coast (Gunderson and Vetter 2006). Of the approximately 65 species of rockfish that occur along the US west coast, most release larvae in winter prior to the spring upwelling season. A few, primarily species within the *Pteropodus* subgenus, release larvae in spring, while others, primarily the *Sebastomus* subgenus, release larvae in summer (Love et al. 2002; Hyde and Vetter 2007). Although there is no agreement on a single month of peak parturition for vermilion rockfish (Lea et al. 1999; Love et al. 2002), an observation perhaps confounded by the presence of a cryptic species, personal observations and published information show that the bulk of parturition occurs in the fall (November–December), the time of weakest alongshore flow and upwelling in the California Current (Longhurst 2007).

Due to severe overexploitation of several rockfish species (i.e., Pacific ocean perch (*Sebastes alutus*), bocaccio (*Sebastes paucispinis*), canary rockfish (*Sebastes pinniger*), cowcod (*Sebastes levis*), darkblotched rockfish (*Sebastes crameri*), widow rockfish (*Sebastes entomelas*), and yelloweye rockfish (*Sebastes ruberrimus*)), a series of depth restricted management areas have been created. These closures began in 2001 with the establishment of the 4300 mi^2 Cowcod Conservation Area in Southern California, soon followed in 2002 with the creation of the California Rockfish Conservation Area, together restricting much of the fishery, both temporally and regionally, with restrictions varying between 36 and 110 m as the maximum allowable fishing depth. These closures have resulted in the near-total protection of the deeper-living sunset rockfish while placing increased fishing effort upon the already heavily exploited nearshore populations of "true" vermilion rockfish.

Together, sunset and vermilion rockfish represent a significant portion of the historic and current commercial and recreational fishery along much of the US west coast (Phillips 1964; www.psmfc.org/recfin). During the period 2002–2006, the vermilion rockfish complex ranked as the number one caught rockfish in the southern California recreational fishery and third statewide. The first stock assessment for vermilion rockfish was conducted by MacCall (2005) but not formally accepted by the Pacific Fisheries Management Council (www.pcouncil.org/groundfish/gfsafe0406/gfsafe0406.html) due to emerging evidence of the cryptic species issue. Despite being overfished in the 1990s, MacCall (2005) suggested that abundance estimates are currently above the precautionary management threshold. However, catch values and biomass estimates used in the 2005 stock assessment were based on the assumption of a single species, a critical management error. Although not currently overfished, at least when assessed as a species complex, vermilion rockfish populations have shown severe declines in both size and age frequencies since the early 1980s with a near complete loss of larger size classes (Love et al. 1998). Such a loss of older and larger fish can be detrimental to the future reproductive quality and capacity of populations (e.g., Berkeley et al. 2004).

The understanding of population connectivity is key to the development of biologically relevant management units and other conservation efforts. This topic is especially relevant, with the establishment of Marine Life Protected Area networks throughout California (www.dfg.ca.gov/mlpa/masterplan.asp) and Oregon as a partial solution to marine fisheries management weaknesses (e.g., Polacheck 1990; McArdle 1998; Murray et al. 1999). However, great care must be taken so that Marine Life Protected Area networks and management regions are designed to properly preserve population connectivity while also providing an exploitable fishery resource. In this paper, we use DNA sequence data from the mitochondrial cytochrome *b* gene to examine population connectivity among "true" vermilion rockfish (sensu Hyde et al. 2008) populations throughout the species' range. We test for barriers to gene flow, provide estimates of average larval dispersal, and compare observed metapopulation structure with oceanographically defined geographic compartments within the California Current Ecological Province as defined by Longhurst (2007).

Fig. 1. Sampling locations and sample size for vermilion rockfish (*Sebastes miniatus*) used in this study with pie charts depicting relative one-step clade (see Fig. 4) content at each site. The 0–100 m bathymetric contour is highlighted yellow to depict possible habitat for vermilion rockfish.

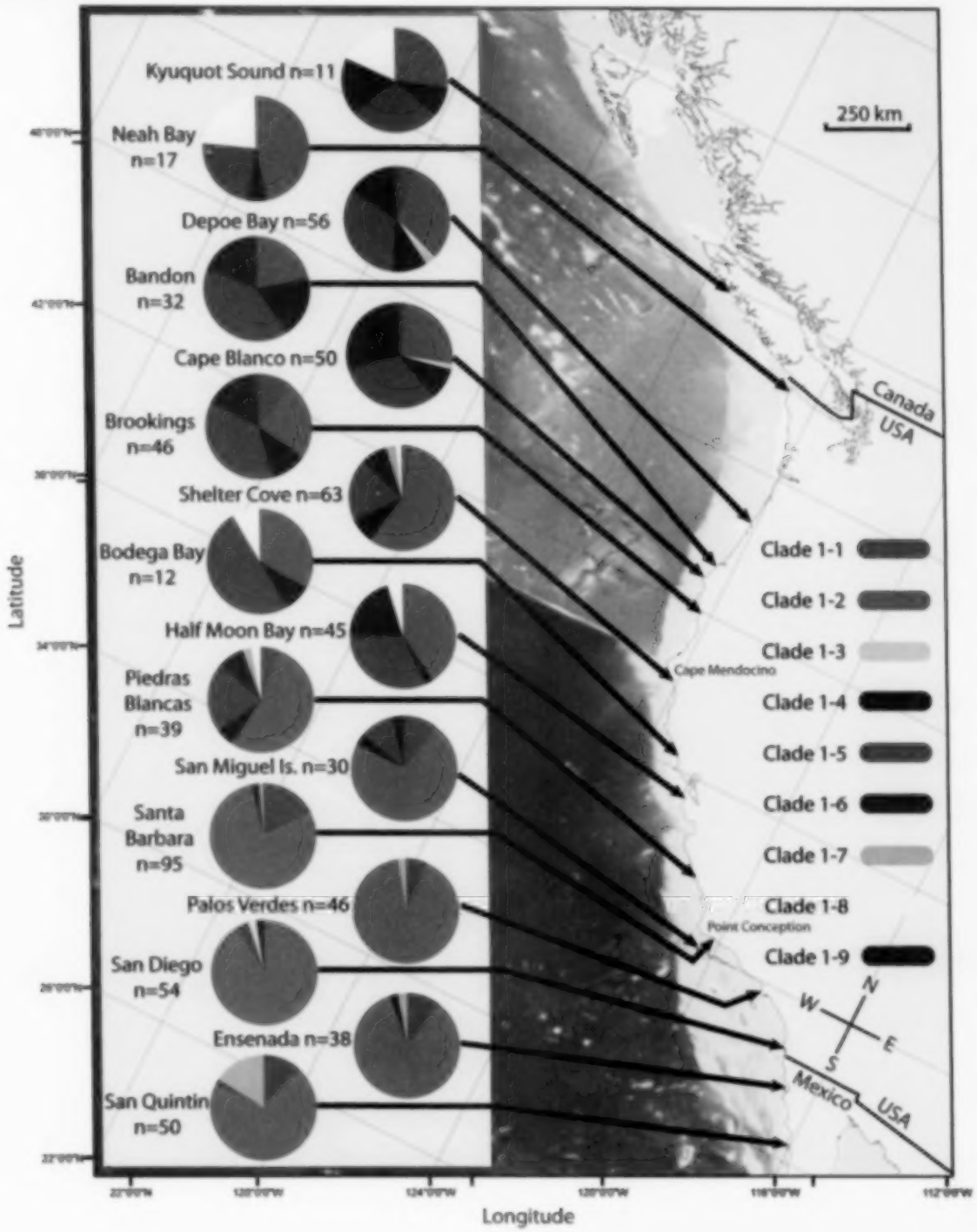

Table 1. Measures of molecular diversity for *Sebastes miniatus*.

Sampling location	*n*	No. of haplotypes	Haplotype diversity	Nucleotide diversity	Tajima's *D*	% haplotype 1
Kyuquot Sound, Canada	11	5	0.855±0.066	0.002±0.001	–0.25	27.3
Neah Bay, Washington	17	5	0.757±0.067	0.001±0.001	–0.47	41.2
Depoe Bay, Oregon	56	11	0.844±0.028	0.002±0.001	–0.72	28.6
Bandon, Oregon	32	8	0.869±0.027	0.002±0.002	0.03	21.9
Cape Blanco, Oregon	50	9	0.856±0.019	0.002±0.002	0.03	22
Brookings, Oregon	46	9	0.853±0.027	0.002±0.001	–0.37	21.7
Shelter Cove, California	63	16	0.776±0.049	0.002±0.001	–1.90*	44.4
Bodega Bay, California	12	6	0.879±0.060	0.002±0.001	–0.14	16.7
Half Moon Bay, California	45	10	0.785±0.036	0.001±0.001	–1.24	33.3
Piedras Blancas, California	39	10	0.832±0.042	0.002±0.001	–1.61*	35.9
San Miguel Island, California	30	9	0.635±0.097	0.001±0.001	–1.96*	60
Santa Barbara, California	95	13	0.489±0.056	0.001±0.001	–2.05*	69.5
Palos Verdes, California	46	10	0.390±0.092	0.001±0.001	–2.19*	78.3
San Diego, California	54	12	0.452±0.085	0.001±0.001	–2.27*	74.1
Ensenada, Mexico	38	11	0.499±0.100	0.001±0.001	–2.05*	71.1
San Quintin, Mexico	50	9	0.598±0.075	0.001±0.001	–1.39	62
Overall	684	42	0.751±0.022	0.002±0.001	–1.16	48.6

Note: An asterisk indicates values significant at the $\alpha = 0.05$ level.

Materials and methods

Sample collection

Fish were collected throughout the common range of the species using various techniques (i.e., hook and line, bottom trawl, pole spear) and identified to species using Love et al. (2002) and genetic species assignment (Hyde et al. 2008). Sampling locations were chosen to represent regions of the west coast that correspond to either current management zones (i.e., Northern, Central, and Southern, www.dfg.ca.gov/marine) or areas between putative phylogeographic breaks recognized for other species of *Sebastes* in this region (e.g., Cope 2004; Matala et al. 2004; Buonaccorsi et al. 2005; J. Hess, National Oceanic and Atmospheric Administration, National Marine Fisheries Service, Northwest Fisheries Science Center, 2725 Montlake Boulevard East, Seattle, WA 98112, USA, personal communication) (Fig. 1). Tissues, either white muscle or pectoral fin clips, were preserved in 95% ethanol pending DNA extraction.

DNA extraction

DNA was extracted from preserved tissue using various protocols. For the majority of samples, DNA was extracted using a proteinase K digestion followed by a lithium chloride – chloroform nucleic acid purification and subsequent ethanol precipitation (Gemmell and Akiyama 1996). DNA from the remaining samples was extracted using either a DNeasy kit (Qiagen) following the manufacturer's protocol or a Chelex (BioRad Laboratories) boiling technique (Walsh et al. 1991; Hyde et al. 2005).

PCR amplification

The mitochondrial cytochrome *b* gene was chosen for this study, as it exhibits a moderate rate of evolution in *Sebastes* species (Hyde and Vetter 2007, J.R. Hyde, unpublished data) and therefore should provide a better signal for population studies than a more variable gene such as the mitochondrial control region, which can exhibit exceedingly high haplotypic diversity in *Sebastes* species (e.g., Rocha-Olivares and Vetter 1999). DNA was amplified for sequencing using primers GluRF2 (5′-AACCATCGTTGTTATTCAACTACAAGAACC) and CB3RF2 (5′-CGAACAGGAARTATCAYTCTGG) in a 10 µL reaction volume containing 67 mmol/L Tris–HCl (pH 8.8), 16.6 mmol/L $(NH_4)_2SO_4$, 10 mmol/L β-mercaptoethanol, 2 mmol/L $MgCl_2$, 800 µmol/L dNTPs, 0.4 µmol/L each primer, 0.5 unit *Taq* DNA polymerase (New England Biolabs), and 50–100 ng of DNA template and amplified using the following temperature profile in a PTC200 DNA Engine (MJ Research): 94 °C for 2 min and 35 cycles of 94 °C for 0.5 min, 59 °C for 1 min, and 72 °C for 1 min followed by 72 °C for 3 min. All PCR batches contained at least one no-template negative control to monitor for possible DNA contamination. Products were electrophoresed through a 2% (*w*/*v*) agarose gel in 1X Tris–borate–EDTA buffer, stained with ethidium bromide, and visualized via a UV transilluminator. Reactions were digested using ExoSAP-IT (USB Corp.) to remove unincorporated primers and deoxynucleotides prior to cycle sequencing. PCR products were sequenced in both forward and reverse directions using BigDye version 3.1 dye terminators (Applied Biosystems) and analyzed on an ABI 3130XL automated capillary sequencer (Applied Biosystems). DNA sequences from both strands were aligned and edited using Sequencher version 4.5 (GeneCodes, Inc). Individual sequences were trimmed to include the first 782 bp of the cytochrome *b* gene for all subsequent analyses.

Genetic analyses

Measures of molecular diversity

Standard indices of molecular diversity, including haplotype (h) and nucleotide diversity (π), were calculated for individual sample sites and the data set as a whole using Arlequin version 3.11 (Excoffier et al. 2005). Tajima's D statistic was calculated using Arlequin and significance tested

Fig. 2. Plots of Φ_{CT} (black) and F_{CT} (gray) values generated during adjacent sample pooling analyses based on subdivision of (*a*) all sample sites and sites (*b*) north and (*c*) south of Point Conception into two groups. Vertical gray lines denote peaks of Φ_{CT} and F_{CT}, which were subsequently analyzed by AMOVA to test for population subdivision.

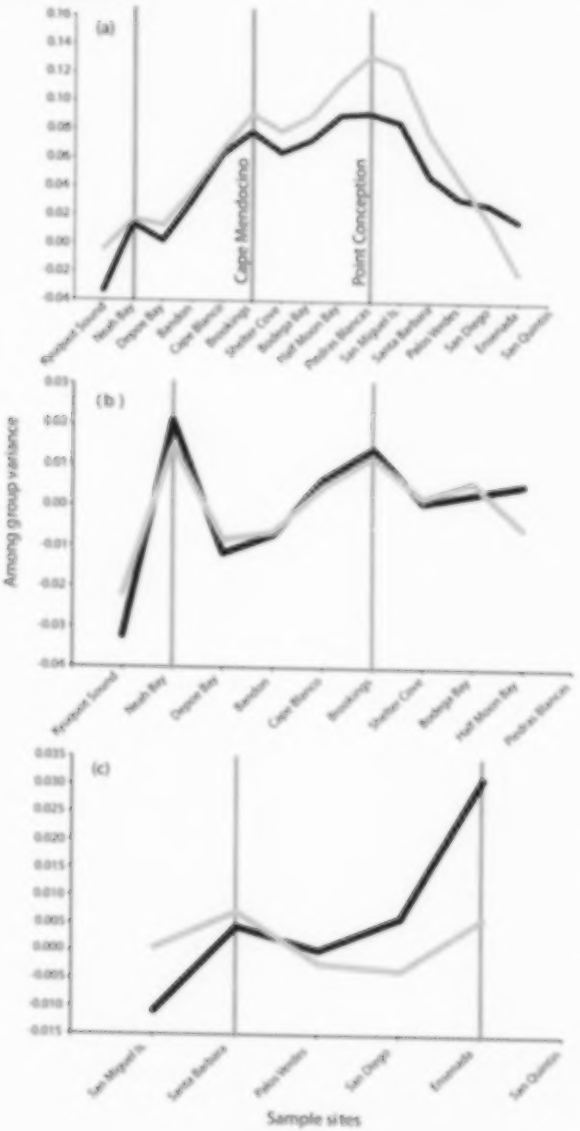

using 10 000 bootstrap replicates. Demographic history can be estimated using the *D* statistic, with negative values signaling an excess of low-frequency haplotypes, possibly due to recent demographic expansion or selective sweeps.

Population structure and gene flow

Pairwise comparisons between all samples of Φ_{ST} and F_{ST} were calculated using Arlequin to assess the level of gene flow between populations. Although Φ and *F* statistics are generally analogous, their differences can help uncover the dynamics of population differentiation. As Φ statistics incorporate measures of genetic distance with the frequency-based analysis of *F* statistics, it is expected that Φ_{ST} values will be greater than F_{ST} values with increasing time since cessation and reduction of gene flow as novel mutations arise. Conversely, recent population subdivision without sufficient time to accumulate novel mutations should result in generally higher values of F_{ST} compared with Φ_{ST}.

As small sample sizes can lead to spurious calculations of Φ_{ST} and F_{ST}, we chose to exclude population samples with $n < 30$ from the isolation by distance analyses. Values of Φ_{ST} and F_{ST} from populations with adequate sample size (i.e., $n \geq 30$) were linearly transformed (i.e., $\Phi_{ST}/(1 - \Phi_{ST})$) (Slatkin 1993) and plotted against geographic distance data obtained using the path measurement tool in Google Earth (earth.google.com). A Mantel test (100 000 permutations) was performed to test the correlation between genetic and geographic distance. The slope of the resultant regression was used to calculate values for average larval dispersal distance. Buonaccorsi et al. (2004, 2005) suggested that the slope of this relationship, combined with estimates of adult density, assuming linear habitat, is amenable to the calculation of average larval dispersal distance for nearshore species of *Sebastes*. Rousset (1997) suggested that habitat could be treated as linear when the habitat width is much less than the distance over which it is compared. Although vermilion rockfish are found in low abundance on offshore banks (Hyde et al. 2008) and around islands in the Southern California Bight, their distribution along much of the coast is primarily within a narrow band of moderately shallow (10–100 m, Fig. 1), nearshore rocky habitat (Love et al. 2002; Williams and Ralston 2002; Hyde et al. 2008), conforming well to Rousset's requirement. By comparing the inverse of the slope of the genetic and geographic regression with the product $D(\sigma^2)$, while inserting reasonable values for adult density (D), the standard deviation or average dispersal distance (σ) can be calculated. Using this relationship, we calculated values of average larval dispersal for a wide range of reasonable adult densities assuming symmetrical, exponential dispersal along a linear habitat.

To assess the geographic partitioning of genetic variance, a hierarchical analysis of molecular variance (AMOVA) was performed using Arlequin version 3.11 (Excoffier et al. 2005). To investigate whether previously proposed phylogeographic breaks may act to restrict gene flow, samples were evaluated using an adjacent sample pooling analysis (sensu Buonaccorsi et al. 2004, 2005). If such a barrier to gene flow exists, it would be expected that populations on either side would be relatively homogeneous, while populations across the barrier would be distinct. By this method, adjacent samples were pooled to create two or more groups in all possible combinations. The best grouping of populations would show the greatest and most significant levels of among-group heterogeneity (Φ_{CT} and F_{CT}) while at the same time showing the smallest and least significant levels of within-group heterogeneity (Φ_{SC} and F_{SC}). Plots of Φ_{CT} and F_{CT} from the adjacent sample pooling analysis were constructed and examined for peaks that may indicate significant barriers to gene flow. Partitioning of samples based on these peaks was assessed by AMOVA.

Table 2. Pairwise Φ_{ST} and F_{ST} comparisons between sampling sites below the diagonal and associated p values above the diagonal.

Sample site	Kyuquot Sound	Neah Bay	Depoe Bay	Bandon	Cape Blanco	Brookings	Shelter Cove	Bodega Bay
Φ_{ST}								
Kyuquot Sound	—	0.741	0.555	0.404	0.251	0.512	0.582	0.192
Neah Bay	–0.03845	—	0.05	**0.027**	**0.01**	**0.036**	0.128	0.075
Depoe Bay	–0.01252	0.04358	—	0.647	0.289	0.848	0.12	0.113
Bandon	–0.00116	0.06842	–0.00886	—	0.375	0.637	**0.014**	0.312
Cape Blanco	0.01594	0.09463	0.00359	-1×10^{-5}	—	0.198	**0.002**	0.07
Brookings	–0.00933	0.05376	–0.01141	–0.0093	0.00931	—	**0.033**	0.185
Shelter Cove	–0.01116	0.01888	0.01073	0.04031	0.0561	0.02388	—	**0.012**
Bodega Bay	0.03969	0.07416	0.03536	0.00802	0.05995	0.02276	0.08008	—
Half Moon Bay	–0.03277	0.03922	0.00344	0.02198	0.02976	0.00608	0.0129	0.07304
Piedras Blancas	–0.00983	0.02013	0.02059	0.0559	0.0721	0.02872	–0.01104	0.08264
San Miguel Is.	0.04492	0.05601	0.04245	0.10002	0.09719	0.05904	–0.00288	0.16344
Santa Barbara	0.1818	0.16896	0.14247	0.243	0.21472	0.16369	0.06689	0.34251
Palos Verdes	0.16463	0.1419	0.11861	0.20339	0.17974	0.1485	0.04174	0.31998
San Diego	0.12503	0.10819	0.09959	0.17577	0.16016	0.13126	0.02577	0.26385
Ensenada	0.1026	0.10357	0.0959	0.16279	0.14523	0.11757	0.0366	0.23849
San Quintin	0.12766	0.12116	0.11641	0.18401	0.17071	0.13621	0.04767	0.24975
F_{ST}								
Kyuquot Sound	—	0.737	0.444	0.577	0.199	0.641	0.207	0.472
Neah Bay	–0.03778	—	0.117	0.063	**0.009**	0.054	0.203	0.169
Depoe Bay	–0.00337	0.02521	—	0.799	0.321	0.694	0.109	0.315
Bandon	–0.01159	0.04194	–0.01129	—	0.766	0.808	**0.033**	0.666
Cape Blanco	0.02227	0.06963	0.00269	–0.0113	—	0.229	**0.003**	0.301
Brookings	–0.01536	0.04153	–0.00677	–0.0126	0.00698	—	**0.013**	0.451
Shelter Cove	0.01623	0.01232	0.01145	0.03102	0.04753	0.03453	—	**0.042**
Bodega Bay	–0.00362	0.03759	0.00713	–0.0166	0.0099	–0.0024	0.05681	—
Half Moon Bay	–0.03824	0.01444	0.01197	0.01487	0.04315	0.00855	0.01875	0.03854
Piedras Blancas	–0.0184	0.00431	0.00587	0.01978	0.04431	0.0121	–0.00586	0.02856
San Miguel Is.	0.08966	0.04658	0.06274	0.10391	0.10925	0.09583	0.00325	0.14217
Santa Barbara	0.21898	0.15231	0.16609	0.22447	0.21623	0.20283	0.0776	0.28417
Palos Verdes	0.27543	0.1855	0.19595	0.25598	0.24305	0.24534	0.09617	0.33982
San Diego	0.23029	0.1498	0.16899	0.22225	0.2153	0.21756	0.07224	0.28823
Ensenada	0.19698	0.12623	0.14436	0.19222	0.18495	0.19004	0.05829	0.25775
San Quintin	0.14494	0.09351	0.11076	0.15438	0.15362	0.1436	0.03603	0.20027

Note: Values significant at the $\alpha = 0.05$ level are highlighted in bold.

Similarly, Monmonier's (1973) maximum difference algorithm was implemented using the program Barriers version 2.2 (Manni et al. 2004) to search for barriers to gene flow. This method uses Delaunay triangulation to connect a series of sample localities in conjunction with a distance matrix (i.e., Φ_{ST} or F_{ST}) to locate areas of maximum change, suggesting the existence of a barrier. As this method is sensitive to inaccurate measures of genetic distance, particularly in the middle of the sample distribution, only samples of $n \geq 30$ were used.

Statistical parsimony and nested clade phylogeographic analysis

The computer program TCS version 1.21 (Clement et al. 2000) was used to generate a statistical parsimony network among all vermilion haplotypes, rooted with the most common sunset rockfish haplotype, and using the default 95% parsimony connection limit. Loop structures were resolved following Pfenninger and Posada (2002). The resultant haplotype network was then partitioned into sequentially nested groupings of one-step clades following Templeton et al. (1995). Nested clade phylogeographic analysis was performed using the program GeoDis version 2.5 (Templeton et al. 1995) in conjunction with the geographic distance matrix used in the isolation by distance analysis. The results of this analysis were interpreted using the dichotomous key provided on the GeoDis Web site (darwin.uvigo.es/).

Results

Haplotype and nucleotide diversity

In total, 782 bp of DNA sequence were analyzed from 684 individuals from 16 geographic locations throughout the entirety of the species' common range (Table 1). We found 42 unique haplotypes among the 16 sites. The 39 variable sites were primarily distributed across third-position sites ($n = 32$); however, there were seven mutations at first-position sites. Only one of the haplotypes resulting from the seven first-position mutations, "Haplotype 8", is relatively common in any population, occurring primarily in populations in the northern half of the study area. Haplotype sequences have been deposited in GenBank, accession Nos.

Half Moon Bay	Piedras Blancas	San Miguel Is.	Santa Barbara	Palos Verdes	San Diego	Ensenada	San Quintin
0.818	0.561	0.083	**0.002**	**<0.001**	**0.002**	**0.01**	**0.006**
0.076	0.146	**0.024**	**<0.001**	**<0.001**	**<0.001**	**<0.001**	**0.002**
0.287	0.064	**0.019**	**<0.001**	**<0.001**	**<0.001**	**<0.001**	**<0.001**
0.102	**0.008**	**<0.001**	**<0.001**	**<0.001**	**<0.001**	**<0.001**	**<0.001**
0.048	**0.002**	**0.001**	**<0.001**	**<0.001**	**<0.001**	**<0.001**	**<0.001**
0.24	**0.038**	**0.008**	**<0.001**	**<0.001**	**<0.001**	**<0.001**	**<0.001**
0.103	0.926	0.525	**<0.001**	**<0.001**	**0.006**	**0.002**	**<0.001**
0.039	**0.02**	**0.001**	**<0.001**	**<0.001**	**<0.001**	**<0.001**	**<0.001**
—	0.177	**0.012**	**<0.001**	**<0.001**	**<0.001**	**<0.001**	**<0.001**
0.01027	—	0.586	**<0.001**	**<0.001**	**0.008**	**0.002**	**<0.001**
0.05554	–0.00531	—	0.167	0.253	0.328	0.351	**0.045**
0.16602	0.07403	0.01026	—	0.095	**0.002**	0.15	**0.006**
0.13815	0.05317	0.00463	0.01498	—	0.548	0.645	**0.023**
0.10887	0.03206	0.00277	0.04129	–0.00192	—	0.062	**0.002**
0.1119	0.04247	0.00191	0.0099	–0.00576	0.0142	—	0.05
0.13599	0.05548	0.02961	0.04124	0.03173	0.04259	0.02439	—
0.913	0.660	**0.033**	**0.002**	**<0.001**	**<0.001**	**0.002**	**0.006**
0.229	0.325	0.069	**0.001**	**<0.001**	**0.001**	**0.003**	**0.01**
0.135	0.236	**0.006**	**<0.001**	**<0.001**	**<0.001**	**<0.001**	**<0.001**
0.150	0.098	**0.001**	**<0.001**	**<0.001**	**<0.001**	**<0.001**	**<0.001**
0.008	**0.006**	**<0.001**	**<0.001**	**<0.001**	**<0.001**	**<0.001**	**<0.001**
0.201	0.149	**<0.001**	**<0.001**	**<0.001**	**<0.001**	**<0.001**	**<0.001**
0.070	0.630	0.289	**<0.001**	**<0.001**	**<0.001**	**0.004**	**0.014**
0.113	0.148	**0.005**	**<0.001**	**<0.001**	**<0.001**	**<0.001**	**<0.001**
—	0.507	**0.007**	**<0.001**	**<0.001**	**<0.001**	**<0.001**	**<0.001**
–0.00425	—	0.072	**<0.001**	**<0.001**	**<0.001**	**<0.001**	**0.003**
0.07363	0.02843	—	0.237	0.079	0.143	0.253	0.48
0.17741	0.12323	0.00595	—	0.101	0.059	0.133	0.184
0.20418	0.15589	0.02734	0.01597	—	0.867	0.771	0.057
0.17301	0.12454	0.0142	0.02026	–0.01017	—	0.769	0.071
0.15358	0.10705	0.00515	0.01311	–0.01065	–0.00915	—	0.178
0.12237	0.07053	–0.004	0.00759	0.02675	0.02031	0.00977	—

EF587183–EF587231. The most common haplotype, "Haplotype 1", was found in high abundance in all populations and dominated the samples south of Point Conception (Table 1). Sites south of Point Conception had lower haplotype diversity than those to the north. Values for Tajima's D were significantly negative at several locations (Table 1), particularly the southern California sample sites, suggesting recent demographic expansion in this region.

Population subdivision as revealed by mitochondrial DNA sequence

AMOVA revealed significant partitioning of genetic variance across multiple geographic features within the study area. Adjacent sample pooling analysis (Fig. 2*a*) indicated that the strongest population subdivision occurred between groups of populations across the biogeographic barrier at Point Conception (two groups: $\Phi_{CT} = 0.0923$, $p < 0.001$ and $F_{CT} = 0.0135$, $p < 0.001$). To remove the effect of this barrier, the sample set was split into a northern and southern set and adjacent sample pooling analysis was performed on each set (Figs. 2*b* and 2*c*). AMOVA showed that the groups delineated in Figs. 2*b* and 2*c* were significant for both the northern set ($\Phi_{CT} = 0.0267$, $p = 0.004$ and $F_{CT} = 0.0209$, $p < 0.01$) and the southern set ($\Phi_{CT} = 0.0230$, $p = 0.049$ and $F_{CT} = 0.0200$, $p = 0.039$). All alternate groupings of these data sets produced smaller and insignificant values of Φ_{CT} and F_{CT}. Overall AMOVA results considering six partitions were $\Phi_{ST} = 0.0845$ ($p < 0.001$) and $F_{ST} = 0.1031$($p < 0.001$), $\Phi_{CT} = 0.0776$ ($p < 0.001$) and $F_{CT} = 0.1017$ ($p < 0.001$), and $\Phi_{SC} = 0.007$ ($p = 0.168$) and $F_{SC} = 0.0002$ ($p = 0.454$). The Monmonier maximum difference algorithm produced identical results to the AMOVA-based adjacent sample pooling analysis (data not shown).

Pairwise Φ_{ST} and F_{ST} values were highly significant between most population pairs across the biogeographic break at Point Conception, even after Bonferroni correction for multiple comparisons (Table 2). The nonsignificant comparisons involved comparison with the San Miguel Island site, perhaps suggesting that this is a zone of overlap. The greatest difference between Φ_{CT} and F_{CT} in the AMOVA-based adjacent sample pooling analysis occurs at San Miguel Island, further suggesting that this is a contemporary zone of

Fig. 3. Plots of linearized (Slatkin 1993) genetic distance (Φ_{ST} and F_{ST}) between pairwise comparisons of sampling sites ($n \geq 30$) in relation to geographic distance. Relationships are presented for (*a*) all sampling sites, (*b*) only sites north of Point Conception, and (*c*) only sites south of Point Conception.

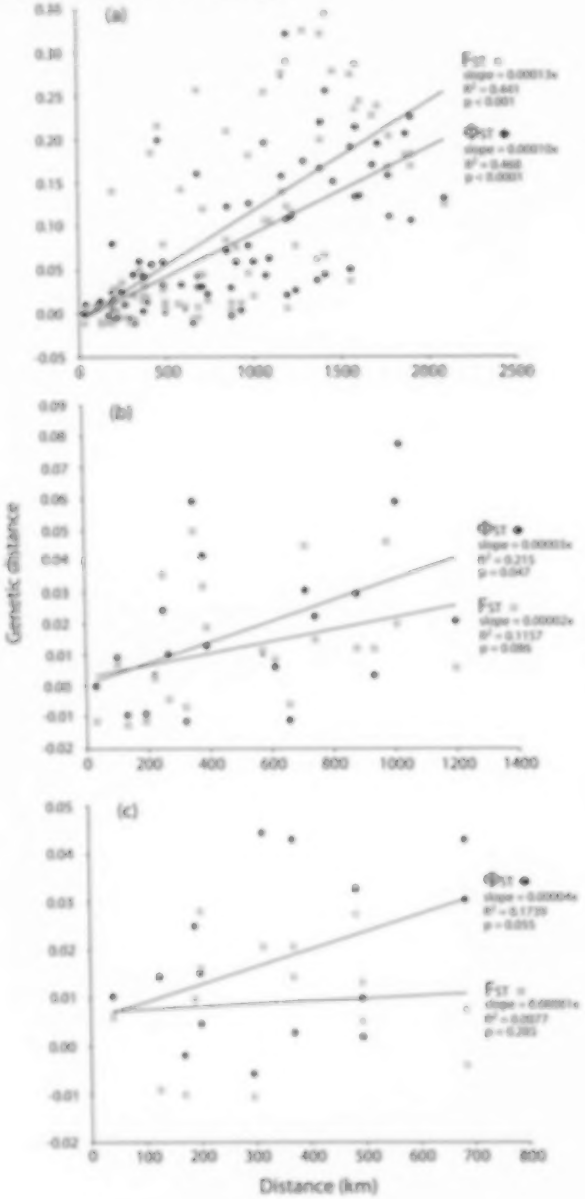

overlap. Comparisons between adjacent population pairs north of Point Conception were typically not significant at the $\alpha = 0.05$ level; however, significance was usually obtained at greater geographic distance. South of Point Conception, the San Quintin sample set was significantly different from all sites for pairwise comparisons of Φ_{ST} except the adjacent Ensenada sample set ($p = 0.05$); pairwise F_{ST} comparisons were not significant.

Table 3. Calculations of average larval dispersal distance based on isolation by distance regression from all sample sites, sites north of Point Conception, and sites south of Point Conception.

σ^2	D	Average dispersal (km)
All sites		
1010.1	10	22.5
101.1	100	7.1
10.1	1000	2.2
1.0	10000	0.7
Sites north of Point Conception		
2941.2	10	38.3
294.1	100	12.1
29.4	1000	3.8
2.9	10000	1.2
Sites south of Point Conception		
2702.7	10	36.8
270.3	100	11.6
27.0	1000	3.7
2.7	10000	1.2

Note: Various values for adult density per kilometre of linear coastline (D) and associated dispersal values are presented.

Isolation by distance analyses revealed a significant positive correlation between increasing genetic and geographic distance when all sample locations were compared (Fig. 3*a*) and also when the subdivided northern and southern data sets were analyzed separately (Figs. 3*b* and 3*c*). The plotted relationships between Φ_{ST} and geographic distance produced a regression with a slope of $\Phi_{ST} = 0.099$ per 1000 km when all samples were compared and a $\Phi_{ST} = 0.034$ per 1000 km (northern sites) and $\Phi_{ST} = 0.037$ per 1000 km (southern sites) when the northern and southern sites were analyzed separately.

As the AMOVA indicated genetic breaks within the data set, the application of a generalized regression for isolation by distance should be viewed with caution, especially across strong breaks such as Point Conception. However, these regressions may still be useful to estimate larval dispersal when major genetic breaks are removed from the analysis. Using a range of adult densities, we calculated possible values for average larval dispersal distance (σ) for both the entire data set and the northern and southern data sets (Table 3). Values for average larval dispersal distance varied from 0.7–22.5 km when the data set was analyzed as a whole to 1.2–38.3 and 1.2–36.8 km when the northern and southern data sets, respectively, were analyzed. Such values are similar to those found for other nearshore *Sebastes* species using this method (i.e., Taylor 2004; Buonaccorsi et al. 2005).

Nested clade phylogeographic analysis

Nested clade phylogeographic analysis revealed a significant pattern of restricted gene flow with isolation by distance both at the total cladogram scale and at the scale of one-step and two-step clade analysis (Fig. 4; Table 4). This

Fig. 4. Statistical parsimony network among 42 *Sebastes miniatus* haplotypes rooted with a single *Sebastes crocotulus* haplotype. Node size is proportional to overall haplotype frequency; solid circles indicate intermediate haplotypes that were not sampled in this study. Haplotypes are grouped by one-step clade assignment used for nested clade phylogeographic analysis.

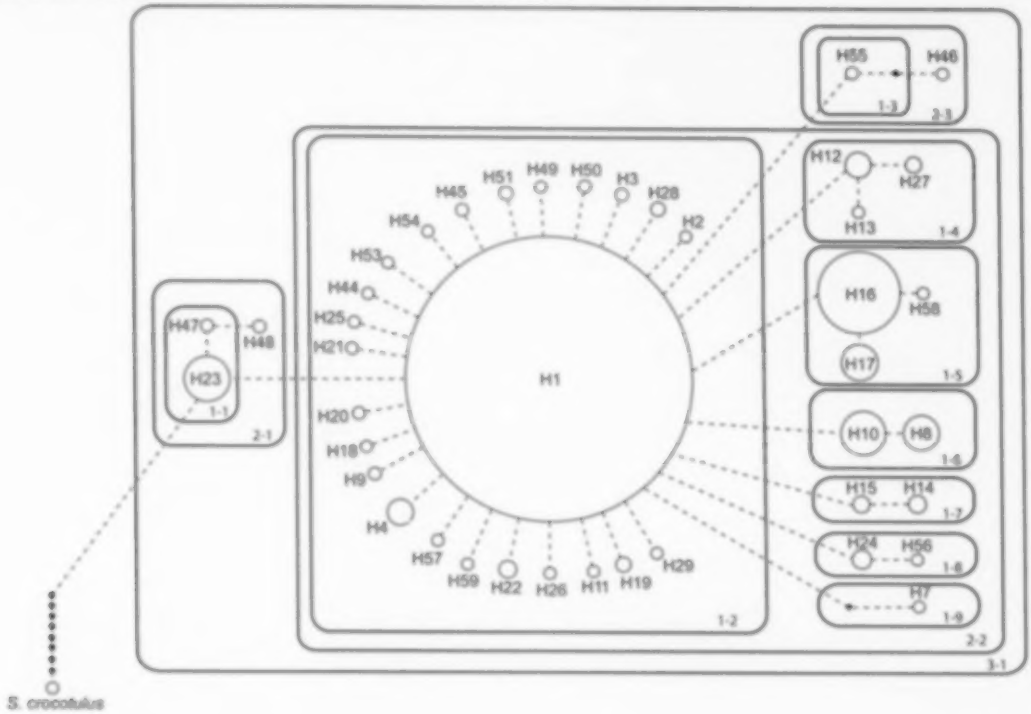

Table 4. Results of nested clade phylogenetic analysis.

Clade	
One-step	
Clade 1-1	Inconclusive outcome
Clade 1-2	**Restricted gene flow with isolation by distance**
Clade 1-3	Inconclusive outcome
Clade 1-4	Inconclusive outcome
Clade 1-5	**Restricted gene flow with isolation by distance**
Clade 1-6	**Restricted gene flow with isolation by distance**
Clade 1-7	**Contiguous range expansion**
Clade 1-8	Inconclusive outcome
Clade 1-9	Inconclusive outcome
Two-step	
Clade 2-1	Inconclusive outcome
Clade 2-2	**Restricted gene flow but with some long distance dispersal**
Clade 2-3	Inconclusive outcome
Total cladogram	
Clade 3-1	**Restricted gene flow with isolation by distance**

Note: Clades refer to those designated in Fig. 4. Significant conclusions are highlighted in bold type.

pattern was driven by the near-complete restriction of 19 haplotypes to populations north of Point Conception and a progressive change, with latitude, in the relative frequencies of several dominant haplotypes and one-step haplotype clades (see Fig. 1). This finding is in agreement with the results of the isolation by distance analysis (Table 3). The predominance of several derived haplotypes in northern samples as well as the southern affinity of the ancestral haplotypes suggest that the historical trend of gene flow has been primarily northward.

Fig. 5. Map of National Oceanic and Atmospheric Administration Pathfinder sea surface temperature data averaged over the month of November 2007 (http://coastwatch.pfeg.noaa.gov/). Black lines denote areas across which gene flow was found to be restricted. White arrows indicate end points for Longhurst's (2007) compartments of the California Current Province.

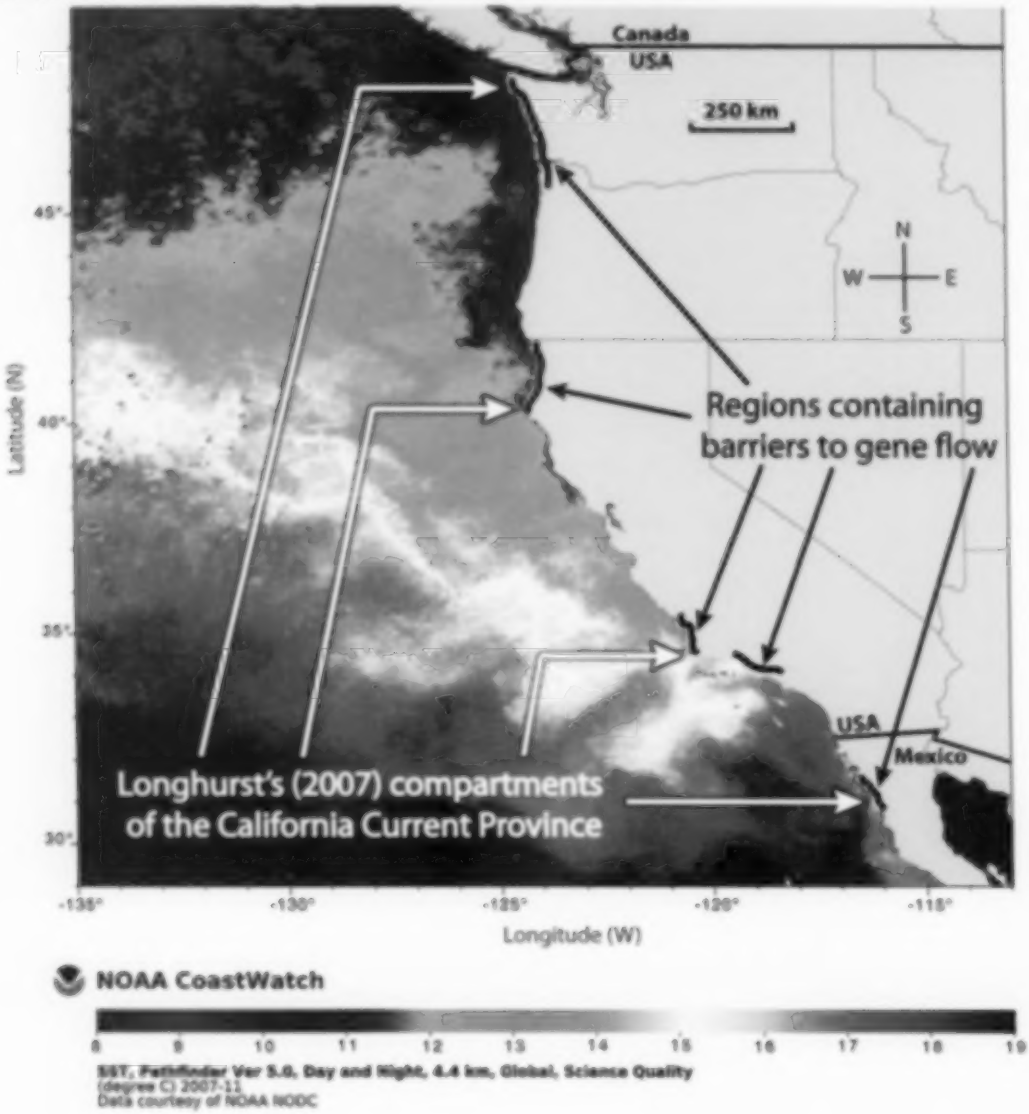

Discussion

Phylogeography and population structure

Analysis of population structure revealed significant genetic heterogeneity throughout the range of vermilion rockfish. Both the Monmonier maximum difference algorithm and AMOVA partitioned the genetic variance within the separate coastal upwelling regions as proposed by Parrish et al. (1981) and Longhurst (2007) with an additional barrier between Santa Barbara and Palos Verdes (Fig. 5). The strongest barrier to gene flow was across Point Conception, a well-documented biogeographic break between the Oregonian and San Diegan provinces (Briggs 1974). Recent studies have suggested that Point Conception may not function as a genetic barrier for all species (e.g., Burton 1998) and that stronger barriers may be present elsewhere within the Southern California Bight. However, this study and studies of other *Sebastes* species have shown that populations north and south of Point Conception are often significantly different (i.e., Buonaccorsi et al. 2004, 2005; Matala et al. 2004). Additional genetic barriers were found in the vicinity of Cape Mendocino, Punta Colnett, Santa Monica Bay, and along the coast of Washington. Several of these oceanographic features have been shown to function as strong ge-

netic barriers for other fishes (e.g., Bernardi 2000), including blue rockfish (*Sebastes mystinus*) (Cope 2004) and yellowtail rockfish (*Sebastes flavidus*) (J. Hess, National Oceanic and Atmospheric Administration, National Marine Fisheries Service, Northwest Fisheries Science Center, 2725 Montlake Boulevard East, Seattle, Washington 98112 USA, personal communication (2006)). Similarly, analysis of catch data from three years of coast-wide pelagic juvenile rockfish surveys showed a low incidence of pelagic juveniles in the offshore jets at Point Conception and Cape Mendocino (Sakuma et al. 2006), further supporting the hypothesis that these features act as barriers to gene flow for many *Sebastes* species.

A significant and positive correlation was found between increasing genetic and geographic distance. This was true when all samples were compared as well as when the samples were divided into two sets to remove the effect of the strong genetic break at Point Conception. The regressions fit to the entire data set and the two subsets differed in their slopes, Φ_{ST} = 0.099, Φ_{ST} = 0.034, and Φ_{ST} = 0.037 per 1000 km. The differences between the entire data set and the two subsets are likely artifacts of comparing populations across the genetic barrier found at Point Conception. We believe that the subset regressions are more accurate for calculating values of larval dispersal distance.

Using the equations of Rousset (1997), the slopes of the isolation by distance regressions, and reasonable values for adult density, we calculated a range of distance values for average larval dispersal. The obtained values were much less than would be expected for a species with a larval and pelagic juvenile phase of 2–3 months. However, studies of other nearshore rockfish species (i.e., Buonaccorsi et al. 2002, 2004, 2005) have produced similar and even lower values for geographic dispersal. Buonaccorsi et al. (2004, 2005) suggested that this limited dispersal may be due in part to the existence of a coastal boundary layer (sensu Largier 2003) acting to retain larvae nearshore, reducing entrainment in the bulk alongshore flow, thereby limiting dispersal.

Vermilion rockfish, in a pattern atypical of most *Sebastes* species, show peak larval release during the fall and early winter months (Love et al. 2002). In contrast with the typical southward flow driven by the California Current throughout much of the year, fall and early winter (September–February) are characterized by weak poleward flow, at least in the nearshore, driven by sporadic pulses of the northerly flowing Davidson Current (Parrish et al. 1981; Longhurst 2007). This pattern of weak northward transport is in agreement with the results of the nested clade and isolation by distance analyses. A plot of average sea surface temperature for November (Fig. 5), the peak month of parturition, shows that discrete water masses at this time largely conform to the barriers to gene flow observed in this study. Larval release during a period of low-level, sporadic poleward flow may help to account for the high degree of population structure and low levels of larval dispersal observed.

Settlement of juveniles to shallow, nearshore habitats followed by an ontogenetic migration to deeper adult habitat is a common theme among *Sebastes* species (Love et al. 1991). Hyde et al. (2008) suggested that a truncation or loss of this ontogenetic migration in a subset of the vermilion rockfish ancestor precipitated the divergence of sunset and vermilion rockfish. It is easy to envision how such a mechanism, when combined with limited adult dispersal (e.g., Miller and Geibel 1973; Lea et al. 1999; Mitamura et al. 2005), may effectively shorten the dispersal capacity of this species.

It is important to acknowledge that a population study using a single, maternally inherited locus carries with it several caveats. Sex-biased dispersal or migrations could strongly influence the results using a purely maternally inherited marker. Tagging studies of vermilion rockfish (e.g., Hartmann 1987; Lea et al. 1999) have shown no movement of tagged individuals, suggesting that larval dispersal is the primary mode of gene flow. Levels of genetic fixation can vary between loci; therefore, averaging over multiple loci can usually provide a more accurate estimation of the true fixation index and may reveal more fine-scale patterns of differentiation. It is possible that the Φ_{CT} and F_{CT} values presented in this study are under- or overestimates of the true values. Preliminary analyses, using multiple microsatellite loci, have produced remarkably similar patterns of genetic subdivision and isolation by distance (J.R. Hyde and J. Budrick, unpublished data).

Management implications

Vermilion rockfish have historically represented an important commercial and recreational fishery in California, Oregon, and Washington. During the 14 year period 1990–2004, the California commercial and recreational fisheries took 2386 and 3341 t, respectively (MacCall 2005). Among recreationally targeted rockfishes, vermilion rockfish are currently the number one caught rockfish in the southern California fishery and third statewide. At current levels of exploitation, there exists a great potential for fishery decline without proper management.

Tajima's *D* statistic was significantly negative at seven sites, including all sites within the Southern California Bight. Negative values of the *D* statistic suggest recent demographic expansion or a selective sweep. This may be due to the high level of exploitation and shift in the demographics of vermilion rockfish in this region (e.g., Love et al. 1998). Since 1999 there have been several large recruitment events in southern California (MacCall 2005; J.R. Hyde, personal observation). The combination of reduced spawning biomass and sweepstakes-like recruitment events could possibly lead to a strong reduction in haplotypic diversity such as that observed at the southern sites. The possibility that human exploitation could result in a measureable reduction in genetic diversity in a long-lived species such as vermilion rockfish is alarming and merits further study.

Isolation by distance analyses suggested that larval dispersal is relatively small (i.e., <38 km), suggesting a stepping-stone model of dispersal between adjacent reefs. This finding has obvious implications for the planning of marine reserve networks and is especially relevant during the current move to establish marine reserves as a solution to fishery management along the California coast. To maintain sustainable populations within the reserves while also providing access and benefit for the fishery, these reserves must be spaced close enough to effectively communicate larvae and maintain gene flow.

Analyses also showed significant barriers to gene flow across several geographic features that impinge into the Cal-

ifornia Current system, suggesting that vermilion rockfish should be managed on a regional scale between these features rather than on a coastwide basis. Currently, vermilion rockfish are managed at the state level under the guidance of the Pacific Fisheries Management Council. The primary management regions within California (i.e., Northern, Central, and Southern) are delineated by Cape Mendocino and Point Conception and conform well to our results. California's Northern management region should be managed together with the Oregon fishery. Although our results suggest that Neah Bay and northward be managed separately, this is likely of little consequence due to the insignificant catch rate of vermilion rockfish in this region. Ideally, California's Southern management region, where the bulk of vermilion rockfish are landed, would be managed together with the fishery in northern Baja, Mexico. This last point has become exceedingly important, as current rockfish closures in southern California have dramatically increased fishing effort in Mexican waters by US fishers (J.R. Hyde, personal observation).

Acknowledgements

The assistance of numerous people in the field collection of fish used in this study is greatly appreciated, in particular M. Lackey and the crew of the F/V *Vagabond*, K. Franke and the crew of the F/V *Outer Limits*, the captain and crew of the F/V *Pacific Queen*, and J. Diamond and the crew of the F/V *Stardust*. D. Bodenmiller (Oregon Department of Fish and Wildlife), J. Budrick (California Department of Fish and Game), J. Butler (National Marine Fisheries Service), T. Carpenter (California Department of Fish and Game), J. Headlee (Oregon Department of Fish and Wildlife), M. Johansson (Oregon State University), N. Kellar (National Marine Fisheries Service), M. Love (University of California at Santa Barbara), J. Marliave (Vancouver Aquarium), M. McCrae (University of California at Santa Barbara), R. Nakamura (California State University In San Luis Obispo), and T. Olive (California State University In San Luis Obispo) also provided invaluable assistance in sample collection. S. Snyder and C. Shultz provided valuable assistance in the laboratory analyses. V. Buonaccorsi provided valuable insight into the population genetic analyses. Comments provided by three anonymous reviewers greatly improved the manuscript. Funding for this project was provided by the Southwest Fisheries Science Center of the National Marine Fisheries Service.

References

Berkeley, S.A., Hixon, M.A., Larson, R.J., and Love, M. 2004. Fisheries sustainability via protection of age structure and spatial distribution of fish populations. Fisheries, **29**(8): 23–32. doi:10.1577/1548-8446(2004)29[23:FSVPOA]2.0.CO;2.

Bernardi, G. 2000. Barriers to gene flow in *Embiotoca jacksoni*, a marine fish lacking a pelagic larval stage. Evolution, **54**(1): 226–237. PMID:10937199.

Briggs, J.C. 1974. Marine zoogeography. McGraw-Hill, New York.

Buonaccorsi, V.P., Kimbrell, C.A., Lynn, E.A., and Vetter, R.D. 2002. Population structure of copper rockfish (*Sebastes caurinus*) reflects postglacial colonization and contemporary patterns of larval dispersal. Can. J. Fish. Aquat. Sci. **59**(8): 1374–1384. doi:10.1139/f02-101.

Buonaccorsi, V.P., Westerman, M., Stannard, J., Kimbrell, C., Lynn, E., and Vetter, R.D. 2004. Molecular genetic structure suggests limited larval dispersal in grass rockfish, *Sebastes rastrelliger*. Mar. Biol. (Berl.), **145**: 779–788.

Buonaccorsi, V.P., Kimbrell, C.A., Lynn, E.A., and Vetter, R.D. 2005. Limited realized dispersal and introgressive hybridization influence genetic structure and conservation strategies for brown rockfish, *Sebastes auriculatus*. Conserv. Biol. **6**: 697–713.

Burton, R.S. 1998. Intraspecific phylogeography across the Point Conception biogeographic boundary. Evolution, **52**(3): 734–745. doi:10.2307/2411268.

Clement, M., Posada, D., and Crandall, K.A. 2000. TCS: a computer program to estimate gene genealogies. Mol. Ecol. **9**(10): 1657–1659. doi:10.1046/j.1365-294x.2000.01020.x. PMID: 11050560.

Cope, J.M. 2004. Population genetics and phylogeography of the blue rockfish (*Sebastes mystinus*) from Washington to California. Can. J. Fish. Aquat. Sci. **61**(3): 332–342. doi:10.1139/f04-008.

Excoffier, L., Laval, G., and Schneider, S. 2005. Arlequin (version 3.0): an integrated software package for population genetics data analysis. Evol. Bioinform. Online, **1**: 47–50. PMID:19325852.

Gemmell, N.J., and Akiyama, S. 1996. An efficient method for the extraction of DNA from vertebrate tissues. Trends Genet. **12**(9): 338–339. doi:10.1016/S0168-9525(96)80005-9. PMID:8855658.

Gomez-Uchida, D., and Banks, M.A. 2005. Microsatellite analyses of spatial genetic structure in darkblotched rockfish (*Sebastes crameri*): is pooling samples safe? Can. J. Fish. Aquat. Sci. **62**(8): 1874–1886. doi:10.1139/f05-084.

Gunderson, D.R., and Vetter, R.D. 2006. Temperate rocky reef fishes. *In* Marine metapopulations. *Edited by* P.F. Sale and J.P. Kritzer. Academic Press, San Diego, Calif. pp. 69–117.

Hartmann, A.R. 1987. Movement of scorpionfishes (Scorpaenidae: *Sebastes* and *Scorpaena*) in the southern California Bight. Calif. Fish Game, **73**: 68–79.

Hyde, J.R., and Vetter, R.D. 2007. The origin, evolution, and diversification of rockfishes of the genus *Sebastes* (Cuvier). Mol. Phylogenet. Evol. **44**(2): 790–811. doi:10.1016/j.ympev.2006.12.026. PMID:17320419.

Hyde, J.R., Lynn, E., Humphreys, R., Jr., Musyl, M., West, A.P., and Vetter, R. 2005. Shipboard identification of fish eggs and larvae by multiplex PCR, and description of fertilized eggs of blue marlin, shortbill spearfish, and wahoo. Mar. Ecol. Prog. Ser. **286**: 269–277. doi:10.3354/meps286269.

Hyde, J.R., Kimbrell, C.A., Budrick, J.E., Lynn, E.A., and Vetter, R.D. 2008. Cryptic speciation in the vermilion rockfish (*Sebastes miniatus*) and the role of bathymetry in the speciation process. Mol. Ecol. **17**(4): 1122–1136. doi:10.1111/j.1365-294X.2007.03653.x. PMID:18261052.

Jordan, D.S., and Gilbert, C.H. 1880. Description of a new species of *Sebastichthys* (*Sebastichthys miniatus*) from Monterey Bay, California. Proc. U.S. Nat. Mus. **3**: 70–73.

Jorgensen, S.J., Kaplan, D.M., Klimley, A.P., Morgan, S.G., O'Farrell, M.R., and Botsford, L.W. 2006. Limited movement in blue rockfish (*Sebastes mystinus*): internal structure of the home range. Mar. Ecol. Prog. Ser. **327**: 157–170. doi:10.3354/meps327157.

Largier, J.L. 2003. Considerations in estimating larval dispersal distances from oceanographic data. Ecol. Appl. **13**(Suppl.): S71–S89. doi:10.1890/1051-0761(2003)013[0071:CIELDD]2.0.CO;2.

Lea, R.N., McAllister, R.D., and VenTresca, D.A. 1999. Biological aspects of nearshore rockfishes of the genus *Sebastes* from central California with notes on ecologically related sport fishes. Calif. Fish Game Fish. Bull. **177**: 1–112.

Longhurst, A. 2007. Ecological geography of the sea. Academic Press, San Diego, Calif.

Love, M.S., Carr, M., and Haldorson, L. 1991. The ecology of substrate-associated juveniles of the genus *Sebastes*. Environ. Biol. Fishes, **30**(1-2): 225–243. doi:10.1007/BF02296891.

Love, M.S., Caselle, J.E., and Buskirk, W.V. 1998. A severe decline in the commercial passenger fishing vessel rockfish (*Sebastes* spp.) catch in the Southern California Bight, 1980–1996. CCOFI Rep. **39**: 180–195.

Love, M.S., Yaklovich, M., and Thorsteinson, L. 2002. The rockfishes of the Northeast Pacific. University of California Press, Berkeley, California.

MacCall, A. 2005. Assessment of vermilion rockfish in southern and northern California. Available from www.pcouncil.org/groundfish/gfstocks/vermassmtfinal.pdf [accessed 25 February 2009].

Manni, F., Guérard, E., and Heyer, E. 2004. Geographic patterns of (genetic, morphologic, linguistic) variation: how barriers can be detected by using Monmonier's algorithm. Hum. Biol. **76**(2): 173–190. doi:10.1353/hub.2004.0034. PMID:15359530.

Matala, A.P., Gray, A.K., Gharrett, A.J., and Love, M.S. 2004. Microsatellite variation indicates population genetic structure of bocaccio. N. Am. J. Fish. Manag. **24**(4): 1189–1202. doi:10.1577/M03-061.1.

McArdle, D.A. 1998. The status of California marine protected areas. *In* California and the world ocean '97. Taking a look at California's ocean resources: an agenda for the future. *Edited by* O.T. Magoon, H. Converse, B. Baird, and M. Miller-Henson. American Society of Civil Engineers, Reston, Va. pp. 74–85.

Miller, D.J., and Geibel, J.J. 1973. Summary of blue rockfish and lingcod life histories; a reef ecology study; and giant kelp, *Macrocystis pyrifera*, experiments in Monterey Bay, California. Calif. Fish Game Fish. Bull. **158**: 1–135.

Mitamura, H., Arai, N., Sakamoto, W., Mitsunaga, Y., Tanaka, H., Mukai, Y., Nakamura, K., Sasaki, M., and Yoneda, Y. 2005. Role of olfaction and vision in homing behaviour of black rockfish *Sebastes inermis*. J. Exp. Mar. Biol. Ecol. **322**(2): 123–134. doi:10.1016/j.jembe.2005.02.010.

Monmonier, M. 1973. Maximum-difference barriers: An alternative numerical regionalization method. Geogr. Anal. **3**: 245–261.

Murray, S.N., Ambrose, R.R., Bohnsack, J.A., Botsford, L.W., Carr, M.H., Davis, G.E., Dayton, P.K., Gotshall, D., Gunderson, D.R., Hixon, M.A., Lubchenco, J., Mangel, M., MacCall, A., McArdle, D.A., Ogden, J.C., Roughgarden, J., Starr, R.M., Tegner, M.J., and Yoklavich, M.M. 1999. No-take reserve networks: sustaining fishery populations and marine ecosystems. Fisheries, **24**(11): 11–25. doi:10.1577/1548-8446(1999)024<0011:NRNS>2.0.CO;2.

Parker, S.J., Rankin, P.S., Olson, J.M., and Hannah, R.W. 2007. Movement patterns of black rockfish (*Sebastes melanops*) in Oregon coastal waters. *In* Biology, assessment, and management of North Pacific rockfishes. *Edited by* J. Heifetz, J. Dicosimo, A.J. Gharrett, M.S. Love, V.M. O'Connell, and R.D. Stanley. Alaska Sea Grant College Program, University of Alaska Fairbanks, Fairbanks, Alaska. pp. 39–57.

Parrish, R.H., Nelson, C.S., and Bakun, A. 1981. Transport mechanisms and reproductive success of fishes in the California Current. Biol. Oceanogr. **1**: 175–203.

Pfenninger, M., and Posada, D. 2002. Phylogeographic history of the land snail *Candidula unifasciata* (Helicellinae, Stylommatophora): fragmentation, corridor migration, and secondary contact. Evolution, **56**(9): 1776–1788. PMID:12389722.

Phillips, J.B. 1964. Life history studies on ten species of rockfish (genus *Sebastodes*). Calif. Fish Game Fish. Bull. **126**: 1–70.

Polacheck, T. 1990. Year around closed areas as a management tool. Nat. Resour. Model. **4**: 327–355.

Rocha-Olivares, A., and Vetter, R.D. 1999. Effects of oceanographic circulation on the gene flow, genetic structure, and phylogeography of the rosethorn rockfish (*Sebastes helvomaculatus*). Can. J. Fish. Aquat. Sci. **56**(5): 803–813. doi:10.1139/cjfas-56-5-803.

Rousset, F. 1997. Genetic differentiation and estimation of gene flow from *F*-statistics under isolation by distance. Genetics, **145**(4): 1219–1228. PMID:9093870.

Sakuma, K.M., Ralston, S., and Wespetad, V.G. 2006. Interannual and spatial variation in the distribution of young-of-the-year rockfish (*Sebastes* spp.): expanding and coordinating a survey sampling frame. CCOFI Rep. **47**: 127–139.

Slatkin, M. 1993. Isolation by distance in equilibrium and non-equilibrium populations. Evolution, **47**(1): 264–279. doi:10.2307/2410134.

Starr, R.M., Heine, J.N., Felton, J.M., and Caillet, G.M. 2002. Movements of bocaccio (*Sebastes paucispinis*) and greenspotted (*S. chlorostictus*) rockfishes in a Monterey submarine canyon: implications for the design of marine reserves. Fish. Bull. U.S. **100**: 324–337.

Taylor, C.A. 2004. Patterns of early-stage pelagic dispersal and gene flow in rockfish species from the southern California bight. Ph.D. thesis, Scripps Institution of Oceanography, University of California, San Diego, Calif.

Templeton, A.R., Routman, E., and Phillips, C.A. 1995. Separating population structure from population history: a cladistic analysis of the geographical distribution of mitochondrial DNA haplotypes in the tiger salamander, *Ambystoma tigrinum*. Genetics, **140**(2): 767–782. PMID:7498753.

Walsh, P.S., Metzger, D.A., and Higuchi, R. 1991. Chelex® 100 as a medium for simple extraction of DNA for PCR-based typing from forensic material. Biotechnol. Tech. **10**: 506–513.

Williams, E.H., and Ralston, S. 2002. Distribution and co-occurrence of rockfishes (family: Sebastidae) over trawlable shelf and slope habitats of California and southern Oregon. Fish. Bull. U.S. **100**: 836–855.

Mechanisms regulating oocyte recruitment and skipped spawning in Northeast Arctic cod (*Gadus morhua*)

Jon Egil Skjæraasen, James Kennedy, Anders Thorsen, Merete Fonn, Bente Njøs Strand, Ian Mayer, and Olav Sigurd Kjesbu

Abstract: To examine mechanisms that affect fecundity, atresia, and skipped spawning in Northeast Arctic cod (*Gadus morhua*), we conducted an experiment where wild-caught cod (>60 cm) kept under restricted food regimes were subjected to monthly biopsies and hormonal and physical measurements. The power of body weight as a fecundity proxy increased until the presumed end of follicle proliferation in early November; thereafter, it remained stable. Atresia occurred in most females, but for maturing females, mainly close to spawning. Eighteen percent of the females had small gonads with predominantly previtellogenic oocytes at sacrifice in January. These females were past-spawners, verified by postovulatory follicles in their gonads. These "skippers" had lower condition than maturing cod from December, smaller livers upon sacrifice, and lower plasma 17β-estradiol values from early November. Until November, oocytes developed similarly for all females, but in November, oocyte development was arrested at the early cortical alveoli stage and atresia occurred in all skippers. In summary, fecundity and skipped spawning seem highly influenced by energy reserves during early vitellogenesis and was limited to females only. Finally, skippers were identifiable long before the predicted onset of spawning, which could have implications for forecasting of egg production and hence stock–recruitment relationships.

Résumé : Afin d'étudier les mécanismes qui affectent la fécondité, l'atrésie et l'omission de fraie chez les morues (*Gadus morhua*) du nord-est de l'Arctique, nous avons mené une expérience dans laquelle des morues (>60 cm), capturées en nature et gardées en régime de restriction de nourriture, ont été soumises à chaque mois à des biopsies et des mesures hormonales et physiques. La valeur de la masse corporelle comme variable de substitution de la fécondité augmente jusqu'à la fin présumée de la prolifération des follicules au début de novembre et demeure stable par la suite. Il se produit une atrésie chez la plupart des femelles; mais, chez les femelles en maturation, l'atrésie a lieu surtout près du moment de la fraie. Au moment de leur dissection en janvier, 18 % des femelles ont de petites gonades avec une prédominance d'oocytes prévitellogéniques. Ces femelles avaient frayé dans le passé, ce que confirme la présence de follicules post-ovulatoires dans leurs gonades. Ces femelles qui sautent la fraye ont une condition plus basse que les morues en maturation à partir de décembre; leur foie est plus petit lors de la dissection et leur concentration plasmatique de 17β-estradiol plus faible depuis le début de novembre. Jusqu'en novembre, les oocytes se développent de façon semblable chez toutes les femelles, mais chez toutes les femelles qui sautent la fraie, le développement des oocytes s'arrête au début du stade des alvéoles corticales et il se produit une atrésie. En résumé, la fécondité et l'omission de la fraie semblent être fortement influencées par les réserves énergétiques au début de la vitellogenèse; le phénomène semble restreint aux femelles. Finalement, les femelles qui sautent la fraie peuvent être identifiées bien avant le début prévu de la fraie, ce qui peut avoir des conséquences sur la prédiction de la production d'œufs et ainsi sur les relations stock–recrutement.

[Traduit par la Rédaction]

Introduction

The energy available for reproduction and growth in iteroparous spawners is surplus energy after energetic requirements for basic metabolic needs have been fulfilled (Rijnsdorp 1990). The energy state of each fish therefore influences its reproductive investment (Kjesbu and Witthames 2007). Consequently, recent models of total egg production and recruitment have also included various indices of individual condition (Marshall et al. 1999, 2000; Scott et al.

Received 12 December 2008. Accepted 22 May 2009. Published on the NRC Research Press Web site at cjfas.nrc.ca on 9 September 2009.
J20876

J.E. Skjæraasen.[1] Department of Biology, University of Bergen, N-5020 Bergen, Norway.
J. Kennedy. Department of Biology, University of Bergen, N-5020 Bergen, Norway; Møreforskning Ålesund, P.O. Box 5075, 5021 Ålesund, Norway.
A. Thorsen, M. Fonn, B.N. Strand, and O.S. Kjesbu. Institute of Marine Research, P.O. Box 1870 Nordnes, N-5817 Bergen, Norway.
I. Mayer. Department of Biology, University of Bergen, N-5020 Bergen, Norway; Norwegian School of Veterinary Science, P.O. Box 8146, N-0033 Oslo, Norway.

[1]Corresponding author (e-mail: jon.skjaeraasen@bio.uib.no).

2006). This has shown the potential merit in incorporating basic biological knowledge for construction of realistic population dynamics models.

The major event responsible for energy transfer into developing oocytes and thereby oocyte growth in marine fish is vitellogenesis (Tyler and Sumpter 1996). During vitellogenesis, vitellogenin is sequestered into the developing oocytes, which thereby are recruited to the maturing pool to become the year's potential egg production. Both the hepatic synthesis of vitellogenin and its subsequent uptake by growing oocytes are under hormonal control by the gonadal steroid 17β-estradiol (Tyler and Sumpter 1996). Marine fish can be broadly distinguished into two different categories depending on their reproductive mode: indeterminate and determinate spawners (Hunter et al. 1992; Murua and Saborido-Rey 2003). Indeterminate spawners, such as anchovies (*Engraulis* sp.) (Motos 1996) and swordfish (*Xiphias gladius*) (Arocha 2002), recruit new oocytes throughout the spawning season. Determinate spawners on the other hand, e.g., Atlantic cod (*Gadus morhua*), recruit a finite number of oocytes to the maturing pool prior to spawning. With this type of reproductive strategy, the completion of oocyte recruitment marks the point of maximum potential fecundity. Subsequent alteration of potential fecundity is only possible through "down-regulation" of oocytes through the process of atresia, i.e., reabsorbtion of vitellogenic oocytes (Woodhead and Woodhead 1965; Kjesbu et al. 1991; Thorsen et al. 2006). Atresia seems to take place within a specific oocyte diameter range, i.e., the atretic window (Witthames and Greer Walker 1995; Óskarsson et al. 2002; Kurita et al. 2003).

Given that oocyte recruitment to the maturing pool in principle occurs only during early vitellogenesis in determinate spawners, their potential fecundity should be influenced by individual energy reserves around the same time. A study on rainbow trout (*Oncorhynchus mykiss*) found that fecundity was unaffected in fish that were fed on a low diet during the later stages of vitellogenesis, while it was significantly reduced for females fed a reduced ration during early vitellogenesis (Bromage et al. 1992). Conversely, cod fed on a low ration prior to the start of vitellogenesis followed by a high ration during early vitellogenesis had fecundities similar to those of fish fed on a high ration over the entire duration (Kjesbu and Holm 1994). Skjæraasen et al. (2006) found that energy reserves during early vitellogenesis were significantly correlated with potential fecundity at the time of spawning. In summary, these studies suggest that fecundity is indeed correlated with individual energy reserves during early vitellogenesis. However, in addition to their influence on fecundity, energy reserves at this time may also be linked to the phenomenon of skipped spawning, which also can have considerable bearing on stock reproductive potential and thereby the stock–recruitment relationship.

Skipped spawning can be defined as the failure of iteroparous spawners to spawn every year following sexual maturity (Rideout et al. 2005). For cod, this phenomenon and its potential importance for spawning stock size assessment and stock–recruitment relationships have received limited attention until recently (Rideout and Rose 2006; Morgan 2008), although reported as early as the 1960s for cod captured in the Barents Sea, i.e., Northeast Arctic cod (Woodhead and Woodhead 1965), and again in the 1990s (Oganesyan (1993) and experimentally for Norwegian Coastal cod in the early 1990s (Kjesbu et al. 1991). Jørgensen et al. (2006) used a state-dependent life history model (Jørgensen and Fiksen 2006) to model the occurrence of skipped spawning in Northeast Arctic cod and predicted that as much as 30% of the sexually mature population may skip spawning, which largely agreed with observations made by Rideout and Rose (2006) on Northern cod following the stock collapse. However, skipped spawning may be common in many important commercial fish, as reviewed by Nikolskii (1969) and Rideout et al. (2005).

It is possible that not only fecundity but also the proportion of skipped spawners is linked to energy reserves of the spawning stock, in particular during early vitellogenesis. To target these questions, we studied gonad investment and the incidence of skipped spawning in Northeast Arctic cod subjected to temporal changes in food availability under a controlled laboratory setting. This allowed us to examine how temporal changes in energy reserves during the maturation cycle affect fecundity and the incidence of atresia. Further, as skipped spawning in this species appears to be linked to individual energy reserves (Kjesbu et al. 1991; Rideout et al. 2005; Rideout and Rose 2006), we chose rations that would generate condition factors resembling those of wild cod in an attempt to induce skipped spawning under experimental conditions. Further, by following individuals for a prolonged period before spawning and continually assessing both oocyte development and sex steroid profiles, we hoped to determine when skippers "separate" from maturing females. This knowledge could have considerable implications for forecasting stock reproductive potential.

Materials and methods

History of fish

To target large cod with a high probability of having spawned at least once before, approximately 200 cod were caught by trawl on the main spawning grounds of Northeast Arctic cod near Vesterålen, northern Norway (67°38′N, 01°30′E), on 8 April 2006 by the research vessel *Johan Hjort*. Aboard the vessel, cod were kept in a 1–3 m^3 aerated tank after capture and transported to Bergen (60°23′N, 05°20′E) where they arrived on 17 April. Fish were then immediately transferred to two identical 30 m^3 tanks at the Institute of Marine Research research facility at Nordnes, Bergen. Fish health was monitored daily and any fish showing signs of injury, stress, or discoloration were removed. During this initial acclimation period, cod were fed a mixture of shrimps (*Pandalus borealis*), Atlantic herring (*Clupea harengus*), and pellets ad libitum with the goal of entraining fish to a pellet-only diet for the upcoming experiment. On 24 May, all cod were weighed (±1 g), measured (±1 cm), and passive integrated transponder (PIT) tagged for individual identification. Fish were then allowed 4 more weeks of recovery before the experiment started on 22 June.

The experiment

On 22 June, all cod were sedated with benzocain (60 ppm), measured, and weighed. In addition, a 2 mL blood sample was obtained from the caudal vein of every

fish. After these measurements, fish <70 cm in total length were transported to the High Technology Centre of Bergen and distributed randomly between two identical 7 m^3 tanks. The remaining fish, between 70 and 99 cm, were distributed randomly between the two bigger 30 m^3 tanks at the Institute of Marine Research. Subsequently, one tank at the Institute of Marine Research and one tank at the High Technology Centre of Bergen were subjected to a medium-ration food regime, hereafter denoted as the ML group, and the two remaining tanks to a low-ration food regime, hereafter denoted as the LM group. The medium ration was calculated as a daily portion of 0.25% of the wet fish biomass in the tanks given as pellets (Europa Marin 17; Skretting AS: www.skretting.no/Internet/SkrettingNorway/webInternet.nsf/main?readForm) twice a week (Kjesbu et al. 1991), i.e., 0.875% of the biomass in the tank per feeding. The low feeding ration was calculated as a daily portion of 0.125% of the biomass given twice a week, i.e., 0.4375% of the biomass in the tank per feeding. The goal was to feed the cod a pellet-only diet during the entire experiment. However, after the experiment was begun, some fish showed a reduced appetite and did not partake in the feeding sessions, leaving substantial amounts of pellets in the tanks. Therefore, the food regime was altered from 7 August on. From this date, cod were given a mixed diet of herring and dry pellets. The new feed ration was calculated so that herring would contribute 80% of the solids (mainly fat and protein) that the cod received. Assuming that dry pellets contain approximately twice the amount of solids (88%, cf. www.skretting.no/Internet/SkrettingNorway/webInternet.nsf/main?readForm) per unit weight compared with fresh herring (20%–40%) (Kent 1990), the new medium ration given twice per week was 1.4% of the biomass in the tank in herring wet weight and 0.175% of the biomass in pellets. The corresponding new low ration was 0.7% of the biomass in herring wet weight and 0.0875% given as pellets. The fish were then subjected to monthly measurements and blood collection (Table 1). After each measurement, the food ration was adjusted according to the new biomass in the tank. In all tanks, cod were kept under a natural photoperiod for Bergen, while temperature was kept at 5–6 °C, which although at the upper limit is within the natural range that Northeast Arctic cod experience in the Barents Sea (Godø and Michalsen 2000).

Originally, the plan was to obtain an ovarian biopsy sample (Kjesbu et al. 1996) at every measurement date. However, in June and August, the pores of the urogenital papilla of the initial five fish examined were greatly restricted in size, and due to the risk of physical damage, further attempts to obtain a biopsy sample were aborted on these dates. From September on, successful biopsies were completed (Table 1).

The ML group received the medium ration until the October measurement after which they were switched to the low ration, whereas the LM group was given the reverse treatment. In October, a subsample of seven males and three females from the ML group and five males and four females from LM group were sacrificed to compare gonadal development and energy reserves at this stage.

Cod were monitored daily and any fish developing signs of injury or stress, i.e., discoloration or loss of appetite, were removed from the tanks. Any fish that were removed or that succumbed at any time during the experiment were omitted from all analyses, tables, and graphs. In total, we obtained data from 16 females and 33 males in the ML group and 36 males and 13 females in the LM group (Table 2). Examination of the female biopsies from 10 and 11 January 2007 indicated that some females were only a few weeks from the start of spawning (see Oocyte measurements section below). All cod were therefore sacrificed between 18 and 23 January. All fish sacrificed at any date was subjected to the same protocol. Total weight and gonad and liver weight were measured and a blood sample was collected from the caudal vein. A section of the gonad was also fixed in 3.6% neutral phosphate-buffered formaldehyde for later histological analyses. For females, the tissue sample was taken from the middle part of the right ovarian lobe for standardization. Finally, otoliths were removed from all fish for ageing, classification of fish into Northeast Arctic and coastal cod, and examination of past spawning history (Rollefsen 1933).

Oocyte measurements

All biopsy samples (n = 150) and the final gonad samples (n = 22) were subjected to digital image analyses (Thorsen and Kjesbu 2001). This method uses the contrast between previtellogenic oocytes and vitellogenic oocytes in relation to the set background to specifically select and measure the diameter of the last category of oocytes. However, oocytes at the very beginning of vitellogenesis, i.e., the early cortical alveoli (E-CA) stage, may not be picked up by this method. By combining the results of the histological (see Histological analyses section below) and digital analyses, we were able to separate between the various stages of previtellogenic (PV), E-CA, late cortical alveoli (L-CA), and yolk granule (YG) oocytes. For each sample containing vitellogenic oocytes that could be measured with the digital image analyses, the size of 200 oocytes was measured. Also, from these data, the average size of the leading cohort (LC_{20}) (average of the largest 10% of the oocytes) was calculated in each sample. From the final gonad sample obtained at the time of sacrifice, we calculated potential fecundity as

$$(1) \qquad F_p = 2.139 \times 10^{11} \times \mathrm{OD}^{-2.7} \times \mathrm{OW}$$

based on Thorsen and Kjesbu (2001) and protocols therein, where F_p is potential fecundity, OD is average vitellogenic oocyte diameter estimated by the digital image analysis, and OW is ovary weight (grams) at the time of sacrifice.

Hormonal samples

Female blood plasma concentrations of the steroids testosterone (T) and 17β-estradiol (E2) were measured by radioimmunoassay (RIA) according to Schulz (1985). In brief, steroids were extracted from 200 μL of plasma with 4 mL of diethylether. The aqueous phase was frozen on dry ice, after which the organic phase was transferred to a glass tube, evaporated in a water bath, and then reconstituted with 600 μL of assay buffer. Samples were assayed in duplicate. Unfortunately, a technical problem with one of the freezers led to the loss of the samples obtained on the final two sampling dates for the cod housed at the High Technology Centre of Bergen.

Table 1. Northeast Arctic cod (*Gadus morhua*) sampling dates and protocol on different dates.

Date(s)	Protocol
22 June 2006	Weight, length, blood sample
8 and 9 August 2006	Weight, length, blood sample
5 and 6 September 2006	Weight, length, blood sample and biopsy
3 and 4 October 2006	Weight, length, blood sample and biopsy, subsample of fish sacrificed, food rations switched
8 and 9 November 2006	Weight, length, blood sample and biopsy
5 and 12 December 2007	Weight, length, blood sample and biopsy
10 and 11 January 2007	Weight, length, blood sample and biopsy
18, 19, and 23 January 2007	Weight, length, blood sample and biopsy, all fish sacrificed

Table 2. Number and average weight and length of Northeast Arctic cod (*Gadus morhua*) males and females in the medium-ration food regime (ML) and low-ration food regime (LM) groups housed at the Institute of Marine Research (IMR) and High Technology Centre of Bergen (HiB).

	ML				LM		
	IMR		HiB		IMR		
	Males (20)	Females (11)	Males (13)	Females (5)	Males (20)	Females (13)	HiB, males (16)
Weight	3620	4373	1975	2056	3353	3720.5	1920
Length	77.6	83.4	62.0	63.2	77.6	79.4	61.7

Note: Numbers of individuals in each subcategory are given in parentheses. Weight and length are the average values at the start of the experiment.

Histological analyses

Histology was done only for female ovaries, which were processed using standard protocols for resin embedding (Technovit 7100), producing 4 μm sections stained with 2% toluidine blue and 1% sodium tetraborate. Oocytes were classified into stages as described above. In addition, the PV oocyte stage was divided into the following three substages based on the classification of Shirokova (1977): phases 4A (indistinct circumnuclear ring located centrally in the cytoplasm), 4B (distinct circumnuclear ring located centrally in the cytoplasm), and 4C (circumnuclear ring located in the periphery of the cytoplasm). The distinction between 4A and 4B was considered in several cases to be ambiguous, so the two phases were presently combined into phase 4AB. Taken together, 4AB and 4C refer to the so-called perinucleuolus stage or advanced PV oocytes. In this line, the appearance of the circumnuclear ring was considered to be an early indication of intracellular preparation for further oocyte growth (see Kjesbu and Kryvi 1989 and citations therein). All sections were carefully screened for postovulatory follicles produced by past-spawning females (Saborido-Rey and Iunquera 1998; Witthames et al. 2009). The prevalence of atresia was noted as the number of "females with atresia" (see Table 3). The intensity of atresia was taken as the percentage of atretic oocytes within the total number of oocytes taken from standard profile counts. In the case of vitellogenic (YG) atresia, the total number of YG and atretic YG oocytes examined was approximately 150. Characterized atretic cells were either in the alpha stage (i.e., containing yolk) or in the beta stage (without yolk) (Hunter and Macewicz 1985). Ovaries showing only the latter stage were specially noted. A similar type of estimation at the PV oocyte and CA stage included examination of a significantly higher number of cells, but nevertheless, the estimate was considered as being less precise, as it was based on an overall judgment of relative cell numbers present. Consequently, all data were grouped into four atretic intensity classes resembling the system introduced by Hunter and Macewicz (1985) for fully mature northern anchovy (*Engraulis mordax*): 0–5, 5–25, 25–50, and >50%. In all cases, the intensity listed was oocyte stage specific, i.e., considering the stages 4AB and 4C, CA, and YG separately. For females containing atretic YG oocytes upon sacrifice and thereby used to estimate fecundity, we applied a stereological correction factor to account for differences in size of healthy and atretic cells, which therefore have unequal chances of being hit in a two-dimensional plane, i.e., during profile counting (Andersen 2003; Kurita et al. 2003; O.S. Kjesbu, unpublished data).

Data analyses

Growth

Length, weight, and condition (condition defined as the residuals of a simple regression of ln length against ln weight, e.g., Scott et al. 2006) development during the experiment was examined by the following mixed-effects model:

$$(2) \qquad y_{ijl} = \mu_0 + \beta_{0l} + b_{0i} + (\mu_1 + \beta_{1l} + b_{1i})t_j + e_{ijl}$$

where y_{ijl} refers to the measurement, i.e., length, weight, or condition, of the ith fish at the jth time t_j. Subscript l denotes feeding regimes (ML and LM) and e_{ijl} is the unexplained error. Subscript 1 refers to a slope and 0 to a constant (i.e., intercept). A Greek letter denotes a fixed effect and a Latin letter denotes a random effect. The time intervals between measurements were fairly equal except between the last two measurements (Table 1) and were coded as 0, 1, 2, 3, 4, 5, 6, 7, and 7.3. Males and females and each feeding period were tested separately.

Hepatosomatic index (HSI) (100 × liver weight × (total weight – gonad weight)$^{-1}$) and gonadosomatic index (GSI)

Table 3. Maturation stage and number of samples containing atretic oocytes during the experiment for Northeast Arctic cod (*Gadus morhua*) females that were maturing, i.e., would have spawned, were sacrificed in October, and would have skipped spawning.

	Most advanced stage						
	Previtellogenic		Vitellogenic				
Date	3	4AB and 4C	E-CA	L-CA	YG	Number of females with atresia	Number finished
Maturing							
September	4	1	9	4		1	4
October			8	5	5	1	8
November				3	15	5	15
December					18	7	17
1 January					18	6	17
2 January					18	5	18
Sacrificed							
September	1	1	2	2		0	
October			2	2	1	1	
Skipped							
September		2				1	
October			3			0	
November		1	2			3	
December		2	1			2	
January		3				2	
2 January		3	1			4	

Note: The stage was decided mainly by histological analyses, but we also used the results of image analyses to separate between early (E-CA) and late (L-CA) cortical alveoli stages. YG denotes the yolk granule stage. Number of females with atresia is the number of females for which at least one atretic oocyte was found in their biopsy sample and number finished is the number of females deemed to have finished oocyte recruitment for a given date.

(100 × gonad weight × total weight^{-1}) were compared between sexes in the different feeding regimes with two-tailed *t* tests. This was done both for fish sacrificed in October and at the end of the experiment.

Oocyte recruitment and atresia

First, we wanted to compare the oocyte size of the leading cohort between females possessing CA and YG oocytes and, second, whether females possessing YG oocytes had finished their oocyte recruitment to the maturing pool. To do this, we first plotted all biopsy data to see if we could find a leading cohort threshold after which all oocytes had reached the YG stage. When females have finished recruiting oocytes to the maturing pool, there becomes a gap between the vitellogenic sizes present and the smallest possible sizes of vitellogenic oocytes, i.e., 250 µm for cod (Kjesbu 1991). Using the oocyte size–frequency distribution curve obtained from the image analyses, we therefore further classified vitellogenic females as either (*i*) still recruiting oocytes to this year's maturing pool, defined as >5% of the measured oocytes being <300 µm, or (*ii*) having finished recruitment, defined as <5% of the oocytes being <300 µm (see Table 3).

To clarify if atresia in maturing females was linked to individual energy reserves, we first divided females into three categories: (*i*) females for which no atresia was detected in any of the biopsy samples, (*ii*) females for which atresia was confined to stages no more advanced than the CA stage, and (*iii*) females that at one or more sampling points had atretic YG oocytes. We first examined if HSI at sacrifice was different between these categories or if intensity of YG atresia at this time was correlated with HSI. We then examined if atresia could be related to short-term changes in condition by examining if there had been a decline in residual condition in the past month for the female for which atresia was found in the sample.

Finally, we wanted to examine how temporal changes in energy reserves affected fecundity. For these tests, we employed simple regressions for each month separately. Total weight was used as the independent variable and potential fecundity (F_p) and potential fecundity adjusted for the atretic loss (F_{pa}) in the final sample (calculated from the histological sections, i.e., $F_{pa} = F_p \times$ (1 – intensity of YG atresia) were used as the dependent variables. For these tests, female weight and both measures of fecundity were ln transformed before applying the regression model.

Skipping spawning in relation to hormonal values and energy reserves

The values and distribution of hormonal samples for skipping and spawning females were compared for each sampling date with two-tailed *t* tests. On some dates, some females had hormonal values so low that they were undetectable in the assays. These were given the same value as the lowest detected value in all analyses and graphs, i.e., 0.17 ng·mL^{-1} for E2 and 0.3 ng mL^{-1} for T. Since we had multiple comparisons, significance was assigned at 0.0064 according to Dunn–Šidák's method (Ury 1976). Similarly, we used our estimate of residual condition to compare energy reserves throughout the experiment with a two-tailed *t*

Fig. 1. Histological sections from a maturing female and a skipping female Northeast Arctic cod (*Gadus morhua*) obtained from gonad samples taken at sacrifice on 19 January 2007. Postovulatory follicles clearly show that both females are past-spawners. However, whereas (*a*) female cdfo possesses large yolk granule (YG) oocytes, (*b*) female cd1e's most advanced stage is previtellogenic 4A oocytes. POF, postovulatory follicle. Scale bar = 100 μm.

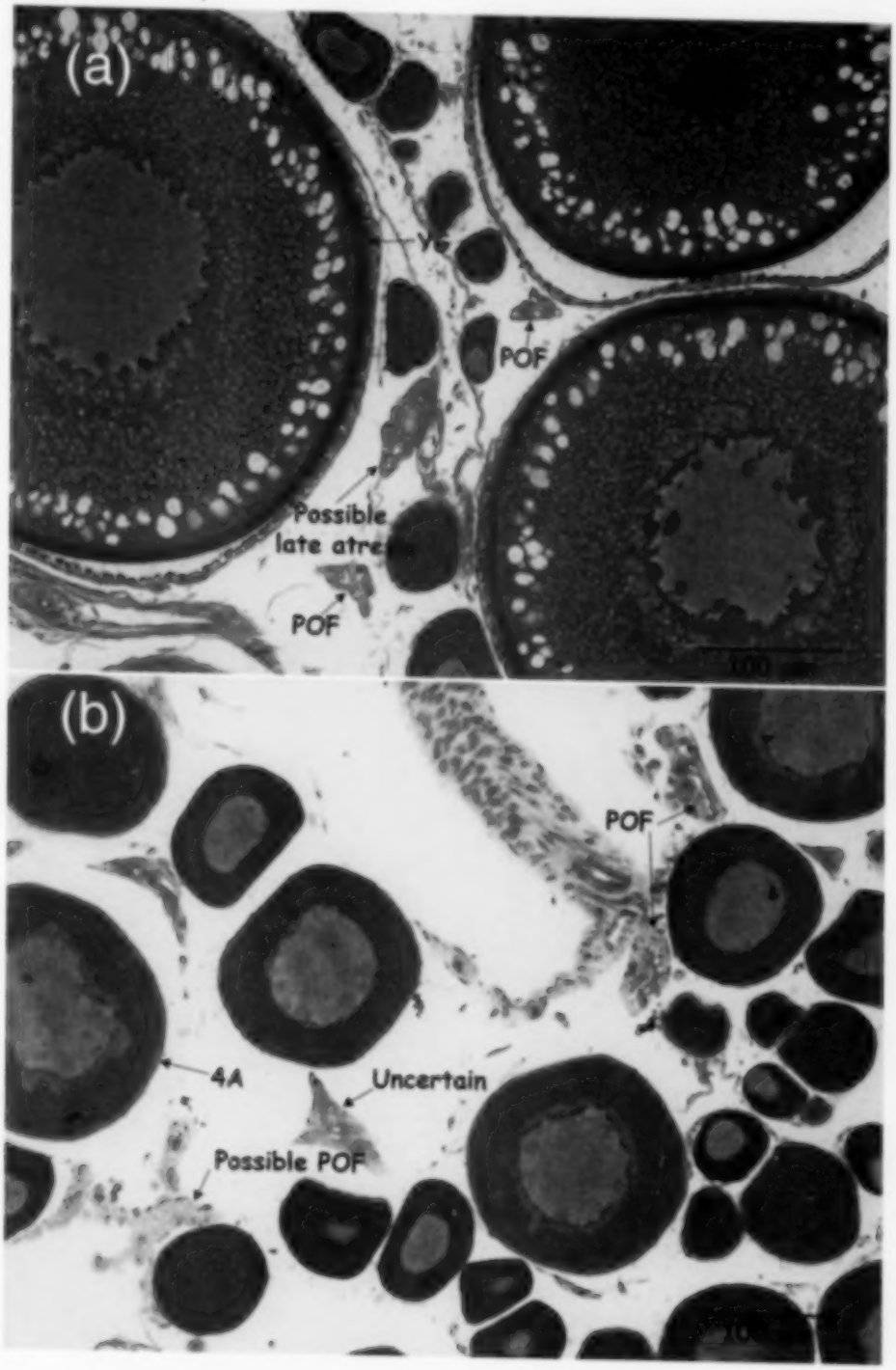

test and again assigned significance at 0.0064. At sacrifice, we compared the HSI of skipping and maturing fish.

Results

Postovulatory follicles were discovered in all biopsy samples from all female ovaries (e.g., Fig. 1). In total, 27 of the 69 males were deemed to be recruit spawners based on the absence of a spawning check. Based on the otolith pattern, 44 of the 64 males were considered to be Northeast Arctic cod, whereas 22 of the 28 females were deemed to be Northeast Arctic cod. The remaining cod had otolith shapes typical of Norwegian coastal cod.

Growth

At the start of the experiment, there was no difference in length, weight, or condition in the LM and ML groups between either males or females (two-tailed t tests, all $p > 0.17$) (Fig. 2). As expected, the different feed regimes caused differences between the groups. During the first feeding period, 22 June to 3 October, females in the ML group increased significantly more in weight than the LM group (eq. 2, df = 85, $p < 0.05$) (Fig. 2) and nearly had significantly larger increments in condition development (eq. 2, df = 85, $p = 0.07$) (Fig. 2). There was no difference in length growth (Fig. 2). ML males had significantly larger increments in condition, weight, and length than LM males (eq. 2, df = 211, all $p < 0.05$) (Fig. 2). The following switch in food regimes caused a reverse situation, and during the latter period, both male and female LM cod increased significantly more in weight and condition (eq. 2, all $p < 0.05$) (Fig. 2) but not in length. Upon sacrifice, there was no difference between either sex in length, weight, or condition (all $p > 0.05$).

In October, GSI values were similar between sexes and groups (Fig. 3). Upon sacrifice in January, there were no differences between maturing males and females between groups, but GSI values were generally higher in males (two-tailed t test, sexes pooled across groups, df = 66, $p < 0.05$).

HSI values appeared to be somewhat higher in the ML group for fish sacrificed in October, but this was not significant when pooling the results across sexes (two-tailed t test, df = 18, $p = 0.17$) (Fig. 3). Upon sacrifice, there was no difference between maturing females or males between groups, but females had significantly higher HSI values than males (two tailed t test, sexes pooled across groups, df = 66, $p < 0.0001$) (Fig. 3).

Oocyte recruitment and atresia in maturing females

Oocyte recruitment

The combined digital image and histology analyses showed that in September, the ovaries of only four females had reached the late CA stage, while nine females were at the early CA stage and five females possessed only PV oocytes (Table 3). However, by November, 15 females had reached the YG stage, with the remaining fish possessing advanced CA oocytes (Table 3). Based on our definition, fish had generally finished oocyte recruitment when they reached the YG stage (Table 3). Hormonally, E2 and T values above 2 ng·mL^{-1} were associated with yolk granules

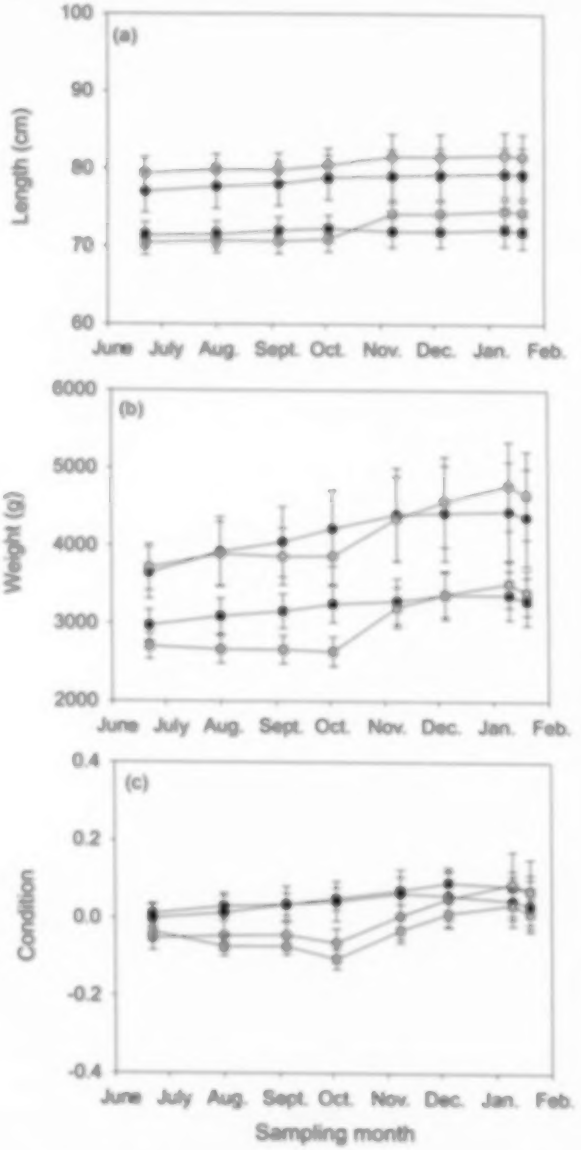

Fig. 2. (*a*) Length, (*b*) weight, and (*c*) condition development during the course of the experiment for ML (solid) and LM (shaded) male (squares) and female (circles) Northeast Arctic cod (*Gadus morhua*).

only, reaching a maximum level of approximately 7.5 and 6 ng·mL^{-1}, respectively. Lower values were associated with PV, CA, or YG oocytes (Fig. 4). Comparing the leading cohort size of females possessing YG and CA oocytes, there was great overlap at <400 μm but, with only one exception, once the leading cohort was >400 μm, the oocytes had reached the YG stage (Fig. 5).

Atresia

In the initial measurements, very few maturing females showed any signs of atresia (Table 3). However, from No-

Fig. 3. (*a*) Gonadosomatic index(GSI = 100 × gonad weight × total weight^{-1} and (*b*) hepatosomatic index (HSI = 100 × liver weight × (total weight – gonad weight)$^{-1}$) for Northeast Arctic cod (*Gadus morhua*) sacrificed in October and at the end of January. ML, medium-ration food regime; LM, low-ration food regime.

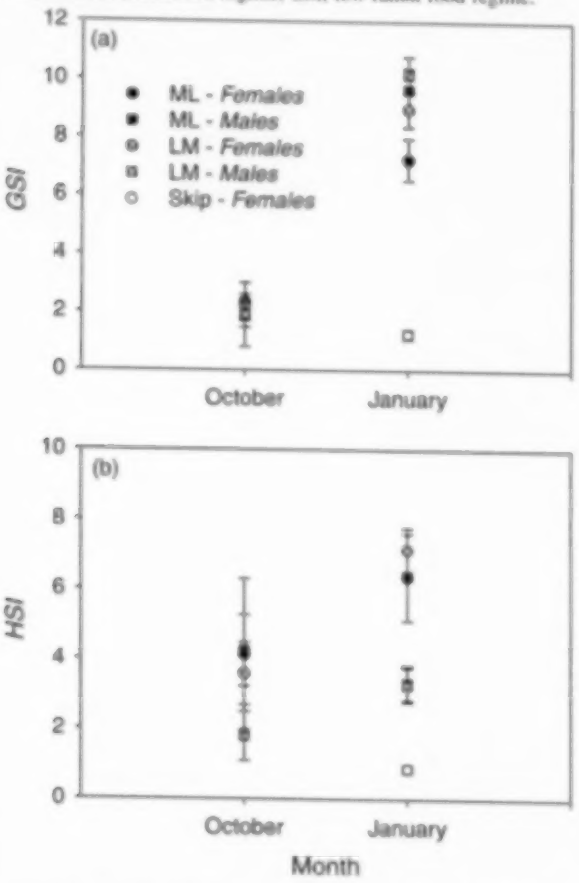

vember onwards, five to seven of the 18 maturing females possessed atretic oocytes at each monthly measurement. Only five of the 18 females showed no signs of atretic loss at any stage. For the remaining 13 females, oocyte atresia was confined to the PV and CA stage in five females, while atretic YG oocytes were observed in eight females at one or more samplings (Table 4). There was no indication of any link between female atresia and energy (one-way ANOVA, $F_{[2,15]} = 0.041$, $p = 0.96$; data not shown) or of any link between HSI at sacrifice and intensity of YG atresia at sacrifice (simple regression, df = 5, $p = 0.49$; data not shown). Further, short time changes in residual condition factor were not associated with atresia, i.e., females were as likely to have increased as decreased in condition just prior to the sample where atresia was discovered (data not shown), nor was any particular form of atresia more prevalent in ML than in LM females. There was no indication of any of the maturing females undergoing mass atresia and aborting spawning, as YG atresia at sacrifice was never above 22% for any female at the final sampling. YG atresia was confined to leading cohort sizes of 415–640 μm.

Fig. 4. Relationship between Northeast Arctic cod (*Gadus morhua*) leading oocyte cohort diameter (LC_{20}) grouped into previtellogenic (PV), cortical alveoli (CA), and yolk granule (YG) oocytes, and (*a*) 17β-estradiol and (*b*) testosterone hormonal values. The horizontal line depicts a sex steroid value of 2 ng·mL^{-1}.

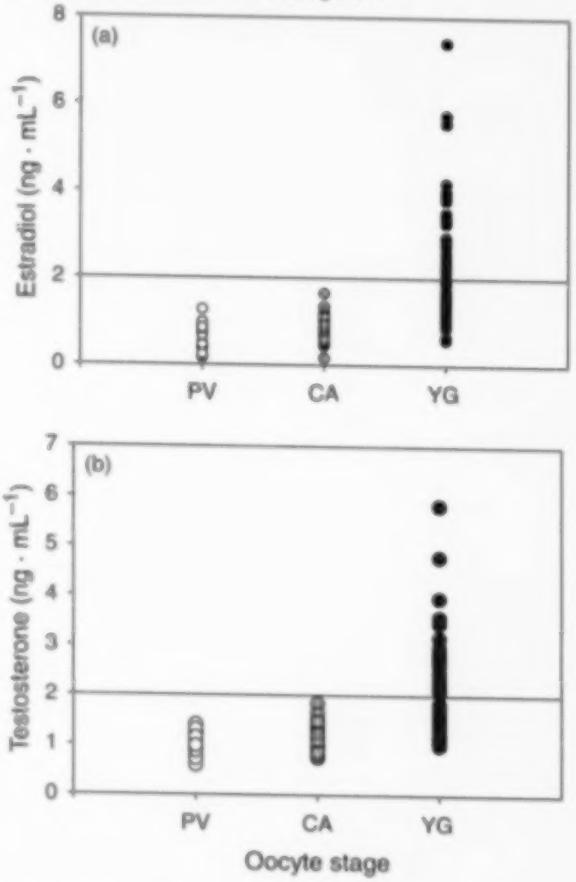

Proxies to fecundity

Generally, female weight at all months was strongly correlated with potential fecundity and potential fecundity controlled for atresia (Table 5). However, even so, temporal patterns were detectable. The explanatory power of weight generally increased from the June measurements until November (Fig. 6), and from this date onwards, the explanatory power remained more or less the same (Table 5). Adjusting for atretic loss generally decreased the variation explained for each month compared with nonadjusted values, but the between-month variation remained very similar to that of the unadjusted values (Table 5). The pattern of explanatory power did not change if we included only cod that were deemed to be Northeast Arctic cod based on their otolith shape.

Skipped spawning

Of the 22 females that were sacrificed in January, four would have skipped spawning. These females had ovaries containing oocytes no more advanced than the 4AB and 4C

Fig. 5. Relationship between Northeast Arctic cod (*Gadus morhua*) leading cohort size (LC_{20}) and cortical alveoli (CA) and yolk granule (YG) oocytes. The horizontal line depicts an LC_{20} value of 400 μm.

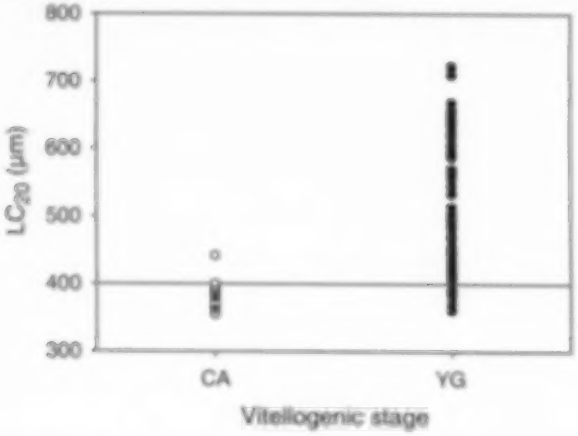

or early CA stages (Table 3) and had lower GSI values at sacrifice (two-tailed *t* test with unequal variances, $p < 0.001$) (Fig. 3). These females also had significantly lower HSI values than the maturing females at sacrifice (two-tailed *t* test with unequal variances, $p < 0.001$) (Fig. 3). Tracing the residual condition of these females back to the experimental start, they were in significantly lower condition than the maturing females from December onwards (all $p < 0.005$) (Fig. 7). Skipping females were present in both the ML and LM groups and had undergone a gradual decline in condition throughout the experiment, whereas maturing females generally had increased their condition (Fig. 7). Plasma E2 levels were significantly lower for these skippers compared with the maturing females from November onwards (two-tailed *t* test with unequal variances, all $p < 0.006$) (Fig. 7). In fact, E2 levels had decreased from October to November in the skipping females (Fig. 7). T levels were only significantly lower for the skippers in the final January samples ($p < 0.001$) (Fig. 7). The results of the combined histological and image analyses closely reciprocated the hormonal data. In October, the skipping females possessed oocytes at the early CA stage and no atresia was evident. This was similar to the maturing females (Table 3). However, in November, none of the skipping females had advanced beyond this stage; in fact, one female now only possessed PV oocytes (Table 3), whereas 15 of the 18 maturing females possessed yolk granules and the remaining three had reached the advanced CA stage (Table 3). Further, at this time, all skipping females showed signs of atresia, whereas only five of 18 maturing females possessed any atretic oocytes (Poisson test, $m = 18$, $p < 0.05$). At the final sampling in January, three of the four skipping females only had PV oocytes. One of the skipping females was deemed to be a coastal cod based on otolith shape. However, removing this female from the analyses did not change the results of any of our analyses, as there was great coherence between oocyte stage and hormonal values in all skipping females (Table 3; Fig. 7). Even though males had on average lower energy reserves than females (Fig. 3), only one of 64 males did not mature. This male was, however, deemed to be an immature cod based on the absence of a spawning check.

Discussion

To our knowledge, this is the first study examining the maturation cycle of Northeast Arctic cod in a controlled laboratory setting with an emphasis on the underlying principles behind the phenomenon of skipped spawning. Even though the Northeast Arctic cod is now the largest and most important commercial cod stock in the world (International Council for the Exploration of the Sea 2008), the large sizes of sexually mature individuals (>60 cm; Nash et al. 2008), coupled with the often long transport routes to suitable tank facilities following capture, have made virtually all studies on adults restricted to the field. Thus, even though we only had a total of 28 females and 69 males in the present experiment, the results still represent a significant advance in the knowledge of mechanisms affecting oocyte recruitment, atresia, and skipped spawning in this stock. We further demonstrate the usefulness of postovulatory follicles as a reliable longlasting marker of past spawning in Northeast Arctic cod, in agreement with the results of Saborido-Rey and Junquera (1998) and Witthames et al. (2009).

Hormonal values, oocyte recruitment, and atresia

As expected, there was an increase in hormonal values concurrent with oocyte development in maturing females. Overall, these results closely mimic those found by Dahle et al. (2003) for E2, whereas present T values are higher than those reported by both Dahle et al. (2003) and Skjæraasen et al. (2004) working on captive Norwegian coastal cod. While female fish generally produce large amounts of T during sexual maturation, the exact physiological role of this androgen is still uncertain (Borg 1994; Senthilkumaran et al. 2004). Through its influence on GnRH release, T facilitates the massive release of LH prior to ovulation. Also, T is the precursor for E2 biosynthesis, and it is believed that these two steroids act in concert during oogenesis. Further, the rather steady increase in plasma T and E2 levels prior to spawning, as also noticed presently for nonskippers, is known to be replaced by highly cycling and significantly larger values during spawning, i.e., during the process of final maturation and egg formation (Kjesbu et al. 1996), in agreement with studies on other batch spawners such as Atlantic halibut (*Hippoglossus hippoglossus*) (Methven et al. 1992). Thus, the present actual levels were more of interest in the comparison between skippers and nonskippers and clearly show that plasma levels of both steroids remained low (<1 ng·mL^{-1}) in the former. Maturing females went from previtellogenic to the YG stage in the course of 2 or in some cases 3 months. When females had reached the YG stage, oocyte recruitment seemed to be effectively finished, i.e., the time window for oocyte recruitment was in most cases 2 months in our experiment. The CA stage oocytes were, as expected, prevalent at the earlier stages and persisted at the most until the leading cohort size had reached 400 μm. The smallest YG oocytes were found at a leading cohort size of 350 μm and the range 350–400 μm therefore represented a transitional zone between the CA and YG

Table 4. Occurrence of Northeast Arctic cod (*Gadus morhua*) atresia divided into cell stage and intensity.

		% atresia stage 4AB and 4C				% atresia stage CA				% atresia stage YG				
Fish	Date	0–5	5–25	25–50	>50	0–5	5–25	25–50	>50	0–5	5–25	25–50	>50	Comment
3025	8 November 2006			×										
3025	5 December 2006				×	×								Few 4AB and 4C
3571	5 December 2006	×				×								
3571	10 January 2007									×				
8259	20 January 2007		×			×								
3e11	7 November 2006			×										
3e11	05 December 2006	×												
3e11	10 January 2007	×												
3e11	18 January 2007	×												
9e12	5 December 2006	×												
9e65	7 November 2006	×												
9e65	10 November 2006									×				
9e65	18 January 2007									×				
2dfb	3 October 2006	×												
5c14	3 October 2006	×												
5c14	18 January 2007									×				
605a	05 December 2006		×											
7cbd	8 November 2006			×										
9b99	10 January 2007									×				
9b99	18 January 2007										×			
a3b7	7 November 2006	×												
a3b7	5 December 2006					×								
a3b7	10 January 2007									×				
adf8	7 November 2006	×												
adf8	18 January 2007										×			
af03	6 September 2006													Beta atresia
af03	6 December 2006			×										Few 4AB and 4C
bea3	5 September 2006	×												
bea3	7 November 2006								×					
bea3	5 December 2006		×											Beta atresia
bea3	11 January 2007		×											
bea3	18 January 2007		×						×					Few CA
c0c7	10 January 2007									×				
cd1e	8 November 2006					×								
cd1e	20 January 2007													Beta atresia
cdf3	5 December 2006	×												Beta atresia
cdf3	10 January 2007									×				
cdf3	18 January 2007										×			

Note: Fish is the PIT tag code for individual females; codes given in italics identify a fish that would have skipped spawning. Beta atresia signifies that the fish had atretic oocytes at the beta stage at the given measurement date. Note that only dates and fish for which we found atresia are given in the table.

Published by NRC Research Press

Table 5. Explanatory power of weight (W_F) as a proxy to potential (F_p) and atresia-adjusted values (F_{pa}) throughout the course of the experiment for Northeast Arctic cod (*Gadus morhua*).

	Potential fecundity (F_p)			Potential fecundity adjusted for atresia (F_{pa})		
Month	Regression formula	R^2 adj	p	Regression formula	R^2 adj	p
June	$F_p = 5.19 + 1.22 \times W_{FJ}$	0.77	$<1.0^{-5}$	$F_{pa} = 5.95 + 1.12 \times W_{FJ}$	0.62	$<1.0^{-4}$
August	$F_p = 6.64 + 1.03 \times W_{FA}$	0.85	$<1.0^{-7}$	$F_{pa} = 7.13 + 0.97 \times W_{FA}$	0.72	$<1.0^{-5}$
September	$F_p = 6.02 + 1.10 \times W_{FS}$	0.86	$<1.0^{-7}$	$F_{pa} = 6.45 + 1.04 \times W_{FS}$	0.74	$<1.0^{-5}$
October	$F_p = 5.97 + 1.11 \times W_{FO}$	0.86	$<1.0^{-7}$	$F_{pa} = 6.40 + 1.05 \times W_{FO}$	0.75	$<1.0^{-5}$
November	$F_p = 5.85 + 1.12 \times W_{FN}$	0.89	$<1.0^{-8}$	$F_{pa} = 6.17 + 1.07 \times W_{FN}$	0.80	$<1.0^{-6}$
December	$F_p = 5.69 + 1.13 \times W_{FD}$	0.89	$<1.0^{-8}$	$F_{pa} = 6.01 + 1.09 \times W_{FD}$	0.79	$<1.0^{-6}$
January	$F_p = 5.78 + 1.12 \times W_{FJa}$	0.88	$<1.0^{-7}$	$F_{pa} = 6.04 + 1.08 \times W_{FJa}$	0.80	$<1.0^{-6}$
Sacrificed	$F_p = 5.58 + 1.14 \times W_{FSa}$	0.88	$<1.0^{-8}$	$F_{pa} = 5.82 + 1.11 \times W_{FSa}$	0.81	$<1.0^{-6}$

Note: R^2 adj is the adjusted explanatory value for the regression. The fecundity measurements and female weight were ln transformed before applying the regression.

Fig. 6. Female Northeast Arctic cod (*Gadus morhua*) weight in (*a*) June and (*b*) November plotted against potential fecundity.

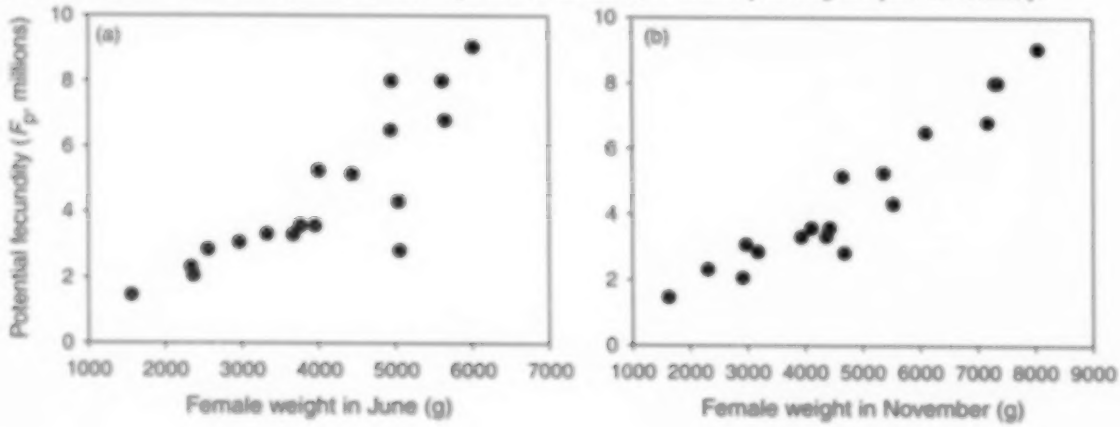

stages in our experiment, very much in agreement with field results on the same stock (Kjesbu 1991).

For the maturing females, atresia was very limited, until oocyte recruitment had finished, when atresia became more frequent and was found in PV, CA, and YG oocytes. This is novel information, as previous studies have mainly focused on prespawning cod, i.e., the YG stage (Kjesbu et al. 1991; Kraus et al. 2008). However, in the earlier study of Kjesbu et al. (1991), there were examples of poor-condition females arrested at the interphase between the PV and CA stages. This type of arrest at an early stage of oogenesis is known to also take part in other species such as winter flounder (*Pseudopleuronectes americanus*, previously *Pleuronectes americanus*) (Burton 1994) and blue whiting (*Micromesistius poutassou*) (Kjesbu 2009). Somewhat surprisingly, we did not find any relationship between our condition proxies and atresia, as atresia generally is negatively correlated with fish condition (e.g., Kjesbu et al. 1991; Kurita et al. 2003; Kraus et al. 2008). However, this finding must be treated with some caution, as (*i*) this analysis referred to the maturing fraction only, (*ii*) atresia levels might be highly fluctuating over time (cf. atretic window), and (*iii*) we actually did not undertake any proximate chemical analyses as in Kjesbu et al. (1991) and Kurita et al. (2003). Although liver index is generally considered a good proxy for liver energy content, there is nevertheless large variation in the specific energy content for a given liver size (Lambert and Dutil 1997).

The explanatory power of weight as fecundity proxy showed a clear temporal pattern, albeit the variation between measurement dates was quite low. This low variation could partly be caused by differences in individual feeding rates, i.e., if some individuals constantly acquired more food than others, this may have masked the effect of the feeding rations at a group level. Even so, explanatory power generally increased until November after which it remained similar. In November, all maturing females had reached either the late CA or YG stages and the majority of females were deemed to be close to the end or to just have finished follicle proliferation. In summary, the results indicate that energy reserves during early vitellogenesis are influential for potential fecundity. This is in agreement with studies on both Norwegian coastal cod (Skjærasen et al. 2006) and European plaice (*Pleuronectes platessa*) (Kennedy et al. 2007).

Skipped spawning

Our study provides experimental evidence of skipped spawning for Northeast Arctic cod. For this stock, this phenomenon has mainly been described from field samples in the Barents Sea (Woodhead and Woodhead 1965; Oganesyan 1993; Marshall et al. 1998). Rideout et al. (2005)

Fig. 7. (*a*) Residual condition, (*b*) 17β-estradiol, and (*c*) testosterone values for female Northeast Arctic cod (*Gadus morhua*) during the experiment. Solid circles indicate maturing females and open circles females that were deemed to be skipping. Asterisks indicate significant differences ($p < 0.0064$) between skipping and maturing females at the date in question.

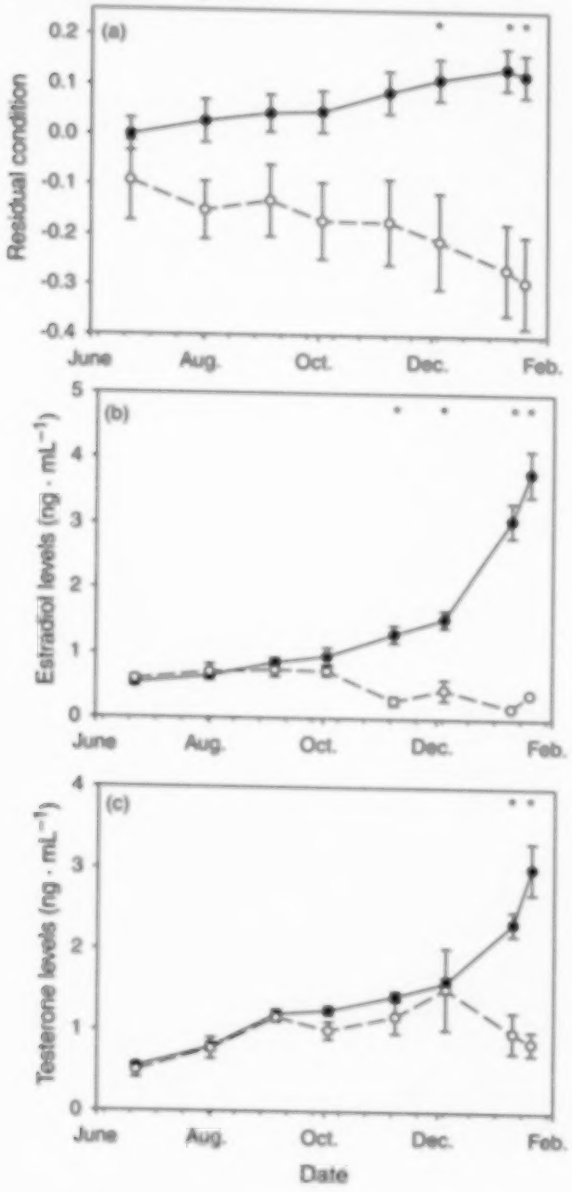

partitioned skipped spawners into retaining, reabsorbing, and resting females. Retaining females do not shed their eggs during the spawning season due to factors such as overcrowding, stress, pollution, and lack of mates. Reabsorbing skippers reabsorb all vitellogenic oocytes prior to spawning, and resting females do not start vitellogenesis at all (sensu Rideout et al. 2005). In our experiment, all skipping females reached the early CA stage, i.e., endogenous vitellogenesis (Wallace and Selman 1981), before further oocyte development was arrested ahead of the main mobilization of energy, i.e., the YG stage (Tyler and Sumpter 1996), or true vitellogenesis (Wallace and Selman 1981). Thus, based on the histology, our females were resting–early-reabsorbing skippers; they only reached the endogenous vitellogenic stage and were clearly on a different trajectory than the maturing females, both hormonally and stage-wise, by early November, the same time the power of weight as a fecundity proxy reached its maximum value for the spawning females. No indication of any cod undergoing mass atresia of yolk granules was found. Previous reports have identified both resting and reabsorbing skippers in Northeast Arctic cod (Woodhead and Woodhead 1965; Oganesyan 1993). Although the data are limited, our results indicate that for the majority of females, the "decision" to skip spawning is taken well ahead of the spawning season. From a life history perspective, this makes sense, given the large distance between spawning and feedings grounds for Northeast Arctic cod. The cost of the spawning migration may push the "decision" to spawn or not forward to a time before the start of the main migration. This implies that for Northeast Arctic cod, skippers remain on the feeding grounds, i.e., in the Barents Sea, and would therefore be unaccounted for in surveys at the spawning grounds, i.e., Lofoten and Vesterålen, and elsewhere along the Norwegian coast (Sundby and Nakken 2008). Tentatively agreeing with this, females with nonmaturing gonads are more or less absent from the long-term fecundity time series from Andenes, Vesterålen (Kjesbu et al. 1996; Thorsen et al. 2006).

Skipped spawning has previously primarily been linked to insufficient energy reserves (Rideout et al. 2005). However, from a life history viewpoint, skipped spawning might also be an adaptive trait, i.e., young females may trade off between investment in growth and, potentially, enhanced future reproductive success at the cost of the present spawning opportunity (Rideout et al. 2005; Jørgensen et al. 2006). Our results clearly support the contention that limited energy reserves cause spawning omission, as skipping females had smaller livers at sacrifice and lower condition from December onwards than maturing cod. Similarly, for Canadian cod, liver energy is the best predictor of spawning probability (Rideout et al. 2006). Due to the limited number of fish in our experiment, we are unable to evaluate if age did influence the likelihood of skipping, but there was no indication of any increased investment in length growth in skipping females. However, very little investment in length growth was observed for any cod through the experiment, which might relate to the present laboratory conditions, as adult Northeast Arctic cod normally grow about 10 cm·year^{-1} in the field (International Council for the Exploration of the Sea 2008).

It might be argued that our strict food regime gave energy reserves that were unnaturally low and that this comparatively high proportion is an artefact caused by the experiment. However, we argue the opposite, as well-fed fish kept in the laboratory usually have condition factors far exceeding those found in natural populations (e.g., Kjesbu 1989). The females in our experiment had an average HSI of approximately 7%, which closely resembles the upper values

seen in the field for the same stock (Marshall et al. 1998). However, we would like to stress that we do not believe that our results can be used to identify thresholds for maturation in the field. In an ongoing large-scale field sampling program, numerous skippers have been identified with liver indexes similar to those of spawning cod in our laboratory experiment (J.E. Skjærasen et al., unpublished data). We speculate that this is caused by differential investment by fish in the laboratory and field where fish kept under low exercise and a low, but reliable, food regime in the laboratory allocate relatively more energy to reproduction and less to growth and maintenance than in the natural situation. However, we do believe that our results represent the general and true mechanism of skipped spawning for Northeast Arctic cod in that (*i*) the main body of skippers separate from maturing females during early vitellogenesis and (*ii*) skipping is highly influenced by individual energy reserves. Further, the complete absence of skipped spawning in males is conspicuous, particularly when considering their overall lower energy reserves.

In summary, both oocyte recruitment and skipped spawning seem to be highly influenced by energy reserves during the critical period of early vitellogenesis for Northeast Arctic cod. This closely mimics the results of Burton (1994) for winter flounder. Skipping was linked to low energy reserves and was clearly more common in females, presumably, because of the larger cost associated with gonad maturation and spawning. Further, hormonally, skippers separated from the maturing fraction long before spawning and oocyte development was arrested at the E-CA stage. This implies that skippers (*i*) can be identified early in the maturation cycle, which is important for forecasting egg production and in recruitment studies, and (*ii*) remain on the feeding grounds in the Barents Sea when the spawning migration starts. If so, estimates of the proportion of skippers at the stock level would, if based on surveys at the spawning grounds, underestimate the proportion of fish that are skipping spawning in any given year.

Acknowledgements

The study was funded by the Research Council of Norway project "Timing and determination of fecundity and skipped spawning: implications for stock–recruitment theory of determinate spawners" (173341/S40) and encouraged by discussion with and the terms of references of the NAFO Working Group on Reproductive Potential and COST Action Fish Reproduction and Fisheries (FA0601). We thank Vemund Mangerud and Maria Krüger-Johnsen for help and assistance during the experiments. Josefin Titelman kindly commented on earlier drafts on the manuscript. The study was approved by and followed the guidelines of the Norwegian Veterinary Authorities for Experimental Research.

References

Andersen, T.E. 2003. Unbiased stereological estimation of cell numbers and volume fraction: the disector and the principles of point counting. *In* Report of the working group on modern approaches to assess maturity and fecundity of warm- and cold-water fish and squids, 4–7 September 2001, Bergen, Norway. *Edited by* O.S. Kjesbu, J.R. Hunter, and P.R. Witthames. Fisken og Havet. No. 12. pp. 11–18.

Arrucha, F. 2002. Oocyte development and maturity classification of swordfish from the north-western Atlantic. J. Fish Biol. **60**(1): 13–27. doi:10.1111/j.1095-8649.2002.tb02385.x.

Borg, B. 1994. Androgens in teleost fishes. Comp. Biochem. Physiol. C. **109**: 219–245.

Bromage, N.R., Jones, J., Randall, C., Thrush, M., Springate, J., Duston, J., and Barker, G. 1992. Broodstock management, fecundity, egg quality and the timing of egg production in the rainbow trout (*Oncorhynchus mykiss*). Aquaculture, **100**(1–3): 141–166. doi:10.1016/0044-8486(92)90355-O.

Burton, M.P.M. 1994. A critical period for nutritional control of early gametogenesis in female winter flounder, *Pleuronectes americanus* (Pisces, Teleostei). J. Zool. (Lond.), **233**(3): 405–415. doi:10.1111/j.1469-7998.1994.tb05273.x.

Dahle, R., Taranger, G.L., Karlsen, Ø., Kjesbu, O.S., and Norberg, B. 2003. Gonadal development and associated changes in liver size and sexual steroids during the reproductive cycle of captive male and female Atlantic cod (*Gadus morhua* L.). Comp. Biochem. Physiol. A. **136**(3): 641–653. doi:10.1016/S1095-6433(03)00215-0.

Godø, O.R., and Michalsen, K. 2000. Migratory behaviour of north-east Arctic cod, studied by use of data storage tags. Fish. Res. **48**(2): 127–140. doi:10.1016/S0165-7836(00)00177-6.

Hunter, J.R., and Macewicz, B.J. 1985. Rates of atresia in the ovary of captive and wild northern anchovy, *Engraulis mordax*. Fish. Bull. U.S. **83**: 119–136.

Hunter, J.R., Macewicz, B.J., Lo, N.C.H., and Kimbrell, C.A. 1992. Fecundity, spawning, and maturity of female Dover sole *Microstomus pacificus*, with an evaluation of assumptions and precision. Fish. Bull. U.S. **90**: 101–128.

International Council for the Exploration of the Sea. 2008. Report of the Arctic Fisheries Working Group. ICES CM\ACOM:01.

Jorgensen, C., and Fiksen, O. 2006. State-dependent energy allocation in cod (*Gadus Morhua*). Can. J. Fish. Aquat. Sci. **63**(1): 186–199. doi:10.1139/f05-209.

Jorgensen, C., Ernande, B., Fiksen, O., and Dieckmann, U. 2006. The logic of skipped spawning in fish. Can. J. Fish. Aquat. Sci. **63**(1): 200–211. doi:10.1139/f05-210.

Kennedy, J., Witthames, P.R., and Nash, R.D.M. 2007. The concept of fecundity regulation in plaice (*Pleuronectes platessa*) tested on three Irish Sea spawning populations. Can. J. Fish. Aquat. Sci. **64**(4): 587–601. doi:10.1139/F07-034.

Kent, M. 1990. Hand-held instrument for fat/water determination in whole fish. Food Contr. **1**(1): 47–53. doi:10.1016/0956-7135(90)90121-R.

Kjesbu, O.S. 1989. The spawning activity of cod, *Gadus morhua* L. J. Fish Biol. **34**(2): 195–206. doi:10.1111/j.1095-8649.1989.tb03302.x.

Kjesbu, O.S. 1991. A simple method for determining the maturity stages of Northeast Arctic cod (*Gadus morhua* L.) by *in vitro* examination of oocytes. Sarsia, **75**: 335–338.

Kjesbu, O.S. 2009. Applied fish reproductive biology: contribution of individual reproductive potential to recruitment and fisheries management. *In* Fish reproductive biology and its implications for assessment and management. *Edited by* T. Jakobsen, M. Fogarty, B.A. Megrey, and E. Moksness. Blackwell Science Ltd., Oxford, U.K. pp. 293–332.

Kjesbu, O.S., and Holm, J.C. 1994. Oocyte recruitment in first-time spawning Atlantic cod (*Gadus morhua*) in relation to feeding regime. Can. J. Fish. Aquat. Sci. **51**(8): 1893–1898. doi:10.1139/f94-189.

Kjesbu, O.S., and Kryvi, H. 1989. Oogenesis in cod, *Gadus morhua* L., studied by light and electron-microscopy. J. Fish Biol. **34**(5): 735–746. doi:10.1111/j.1095-8649.1989.tb03353.x.

Kjesbu, O.S., and Witthames, P.R. 2007. Evolutionary pressure on reproductive strategies in flatfish and groundfish: relevant concepts and methodological advancements. J. Sea Res. **58**(1): 23–34. doi:10.1016/j.seares.2007.02.001.

Kjesbu, O.S., Klungsøyr, J., Kryvi, H., Witthames, P.R., and Greer Walker, M. 1991. Fecundity, atresia, and egg size of captive Atlantic cod (*Gadus morhua*) in relation to proximate body composition. Can. J. Fish. Aquat. Sci. **48**(12): 2333–2343. doi:10.1139/f91-274.

Kjesbu, O.S., Kryvi, H., and Norberg, B. 1996. Oocyte size and structure in relation to blood plasma steroid hormones in individually monitored, spawning Atlantic cod. J. Fish Biol. **49**(6): 1197–1215. doi:10.1111/j.1095-8649.1996.tb01789.x.

Kraus, G., Tomkiewicz, J., Dickmann, R., and Köster, F.W. 2008. Seasonal prevalence and intensity of follicular atresia in Baltic cod *Gadus morhua callarias* L. J. Fish Biol. **72**(4): 831–847. doi:10.1111/j.1095-8649.2007.01760.x.

Kurita, Y., Meier, S., and Kjesbu, O.S. 2003. Oocyte growth and fecundity regulation by atresia of Atlantic herring (*Clupea harengus*) in relation to body condition throughout the maturation cycle. J. Sea Res. **49**(3): 203–219. doi:10.1016/S1385-1101(03)00004-2.

Lambert, Y., and Dutil, J.D. 1997. Can simple condition indices be used to monitor and quantify seasonal changes in the energy reserves of Atlantic cod (*Gadus morhua*)? Can. J. Fish. Aquat. Sci. **54**(Suppl. 1): 104–112. doi:10.1139/cjfas-54-S1-104.

Marshall, C.T., Kjesbu, O.S., Yaragina, N.A., Solemdal, P., and Ulltang, Ø. 1998. Is spawner biomass a sensitive measure of the reproductive and recruitment potential of Northeast Arctic cod? Can. J. Fish. Aquat. Sci. **55**(7): 1766–1783. doi:10.1139/cjfas-55-7-1766.

Marshall, C.T., Yaragina, N.A., Lambert, Y., and Kjesbu, O.S. 1999. Total lipid energy as a proxy for total egg production by fish stocks. Nature, **402**(6759): 288–290. doi:10.1038/46272.

Marshall, C.T., Yaragina, N.A., Ådlandsvik, B., and Dolgov, A.V. 2000. Reconstructing the stock–recruit relationship for Northeast Arctic cod using a bioenergetic index of reproductive potential. Can. J. Fish. Aquat. Sci. **57**(12): 2433–2442. doi:10.1139/cjfas-57-12-2433.

Methven, D.A., Crim, L.W., Norberg, B., Brown, J.A., Goff, G.P., and Huse, I. 1992. Seasonal reproduction and plasma-levels of sex steroids and vitellogenin in Atlantic halibut (*Hippoglossus hippoglossus*). Can. J. Fish. Aquat. Sci. **49**(4): 754–759. doi:10.1139/f92-084.

Morgan, M.J. 2008. Integrating reproductive biology into scientific advice for fisheries management. J. Northwest Atl. Fish. Sci. **41**: 37–51. doi:10.2960/J.v41.m615.

Motos, L. 1996. Reproductive biology and fecundity of the Bay of Biscay anchovy population (*Engraulis encrasicolus* L.). Sci. Mar. **60**: 195–207.

Murua, H., and Saborido-Rey, F. 2003. Female reproductive strategies of marine fish species of the North Atlantic. J. Northwest Atl. Fish. Sci. **33**: 23–31. doi:10.2960/J.v33.a2.

Nash, R.D.M., Kjesbu, O.S., Trippel, E.A., Finden, H., and Geffen, A.J. 2008. Potential variability in the paternal contribution to stock reproductive potential of Northeast Arctic cod (*Gadus morhua*). J. Northwest Atl. Fish. Sci. **41**: 71–83. doi:10.2960/J.v41.m619.

Nikolskii, G.V. 1969. Theory of fish population dynamics as the biological background for rational exploitation and management of fishery resources. Oliver and Boyd, Edinburgh, U.K.

Oganesyan, S.A. 1993. Periodicity of the Barents Sea cod reproduction. ICES C.M. 1993/G: 64.

Óskarsson, G.J., Kjesbu, O.S., and Slotte, A. 2002. Predictions of realised fecundity and spawning time in Norwegian spring-spawning herring (*Clupea harengus*). J. Sea Res. **48**(1): 59–79. doi:10.1016/S1385-1101(02)00135-1.

Rideout, R.M., and Rose, G.A. 2006. Suppression of reproduction in Atlantic cod *Gadus morhua*. Mar. Ecol. Prog. Ser. **320**: 267–277. doi:10.3354/meps320267.

Rideout, R.M., Rose, G.A., and Burton, M.P.M. 2005. Skipped spawning in female iteroparous fishes. Fish Fish. **6**: 50–72.

Rideout, R.M., Morgan, M.J., and Lilly, G.R. 2006. Variation in the frequency of skipped spawning in Atlantic cod (*Gadus morhua*) off Newfoundland and Labrador. ICES J. Mar. Sci. **63**: 1101–1110.

Rijnsdorp, A.D. 1990. The mechanism of energy allocation over reproduction and somatic growth in female North Sea plaice, *Pleuronectes platessa* L. J. Sea Res. **25**: 279–290.

Rollefsen, G. 1933. The otoliths of the cod. Fiskeridir. Skr. Ser. Havunders. **4**: 1–14.

Saborido-Rey, F., and Junquera, S. 1998. Histological assessment of variations in sexual maturity of cod (*Gadus morhua* L.) at the Flemish Cap (north-west Atlantic). ICES J. Mar. Sci. **55**(3): 515–521. doi:10.1006/jmsc.1997.0344.

Schulz, R. 1985. Measurement of five androgens in the blood of immature and maturing male rainbow trout, *Salmo gairdneri* (Richardson). Steroids, **46**(2-3): 717–726. doi:10.1016/0039-128X(85)90051-0. PMID:3837411.

Scott, B.E., Marteinsdottir, G., Begg, G.A., Wright, P.J., and Kjesbu, O.S. 2006. Effects of population size/age structure, condition and temporal dynamics of spawning on reproductive output in Atlantic cod (*Gadus morhua*). Ecol. Model. **191**(3-4): 383–415. doi:10.1016/j.ecolmodel.2005.05.015.

Senthilkumaran, B., Yoshikuni, M., and Nagahama, Y. 2004. A shift in steroidogenesis occurring in ovarian follicles prior to oocyte maturation. Mol. Cell. Endocrinol. **215**(1-2): 11–18. doi:10.1016/j.mce.2003.11.012. PMID:15026170.

Shirokova, M.Y. 1977. Peculiarities of the sexual maturation of females of the Baltic cod, *Gadus morhua callarias*. J. Ichthyol. **17**: 574–581.

Skjæraasen, J.E., Salvanes, A.G.V., Karlsen, Ø., Dahle, R., Nilsen, T., and Norberg, B. 2004. The effect of photoperiod on sexual maturation, appetite and growth in wild Atlantic cod (*Gadus morhua* L.). Fish Physiol. Biochem. **30**(2): 163–174. doi:10.1007/s10695-005-4319-6.

Skjæraasen, J.E., Nilsen, T., and Kjesbu, O.S. 2006. Timing and determination of potential fecundity in Atlantic cod (*Gadus morhua*). Can. J. Fish. Aquat. Sci. **63**(2): 310–320. doi:10.1139/f05-218.

Sundby, S., and Nakken, O. 2008. Spatial shifts in spawning habitats of Arcto-Norwegian cod related to multidecadal climate oscillations and climate change. ICES J. Mar. Sci. **65**(6): 953–962. doi:10.1093/icesjms/fsn085.

Thorsen, A., and Kjesbu, O.S. 2001. A rapid method for estimation of oocyte size and potential fecundity in Atlantic cod using a computer-aided particle analysis system. J. Sea Res. **46**(3-4): 295–308. doi:10.1016/S1385-1101(01)00090-9.

Thorsen, A., Marshall, C.T., and Kjesbu, O.S. 2006. Comparison of various potential fecundity models for north-east Arctic cod, *Gadus morhua* L., using oocyte diameter as a standardizing factor. J. Fish Biol. **69**(6): 1709–1730. doi:10.1111/j.1095-8649.2006.01239.x.

Tyler, C.R., and Sumpter, J.P. 1996. Oocyte growth and development in teleosts. Rev. Fish Biol. Fish. **6**(3): 287–318. doi:10.1007/BF00122584.

Ury, H.K. 1976. A comparison of four procedures for multiple comparisons among means (pairwise contrasts) for arbitrary

sample sizes. Technometrics, **18**(1): 89–97. doi:10.2307/1267921.

Wallace, R.A., and Selman, K. 1981. Cellular and aspects of oocyte growth in teleosts. Am. Zool. **21**: 325–343.

Witthames, P.R., and Greer Walker, M.G. 1995. Determinacy of fecundity and oocyte atresia in sole (*Solea solea*) from the Channel, the North Sea and the Irish Sea. Aquat. Living Resour. **8**(1): 91–109. doi:10.1051/alr:1995007.

Witthames, P.R., Thorsen, A., Fonn, M., Greenwood, L.N., Saborido-Rey, F., Dominguez, R., Murua, H., Korta, M., and Kjesbu, O.S. 2009. Advances in fecundity methodology applied to some marine fish. Fish. Bull. U.S. **107**: 148–164.

Woodhead, A.D., and Woodhead, P.M.J. 1965. Seasonal changes in the physiology of Barents Sea cod, *Gadus morhua* L., in relation to its environment. 1. Endocrine changes particularly affecting migration and maturation. ICNAF Spec. Publ. **6**: 691–715.

The role of wind in determining the timing of the spring bloom in the Strait of Georgia

A. Kathleen Collins, Susan E. Allen, and Rich Pawlowicz

Abstract: A coupled biophysical model of the Strait of Georgia (SoG), British Columbia, Canada, has been developed and successfully predicts the timing of the spring phytoplankton bloom. The physical model is a one-dimensional vertical mixing model, using a K-profile parametrization of the boundary layer, forced with high frequency meteorological data. The biological model includes one phytoplankton class (microphytoplankton) and one nutrient source (nitrate). The spring bloom in the SoG occurs when phytoplankton receive enough light that their growth rates exceed their loss rates. The amount of light that the phytoplankton receive is a function of solar radiation and the depth of mixing. The model was used to determine what physical factors are controlling the phytoplankton losses and the light received by the phytoplankton. Wind was found to control the spring bloom arrival time, with strong winds increasing the mixing-layer depth and delaying the bloom. The amount of incoming solar irradiance, through amount of cloud cover, had a secondary effect. The freshwater input (primarily Fraser River discharge) had an insignificant effect on the timing. Increased freshwater flux increases the buoyancy flux and thus decreases the mixing-layer depth but also increases the strength of the estuarine circulation, increasing the advective loss.

Résumé : Nous avons élaboré un modèle biophysique couplé du détroit de Géorgie (SoG), Colombie-Britannique, Canada, qui prédit avec succès le moment de la prolifération printanière du phytoplancton. Le modèle physique est un modèle de brassage vertical unidimensionnel, avec un paramétrage du profil K de la couche limite, forcé par des données météorologiques de haute fréquence. Le modèle biologique comprend une classe de phytoplancton (le microphytoplancton) et une source de nutriments (le nitrate). La prolifération printanière dans le SoG se produit lorsque le phytoplancton reçoit assez de lumière pour que son taux de croissance surpasse son taux de perte. La quantité de lumière reçue par le phytoplancton est fonction de la radiation solaire et de la profondeur du brassage. Le modèle a servi à déterminer quels facteurs physiques contrôlent les pertes du phytoplancton et la lumière reçue par le phytoplancton. Le vent contrôle le moment de l'arrivée de la prolifération printanière; cependant, les vents forts augmentent la profondeur de la couche de mélange et retardent la prolifération. La quantité d'éclairement solaire incident a un effet secondaire selon l'importance de la couverture nuageuse. L'apport d'eau douce (principalement le débit du Fraser) a un effet négligeable sur le calendrier de la prolifération. L'apport accru d'eau douce augmente le flux de flottabilité et diminue ainsi la profondeur de la couche de mélange, mais augmente aussi la force de la circulation dans l'estuaire, accroissant ainsi les pertes par advection.

[Traduit par la Rédaction]

Introduction

The Strait of Georgia (SoG) is a semi-enclosed, deep sea (maximum depth 400 m) located off the coast of mainland British Columbia, Canada (Fig. 1). In the southern SoG, the near-surface physical oceanography is dominated by the Fraser River plume and the estuarine flow it produces (Pawlowicz et al. 2007). The SoG is too large to be considered a classic estuary, but its dynamics are similar to those of smaller fjord estuaries. It is productive (yearly average productivity 1.6 g C·m^{-2}·day^{-1}) and, being a temperate sea, has a classic diatom-dominated spring bloom and a weaker fall bloom (R. Pawlowicz, A.R. Sastri, S.E. Allen, D. Cassis, O. Riche, M. Halverson, R. El-Sabaawi, and J.F. Dower, unpublished data). The timing of the spring bloom has been observed to vary interannually by as much as 6 weeks, with blooms as early as February and as late as mid-April (R. Pawlowicz, A.R. Sastri, S.E. Allen, D. Cassis, O. Riche, M. Halverson, R. El-Sabaawi, and J.F. Dower, unpublished data). The timing of the bloom is believed to be influential in the survival of various higher trophic levels, including, for example, Pacific herring (*Clupea pallasi*) and the historically dominant copepod *Neocalanus plumchrus*. The larval stages of Pacific herring have a fixed spawning time (Beamish et al. 2004), which may or may not coincide with the increased food supply associated with the bloom. Nauplii of *N. plumchrus* migrate to the surface in the spring. If the spring bloom is very early, the nauplii can miss the

Received 12 June 2008. Accepted 30 March 2009. Published on the NRC Research Press Web site at cjfas.nrc.ca on 9 September 2009. J20616

Paper handled by Associate Editor Gary Sprules.

A.K. Collins,[1] S.E. Allen,[2] and R. Pawlowicz. Department of Earth and Ocean Sciences, University of British Columbia, 6339 Stores Road, Vancouver, BC V6T 1Z4, Canada.

[1]Present address: Bedford Institute of Oceanography, Fisheries and Oceans Canada, P.O. Box 1006, Dartmouth, NS B2Y 4A2, Canada.
[2]Corresponding author (e-mail: sallen@eos.ubc.ca).

Fig. 1. Study region including sampling stations S3 and S2-2, the Fraser River, Parksville, Vancouver, Halibut Buoy, Sandheads Meteorological Station, and Vancouver International Airport (YVR).

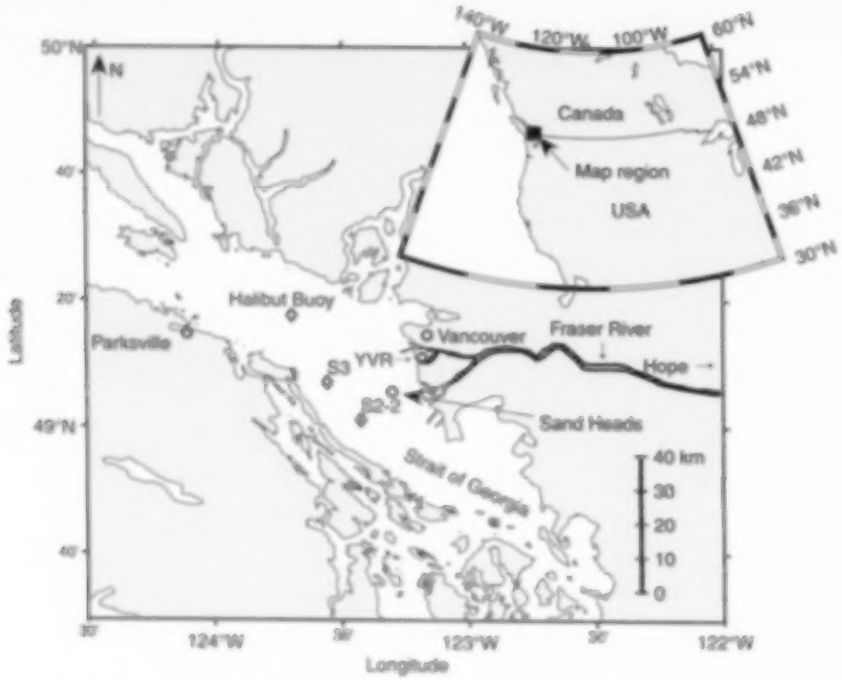

spring bloom and rely solely on postbloom plankton, which are less nutritious (El-Sabaawi et al. 2009). Here we use a numerical model to investigate what processes cause variation in the timing of the spring bloom and develop a simple method for predicting that time.

The spring bloom is a time of rapid accumulation of phytoplankton biomass, which occurs after the relatively low biomass observed in the winter. This accumulation arises because growth rates exceed loss rates for a period of time. We will first discuss factors influencing growth rates and then consider losses. Growth rates can be limited by light or nutrients and retarded by cold temperatures. In the summer, productivity in the SoG can be limited by lack of nitrate (Yin et al. 1997*a*). Other nutrient limitations have not been measured directly, though in some years, silicon is near limiting values towards the end of the spring bloom (R. Pawlowicz, A.R. Sastri, S.E. Allen, D. Cassis, O. Riche, M. Halverson, R. El-Sabaawi, and J.F. Dower, unpublished data). However, in the winter, both these nutrients are well above saturation (R. Pawlowicz, A.R. Sastri, S.E. Allen, D. Cassis, O. Riche, M. Halverson, R. El-Sabaawi, and J.F. Dower, unpublished data), and so phytoplankton growth must be limited by light. Assuming a secondary role for changes in losses, the spring bloom must be initiated by an increase in the net daily light experienced by phytoplankton.

The amount of light that a phytoplankter experiences will be set by a number of factors: (*i*) those that influence the amount of light entering the surface water (length of day, sun angle, amount of cloud in the atmosphere, and surface albedo); (*ii*) those that absorb or reflect light in the water, changing the light extinction coefficient in the water, and (*iii*) the depth of the phytoplankter. The phytoplankton near the surface will always receive the most light, but due to vertical mixing, no phytoplankton is likely to stay at the surface for very long. So a key factor in the amount of light that a phytoplankter receives is the mixing near the surface.

Sverdrup (1953) expressed this effect as critical depth, which was compared with the mixed-layer depth. If critical depth, defined as the depth at which integrated growth equals the integrated respiration, is deeper than the mixed-layer depth, then net growth and a possible bloom are expected. However, the mixed layer, defined as a region near the surface that is well mixed with respect to salinity and temperature, is not always equivalent to the mixing layer, i.e., the layer that is actively mixing. Results from cases in which the mixing layer is shallower than a residual mixed layer can lead to blooms even where the mixed layer is deeper than the critical depth (Huisman et al. 1999). In the SoG, we have the opposite effect. Mixing is occurring without homogenization of properties because there is a significant buoyancy flux into the upper water column. This effect has been seen previously in other regions and authors have assumed that active mixing is occurring down to the strong halocline (Erga and Heimdal 1984). The terminology of a mixing layer as opposed to a mixed layer is carefully used, for example, in Parsons et al. (1984). Mixing-layer depth is a function of processes adding kinetic turbulent energy, which deepens and attempts to homogenize the layer (wind, cooling), and processes adding potential energy, which shallows and attempts to restratify the layer (freshwater influx, warming).

Losses to the phytoplankton biomass can occur due to ad-

vection, sinking, grazing, and viral lysis. A sharp decrease in the loss rate could generate a spring bloom. However, advection changes slowly in the SoG, and the remaining terms are more likely to change in response to the accumulation of biomass rather than causing it. The estuarine circulation in the SoG causes vertical entrainment of deeper water into the surface layer and horizontal advective loss. The strength of this circulation is determined by the freshwater flux into the SoG, which varies on time scales of weeks.

Thus we expect a central role in the timing of the spring bloom for the amount of light reaching the SoG and for the mixing-layer depth and a secondary role for the advective loss. In this paper, we will investigate the role of the principal physical forcings on the SoG, which vary interannually (wind, freshwater flux, and cloud fraction). We wish to determine which of these physical forcings, within the observed variation of the forcing, most strongly influence the timing of the spring bloom.

To directly observe mixing-layer depth, one can use various instantaneous turbulence measurements, but it is much harder to maintain measurements over an extended period, and unlike mixed depth, which is due to the integrative effects of mixing, mixing-layer depth varies rapidly. Here, the depth of the mixing layer will be calculated using a turbulence closure model designed for the surface ocean (Large et al. 1994). Recent one-dimensional (1D) models have considered the timing of the spring bloom in Prince William Sound (Eslinger et al. 2001) and the Bering Sea (Jin et al. 2006). In both cases, the phytoplankton is light-limited and the initiation of the bloom is due to reduced mixing and increased stratification. In the Bering Sea, ice is usually a controlling factor, but in ice-free years, Jin et al. (2006) showed that wind mixing and thermal stratification controlled the mixing-layer depth and thus the timing of the bloom. They were limited in their investigation of interannual variations as they had only one year of ice-free data. Using three years of data in Prince William Sound, Eslinger et al. (2001) showed that, again, wind mixing controlled the mixing-layer depth and the timing of the spring bloom. In both these regions, thermal stratification dominates over salinity stratification; whereas in the SoG, salinity stratification dominates due to the large freshwater fluxes. For the SoG, it has therefore been postulated that the beginning of the large freshwater flux due to snowmelt (the freshet) is necessary for the mixing layer to shallow and the bloom to begin (Yin et al. 1997*b*).

Recently, an extensive set of physical and biological data has been collected for the southern portion of the Strait. These data include meteorological parameters, hydrological data, and a vast set of hydrographic and biological data collected as part of the STRATOGEM (Strait of Georgia Ecosystem Modeling) program, including three years of monthly or more frequent surveys and four years of continuous data collection from the ferries crossing the SoG (Pawlowicz et al. 2007). The high quality and high frequency data from the STRATOGEM project provide an opportunity to develop a coupled biophysical model that includes high frequency (hourly) variations of atmospheric forcing. In the work reported here, the biological model is optimized to find the timing of the spring bloom. The spring bloom is initiated as light limitation lifts, leading to a diatom bloom that is terminated by nitrate exhaustion. Thus our biological model only includes one nutrient type (nitrate) and one phytoplankton (a diatom).

We have chosen to use a high resolution 1D (vertical) coupled biophysical model to correctly model the surface mixing layer. Spatial variations in bloom timing are relatively small: data from the ferries crossing the SoG show that the spring bloom occurs nearly simultaneously (within 3 days) across the Strait. Survey data show that although patchy, chlorophyll distributions are reasonably similar throughout the southern Strait. Two-layer models of the SoG (St. John et al. 1993; Li et al. 2000) cannot capture the details near the surface, and 3D models of the SoG (Masson and Cummins 2004) have limited resolution near the surface. The knowledge from previous studies and the high quality data collected as part of STRATOGEM allow us to parametrize the necessary 2D physical processes and tune the 1D model to correctly represent the SoG physics. We use physical dynamical understanding to ensure that these parametrizations have correct properties beyond the observed values. This then provides a simple, fast-running model that we can use both in interpolative mode for the observed years and in extrapolative mode for years without data and for hypothetical physical forcings. This latter facility allows us to vary wind speed, cloud fraction, and freshwater flux individually to determine their separate impacts on the timing of the spring bloom.

Material and methods

Site

The Fraser River is the largest river in British Columbia and contributes 60% to 70% of the freshwater entering the Strait (Herlinveaux and Tully 1961; Pawlowicz et al. 2007). Flow is relatively low during the winter months (average winter flow at Hope, 150 km upstream, is 8.5×10^2 $m^3 \cdot s^{-1}$ (Environment Canada 2006)), begins to increase in April–May, and then peaks in June when the mountain snowpack melts; this is termed the freshet (average freshet at Hope is 8×10^3 $m^3 \cdot s^{-1}$).

Winds are generally weak in the SoG compared with in the open coastal ocean; average wind speed is 5.2 $m \cdot s^{-1}$ between 2001 and 2005 (Environment Canada 2002) at Sandheads (Fig. 1). The winds follow a seasonal pattern, with the strongest winds occurring during winter storms and very weak wind conditions occurring during high pressure periods in the summer. Cloud cover in the SoG region typically follows a pattern of obscured skies throughout much of the winter months and clear skies during the summer.

The biological community in the SoG is characterized by a phytoplankton bloom of average magnitude 30 mg $Chl \cdot m^{-3}$ that typically occurs in the early spring, followed by an increase in zooplankton grazers and nutrient depletion (Harrison et al. 1983). The spring bloom is initially composed of the chain-forming diatom *Thalassiosira* spp. and progresses with the explosion of *Skeletonema costatum*, with the diatom *Chaetoceros convolutus* blooming more slowly (Harrison et al. 1983; Hobson and McQuoid 1997). Ammonium and urea concentrations are low in the SoG (NH_4^+ concentrations of 0.5 to 2 $\mu mol \cdot L^{-1}$ directly after the spring bloom (Yin et al. 1996)) compared with nitrate, which is

abundant (30 μmol·L^{-1}; R. Pawlowicz, A.R. Sastri, S.E. Allen, D. Cassis, O. Riche, M. Halverson, R. El-Sabaawi, and J.F. Dower, unpublished data) and is an important nutrient source for phytoplankton throughout the year and probably the primary nutrient during the bloom (Harrison et al. 1983). Average yearly *f* ratios have been estimated at 0.3–0.4 (Mackas and Harrison 1997) and, more recently, 0.5 (R. Pawlowicz, A.R. Sastri, S.E. Allen, D. Cassis, O. Riche, M. Halverson, R. El-Sabaawi, and J.F. Dower, unpublished data). The surface macrozooplankton community in the SoG is mainly composed of copepods and was historically dominated by the large calanoid copepod *Neocalanus plumchrus* (Harrison et al. 1983). *Neocalanus plumchrus* depends on phytoplankton biomass for survival and growth (Kobari and Ikeda 2001) and is perhaps a substantial food source for salmon (Parsons et al. 1984).

Data

The field data used in this study were collected over four years at nine stations in the SoG. The nominal location being modeled is station S3 (Fig. 1). Sampling took place approximately once per month and more frequently during the spring phytoplankton bloom. Casts were taken with a conductivity–temperature–depth (CTD) sensor; variables recorded at each station included chlorophyll fluorescence, photosynthetically active radiation (I_{PAR}), temperature, and salinity. Nitrate, chlorophyll, salinity, oxygen, and taxonomy samples were taken at depths of 0, 5, 10, and 30 m. The chlorophyll samples were filtered and size-fractionated, and the largest fraction (>20 μm) was used for model comparison. Continuous surface salinity, temperature, and chlorophyll fluorescence data are available from a sampling program aboard several BC Ferries vessels, one of which passes near station S3. Fluorescence data from within a 2 min latitude by × 2 min longitude box centered on S3 were used to compare with model output.

Wind speed and direction were obtained from Environment Canada's weather station at Sandheads CS, an exposed site at the edge of the mud flats of the Fraser River delta (all locations, Fig. 1) (Environment Canada 2002). Other meteorological data not available from the automatic station at Sandheads (hourly humidity, air temperature, cloud fraction) were obtained from Environment Canada's weather station at the Vancouver International Airport (Environment Canada 2002). Fraser River flow is measured daily at Hope, BC, 150 km upstream of where the river enters the Strait, and Englishman River flow is measured daily at Parksville, BC (Environment Canada 2006). Downward shortwave radiation data measured by the UBC Department of Agroecology was used for the parametrization of the cloud model that will be described in the next section. Irradiance data from Halibut Bank Buoy were used to verify the cloud model.

The physical model

The physical model used is an adapted version of the K-profile parametrization (KPP) nonlocal boundary-layer model (Large et al. 1994). The model represents mixing due to turbulent vertical velocities of unresolved eddies and calculates numerical values for the horizontal velocities, temperature, salinity, and diffusivity in time and space. The fine vertical grid resolution available from a 1D model enables the careful evaluation of near-surface mixing and its importance on phytoplankton growth; the speed of calculations allows for many model runs.

We will neglect the tides in the model. Tides in the central SoG are of maximum velocity 0.5 m·s^{-1} but contribute little mixing to the system because of the depth of the Strait (200–400 m) (Thomson 1994). This is in direct contrast to the strong tidal mixing that occurs to the south and north of the SoG in narrow, shallow, and complicated channels. In the SoG, tidal excursions are on the order of 10 km, which is small compared with the size of the central SoG and so the advective role of the tides is not a dominant factor because variations within the tidal excursion are small.

The KPP model has been incorporated into a number of large 3D models (ROMS, e.g., Durski et al. (2004); HYCOM, e.g., Chassignet et al. (2003); MITgcm, e.g., Campin et al. (2008)). Some results show stronger mixing for the KPP model than for the Mellor–Yamada 2.5 turbulence closure scheme (Durski et al. 2004) that had been used by Denman and Peña (2002), for example, to model phytoplankton cycles in the Northeast Pacific Ocean. Other results show weaker mixing and suggest better agreement with turbulence measurements (Kettle 2005). KPP and Mellor–Yamada 2.5 models are the most commonly used turbulent parametrizations.

To use any 1D mixing models in the SoG requires incorporation of additional processes. The SoG has a number of important horizontal processes, including the estuarine circulation and baroclinic pressure gradients. These processes must be parametrized in the physical model, are additions to the standard KPP model, and are explained in detail below.

The equations for across-strait and along-strait velocity, salinity, and temperature can be represented as, respectively,

$$(1a)\quad \frac{\partial u}{\partial t} - fv = -\frac{1}{\rho_0}\frac{\partial p}{\partial x} - \frac{\partial}{\partial z}(w_e u) + \mathcal{V}(u)$$

$$(1b)\quad \frac{\partial v}{\partial t} + fu = -\frac{1}{\rho_0}\frac{\partial p}{\partial y} - \frac{\partial}{\partial z}(w_e v) + \mathcal{V}(v)$$

$$(1c)\quad \frac{\partial S}{\partial t} = -\frac{\partial}{\partial z}(w_e S) + J_s \exp(\gamma z) + \mathcal{V}(S)$$

$$(1d)\quad \frac{\partial T}{\partial t} = -\frac{\partial}{\partial z}(w_e T) + \frac{I_{TOTAL}(z)}{c_p\,\rho(z)} + \mathcal{V}(T)$$

where u and v are the across- and along-strait velocities, respectively, S is salinity, T is temperature, t is time, x and y are along- and across-strait distances, respectively, z is vertically upward distance starting at the sea surface (so all z values are negative), f is the Coriolis parameter, $\mathcal{V}$ is the mixing prescribed by the KPP model (Large et al. 1994), p is the baroclinic pressure, ρ is the density of water, ρ_0 is a constant reference density, c_p is the specific heat at constant pressure, w_e is a vertical upwelling flux, J_s is an added freshwater flux, $1/\gamma$ is the scale depth of the freshwater flux, and I_{TOTAL} is the incoming shortwave radiation. Surface boundary conditions for the momentum equations include wind stress, and those for the temperature include the longwave radiation balance and the sensible and latent heat

Fig. 2. (*a*) Fraser River (left axis) and Englishman River (right axis) flow for January 2002 – June 2005. (*b*) Salinity fit based on Fraser River and Englishman River flow data and observations of surface salinity at station S3.

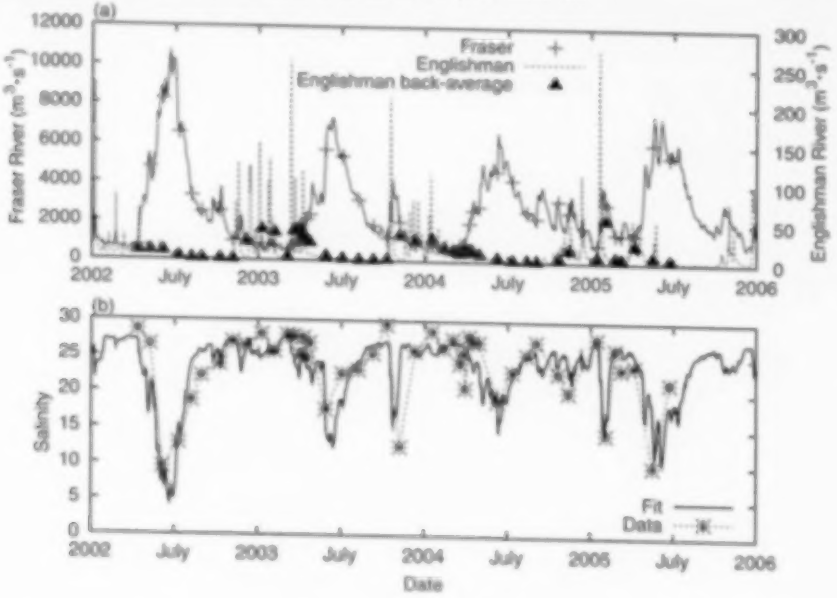

flux. The underlined terms are those additional to the standard KPP model, and they and the incoming shortwave radiation are discussed in the next three subsections.

Estuarine flow

The effect of the estuarine flow is seen in the two underlined terms of the salinity equation (eq. 1*c*). Estuarine flow has two effects. First, the freshwater flow into the Strait keeps the surface relatively fresh and is the main stratifying influence (J_s). In the model, freshwater is added to the surface layer based on a parametrization of total freshwater flow into the Strait. Second, estuarine entrainment from the deeper water into the surface layer causes a slow upwelling of the water column (w_e).

Empirically, we find that the surface salinity at station S3 is well correlated with the input of freshwater into the SoG. This input is composed of the Fraser River (with sources in the interior of British Columbia) and a number of smaller rivers that drain coastal areas. Most of these are not measured, but we assume that their effect will be similar to that of the Englishman River. We model the total freshwater flux as

$$(2a) \qquad Q_T = Q_F + a_E Q_E$$

where Q_T is the effective total freshwater flux, Q_F is the Fraser River flux, $a_E = 55.0$, and Q_E is a 20-day back-average of the Englishman River flux (Fig. 2*a*). Then we model the surface salinity at station S3 as

$$(2b) \qquad S_{surface} = S_D \frac{\exp(-Q_T/\alpha_f)}{\gamma_f + \exp(-Q_T/\alpha_f)}$$

where $S_D = 30.0$, $\alpha_f = 2440$ m^3·s^{-1}, and $\gamma_f = 0.0633$ (subscript "f" refers to freshwater flux) (Fig. 2*b*); $R^2 = 0.61$. This allows us to interpolate the observed salinities at station S3 to daily resolution.

Next, to force the surface salinities in the model to these observations, we add a forcing term:

$$(3) \qquad J_s \exp(\gamma z) = F_o S_0 \left(\frac{Q_T}{\overline{Q}}\right)^{\sigma_s} \exp\left(\frac{z}{a_b h_m}\right)$$

where $F_o = 3.0 \times 10^{-6}$ m·s^{-1}, S_0 is the mixed-layer salinity at the previous time step, $\overline{Q} = 3624$ m^3·s^{-1}, $\sigma_s = 1.12$, $a_b = 3.5$, and h_m is the mixing-layer depth determined by the KPP model. The constants F_o, σ_s, and a_b were selected to match the model salinity to the interpolated observed salinity; see the Results section. We see that the scale depth over which the freshwater flux impacts the water column is $1/\gamma = a_b h_m$.

Vertical advection (upwelling) is assumed to be dominated by the estuarine circulation. The vertical velocity was determined using a similarity solution fitted to observations of salinity at stations S3 and S2-2, Knudson relations, and a force balance between the estuarine pressure gradient and the turbulent momentum mixing (see Appendix A):

$$(4) \qquad w_e = w_* \left[2.72 \frac{Q_T}{\overline{Q}} \exp\left(\frac{-Q_T}{\overline{Q}}\right)\right]\left[1 - \left(1 + \frac{z}{2.5\,d}\right)^2\right]$$

where $w_* = 2.5 \times 10^{-5}$ m·s^{-1}, $\overline{Q} = 3624$ m^3·s^{-1}, and $d = 11.7$ m is the average depth at which the cumulative freshwater reaches 67% of its surface value at station S3. Although complex, the primary purpose of these parameterizations is to ensure that the physical parameters of the water column are realistically represented not only for years with observations, but also for years without data and for hypothetical physical forcings.

This vertical velocity controls the vertical advection of salt (eq. 1*c*), temperature (eq. 1*d*), momentum (eqs. 1*a* and

Fig. 3. Sketch of the vertical velocity field as a function of depth (vertical arrows) and the resulting detrained flux of water (horizontal arrows).

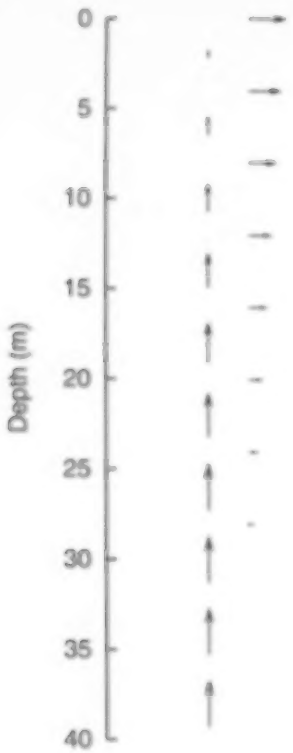

1*b*), nitrate, and phytoplankton. As the vertical velocity has convergence (that is, it is stronger at depth than near the surface), detrainment (removal) of these properties, as well as water, occurs throughout the depth of the model (Fig. 3). This advective loss is a significant loss term for the phytoplankton in winter. The vertical velocity at depth is a function of the river flow (eq. 4); for the river flows observed, this velocity is usually between 1.8 and 2.5 $\times$ 10^{-5} m·s^{-1}, only rarely drops below 1.6 $\times$ 10^{-5} m·s^{-1}, and never goes below 0.95 $\times$ 10^{-5} m·s^{-1}.

Baroclinic pressure gradients

In the open ocean, flow in a given direction in a given layer between isopycnals can continue in a single direction without particular consequences. In a constricted basin it causes an accumulation of mass within that layer downstream and a corresponding baroclinic pressure gradient against the flow. These pressure gradients appear in the momentum eqs. 1*a* and 1*b*.

To include this pressure gradient, it is assumed that (*a*) the basin is shaped like an ellipse with nearly vertical sides; (*b*) station S3 is located in the exact center of the basin; and (*c*) the basin is initially uniformly stratified. A flow in a given isopycnic layer will cause a thickening (thinning) of that layer downstream (upstream):

Fig. 4. Illustration of the scheme used to solve for the *x* and *y* baroclinic pressure gradients. This shows the scheme in one dimension, the same theory applies for two dimensions. Broken lines denote undisturbed isopycnals at the grid spacing, and solid lines denote the instantaneous isopycnals. Flow from left to right, as illustrated in the top layer, causes the layer to thicken to the right, thereby reducing the baroclinic pressure below.

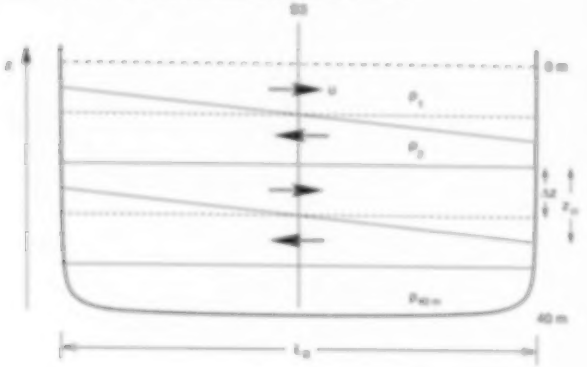

$$(5) \qquad z^{+x}_{+x,i} = \int \frac{U_i dt}{L_x/2} + \Delta z$$

where U_i is the baroclinic velocity $u_i - \langle u_i \rangle$ in the ith layer with $i = 1$ being the top layer, $\langle\ \rangle$ implies the vertical average, L_x is the width of the ellipse, Δz is the undisturbed thickness of the layer, and $z^{+x}_{+x,i}$ is the thickness at the positive x boundary of the ellipse (Fig. 4). The thickness at the positive y boundary is found similarly.

These tilted isobars cause baroclinic pressure gradients at z_i of

$$(6) \qquad \frac{\partial p_i}{\partial x} = \frac{g}{\rho_0 L_x}\left\{\sum_{j=1}^{k}\rho_j z_{+x,j} + \rho_{k+1}\left(\sum_{j=1}^{k} z_{+x,j} - |z_i|\right) - \sum_{j=1}^{i}\rho_j \Delta z\right\}$$

where k is the last full layer just above z_i and the expression inside the parentheses is the fraction of the k+1 layer above z_i. In addition, g is the acceleration due to gravity, ρ_i is the density in the ith layer, and ρ_0 is a constant reference density. The calculation is similar for the pressure gradient in y. These are the pressure gradient terms used in eqs. 1*a* and 1*b*. We use L_x = 60 km and L_y = 240 km, with the ellipse oriented with its major axis northwest–southeast with its northwest end 55° E of North.

Light

The physical model incorporates light in three parts, beginning with a cloud model that filters light from the sun, an albedo, and parametrizations for the deposition of photosynthetically active radiation and for the total light spectrum that is available for heat. All calculations for light use units of W·m^{-2}. To compare I_{PAR} with field data measured in μE·m^{-2}·s^{-1}, these units are converted to W·m^{-2} using a conversion factor of 0.2174, recommended by the I_{PAR} sensor manufacturer (Biospherical Instruments Inc.). This is based on a quanta-to-Watt ratio of 2.77 $\times$ 10^{18} quanta·s^{-1}·W^{-1}.

Table 1. Parameters used in the biological model.

Symbol	Parameter	Value	Source
R_{max} (T_{ref})	Maximum growth rate (24 h)	2.16·day^{-1}	Durbin (1974) and Hitchcock (1980)
T_{ref}	Reference temperature	10 °C	
I_{op}	Optimal light level	38.4 W·m^{-2}	Fit to Steele (1962) and Durbin (1974)
α_T	Temperature effect slope	0.07 °C	Eppley (1972)
κ	Half-saturation, nitrate	0.5 μmol·L^{-1}	Falkowski (1975)
W_1	Sinking rate, nutrient replete	0.5 m·day^{-1}	Cugier et al. (2005)
W_2	Sinking rate, nutrient depleted	1.2 m·day^{-1}	Cugier et al. (2005)
R_M (T_{ref})	Mortality	0.1·day^{-1}	Spitz et al. (2003)
	Maximum temperature for growth	18 °C	Durbin (1974)
	Range of decrease due to temperature	8 °C	
κ_p	Half-saturation, mesozooplankton on diatoms	0.5 μmol N·L^{-1}	From data
$\gamma(T_{ref})$	Maximum ingestion, mesozooplankton	0.6·day^{-1}	Cugier et al. (2005)
Z_w	Winter concentration, zooplankton	0.168 μmol N·L^{-1}	Tuned

The methodology of a cloud model for the open seas of the North Atlantic Ocean (Dobson and Smith 1988) was followed to develop a new cloud model for the SoG using shortwave radiation obtained from the Department of Agroecology Science at UBC (R. Ketler, Department of Agroecology, University of British Columbia, Vancouver, British Columbia, personal communication, 2005).

An albedo value of 18% was calculated for the SoG by measuring I_{PAR} just above and just below the sea surface at nine stations on 11 November 2004. Albedo varies from ~0.03 to 0.4 with season, sea roughness, and water clarity (Jin et al. 2004), so a value of 18% for the productive and turbid SoG is appropriately higher than the open-ocean value of 6% used by Large et al. (1994); we include albedo as a constant value following Large et al. (1994).

The depth distribution of photosynthetically active radiation (I_{PAR}, 400–700 nm) requires a distinction from the total light (300–2500 nm). Integrating the whole light spectrum (Jerlov 1976), we find that 44% is in the photosynthetically available range. Therefore surface irradiance ($I_{PAR}(0\,m)$) is calculated in the model as 44% of the total nonreflected light. Analysis of the SoG irradiance data showed that I_{PAR} follows an exponential decay:

$$I_{PAR}(z) = I_{PAR}(0\,m)\exp(K_{PAR}z) \tag{7}$$

where K_{PAR} is the attenuation coefficient, which is unknown. A parametrization for K_{PAR} will provide the model with an irradiance profile.

Attenuation (K_{PAR}) of light depends on the amount of particulate matter in the water, including organic material such as phytoplankton and inorganic material such as sediment transported by the Fraser River. An empirical relationship between measured light and the phytoplankton quantity in the water (measured from chlorophyll P_c) and Fraser River flow (Q_f) was found to give

$$K_{PAR}(z) = \alpha_i + \beta_i \overline{P}^{0.665} + \left[\gamma_i\left(\frac{Q_f}{\overline{Q}}\right)^{\alpha_i} + \theta_i\right]\exp\left(\frac{z}{d_i}\right) \tag{8}$$

where the exponent of 0.665 on $\overline{P}$ follows Ménesguen et al. (1995) and $\overline{P} = P_c/(1\,mg\,Chl\cdot m^{-3})$. The fit gave α_i = 0.0910·m^{-1}, β_i = 0.0289·m^{-1}, γ_i = 0.00986·m^{-1}, θ_i = 0.445·m^{-1}, and d_i = 2.56 m. The large exponent on the river flow reflects the fact that young river water (less than 1 day old) only reaches station S3 under strong flow conditions.

The fit is done on the light decrease over 1 m steps for 45 PAR profiles and has R^2 = 0.77. It dictates that as particulate matter in the water column (river sediment or phytoplankton) increases, K_{PAR} increases and light is absorbed closer to the surface because there is more matter to absorb it.

The distribution of total light in the water to calculate the nonturbulent heat flux profile is taken from the Jerlov (1976) water classification system, which provides data on the distribution of light with depth; this distribution follows a double exponential decay. For each of Jerlov's five coastal water types, two attenuation coefficients, K_1 and K_2, are estimated. The K_1 and K_2 values are fit separately to the theoretical K_{PAR} values given by Jerlov for each water type, giving us an expression for each of the attenuation coefficients:

$$K_1 = 0.81K_{PAR} + 1.18\,m^{-1} \tag{9a}$$

$$K_2 = 0.82K_{PAR} - 0.088\,m^{-1} \tag{9b}$$

The fits have R^2 = 0.94 and 0.97, respectively. Equations 9*a* and 9*b* are solved during model computations using the value of K_{PAR} (eq. 8). The total light profile can then be generated by integrating

$$\frac{\partial I_1}{\partial z} = K_1 I_1 \qquad \frac{\partial I_2}{\partial z} = K_2 I_2 \tag{10}$$

using initial conditions

$$I_1(0\,m) = 0.70I(0\,m) \qquad I_2(0\,m) = 0.30I(0\,m) \tag{11}$$

based on eqs. 8, 9*a*, 9*b*, and $I(0\,m)$ and where the values 70% and 30% were determined empirically. The value $I_{TOTAL} = I_1 + I_2$ is used for the shortwave radiation in eq. 1*d*.

Wind

Wind speed and direction are measured at a height of 10 m at Sandheads Meteorological Station (Fig. 1) and are transformed from wind speed and direction into meridional (u) and zonal (v) components and rotated to 55° NW to be aligned with the major axis of the SoG. Wind stress is calculated following Large and Pond (1982).

Bottom boundaries

The profile salinity and temperature data at 40 m was fit to constant, seasonal, and bi-seasonal components. The bottle nitrate data at 30 m was averaged and used for the 40 m values as nitrate below 30 m was found to be nearly constant at other stations in the Strait.

The biological model

The objective of the SoG biological model, when coupled with the physical model, is to predict the timing of the spring phytoplankton bloom. The growth rate of phytoplankton and rate of change of nutrient concentration are calculated based on Jeffery (2002), with only one size class of phytoplankton (P) included (microphytoplankton, >20 μm) and nitrate (N) as the sole nutrient modeled. Although phytoplankton use ammonium during the spring bloom, as evidenced by the f ratios, the amount of ammonium available at any time is small and inclusion of ammonium in the model makes no substantial changes to the spring bloom timing and only slightly increases its magnitude. We use the simplest possible model for the spring bloom because the addition of complexity to a model requires the use of more parameters, and in general, biological parameters are poorly constrained. Predictive capability often decreases with model complexity, particularly if the model is only to be used in a single region (e.g., Friedrichs et al. 2006).

All units in the biological model are nitrogen atom concentrations. The phytoplankton and nitrate equations are

$$\frac{\partial P}{\partial t} = \left\{\min[u_c(I_{PAR}), u_n(N)] - R_m - \Upsilon\frac{Z(t,z)}{\kappa_P + P}\right\}P + \frac{\partial}{\partial z}(w_s P) - \frac{\partial}{\partial z}(w_e P) + V(P) \tag{12a}$$

$$\frac{\partial N}{\partial t} = -\left\{\min[u_c(I_{PAR}), u_n(N)]\right\}P - \frac{\partial}{\partial z}(w_e N) + V(N) \tag{12b}$$

where P is the phytoplankton concentration, N is the nitrate concentration, u_c is the growth based on light limitation, u_n is the growth based on nitrate limitation, R_m is the rate of natural mortality, Υ is the maximum ingestion of phytoplankton by zooplankton, Z is the zooplankton concentration, κ_p is the half-saturation for zooplankton grazing, and w_s is the sinking rate of the phytoplankton (positive downward). The last two terms in each equation are, respectively, the estuarine advective loss and the turbulent diffusion determined by the physical model. Further advection terms, due to horizontal currents, cannot easily be incorporated into the 1D model and are neglected as chlorophyll and nitrate distributions are similar throughout the southern Strait.

The values for the biological parameters are provided (Table 1). Each of the biological terms in the two equations will be described below after initialization is discussed. The biological model is a simplified version of the standard NPZD models with origins back to Fasham et al. (1990). The formulation for the nutrient limitation term, the use of a minimum function, and the linear natural mortality are standard formulations for NPZD-type biological models (e.g., Denman and Peña 2002; Cugier et al. 2005). The light limitation term used here is a fit for a particular phytoplankton species, whereas most models use a more general form. We choose a Holling type-II grazing term similar to the Ivlev function used by Cugier et al. (2005), whereas Denman and Peña (2002) use a Holling type-III term.

Initialization

The phytoplankton in the model is initialized using profile fluorescence measurements, which are converted from mg Chl·m^{-3} to μmol N·L^{-1} using a conversion factor of 1.5:1. This ratio was estimated by plotting chlorophyll versus nitrate in the rapid growth time of the spring bloom. It is slightly smaller than, but on order of, the value 2.2 estimated for the Oregon Shelf (Dickson and Wheeler 1995). Ratios of chlorophyll to nitrate vary strongly depending on the health of the phytoplankton. Values at the peak of a bloom can be very high, with lower values especially during nitrate depletion (Parsons et al. 1984). Nutrients are initialized using sampled nitrate bottle data. The data from the bottles (0, 5, 10, and 30 m) is interpolated at 0.5 m intervals to match the grid spacing of the physical model. Nitrate concentrations between depths of 30 m and 40 m are assumed to be constant; this is consistent with observations at other stations in the Strait at which bottle samples were taken at greater depths.

Phytoplankton growth

Phytoplankton growth depends on the availability of light and nutrients and is calculated as a function of whichever is minimum. When nutrients are not limiting, phytoplankton growth depends on light availability:

$$u_c = R_{max}(T)\left[1 - \exp\left(\frac{-I_{PAR}}{0.67I_{opt}}\right)\right]\left[1.8\exp\left(\frac{-I_{PAR}}{2.7I_{opt}}\right)\right] \tag{13}$$

where I_{opt} is the optimum light intensity and $R_{max}(T)$ is the maximum growth rate. The coefficients were chosen to give a Steeles-like shape for low light (Steele 1962) and to fit experimental light curves for *Thalassiosira nordenskioldii* (Durbin 1974) at high light.

When light is not limiting, phytoplankton growth depends on nutrient availability:

$$u_n = R_{max}(T)\frac{N}{\kappa + N} \tag{14}$$

where κ is the half-saturation constant for nitrate (N).

The maximum growth value, R_{max}, for *Thalassiosira nordenskioldii* was measured as 1.4·day^{-1} and 1.0·day^{-1} at 10 °C for a 12 h light – 12 h dark cycle (Hitchcock 1980; Durbin 1974, respectively). The value used in the model (1.06·day^{-1}) was between these values. Sensitivity to this choice is discussed under model limitations in the Discussion.

Table 2. Model runs used to predict the spring blooms of 2002, 2003, 2004, and 2005 with their observed and modeled peak bloom dates.

Run	Start date	End date	Observed bloom	Modeled bloom
R1	20 September 2001	1 November 2002	1 April 2002	30 March 2002
R2	8 October 2002	1 November 2003	27–30 March 2003	27 March 2003
R3	9 October 2003	1 November 2004	17 March 2004	21 March 2004
R4	19 October 2004	1 November 2005	28 February 2005	2 March 2005

Mortality and grazing

Phytoplankton concentration decreases due to mortality and grazing. The rate of natural mortality (R_m) is taken as 0.1-day^{-1} at 10 °C (Spitz et al. 2003). Following Denman and Peña (2002), grazing is based on an annual fit to the observed dry weight of zooplankton. The dry weights used were collected as part of the STRATOGEM surveys using 236 μm mesh SCOR-type net (Sastri and Dower 2009). All tows were done during the day, so it was assumed that all zooplankton in the 100 m to surface tows could reach the euphotic zone to feed to ensure that most diel migrators were included. The 4 years of data were combined and a fit to the values (in μmol N·L^{-1}) was found:

$$\bar{Z} = Z_w + 0.525\exp\left[\frac{-(D-112)^2}{53.8^2}\right] + 0.152\exp\left[\frac{-(D-229)^2}{51.6^2}\right] + 0.0318\exp\left[\frac{-(D-316)^2}{14.6^2}\right] \quad (15)$$

where $\bar{Z}$ is the average zooplankton biomass over the model depth, Z_w is the winter concentration, and D is the day of the year. The weak fall zooplankton bloom has little impact on this study but is expected to be important in later studies considering summer and fall productivity.

Zooplankton are assumed to be able to choose their depth and thus mirror the phytoplankton concentration profile. Thus the zooplankton concentration as a function of depth is

$$Z = \bar{Z}\frac{P}{\bar{P}} \quad (16)$$

where $\bar{P}$ is the average phytoplankton concentration over the model depth.

Grazing is modeled with a hyperbolic growth function with a half-saturation constant κ_p = 1.0 μmol N·L^{-1} of phytoplankton based on observed winter concentrations of 0.5 μmol N·L^{-1} of phytoplankton (converted from total chlorophyll observations). Maximum ingestion Υ equals 0.6-day^{-1} at 10 °C (Cugier et al. 2005). The winter zooplankton concentration Z_w was the single tuned parameter. The fit gave a value of 0.073 μmol N·L^{-1}. The higher, tuned value of 0.168 μmol N·L^{-1} represents, in part, the unknown microzooplankton grazing pressure.

Temperature dependency

A temperature dependency of maximum growth rate, grazing, and mortality is implemented in the model by multiplying each by

$$\exp[\alpha_T(T - T_{ref})] \quad (17)$$

(Eppley 1972), where T_{ref} = 10 °C, α_T = 0.07·°C^{-1}, and T is modeled temperature. These functions are executed at all model depths.

An additional temperature effect is implemented only on the phytoplankton growth rate. *Thalassiosira nordenskioldii* is not observed to grow at temperatures of 18 °C and above (Durbin 1974). Thus the growth rate was multiplied by a linear decrease from one to zero as the temperature increases from 10 °C to 18 °C.

Sinking

Diatoms are negatively buoyant, particularly when nutrient-limited (Waite et al. 1992). Following Cugier et al. (2005), nutrient limitation is calculated as

$$f_N = \frac{N}{\kappa + N} \quad (18)$$

and then sinking speed is

$$w_s = W_1 f_N^{0.2} + W_2(1 - f_N^{0.2}) \quad (19)$$

where W_1 and W_2 are the sinking rates for nutrient-replete and nutrient-depleted diatoms, respectively.

Results

Physical model tuning and sensitivities

The physical model was run independently of the biological model over various time scales and compared with field data. The physical model was considered to be performing adequately when modeled physical profiles resembled observed physical profiles. To achieve this, internal mixing, vertical advection, and freshwater parameters were tuned, as described below. Profiles are generally well matched at depths below 30 m due to the bottom boundary conditions. For each run, the model was initialized with CTD data from either an October or a September cruise (Table 2) in the fall and run for one year and compared with later cruises, so that the model results could be compared with observations.

The value of the vertical advection velocity (adjusted through w_s) was set based on the analytic calculations and agrees with independent estimates in the Strait (Pawlowicz et al. 2007). It was not tuned. The amount of freshwater added to the Strait (F_w and σ_s in eq. 3) was tuned to give surface salinities that matched the empirical relationship (eq. 2*b*). The depth over which the freshwater was added (a_b in eq. 3) was tuned to give a good match between model and observed halocline depth. Most KPP parameters were set to the default values (Large et al. 1994) except the internal wave-mixing values (minimum mixing values) were in-

Fig. 5. Modeled daily-averaged mixing-layer depth (left axis, solid), daily-averaged wind magnitude cubed (right axis, shaded), and Fraser River flow (right axis, solid line) for 1 January to 1 October for each year: (*a*) 2002; (*b*) 2003; (*c*) 2004; and (*d*) 2005. Strong winds deepen the mixing-layer depth, whereas weak winds are associated with shallow mixing-layer depths. The Fraser River freshet coincides with a stable, shallow mixing-layer depth. Mixing-layer depths in January–February were deeper in 2002 (48.0 m) than in 2003 (3.11 m), 2004 (3.55 m), and 2005 (2.41 m), corresponding with stronger winds in 2002 (average wind speed cubed 340 $m^3 \cdot s^{-3}$) than in 2003 (240 $m^3 \cdot s^{-3}$), 2004 (220 $m^3 \cdot s^{-3}$), and 2005 (185 $m^3 \cdot s^{-3}$).

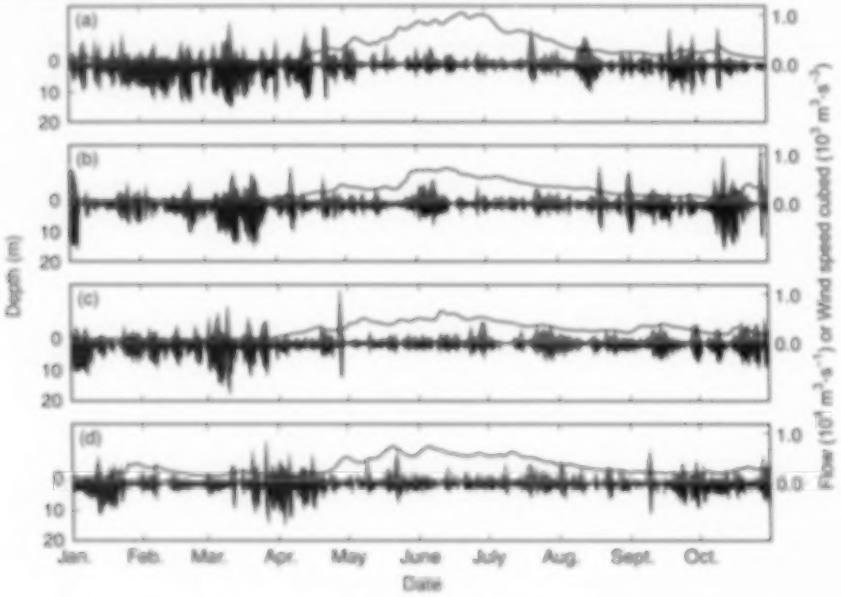

creased by 50% to reduce the strength of the model halocline, which was stronger than observed. This increase is consistent with the fact that the SoG has an active internal wave field due to strong tides over complicated topography to the north and south of the Strait (Gargett 1976). In addition, the shear diffusivity (eq. 28 in Large et al. (1994)) was slightly smoothed by adding 10% of the value above and below to 80% of the value calculated at a given depth; because the gradient Richardson number is a ratio of two differences, it is quite noisy, leading to sharp peaks and troughs in the shear diffusivity.

Physical model results

The KPP model calculates a mixing-layer depth based on a balance between kinetic energy and potential energy (Large et al. 1994). Wind is the sole mechanism through which kinetic energy is introduced into the model. The effect of wind mixing on the mixing-layer depth is expected to be proportional to the cube of wind speed (Fischer et al. 1979). A plot of KPP mixing-layer depth and wind speed cubed shows a clear relationship (Fig. 5). We see the deepest mixing-layer depths coinciding with strong winds, especially in the winter of 2002. A wind event in late August 2003 deepens the stable, shallow mixing layer from less than 1 m to greater than 10 m; the same type of event occurs in late April 2004.

The biggest source for potential energy input into the SoG is the freshwater inflow. The effect of the freshwater flux (which is proportional to the buoyancy flux) on the mixing layer is expected to be proportional to one over the flux (Fischer et al. 1979). In the model, this effect is particularly clear during the freshet when strong freshwater flux stratifies the water column and decreases the mixing-layer depth (Fig. 5). The mixing-layer depth is frequently deeper than 10 m in the fall and winter, but shallows to less than 5 m during the freshet. Wind events can disrupt the stratification produced by the layer of freshwater (late August 2003).

Model-calculated light above the surface compares well with data (Fig. 6) collected at the Halibut Bank Buoy (J. Gower, personal communication, 2005), which measures I_{PAR} at the surface. The correlation between modeled and observed surface irradiance is evidence that the estimation of light at 0 m done by the model — the cloud model and the estimation of how much of the total light is I_{PAR} — is predicting irradiance in the SoG reasonably successfully. Clouds are spatially variable over the Strait, with more clouds over land than water during certain times of the day and year and vice versa during other times. Clouds are also temporally variable. The fact that our model (based on observations at the airport) is agreeing, on average, with values from the Halibut Bank Buoy (Fig. 6) probably reflects the proximity of the airport to the Strait and the fact that prevailing winds bring air from the Strait over the airport.

The model predicts slightly warm temperature (Fig. 7*a*). Modeled and observed surface temperatures vary well together and are consistently within 1.5 °C of each other. Salinity is predicted well by the model, but less consistently than temperature (Fig. 7*a*). Modeled and observed surface salinity are, on average, within 2.1 of each other. The depth and strength of the thermocline and halocline are modeled

Fig. 6. Modeled (dotted lines) and observed (solid lines) surface irradiance for (*a*) 27 July – 5 August 2003, (*b*) 25 October – 16 November 2003; note that each panel is on a different scale: (*a*) during a relatively cloud-free period; (*b*) during cloudier conditions and showing that the model both over- and under-predicts irradiance.

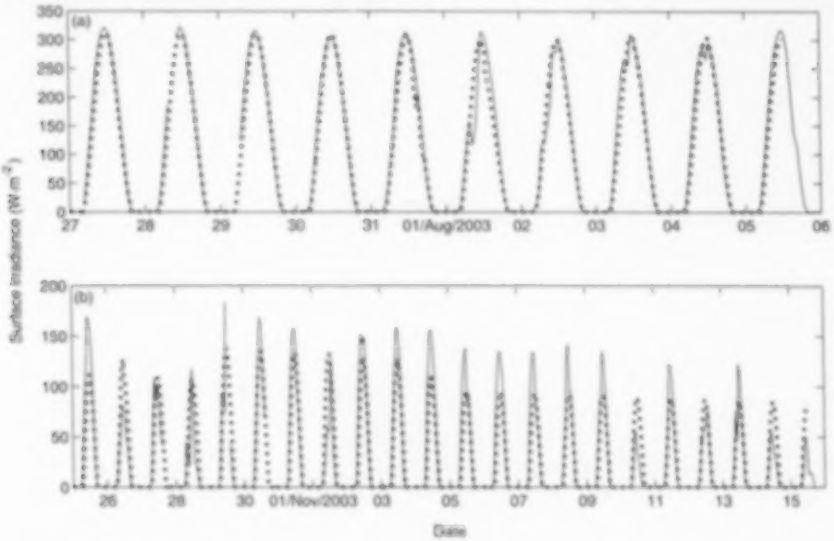

well in most cases. Irradiance profiles are generally well predicted by the model. Density is determined primarily by salinity (Fig. 7*b*). The model shows more evidence of a mixed layer than the data. As discussed above, the mixed layer is not as important as the mixing layer, and therefore more emphasis has been placed on matching the depth and strength of the halocline than the mixed-layer depth.

The model cannot include small-scale random variations that we observe in the SoG. In the example shown, the halocline is about 1 m too deep and the irradiance drops too slowly (Fig. 7). These errors are typical but not systematic; other examples show haloclines that are too shallow and irradiance that drops too fast.

Physical model performance

The manner in which the model responds to varied conditions in meteorological forcing such as high winds or increased freshwater input is a good indication of its success in modeling the physical system of the SoG. The physical model was forced with artificially high winds (low winds) and the mixing layer deepened (shallowed); tests with artificially high (low) Fraser River flow decreased (increased) surface salinity; and tests with forced clear (obscured) skies without changing air temperatures or humidity increased (decreased) water temperatures and light.

Biological model tuning and sensitivities

The SoG coupled biological–physical model was run in 13-month segments from September 2001 to November 2005; each run was initialized in September or October and run until November of the following year (Table 2). The biological model was tuned independently of the physical model. The only parameter tuned was the winter concentration of zooplankton, Z_o. For each of the four 13-month runs, surface modeled P was plotted and compared with both the high frequency ferry record of fluorescence and the discrete bottle-sampled chlorophyll (Fig. 8), and the surface-modeled N was compared with the discrete bottle-sampled nitrate (Fig. 9). The peak of the spring bloom was determined as the date of the maximum phytoplankton concentration within 4 days of the nitrate concentration going below 0.1 μmol·L^{-1}. One value for Z_o was found (Table 1) that produced optimal results for the timing of the spring bloom for the 4 years (Table 2).

The sensitivity of the modeled timing of the bloom to various parameters was determined (Table 3). The timing of the spring bloom was found to be relatively insensitive to the physical model parameters in KPP but strongly sensitive to biological parameters that affected the winter light-limited growth or the mortality. Increasing the optimal light level from 38.4 to 45 W·m^{-2} (17%) postpones the bloom an average of 26 days. Increasing the winter zooplankton concentration from 0.168 to 0.18 μmol N·L^{-1} (6%) postpones the bloom by an average of 6 days, and increasing the natural mortality from 0.1·day^{-1} to 0.11·day^{-1} (10%) postpones the bloom an average of 8 days.

The timing of the spring bloom is relatively insensitive to the initial profiles. Starting the model with a CTD–fluorescence–nitrate profile from a different year had no effect on the timing of the 2002, 2003, and 2004 spring blooms. However, the 2005 spring bloom changes by ±5 days. The 2005 bloom is sensitive to initial conditions because the winter phytoplankton concentrations remain higher than in the other years (Fig. 10) and, in particular, above the half-saturation constant for grazing. Thus, in 2005, the grazing term remains nearly linear and fall phytoplankton concentration information is transmitted through the winter.

Biological model results

The interannual variation of the arrival of the spring phy-

Fig. 7. Comparisons of model-predicted (thin lines) and observed (thick lines and points) data of physical and biological properties for 8 March 2005: (*a*) salinity (solid lines) and temperature (broken lines); (*b*) density (solid lines) and light (broken lines); (*c*) nitrate (solid line and solid circles) and chlorophyll fluorescence (broken lines, and solid diamonds are bottle-sampled chlorophyll $a > 20$ μm). Note that for nitrate there are only discrete samples and so no data line is shown.

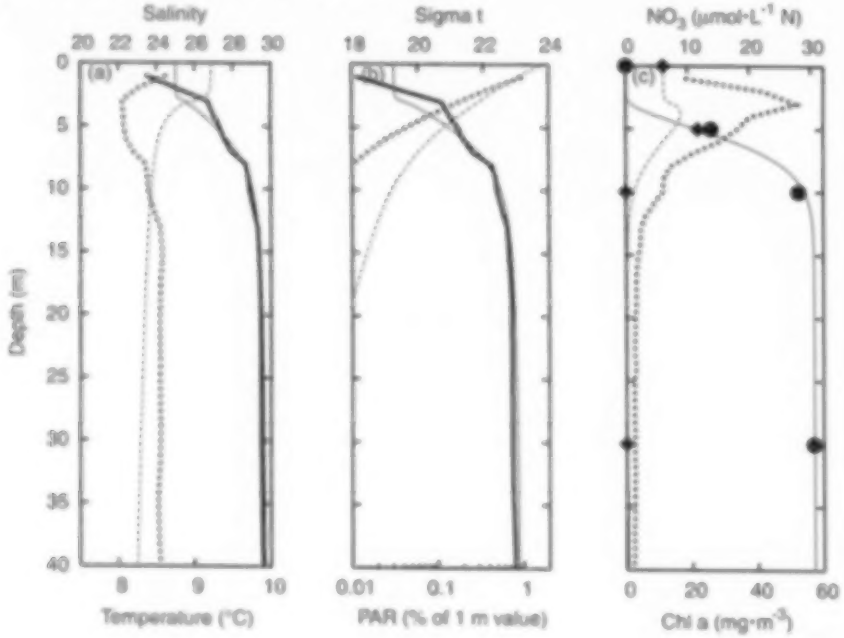

Fig. 8. Modeled surface phytoplankton (dark solid line), ferry fluorescence (shading), and bottle-sampled (>20 μm) chlorophyll (×s connected by broken line) for each year: (*a*) 2002; (*b*) 2003; (*c*) 2004; and (*d*) 2005. Ferry fluorescence absolute scale is poorly known and possibly changed between years. Vertical line marks 1 April each year.

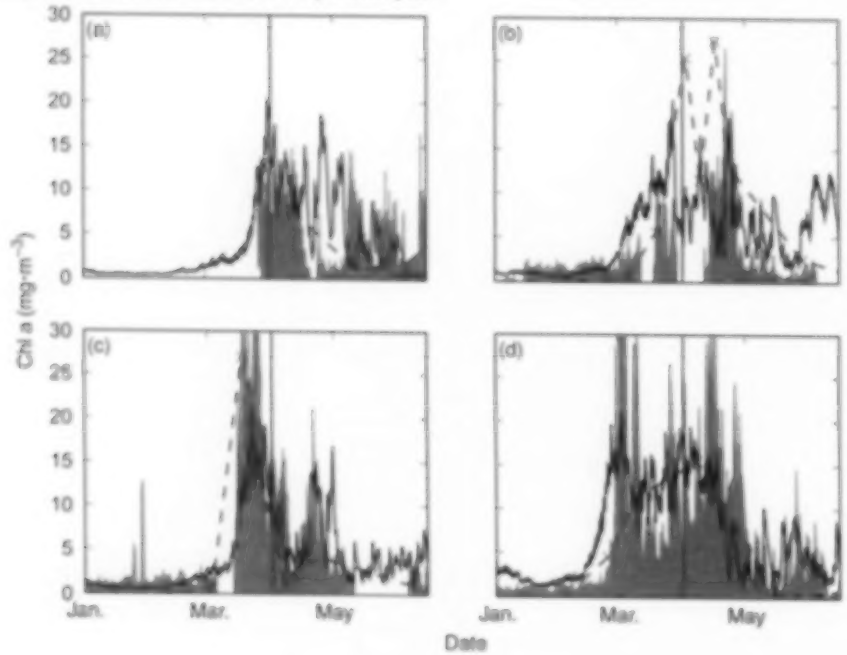

Fig. 9. Modeled surface nitrate (solid lines) and bottle-sampled nitrate (×s) for each year: (*a*) 2002; (*b*) 2003; (*c*) 2004; and (*d*) 2005.

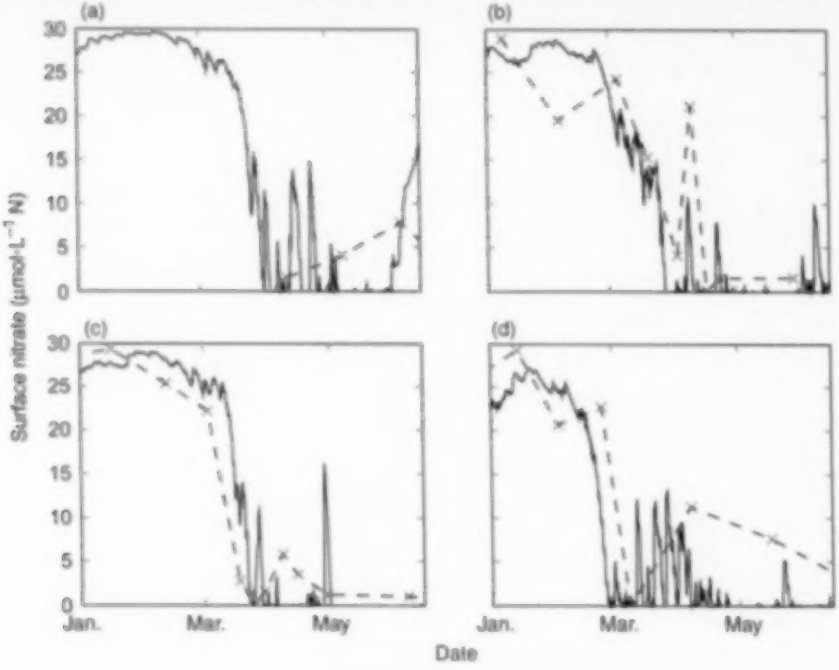

toplankton bloom is predicted successfully by the coupled biophysical model (Figs. 8 and 9). In each of the four sampled years, both the phytoplankton bloom arrival, peak, and decline and the nitrate depletion occur within 3 days of that observed in the field. Nitrate levels throughout the winter increase to levels that are seen in the field, whereas *P* decreases to low levels during the light-limited winter months.

Another measure of the success of the model is the comparison of the modeled biological parameters to the CTD observations (Fig. 7*c*). The nitrate is generally well matched at the surface and through the mixing-layer depth, and the slope of depletion with depth is well predicted (Fig. 7*c*). The model often underpredicts phytoplankton compared with observed fluorescence (CTD) because fluorescence represents all the phytoplankton in the water column and the model only includes diatoms. A better comparison tool is bottle-sampled chlorophyll in the >20 μm size class. During the spring bloom, the >20 μm size class represents 40%–60% of the total measured chlorophyll, which would account for most of the difference seen between the modelled and measured fluorscence chlorophyll values. However, even compared with the bottle-sampled chlorophyll, the magnitude of the bloom is consistently underpredicted by the model (Fig. 8). We suggest that this is due to the absence of the ammonium regeneration loop that provides an alternate food source for phytoplankton and perhaps to using too low a chlorophyll-to-nitrogen ratio for the phytoplankton.

Discussion

Interannual differences in the Strait of Georgia

Variations within the physical and biological environments over the four sampled years were significant. Wind at Sandheads was strongest for the January through March period in 2002 (mean wind speed was 5.62 $m \cdot s^{-1}$), followed closely by 2003 (5.04 $m \cdot s^{-1}$) and 2004 (5.07 $m \cdot s^{-1}$), and was significantly weaker in 2005 (3.24 $m \cdot s^{-1}$); the 30-year mean for this period is 5.16 $m \cdot s^{-1}$ (Environment Canada 2002). The Fraser River freshet was greater than the climatological mean by more than 3×10^3 $m^3 \cdot s^{-1}$ in 2002, and early 2005 flow was four times greater than mean winter flow (Environment Canada 2006); flow in 2003 and 2004 was average. In January 2005, total precipitation was 249.6 mm compared with a 30-year mean of 153.6 mm; February total precipitation was 45.8 mm compared with a 30-year mean of 123.1 mm (Environment Canada 2002). February 2005 had 139.9 h of bright sunshine, a 30-year maximum and far greater than the 30-year mean of 84.6 h (Environment Canada 2002). The arrival of the spring bloom also varied greatly over the sampling period, peaking earliest in 2005 (February 28) and latest in 2002 (April 1).

What factors control the spring bloom?

Before the spring bloom, strong wind speed cubed decreases the surface chlorophyll concentration and indeed the depth-averaged chlorophyll (not shown). As winds increase the mixing-layer depth, the phytoplankton are mixed to depths without sufficient light to grow. Almost every decrease in the time series is correlated with strong wind, and it appears that blooms are significantly delayed after winters with many strong storms. After the spring bloom, strong winds have the opposite effect; they mix nutrients into the nutrient-exhausted surface layer and increase the chlorophyll concentration.

Table 3. Sensitivity of the spring bloom date with regards to various model parameters.

Parameter	Standard value	Substituted value	Average bloom change (days)
Background momentum (scalar) mixing	1.5×10^{-4} (10^{-5}) $m^2 \cdot s^{-1}$	1.0×10^{-4} (10^{-5}) $m^2 \cdot s^{-1}$	+2.5
	1.5×10^{-4} (10^{-5}) $m^2 \cdot s^{-1}$	2.0×10^{-4} (10^{-5}) $m^2 \cdot s^{-1}$	−1
Sheer smoothing (fraction above and below)	0.1	0.15	−1.5
	0.1	0.05	+0.75
Mesozooplankton, winter concentration	0.168 μmol N·L^{-1}	0.15 μmol N·L^{-1}	−14
	0.168 μmol N·L^{-1}	0.18 μmol N·L^{-1}	+6
Mesozooplankton, summer concentration (multiplied by)	1.0	0.9	−8
	1.0	1.1	+5
Mesozooplankton, ingestion	0.6·day^{-1}	0.59·day^{-1}	−3
	0.6·day^{-1}	0.61·day^{-1}	+1.25
Mesozooplankton, half-saturation	1.0 μmol N·L^{-1}	0.75 μmol N·L^{-1}	0
	1.0 μmol N·L^{-1}	1.5 μmol N·L^{-1}	−22
Diatom, I_{opt}	38.4 W·m^{-2}	35.0 W·m^{-2}	−20
	38.4 W·m^{-2}	45.0 W·m^{-2}	+26
Diatom, maximum temperature	18 °C	15 °C	+45
	18 °C	22 °C	0
Diatom, half-saturation nitrate	1.0 μmol N·L^{-1}	0.5 μmol N·L^{-1}	0
	1.0 μmol N·L^{-1}	1.5 μmol N·L^{-1}	−0.25
Diatom, natural mortality	0.1·day^{-1}	0.086·day^{-1}	−17
	0.1·day^{-1}	0.11·day^{-1}	+8

Note: The date of the bloom is most sensitive to parameters directly affecting the light-limited winter growth (optimal light level, maximum temperature for growth (when its low)) and those directly affecting loss terms (natural mortality rate and mesozooplankton concentration, ingestion rate, and half-saturation point (when its high)).

Fig. 10. Daily-averaged wind speed cubed (left axis, shading) and modeled surface chlorophyll (right axis, solid line) for all four years: (*a*) 2002; (*b*) 2003; (*c*) 2004; and (*d*) 2005. Note that chlorophyll is on a log scale. Winds are strongest in 2002 (*a*) and weakest in 2005 (*d*); the bloom is latest in 2002 (*a*) and earliest in 2005 (*d*). (Maximum daily-averaged wind speed cubed reaches 5082 $m^3 \cdot s^{-3}$ in December 2001.)

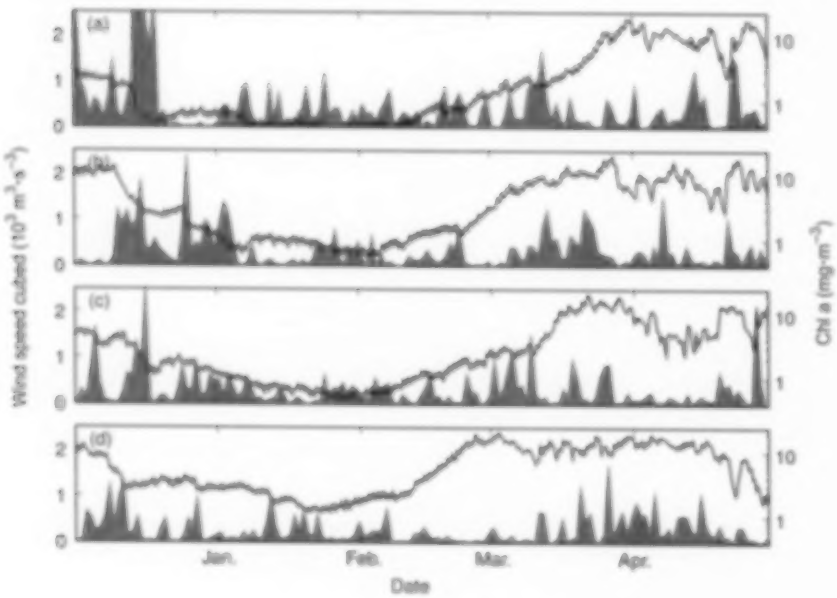

To quantify the effect of different physical forcings on the arrival time of the spring bloom, a series of 74 tests was done using various data sets. In each test, one variable (clouds, Fraser River flow, or wind) was replaced with either artificial data or data from another time period; all other variables remained constant. For example, the run "R1c00" (Table 4) was initialized in September 2001 and run until November 2002 with all data from 2001–2002 except the

Table 4. List of run tests that were done to determine the impact of the various forcing factors.

Code	Base years	Forcing varied	Value of changed forcing
R*wR1	R2, R3, R4	Wind	R1 wind
R*wR2	R1, R3, R4	Wind	R2 wind
R*wR3	R1, R2, R4	Wind	R3 wind
R*wR4	R1, R2, R3	Wind	R4 wind
R*w050	R1, R2, R3, R4	Wind	0.5*wind
R*w080	R1, R2, R3, R4	Wind	0.8*wind
R*w125	R1, R2, R3, R4	Wind	1.25*wind
R*w200	R1, R2, R3, R4	Wind	2*wind
R*cR1	R2, R3, R4	Clouds	R1 clouds
R*cR2	R1, R3, R4	Clouds	R2 clouds
R*cR3	R1, R2, R4	Clouds	R3 clouds
R*cR4	R1, R2, R3	Clouds	R4 clouds
R*c00	R1, R2, R3, R4	Clouds	None
R*c035	R1, R2, R3, R4	Clouds	0.35
R*c10	R1, R2, R3, R4	Clouds	1.0
R*fR1	R2, R3, R4	Freshwater	R1 freshwater
R*fR2	R1, R3, R4	Freshwater	R2 freshwater
R*fR3	R1, R2, R4	Freshwater	R3 freshwater
R*fR4	R1, R2, R3	Freshwater	R4 freshwater
R*f050	R1, R2, R3, R4	Freshwater	0.5*freshwater
R*f200	R1, R2, R3, R4	Freshwater	2*freshwater
R3fR4×2	R3	Freshwater	2*R4 freshwater
R4fR3/2	R4	Freshwater	0.5*R3 freshwater

Note: List of the base runs is given in Table 2. The asterisk (*) in the code is replaced by the number of the base run in column 2.

cloud data, which were set to 0 for the entire run. "R1cR2" was run for the same period, but clouds were replaced with clouds from 2003; this less extreme type of data set produced more realistic results than the data sets that were constant values.

Wind

The bloom arrival times varied significantly with different wind data sets (Fig. 11*a*) such that weak winds cause the bloom to arrive earlier than strong winds, which delay the bloom. Low wind mixing in the SoG provides the stratification necessary for a bloom to develop, whereas strong wind mixing prevents stratification. For realistic average wind speeds (>5 $m \cdot s^{-1}$ and <9 $m \cdot s^{-1}$), there is a linear relationship between wind strength and bloom arrival time (Fig. 11*a*). At both higher and lower wind speeds, the bloom date is a weaker function of wind speed. The linear relationship follows

$$\text{Year day of bloom peak} = 11.3\,\text{days} \cdot \text{m}^{-1} \cdot \text{s} \langle W^3 \rangle^{1/3} + \text{Dec. } 30 \quad (20)$$

where $\langle W^3 \rangle^{1/3}$ is the cubed root of the December to February averaged wind speed cubed. The root mean square of the residuals is 7.3 days. The fit is based on the model results (open symbols in Fig. 11); the four observations (solid symbols in Fig. 11) are within the scatter of model results and are consistent with the same slope. Runs "R1wR4", "R2wR4", and "R3wR4" were forced with 2005 wind and had bloom peak dates of more than 2 weeks earlier than "R1", "R2", and "R3". The half-wind scenarios (R*w050) caused the bloom to arrive earlier than for any other scenario in Table 4.

The historical record (1968–2006) shows variations of 6.0–8.9 $m \cdot s^{-1}$ for the cubed-root December to February averaged cubed wind speed. This would correspond to a variation in spring bloom timing of 33 days due to the wind alone.

Cloud cover

Variations in cloud cover have a weaker effect on the timing of the spring bloom (Fig. 11*b*). When the model is tested with clouds from different years, the bloom peak dates are all within 10 days of each other. However, including no clouds and full cloud cover, a strong trend is evident with more clouds delaying the bloom. The curve is less steep than that for wind, suggesting that wind controls the timing of the bloom with light having a secondary effect.

The historical record (1968–2006) shows variations of 0.60 to 0.85 for the December to February averaged cloud fraction. Given the slope implied here (about 60 days), the historical variation due to cloud fraction would be about 15 days or half that due to the wind speed.

Fraser River flow

Variations in Fraser River flow do not cause a consistent pattern in bloom arrival time (Fig. 11*c*). There is a tendency for high freshwater flow to move the bloom earlier; stronger stratification leads to both a shallower mixing layer and weaker estuarine advection. Also, following any particular run, at low freshwater flow, there is also a tendency to move the bloom earlier; this is probably the response to weaker advection that occurs if the freshwater flow, and thus the estuarine circulation, is weaker. Note that the freshwater flux has a much more direct impact on the stratifica-

Fig. 11. Results of model testing gave different bloom arrival dates for different wind (cubed root of the average December to February wind speed cubed), cloud patterns (average cloud fraction from December to January), and freshwater flow (average effective total freshwater (eq. 2*a*) from December to January). Solid symbols represent actual peak bloom. Open squares, circles, upward triangles, and downward triangles represent R1, R2, R3, and R4 runs, respectively. As wind magnitude increases, the arrival date of the bloom is later; this relationship is strong. Cloud fraction plays a secondary role in the timing of the bloom. There is no clear relationship between date of bloom peak and river flow.

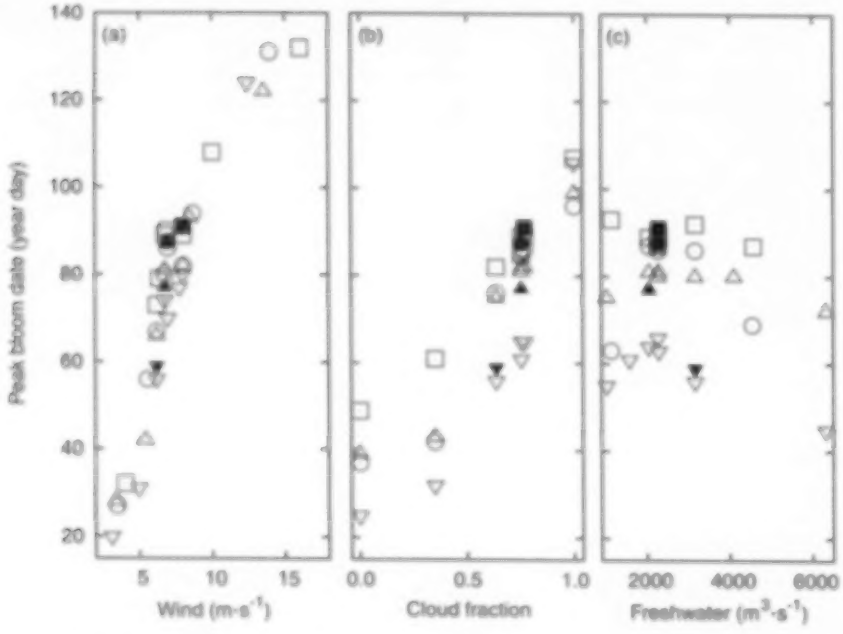

tion, as can be seen by the small mixing-layer depth during the freshet, than it does on the spring bloom timing. For winter–spring phytoplankton in the SoG, the estuarine advection term (a loss term) is as important as the freshwater-induced reduction in mixing-layer depth (which impacts the light levels for the phytoplankton and thus the growth term).

Empirical fit

A linear fit on the cubed root of the average wind speed cubed is a good representation of the bloom date for the runs with wind manipulated. Here we estimate an empirical fit for all the runs in Table 4. The shape of the bloom peak date versus wind strength (Fig. 11*a*) for all winds suggests a decreasing slope at high winds and low winds $A_1\omega^2/(A_2^2+\omega^2)$, where $\omega = \langle W^3 \rangle^{1/3}$ is the cubed root of the mean cubed wind speed and A_1 and A_2 are constants. The bloom date increases with cloud fraction $A_3c_f^2$, where A_3 is another constant and c_f is the cloud fraction. In both cases, the parameters squared gave a better fit than without squaring. Following the structure of the estuarine vertical advection with total freshwater flow, we implement the effect of the freshwater with $A_4(Q_T/\overline{Q})\exp(-Q_T/\overline{Q})$. This gives

$$\text{(21)}\qquad \text{Year day of bloom peak} = \frac{A_1\omega^2}{A_2^2+\omega^2} + A_3c_f^2 + A_4(Q_T/\overline{Q})\exp(-Q_T/\overline{Q}) + A_5$$

where A_5 is another constant. A multiple least squares fit gives

Fig. 12. Comparison of bloom arrival date predicted by eq. 21 with dates predicted from model testing with different cloud, wind, and Fraser River scenarios. Thin lines are ±7 days; plus signs (+) are model results, and solid circles are the observations.

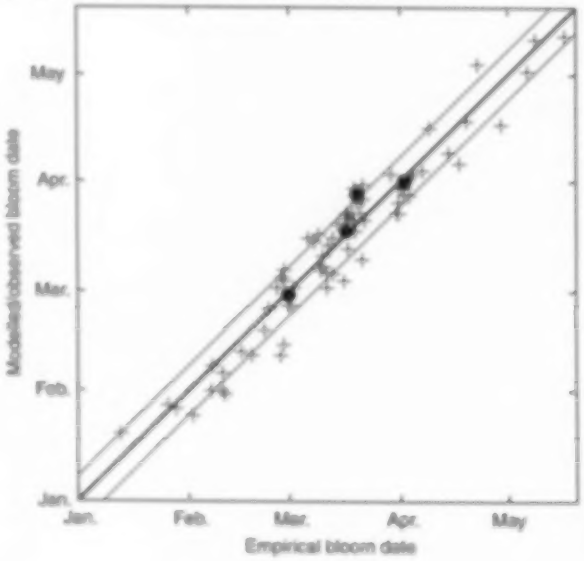

(22) $A_1 = 167$ days, $A_2 = 6.85\ \mathrm{m \cdot s^{-1}}$, $A_3 = 66.0$ days, $A_4 = 34.7$ days, $A_5 = -54.8$ days

with a root mean square of the residuals of 6.6 days (Fig. 12). The empirical fit implies a variation of peak bloom date of 21 days due to the winds, 11 days due to the clouds, and 1.5 days due to the freshwater, over the observed 2002–2005 range of these parameters.

Model limitations

Each parametrization in the physical model for the SoG has inherent limitations. The freshwater flux parametrization was extensive and based on innovative methods and a wide range of data. The surface salinity in the model is calculated based on a regression of daily flow estimates and matched to the 15 min model time step in a smoothing procedure; freshwater flux calculations depend on this value. All these steps introduce the possibility of error and inaccuracy, but well-modeled salinity implies that error introduced by these parametrizations is small.

Uncertainty in the calculation for I_{PAR} is derived from the multivariable nature of the attenuation coefficient (eq. 8). One of these variables is calculated by the model and thus depends on another set of variables and equations and associated uncertainty. The total light scheme depends on eqs. 8, 9*a*, and 9*b*), of which the latter two are based on data from Jerlov (1976).

A diverse biological community inhabits the SoG, including many different sizes and species of both phytoplankton and zooplankton, and a complex regeneration cycle (R. Pawlowicz, A.R. Sastri, S.E. Allen, D. Cassis, O. Riche, M. Halverson, R. El-Sabaawi, and J.F. Dower, unpublished data). Although the biological model includes only one phytoplankton group and one nutrient source, results show that these parameters, arguably the most important in terms of spring bloom development, are adequate to predict interannual variability in the timing of the spring bloom. The growth rate was chosen to lie between published *Thalassiosira* spp. growth rates. To look at the sensitivity of that choice, we also considered growth rates of 1.8-day^{-1}and 2.6-day^{-1} (24 h at 10 °C). For each growth rate, we re-tuned the model by changing the winter zooplankton biomass (to 0.056 μmol N·L^{-1} and 0.287 μmol N·L^{-1}, respectively) and re-ran a subset of the test runs. Then we re-fit the empirical relation between the winds, cloud fraction, freshwater, and the predicted bloom date. For cubed-root of average wind speeds cubed below 8 m·s^{-1}, the results were within 7 days of the base case. For greater wind speeds, lower growth rates predict later blooms than do higher growth rates. The changes in growth rate chosen were large, about ±20%. Even with these changes, only the magnitude of the dependence on the wind and cloud fraction change.

As temperature in the SoG is not important to the stratification, the systematic slightly warm temperatures in the model mainly impact the results through the temperature dependence on growth, mortality, and grazing. Thus the temperature error has an equivalent effect as a change in the biological parameters much smaller than the change in growth rate discussed above.

If we wish to use the model in a predictive mode, we must be conscious of the large sensitivity of the model (and probably the real spring bloom) to the biological parameters and whether these values may change. The largest possible changes would come either from a change in phytoplankton community and thus in growth rate and optimal light levels or from a change in number or species of overwintering zooplankton. If significant shifts occur in either of these communities, the model will not be able to predict the shift in the timing of spring bloom.

Thus the model is not sensitive to the choice of parameters if we re-tune it. The result that the timing of the spring bloom is primarily dependent on the wind speed and secondarily on the cloud fraction is robust to large changes in the parameters. However, shifts in either growth rate or loss parameters that are not balanced will cause "biological" shifts in the timing of the spring bloom that are not dependent on the physical forcings.

Comparison with other results

Previous research on bloom dynamics in the SoG suggests that a stratified water column is necessary for a bloom to occur and that this stratification is achieved by freshwater input and destroyed by winds greater than 4 m·s^{-1} (Yin et al. 1997*b*). Yin et al. (1997*b*) further assert that the bloom will not fully develop until the freshwater discharge is strong enough to overcome wind and tidal mixing and that the bloom arrival is dependent on the freshet arrival (Yin et al. 1996). This theory is not supported by the results presented here, which show that the freshwater flux has no consistent effect on the bloom arrival time (Fig. 11*b*). The relationship between wind and bloom arrival time discussed here agrees with Yin's claim that wind can delay the bloom (Yin et al. 1997*b*). These previous results were based on cruises during 1991, which had a winter (December–February) with similar winds and clouds to 2003 or 2004 but high freshwater flux similar to 2005.

A coupled physical and biological two-layer box model found that plankton populations were insensitive to interannual changes in estuarine circulation caused by variability in Fraser River discharge (Li et al. 2000), a result that agrees with our research. Li et al. (2000) did not explicitly test the model's sensitivity to wind or changes in light availability but suggested that variations in biological parameters could cause interannual timing variations. We would propose that this variability is primarily due to variations in light intensity due to wind mixing or clouds that were not explicitly modeled in Li's study.

A number of models aiming to investigate dependence of the interannual variability in the timing of the spring bloom on the physical environment exist, with varying degrees of similarity to this study. These models are often 1D physical models, whereas biological models range in their complexity. Unlike Prince William Sound and the Bering Sea, the SoG stratification is dominated by salinity variations due to strong freshwater runoff. However, as in Prince William Sound (Eslinger et al. 2001) and the Bering Sea (Jin et al. 2006), we have shown that in the SoG, the dominant influence on the timing of the spring bloom is interannual variations in the wind. On the other hand, a study in an estuary off the UK coast using linear and stepwise regression analyses between chlorophyll *a* concentration and each of mean water column I_{PAR}, river flow, tidal range, and wind speed

found no clear relationship between wind speed and the timing of the spring bloom (Iriarte and Purdie 2004). The authors concluded that the main factor controlling the timing of the bloom in this location is irradiance. Similarly, results from a 1D NPZD model coupled to the finite volume coastal ocean model (FVCOM) showed that over the shallow, well-mixed region of George's Bank, the timing of the bloom depends on light intensity and attenuation (Ji et al. 2006). These results are not surprising as mixing is dominated by tides not winds for both these regions.

Implications

The results for the SoG on the timing of the spring bloom have implications for other regions. First, in regions with strong buoyancy fluxes, the mixing layer may exceed the depth of the mixed layer and thus blooms may not occur even if the Sverdrup critical depth exceeds the mixed-layer depth. Second, in estuaries or other regions with estuarine circulation, the freshwater flux has two opposing effects on the timing of the spring bloom. Increased freshwater flux increases the stratification and thus increases the phytoplankton growth rate but increased freshwater flux also increases estuarine circulation and thus increases the phytoplankton loss rate. Third, considering the results from other regions described above, in regions where wind mixing dominates over tidal mixing, interannual variations in the wind speed will have a significant effect on the interannual variation of the timing of the spring bloom.

The major result of this study is that the spring bloom in the Strait of Georgia is controlled primarily by the wind, with high winds causing a late bloom and weak winds causing an early bloom, and secondarily by the amount of cloud. Edwards and Richardson (2004) assert that changes in the synchrony of timing between primary, secondary, and tertiary production affects marine trophodynamics, including commercially important fish stocks. Mean spring wind speed has decreased over the last 35 years in the Strait of Georgia, but wind forecasts for this region range from rising temperatures leading to reduced global wind fields to rising temperatures leading to increased local wind (Boesch et al. 2000). Although the wind forecast is unclear, this study implies that as wind patterns change, we can expect a change in spring bloom timing, with subsequent effects carrying through to the upper trophic levels.

Acknowledgments

John Gower of Fisheries and Oceans Canada provided the 2001–2005 irradiance at Halibut Bank Buoy data and Rick Ketler of UBC Department of Agroecology provided the 2001–2005 solar radiation data. Kira Jang did the sensitivity studies. Doug Latornell made the model more efficient and prepared a number of the figures. The excellent data set used in this study would not have been collected without the efforts of the crew of the CGS *Siyay* and the many scientists who participated in the cruises. The ferry data were collected from BC Ferries, primarily the *Queen of New Westminster*. The manuscript was significantly improved based on comments from three anonymous reviewers. The second author would like to thank Alain Ménesguen for his useful suggestions and hospitality while she was on sabbatical at IFREMER.

References

Batchelor, G.K. 1967. An introduction to fluid dynamics. Cambridge University Press, Cambridge, UK.

Beamish, R.J., Benson, A.J., Sweeting, R.M., and Neville, C.M. 2004. Regimes and the history of the major fisheries off Canada's west coast. Prog. Oceanogr. **60**(2–4): 355–385. doi:10.1016/j.pocean.2004.02.009.

Boesch, D.F., Field, J.C., and Scavia, D. (*Editors*). 2000. The potential consequences of climate variability and change on coastal areas and marine resources. NOAA Center for Sponsored Coastal Ocean Research, Silver Spring, Maryland. Decision Analysis Series No. 21.

Campin, J.M., Marshall, J., and Ferreira, D. 2008. Sea ice–ocean coupling using a rescaled vertical coordinate z^*. Ocean Model. **24**(1–2): 1–14. doi:10.1016/j.ocemod.2008.05.005.

Chassignet, E.P., Smith, L.T., Halliwell, G.R., and Bleck, R. 2003. North Atlantic simulation with the HYbrid Coordinate Ocean Model (HYCOM): impact of the vertical coordinate choice, reference density, and thermobaricity. J. Phys. Oceanogr. **33**(12): 2504–2526. doi:10.1175/1520-0485(2003)033<2504:NASWTH>2.0.CO;2.

Cugier, P., Ménesguen, A., and Guillaud, J.F. 2005. Three-dimensional (3D) ecological modelling of the Bay of Seine (English Channel, France). J. Sea Res. **54**(1): 104–124. doi:10.1016/j.seares.2005.02.009.

Denman, K.L., and Peña, M.A. 2002. The response of two coupled one-dimensional mixed layer/planktonic ecosystem models to climate change in the NE subarctic Pacific Ocean. Deep Sea Res. Part II Top. Stud. Oceanogr. **49**(24-25): 5739–5757. doi:10.1016/S0967-0645(02)00212-6.

Dickson, M.-L., and Wheeler, P.A. 1995. Nitrate uptake rates in a coastal upwelling regime: a comparison of PN-specific, absolute, and chl *a*-specific rates. Limnol. Oceanogr. **40**: 533–543.

Dobson, F.W., and Smith, S.D. 1988. Bulk models of solar radiation at sea. Q. J. R. Meteorol. Soc. **114**: 165–182.

Durbin, E.G. 1974. Studies on the autecology of the marine diatom *Thalassiosira nordenskioldii* cleve. 1. The influence of day-length, light intensity, and temperature on growth. J. Phycol. **10**: 220–225.

Durski, S.M., Glenn, S.M., and Haidvogel, D.B. 2004. Vertical mixing schemes in the coastal ocean: comparison of the level 2.5 Mellor–Yamada scheme with an enhanced version of the K profile parameterization. J. Geophys. Res. **109**(C1): C01015. doi:10.1029/2002JC001702.

Edwards, M., and Richardson, A.J. 2004. Impact of climate change on marine pelagic phenology and trophic mismatch. Nature (London), **430**(7002): 881–884. doi:10.1038/nature02808. PMID:15318219.

El-Sabaawi, R., Dower, J.F., Kainz, M., and Mazumder, A. 2009. Interannual variability in fatty acid composition of the copepod *Neocalanus plumchrus* in the Strait of Georgia, British Columbia. Mar. Ecol. Prog. Ser. **382**: 151–161. doi:10.3354/meps07915.

Environment Canada. 2002. Climate database [online]. Available at http://www.climate.weatheroffice.ec.gc.ca/climateData/canada_e.html.

Environment Canada. 2006. Hydrometric data [online]. Available at http://www.wsc.ec.gc.ca/.

Eppley, R.W. 1972. Temperature and phytoplankton growth in the sea. Fish. Bull. (Washington, D.C.), **70**(4): 1063–1081.

Erga, S.R., and Heimdal, B.R. 1984. Ecological studies on the phytoplankton of Korsfjorden, western Norway. The dynamics of a spring bloom seen in relation to hydrographical conditions and light regime. J. Plankton Res. **6**(1): 67–90. doi:10.1093/plankt/6.1.67.

Eslinger, D.L., Cooney, R.T., McRoy, C.P., Ward, A., Kline, T.C., Jr., Simpson, E.P., Wang, J., and Allen, J.R. 2001. Plankton dynamics: observed and modelled response to physical conditions in Prince William Sound, Alaska. Fish. Oceanogr. **10**(Suppl. 1): 81–96. doi:10.1046/j.1054-6006.2001.00036.x.

Falkowski, P.G. 1975. Nitrate uptake in marine phytoplankton: comparison of half-saturation constants from seven species. Limnol. Oceanogr. **20**(3): 412–417.

Fasham, M.J.R., Ducklow, H.W., and McKelvie, S.M. 1990. A nitrogen-based model of plankton dynamics in the oceanic mixed layer. J. Mar. Res. **48**: 591–639.

Fischer, H.B., List, E.J., Koh, R.C.Y., Imberger, J., and Brooks, N.H. 1979. Mixing in inland and coastal waters. Academic Press, San Diego, California.

Friedrichs, M.A.M., Hood, R.R., and Wiggert, J.D. 2006. Ecosystem model complexity versus physical forcing: quantification of their relative impact with assimilated Arabian Sea data. Deep Sea Res. Part II Top. Stud. Oceanogr. **53**(5-7): 576–600. doi:10.1016/j.dsr2.2006.01.026.

Gargett, A.E. 1976. Generation of internal waves in the Strait of Georgia, British Columbia. Deep-Sea Res. **23**: 17–20.

Harrison, P.J., Fulton, J.D., Taylor, F.J.R., and Parsons, T.R. 1983. Review of the biological oceanography of the Strait of Georgia: pelagic environment. Can. J. Fish. Aquat. Sci. **40**(7): 1064–1094. doi:10.1139/f83-129.

Herlinveaux, R.H., and Tully, J.P. 1961. Some oceanographic features of the Juan de Fuca Strait. J. Fish. Res. Board Can. **18**: 1027–1071.

Hetland, R.D., and MacDonald, D.G. 2008. Spreading in the near-field Merrimack River plume. Ocean Model. **21**(1–2): 12–21. doi:10.1016/j.ocemod.2007.11.001.

Hitchcock, G.L. 1980. Influence of temperature on the growth rate of *Skeletonema costatum* in response to variations in daily light intensity. Mar. Biol. (Berl.). **57**(4): 261–269. doi:10.1007/BF00387569.

Hobson, L.A., and McQuoid, M.R. 1997. Temporal variations among planktonic diatom assemblages in a turbulent environment of the southern Strait of Georgia, British Columbia, Canada. Mar. Ecol. Prog. Ser. **150**: 263–274. doi:10.3354/meps150263.

Huisman, J., van Oostveen, P., and Weissing, F.J. 1999. Critical depth and critical turbulence: two different mechanisms for the development of phytoplankton blooms. Limnol. Oceanogr. **44**: 1781–1787.

Iriarte, A., and Purdie, D.A. 2004. Factors controlling the timing of major spring bloom events in an UK south coast estuary. Estuar. Coast. Shelf Sci. **61**(4): 679–690. doi:10.1016/j.ecss.2004.08.002.

Jeffery, N. 2002. Modelling a phytoplankton dichotomy in the eastern subarctic Pacific: impact of atmospheric variability, iron surface flux, and life cycle dynamics of the calanoid copepods, *Neocalanus* spp. Ph.D. thesis, University of British Columbia, Vancouver, British Columbia.

Jerlov, N.G. 1976. Marine optics. Vol. 14. Elsevier Oceanography Series, Elsevier Scientific Publishing Company, New York.

Ji, R.B., Chen, C.S., Franks, P.J.S., Townsend, D.W., Durbin, E.G., Beardsley, R.C., Lough, R.G., and Houghton, R.W. 2006. Spring phytoplankton bloom and associated lower trophic level food web dynamics on Georges Bank: 1-D and 2-D model studies. Deep Sea Res. Part II Top. Stud. Oceanogr. **53**(23-24): 2656–2683. doi:10.1016/j.dsr2.2006.08.008.

Jin, Z., Charlock, T.P., Smith, W.L., and Rutledge, K. 2004. A parameterization of ocean surface albedo. Geophys. Res. Lett. **31**(22): L22301. doi:10.1029/2004GL021180.

Jin, M., Deal, C.J., Wang, J., Tanaka, N., and Ikeda, M. 2006. Vertical mixing effects on the phytoplankton bloom in the southeastern Bering Sea mid-shelf. J. Geophys. Res. **111**(C3): C03002. doi:10.1029/2005JC002994.

Kettle, A.J. 2005. Comparison of the nonlocal transport characteristics of a series of one-dimensional oceanic boundary layer models. Ocean Model. **8**(4): 301–336. doi:10.1016/j.ocemod.2004.01.002.

Koburi, T., and Ikeda, T. 2001. Ontogenetic vertical migration and life cycle of *Neocalanus plumchrus* (Crustacea: Copepoda) in the Oyashio Region, with notes on regional variations in body sizes. J. Plankton Res. **23**(3): 287–302. doi:10.1093/plankt/23.3.287.

Large, W.G., and Pond, S. 1982. Sensible and latent heat flux measurements over the ocean. J. Phys. Oceanogr. **12**(5): 464–482. doi:10.1175/1520-0485(1982)012<0464:SALHFM>2.0.CO;2.

Large, W.G., McWilliams, J.C., and Doney, S.C. 1994. Oceanic vertical mixing: a review and a model with a nonlocal boundary layer parameterization. Rev. Geophys. **32**(4): 363–403. doi:10.1029/94RG01872.

Li, M., Gargett, A., and Denman, K. 2000. What determines seasonal and interannual variability of phytoplankton and zooplankton in strongly estuarine systems? Application to the semi-enclosed estuary of Strait of Georgia and Juan de Fuca Strait. Estuar. Coast. Shelf Sci. **50**: 467–488. doi:10.1006/ecss.2000.0593.

MacDonald, D.G., and Geyer, W.R. 2004. Turbulent energy production and entrainment at a highly stratified estuarine front. J. Geophys. Res. **109**(C5): C05004. doi:10.1029/2003JC002094.

Mackas, D.L., and Harrison, P.J. 1997. Nitrogenous nutrient sources and sinks in the Juan de Fuca Strait/Strait of Georgia/Puget Sound estuarine system: assessing the potential for eutrophication. Estuar. Coast. Shelf Sci. **44**(1): 1–21. doi:10.1006/ecss.1996.0110.

Masson, D., and Cummins, P.F. 2004. Observations and modeling of seasonal variability in the Straits of Georgia and Juan de Fuca. J. Mar. Res. **62**(4): 491–516. doi:10.1357/0022240041850075.

Ménesguen, A., Guillard, J.F., Aminot, A., and Hoch, T. 1995. Modeling the eutrophication process in a river plume — the Seine case-study (France). Ophelia, **42**: 206–225.

Parsons, T.R., Takahashi, M., and Hargrave, B. 1984. Biological oceanographic processes. Pergamon Press, New York.

Pawlowicz, R., Riche, O., and Halverson, M. 2007. The circulation and residence time of the Strait of Georgia using a simple mixing-box approach. Atmos.-ocean, **45**(4): 173–193. doi:10.3137/ao.450401.

Sastri, A.R., and Dower, J.F. 2009. Interannual variability in chitobiase-based production rates of the crustacean zooplankton community in the Strait of Georgia, British Columbia, Canada. Mar. Ecol. Prog. Ser. In press.

Spitz, Y.H., Newberger, P.A., and Allen, J.S. 2003. Ecosystem response to upwelling off the Oregon coast: behavior of three nitrogen-based models. J. Geophys. Res. **108**(C3): C03062. doi:10.1029/2001JC001181.

St. John, M.A., Marinone, S.G., Stronach, J., Harrison, P.J., Fyfe, J., and Beamish, R.J. 1993. A horizontally resolving physical–biological model of nitrate concentration and primary productivity in the Strait of Georgia. Can. J. Fish. Aquat. Sci. **50**: 1456–1466. doi:10.1139/f93-166.

Steele, J.H. 1962. Environmental control of photosynthesis in the sea. Limnol. Oceanogr. **7**: 137–150.

Sverdrup, H.U. 1953. On conditions for the vernal blooming of phytoplankton. J. Cons. Cons. Int. Explor. Mer, **18**: 287–295.

Thomson, R.E. 1994. Physical oceanography of the Strait of Geor-

gia – Puget Sound – Juan de Fuca Strait system. *In* Review of the marine environment and biota of the Strait of Georgia, Puget Sound, and Juan de Fuca Strait. *Edited by* R.C.H. Wilson, R.J. Beamish, F. Aitkens, and J. Bell. Can. Tech. Rep. Fish. Aquatic Sci. No. 1948. pp. 36–100.

Waite, A., Bienfang, P.K., and Harrison, P.J. 1992. Spring bloom sedimentation in a sub-arctic ecosystem. 1. Nutrient sensitivity. Mar. Biol. (Berl.). **114**: 119–129.

Yin, K., Harrison, P.J., Goldblatt, R.H., and Beamish, R.J. 1996. Spring bloom in the central Strait of Georgia: interactions of river discharge, winds and grazing. Mar. Ecol. Prog. Ser. **138**: 255–263. doi:10.3354/meps138255.

Yin, K., Goldblatt, R.H., Harrison, P.J., St. John, M.A., Clifford, P.J., and Beamish, R.J. 1997*a*. Importance of wind and river discharge in influencing nutrient dynamics and phytoplankton production in summer in the central Strait of Georgia. Mar. Ecol. Prog. Ser. **161**: 173–183. doi:10.3354/meps161173.

Yin, K., Harrison, P.J., Goldblatt, R.H., St. John, M.A., and Beamish, R.J. 1997*b*. Factors controlling the timing of the spring bloom in the Strait of Georgia estuary, British Columbia, Canada. Can. J. Fish. Aquat. Sci. **54**: 1985–1995. doi:10.1139/cjfas-54-9-1985.

Appendix A

The 46 CTD profiles from each of stations S2-2 and S3 (Fig. 1) from the surface to depth $D = -40$ m were fitted to similarity solution (see Batchelor 1967) for the cumulative freshwater, where the cumulative freshwater is defined as

$$(A1) \qquad F_{cum}(z) = \int_D (S_D - S)\,dz'$$

where $S_D = 30$ is the deep-water salinity, $S(z)$ is the salinity at depth z, and z is the vertical distance measured upward from the sea surface so that all values of z are negative. The similarity solution has two parameters: F, the surface value of the cumulative freshwater, and d, the depth at which F_{cum} is 67% of the surface value. Each of the two parameters was fitted to the data assuming a separable fit to the total freshwater Q_T and the distance r from the mouth of the Fraser River (taken here to be Sandheads). That the cumulative freshwater fit has the same form at stations S2-2 and S3 supports this relationship. So

$$(A2a) \qquad F_{cum} = F\mathcal{F}\left(\frac{z}{d}\right)$$

$$(A2b) \qquad F = F_*\mathcal{F}_r\left(\frac{r}{r_3}\right)\mathcal{F}_T\left(\frac{Q_T}{\bar{Q}_T}\right)$$

$$(A2c) \qquad d = d_*\mathcal{D}_r\left(\frac{r}{r_3}\right)\mathcal{D}_T\left(\frac{Q_T}{\bar{Q}_T}\right)$$

where $F_* = 57.6$ m, $r_3 = 21.4$ km is the distance to station S3, $\bar{Q}_T = 3231$ m^3·s^{-1} is the mean total freshwater, $d_* = 11.7$ m, and $\mathcal{F}$ is a fitted polynomial function from the surface to the bottom of the plume at $2.5d$.

Consider quasi-steady Knudsen relations for conservation of mass and salt from the river mouth to some position r where we assume that the plume spreads as r^β with $\beta = 1.2$ (following Hetland and MacDonald 2008) and forms a fraction $c \approx 1/3$ of a circle at station S3. Then

$$(A3) \qquad S_D Q_T = 2\pi c r \int_{2.5d}^{0} V(S_D - S)\,dz$$

where V is the radial velocity, also assumed to be a separable function of Q_T and r. Balancing the variation with respect to Q_T on the two sides of eq. A3 gives

$$(A4) \qquad V \propto \frac{Q_T}{\mathcal{F}_T}$$

and from conservation of mass, the upwelling velocity must be

$$(A5) \qquad w \propto \frac{Q_T \mathcal{D}_T}{\mathcal{F}_T}$$

Fitting $\mathcal{D}_T/\mathcal{F}_T$ to Q_T gives the second term in eq. 4.

Assuming that the pressure is hydrostatic and that pressure gradients are small at depth, the pressure gradient directed away from the mouth of the river can be directly calculated from the cumulative freshwater. This pressure gradient is large enough that it can be balanced only by turbulent momentum mixing. We assume a parabolic eddy viscosity profile, consistent with the KPP eddy viscosity profile and with observations near the mouth of the Fraser River (MacDonald and Geyer 2004). For mean river flow and at station S3, we assume a minimum eddy viscosity at the surface and at $2.5d$ of 8×10^{-4} m^2·s^{-1} and a maximum (at $1.25d$) of 4 to 6.5×10^{-3} m^2·s^{-1}. From this balance and estimating the spatial derivatives using differences between stations S2-2 and S3, the vertical profile of the horizontal velocity can be found. Conservation of mass then gives the vertical profile of the vertical velocity, which fits closely to the third term in eq. 4.

The value for w_* was found using eq. A3, estimating the integral using the vertical profile found from the pressure–turbulent mixing balance, taking $c = 1/3$ and, because the absolute value of the freshwater flux was needed, correcting Q_T for flow into the Fraser River after Hope (a factor of 1.66; Pawlowicz et al. 2007).

References

Batchelor, G.K. 1967. An introduction to fluid dynamics. Cambridge University Press, Cambridge, UK.

Hetland, R.D., and MacDonald, D.G. 2008. Spreading in the near-field Merrimack River plume. Ocean Model. **21**(1-2): 12–21. doi:10.1016/j.ocemod.2007.11.001.

MacDonald, D.G., and Geyer, W.R. 2004. Turbulent energy production and entrainment at a highly stratified estuarine front. J. Geophys. Res. **109**(C5): C05004. doi:10.1029/2003JC002094.

Pawlowicz, R., Riche, O., and Halverson, M. 2007. The circulation and residence time of the Strait of Georgia using a simple mixing-box approach. Atmos.-ocean, **45**(4): 173–193. doi:10.3137/ao.450401.

How different is different? Defining management and conservation units for a problematic exploited species

Andrea M. Bernard, Moira M. Ferguson, David L.G. Noakes, Bruce J. Morrison, and Chris C. Wilson

Abstract: Discontinuous genetic structure is widely used to delineate local, regional, and phylogenetic groups within species for conservation and management purposes. We used microsatellite markers to assess the genetic distinctiveness of putative stocks and populations of lake whitefish (*Coregonus clupeaformis*) in Ontario waters. Analysis of spawning aggregations in eastern Lake Ontario showed fish from Chaumont Bay, New York, to be weakly differentiated from spawning whitefish in and near the Bay of Quinte, Ontario. No significant differences were found between lake- and bay-spawning aggregations within the Bay of Quinte. These same genetic tools were used to test the distinctiveness and evolutionary significance of Lake Simcoe lake whitefish as a designatable unit (DU) under guidelines established by the Committee on the Status of Endangered Wildlife in Canada (COSEWIC). Although there was marked differentiation among populations from across Ontario, the Lake Simcoe population was closely allied with lake whitefish populations from Lake Ontario and Lake Huron, suggesting that a distinct status is not warranted on genetic grounds. This work demonstrates how assessing hierarchical diversity under COSEWIC's framework can provide key information of the status of exploited populations for fishery management.

Résumé : Les structures génétiques discontinues servent couramment à délimiter les groupes locaux, régionaux et phylogénétiques au sein des espèces pour des fins de conservation et de gestion. Nous utilisons des marqueurs microsatellites afin d'évaluer le caractère distinctif de stocks présumés et de populations de grands corégones (*Coregonus clupeaformis*) dans les eaux ontariennes. Une analyse des rassemblements de fraie dans l'est du lac Ontario indique que les poissons de Chaumont Bay, New York, sont faiblement différenciés des corégones qui frayent dans la baie de Quinte, Ontario, et les environs. Au sein de la baie de Quinte, il n'y a pas de différence significative entre les rassemblements qui frayent dans le lac et ceux qui le font dans la baie. Les mêmes outils ont servi à tester le caractère distinctif et l'importance évolutive des grands corégones du lac Simcoe en tant qu'unité désignable (DU) selon les principes établis par le Comité sur situation des espèces en péril au Canada (COSEPAC). Bien qu'il existe une nette différenciation entre les populations réparties sur l'ensemble de l'Ontario, la population du lac Simcoe est fortement apparentée aux populations de grands corégones des lacs Ontario et Huron, ce qui laisse croire qu'il n'est pas justifié de lui attribuer un statut distinct d'après les critères génétiques. Notre travail démontre comment l'évaluation de la diversité génétique dans le cadre fourni par le COSEPAC peut apporter des renseignements sur le statut des populations exploitées essentiels pour la gestion des pêches.

[Traduit par la Rédaction]

Introduction

Recognizing biological units and understanding the formative roles of the evolutionary and ecological processes that influence them are key issues for sustainable management and conservation of exploited species. Since exploitation may result in evolutionary changes to the productivity and growth rates of species (Conover and Munch 2002), which may vary among intraspecific population units (Carvalho and Hauser 1994), recognition of distinct self-sustaining groups is essential for their long-term management. Resolving biologically meaningful spatiotemporal groupings is particularly important for exploited species to prevent their overexploitation and loss as well as the subsequent ecological and economic consequences (Begg and Waldman

Received 7 October 2008. Accepted 31 May 2009. Published on the NRC Research Press Web site at cjfas.nrc.ca on 9 September 2009. J20810

Paper handled by Associate Editor Eric Taylor.

A.M. Bernard,[1,2] M.M. Ferguson, and D.L.G. Noakes.[3] Department of Integrative Biology, University of Guelph, Guelph, ON N1G 2W1, Canada.
B.J. Morrison. Ontario Ministry of Natural Resources, Glenora Fisheries Station, Picton, ON K0K 2T0, Canada.
C.C. Wilson. Aquatic Research Section, Ontario Ministry of Natural Resources, Trent University, 2140 East Bank Drive, Peterborough, ON K9J 7B8, Canada.

[1]Corresponding author (e-mail: andrbern@nova.edu).
[2]Present address: Oceanographic Center, Nova Southeastern University, 8000 North Ocean Drive, Dania Beach, FL 33004, USA.
[3]Present address: Oregon Hatchery Research Center, Oregon State University, 104 Nash, Corvallis, OR 97331, USA.

1999; Begg et al. 1999). Although both the terms "population" and "evolutionarily significant unit" (ESU) refer to self-sustaining biological units of individuals below the species level, establishing operational definitions for either is challenging (Schaefer 2006). The former is used to describe individuals that require separate management with respect to exploitation, and the latter is used to identify groups of individuals of special interest with respect to conservation. Within Canada, the assessment and recognition of evolutionarily distinct population segments (e.g., ESUs) or "designatable units" (DUs) is performed by the Committee on the Status of Endangered Wildlife in Canada (COSEWIC); delineation of DUs requires that a population must be first recognized as "discrete" followed by consideration of whether such discreteness should be interpreted as "significant" (COSEWIC 2008). Given the importance of managing and conserving species effectively, debate persists on how to pragmatically implement these above concepts to identify discrete biologically significant intraspecific units.

Conceptual population definitions range across a continuum of varying spatial and temporal stability and connectivity (Ihssen et al. 1981*a*; Carvalho and Hauser 1994) and tend to champion either evolutionary or ecological paradigms (Waples and Gaggiotti 2006). Definitions such as Moritz's (1994) management unit (MU) tend to rely on strictly genetic criteria rather than demographic or ecological processes to identify population structure, although this has been widely criticized (Paetkau 1999; Taylor and Dizon 1999). Although past ESU concepts have emphasized adaptive variation (Ryder 1986), reproductive isolation and evolutionary potential or legacy (Waples 1991, 1995), and historical isolation (Moritz 1994; Dimmick et al. 1999), COSEWIC's (2008) DU concept has adopted a more holistic, hypothesis-driven measure of distinctiveness. Akin to several other population and ESU concepts that have been tailored for operational use (Moritz 1994; Crandall et al. 2000; Fraser and Bernatchez 2001), the DU approach makes use of testable hypotheses, allowing for a more consistent practical application of the concept. This practice, however, requires managers to determine the degree of statistical differentiation required to constitute biological significance (Hedrick 1999; Goldstein et al. 2000), thereby exasperating consistent delineation (Palsbøll et al. 2007). To circumvent this problem, many have suggested the use of phenetic concepts (e.g., Bowen et al. 1991), as they illustrate differences in terms of relative degrees of differentiation, allowing for the correspondence among independent data sources (e.g., morphological and genetic) to act as an indicator of conservation status (Vogler and DeSalle 1994). While the amount of intraspecific variation differs across species and markers (Avise 2000), a comparison of intraspecific variation among neighboring populations using shared markers may help to expose highly differentiated biological units.

In this study, we evaluated the ability to apply population and DU concepts to a natural data set and the relative abilities of these concepts to elucidate biologically significant divergence. We examined a heavily exploited species, the lake whitefish (*Coregonus clupeaformis*), from Great Lakes and inland populations across Ontario, Canada. Coregonids provide an exceptional example of the difficulties associated with inferring population structure from genetic and phenotypic information, with varying degrees of documented conflict and congruence among informative characters (Casselman et al. 1981; Turgeon et al. 1999; Østbye et al. 2005) and high levels of documented phenotypic plasticity (Brooks 1957; Lindsey 1981; Bernatchez 1995). Populations of lake whitefish in the Great Lakes have undergone substantial fluctuations as a result of high levels of exploitation, competition with exotic species, and eutrophication (Mohr and Nalepa 2005), underscoring the need for population discrimination for sustainable management.

We used microsatellite DNA loci to assess the population structure of sympatric lake whitefish stocks in eastern Lake Ontario using collections from two temporal intervals that have been previously described based on morphometric and osseometric differences (the term "osseometric" pertains to calcified structures, e.g., scales and otoliths (Casselman et al. 1981)) (Ihssen et al. 1985; Brown and Casselman 1992). The descriptive outcomes of these previous studies were considered as testable hypotheses for detecting genetic differentiation among stocks, as was the null hypothesis of a single panmictic population in Ontario and New York waters of eastern Lake Ontario. In addition, these data were also used to quantitatively assess whether spawning groups constituted genetically differentiated MUs based on published criteria (Moritz 1994; Palsbøll et al. 2007).

A similar hypothesis-based approach was used to assess the evolutionary distinctiveness of lake whitefish in Lake Simcoe, Ontario. The Lake Simcoe population of lake whitefish was originally designated as "threatened" in 1987 by COSEWIC, in part because of genetic information suggesting its distinctiveness from allopatric Great Lakes populations (Ihssen et al. 1981*b*; Evans et al. 1988). This designation was changed in 2005 to "data deficient" due to uncertainty regarding the biological distinctiveness of this population (COSEWIC 2005). We evaluated hypotheses concerning the genetic distinctiveness of the Lake Simcoe lake whitefish by using neutral genetic markers to exemplify the challenges associated with the operational implementation of the DU concept. The findings from both case studies highlight the differential applicability of demographically sensitive neutral genetic markers in contiguous versus isolated habitats.

Materials and methods

Sample collections

Scale samples, muscle biopsies, and fin clips were collected from 428 individuals from several sample sites across Ontario waters (Table 1; Fig. 1). All Lake Ontario samples except those from Chaumont Bay, New York, were obtained from spawning adults; Chaumont Bay samples consisted of a mixture of dried scales from spawning adults ($n = 10$) and frozen 2004 young-of-the-year ($n = 31$). Lake Simcoe whitefish samples were obtained from the Ontario Ministry of Natural Resources (OMNR) Fisheries Research Facility in Codrington, Ontario (OMNR Fish Culture broodstock lot 98–927); these individuals were the progeny of eight families (16 spawning adults) collected in 1997 near Strawberry Island, Lake Simcoe, by the OMNR Lake Simcoe Fishery Assessment Unit. Lake Simcoe hatchery whitefish were used in this study, as stocked fish now comprise the major-

Table 1. Summary of sample locations for genetic analysis showing lake of origin, collection site (within lake), sample sizes (*n*), collection year, and type of tissue and method of tissue preservation.

Lake	Collection site	*n*	Collection year	Type of tissue and method of preservation
Lake Ontario	Bay of Quinte, Big Bay (Bay)	57	2003	Fin clips in 95% ethanol
				Dried scales
	South shore Prince Edward County (Lake)	84	2003	Fin clips in 95% ethanol
				Dried scales
	Bay of Quinte (Bay)	38	1992	Dried scales
	Long Point, Prince Edward County (Lake)	34	1992	Dried scales
	Chaumont Bay (CB)	10	2004	Dried scales
		31		Frozen tissue
Lake Huron, Georgian Bay	Owen Sound	30	2005	Fin clips in 95% ethanol
	Cape Rich	18		
Lake Simcoe	Strawberry Island	65	1997	Frozen muscle tissue
Lake Opeongo	—	29	2005	Fin clips in 95% ethanol
Hogan Lake	—	8	2005	Fin clips in 95% ethanol
Lake of the Woods	Whitefish Bay	24	2004	Fin clips in 95% ethanol

Note: A dash indicates that a more precise sample location is not available. Site locations are shown in Fig. 1.

ity of the Lake Simcoe whitefish population due to successive years of lake whitefish recruitment failure (COSEWIC 2005).

Genetic analyses

Extraction of genomic DNA from preserved and frozen tissue was performed using a modified 96-well plate isopropanol extraction protocol (Wilson et al. 2007). For archival scales (1992 sample collection date), genomic DNA was purified using a Qiagen DNeasy tissue kit (Qiagen Inc.) with a final elution volume of 20 µL. Ten microsatellite loci were amplified using fluorescently labeled primers developed by Rogers et al. (2004). A subset of five of these markers was used to amplify the historical Lake Ontario scale samples. The polymerase chain reaction was performed in 10 µL reaction volumes with 20 ng of DNA, 1 µL of reaction buffer (New England BioLabs) (10× concentration, 20 mmol/L $MgSO_4$), 1.0 µL of bovine serum albumin (10× 2 mg/mL), 0.2 µL (10 mmol/L) of deoxynucleotide triphosphates, 1 U of *Taq* DNA polymerase (New England BioLabs), and 0.2–0.5 µL (10 µmol/L) of each primer. Reactions were conducted in a PTC-100 thermocycler (MJ Research Inc.). Thermocycler profiles consisted of a denaturation period of 11 min at 95 °C followed by 29–39 cycles for 30 s at 94 °C, 1 min at the primer annealing temperature (*Cocl-Lav*4, 6, 18, 28, 45, 52, and 68 at 59 °C, *Cocl-Lav*224 at 60 °C, and *Cocl-Lav*19 and 32 at 61 °C), and 1 min at 72 °C with a final extension step at 60 °C for 45 min. Electrophoresis was performed using an ABI 377 automated sequencer on a 4.5% polyacrylamide gel; allelic data were collected and scored using GeneScan version 3.1.2 and GenoTyper 2.5 (Applied Biosystems Inc.).

Hypothesis testing as a means to define management and conservation units

To assess the intralake population structure of lake whitefish within the eastern basin of Lake Ontario, we tested the null hypothesis of individuals across sampling locations comprising a single panmictic population against two alternative hypotheses: (*i*) the Bay and Lake individuals encompass a single reproductively discrete unit, while the Chaumont Bay individuals comprise a second genetically distinguishable population and (*ii*) each of the three sampling locations (Bay, Lake, Chaumont Bay) comprises a reproductively discrete population. Statistically significant genetic differentiation among sampling locations was inferred as evidence to support the identification of discrete MUs (sensu Moritz 1994).

We used criteria set forth by COSEWIC (2008) to assess the distinctiveness of the lake whitefish population in Lake Simcoe. COSEWIC's guidelines for the identification of DUs involve examining the discreteness and significance of biological units. Discreteness may be assessed by testing for (*i*) genetic distinctiveness, (*ii*) natural disjunction between portions of the species' geographic range, or (*iii*) the occupation of separate aquatic biogeographic zones (COSEWIC 2008). If a population is found to be discrete, significance of the population is assessed using any or all of the four following criteria: (*i*) deep phylogenetic divergence, (*ii*) evidence of unique ecological traits or local adaptations, (*iii*) a determination of whether the population represents the only surviving natural occurrence of the species, and (*iv*) whether the loss of the population would result in an extensive gap in the range of the species in Canada (COSEWIC 2008). To assess the conservation status of the lake whitefish population in Lake Simcoe, a series of testable hypotheses were developed within the COSEWIC framework to address the DU criteria of genetic distinctiveness under the null hypothesis that Lake Simcoe whitefish were no more distinct than any other Great Lakes population. Hypotheses for both studies were tested by assessing the genetic diversity and divergence among putative groups and testing predicted groupings against empirical data interpretations from population- and individual-based analyses.

Statistical analysis

Allele frequencies and expected (H_E) and observed (H_O) heterozygosities were calculated using GENEPOP on the web (Raymond and Rousset 1995*a*; http://genepop.curtin.edu.au/) for all populations and sampling periods. Depar-

Fig. 1. Map of study locations used to assess genetic diversity and divergence among lake whitefish (*Coregonus clupeaformis*) populations in Lake Ontario (A), Lake Huron (B), Lake Simcoe (C), Lake Opeongo (D), Hogan Lake (E), and Lake of the Woods (F). The left inset shows the location of the Great Lakes region in Canada and the United States. The right inset of Lake Ontario shows spawning site and sampling locations for the three hypothesized lake whitefish stocks in eastern Lake Ontario: Bay of Quinte (1) (two sampling points), south shore of Prince Edward County (2), Long Point (3), and Chaumont Bay, New York (4).

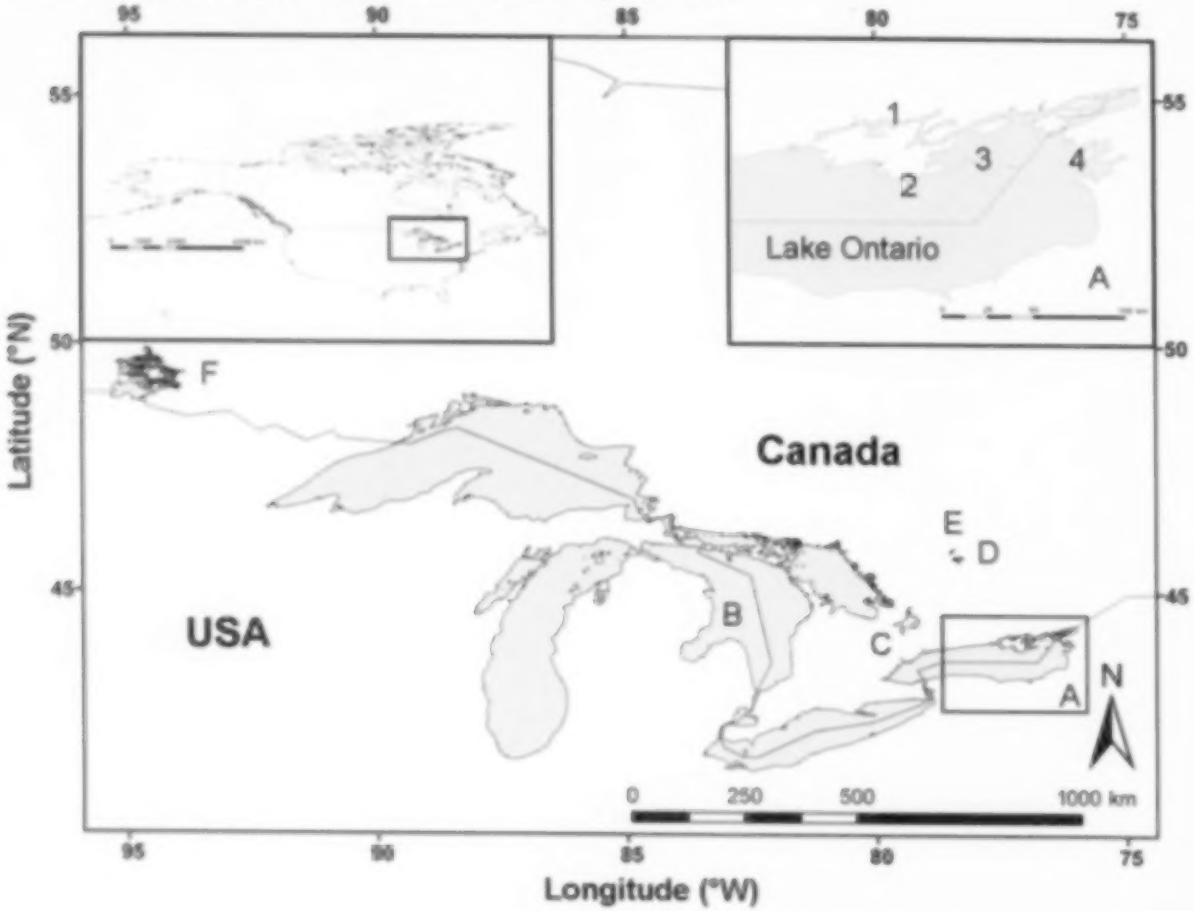

tures from Hardy–Weinberg proportions (HWE) across all loci and populations were tested using Fisher's exact test (Raymond and Rousset 1995*b*). Significance values were computed using 1000 Markov chain iterations (Guo and Thompson 1992) and adjusted using sequential Bonferroni correction (Rice 1989). Global exact tests (Raymond and Rousset 1995*b*) for departures from HWE were performed under the alternative hypothesis of heterozygote deficiency (1000 iterations). El Mousadik and Petit's (1996) allelic richness index (R_S) was estimated for each population using FSTAT 2.9.3.2 (Goudet 2002) to allow for comparison of diversity across populations independent of sample size. A nonparametric Kruskal–Wallis test was used to compare H_O, H_E, and R_S among interlake populations using SPSS 10.0.7 statistical software (SPSS Inc., Chicago, Illinois).

Estimated population divergences were computed using both Weir and Cockerham's (1984) F_{ST} analogue (θ) and R_{ST} (Rousset 1996). Both estimators (θ and R_{ST}) incorporate information regarding the mutational process (infinite allele model and stepwise mutation model, respectively). Given the lack of consensus regarding the most appropriate mutational model to describe the evolution of microsatellites (Gaggiotti et al. 1999), both test statistics were adopted for use in this study. Global and pairwise values of θ (Weir and Cockerham 1984) and R_{ST} (Rousset 1996) were estimated separately for the intralake (Lake Ontario) and interlake samples using FSTAT 2.9.3.2 (Goudet 2002) and GENEPOP, respectively. Significance of pairwise population differentiation estimates was tested in FSTAT 2.9.3.2 using 1000 permutations and sequential Bonferroni correction (Rice 1989). The temporal stability of allele frequencies at each Lake Ontario sampling location was tested using Pearson's correlation coefficient as implemented in SPSS 10.0.7 statistical software (SPSS Inc., Chicago, Illinois). An unrooted neighbor-joining dendrogram was constructed using Nei et al.'s (1983) D_A, as Takezaki and Nei (1996) concluded that this measure, in conjunction with neighbor-joining, would generate the most appropriate topology when

utilizing microsatellite genetic markers. The neighbor-joining dendrogram was generated using Populations 1.2.28 (Langella 2002) and visualized using TREEVIEW 1.6.6 (Page 1996); significance of branch points was tested using 10 000 bootstrap replicates across loci. In addition, an unrooted UPGMA tree (unweighted pair group method with arithmetic mean, 10 000 bootstraps over all loci) was also constructed using Cavalli-Sforza and Edwards' (1967) chord distance (D_C) for comparison with the UPGMA tree generated from previous allozyme data (Ihssen et al. 1981*b*).

The population-level analyses were complemented by individual-based assignment tests without a priori population assignment to assess the genetic support for putative population groupings. The program *structure* 2.1 (Pritchard et al. 2000) was employed to perform multilocus cluster analysis to estimate the number of populations (k) within the Lake Ontario data set and the number of distinct clusters (k) among the genotypic data from all six lakes. The Bayesian model aims to assign individuals into clusters that are in HWE and linkage equilibrium and assumes no mutational process (Pritchard et al. 2000). Five independent runs were performed on the Lake Ontario data set at k = 1 to 4, each with 50 000 dememorizations and Markov chain Monte Carlo (MCMC) repetitions, using no prior information and assuming correlated allele frequencies and admixture (Falush et al. 2003). These values of k were selected to test contrasting hypotheses of panmixia (k = 1), jurisdictional stocks (k = 2), or each sampling location as a reproductively isolated group of individuals (k = 3) and allowed for the possibility of a currently undescribed population within eastern Lake Ontario (k = 4). Similarly, individual-based analyses among the six study lakes were performed via four independent runs of k = 1 to 9 at 50 000 dememorizations and 50 000 MCMC repetitions, again using no prior information and assuming correlated allele frequencies and no admixture to reflect the reciprocal geographic isolation among populations. To assess the robustness of the probabilities for different solutions of k, the length of the MCMC burn-in and resampling periods were adjusted (10 000, 50 000, 75 000, and 100 000) until the variation across independent replicates was minimized. Subsequent to the individual-based analyses of the genetic data from the six study lakes, net nucleotide distances were estimated among all identified clusters using the most recent version of the program *structure* (version 2.2).

Results

Identifying units for management: intralake comparison of lake whitefish populations

Preliminary screening of the data indicated that two of the 10 loci screened (*Cocl-Lav28* and *Cocl-Lav32*) appeared to be duplicated, as some individuals exhibited three or four alleles at each locus. Further screening revealed that these same two loci exhibited significant departures from HWE expectations ($p < 0.05$) after sequential Bonferroni correction (Rice 1989). These two loci were therefore excluded from all further analyses due to the potential for errors in scoring and data interpretation. Within the Lake Ontario data set, four loci exhibited significant deviation from HWE expectations at $p < 0.05$, although these differences were not significant after sequential Bonferroni correction (Table 2). As allele frequency differences were not found between the two sampled Chaumont Bay spawning cohorts (adults and larvae from 2004, $p = 0.095$), these were pooled for all subsequent analyses.

The data from lake whitefish in eastern Lake Ontario showed mixed evidence of weak genetic structure (Table 3*a*). A global exact test of heterozygote deficiency found a significant departure from HWE among pooled contemporary Lake, Bay, and Chaumont Bay individuals (p = 0.003), suggesting possible subdivision (Wahlund effect) among the a priori stocks; when the Chaumont Bay stock was removed from the analysis, the pooled Lake and Bay samples met HWE expectations ($p = 0.143$).

Following sequential Bonferroni correction (table-wide), the 2003 Lake and Chaumont Bay populations were the only contemporary groups to demonstrate significant differentiation at $p < 0.05$. In addition, a post hoc comparison between the pooled individuals of the Lake and Bay stocks versus the Chaumont Bay individuals detected significant differences (θ, $p = 0.003$). For the 1992 sampled cohorts, no evidence of genetic differentiation was detected among the Lake and Bay spawning individuals ($p < 0.05$) after sequential Bonferroni correction. Allele frequencies appeared to be temporally stable within a priori identified populations; Pearson's correlation coefficient revealed statistically significant correlations ($r > 0.98$, $p < 0.01$) among temporal comparisons. Pairwise estimates of θ and R_{ST} across temporal periods (and between the same putative stocks) were similarly low and stable (Table 3*a*). Global estimates of θ and R_{ST} for all 2003 and 2004 Lake Ontario populations were 0.012 and 0.0163, respectively. Overall, pairwise θ and R_{ST} estimates revealed minor intralake differences among the Lake and Bay stocks, with more pronounced differences between each of these and the Chaumont Bay stock (Table 3*a*).

In contrast with the population-level comparisons, Bayesian individual assignment tests showed no evidence of structure among the putative contemporary Lake Ontario populations. The estimated likelihood of each k ($L(k)$) varied considerably between independent runs, despite varying the length of the burn-in period and the number of MCMC repetitions. The highest mean likelihood for contemporary samples was found at k = 1 (ln $P(K|X)$ = –3689.4) and lowest at k = 3 (ln $P(K|X)$ = –3867.32). Estimated posterior probabilities strongly suggested the existence of a single panmictic population within the eastern basin ($P(K|X) > 0.999$). In addition, at k values >1, individual assignment values (q) and mean proportion of membership were roughly symmetrical ($q = 1/k$) across all populations and no single individual was strongly assigned a single cluster ($q < 0.75$). Equivalent membership to all clusters, on both a population and an individual level, has been determined to be indicative of an absence of structure (Pritchard and Wen 2004). Mean likelihood values and posterior probabilities for the 1992 Bay and Lake collections peaked at k = 4 (–872.2 and 0.997, respectively). However, the mean likelihood values derived from k = 1 to 4 fell within a narrow range (–872.2 to –881.5), and individual and population assignments were highly symmetric across all hypothesized populations ($q = 1/k$), suggesting an absence of substructure.

Table 2. Summary statistics for eight microsatellite loci among lake whitefish (*Coregonus clupeaformis*) samples.

Sample	Locus								
	*Cocl-Lav*6	*Cocl-Lav*45	*Cocl-Lav*52	*Cocl-Lav*4	*Cocl-Lav*68	*Cocl-Lav*18	*Cocl-Lav*224	*Cocl-Lav*19	Average
1992 Bay									
n	38	—	38	33	38	—	—	35	
A	6	—	22	4	3	—	—	5	8
RPT	125–145	—	98–162	148–154	176–182	—	—	251–263	
R_S	3.2	—	10.4	3.2	2.1	—	—	3.9	
H_O	0.37	—	0.87	0.70	0.26	—	—	0.60	0.56
H_E	0.37	—	0.93	0.64	0.27	—	—	0.60	0.56
HW	0.64	—	0.12	0.92	1.00	—	—	1.00	0.87
1992 Lake									
n	31	—	29	26	33	—	—	24	
A	7	—	18	4	2	—	—	5	7.2
RPT	129–145	—	98–148	150–158	176–180	—	—	251–265	
R_S	4.1	—	9.2	3.3	1.8	—	—	3.9	
H_O	0.55	—	0.86	0.62	0.18	—	—	0.63	0.57
H_E	0.52	—	0.91	0.69	0.17	—	—	0.65	0.59
HW	0.78	—	0.21	0.77	1.00	—	—	0.80	0.92
2003 Bay									
n	54	48	57	57	57	55	46	51	
A	5	6	19	3	2	3	16	8	8.5
RPT	129–145	214–255	98–160	150–158	176–182	150–158	211–243	251–271	
R_S	3.2	4.4	8.8	3.1	2.1	2.3	8.7	4.4	
H_O	0.44	0.63	0.88	0.65	0.28	0.58	0.93	0.63	0.63
H_E	0.43	0.67	0.88	0.64	0.27	0.50	0.89	0.64	0.62
HW	0.41	0.03	0.20	0.66	1.00	0.23	0.44	0.33	0.24
2003 Lake									
n	81	81	81	77	83	82	80	69	
A	7	7	21	4	4	2	17	7	8.75
RPT	129–147	235–255	96–164	148–154	174–186	150–156	207–243	251–265	
R_S	3.7	3.7	9.0	3.2	1.9	2.0	7.1	3.9	
H_O	0.48	0.48	0.91	0.69	0.16	0.40	0.75	0.54	0.57
H_E	0.46	0.46	0.90	0.67	0.17	0.46	0.83	0.57	0.58
HW	0.89	0.35	0.88	0.09	0.50	0.33	0.54	0.03	0.26
2004 CB									
n	41	40	40	41	40	27	38	38	
A	7	6	17	3	3	3	13	5	7.13
RPT	129–147	239–255	102–146	150–154	176–182	150–156	211–243	251–265	
R_S	3.2	2.8	9.6	3.0	2.2	2.5	7.7	3.6	
H_O	0.37	0.58	0.98	0.76	0.30	0.37	0.97	0.68	0.62
H_E	0.34	0.46	0.92	0.67	0.36	0.52	0.87	0.69	0.60
HW	0.21	0.00	0.83	0.60	0.48	0.02	0.44	0.47	0.03

Published by NRC Research Press

Table 2 (*continued*).

Sample	Locus								
	Cocl-Lav6	*Cocl-Lav45*	*Cocl-Lav52*	*Cocl-Lav4*	*Cocl-Lav68*	*Cocl-Lav18*	*Cocl-Lav224*	*Cocl-Lav19*	Average
ONT									
n	170	166	178	175	180	164	164	158	
A	8	9	26	5	5	5	14	4	9.38
RPT	129–147	235–255	96–164	148–158	174–186	150–158	207–243	251–271	
R_S	3.4	4.2	9.1	3.1	2.1	2.1	7.9	4	
H_O	0.46	0.60	0.92	0.69	0.23	0.46	0.85	0.59	0.60
H_E	0.44	0.61	0.90	0.66	0.25	0.48	0.87	0.63	0.60
HW	0.33	0.01	0.34	0.06	0.56	0.01	0.64	0.13	**0.00**
HUR									
n	48	46	48	40	35	47	35	47	
A	3	6	18	3	3	2	11	6	6.5
RPT	129–143	239–255	100–144	150–154	176–182	150–156	213–277	251–267	
R_S	2.7	3.7	9.1	2.9	1.8	2.0	7.0	4.0	
H_O	0.46	0.61	0.90	0.53	0.11	0.32	0.83	0.60	0.54
H_E	0.42	0.59	0.91	0.60	0.11	0.30	0.83	0.58	0.54
HW	1.00	0.91	0.70	0.49	1.00	1.00	0.42	0.50	0.99
SIM									
n	65	56	57	60	61	54	61	55	
A	5	5	17	3	3	4	8	4	6.13
RPT	129–143	241–255	102–152	150–154	176–182	146–156	213–237	251–263	
R_S	2.7	3.7	9.2	2.9	1.8	2.5	5.3	2.4	
H_O	0.29	0.76	1.0	0.67	0.16	0.61	0.87	0.18	0.57
H_E	0.32	0.68	0.89	0.66	0.15	0.52	0.80	0.22	0.53
HW	0.02	**0.00**	0.00	0.70	1.00	**0.00**	0.15	0.00	0.00
OPE									
n	27	25	18	24	28	29	16	24	
A	3	4	11	2	1	1	5	3	3.75
RPT	135–143	241–255	116–146	152–154	180	156	217–269	255–263	
R_S	2.3	2.9	7.8	2.0	1.0	1.0	4.7	2.5	
H_O	0.48	0.40	0.95	0.50	—	—	0.56	0.38	0.41
H_E	0.48	0.51	0.87	0.51	—	—	0.78	0.32	0.43
HW	1.00	0.37	0.26	1.00	—	—	0.01	1.00	0.32
HOG									
n	8	8	8	8	8	8	8	8	
A	2	2	5	4	2	2	3	2	2.75
RPT	129–135	241–253	102–140	148–154	176–180	150–156	233–237	255–263	
R_S	2.0	2.0	5.0	4.0	2.0	2.0	3.0	2.0	
H_O	0.13	0.38	0.50	0.88	0.50	0.25	0.25	0.38	0.41
H_E	0.53	0.33	0.79	0.76	0.40	0.40	0.34	0.33	0.48
HW	0.05	1.00	0.01	1.00	1.00	0.39	0.20	1.00	0.21

Published by NRC Research Press

Table 2 (*concluded*).

Sample	Locus										
	Cocl-Lav6	*Cocl-Lav45*	*Cocl-Lav52*	*Cocl-Lav4*	*Cocl-Lav68*	*Cocl-Lav18*	*Cocl-Lav224*	*Cocl-Lav19*	Average
LOW									
n	21	24	22	19	19	24	20	24	
A	4	3	16	3	2	2	3	6	6.13
RPT	129–143	241–255	102–148	150–154	176–180	150–156	205–267	251–271	
R_S	3.6	3.0	8.9	2.8	1.8	2.0	7.5	4.3	
H_O	0.29	0.92	0.77	0.53	0.16	0.38	0.90	0.45	0.55
H_E	0.57	0.65	0.87	0.48	0.15	0.47	0.84	0.54	0.57
HW	0.00	0.03	0.01	0.80	1.00	0.39	0.37	0.14	0.00

Notes: Bay, Bay of Quinte; Lake, Prince Edward County; CB, Chantrey Bay, New York; ONT, Lake Ontario (pooled 2003 and 2004); HUR, Lake Huron; SIM, Lake Simcoe; OPE, Lake Opeongo; HOG, Hogan Lake; LOW, Lake of the Woods; Average, average across all loci; *n*, number of individuals; *A*, number of alleles; RPT, size range of alleles; R_S, standardized allelic richness; H_O, observed heterozygosity; H_E, expected heterozygosity; HW, probability of concordance with Hardy–Weinberg expectation. Absence of data is represented by a dash. Values in bold are significant after correction for multiple tests (initial $\alpha = 0.0562$; $\alpha = 0.0006$).

Identifying units for conservation: interlake comparison of lake whitefish populations

The genetic diversity observed varied considerably among the surveyed populations (Table 2). No significant allele frequency differences were found between the two sample locations within Georgian Bay, Lake Huron (Cape Rich and Owen Sound, $p = 0.992$), which were therefore pooled for subsequent analyses. Subsequent to correction for multiple comparison testing, all populations and loci were found to be within HWE ($p < 0.05$) except for Lake Simcoe (*Cocl-Lav*45 and *Cocl-Lav*18) and the pooled Lake Ontario data (Table 2). Although the surveyed populations showed differences in allele frequencies at the eight microsatellite loci, no fixed differences in alleles were observed.

Estimates of within-population diversity (H_O and R_S) were lowest for Lake Opeongo and Hogan Lake ($H_O = 0.41$) and highest within Lake Ontario ($H_O = 0.60$). Samples obtained from Lake Opeongo had no detectable variation at two loci, and the average number of alleles per locus was quite small at $A = 3.8$ (Table 2). Despite the apparent lower diversity of fish from the two Algonquin lakes, standardized estimates of allelic richness after correction for sample size showed comparable diversity among sampled populations (Table 2). Differences in H_E, H_O, and R_S were not statistically significant using Kruskal–Wallis tests (df = 5, $p = 0.77$, 0.58, and 0.43, respectively).

Testing of the relative degrees of divergence among populations revealed strong and consistent levels of differentiation. All pairwise population comparisons of genotypic frequencies among lakes yielded highly significant values ($p < 0.001$) (see Bernard 2006 for allele frequency data). Global interlake estimates of θ (Weir and Cockerham 1984) and R_{ST} (Rousset 1996) were much higher than those within Lake Ontario and were estimated as 0.110 (95% CI = 0.067, 0.166) and 0.140, respectively. Pairwise estimates of θ (Weir and Cockerham 1984) and R_{ST} (Rousset 1996) among lakes varied greatly (Table 3). The neighbor-joining dendrogram of pairwise D_A genetic distances showed only minor differentiation between Lakes Huron and Ontario relative to all other surveyed populations (Fig. 2), whereas inland populations showed substantial divergence. Genetic differentiation and bootstrap support were most pronounced for the populations in Algonquin Park (Lake Opeongo and Hogan Lake) and showed much divergence from all other surveyed populations. The UPGMA dendrogram of pairwise D_C distances was highly congruent with published allozyme data (Ihssen et al. 1981*b*). Both marker systems showed close grouping among Lakes Ontario, Huron, and Simcoe, whereas Lake Opeongo lake whitefish were highly differentiated from all other sampled populations (Fig. 3).

Individual-based analysis of differentiation among the sampled lake whitefish groups largely mirrored the population-level comparisons. *structure* identified disparate subgroupings among the lake whitefish populations. Mean estimated likelihood values and posterior probabilities peaked at $k = 4$ (–6797.45 and >0.999, respectively). Post hoc inspection of the variance of $L(k)$ between independent runs also revealed a large increase at $k > 4$, suggesting an inability of the program to detect and delineate appropriate clusters beyond $k = 4$. At $k = 4$, three of the six populations (Lake Simcoe, Hogan Lake, and Lake Opeongo) were

Table 3. Pairwise genetic divergence estimates as measured by Weir and Cockerham's (1984) θ values (upper triangular matrix) and Rousset's (1996) R_{ST} (lower triangular matrix) (*a*) among within-lake lake whitefish (*Coregonus clupeaformis*) spawning populations (Ontario) at two temporal sampling periods and (*b*) among spawning populations from separate Ontario lakes.

(*a*) Among within-lake spawning populations (Ontario) at two temporal sampling periods

Sample location	Bay 1992	Lake 1992	Bay 2003	Lake 2003	CB 2004
Bay 1992	—	0.006	0.000	**0.005**	0.012
Lake 1992	0.011	—	0.004	–0.002	0.005
Bay 2003	–0.007	0.019	—	0.005	0.013
Lake 2003	–0.003	–0.005	0.013	—	**0.020**
CB 2004	0.044	–0.003	0.043	0.016	—

(*b*) Among spawning populations from separate Ontario lakes

Sample location	ONT	HUR	SIM	OPE	HOG	LOW
ONT	—	**0.064**	**0.045**	**0.232**	**0.166**	**0.063**
HUR	0.018	—	**0.101**	**0.219**	**0.233**	**0.051**
SIM	0.035	0.020	—	**0.247**	**0.206**	**0.083**
OPE	0.316	0.266	0.249	—	**0.282**	**0.213**
HOG	0.252	0.247	0.194	0.075	—	**0.157**
LOW	0.108	0.068	0.041	0.114	0.052	—

Note: Bay, Bay of Quinte; Lake, Prince Edward County; CB, Chaumont Bay, New York; ONT, Lake Ontario (pooled 2003 and 2004); HUR, Lake Huron; SIM, Lake Simcoe; OPE, Lake Opeongo; HOG, Hogan Lake; LOW, Lake of the Woods. Values in bold (θ) are significant after correction for multiple tests (Lake Ontario, initial $\alpha = 0.05/10 = 0.005$; interlake comparisons, initial $\alpha = 0.05/15 = 0.003$).

Fig. 2. Neighbor-joining dendrogram of genetic distance estimates among lake whitefish (*Coregonus clupeaformis*) populations from Lake Ontario, Lake Huron, Lake Simcoe, Lake Opeongo, Hogan Lake, and Lake of the Woods using Nei et al.'s (1983) D_A genetic distance for data from eight microsatellite loci. Numbers at branch nodes represent percent bootstrap support from 10 000 iterations; only values >50% are shown.

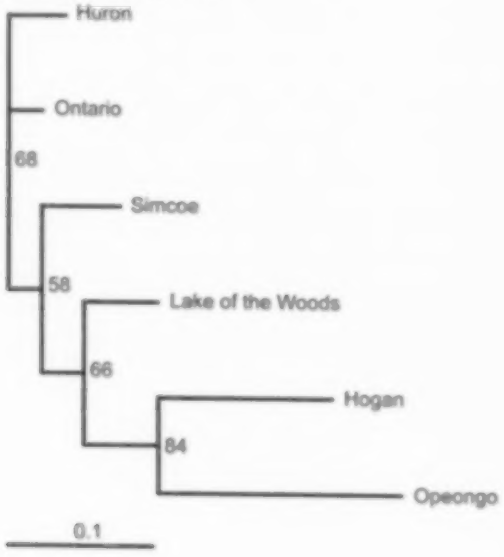

strongly assigned to single clusters ($q > 0.72$). Hogan Lake and Lake Opeongo assigned strongly to the same cluster (cluster 1) across independent runs (average membership coefficients were $q = 0.72$ and $q = 0.99$, respectively), while individuals from Lake Simcoe were consistently assigned to an exclusive cluster (cluster 2) at an average of $q = 0.81$. Membership probabilities for lake whitefish from Lake Huron, Lake Ontario, and Lake of the Woods were largely shared between the third and fourth groups, with membership coefficients of individual fish being largely symmetrical (i.e., similar membership probabilities) for clusters 3 and 4. Within this set, individuals from Lakes Huron and Ontario were predominately assigned to cluster 3, whereas whitefish from Lake of the Woods appeared to belong more strongly to cluster 4. Since assignment of individuals from Lakes Huron and Ontario were quite symmetrical across clusters 3 and 4, recognizable genetic differences among lake whitefish from these two lakes appear to be minor. The net nucleotide distance among identified clusters at $k = 4$ exemplified the strong differentiation of the sampled inland lakes (Lake Opeongo and Hogan Lake) relative to all other populations, in contrast with the relatively minor differentiation of the Lake Simcoe individuals. Net nucleotide distances of the Algonquin cluster populations relative to all other identified clusters ranged from 0.72 to 0.88, while differentiation of the Lake Simcoe cluster to the remaining two clusters was substantially lower (0.13 and 0.17).

Discussion

Both components of our study exemplified the operational simplicity of utilizing neutral genetic markers to identify both MUs and DUs as well as the limitations of relying on a purely genetic approach. Relying strictly on neutral genetic evidence to identify lake whitefish MUs (sensu Moritz 1994) in Lake Ontario proved to be problematic, indicating that evidence of demographic independence may be more readily applicable in recently diverged populations or in circumstances with high historical gene flow (Palsbøll et al. 2007). The population-level analysis of Lake Ontario spawning aggregations rejected the null hypothesis of a single pan-

Fig. 3. UPGMA dendrograms of genetic distance estimates among lake whitefish (*Coregonus clupeaformis*) populations from Lake Ontario, Lake Huron, Lake Simcoe, Lake Opeongo, Hogan Lake, and Lake of the Woods based on (left) Cavalli-Sforza and Edwards (1967) chord distance (D_C) of microsatellite data and (right) Nei's (1972) standard genetic distance (D_S) of allozyme data for populations from Lake Ontario, Lake Huron, Lake Simcoe, Lake Opeongo, and Lavieille Lake (Algonquin Park) modified from Ihssen et al. (1981*b*). Numbers at branch nodes represent percent bootstrap support from 10 000 iterations; only values >50% are shown.

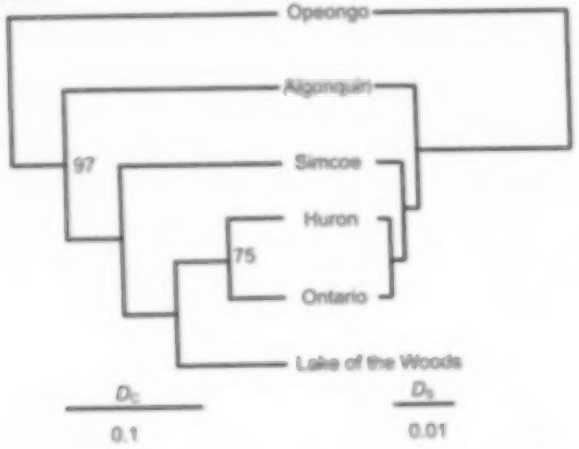

mictic stock but did not support the putative distinction between "Bay" and "Lake" stocks in the Bay of Quinte region. In contrast, delineating DUs by means of ranking their relative neutral genetic differentiation provided clear levels of divergence among populations in the second case study, greatly facilitating conservation-oriented management decisions. Analyses of Great Lakes and inland populations of lake whitefish demonstrated that the population in Lake Simcoe has less merit as a DU on genetic grounds than populations in Algonquin Park.

Identifying units for management: intralake comparison of lake whitefish populations

Population-based divergence measures (θ and R_{ST}) identified two genetically discrete MUs among the eastern Lake Ontario whitefish: a unit comprising both the Bay and Lake spawning aggregations and a unit within Chaumont Bay, New York. The identification of two distinct and temporally stable MUs is congruent with previous allozyme data, which failed to detect significant differentiation between the Bay and Lake populations (Ihssen et al. 1985). Conversely, analysis with *structure* suggested a single panmictic population with no evidence of substructure. This apparent discrepancy between the population- and individual-based analyses is consistent with other studies, as *structure* and other individual-based analyses have a limited ability to discriminate among weakly differentiated populations (Latch et al. 2006; Waples and Gaggiotti 2006; Pritchard et al. 2007). This may also be exacerbated by high levels of gene flow (Waples and Gaggiotti 2006), which are consistent with the high variance estimates for the likelihoods from *structure* runs at $k > 1$.

The lack of consistent detectable genetic resolution between the contemporary Bay and Lake spawning groups in Lake Ontario does not refute the hypothesis of ecologically and demographically distinct stocks, however, and may reflect historical demographic instability and moderate levels of contemporary gene flow (Palsbøll et al. 2007). Distinct population crashes marred the demographic history of lake whitefish over the past century, most notably in the early 1960s (Christie 1972; Casselman et al. 1996). Subsequent to this collapse, asymmetric recovery of the Lake and Bay stocks in the late 1970s may have allowed for extensive mixing, as lake whitefish stock recovery began initially in 1977 at the Lake spawning shoal, while recovery was delayed within the Bay until 1979 (Casselman et al. 1996). Casselman et al. (1996) suggested that this asymmetric recovery might be indicative of recolonization of the Bay of Quinte spawning shoals by immigrants originating from the Lake population. The very modest genetic differentiation currently detected among sampling sites may therefore be due to the quite recent separation of these two recently reestablished spawning aggregates as well as some degree of mixing. Mark–recapture and osseometric evidence suggests that mixing between the Lake and Bay spawning aggregations ranges between 5% and 12% (Christie 1967; Ihssen et al. 1985; Brown and Casselman 1992). Gene flow of this magnitude would likely homogenize their neutral genetic variation (Martien and Taylor 2003; Waples and Gaggiotti 2006) but may not impede their demographic independence and subsequent need for separate management (Palsbøll et al. 2007).

The ecological distinction of the Bay and Lake spawning aggregations is suggested by meristic and morphometric differences (Ihssen et al. 1985) and osseometric analysis (Brown and Casselman 1992), despite negligible genetic differentiation. Accordingly, the adoption of a disparate population concept that relies on phenotypic data as well as neutral genetic markers (Bernatchez 1995) would support the delineation of three distinct MUs in the eastern basin rather than the two genetically derived MUs. Given the phenotypic plasticity of coregonids (Brooks 1957; Lindsey 1981), however, environmental heterogeneity among spawning sites within the eastern basin may have induced apparent (plastic) phenotypic differentiation rather than adaptive or demographic divergence. As such, utilizing a population concept that relies on plastic characters does not offer the reliability of tracking distinct groups of individuals from generation to generation, thereby decreasing the utility of such a concept for the purposes of lake whitefish fisheries management. Given such ambiguities, the adoption of genetically differentiated populations (e.g., Moritz's (1994) MU concept) would appear to be the most appropriate method to identify demographically independent stocks at this time (also see Palsbøll et al. 2007).

The limitations of relying solely on genetic criteria may be exacerbated when population histories include severe population fluctuations and environmental degradation. Both are known to have occurred for lake whitefish in Lake Ontario (Christie 1972; Casselman et al. 1996), which may have compromised historical stock structure and past genetic differentiation. Thus, utilizing a single concept to delineate population structure in an unstable system is not advisable.

Given the known phenotypic plasticity of coregonids and unstable demographic history of the Lake Ontario lake whitefish, methods such as stable isotope or life history analyses used in conjunction with genetic analyses may offer better resolution of population discrimination for fisheries management. In addition, evidence of heritable differences in documented morphometric traits would greatly enhance their value for long-term population discrimination.

Although the use of holistic stock discrimination techniques or multiple concepts is often advocated (Paetkau 1999), their application can be extremely complex, as integrating data from genetic and ecological sources can be difficult (Dizon et al. 1992; Paetkau 1999; Miller et al. 2005). To circumvent this complexity, Vogler and DeSalle (1994) suggested using molecular markers for initial demarcation of biological units with subsequent mapping of nonmolecular characters onto genetically defined units to test for congruence. To compensate for such uncertainties, scientists and managers should focus on developing policies that recognize uncertainties and strategic research to reduce those uncertainties (e.g., Peterman 2004).

Identifying units for conservation: interlake comparison of lake whitefish populations

The results of this study, in conjunction with previous analyses, suggest that the Lake Simcoe whitefish do not qualify as a DU based on COSEWIC's two key criteria of discreteness and significance (COSEWIC 2008). Although both population- and individual-based genetic analyses showed the Lake Simcoe population to be significantly differentiated (discrete) from comparison populations, both analytical approaches showed it to be less divergent than other inland populations. More importantly, no available data show evidence of the population having unique evolutionarily significant traits; rather, the Lake Simcoe population has life history and morphological traits similar to those in the nearby Great Lakes (Ihssen et al. 1981*b*).

The comparison among inland lacustrine populations highlights a special difficulty for COSEWIC's "discreteness" criterion, as habitat restrictions and reciprocal isolation may result in more pronounced differences among geographic isolates than may be the case for terrestrial or marine organisms due to reduced opportunities for dispersal and gene flow. Populations of freshwater fishes typically show more pronounced differences compared with anadromous and marine species (Ward et al. 1994), despite recent shared phylogeographic ancestry in many cases (Bernatchez and Wilson 1998). The criterion of geographic disjunction, while intuitively appealing, is similarly challenged (COSEWIC 2008), as natural disjunction is characteristic of many freshwater systems, decreasing its utility as an informative criterion for delineating conservation units. This difficulty is recognized and partly offset by COSEWIC's (2008) third discreteness criterion, the persistence of populations in varying aquatic biogeographic regions, which recognizes not only geographic disjunction but also separation among major watersheds and historical dispersal or distinction (COSEWIC 2008); however, further deliberation of how to properly assess biota inhabiting disjunct aquatic areas may be required to ensure consistent delineation. Consideration must therefore be given when applying this framework to many fishes where barriers exist between populations.

Occurrence of populations within separate aquatic biogeographic zones is recognized as a useful measure of discreteness, as this separation may reflect differing contemporary local adaptations in response to variable ecological conditions, limited gene flow, or different postglacial origins (COSEWIC 2008). With the exception of the population in Lake of the Woods, which occurs within the Saskatchewan – Nelson River biogeographic zone, all of the surveyed populations occurred within the Great Lakes – Upper St. Lawrence freshwater biogeographic zone (COSEWIC 2008). It is therefore perhaps ironic that greater genetic divergence, as measured by microsatellite DNA markers, was present within this region than between Lake of the Woods and the Great Lakes populations.

Despite meeting the first DU criterion of discreteness, we found no evidence to suggest that the Lake Simcoe population warrants designation as "significant", as defined by COSEWIC (2008). First, there is no evidence to suggest the presence of deep phylogenetic divergence between the population in Lake Simcoe and those in Lakes Huron and Ontario. By comparison, the population in Lake Opeongo was substantially more divergent from the Great Lakes populations. This finding is congruent with the comparative study by Ihssen et al. (1981*b*), which assessed genetic, morphometric, and life history characteristics and showed that whitefish in Lake Simcoe were not significantly differentiated from those in Lakes Huron and Ontario versus the Lake Opeongo population, which was notably distinct from all others in the study. One limitation of our study was the small sample sizes available, as several sample sets fell short of those typically considered as robust for strong statistical power for microsatellite studies (Ruzzante 1998). Low sample sizes can invalidate parameter estimates such as F_{ST} due to increased statistical variance (Ruzzante 1998); however, this did not annul the significant population-level divergences found among all interlake comparisons.

Frequency-based differences for rapidly evolving genetic markers such as microsatellites have inherent limitations for identifying divergent groups, and fixed differences at multiple loci are preferable for identifying significantly divergent lineages (Palsbøll et al. 2007; COSEWIC 2008). The absence of fixed genetic differences at any of the loci used in this study suggests that all of the populations share a common phylogeographic ancestry (Ihssen et al. 1981*b*; Bernatchez and Dodson 1991), with subsequent divergence influenced by carrying capacities of local habitats and local adaptation (Bernatchez 1995; Bernatchez and Wilson 1998). Accordingly, populations in large connected lakes such as Lakes Huron and Ontario showed relatively minor differences at neutral loci (Ihssen et al. 1981*b*). Similarly, the large carrying capacity and recent evolutionary time since separation have buffered neutral differentiation for lake whitefish in Lake of the Woods, whereas the observed lower diversity in smaller inland populations reflects divergence in ecological rather than evolutionary time through genetic drift. The more pronounced divergences of lake whitefish populations in Algonquin Park compared with Lake Simcoe may reflect stronger founder effects, shorter periods of colonization op-

portunity (Mandrak and Crossman 1992, 2003), and (or) smaller habitat volumes, whereas the geographic proximity of Lake Simcoe to Lake Huron would have facilitated colonization, with lake whitefish likely arriving in Lake Simcoe from the Great Lakes basin approximately 12 000 years ago (Ihssen et al. 1981*b*; Evans et al. 1988; Mandrak and Crossman 1992).

No firm evidence exists to suggest that the Lake Simcoe whitefish meet any other of the three COSEWIC significance criteria (persistence of the population in a unique ecological setting conducive to local adaptation, evidence that the Lake Simcoe population represents the only surviving natural occurrence of the species, or evidence that its loss would result in an extensive gap in the range of the species in Canada) despite some earlier arguments supporting their listing (Evans et al. 1988). Lake Simcoe itself does not appear to offer a unique ecological setting that would support diversification through local adaptation, and the Lake Simcoe whitefish population exhibits life history and morphological characteristics comparable with those of the Great Lakes populations (Ihssen et al. 1981*b*). By contrast, the clear distinction of the Lake Opeongo population for multiple traits (e.g., meristics, genetics, and life history (Ihssen et al. 1981*b*)) may indicate that adaptive differentiation has played some role in its divergence. Furthermore, lake whitefish are broadly distributed across Ontario and much of Canada (Bernatchez and Dodson 1991); although the whitefish's extirpation from Lake Simcoe would represent a substantial economical and ecological loss, it would not result in an extensive gap in the range of the species in Canada. Although it was not the focus of this study, combined morphometric, meristic, genetic, and life history evidence (Ihssen et al. 1981*b*) indicates that lake whitefish in Lake Opeongo may warrant possible investigation as a DU.

Despite not meeting COSEWIC's DU requirements, the observed differentiation among populations in this study reflects varying degrees of independent evolutionary trajectories. Although decisions of how much neutral divergence is required for evolutionary significance can be somewhat subjective (Goldstein et al. 2000; Palsbøll et al. 2007), the comparative analysis performed in this study clearly elucidated the most divergent lineages among the studied populations. Arguments for a combined approach to defining units for conservation are not new. Bernatchez (1995) suggested that measuring both historical and adaptive divergence based on molecular and quantitative (phenotypic or physiological) genetic characters would be a more robust approach than relying on any single method, and Palsbøll et al. (2007) argued for the inclusion of demographic and ecological traits in identifying relevant MUs. Accordingly, COSEWIC's (2008) DU guidelines represent a significant advance towards adopting a unified approach to conservation management and a useful tool for recognizing biologically significant units of conservation.

The two systems presented here exemplify the challenges involved in recognizing significant intraspecific groupings for management and conservation as well as the utility and limitations of applying molecular markers to delineate appropriate biological units. Although having a single broadly applicable concept or tool to delineate management and conservation units would seem highly desirable to ensure consistency across studies, this may not be achievable based on the highly variable nature of some species and their evolutionary histories (Fraser and Bernatchez 2001). Neutral genetic markers provide valuable tools to identify the demographic independence of putative population units for fisheries management and historically divergent populations for conservation but are also subject to overinterpretation (Palsbøll et al. 2007). Accordingly, genetic data should be considered together with the ecology, demography, and history of populations prior to the adoption of management strategies (Bernatchez 1995; Palsbøll et al. 2007; COSEWIC 2008). This combined approach, using appropriate tools to identify meaningful biological units at different management scales, will help ensure the future as well as historical legacies of populations and species.

Acknowledgements

This work was facilitated and supported by the Ontario Ministry of Natural Resources (OMNR) and the New York State Department of Environmental Conservation. John Casselman, Glenn Forward, Yolanda Morbey, Lee Murray, Gary Ridout, Lori Skitt, and Bill Sloan (OMNR) generously provided samples for this study. Technical advice was provided by Mike Lavender, Mike Halbisen, Jim Hoyle, and Jay Dietrich (OMNR). We thank the two anonymous reviewers for their valuable suggestions for improvement of this manuscript. Funding for this project was provided by OMNR and the Canada–Ontario Agreement respecting the Great Lakes Ecosystem. This paper is dedicated to Bev Scott, a pioneer in studies of whitefish, as he enters his 92nd year with continued dedication to fish research.

References

Avise, J.C. 2000. Phylogeography: the history and formation of species. Harvard University Press, Cambridge, Mass.

Begg, G.A., and Waldman, J.R. 1999. An holistic approach to fish stock identification. Fish. Res. **43**(1–3): 35–44. doi:10.1016/S0165-7836(99)00065-X.

Begg, G.A., Friedland, K.D., and Pearce, J.B. 1999. Stock identification and its role in stock assessment and fisheries management: an overview. Fish. Res. **43**(1–3): 1–8. doi:10.1016/S0165-7836(99)00062-4.

Bernard, A. 2006. Cryptic structure and diversity of lake whitefish (*Coregonus clupeaformis*) in Ontario waters. M.Sc. thesis, Department of Integrative Biology, University of Guelph, Guelph, Ont.

Bernatchez, L. 1995. A role for molecular systematics in defining evolutionarily significant units in fishes. *In* Evolution and aquatic ecosystems: defining unique units in population conservation. *Edited by* J.L. Nielson. American Fisheries Society Symposium 17. American Fisheries Society, Bethesda, Md. pp. 114–132.

Bernatchez, L., and Dodson, J.J. 1991. Phylogeographic structure in mitochondrial DNA of the lake whitefish (*Coregonus clupeaformis*) and its relation to Pleistocene glaciations. Evolution, **45**(4): 1016–1035. doi:10.2307/2409706.

Bernatchez, L., and Wilson, C.C. 1998. Comparative phylogeography of Nearctic and Palearctic fishes. Mol. Ecol. **7**(4): 431–452. doi:10.1046/j.1365-294x.1998.00319.x.

Bowen, B.W., Meylan, A.B., and Avise, J.C. 1991. Evolutionary distinctiveness of the endangered Kemp's ridley sea turtle. Nature, **352**(6337): 709–711. doi:10.1038/352709a0. PMID: 1876185.

Brooks, J.L. 1957. The species problem in freshwater animals. *In* The species problem. *Edited by* E. Mayr. American Association for the Advancement of Science, Washington, D.C. pp. 81–123.

Brown, D.M., and Casselman, J.M. 1992. Research project: development of criteria for discriminating among lake whitefish stocks in Eastern Lake Ontario. Lake Ontario Fisheries Unit 1991 Annual Report. Ontario Ministry of Natural Resources, Picton, Ont. Section 21, pp. 1–9.

Carvalho, G.R., and Hauser, L. 1994. Molecular genetics and the stock concept in fisheries. Rev. Fish Biol. Fish. **4**(3): 326–350. doi:10.1007/BF00042908.

Casselman, J.M., Collins, J., Crossman, E., Ihssen, P., and Spanger, G. 1981. Lake whitefish (*Coregonus clupeaformis*) stocks of the Ontario waters of Lake Huron. Can. J. Fish. Aquat. Sci. **38**(12): 1772–1789. doi:10.1139/f81-225.

Casselman, J.M., Brown, D.M., and Hoyle, J.A. 1996. Resurgence of lake whitefish, *Coregonus clupeaformis*, in Lake Ontario in the 1980s. Great Lakes Res. Rev. **2**: 20–28.

Cavalli-Sforza, L.L., and Edwards, A.W.F. 1967. Phylogenetic analysis. Models and estimation procedures. Am. J. Hum. Genet. **19**(3 Pt. 1): 233–257. PMID:6026583.

Christie, W.J. 1967. Vital statistics of Lake Ontario whitefish. File Report. Ontario Ministry of Natural Resources, Glenora Fisheries Station, 41 Hatchery Lane, R.R. 4, Picton, Ont.

Christie, W.J. 1972. Lake Ontario: effects of exploitation, introductions, and eutrophication on the salmonid community. J. Fish. Res. Board Can. **29**: 913–929.

Conover, D.O., and Munch, S.B. 2002. Sustaining fisheries yields over evolutionary time scales. Science, **297**(5578): 94–96. doi:10.1126/science.1074085. PMID:12098697.

COSEWIC. 2005. COSEWIC assessment and update status report on the lake whitefish (Lake Simcoe population) *Coregonus clupeaformis* in Canada. Committee on the Status of Endangered Wildlife in Canada. Ottawa, Ontario.

COSEWIC. 2008. Guidelines for recognizing designatable units below the species level (approved by COSEWIC November 2008.) [Online.] Available from www.cosewic.gc.ca/eng/sct2/sct2_5_e.cfm [accessed 7 February 2009].

Crandall, K.A., Bininda-Emonds, O.R.P., Mace, G.M., and Wayne, R.K. 2000. Considering evolutionary processes in conservation biology. Trends Ecol. Evol. **15**(7): 290–295. doi:10.1016/S0169-5347(00)01876-0. PMID:10856956.

Dimmick, W.W., Ghedotti, M.J., Grose, M.J., Maglia, A.M., Meinhardt, D.J., and Pennock, D.S. 1999. The importance of systematic biology in defining units of conservation. Conserv. Biol. **13**(3): 653–660. doi:10.1046/j.1523-1739.1999.98193.x.

Dizon, A.E., Lockyer, C., Perrin, W.F., Demaster, D.P., and Sisson, J. 1992. Rethinking the stock concept: a phylogenetic approach. Conserv. Biol. **6**(1): 24–36. doi:10.1046/j.1523-1739.1992.610024.x.

El Mousadik, A., and Petit, R.J. 1996. High levels of genetic differentiation for allelic richness among populations of argan tree [*Argania spinosa* (L.) Skeels] endemic to Morocco. Theor. Appl. Genet. **92**(7): 832–839. doi:10.1007/BF00221895.

Evans, D.O., Houston, J.J., and Meredith, G.N. 1988. Status of the Lake Simcoe whitefish, *Coregonus clupeaformis*, in Canada. Can. Field-Nat. **102**: 103–113.

Falush, D., Stephens, M., and Pritchard, J.K. 2003. Inference of population structure using multilocus genotype data: linked loci and correlated allele frequencies. Genetics, **164**: 1567–1587. PMID:12930761.

Fraser, D.J., and Bernatchez, L. 2001. Adaptive evolutionary conservation: towards a unified concept for defining conservation units. Mol. Ecol. **10**(12): 2741–2752. PMID:11903888.

Gaggiotti, O.E., Lange, O., Rassmann, K., and Gliddon, C. 1999. A comparison of two indirect methods for estimating average levels of gene flow using microsatellite data. Mol. Ecol. **8**(9): 1513–1520. doi:10.1046/j.1365-294x.1999.00730.x. PMID:10564457.

Goldstein, P.Z., DeSalle, R., Amato, G., and Vogler, A.P. 2000. Conservation genetics at the species boundary. Conserv. Biol. **14**(1): 120–131. doi:10.1046/j.1523-1739.2000.98122.x.

Goudet, J. 2002. FSTAT (version 2.9.3.2): a computer program to calculate *F*-statistics (updated from Goudet 1995) [online]. Available from www2.unil.ch/popgen/softwares/fstat.htm [accessed 18 July 2007].

Guo, S.W., and Thompson, E.A. 1992. Performing the exact test of Hardy–Weinberg proportion for multiple alleles. Biometrics, **48**(2): 361–372. doi:10.2307/2532296. PMID:1637966.

Hedrick, P.W. 1999. Perspective: highly variable loci and their interpretation in evolution and conservation. Evolution, **53**(2): 313–318. doi:10.2307/2640768.

Ihssen, P.E., Booke, H.E., Casselman, J.M., McGlade, J.M., Payne, N.R., and Utter, F.M. 1981*a*. Stock identification: materials and methods. Can. J. Fish. Aquat. Sci. **38**(12): 1838–1855. doi:10.1139/f81-230.

Ihssen, P.E., Evans, D.O., Christie, W.J., Reckahn, J.A., and Desjardine, R.L. 1981*b*. Life history, morphology, and electrophoretic characteristics of five allopatric stocks of lake whitefish (*Coregonus clupeaformis*) in the Great Lakes region. Can. J. Fish. Aquat. Sci. **38**(12): 1790–1807. doi:10.1139/f81-226.

Ihssen, P.E., Christie, W.J., Martin, G.W., and Radford, J. 1985. Morphological and biochemical differentiation of two sympatric whitefish (*Coregonus clupeaformis*) stocks of eastern Lake Ontario. Ontario Ministry of Natural Resources, Glenora Fisheries Station, 41 Hatchery Lane, R.R. 4, Picton, Ont.

Langella, O. 2002. Populations 1.2.30 [online]. Available from http://bioinformatics.org/~tryphon/populations/ [accessed 15 January 2008].

Latch, E.K., Dharmarajan, G., Glaubitz, J.C., and Rhodes, O.E., Jr. 2006. Relative performance of Bayesian clustering software for inferring population substructure and individual assignment at low levels of population differentiation. Conserv. Genet. **7**(2): 295–302. doi:10.1007/s10592-005-9098-1.

Lindsey, C.C. 1981. Stocks are chameleons — plasticity in gill rakers of coregonid fishes. Can. J. Fish. Aquat. Sci. **38**(12): 1497–1506. doi:10.1139/f81-202.

Mandrak, N.E., and Crossman, E.J. 1992. Postglacial dispersal of freshwater fishes into Ontario. Can. J. Zool. **70**(11): 2247–2259. doi:10.1139/z92-302.

Mandrak, N.E., and Crossman, E.J. 2003. Fishes of Algonquin Provincial Park. Ontario Parks, Toronto, Ont.

Martien, K.K., and Taylor, B.L. 2003. Limitations to hypothesis-testing in defining management units for continuously distributed species. J. Cetacean Res. Manag. **5**: 213–218.

Miller, J.A., Banks, M.A., Gomez-Uchida, D., and Shanks, A.L. 2005. A comparison of population structure in black rockfish (*Sebastes melanops*) as determined with otolith microchemistry and microsatellite DNA. Can. J. Fish. Aquat. Sci. **62**(10): 2189–2198. doi:10.1139/f05-133.

Mohr, L.C., and Nalepa, T.F. (*Editors*). 2005. Proceedings of a Workshop on the Dynamics of Lake Whitefish (*Coregonus clupeaformis*) and Amphipod *Diporeia* spp. in the Great Lakes. Great Lakes Fish. Comm. Tech. Rep. 66.

Moritz, C. 1994. Defining 'Evolutionary Significant Units' for conservation. Trends Ecol. Evol. **9**(10): 373–375. doi:10.1016/0169-5347(94)90057-4.

Nei, M. 1972. Genetic distance between populations. Am. Nat. **106**(949): 283–292. doi:10.1086/282771.

Nei, M., Tajima, F., and Tateno, Y. 1983. Accuracy of estimated phylogenetic trees from molecular data. II. Gene frequency data. J. Mol. Evol. **19**(2): 153–170. doi:10.1007/BF02300753. PMID:6571220.

Østbye, K., Naesje, T.F., Bernatchez, L., Sandlund, O.T., and Hindar, K. 2005. Morphological divergence and origin of sympatric populations of European whitefish (*Coregonus lavaretus* L.) in Lake Femund, Norway. J. Evol. Biol. **18**(3): 683–702. doi:10.1111/j.1420-9101.2004.00844.x. PMID:15842498.

Paetkau, D. 1999. Using genetics to identify intraspecific conservation units: a critique of current methods. Conserv. Biol. **13**(6): 1507–1509. doi:10.1046/j.1523-1739.1999.98507.x.

Page, R.D.M. 1996. TreeView: an application to display phylogenetic trees on personal computers. Comput. Appl. Biosci. **12**(4): 357–358. PMID:8902363.

Palsbøll, P.J., Bérubé, M., and Allendorf, F.W. 2007. Identification of management units using population genetic data. Trends Ecol. Evol. **22**(1): 11–16. doi:10.1016/j.tree.2006.09.003. PMID:16982114.

Peterman, R.M. 2004. Possible solutions to some challenges facing fisheries scientists. J. Mar. Sci. **61**: 1331–1343.

Pritchard, J.K., and Wen, X. 2004. Documentation for *structure* software: version 2 [online]. Available from http://pritch.bsd.uchicago.edu/software/readme_2_1/readme.html [accessed 12 April 2008].

Pritchard, J.K., Stephens, M., and Donnelly, P. 2000. Inference of population structure using multilocus genotype data. Genetics, **155**(2): 945–959. PMID:10835412.

Pritchard, J.K., Wen, X., and Falush, D. 2007. Documentation for *structure* software: version 2.2 [online]. Available from http://pritch.bsd.uchicago.edu/software [accessed 7 January 2007].

Raymond, M., and Rousset, F. 1995*a*. GENEPOP (version 1.2): population genetics software for exact tests and ecumenicism. J. Hered. **86**: 248–249.

Raymond, M., and Rousset, F. 1995*b*. An exact test for population differentiation. Evolution, **49**(6): 1280–1283. doi:10.2307/2410454.

Rice, W.R. 1989. Analyzing tables of statistical tests. Evolution, **43**(1): 223–225. doi:10.2307/2409177.

Rogers, S.M., Marchand, M.-H., and Bernatchez, L. 2004. Isolation, characterization and cross-salmonid amplification of 31 microsatellite loci in the lake whitefish (*Coregonus clupeaformis*, Mitchill). Mol. Ecol. Notes, **4**(1): 89–92. doi:10.1046/j.1471-8286.2003.00578.x.

Rousset, F. 1996. Equilibrium values of measures of population subdivision for stepwise mutation processes. Genetics, **142**(4): 1357–1362. PMID:8846911.

Ruzzante, D.E. 1998. A comparison of several measures of genetic distance and population structure with microsatellite data: bias and sampling variance. Can. J. Fish. Aquat. Sci. **55**(1): 1–14. doi:10.1139/cjfas-55-1-1.

Ryder, O.A. 1986. Species conservation and systematics: the dilemma of subspecies. Trends Ecol. Evol. **1**(1): 9–10. doi:10.1016/0169-5347(86)90059-5.

Schaefer, J.A. 2006. Towards maturation of the population concept. Oikos, **112**(1): 236–240. doi:10.1111/j.0030-1299.2006.13763.x.

Takezaki, N., and Nei, M. 1996. Genetic distances and reconstruction of phylogenetic trees from microsatellite DNA. Genetics, **144**(1): 389–399. PMID:8878702.

Taylor, B.L., and Dizon, A.E. 1999. First policy then science: why a management unit based solely on genetic criteria cannot work. Mol. Ecol. **8**(Suppl.): S11–S16. doi:10.1046/j.1365-294X.1999.00797.x. PMID:10703548.

Turgeon, J., Estoup, A., and Bernatchez, L. 1999. Species flock in the North American Great Lakes: molecular ecology of Lake Nipigon ciscoes (Teleostei: Coregonidae: *Coregonus*). Evolution, **53**(6): 1857–1871. doi:10.2307/2640446.

Vogler, A.P., and DeSalle, R. 1994. Diagnosing units of conservation management. Conserv. Biol. **8**(2): 354–363. doi:10.1046/j.1523-1739.1994.08020354.x.

Waples, R.S. 1991. Pacific salmon, *Oncorhynchus* spp., and the definition of "species" under the Endangered Species Act. Mar. Fish. Rev. **53**: 11–22.

Waples, R.S. 1995. Evolutionary significant units and the conservation of biological diversity under the Endangered Species Act. Am. Fish. Soc. Symp. **17**: 8–27.

Waples, R.S., and Gaggiotti, O. 2006. What is a population? An empirical evaluation of some genetic methods for identifying the number of gene pools and their degree of connectivity. Mol. Ecol. **15**(6): 1419–1439. doi:10.1111/j.1365-294X.2006.02890.x. PMID:16629801.

Ward, R.D., Woodwark, M., and Skibinski, D.O.F. 1994. A comparison of genetic diversity levels in marine, fresh-water, and anadromous fishes. J. Fish Biol. **44**(2): 213–232. doi:10.1111/j.1095-8649.1994.tb01200.x.

Weir, B.S., and Cockerham, C.C. 1984. Estimating *F*-statistics for the analysis of population structure. Evolution, **38**(6): 1358–1370. doi:10.2307/2408641.

Wilson, C.C., Lavender, T.M., and Black, J. 2007. Genetic assessment of walleye (*Sander vitreus*) restoration efforts and options in Nipigon Bay and Black Bay, Lake Superior. J. Great Lakes Res. **33**(Suppl. 1): 133–144. doi:10.3394/0380-1330(2007)33[133:GAOWSV]2.0.CO;2.

CORRIGENDUM / RECTIFICATIF

Corrigendum: Differences in predicted catch composition between two widely used catch equation formulations

Trevor A. Branch

Ref.: Ref: Can. J. Fish. Aquat. Sci. **66**: 126–132, 2009.

I correct three related typographical errors in the introduction of this paper, which were brought to my attention by T. Garrison (University of Washington, School of Aquatic and Fishery Sciences, Seattle, WA 98195, USA). In each case the e^{-X} term should have been $1 - e^{-X}$:

Eq. 2. Original : $C_t = \frac{F}{M+F} N_t e^{-M-F}$ Corrected : $C_t = \frac{F}{M+F} N_t (1 - e^{-M-F})$

Eq. 4. Original : $C_{a,t} = \frac{S_a F_t}{M + S_a F_t} N_{a,t} e^{-M-S_a F_t}$ Corrected : $C_{a,t} = \frac{S_a F_t}{M + S_a F_t} N_{a,t} (1 - e^{-M-S_a F_t})$

Eq. 6. Original : $C_{a,t} = \frac{S_a F_t}{M + S_a F_t} A_a N_{a,t} e^{-M-S_a F_t}$ Corrected : $C_{a,t} = \frac{S_a F_t}{M + S_a F_t} A_a N_{a,t} (1 - e^{-M-S_a F_t})$

In these equations, t refers to time, a refers to age group, M is instantaneous natural mortality rate, N is fish abundance, F is instantaneous fishing mortality rate, C is observed catch, S is gear selectivity, and A is availability to the fishing gear.

Received 8 July 2009. Accepted 8 July 2009. Published on the NRC Research Press Web site at cjfas.nrc.ca on 9 September 2009. J21301

T.A. Branch. School of Aquatic and Fishery Sciences, Box 355020, University of Washington, Seattle, WA 98195, USA (e-mail: tbranch@gmail.com).

 doi:10.1139/F09-107

ERRATUM / ERRATUM

Erratum: Lead–radium dating of orange roughy (*Hoplostethus atlanticus*): validation of a centenarian life span

Allen H. Andrews, Dianne M. Tracey, and Matthew R. Dunne

Ref.: Can. J. Fish. Aquat. Sci. **66**: 1130–1140, 2009.

An error occurred during typesetting of the article that mistakenly reported radon-222 (^{222}Rn) as radium-222 (^{222}Ra). All instances of ^{222}Ra in four paragraphs on pp. 1136–1137 of the Discussion should be ^{222}Rn. These paragraphs have been corrected and reprinted below.

The seminal radiometric study on orange roughy by Fenton et al. (1991) used pooled whole otolith samples and an approach that made it necessary to make some educated assumptions. The study did not perform any growth zone derived age estimations, but instead sought to independently determine age for groups of fish with similar length and otolith weight. For the method to work, there needed to be little or no (*i*) between-individual variability in otolith mass growth rate and (*ii*) variability in ^{226}Ra uptake throughout the growth of the otolith. In addition to these factors, there were important assumptions about the very nature of the lead–radium dating technique; the otolith needed to be a closed system to (*i*) the ingrowth of ^{210}Pb from ^{226}Ra with no loss of ^{226}Ra daughter products and (*ii*) the incorporation of exogenous sources of the decay series radionuclides (not from the decay of incorporated ^{226}Ra). Within these assumptions, the most conceivable problems were (*i*) the potential loss of ^{222}Rn (daughter product of ^{226}Ra and a noble gas) and (*ii*) the incorporation of exogenous ^{210}Pb or polonium-210 (used as a proxy for ^{210}Pb in alpha-spectrometry). These concerns could not be thoroughly addressed when Fenton et al. (1991) performed the analyses on orange roughy otoliths, but subsequent studies have provided support for the assumptions that were necessary (Francis 1995; Smith et al. 1995). In some cases, the assumptions have been tested directly.

The veracity of the lead–radium technique was questioned by a number of papers addressing the assumptions. In a perspective paper, West and Gauldie (1994) argued that there were uncontrollable errors that invalidated the technique for fish age estimation but provided a series of observations and conclusions that failed to consider equally viable explanations that do not discredit the radiometric technique. In an attempt to measure loss of ^{222}Rn from orange roughy otoliths, Gauldie and Cremer (1998) openly recognized anomalous results, a faulted technique, and negative values that imply the contrary; nevertheless, they concluded from weak trends in rather dubious data that loss of ^{222}Rn was a problem and that this invalidated old ages. The inconclusive quality of those data was reiterated in a follow-up application that reported a loss of 26%–28% (Gauldie and Cremer 2000), but these findings are inconsistent with determinations made in this study because large losses as such would create an upper limit to the measured lead–radium ratios. Furthermore, evidence supporting the author's conclusions was cited (e.g., incomplete concepts from a report by Whitehead and Ditchburn (1996)), but a prior publication that (*i*) specifically addressed ^{222}Rn diffusion from orange roughy otoliths and (*ii*) provided evidence to support a long life span (Whitehead and Ditchburn 1995) was ignored (i.e., Gauldie and Cremer 1998, 2000; Gauldie and Romanek 1998).

Perhaps the most scientifically robust study to date on potential loss of ^{222}Rn from otoliths was performed on red snapper (*Lutjanus campechanus*) and red drum (*Sciaenops ocellatus*) from the Gulf of Mexico (Baker et al. 2001). In this study, two species with relatively large otoliths and some of the highest ^{226}Ra activities recorded from otolith material were analyzed; the study resulted in low (≤4.1%) to no loss of ^{222}Rn. The measured loss was further considered more of a surface emanation because larger otoliths liberated relatively less ^{222}Rn. They concluded that such losses were probably insignificant relative to other sources of error associated with lead–radium dating. This would be

Received 30 July 2009. Accepted 30 July 2009. Published on the NRC Research Press Web site at cjfas.nrc.ca on 9 September 2009. J21329

A.H. Andrews.[1,2] Rhodes University, Department of Ichthyology and Fisheries Science, Grahamstown 6140, South Africa.
D.M. Tracey and M.R. Dunne. National Institute of Water and Atmospheric Research, P.O. Box 14-901, Kilbirnie, Wellington, New Zealand.

[1]Corresponding author (e-mail: andrews@mlml.calstate.edu).
[2]Present address: Age and Longevity Research Laboratory, Moss Landing Marine Laboratories, California State University, 8272 Moss Landing Road, Moss Landing, CA 95039, USA.

especially true in the case of otolith cores because the loss would be temporary and much less significant with time. In another study, Pacific halibut (*Hippoglossus stenolepis*) otoliths revealed no evidence of ^{222}Rn loss, but experimental error from low lead–radium levels led to somewhat inconclusive results (Kastelle and Forsberg 2002).

Another scenario to consider with regard to loss of ^{222}Rn is the potential affect on the measured lead–radium ratio as age approaches 100 years. In a study performed on yelloweye rockfish (*Sebastes ruberrimus*), otolith cores provided measured lead–radium ratios that were very close to secular equilibrium (Andrews et al. 2002). If there was a consistent problem with the loss of ^{222}Rn throughout the period of otolith growth, then secular equilibrium would not and could not be attained. It was at approximately 99 years that secular equilibrium was approached to within 95% for the ingrowth model used in the present study (core age of 4 years). Provided that there was a ^{222}Rn loss on the order of 25% for the oldest orange roughy age group (90–108 years with an average age of 98 years), the measured ratio (1.007, 2 SE low of 0.9461) would have been far less, approximately 0.675 and a radiometric age of 30–40 years. In addition, none of the samples analyzed in this study, as well as other studies (e.g., Andrews et al. 2002), would have exceeded this ratio. The findings presented here for orange roughy support the hypothesis that loss of ^{222}Rn was not a significant factor in the determination of age from lead–radium dating.

NRC·CNRC

National Research Council Canada | Conseil national de recherches Canada

Canadian Journal of Fisheries and Aquatic Sciences 1980–1995 back issues now available on the Web!

Archives du Journal canadien des sciences halieutiques et aquatiques (1980–1995) maintenant accessibles sur le Web!

NRC Research Press is currently taking orders for the one-time purchase of the *Canadian Journal of Fisheries and Aquatic Sciences* back files (1980–1995), 15 years of fully indexed digitized articles are available!

This monthly journal publishes manuscripts reporting significant new knowledge and understanding of fisheries and aquatic sciences. They cover a range of disciplines including biology and ecology of marine and freshwater organisms, limnology, oceanography, physiology, toxicology, genetics, economics, disease, and management. CJFAS is one of 16 journals published by NRC Research Press, Canada's foremost scientific publisher.

Since this is a cost-recovery initiative, once costs are fully recovered, we would like to make our content more widely available by making the back files completely open in late 2009. We hope that libraries and the STM community share this goal and will partner with us to make this initiative a success.

ISSN: 1205-7533

CJFAS Web site: cjfas.nrc.ca

Frequency: Monthly (12 times/year)

Price: $2000.00

Les Presses scientifiques du CNRC acceptent maintenant les commandes pour l'achat en bloc des archives du *Journal canadien des sciences halieutiques et aquatiques* (1980–1995), 15 années d'articles numérisés et indexés!

Cette revue mensuelle publie des articles contribuant, via l'apport de nouvelles connaissances d'importance ou d'une compréhension approfondie, à l'enrichissement des sciences halieutiques et aquatiques. Ceux-ci traitent de disciplines variées, y compris la biologie et l'écologie des organismes d'eau douce et d'eau salée, la limnologie, l'océanographie, la physiologie, la toxicologie, la génétique, l'économie, les maladies et la gestion. Elle est l'une des 16 revues des Presses scientifiques du CNRC, la maison d'édition scientifique la plus importante au Canada.

Il s'agit d'une initiative en recouvrement de coûts. Ainsi, nous aimerions élargir l'accès à nos collections en offrant les archives tout à fait gratuitement vers la fin de 2009, une fois les coûts entièrement recouvrés. Nous espérons que le milieu STM et les bibliothèques appuieront notre objectif et contribueront au succès de cette initiative.

ISSN : 1205-7533

Site Web : jcsha.cnrc.ca

Fréquence : mensuelle (12 numéros par année)

Tarif : 2000 $

Contact **Mike Boroczki** at **613-993-9108**
or mike.boroczki@nrc-cnrc.gc.ca for further information.

Communiquez avec **Mike Boroczki** au **613-993-9108**
ou mike.boroczki@nrc-cnrc.gc.ca pour obtenir des renseignements supplémentaires.

NRC Research Press
ANNOUNCEMENT

An NRC Research Press
JOURNAL
Une REVUE des
Presses scientifiques du CNRC

Presses scientifiques du CNRC
ANNONCE

OpenArticle

LibreArticle

NRC Research Press is pleased to announce a new publishing option in support of authors who wish or need to sponsor open access to their published research articles. The ***OpenArticle*** option establishes a fee-based mechanism for individual authors or their research funding agencies to sponsor the open availability of their articles on the Web at the time of online publication. Under this new policy, to be implemented January 2008, NRC Research Press will enable unrestricted Web access to a contributing author's publication from the NRC Research Press Web site, in exchange for a fixed payment from the sponsoring author. The base fee for the ***OpenArticle*** option will be initially set at a subsidized price of $3000 for all NRC Research Press journals.

The ***OpenArticle*** option will be offered to authors after editorial acceptance. Upon an author's payment to sponsor the ***OpenArticle*** option, NRC Research Press will make the article freely available upon Web publication.

NRC Research Press is Canada's foremost scientific publisher, publishing 16 international STM journals, monographs, and a growing number of affiliated journals for clients.

For further information, please contact:

Mike Boroczki, Business Manager
NRC Research Press
National Research Council Canada
Ottawa, ON K1A 0R6, Canada
mike.boroczki@nrc-cnrc.gc.ca (email)
613-993-9093 (T)/613-952-7656 (F)
http://researchpress.nrc.ca (Web site)

Les Presses scientifiques du CNRC (Presses) sont ravies d'offrir une nouvelle option pour appuyer les auteurs qui désirent (ou doivent) financer le libre accès à leurs résultats de recherche. Grâce à l'option ***LibreArticle***, les auteurs ou les organismes subventionnaires de recherche bénéficient d'un mécanisme tarifé pour commanditer le libre accès à leurs articles dès leur parution sur le Web. L'entrée en vigueur de cette nouvelle option est prévue pour janvier 2008. Ainsi, les Presses offriront le libre accès Web à la publication d'un auteur collaborateur à partir du site Web des Presses, moyennant un paiement fixe de la part de l'auteur commanditaire. Le tarif de base pour l'option ***LibreArticle*** est initialement fixé au prix subventionné de 3 000 $ pour l'ensemble des revues des Presses.

Par ailleurs, les auteurs pourront uniquement bénéficier de l'option ***LibreArticle*** une fois le processus d'édition terminé. À la réception de leur paiement, les Presses offriront le libre accès à l'article dès sa parution sur le Web.

Principal éditeur scientifique du Canada, les Presses scientifiques du CNRC publient 16 revues STM de renommée internationale, des monographies et un nombre grandissant de revues affiliées.

Pour de plus amples renseignements, communiquez avec :

Mike Boroczki, gestionnaire des Affaires commerciales
Presses scientifiques du CNRC
Conseil national de recherches du Canada
Ottawa (Ontario) K1A 0R6, Canada
Courriel : mike.boroczki@nrc-cnrc.gc.ca
Tél. : 613-993-9093; téléc. : 613-952-7656
Site Web : http://pressesscientifiques.cnrc.ca

National Research Council Canada | Conseil national de recherches Canada

NRC·CNRC

NRC·CNRC
From Discovery to Innovation...
De la découverte à l'innovation...
La Science à l'œuvre pour le Canada
at work for Canada

New release / Nouvelle parution

Late Ordovician Orthide and Billingsellide Brachiopods

from Anticosti Island, Eastern Canada: Diversity Change Through a Mass Extinction

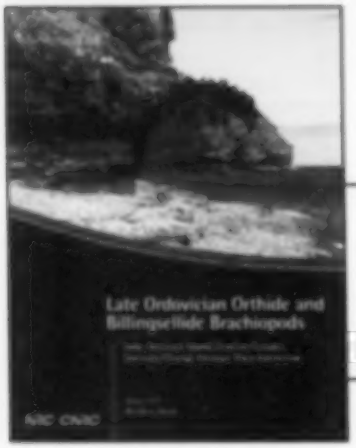

By / De

Jisuo Jin and Renbin Zhan

Softcover / Édition brochée
ISBN: 978-0-660-19789-0
NRC / CNRC : 46858
$69.95 CAN; Other countries $69.95 US
59,95 $CAN; À l'étranger : 59,95 $US

This monographic study deals with a major marine faunal turnover during the Late Ordovician global greenhouse/icehouse episodes. The Late Ordovician was marked by one of the two greatest global sea-level rises and inundations of the North American paleocontinent during the Phanerozoic (last 544 million years), accompanied by a rapid diversification of invertebrate faunas in shallow, tropical, epicontinental seas. Toward the end of the Late Ordovician, continental glaciation in the southern hemisphere (Gondwana landmass) caused a major sea-level drop and marine regression from North America, bringing about the first of the five major mass extinction events in life history. Anticosti Island was part of the larger Anticosti basin, located on the eastern continental shelf of the North America paleocontinent, and was covered by a shallow, tropical sea in the Late Ordovician epoch. During the latest Ordovician global mass extinction event, the marine shelly benthos (bottom) of the Anticosti basin experienced a significant local radiation. This provides a great opportunity for us to investigate the response of marine life to a major environmental crisis. This monographic study aims to document the diversity change of brachiopods (one of the major groups of marine life during the Ordovician Period) from pre-extinction to extinction times.

Cette étude monographique porte sur un renouvèlement majeur de la faune marine survenu à la suite d'épisodes planétaires d'effet de refroidissement et de réchauffement lors de l'Ordovicien tardif. Cette période a d'ailleurs été marquée par l'une des deux plus importantes élévations du niveau de la mer mondial et inondations du paléocontinent nord-américain du Phanérozoïque (les 544 derniers millions d'années). Ce bouleversement a aussi été accompagné par une diversification rapide de la faune d'invertébrés dans les mers épicontinentales tropicales et peu profondes. Vers la fin de l'Ordovicien tardif, la glaciation continentale dans l'hémisphère méridional (masse terrestre du Gondwana) a causé un important rabattement du niveau de la mer et une régression marine en Amérique du Nord, phénomènes qui ont mené à la première des cinq plus importantes extinctions massives de l'évolution biologique. L'île d'Anticosti faisait alors partie du bassin d'Anticosti, entité géographique plus imposante, située sur la partie est du plateau continental du paléocontinent nord-américain, et était couverte d'une mer tropicale peu profonde. Lors de la dernière extinction massive planétaire de l'Ordovicien tardif, le benthos coquiller marin du bassin d'Anticosti a connu une expansion locale considérable, ce qui nous offre une occasion idéale d'étudier les façons dont la vie marine réagit à une crise environnementale majeure. Cette étude monographique fait état des changements dans la diversité des brachiopodes (l'un des principaux groupes d'organismes marins de l'Ordovicien) de la préextinction à l'extinction.

To order books / Pour commander

Order Office / Bureau des commandes
NRC Research Press / Presses scientifiques du CNRC, National Research Council / Conseil national de recherches
Ottawa, ON K1A 0R6, Canada. Telephone / Téléphone : 613-990-2254; Fax / Télécopieur : 613-952-7656
E-mail / Courriel : pubs@nrc-cnrc.gc.ca; Order online / Commandes en ligne : http://pubs.nrc-cnrc.gc.ca

Shipping and handling extra.
Canadian customers add GST. Prepayment required unless order is accompanied by a purchase order number. Cheques or money orders should be made payable to: **"Receiver General for Canada, Credit NRC"**. For all orders outside Canada, rates are in U.S. dollars. All sales are final.

Frais d'expédition et de manutention en sus.
Clients du Canada, ajoutez la TPS. Les commandes doivent être payées d'avance à moins qu'elles ne soient accompagnées d'un numéro de bon de commande. Les chèques ou mandats doivent être libellés à l'ordre du « **Receveur général du Canada, crédit du CNRC** ». Pour les commandes hors-Canada, les tarifs sont en dollars américains. Vente ferme.

01/09/2008

National Research Council Canada / Conseil national de recherches Canada

Canada

Joshua A. Israel, K. Jun Bando, Eric C. Anderson, and Bernie May	**1491–1504**	Polyploid microsatellite data reveal stock complexity among estuarine North American green sturgeon (*Acipenser medirostris*)
David G. Hankin, Jacqueline Fitzgibbons, and Yaming Chen	**1505–1521**	Unnatural random mating policies select for younger age at maturity in hatchery Chinook salmon (*Oncorhynchus tshawytscha*) populations
M. Demarty and Y.T. Prairie	**1522–1531**	In situ dissolved organic carbon (DOC) release by submerged macrophyte–epiphyte communities in southern Quebec lakes
Brianna Wyn, Karen A. Kidd, Neil M. Burgess, and R. Allen Curry	**1532–1545**	Mercury biomagnification in the food webs of acidic lakes in Kejimkujik National Park and National Historic Site, Nova Scotia
Shawn R. Garner, John W. Heath, and Bryan D. Neff	**1546–1553**	Egg consumption in mature Pacific salmon (*Oncorhynchus* spp.)
Rebecca Whitlock and Murdoch McAllister	**1554–1568**	A Bayesian mark–recapture model for multiple-recapture data in a catch-and-release fishery
John R. Hyde and Russell D. Vetter	**1569–1581**	Population genetic structure in the redefined vermilion rockfish (*Sebastes miniatus*) indicates limited larval dispersal and reveals natural management units
Jon Egil Skjæraasen, James Kennedy, Anders Thorsen, Merete Fonn, Bente Njøs Strand, Ian Mayer, and Olav Sigurd Kjesbu	**1582–1596**	Mechanisms regulating oocyte recruitment and skipped spawning in Northeast Arctic cod (*Gadus morhua*)
A. Kathleen Collins, Susan E. Allen, and Rich Pawlowicz	**1597–1616**	The role of wind in determining the timing of the spring bloom in the Strait of Georgia
Andrea M. Bernard, Moira M. Ferguson, David L.G. Noakes, Bruce J. Morrison, and Chris C. Wilson	**1617–1630**	How different is different? Defining management and conservation units for a problematic exploited species
	CORRIGENDUM	RECTIFICATIF
Trevor A. Branch	**1631**	Corrigendum: Differences in predicted catch composition between two widely used catch equation formulations
	ERRATUM	ERRATUM
Allen H. Andrews, Dianne M. Tracey, and Matthew R. Dunne	**1632–1633**	Erratum: Lead–radium dating of orange roughy (*Hoplostethus atlanticus*): validation of a centenarian life span

National Research Council Canada
Ottawa, Canada K1A 0R6

Conseil national de recherches Canada
Ottawa, Canada K1A 0R6

Postage paid at Ottawa
Publications mail
Registration No. 40062591

Port payé à Ottawa
Poste-publication
Enregistrement n° 40062591

USPS periodical postage paid at Plattsburgh, NY 12901, USA

Canadian Journal of

FISHERIES AND AQUATIC SCIENCES

Volume 66, Number 9, September 2009

Journal canadien des

SCIENCES HALIEUTIQUES ET AQUATIQUES

Volume 66, numéro 9, septembre 2009

RAPID COMMUNICATIONS — COMMUNICATIONS RAPIDE

Robert S. Schick, Patrick N. Halpin, Andrew J. Read, Christopher K. Slay, Scott D. Kraus, Bruce R. Mate, Mark F. Baumgartner, Jason J. Roberts, Benjamin D. Best, Caroline P. Good, Scott R. Loarie, and James S. Clark **1399–1403** Striking the *right* balance in right whale conservation

Hamish J. Moir, Christopher N. Gibbins, John M. Buffington, John H. Webb, Chris Soulsby, and Mark J. Brewer **1404–1408** A new method to identify the fluvial regimes used by spawning salmonids

ARTICLES — ARTICLES

Timothy Loher and Calvin L. Blood **1409–1422** Seasonal dispersion of Pacific halibut (*Hippoglossus stenolepis*) summering off British Columbia and the US Pacific Northwest evaluated via satellite archival tagging

Mikio Inoue, Hiroshi Miyata, Yousuke Tange, and Yoshinori Taniguchi **1423–1434** Rainbow trout (*Oncorhynchus mykiss*) invasion in Hokkaido streams, northern Japan, in relation to flow variability and biotic interactions

Courtney R. Salm, Jasmine E. Saros, Sherilyn C. Fritz, Christopher L. Osburn, and David M. Reineke **1435–1448** Phytoplankton productivity across prairie saline lakes of the Great Plains (USA): a step toward deciphering patterns through lake classification models

Chris J. Harvey **1449–1461** Effects of temperature change on demersal fishes in the California Current: a bioenergetics approach

Adam Langley, Karine Briand, David Seán Kirby, and Raghu Murtugudde **1462–1477** Influence of oceanographic variability on recruitment of yellowfin tuna (*Thunnus albacares*) in the western and central Pacific Ocean

J.A. Galarza, G.F. Turner, E. Macpherson, and C. Rico **1478–1490** Patterns of genetic differentiation between two co-occurring demersal species: the red mullet (*Mullus barbatus*) and the striped red mullet (*Mullus surmuletus*)

Continued on inside back cover / Suite au verso

Front cover: Ikoko Saito/Toshiyuki Tajima/Dex Image/Getty Images.

Page couverture : Ikoko Saito/Toshiyuki Tajima/Dex Image/Getty Images.

Canada

Printed in Canada by / Imprimé au Canada par NRC Reprographic Services / Service de reprographie CNRC
Page production by / Mise en page par NRC Research Press / Presses scientifiques du CNRC

0706-652X(20090966:9:1-8